# The use of miR-92a inhibitor to enhance endothelial progenitor cell-mediated regeneration of injured arteries

**Jorge Manuel Arsénio dos Santos Ruivo**

2018

Centre for Cardiovascular Biology and Medicine

Division of Medicine

**University College London**

A thesis submitted to University College London for the degree of Doctor of Philosophy (Ph.D.)

# Declaration

*I, Jorge Manuel Arsénio dos Santos Ruivo, confirm that the work presented in this thesis is my own. Where information has been derived from other sources, I confirm that this has been indicated.*

Signed

Jorge Ruivo

# Abstract

Restenosis, a pathological condition characterised by neointima formation and lumen narrowing, can occur in some patients submitted to percutaneous coronary intervention. Reducing its incidence remains an important medical issue.

Circulating endothelial precursor cells (EPCs) home to the vascular injury site and contribute to re-endothelialisation and neointima attenuation. However, the engraftment and repair capacity of EPCs from patients with cardiovascular disease are typically impaired.

Priming strategies to increase EPCs' engraftment may improve post-injury outcomes. Anti-angiogenic miR-92a is upregulated in EPCs of cardiovascular patients, contributing to their reduced regenerative capacity. It was hypothesized that miR-92a antagonism in EPCs could result in a more favourable angiogenesis profile, with the rationale of developing a future functional priming strategy before cell transplantation which could lead to increased engrafting/thriving and accelerated re-endothelialisation on injured segments, hence, contributing towards post-PCI restenosis prevention.

The aims of the work were: 1) to differentiate and characterise $CD34^+$-derived late-outgrowth EPCs from an enriched progenitor human source; 2) to characterise target gene expression and demonstrate *in vitro* the functional priming following the treatment of EPCs with miR-92a inhibitor and relate it to the ensueing integrin α5 subunit (ITGA5) derepression.

A human EPC culture was obtained following differentiation of cord blood $CD34^+$ cells. miR-92a inhibitor treatment using oligofectamine in $CD34^+$-derived late-outgrowth EPCs revealed pro-angiogenic,-migratory,-proliferative, and -adhesive effects *in vitro*, which was accompanied by the derepression of integrin α5 (ITGA5). Remarkably, siRNA ITGA5 abrogated the enhanced matrix adhesion in primed EPCs, highlighting the role of the miR-92a downstream target in EPC engraftment. Preliminary intraluminal transplantation results suggested enhanced engraftment capacity of primed EPCs in the rat carotid balloon angioplasty model.

# Acknowledgements

I am very thankful to Prof. Ian Zachary, my P.hD. supervisor for the opportunity, patience and support that he gave me to complete my Ph.D. in his research group, as well as for his supervision and invaluable suggestions during this project.

I am very grateful to Prof. John Martin, my P.hD. co-supervisor for his esteemed support and overall for believing in me. From him I have learnt a great deal about scientific reasoning from the clinician perspective, a vital skill which I will take with me in my future career.

I am immensely thankful to Dr Vedanta Mehta, who has since become a dear friend, for the generosity with which he gave his time to answer my questions, guided me through the lab and for having a wonderfully calm and pleasant presence which was a pleasure to work alongside.

I want to express my deep gratitude to Dr Caroline Pellet-Many and Dr. Ian Evans for teaching me the practical techniques, their assistance and discussions during this project. Additionally, I want to thank Dr. Paul Frankel, Dr. Katya Paliashvili, Dr. Laura Fields, Dr. Marwa Mahmoud, Dr. Marie C. Ramel, Dr. Dan Liu, Dr. Carla Milagre, Dr. Andy O'Leary for their help in the laboratory and my fellow PhD colleagues Rudina Tahiri, Angela Barrett, Nicola Lockwood, Vanessa Lowe and Tonya Frolov for the constructive and enjoyable discussions. I would like to also express gratitude to former members of the CVB group. I thank Dr Maiko Yamaji for her friendship and ever-present willingness to help and advise me. My thanks additionally go to Dr Birger Herzog, who was an impeccable help. I also wish to thank Dr Lili Cheng and Dr Haiyan Jia for their advice. I consider myself extremely fortunate to have worked alongside so many wonderful and helpful colleagues, all of whom contributed to my completion of this thesis in their own ways.

I am also grateful to the fellows who hosted me in Biocant (Portugal) during my first PhD year and for their advice and invaluable support during this time, namely Prof. Lino Ferreira, Dr. Ricardo Neves, Dr. Sezin Aday, Carlos Boto and José Paiva, who became a dear friend.

UCL funded my research consumables through an European Union's Seventh Programme for research, technological development and demonstration under grant agreement No 278313 awarded to the Cardiovascular Biology group for the Biomasgcar project. The Portuguese Fundação Calouste Gulbenkian and Fundação para a Ciência e Tecnologia funded my salary and tuition fees through two individual PhD scholarships. I am extremely grateful to all these Institutions for financing the work in this project. From Fundação Calouste Gulbenkian I would like to additionally acknowledge the help and wisdow of Prof. Leonor Parreira and Prof. João Ferreira, who have scientifically inspired me.

Last but certainly first, I give my sincere thanks to my family who give sense to my life and motivate me to reach my dreams. In particular, to my parents and brother who have supported me throughout this journey, and a special thanks to my lovely wife, that gave up so many of her dreams to help me persuade mine, ultimately, even changing her country of residence for me.

# Table of Contents

# List of Figures

# List of Tables

# List of Abbreviations

**acLDL:** acetylated low-density lipoprotein
**ACTB:** β-actin
**AGO2:** Argonaute 2
**Akt:** Protein kinase B
**AMI:** Acute myocardial infarction
**ATP:** Adenosine triphosphate
**BM:** Bone marrow
**BMB:** Bone marrow blood
**BSA:** Bovine serum albumin
**CAD:** Coronary artery disease
**CCA:** Common carotid artery
**CD:** Cluster of differentiation
**CEC:** Circulating endothelial cell
**CFU:** Colony forming unit
**$CO_2$:** Carbon dioxide
**CRP:** C-reactive protein
**CVD:** Cardiovascular disease
**DAPI:** 4',6-diamidino-2-phenylindole
**DLS:** Dynamic light scattering
**EBM:** Endothelial basal médium
**EC:** Endothelial cell
**ECA:** External carotid artery
**ECM:** Extracellular matrix
**EGM:** Endothelial growth medium
**eNOS:** Endotelial Nitric oxid synthase
**EPC:** Endothelial precursor cell
**ERK:** Extracellular signal–regulated kinase
**FAK:** Focal adhesion kinase
**FACS:** Fluorescence-activated cell sorting
**FBS:** Fetal bovine serum
**FITC:** Fluorescein isothiocyanate
**Flt3:** Fms-related tyrosine kinase 3 ligand
**FN:** Fibronectin
**FSC:** Forward scatter
**G-CSF:** Granulocyte colony stimulating factor
**HAEC:** Human aortic endothelial cell
**HRP:** Horse-radish peroxidase
**HSC:** Hematopoietic stem cell
**HUVEC**: Human umbilical vein endothelial cell
**ICA:** Internal carotid artery
**IF:** Immunofluorescence
**IgG:** Immunoglobulin
**IL-8:** Interleukin 8
**I/M:** Intima-to-media ratio
**ITGA5:** Integrin α5 subunit
**ITGAV:** Integrin αv subunit
**KDR:** Kinase insert domain receptor
**KLF2:** Krüppel-like factor 2
**KLF4:** Krüppel-like factor 4

**LDL:** Low density lipoprotein
**MAC:** Myeloid angiogenic cell
**MACS:** Magnetic activated cell sorting
**MAPK:** Mitogen-activated protein kinase
**MKK4:** Mitogen-activated protein kinase kinase 4
**MMP9:** Matrix metalloproteinase-9
**MNC:** Mononuclear cell
**miR:** micro ribonucleic acid
**miRNA:** micro ribonucleic acid
**mRNA:** Ribonucleic acid Messenger
**MSC:** Mesenchymal stem cell
**MVB:** Multivesicular bodies
**ncRNA:** Non-coding RNA
**NO:** Nitric oxide
**NP:** Nanoparticle
**$O_2$:** Oxygen
**OF:** Oligofectamine
**PAC:** Proangiogenic cell
**PB:** Peripheral blood
**PBS:** Phosphate buffered saline
**PBS-T:** Phosphate buffered saline plus tween 20
**PCI:** Percutaneous coronary intervention
**PdI:** Polydispersity index
**PE:** Phycoerythrin
**PFA:** Paraformaldehyde
**PFCE:** Perfluoro-1,5-crown ether
**PLGA:** Poly(lactic-co-glycolic acid)
**PVA:** Polyvinyl alcohol solution
**RF:** Risk factor
**RIPA:** Radio-Immunoprecipitation Assay
**RISC:** RNA-induced silencing complex
**RNA:** Ribonucleic acid
**RT:** Room temperature
**rt-PCR**: Real time polymerase chain reaction
**SCF:** Stem cell factor
**SDF:** Stromal derived factor
**SEM:** Standard error of the mean
**siRNA:** Small interference ribonucleic acid
**SIRT1:** Sirtuin 1
**SMC:** Smooth muscle cell
**SP:** Side population
**SSC:** Side scatter
**TNF:** Tumour necrosis factor
**TFE:** Trifluoroethanol
**UCB:** Umbilical cord blood
**VECAD:** Vascular endothelial cadherin
**VEGF:** Vascular endothelial growth factor
**VEGFR:** Vascular endothelial growth factor receptor
**VSMC:** Vascular smooth muscle cell
**WB:** Western blot
**vWF:** von Willebrand factor

# Chapter 1: Endothelial progenitor cells for vascular repair after angioplasty

Coronary artery disease (CAD) is the principal cause of death in industrialised nations and expected to become so in emerging countries by 2020 (Bassand et al., 2007). Atherosclerotic plaque stenosis or rupture, with differing degrees of superimposed thrombosis and distal embolization, is the substrate for the acute or chronic ischemia seen in these patients. For both, the advent percutaneous coronary intervention (PCI) inaugurated a new era of clinical management. PCI is considered a minimally invasive, endovascular procedure to widen stenotic or (partially) occluded arteries, usually subsequent to arterial atherosclerosis. A deflated balloon attached to a catheter is passed over a guide-wire into the narrowed vessel and then inflated to a fixed size. The balloon forces expansion of the blood vessel and the surrounding muscular wall, allowing an improved blood flow (angioplasty). A stent may be inserted at the time of ballooning to ensure the vessel remains open, and the balloon is then deflated and withdrawn. Still, PCI can often fail because of restenosis, thrombosis, and vasospasm (Bennett & O'Sullivan, 2001). In this introductory chapter, I will review some of the principles behind (1.1) post-PCI restenosis, the (1.2) contribution of Endothelial precursor cells (EPCs) for vascular repair and (1.3) the role of miR-92a for priming EPCs.

# 1.1 Restenosis

## Post-injury arterial restenosis is a prevalent condition among certain risk groups

PCI has become widely accepted as an efficient and safe treatment modality for CAD, leading to improved perfusion, quality of life and survival (Kolh & Wijns, 2011). However, being an invasive technique, there is a risk of complications. As the balloon is inflated to high atmospheric pressures to restore normal coronary blood flow and compress the atheroma plaque, it also eccentrically distends the vessel. Mechanical injury is necessarily a feature of PCI, resulting from the barotrauma and vigorous opposition of stent struts against the vessel wall if a stent is also deployed. Consequently, a comprehensive inflammatory and proliferative reaction, involving several different cellular players, is set in motion. Although this response is physiological, it can be exaggerated in some patients, resulting in lumen re-narrowing or restenosis. PCI success can be limited by restenosis of the target vessel in 30–60% of patients, particularly if multi-vessel disease or diabetes is present (Rajagopal & Rockson, 2003), while the incidence of in-stent restenosis has been reported to be as high as 29% in high-risk populations using bare metal stents (Mauri et al., 2008). This complication is defined by angiographic or clinical criteria and prompts revascularization (Cutlip et al., 2007). To date, many predictive clinical, biological, (epi)genetic, lesion-related and procedural risk factors (RFs) have been recognized (Jukema, Verschuren, Ahmed, & Quax, 2012). Defining risk markers is not only helpful for risk stratification and prognosis, helping in the identification of those that could benefit from additional treatment modalities, but also provides valuable information on the underlying molecular and cellular mechanism of restenosis, with implications for new therapies.

## Restenosis pathophysiology involves a complex interplay of endothelial cells, platelets, leukocytes, vascular smooth muscle cells, mesenchymal and endothelial precursor cells

The reason why restenosis remains largely unsolved clinically is likely attributed to its complex mechanisms. The vascular endothelium is a dynamic border between circulating blood elements and the surrounding tissue. The entire endothelial cell (EC) monolayer comprises $10^{13}$ ECs and covers approximately $7m^2$ in an average adult (Cines et al., 1998). It regulates nutrient and blood component traffic and participates in many other complex physiologic events such as angiogenesis and inflammation (Y. Lin, Weisdorf, Solovey, & Hebbel, 2000). Moreover, it has pivotal roles in coagulation, inflammation, vasodilatation and vasoconstriction through a variety of important regulatory substances, including prostaglandins and nitric oxide (NO) (Cines et al., 1998). In healthy subjects, a low level of endothelial turnover occurs basally (Hristov & Weber, 2008). However, in acute vascular injury (as in PCI), there is a significant (potentially reversible) impairment of the endothelial monolayer. Under normal circumstances, the cellular and molecular processes that control vascular injury responses result in vascular healing. In pathological conditions, dysregulation of vascular repair results in persistent vascular inflammation. These cases may cause irreversible structural damage, i.e. a restenotic obstruction of the lumen, which can constitute a medical condition on its own. The cascade of complex biological events leading to restenosis comprises two major processes: *neointimal hyperplasia* and *constrictive remodelling* **(Figure 1)**. Its putative causal mechanisms have not yet been fully identified, but are thought to include inflammation, vascular smooth muscle cell (VSMC) proliferation, and matrix remodelling (Jukema, Verschuren, et al., 2012).

**Figure 1 | Restenosis**
Intravascular ultrasound images of the various stages of coronary artery disease. Indicated are the outer border of the vessel (green), the lumen (red), and the coronary stent (pink). Schematic representations are shown to the right of these images. The processes occurring in the vessel immediately after PCI (with stent placement) are highlighted in detail. Adapted from (Jukema, Verschuren, et al., 2012). ECM, extracellular matrix; PCI - Percutaneous coronary intervention.

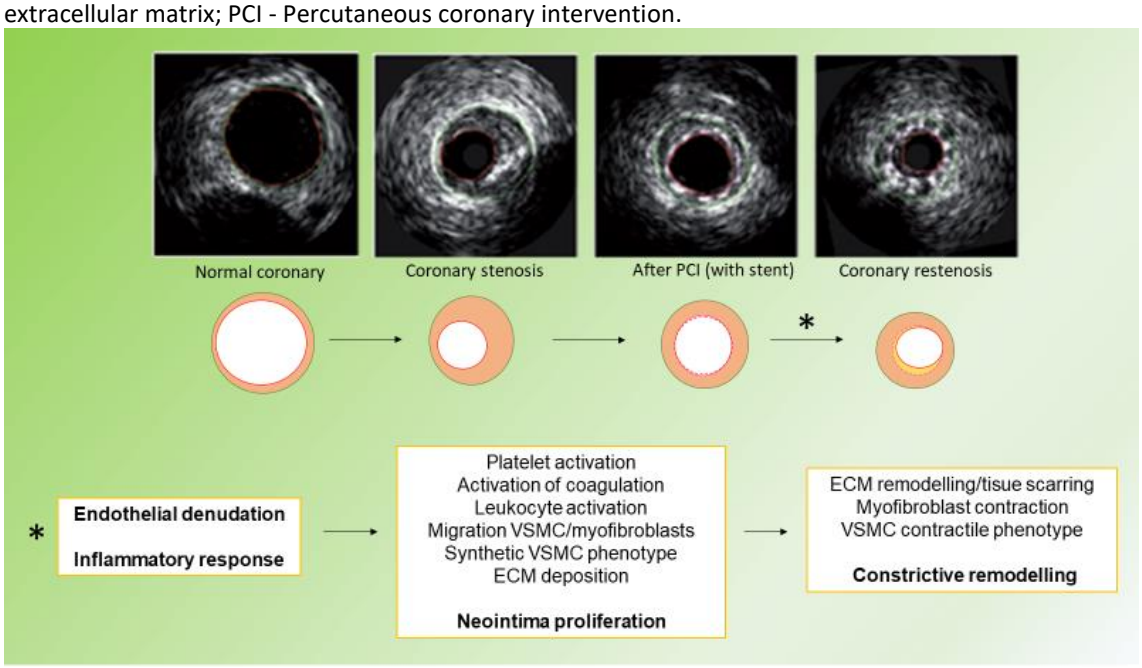


A functionally intact endothelium is a pre-requisite for the inhibition of intimal hyperplasia (Kipshidze et al., 2004), which is attributed to the potent inhibitory effects of endothelium-derived NO (von der Leyen et al., 1995). The endovascular laceration due to rigid stent struts and high-pressure balloon inflations is considered the initiating event of neointimal hyperplasia after balloon angioplasty (Behrendt & Ganz, 2002), since it determines the loss of a significant anti-thrombogenic cap, triggering an intense local inflammatory response. Then, there is dysfunction of neighbouring ECs, which undergo apoptosis. The resulting endothelial denudation and fragmentation of the internal elastic lamina result in a rapid influx of leukocytes and in the exposure of circulating platelets to the sub-endothelial matrix (Inoue et al., 2011). The exposed deeper matrix contains many platelet-activating factors (Fager, 1995), which give rise to microthrombus formation. Activated platelets, dysfunctional ECs, and macrophages within thrombi are a primary source of reactive oxygen species, chemotactic and mitogenic factors which can induce a VSMC phenotypic transition (Durham, Speer, Scatena, Giachelli, & Shanahan, 2018; Pakala, Willerson, & Benedict, 1997). Mature, differentiated VSMCs express a unique repertoire of contractile proteins (Owens, 1995), enabling them to perform their contractile functions. VSMCs are highly plastic cells and

can undergo de-differentiation upon environmental modulation, a change that is reversible. Within one week after endothelial denudation, the shortage of arterioprotective factors, such as NO, and the increased production of growth factors, such as platelet-derived growth factor (PDGF-BB), drive the VSMCs in the innermost part of the media to switch back to a more synthetic phenotype (N. M. Liu, Siu, Youn, & Cai, 2016). Synthetic VSMCs are characterised by a reduced contractile protein content, an increased rate of proliferation, and increased secretion of extracellular matrix (ECM) proteins and cytokines (Doran, Meller, & McNamara, 2008). The disassembly of stress fibres and the rearrangement of actin filaments, drive the transformed VSMCs to acquire a polarised asymmetric shape, facilitating the migratory activity towards the tunica intima, the source of chemoattractants (cytokines, growth factors, ECM components). Later on, the neointima is developed by excessive matrix deposition and the accumulation of migrated VSMCs, circulating progenitor cells (Psaltis, Harbuzariu, Delacroix, Holroyd, & Simari, 2011; Sata et al., 2002) and myofibroblasts (Y. Shi et al., 1996; D. Wang, Li, Dai, Wang, & Li, 2018).

Neointima formation is followed by inward remodelling of the vessel, a process called constrictive remodelling. The proposed underlying mechanisms for this process include media matrix remodelling (Riessen, Wight, Pastore, Henley, & Isner, 1996), migration of myofibroblasts towards the intima (Zargham, 2008), and restoration of the VSMC contractile phenotype within the neointima (Shanahan & Weissberg, 1998). Whereas PDGF signalling promotes the synthetic phenotype, activation of TGF-β pathways favours their differentiation back into contractile VSMCs (Nazari-Jahantigh, Wei, & Schober, 2012). It seems likely that there is a disturbed blood flow after neointima outgrowth that may lead to chronic TGF-β mediated deposition of collagen and FN (Zargham, 2008). This matrix composition will activate specific integrin receptors in VSMC, such as α1β1 and α8β1 (Zargham, Pepin, & Thibault, 2007), eliciting re-expression of differentiated contractile markers (Shanahan & Weissberg, 1998), resulting in scar contraction and late luminal loss. The latter suggests that the pathophysiology of restenosis may be different in the early and late phases after vascular injury.

Given its complexity, the development of innovative therapeutic approaches to restenosis lies in a detailed understanding of the events and timings causing both

neointimal thickening and vascular remodelling, including all cellular sources. The restenosis process was formerly ascribed to vascular SMCs and ECs only, however diverse vascular wall progenitor cells with specific mural distribution **(Figure 2)** are also implicated in vascular disease and repair (Vono, Spinetti, Gubernator, & Madeddu, 2012; D. Wang et al., 2018) through their intrinsic endothelial, smooth muscle, hematopoietic or mesenchymal differentiation potential (Psaltis & Simari, 2015).

**Figure 2 | Mural distribution of postnatal vascular wall and bone marrow derived progenitor cells implicated in vascular repair.**
Different types of progenitor cells have been identified within all mural layers of arteries and veins, as well as derived from the circulation. AMPC – adventitial macrophage progenitor cell; BM - bone marrow; EPC – endothelial precursor cell; CVC - calcifying vascular cells; HPC/HSC – hematopoietic progenitor/stem cell; MVSC – multipotent vascular stem cell; SVP - saphenous vein-derived progenitor cells; SPC – smooth muscle progenitor cell; VW-MSC – vascular wall mesenchymal stem cell.

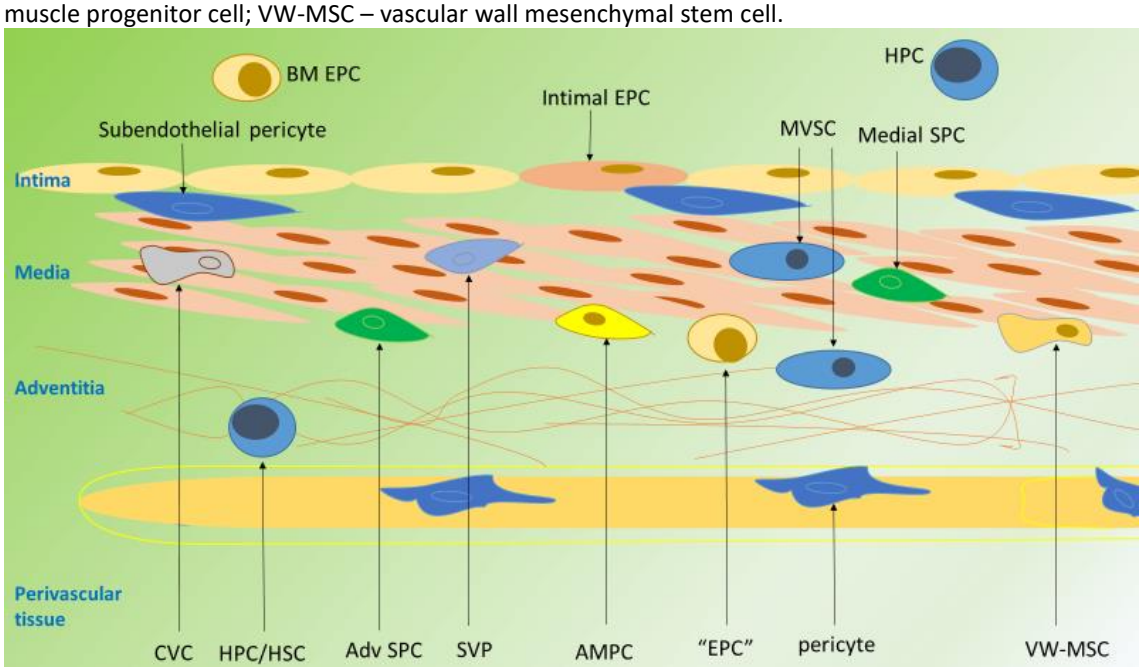


### *Vascular wall progenitors*

The *adventitia*, the outermost layer of the blood vessel, is composed of a collagen-rich extracellular matrix embedded with a mixture of cells. It provides an interface to the highly cellular and cytokine-rich perivascular connective/adipose tissue and with *vasa vasorum* (Stenmark et al., 2013). Evidence for vascular stem/progenitor cell enrichment in the adventitia, specifically along its border with the media (vasculogenic zone), is robust (Halper, 2018). Namely, the presence of cells with endothelial potential ($CD34^{+}CD31^{-}$) in the so-called vasculogenic zone of the inner adventitia has been inferred from arterial ring sprouting assays (Zengin et al., 2006).

Also, adventitial macrophage progenitor cells (AMPCs) proliferate and differentiate in response to growth factors to generate macrophages and dendritic cells locally in the adventitia (Halper, 2018).

In addition, a specific population of $Sox10^{+}$ multipotent vascular stem cell (MVSCs) is activated upon vascular injury, becomes proliferative, and can migrate from both medial and adventitial layers to contribute to neointima formation and microvessel formation during tissue repair and regeneration (D. Wang et al., 2017).

Highly proliferative progenitors have also been isolated from human veins, and termed "saphenous vein-derived progenitor cells" (SVPs). These cells are localized around adventitial vasa vasorum and co-express CD34, pericyte/mesenchymal antigens and stem cell marker Sox2 (D. Wang et al., 2018). SVPs improve neovascularization and blood flow recovery (Campagnolo et al., 2010).

Vascular wall multipotent stem cells (VW-MPSCs), which co-express certain MSC markers (CD44, CD73, CD105, CD90, Stro1 and CD29) and stemness markers Oct4 and Sox2 (D. Klein et al., 2011), when transplanted with human umbilical vein endothelial cells (HUVECs) into matrigel plugs in immunodeficient mice, lead to new vessel formation covered with MPSC-derived pericyte- and smooth muscle-like cells (D. Klein et al., 2011). MPSCs include two cell types: (1) Perycites are contractile cells that surround and appose microvascular ECs, with which they share a basement membrane that separates much of the pericyte–endothelial interface, except at discrete intercellular contact points. Perycites serve to pattern vascular networks and facilitate EC growth and differentation, while regulating vessel tone, caliber, permeability and providing mechanical stability in established vessels (Psaltis & Simari, 2015), therefore, facilitating neovascularization and angiogenesis (Katare et al., 2011). However, pericytes can also differentiate into myofibroblasts and are another important cellular source of vascular/organ fibrosis (Katare et al., 2011). (2) VW-MSCs also occupy the perivascular niche supporting angiogenesis, and they have multilineage differentiation potential into mature pericytes, SMCs, and perhaps even ECs, help mediate vascular tissue homeostasis and repair (Psaltis & Simari, 2015). This is achieved by trophic support of other vascular cells, vasa vasorum expansion, differentiation into SMCs, pericytes and adventitial fibroblasts, and production of mineral and fat deposits, collagen and extracellular matrix in both adventitia and atheroma.

The *media* also harbors MVSCs and side population (SP) progenitors, both of which have smooth muscle cell-forming potential. This small population of Sca-1+, c-kit (-/low), Lin-, CD34-/low cells from the media layer, can give rise to ECs and SMCs cultured with vascular endothelial growth factor (VEGF) and transforming growth factor β1 (TGF-β1)/platelet-derived growth factor BB (PDGF-BB) respectively. A population of calcifying vascular cells (CVCs) which can be found in human atherosclerotic lesions in the arterial media is also known to to differentiate into SMC, osteogenic, and chondrogenic lineages (Tintut et al., 2003).

In the *intima* progenitor cells with endothelial potential have been described (cKit+ SP), and subendothelial pericytes also identified in the intima in human arteries of all sizes (Psaltis & Simari, 2015).

***Bone marrow progenitors***

While the before mentioned progenitor populations are locally derived or maintained in the vessel wall itself, the vascular repair process seems to be partially governed by cells derived from the bone marrow (BM) too (Bianconi et al., 2018; Sata et al., 2002). It is understood that the participation of the BM in arterial remodelling after injury is not only limited to the inflammatory stage of the vascular remodelling process driven by mononuclear cells (MNCs) and macrophages. A minor population of BM-derived VSMCs within the neointima has also been identified (Rodriguez-Menocal et al., 2009), as well as, circulating BM-derived endothelial progenitor cells (EPCs) recruited to sites of vascular injury, where they encourage healing by resident ECs, thereby significantly contributing to re-endothelialisation and limiting neointimal formation (Haider, Aziz, & Al-Reshidi, 2017; Szmitko, Kutryk, Stewart, Strauss, & Verma, 2006). Only EPCs will merit our focus for the PhD work.

## 1.2 The role of EPCs in restenosis

There is widespread consensus that there are circulating blood cells termed EPCs that are involved in the process of forming new blood vessels and repairing injured ones. Since Asahara first identified them in 1997 (Asahara et al., 1997), mounting evidence suggests that this cell population functionally contributes to pathological changes in cardiovascular disease (CVD) models of peripheral vascular disease (Vaughan et al., 2012), stroke (Y. Fan et al., 2010; Takizawa, Nagata, Nakayama, Masuda, & Asahara, 2016), retinopathy (X. Liu et al., 2010), myocardial and limb ischemia (Bonauer et al., 2009), atherosclerosis (Torsney, Mandal, Halliday, Jahangiri, & Xu, 2007; Q. Xu, 2008) and tumour vascular associated-growth (Lyden et al., 2001; Patenaude, Parker, & Karsan, 2010), which makes them therapeutically promising for vascular repair (Balaji, King, Crombleholme, & Keswani, 2013). These precursor cells are mobilised mainly from the BM, and are then recruited to sites of ischemic (Zampetaki, Kirton, & Xu, 2008), atherosclerotic (Pelliccia et al., 2010) or endothelial (Werner et al., 2002) distress, and there contribute to angiogenesis (Takahashi et al., 1999) and re-endothelialisation (Pelliccia et al., 2010). Their regeneration potential is associated with an inherent ability to incorporate within the vessel and secrete pro-angiogenic factors (Zampetaki et al., 2008) and to terminally differentiate into proliferative mature ECs (Lev et al., 2010). Consequently, autologous EPC transplantation to improve neovascularization and vascular repair has been sought, as well as epigenetic and genetic techniques aimed at enhancing their *ex vivo* expansion and therapeutic potential (Balaji et al., 2013). However, so far, there is still substantial ambiguity regarding the origin, definition, and identification of EPCs (Hristov, Erl, & Weber, 2003; Simard et al., 2017).

## EPC origin

Adult stem cells are unspecialized cells capable of replicating or self-renewing themselves, and are able to give rise to mature cell types that have characteristic morphologies and specialised functions **(Figure 3)** (Bautch, 2011). A precursor or progenitor cell is an intermediately undifferentiated cell type but lacks self-renewing ability (Bautch, 2011). Such cells are usually regarded as "committed" to differentiating along a specific cellular development pathway. EPCs are a putative kind of adult progenitor cells committed to differentiate into mature ECs when triggered (Bai & Wang, 2008), but they do not have baseline characteristics of mature ECs. According to various *in vitro* and *in vivo* studies (Gunsilius et al., 2000), EPCs and hematopoietic progenitor cells (HPCs) are believed to derive from a common stem cell called hemangioblast (A. M. Muller, Medvinsky, Strouboulis, Grosveld, & Dzierzak, 1994), since both lineages share similar cell-surface antigens, including Kinase insert domain receptor (KDR), Tie-2, and CD34 (Flamme & Risau, 1992). Specifically, $CD34^+KDR^+$ cells have been shown to give rise to both HPC and EPCs with long-term proliferative potential (Pelosi et al., 2002). CD34 antigen expression is then gradually reduced as hematoendothelial lineages maturate (Sidney, Branch, Dunphy, Dua, & Hopkinson, 2014). CD45 expression seems to be a distinctive feature since $CD34^+$ cells are known not to express CD45 during hematoendothelial development, rather acquiring it during differentiation into HPC, except if they are destined to differentiate into ECs (Timmermans et al., 2009). To make things more complex, the potential of BM-derived HPCs to transdifferentiate *in vivo* and *in vitro* into EPCs has also been documented by some research groups (Gehling et al., 2000; Grant et al., 2002). Understanding the endothelial-to-hematopoietic transition will have significant implications for the interpretation of the EPC phenotype and vascular biology in general since there is considerable overlap between these cellular players.

**Figure 3 | Hemangioblast model.**
Development of ECs from EPC (precursor cell) and angioblast (stem cell). HPC – hematopoietic progenitor cell; HSC – hematopoietic stem cell; EPC – endothelial precursor cell; SMC – smooth muscle cell. Adapted from (Bautch, 2011).

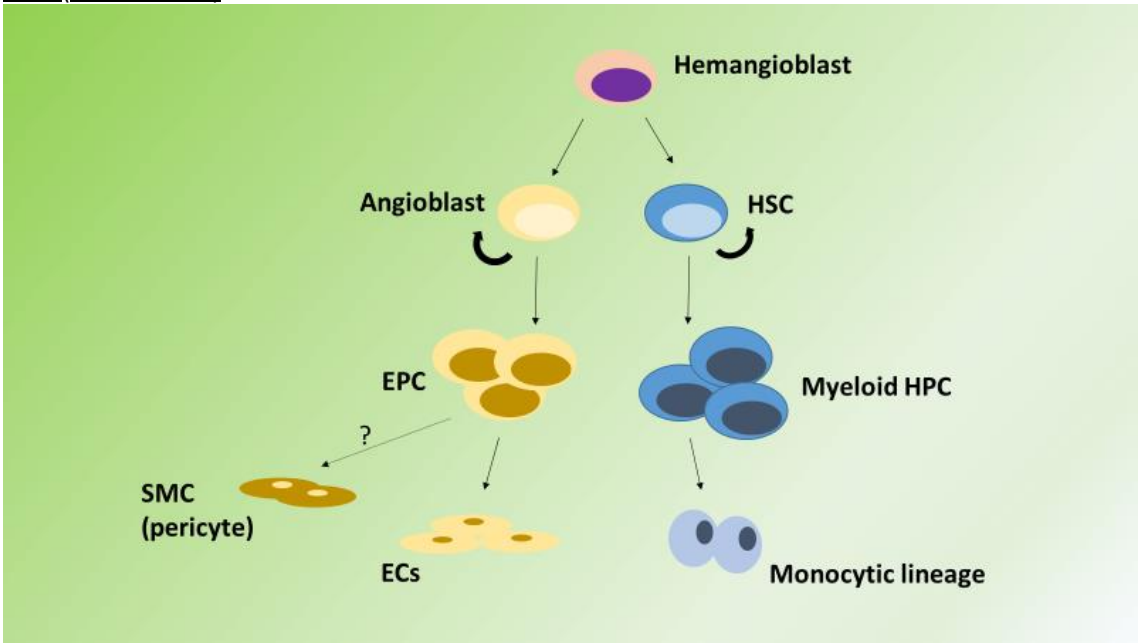


## EPC definition

Controversy still exists whether cells with numerous hematopoietic features that also participate in the process of new blood vessel formation and vascular repair ought to be called EPCs or not. Should the term EPC be reserved for a progenitor for the endothelial lineage alone? The answer is yes, and to date, some defining properties have been proposed for EPCs (Patel, Donovan, & Khosrotehrani, 2016; Simard et al., 2017; Yoder, 2012). It must be a circulating cell that gives rise to progeny exhibiting clonal proliferation and differentiation restricted to the endothelial lineage. Moreover, it can generate capillary-like structures with a lumen *in vitro* (cytoplasmic vacuolation). It should have the capability to form stable blood vessels (cells must secrete a basement membrane) when implanted into tissues, to become an integrated part of the host circulatory system and to present the potential to undergo remodelling to form the intima of the vessel. Most circulating BM-derived cells identified so far fail to do so (Hirschi, Ingram, & Yoder, 2008). Thus their EPC designation should be revisited. Finding a unique cell surface marker that would allow prospective isolation and enrichment of cells displaying the above activities would certainly help clarify the EPC identity and must remain a focus for the field.

## EPC identification

To date, putative EPCs have been identified using two general approaches: surface and functional phenotyping. Nevertheless, the precise identification of EPCs remains tentative (Hristov et al., 2003; Patel et al., 2016; Simard et al., 2017), since many of the (nonspecific) markers used in phenotyping these cells are shared by both HPCs and mature ECs. Their multiple roles in vascular homoeostasis, redundant sources (Urbich & Dimmeler, 2004), broad plasticity (Asahara et al., 1997) and general uncertainty about tissue culture modulation on phenotype add to the uncertainty around the identification so far. All the afore-mentioned factors have resulted in various proangiogenic subsets being used in basic research and clinical trials (Chong, Ng, & Chan, 2016; Rafii & Lyden, 2003; Sekiguchi, Ii, & Losordo, 2009) with inconsistent therapeutic outcomes (Beeres, Atsma, van Ramshorst, Schalij, & Bax, 2008; Chong et al., 2016).

### Cell surface phenotype

EPC antigen characterization has been evolving thanks to the contribution of modern flow cytometry, which now uses multiple simultaneous fluorochromes properly compensated, linear scale analysis of low-intensity staining regions, gate exclusion of false signals by erythrocyte or monocyte specific staining as well as by positive nDNA staining, a feature lacking in microparticles (Pober, 2012).

Historically, EPCs have been thought to be derived from $CD34^+$ cells, which subsequently differentiated into cells expressing definitive endothelial markers (Asahara et al., 1997) and which play a role in regenerative angiogenesis (Fadini et al., 2008). This was further supported by the findings by Kawamoto and colleagues, who demonstrated that $CD34^-$ cells lacked proangiogenic potential (Kawamoto et al., 2006). The transmembrane phosphoglycoprotein CD34 belongs to the CD34-superfamily, which also comprises podocalyxin and endoglycan (Nielsen & McNagny, 2008). CD34 has a molecular weight of 115 kDa and possesses an extracellular domain that is heavily sialylated, O-linked glycosylated and contains several N-linked glycosylation sites (Sidney et al., 2014). l-Selectin (CD62L), E-selectin and CrkL are the most commonly described ligands for CD34

(Baumheter et al., 1993; Felschow, McVeigh, Hoehn, Civin, & Fackler, 2001). The CD34 antigen was first identified on hematopoietic stem cells (HSCs) (and then on mesenchymal stem cells or MSCs), but it is not restricted to these cell types. Several other non-hematopoietic cell types coexpress tissue-specific markers alongside CD34, suggesting that the presence of CD34 may indicate a specific progenitor for that tissue. Evidence for this is certainly apparent in muscle satellite cells, epithelial progenitors, corneal keratocytes, and interstitial cells (Sidney et al., 2014). It has been hypothesised that CD34 plays a role in trafficking of HSCs to niches within the BM (Nielsen & McNagny, 2008, 2009). Additionally, CD34 is involved in cytoadhesion, regulation of cell differentiation and proliferation processes (Healy et al., 1995; Nielsen & McNagny, 2008, 2009). Its role in enhancing cell proliferation and/or blocking differentiation is corroborated by its progressive decline in surface density from multipotent hematopoietic progenitors to more mature cells, suggesting a role in the maintenance of the undifferentiated progenitor phenotype (Krause, Fackler, Civin, & May, 1996). Moreover, there are fewer HPCs in embryonic and adult tissues in CD34-knockout mice compared with wild-type animals, while adult-derived progenitors seem to harbour a proliferation defect (J. Cheng et al., 1996). Despite the hematopoietic changes, the CD34 knockout mice are viable and show a typical hematopoietic profile of adult blood (Salati et al., 2008). Nevertheless, their vascular phenotype is abnormal, given that CD34 is also expressed on all vascular ECs of both adults and embryos (Baumhueter, Dybdal, Kyle, & Lasky, 1994; Young, Baumhueter, & Lasky, 1995). Gene deletion studies have demonstrated the pivotal role of CD34 in the development and integrity of blood vessels. $CD34^{-/-}$ mice are prone to autoimmune arthritis because of increased vascular permeability (Blanchet et al., 2010). Loss of CD34 results in altered vessel structure and vascular integrity within developing tumors (Maltby et al., 2011). Moreover, during early embryogenesis, the loss of CD34 was sufficient to delay the opening of the nascent lumen of the aorta (Strilic et al., 2009).

Exactly, because CD34 expression has also been reported in microvasculature mature ECs (Timmermans et al., 2009), other groups have suggested the use of a more immature marker for putative EPCs (Gehling et al., 2000). CD133 was considered a good candidate since it is expressed on HSCs but, unlike CD34, not on mature ECs (Handgretinger et al.,

2003). In fact, virtually all mature hematopoietic cells, including megakaryocytes, mature myeloid, lymphoid and erythroid cells fail to express CD133 (Miraglia et al., 1997). Since the discovery of CD133, also called Prominin-1, as a transmembrane glycoprotein in human HSCs and mouse neuroepithelial cells (Z. Li, 2013), many studies have demonstrated that its expression is associated with progenitor/stem activity, tumorigenesis, regeneration, differentiation, and metabolism (Z. Li, 2013). Among other processes, CD133 is particularly involved in glucose and transferrin uptake, autophagy, membrane-membrane interaction, and as a matrix metalloproteinase (Z. Li, 2013). $CD133^+$ cells are kept at relatively constant numbers in BM, blood, different tissues and even tumours, due to a dynamic and reversible expression in response to the changes of cell microenvironment. Typically, when cellular damage occurs via chemical, physical or mutational insults, $CD133^+$ progenitor or stem cells are activated, differentiate and start proliferating to promote neuronal, bone, muscle or vascular regeneration (Cao et al., 2013; Kijima et al., 2009; M. Shi et al., 2009). In the hematopoietic system, its expression seems to be more restricted to a subset of CD34 bright progenitor cells in human fetal liver, BM, umbilical cord blood (UCB) and peripheral blood (PB) (Buhring et al., 1999). $CD133^+$ cells isolated from UCB have been reported to undergo *in vitro* pre-angiogenic process, form pseudo-vessel structures and present angiogenesis under hypoxic conditions (Paprocka et al., 2011), but there are contradictory reports concerning their EC differentiation (Case et al., 2007; Peichev et al., 2000). *In vivo*, $CD133^+$ cells seem to support neovascularization of ischemic tissues in animal models (Bartunek et al., 2005; Y. X. Cui, Kafienah, Suleiman, & Ascione, 2013; Perin & Silva, 2009), but generally speaking, total $CD133^+$ cells should not be regarded as EPCs because they lack endothelial markers and mostly represent HPCs (Gehling et al., 2000). In summary, the relative non-specificity of this marker, the rarity of these cells in human BM and UCB (Y. X. Cui et al., 2013), and different differentiation results have been limiting factors for its use.

Unfortunately, no single specific surface marker has been found to distinguish EPCs. Currently, investigators characterise EPCs by including hematopoietic stemness markers in combination with markers demonstrating endothelial commitment, but this has resulted in an extensive list of putative EPCs immunophenotypes (Timmermans et al.,

2009). The most studied one reflects the co-expression of CD34 and Kinase insert domain receptor (KDR), considered to be immature cells with endothelial priming (Balaji et al., 2013) able to generate ECs *in vitro* (Asahara et al., 1997; Bompais et al., 2004). KDR is also known as vascular endothelial growth factor receptor 2 (VEGFR-2), CD309 or Flk1 (Fetal Liver Kinase 1). KDR, the human gene that encodes the type III transmembrane kinase receptor, is located in chromosome 4q11–q12 (Holmes, Roberts, Thomas, & Cross, 2007). VEGFR-2 is the principal receptor transmitting VEGF signals in the vascular endothelium (and aslo lymphatic endothelium). Therefore it has a critical role in vascular development, which is highlighted by the fact that VEGFR-2 knockout mice die at E8.5-9.5 due to defective development of blood islands, endothelial cells and haematopoietic cells (Shalaby et al., 1995). VEGFR-2 binds all VEGF-A isoforms, VEGF-C, -D and -E. Ligand binding induces receptor dimerisation and autophosphorylation. Downstream effects of VEGFR-2 activation in the vascular endothelium include cell proliferation, migration, permeability and survival, resulting in vasculogenesis and angiogenesis, through a number of genes with known roles in angiogenesis, such as Cox-2, Down syndrome critical region-1 (DSCR-1), Endocan, Decay-accelerating factor (DAF), Egr3, Ets-1, MMP-1 or Flt-1 (Sato et al., 2000).

One major problem is that $CD34^+KDR^+$ cells are so rare in the steady-state PB that they can usually be sorted only from CB or mobilised PB (Fadini et al., 2008). Moreover, there is also substantial debate concerning this definition, because none of the markers is specific (Peichev et al., 2000) and $CD34^+KDR^+$ phenotype may represent mature ECs in microvascular endothelia or circulating mature ECs (CECs) sloughed from vasculature as well (Kachamakova-Trojanowska, Bukowska-Strakova, Zukowska, Dulak, & Jozkowicz, 2015; Timmermans et al., 2009).

As some mature ECs may detach from the vessel wall and enter the circulation of healthy and diseased human subjects (Blann et al., 2005), Peichev *et al.* attempted to devise a separation protocol to distinguish circulating EPCs from CECs (Peichev et al., 2000). Since mature ECs do not express CD133 (Gehling et al., 2000), the authors, in addition to CD34 and KDR positivity, included CD133 expression as a discriminating marker. According to their results, only a small subset of $CD34^+$ cells derived from hematopoietic sources expressed CD133 and KDR (2% percentage of total circulating $CD34^+$ cells). The

restrictive triple expression pattern was also observed in some cells coating the luminal surface of implanted left ventricular assist devices in human subjects, suggesting that one could use CD34, CD133, KDR as markers for circulating EPC in human subjects. Therefore, they extrapolated that $CD34^{+}KDR^{+}$ cells that coexpress the more immature CD133 might represent the true EPC population. Remarkably, $CD34^{+}CD133^{+}KDR^{+}$ cells have been shown to facilitate tumour microvasculature growth (Bertolini, Mancuso, & Kerbel, 2005; D. Gao et al., 2008), yet there is no evidence that these cells differentiate into ECs and directly incorporate into the vessels. In fact, $CD34^{+}CD133^{+}KDR^{+}$ cells do not contribute to the formation of ECs *in vitro* (Case et al., 2007), nor do they spontaneously form capillary-like structures *in vitro* or *in vivo* (Case et al., 2007; Timmermans et al., 2007). Interestingly, Peichev and colleagues back in 2000 (Peichev et al., 2000) did not test the triple positive cells for expression of CD45, a common leukocyte antigen. Case and colleagues subsequently reported that $CD34^{+}CD133^{+}KDR^{+}$ cells represent an enriched population of $CD45^{+}$ cells using *in vitro* hematopoiesis assays. It is clearer now that the proangiogenic $CD34^{+}CD133^{+}KDR^{+}$ cells are of haematopoietic origin and may not be true EPCs (Case et al., 2007; Simard et al., 2017) since they do not possess the postnatal vasculogenic profile that is proposed for a cell with endothelial progenitor properties (Estes et al., 2010; Medina et al., 2017). While these proangiogenic HPCs may be recruited to denuded vessels early in the process of vascular repair, it is more probable that they promote angiogenesis via paracrine mechanisms (Estes et al., 2010; Medina et al., 2017; Medina et al., 2010; Richardson & Yoder, 2011). Since the evidence does not support the use of CD133, another marker is needed to discriminate circulating $CD34^{+}KDR^{+}$ precursors from mature CECs, which also express CD34 and KDR.

Lately, the combined analysis of CD45 expression has also been proposed to identify EPCs. Most $CD34^{+}$ cells express CD45 at low intensity ($CD45^{dim}$) (Fadini, Losordo, & Dimmeler, 2012). Timmermans and colleagues (Timmermans et al., 2007) used Magnetic activated cell sorting (MACS) preenriched UCB $CD34^{+}$ cells (mean purity 94,3%) and sorted them into $CD34^{+}CD45^{+}$ HPCs (mean purity 99.5%) and a small (2% of total $CD34^{+}$ cells) $CD34^{+}CD45^{-}$ cell fraction (mean purity 99.2%) from the same blood unit, using stringent flow cytometry gates. The cell fractions were then cultured separately in M199 or EBM2 media. Their experiences revealed that *in vitro* EC-like cells derived only

from the $CD34^+CD45^-$ cells, whereas $CD34^+CD45^+$ HPCs did not generate cells with endothelial phenotype in culture (Timmermans et al., 2007). They also showed that the $CD34^+CD45^-$ cell fraction expressed KDR, unlike $CD34^+CD45^+$ HPC cells. Intriguingly, Case (Case et al., 2007) and Timmermans's (Timmermans et al., 2007) findings seem to clash, since Case advocated by Fluorescence-activated cell sorting (FACS) that MACS $CD34^+$-enriched $CD133^+KDR^+$-FACS sorted are universally positive for CD45, while Timmermans could not find KDR expression by real time polymerase chain reaction (RT-PCR) in $CD34^+CD45^+$ cells. It may be that Timmermans' group while sorting for MACS $CD34^+$-enriched $CD45^+$-FACS sorted cells did not manage to gate in the limited $CD34^+CD133^+KDR^+$ cell subset, or that the KDR cDNA numbers were too low to start PCR amplification. Both hypotheses could explain a negative KDR expression in RT-PCR. More recently, Lanuti *et al.* using rigorous polychromatic flow cytometry settings, came to the same observation, that $CD45^+CD34^+CD133^+KDR^+$ could not be found in any PB or CB sample since KDR expression could not be detected on the surface of $CD45^+CD34^+CD133^+$ cells (Lanuti et al., 2016). Irrespective of the contribution of the small triple positive population, the data presented by Timmermans *et al.* are consistent with the previous observation that $CD34^+KDR^+$, but not $CD34^+KDR^-$ cells, are endothelial precursors (Pelosi et al., 2002). Because analysis of the hematopoietic marker CD45 was not performed in the initial description of $CD34^+KDR^+$ precursors (Asahara et al., 1997; Peichev et al., 2000; Pelosi et al., 2002; Q. Shi et al., 1998) it is likely that $CD34^+KDR^+$ cells in these studies were confined to the $CD34^+CD45^-$ cell fraction, which probably comprises the true origin of EPCs (Medina et al., 2017; Simard et al., 2017; Timmermans et al., 2007). In fact, $CD34^+KDR^+$ cells show improved association with CAD and response to statin therapy if restricted to the $CD45^{dim}$ gate (Schmidt-Lucke et al., 2010).

Looking for a more accurate EPC phenotype, CD146, a transmembrane glycoprotein described as a component of the endothelial junction involved in cell adhesion, permeability and transmigration (Kebir et al., 2010), has also gathered recent interest. CD146 was initially implicated in melanoma growth and metastasis (L. Mills et al., 2002), yet it has shown links to angiogenesis as well (Y. Kang et al., 2006). In their article, Tura *et al.* (Tura et al., 2013) confirmed that endothelial colony-generating EPCs were present only in the $CD34^+CD133^-$ MNC fraction. Following further enrichment using CD146 they

found that only the $CD34^+CD133^-CD146^+$ subset gave rise to colonies with true endothelial characteristics, unlike CD146 negative. These findings are in line with a recent study by Mund *et al.* who also reported that EPC colonies express CD146 (Mund, Estes, Yoder, Ingram, & Case, 2012). Unfortunately, Tura *et al.* did not assay for KDR expression in their subsets. Moreover, another critical issue remains unresolved: the cell marker CD146 used to identify putative EPC is not able to distinguish them from circulating mature cells, since CD146 is constitutively expressed on mature ECs too (Boos, Lip, & Blann, 2006).

In summary, our best attempt to identify a putative EPC surface phenotype is presented in **Figure 4**.

**Figure 4 | Simplified Venn diagram depicting subgrouping of different progenitor cell phenotypes**
HPC-comprehending subsets: $CD34^+CD133^+KDR^+$(Case et al., 2007); $CD34^-CD133^+KDR^+$ (Reyes et al., 2002); $CD34^+CD45^+$($CD133^+$) (Timmermans et al., 2007), (Case et al., 2007); EPC-comprehending subsets: $CD34^+CD45^-$($KDR^+CD133^-$) (Timmermans et al., 2007)); $CD34^+KDR^+$ (Pelosi et al., 2002), (Tura et al., 2013). The question mark represents the putative region with EPC potential. Alternatively, EPCs could arise from two distinct subsets, $CD34^+CD146^+$ and $CD34^+KDR^+$. No single marker is known to date to distinguish EPCs from ECs. CD – cluster of differentiation; HPC – hematopoietic progenitor cell; EC – endothelial cell; EPC – endothelial precursor cell; KDR – kinase insert domain receptor.

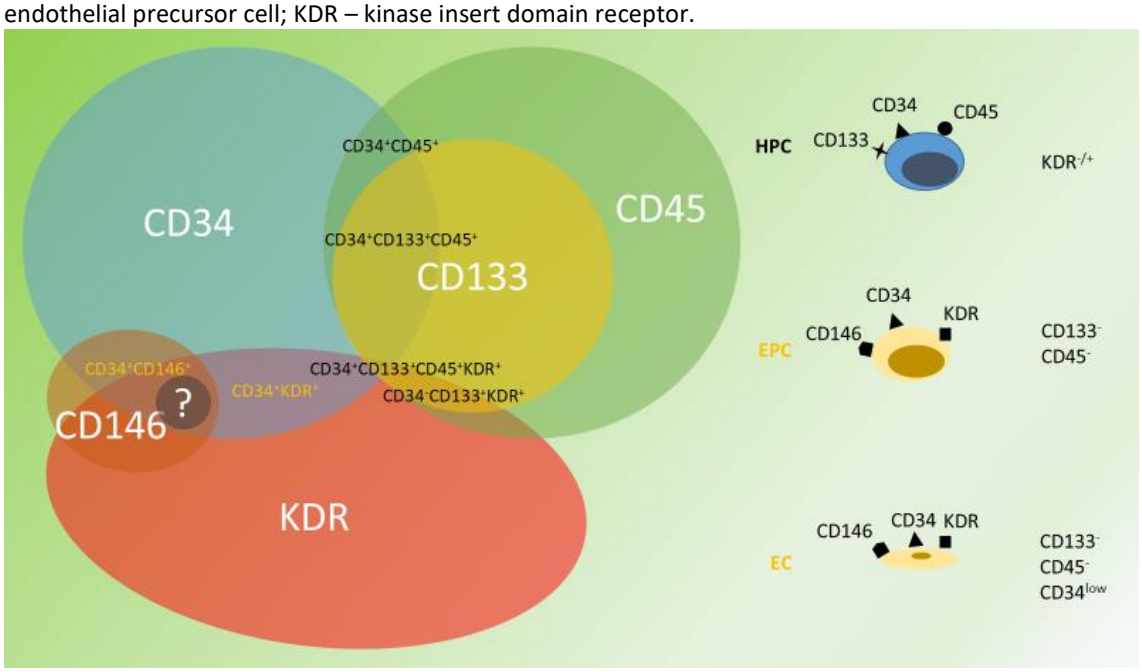


Altogether, it seems that the $CD34^+KDR^+$ phenotype represents the best compromise regarding detection accuracy, biological meaning and clinical usefulness. It is possible that a distinctive marker or marker combination is still to be found. Until then, the use of heterogeneous marker combinations to define EPCs (and even gating strategies which

are not standardised), makes the significance of flow cytometric studies difficult to interpret, creates obstacles to the direct comparison of data between researchers, and may result in discrepancies in the interpretations of study results among different groups. It is now clear that hematopoietic and vascular endothelial progenitors display the same set of antigens and can only be discriminated by extensive testing. Therefore, one should strongly consider that any putative EPC, whatever its surface phenotype, be carefully assessed by gene expression and validating its endothelial potential *in vitro* and *in vivo* (morphology, clonogenicity, functionality).

## Functional phenotype

Inferring the presence of endothelial precursors within a given cell population by the identification of cells bearing mature endothelial characteristics after a period of culture under pro-angiogenic conditions is another approach to identifying (and isolating) EPCs. This was first attempted by Asahara *et al.* (Asahara et al., 1997) in 1997 by isolating human PB $CD34^+$ cells (15.7% enrichment) and culturing them in fibronectin (FN)-coated dishes. They reported that CD34-enriched cells had a spindle-shaped morphology and clustered together similarly to blood island-like clusters found in the embryonic yolk sac. The putative EPCs expressed numerous cell surface proteins typically present in human umbilical vein endothelial cells (HUVECs). They interpreted this endothelial-like outgrowth as constituting evidence for the presence of circulating post-natal angioblasts which could generate EPCs. Further studies revealed that KDR expressing putative EPCs (enriched to 20%) improved microvascular density after infusion into nude mice with induced hindlimb ischemia. Although the results were ground-breaking, potential limitations of this study have been discussed. These included the lack of sufficient cellular pre-enrichment to constitute a purified cell population, failure to perform clonal analytical studies and lack of high cellular resolution evidence that the infused putative EPCs directly formed the new blood vessels in the ischemic tissues of the mice with induced vascular injury.

Three optimised culture methods inspired by the original Asahara assay (Asahara et al., 1997) have been proposed as an alternative to FACS antigen analysis (Fadini et al., 2012; Williamson, Stringer, & Alexander, 2012) **(Figure 5)**.

The first one developed by Kalka *et al.* (Kalka, Masuda, Takahashi, Kalka-Moll, et al., 2000) involves plating MNCs on FN-coated dishes and incubating them with medium containing endothelial growth factors and serum. After three days in culture, the non-attached cells were removed and the adherent cells kept in culture for 14 days. Two types of cell populations were generated sequentially by the *EPC culture assay*. The cells initially seeded were round, and after 3 to 5 days started grouping in clusters. These were comprised of elongated cells which had a spindle shape like that of the EPC first reported by Asahara (Asahara et al., 1997). These cells were termed early EPC, given their short culture time. They showed peak growth at 2 to 3 weeks and after that, they did not replicate *in vitro* and gradually disappeared after four weeks in culture.

**Figure 5 | An overview of the most common methods to isolate EPCs.**
Adapted from (Fadini et al., 2012). CD – cluster of differentiation; EC – endothelial cell; EC-CFU - endothelial cell colony-forming unit; ECFC - endothelial colony-forming cell; eNOS – endothelial nitric oxide synthase; EPC – endothelial precursor cell; KDR – kinase domain insert receptor; LDL – low-density lipoprotein; MNC – mononuclear cell; vWF – von Willebrand factor.

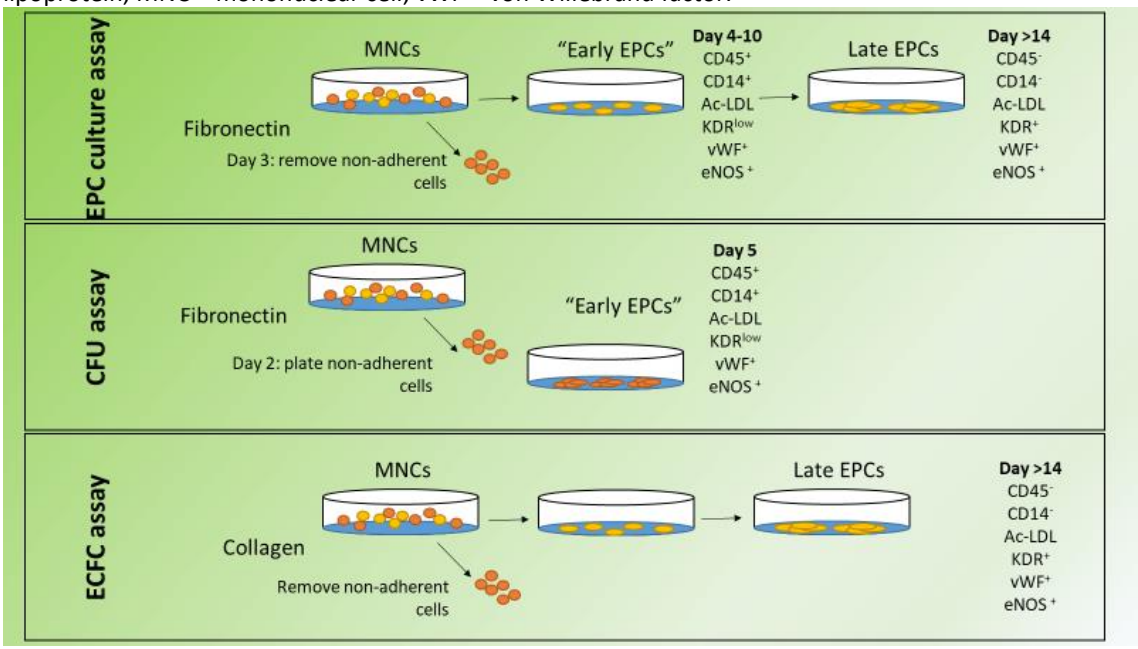


Another population of cells with different morphology and growth pattern appeared in 2 to 3 weeks after plating and were defined as late-outgrowth EPCs. These were firmly attached to the plate and rapidly replicated from several cells to colonies with

cobblestone appearance like ECs. They exhibited multiple population doublings without senescence resulting in exponential growth at 4 to 8 weeks and lived up to 12 weeks. Remarkably, both cell types internalised acetylated-low density lipoproteins (ac-LDL). Despite its simplicity, this isolating method seems flawed by the lack of specificity of the cells obtained. Several blood cells (stem, progenitor, or mature lineages) also possess integrin receptors for FN which promote their attachment to the culture matrix. Remarkably, adherent monocytes when cultured in media containing endothelial growth factors are known to express a variety of proteins typically associated with ECs (von Willebrand factor - vWF, endothelial nitric oxide synthase - eNOS, CD31 and KDR) (Schmeisser et al., 2001; Schmeisser, Graffy, Daniel, & Strasser, 2003). Hence, this very straightforward assay of adherent MNCs growth did not promote the exclusive emergence of EPCs.

Hill and colleagues optimised the previous assay by attempting to deplete the early-adherent MNCs, macrophages and circulating mature ECs from the putative EPC system (Hill et al., 2003). To do this, they allowed a 48h incubation before replating the non-adherent cells on fresh FN-coated dishes. In 5-7 days, central clusters of round cells surrounded by multiple spindle-shaped cells emerged and were scored as endothelial cells colony-forming units (EC-CFUs). Subsequent transcriptome, proteomic, and functional analysis have revealed that cells generated by the *CFU assay* are more closely related to hematopoietic cells than to ECs (Yoder, 2012). Although worthy in intent, the failure to show that all hematopoietic cells were depleted by the preplating step diminished the interest on this method to isolate putative EPCs.

Later, a different type of colony derived from an *ECFC assay* developed by Ingram *et al.* (Ingram et al., 2004) and further improved by Yoder *et al.* (Yoder et al., 2007) was described. In contrast to EC-CFUs, the ECFC colonies emerged from the adherent fraction on type I collagen following the removal of the non-attached population within the first 24h, after 14–21 days in culture (Ingram et al., 2004; Y. Lin et al., 2000). According to Lin and colleagues (Y. Lin et al., 2000), who have subsequently replicated the assay, the discarding of non-adherent cells leaves 19 ± 9 attached cells with endothelial-like morphology and positive for anti-endothelial monoclonal antibody P1H12 staining, plus 100–200 other MNCs which die out within the first two weeks of

culture. The outgrowth colonies are composed of $CD34^+$ ECFCs (Timmermans et al., 2007) which are morphologically indistinguishable from mature ECs, but present a delayed robust proliferative potential, with some colonies growing to more than 10,000 progeny from a single cell plated 14 days earlier (Ingram, Caplice, & Yoder, 2005; Ingram et al., 2004).

Although both short and long-term cultured cells arising from EC-CFU and ECFC assays share mutual properties, such as expression of CD31, CD34, lectin binding, and acetylated low-density lipoprotein (acLDL) uptake, they possess distinctive phenotypes regarding morphology, proliferative and functional potential (Medina et al., 2017; Timmermans et al., 2007) **(Table 1)**.

**Table 1 | Progeny characteristics following EC-CFU and ECFC assays.**
EC-CFUs or "early EPCs" are generated from a non-adherent population of MNCs cultured on fibronectin and appear some 5 to 7 days in culture. EC-CFUs exhibit endothelium-like surface characteristics, however, they are composed of monocytes and angiogenic lymphocytes and have little capacity to form perfusing vessels or incorporate directly into vascular structures. EC-CFUs exhibit phagocytic activity and avidly secrete angiogenic growth factors. Contrastingly, ECFCs or late-outgrowth EPCs are generated from adherent MNCs grown on type I collagen and appear after 2 to 3 weeks of cell culture. ECFCs are morphologically indistinguishable from mature ECs and are derived from non-hematopoietic ($CD45^-$) cells expressing CD34. ECFCs have robust proliferative potential and the capacity to form perfusing blood vessels in vitro. Adapted from (Timmermans et al., 2009), (Fadini et al., 2012), (Tura et al., 2013), (Balaji et al., 2013; Medina et al., 2017). CD – cluster of differentiation; EC – endothelial cell; EC-CFU - endothelial cell colony-forming unit; ECFC - endothelial colony-forming cell; MACs- myeloid angiogenic cells; MNC – mononuclear cell; PAC – proangiogenic cells.

| Characteristics | EC-CFU / "early EPCs"/ PACs / MACs | ECFC / late outgrowth EPCs |
|---|---|---|
| **Adhesive protein** | Fibronectin | Collagen |
| **Precursor** | $CD45^+CD14^+CD34^+KDR^+$ $CD146^-$ | $CD34^+KDR^+CD146^+$ $CD45^-CD14^-$ |
| **Appearance in culture** | 5-7 days | 14-21 days |
| **Proliferative potential** | Low | High |
| **Phagocytic function** | Yes | No |
| **Ability to form vascular networks on Matrigel** | Low | High |
| **Incorporation into vessels** | Low, preferentially perivascular | High |

| | | |
|---|---|---|
| **Cytokine and growth factor release** | High | Low |
| **Improve neovascularization *in vivo*** | Yes | Yes |
| **Morphology** | Mass of round and spindle-shaped cells 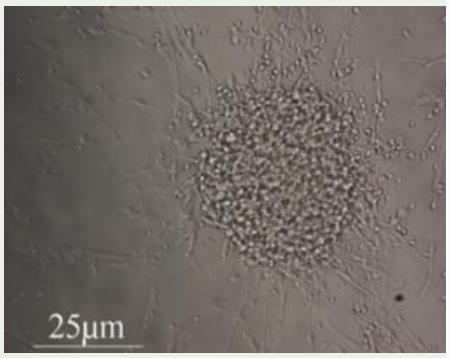  | polygonal cells in cobblestone monolayer 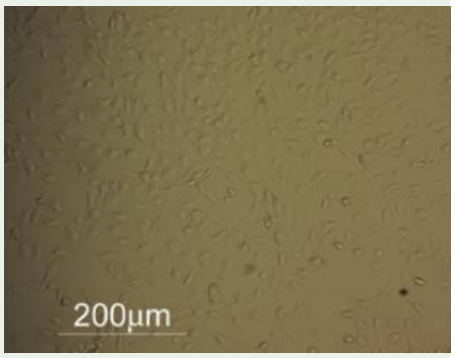  |

Short-term cultured EC-CFUs, historically termed “early EPCs”, are forced within a few days in culture to express endothelial markers, such as eNOS, CD31, CD105, CD141, CD144, CD146, vWF, Tie-2, KDR, and E-selectin, while preserving CD34 positivity (Padfield, Newby, & Mills, 2010; Yoder et al., 2007; Zampetaki et al., 2008). Therefore, they were thought to be cells with EC fate derived from circulating HPCs (Hirschi et al., 2008). However, the coexpression of endothelial markers by EC-CFUs has been a topic of controversy. There is evidence that the detection of endothelial markers might result from contamination with microparticles deriving from platelets which fuse with MNCs leading to false-positive events in FACS analysis (Prokopi et al., 2009), which would mean that isolated HPCs do not differentiate at all into an endothelial lineage as some groups have hinted (Yoder et al., 2007). The lack of an endothelial predetermination is further supported by the discovery that the endothelial genes in EC-CFUs are epigenetically repressed (Ohtani et al., 2011). Silencing of promoters of specific endothelial commitment genes (eNOS, KDR, vWF, and VE-cadherin) seems to occur at the level of histones and DNA methylation (Ohtani et al., 2011). In fact, it is well established now that the colonies arising from the CFU-Hill assay are, in fact, composed of a heterogenic population that mainly originates from myeloid hematopoietic cells, and shares common features with monocyte/macrophages, such as spindle morphology (Yoder et al., 2007), bacteria phagocytic ability (Hur et al., 2007), and colony stimulating factor-1

receptor and expression of nonspecific esterase that is inhibited by sodium fluoride (Yoder et al., 2007). These colonies are in fact a combination of core $CD3^+CD31^+CXCR4^+$ angiogenic T-cell lymphocytes and monocytes at the periphery (Hur et al., 2007; Rohde et al., 2007). EC-CFUs are generated from $CD14^+$ cells (Urbich et al., 2003) since depletion of $CD14^+$ cells prevents their formation (Rohde et al., 2006). Their numbers are high after isolation, but they have a low proliferative potential (Zampetaki et al., 2008), and thus cannot be further expanded. Despite being able to incorporate into the endothelial monolayer, they fail to form perfused vessels *in vivo* (Yoder et al., 2007; Zampetaki et al., 2008). It is thought that "early EPCs" support neovascularization *in vivo* in an indirect fashion, by producing specific growth factors and chemokines, since they do not seem to adopt a typical endothelial phenotype *in vitro* (Timmermans et al., 2007). Hypothetically, "early EPCs" are recruited to damaged sites and secrete regulatory cytokines that help vessel repair by local neighbour (Ingram, Mead, et al., 2005) or circulating (Timmermans et al., 2009) cells with endothelial progenitor potential. The paracrine secretion of pro-angiogenic substances like VEGF, stromal derived factor 1 (SDF-1), interleukin 8 (IL-8), matrix metalloproteinase 9 (MMP-9), granulocyte and granulocyte-monocyte colony stimulating factors (G-CSF and GM-CSF) by these cells has been extensively demonstrated, all of which are implicated in the mobilisation of BM progenitors (Hur et al., 2007; Inoue et al., 2011; Rehman, Li, Orschell, & March, 2003) and in support of tissue-residing cells contributing indirectly to angiogenesis and vascular repair (Simard et al., 2017; Urbich & Dimmeler, 2004; Ziegelhoeffer et al., 2004). Based on their ability to support angiogenesis, not necessarily associated with any definitive endothelial commitment (Rehman et al., 2004), early EPCs should be redefined (Fadini et al., 2012) as proangiogenic cells (PACs) or myeloid angiogenic cells (MACs) instead, as some researchers have already suggested (Medina et al., 2017; Yoder et al., 2007).

In contrast, ECFCs or late-outgrowth EPCs display similar endothelial features *in vitro* and were reported to contribute to neovascularization by incorporating as newly matured ECs into vessels *in vivo* (Yoder et al., 2007), and therefore probably act more as true EPCs (Ingram et al., 2004; Y. Lin et al., 2000; Medina et al., 2017; Yoder et al., 2007). The number of late-outgrowth EPCs is extremely low after isolation, with approximately

1 colony arising per $10^8$ mononuclear cells plated (Fadini et al., 2012). However, while short-term cultured PACs can only support vascular network formation, long-term outgrowing EPCs can form vascular structures *in vitro* in the absence of co-culture (Sieveking, Buckle, Celermajer, & Ng, 2008). Unlike PACs which have a spindle-shaped morphology, these clusters appear as tightly adherent colonies with cobblestone appearance, which begin to proliferate only 2–3 weeks after seeding at a high proliferation rate (Ingram et al., 2004; Zampetaki et al., 2008), and can be maintained in culture extensively (Zampetaki et al., 2008). In fact, in compliance with the notion that the hallmark of progenitor cells is their ability to proliferate and to give rise to progeny, Ingram and colleagues demonstrated that the late EPCs could achieve ≥100 population doublings (Ingram et al., 2004). These cells do not exhibit the pan-leukocyte marker CD45 (Timmermans et al., 2007), the myeloid/macrophage markers CD14 (Padfield et al., 2010), CD11 (Padfield et al., 2010) and CD133 (Timmermans et al., 2007), nor do they have phagocytic behaviour (Padfield et al., 2010). In fact, there is no ECFC growth starting from $CD45^+$ or $CD14^+$ enriched populations (Gulati et al., 2003; Timmermans et al., 2007), clearly indicating the need for a $CD45^-CD14^-CD34^+$ origin. Remarkably, late-outgrowth EPCs, unlike PACs, do not produce an enormous amount of angiogenic growth factors (Hur et al., 2004). Medina and colleagues compared PACs and late EPCs by genome-wide transcriptional profiling and 2D protein electrophoresis and discovered they displayed strikingly different gene expression signatures (Medina et al., 2010). PACs highly expressed haematopoietic specific transcripts (WAS, RUNX1, LYN) with links to immunity and inflammation (TLRs, HLAs), whereas late-outgrowth EPCs expressed many transcripts involved in angiogenesis-related signalling pathways (Tie2, eNOS, Ephrins). Proteomic comparison between PACs and MNCs indicated that 77% of the proteins isolated by 2-D gels are also expressed by monocytes, while 90% of spots identified are common between late-outgrowth EPCs and ECs (Medina et al., 2010). Therefore, PACS are haematopoietic cells with a monocytic-like molecular profile, while late-outgrowth EPCs have a molecular fingerprint which suggests a close association to the endothelial lineage. In concordance with the latter, while short-term cultured PACs can only support vascular network formation, long-term outgrowing EPCs can form vascular structures *in vitro* (Sieveking et al., 2008). The ability of the ECFCs to display spontaneous vasculogenic properties distinguishes this EPC from all other types of cells that have

been given this term. They are mobilised upon injury insults (Massa et al., 2009), have proliferative capacity (Ingram et al., 2004), adopt an EC phenotype, and are capable of forming perfusing vessels *in vivo* (Yoder et al., 2007).

Altogether, late-outgrowth EPCs most accurately fulfil the criteria of an EPC suitable for endogenous vascular repair. However, and even though the cells obtained by the protocols differ in their capacity to differentiate in ECs and to physically form new blood vessels, most of the published short-term or long-term culture methods yielded cells with the ability to improve neovascularization in preclinical models (Hur et al., 2004; Urbich & Dimmeler, 2004; Yoder et al., 2007; Yoon et al., 2005). Consequently, it could be suggested that both phenotypes have a complementary role in vascular repair (Chong et al., 2016; Urbich, Aicher, et al., 2005), where the low proliferative potential PACs act to secrete angiogenic factors stimulating the proliferative capability of the late outgrowth EPCs (Zampetaki et al., 2008). In fact, the simultaneous injection of both cells types has been shown to significantly promote greater tissue repair (Yoon et al., 2005), highlighting their synergistic role in improving physiological angiogenesis.

## EPC sources and mobilisation

Despite the advance in EPC research, the primary sources of these cells and differentiation pathways of late-outgrowth EPCs are still under debate (Simard et al., 2017) **(Figure 6)**.

**Figure 6 | Origin and differentation of EPCs.**
Scheme depicts the possible origin and differentiation of EPCs from hematopoietic and non-hematopoietic cells. EPCs give rise to endothelial cell lineage, including late-outgrowth EPCs and ECs. HPCs give rise to blood cells, such as monocytes and PACs. Whether monocytes can act as PACs and vice versa is still controversial. CECs can arise from the detachment of mature ECs and repair other areas of endothelium damage or can stem from the differentiation of PACs. Adapted from (Urbich & Dimmeler, 2004), (Timmermans et al., 2009), (Balaji et al., 2013), (Marcola & Rodrigues, 2015), (Cappellari, D'Anna, Avogaro, & Fadini, 2016). CD – cluster of differentiation; CEC – circulating endothelial cell; EC - endothelial cells; EPC – endothelial precursor cell; HPC – hematopoietic progenitor cell; KDR – kinase insert domain receptor; PAC – proangiogenic cell.

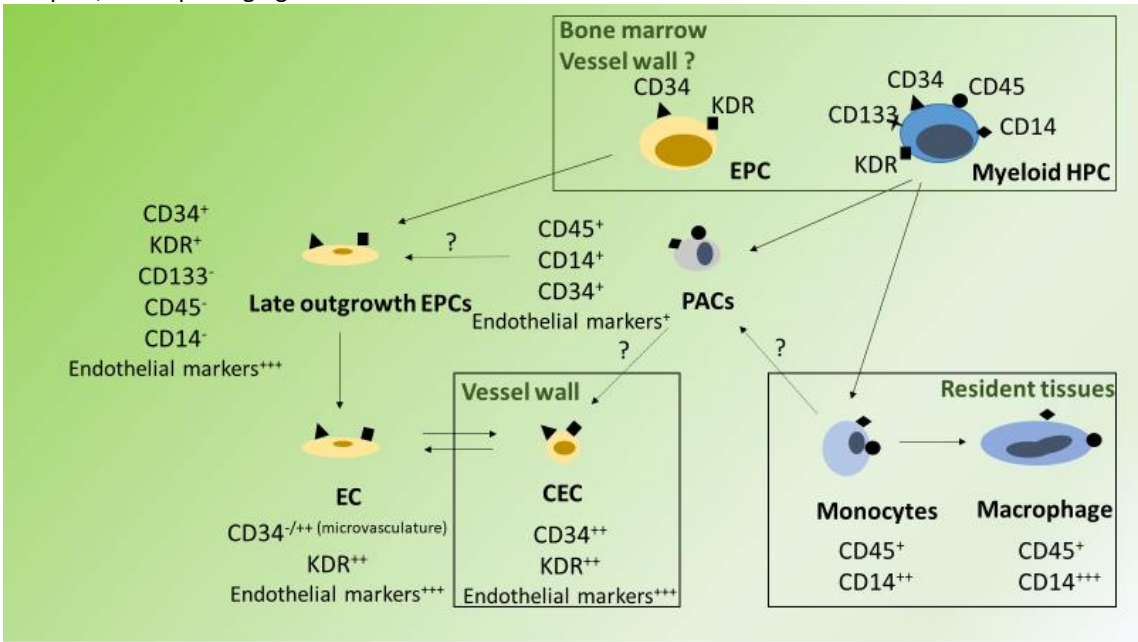


Initially, late EPCs were ascribed to BM-derived circulating angioblasts (Y. Lin et al., 2000). At the BM, EPCs reside in a special osteoblastic niche characterised by low oxygen tension and high SDF-1α level and from there are repeatedly mobilised in response to peripheral stimuli (Hristov et al., 2003) for supporting re-endothelialisation and angiogenesis **(Figure 7)**. The interaction between stem cells and stromal cells (osteoblasts, ECs, fibroblasts) are amplified by membrane-anchored cytokines which transduce proliferation and or differentiation signals, or by the maintenance of progenitors in a quiescent state under the constraints of limited growth factor

concentrations. Rapid availability of cytokines is essential for the recruitment of quiescent EPCs to a permissive vascular niche where they can proliferate, differentiate, and be released into circulation. EPC recruitment has been demonstrated to be impaired in $eNOS^{-/-}$ mice (Aicher, Heeschen, et al., 2003). Therefore, the mobilization is believed to be chiefly dependent on the activation of eNOS (Heissig et al., 2002) produced by osteoblasts and ECs in the presence of several mobilizing factors. These include insulin, G-CSF, HIF1-α, VEGF, erythropoietin, SDF-1, placental growth factor, estrogen and SDF-1α (also known as CXCL12), which get upregulated upon tissue hypoxia, or wound-healing conditions to a concentration greater than that in the BM (Aicher, Heeschen, et al., 2003; Balaji et al., 2013; De Falco et al., 2004; B. Li et al., 2006; Shim, Nam, Hyuk, Yoon, & Song, 2015). All these factors act via the phosphoinositide 3-kinase/protein kinase B (Akt) pathway resulting in eNOS activation (Dimmeler et al., 1999). In turn, the increased bioavailability of NO upregulates the enzymatic activity of elastase, cathepsin G and MMPs, which then cleave the intercellular bonds between the stem and stromal cells (Dimmeler et al., 1999; Urbich & Dimmeler, 2004). Particularly, MMP-9 activation results in the release of a soluble kit ligand in the BM niche, which cleaves adhesive bonds on stromal cells, leading to EPC migration into the vascular zone, and subsequent proliferation and PB mobilisation via transendothelial migration (Heissig et al., 2002).

**Figure 7 | EPC mobilisation from BM.**
The BM-derived EPCs reside in an osteoblastic microenvironment where they can readily sense and respond to the stress-induced demands for supporting re-endothelialisation and angiogenesis. The NO-induced activation of MMP-9, which cleaves adhesion/survival-promoting membrane-bound Kit ligand (mKitL) into a survival/motogenic soluble Kit ligand (sKitL), constitutes an early step in this process. Subsequently, cKit-positive stem and progenitor cells, including the common hemangioblast, move to the vascular zone of the BM microenvironment, where they switch from a quiescent to a proliferative state and are released into circulation. Adapted from (Heissig et al., 2002) and (Balaji et al., 2013). BM – bone marrow; CD – cluster of differentiation; EC - endothelial cells; eNOS – endothelial nitric oxide synthase; EPC – endothelial precursor cell; EPO – erythropoietin; G-CSF – granulocyte colony stimulating factor; GM-CSF – granulocyte-monocyte colony stimulating factor; HPC – hematopoietic progenitor cell; KDR – kinase insert domain receptor; MMP9 – matrix metalloproteinase-9; PAC – proangiogenic cell; SDF-1- stromal derived factor 1; VEGF – vascular endothelial growth factor.

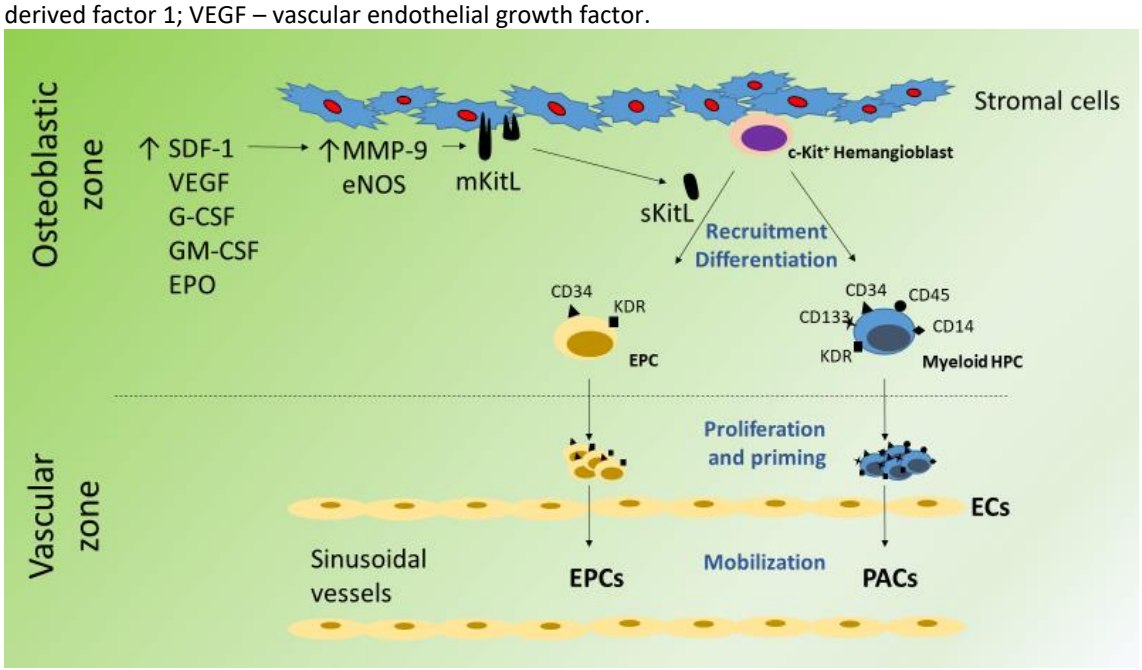


Irrespective of the BM contribution to an EPC circulatory pool, the possible existence of specific niche(s) of vascular wall EPCs locally derived or maintained should also be considered. Indeed, during the past decade evidence of an array of progenitor cells resident within the mural layers which could contribute towards the endothelial homoeostasis **(Figure 8)** has emerged (Psaltis & Simari, 2015).

**Figure 8 | Hypothetical scheme of vascular wall EPC zones.**
This scheme illustrates the concept of vascular mural zones containing EPCs and HPCs capable of differentiating into endothelial cells and form capillary-like sprouts from the vascular wall, and immune cells, respectively. Additionally, lineage-committed MSCs, SPCs, MVSCs and AMPCs have also been described to reside within the mural layers of vessels. Dashed lines correspond to internal and external elastic laminas. Adapted from (Ingram, Mead, et al., 2005), (Zengin et al., 2006), (Naito, Kidoya, Sakimoto, Wakabayashi, & Takakura, 2012), (S. Fang, Wei, Pentinmikko, Leinonen, & Salven, 2012) and (Psaltis & Simari, 2015). ABC - ATP-binding cassette; AMPC - adventitial macrophage progenitor cells; CD – cluster of differentiation; EPC – endothelial precursor cell; HPC – hematopoietic precursor cell; HP-ECFC – high potential endothelial colony forming cell; KDR – kinase domain receptor; MSC – mesenchymal stem cell; MVSC - multipotent vascular stem cell; SP – side population; SPC - smooth muscle progenitor cell; VE-cad – vascular endothelial cadherin.

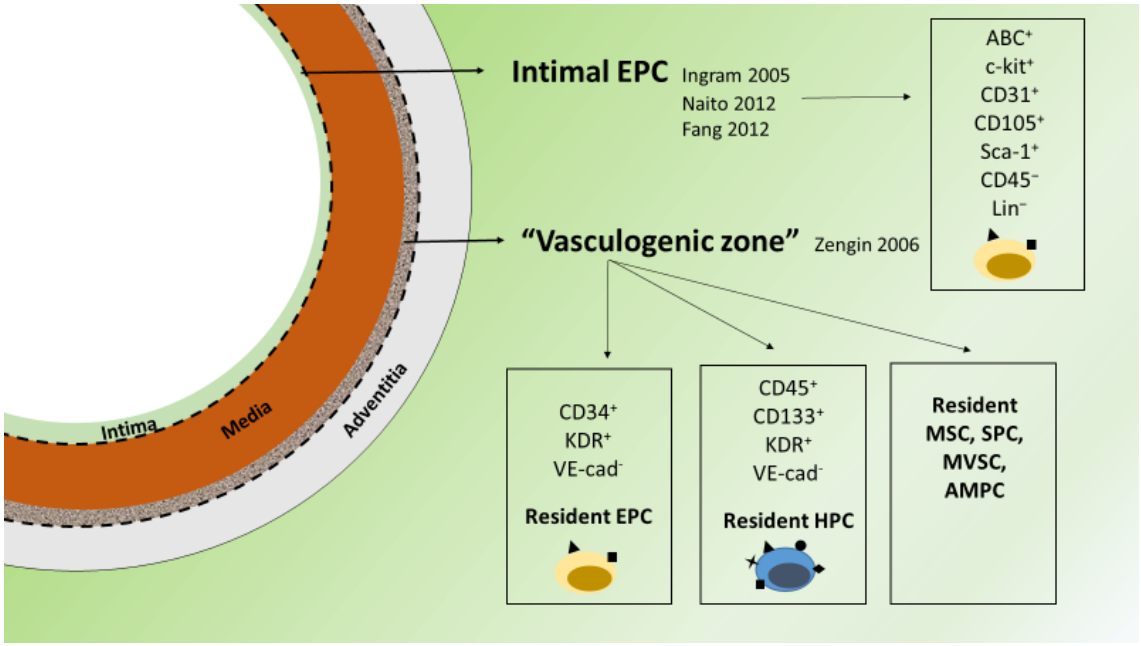


In support of this theory, Zengin and colleagues identified an enriched area of $CD34^+$ and $KDR^+$ cells (aside from the expected positive staining for CD34 in the endothelial layer), located between the smooth muscle and adventitial layers of the vascular wall, in close vicinity to the external elastic membrane (Zengin et al., 2006). Interestingly, this zone did not stain for CD31 and VE-cadherin like in the intima, nor SMA-like in the media. By marking the cells of the vasculogenic zone *ex vivo* with an AdV5-GFP-system, Zengin demonstrated that this vascular wall zone contains a niche of cells capable of forming outward capillary sprouts during an arterial ring assay. During the Matrigel assay, there was a significant accumulation of $CD34^+$ cells not only in the vasculogenic zone but also in the whole adventitia of the vascular wall. During this process, the GFP-$CD34^+$ cells became positive for markers typical of activated (CEACAM1) and tightly-junctional endothelium (occluding, VE-cadherin), but remained negative for CD31. Another minority population that was detected in the vasculogenic zone were cells positive for

CD45. Their number within the wall did not change significantly after the ring assay, nor did they apparently participate in capillary formation, although a few of them migrated into the collagen gel outside the rings. Therefore, it was hypothesised that the vasculogenic zone seemingly contains cells of different subpopulations and $CD45^+$ cells, postulated to be cells of HPC origin, which may act as inflammatory cells relevant for a local immune response or angiogenesis support. Although the observations were compelling towards the existence of a niche of cells within the vessel wall with angiogenic outgrowth potential, this work did not unequivocally identify a putative EPC nor a definitive EPC source. No distinctive antigenic or clonogenic characterization was pursued to differentiate this cells from CECs bearing low proliferative potential, for instance. Moreover, peri-adventitial AdGFP tagging is not sufficient to validate that the outgrowth ECs came from the "vasculogenic zone". Moreover, matrigel-based sprouting assays are not specific for cells of endothelial lineage, and outgrowths from vascular explants contain a mixture of fibroblasts, macrophages, ECs, and pericytes (Zengin et al., 2006; Zorzi, Aplin, Smith, & Nicosia, 2010) making it difficult to differentiate *bona fide* EPCs from other PACs that coexist in the adventitia and possess hematopoietic features (Zengin et al., 2006).

In contrast to the previous study by Zengin, others used rigorous clonal assays to try to identify vascular wall EPCs. Ingram and colleagues described an entire hierarchy of cells that could be isolated from vessel wall-derived cultures (Ingram, Mead, et al., 2005) and which displayed a high proliferative potential similar to that of late-outgrowth EPCs. In endopoiesis, the most proliferative progenitor that can be cultured in the absence of a stromal cell monolayer is designated a high proliferative potential–ECFC (Ingram et al., 2004). Single high proliferative potential-ECFCs are capable of generating colonies that go on to form secondary and tertiary colonies upon replating (Ingram et al., 2004). To compare the clonogenic capacity of single cells derived from UCB or vessel walls, Ingram grew monolayers of UCB-derived late-outgrowth EPCs, HUVECs, and Human aortic endothelial cell (HAECs) and demonstrated that, surprisingly, they could all be passaged for at least 40 population doublings. Then, they performed single cell culture which revealed that both high proliferative potential-ECFCs and low proliferative potential-ECFCs exist among HUVEC and HAEC populations. These intima-derived progenitor cells expressed EC surface markers (CD31, CD141, CD105, CD146, CD144, vWF) and displayed

the similar clonogenic potential to UCB EPCs. The presence of high proliferative potential-ECFCs among HUVECs and HAECs derived from vessel walls could explain the high passage number achieved by otherwise terminally differentiated mature ECs with low proliferative potential (Bompais et al., 2004).

Subsequent data have supported this notion that EC turnover is not a stochastic property of mature ECs, but rather the result of a hierarchical organisation of different endothelial subpopulations categorised by their clonogenic potential (Psaltis & Simari, 2015). Naito and colleagues identified a side population (SP) of $CD31^{+}CD45^{-}$ stem/progenitor-like ECs at the intima of pre-existing blood vessels, based on their ability to efflux lipophilic fluorescent Hoechst 33342 dye via the ATP-binding cassette (ABC) family of cell membrane transporter proteins (Naito et al., 2012). The SP assay is a FACS based method that relies on the fact that while uptake of the DNA binding dye occurs uniformly in all cells through passive diffusion, efflux is an active energy-driven process, and only certain cells expressing a sufficient number of ABC transporters are able to actively efflux the dye out of the cell, which in turn is captured on FACS. Combining the SP assay with cell surface phenotyping lead to the observation that this sub-population of stem/progenitor-like ECs were found to constitute nearly 1% of all $CD31^{+}CD45^{-}$ ECs present in samples of hindlimb muscle, liver, lung and heart, but could not be detected in BM, blood or ECs in culture. Since the SP assay is performed on viable cell populations, this enabled subsequent functional characterization of the cells *in vitro* and *in vivo*. Although quiescent in steady state, the sorting of the SP-ECs revealed within them a colony forming nature, high replication potential compared to other colony-forming ECs, and ability to regenerate mature blood vessels *in vivo* ischemic milieus, as well as a distinct gene expression pattern compared with conventional ECs. Moreover, a high nucleus/cytoplasm ratio and high expression of surface marker CD133 strongly suggest that the SP ECs possessed essential characteristics of stem/progenitor cells. Nevertheless, although ABC transporters are enriched in stem/progenitor cells, several reports document that the SP phenomenon is not restricted to this phenotype (Golebiewska, Brons, Bjerkvig, & Niclou, 2011). Such transporters have also been described in specific differentiated cells where they are thought to play a role in protection against the cytotoxic effects of toxins and xenobiotics (multiple drug

resistance) by limiting toxin/drug entry into certain tissues and promoting their elimination into bile and urine (Fromm, 2000).

Fang and colleagues later identified an intimal population of $Lin^{-}CD31^{+}CD105^{+}Sca\text{-}1^{+}c\text{-}kit^{+}$ ECs from mouse pulmonary vasculature that contained a rare (0.4%) subset of ECFCs. This c-$kit^{+}$ clonal subset was shown by transgenic reporter tracing to be of probably endothelial and non-hematopoietic origin (S. Fang et al., 2012). These cells were recognised by *in situ* immunostaining in the capillaries, arteries, and veins of a range of organs (lung, liver, kidney and subcutaneous tissues), as well as in neovessels in subcutaneous Matrigel plugs, and in murine and human melanoma cells and breast cancer samples. Then, the authors demonstrated that the clonal progeny of single c-$kit^{+}$ ECFCs could generate host-perfused blood vessels *in vivo* within Matrigel plugs, and confirmed their capacity for long-term self-renewal. Phenotyping of c-kit-deficient mice exposed a reduction in ECFC recovery, along with reduced angiogenesis and tumour growth, that notably were not restored by reconstitution of the hematopoietic system with wild-type BM (S. Fang et al., 2012).

These vascular wall EPCs are not to be confused with the reduced outgrowth potential mature intima-derived CECs which get dislodged from the vessel wall. Some so-called circulating EPCs are these injured, or senescent ECs sloughed from the vessel wall into the blood stream **(Figure 6)**. CECs which are $CD146^{+}CD34^{bright}CD45^{-}$ (Cappellari et al., 2016), are described as mature ECs that detach from the endothelial layer into the circulation at angiogenic sites, during increased shear stress (Rowand et al., 2007), veinpuncture (Boos, Lane, et al., 2006) and several clinical disorders that have in common the presence of vascular injury (Blann et al., 2005), such as diabetes (Lombardo et al., 2012). It is estimated that normal adults have 2.6 ± 1.6 CEC/mm of PB. The majority of these CECs are quiescent, and at least half are microvascular as defined by CD36 positivity (A. Solovey et al., 1997). CECs bear no or low proliferative potential in culture (Blann et al., 2005), unlike late EPCs ($CD34^{+}KDR^{+}$). In fact, CECs are currently practically indistinguishable by flow cytometry alone from late-outgrowth EPCs, except for CD34 brightness (Cappellari et al., 2016). Therefore one needs to differentiate them according to their proliferative capacity. Lin *et al.* studying sex-mismatched BM transplant patients

claimed that the majority of the so-called circulating EPCs (95%) were in fact derived from the vessel wall and displayed restricted growth capability (Y. Lin et al., 2000). Briefly, the authors, following the analysis of fluorescence *in situ* hybridization of PB samples from BM transplant recipients who had received gender-mismatched grafts 5–20 months earlier, reported that most circulating $CD146^+$ cells (considered endothelial-committed cells (A. N. Solovey et al., 2001)) exhibited a recipient genotype. Genotype analysis of buffy coat cultures from these subjects revealed an outgrowth of ECs of both donor and recipient genotypes. Remarkably, ECs with recipient genotype had expanded only 17 ± 9–fold after 27 ± 4 days in culture, whereas cells having transplant donor genotype displayed a delayed outgrowth profile but expanded fully 1023 ± 476–fold over the same time window. These findings suggest that the majority of circulating endothelial committed-cells found in fresh PB were derived from the recipient own vessel walls and had limited growth capability (CECs), and the delayed but exuberant endothelial outgrowth in culture stemmed from the rarer donor BM-derived circulating cells (EPCs).

Other groups have suggested that parenchymatous organs, such as the muscle, adipose, dermis, liver, intestine and liver (Aicher et al., 2007), could be alternative EPC source contributing to the circulating progenitor cell pool. However, since an insufficient phenotyping was carried out at the time and in light of subsequent work, it is likely that $CD146^+CD34^-CD133^-Syto16^+$ vascular wall resident ECs could exist in the wall of adult blood vessels of those organs (Ergun & Gehling, 2007).

Moreover, reports that myeloid cells can generate endothelial progeny are also a matter of debate. $CD14^+CD34^{low}$ myeloid cells have been shown to coexpress endothelial markers and form tube-like structures *ex vivo* (Schmeisser et al., 2001). Furthermore, *ex vivo* expansion of purified $CD14^+$ MNCs generated cells with an endothelial phenotype, which incorporated in newly formed blood vessels *in vivo* (Urbich et al., 2003). These data would suggest that myeloid cells may transdifferentiate to the endothelial lineage cells. Nevertheless, it is possible that these assays might have been contaminated by $CD45^-$ cells with true endothelial potential.

In summary, to date, the *in vivo* counterpart of the late-outgrowth EPCs is yet to be unambiguously demonstrated, due to its rarity in circulation and the lack of a marker combination that uniquely identifies these cells. So far, the BM, and possibly the blood vessel vascular wall, are considered the most likely repository and processing EPC compartments (Simard et al., 2017). Alternatively, there is even the possibility that late-outgrowth EPCs are culture artefacts resulting from the *in vitro* selection pressure (Timmermans et al., 2009).

## EPC homing, engraftment and differentiation

Incorporation of circulating EPCs at the injury site (homing) requires a coordinated sequence of multistep adhesive and signalling events including chemoattraction, selectin-mediated rolling, integrin-mediated adhesion, diapedesis through the endothelial monolayer, invasion in the ECM involving integrin-dependent processes and proteases, and finally, differentiation into ECs **(Figure 9)**.

Once mobilised from the BM, EPCs in circulation respond to gradient signalling in the tissues undergoing active remodelling. Some *homing* chemokines and respective EPC receptors upregulated after arterial injury are IL-8 and CXCR2; RANTES/CCL5 and CCR5; growth-regulated oncogene-a and CXCR1; and C-C chemokine and chemokine (C–C motif) receptors 2 and 5 (Balaji et al., 2013; Hristov & Weber, 2008). Platelet adhesion to the injured vascular wall also constitutes a major determinant of re-endothelialisation by inducing the release of SDF-1α (also known as CXCL12) (Massberg et al., 2006; Stellos & Gawaz, 2007). SDF-1α is a chemoattractant that exerts its role through binding with its receptor C-X-C chemokine receptor 4 (CXCR4), expressed on the EPC surface (Walter et al., 2005), thus acting as a sensor for circulating EPC cruising through sites of the microvasculature wherein an SDF-1α gradient is present. Blocking CXCR4 significantly reduces the adhesion of EPCs to mature EC monolayers *in vitro* (Ceradini et al., 2004) and homing of the progenitor cells to the ischemic myocardium (Abbott et al., 2004) or after arterial wire injury *in vivo* (Hristov, Zernecke, Bidzhekov, et al., 2007).

**Figure 9 | Mechanism of EPC homing, engraftment and differentiation.**
Recruitment and incorporation of late-outgrowth EPCs into injured vessels requires a coordinated multistep process including chemoattraction, adhesion, trans-endothelial migration, matrix degradation and *in situ* differentiation. Factors that are proposed to regulate the distinct steps are indicated. Dashed green lines correspond to molecular interactivity. The dashed yellow line corresponds to damaged endothelium. Adapted from (Urbich & Dimmeler, 2004) and (Caiado & Dias, 2012). BM – bone marrow; CD – cluster of differentiation; CXCR2 - C-X-C chemokine receptor type 2; CXCR4 - C-X-C chemokine receptor type 4; EC – endothelial cell; ECM – extracellular matrix; EPC – endothelial precursor cell; GF – growth factors; IGF – insulin –like growth factor, IL – interleukin; MCP1 - Monocyte Chemoattractant Protein-1, MMP - Matrix metalloproteinase, PAC – proangiogenic cell; PDGF – platelet derived growth factor; PSGL1 - P-selectin-glycoprotein ligand-1; SDF – stromal derived factor; VEGF – vascular endothelial growth factor.

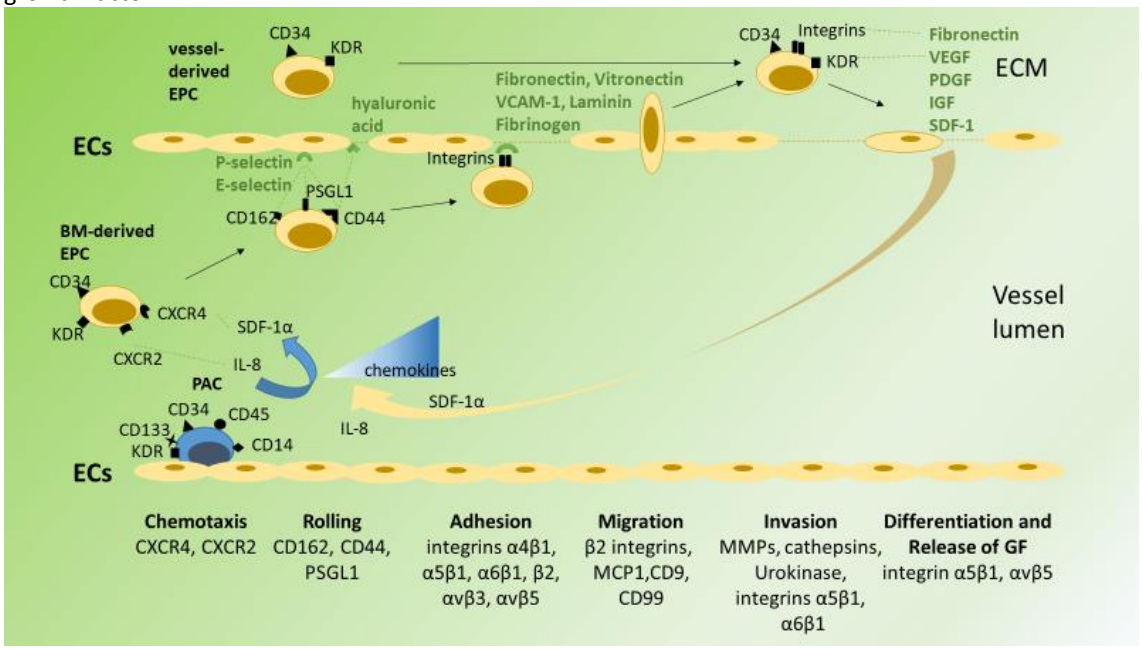


Concordantly, a dysregulation of the SDF-1α/CXCR4 signalling in EPCs from patients with stable chronic CAD has been described (Walter et al., 2005). The intrinsic migratory capacity of EPCs towards SDF-1α even seems to determine the functional improvement of patients receiving stem cell therapy in clinical trials (Britten et al., 2003). The upregulation of SDF-1α transcription factor HIF-1α (Schober, Karshovska, Zernecke, & Weber, 2006) at injured arteries and in hypoxic tissue promotes the recruitment of mobilised EPCs, which characteristically overexpress CXCR4 (Leone et al., 2005), to these sites (Ceradini et al., 2004; Karshovska et al., 2007). Therefore, it is not surprising that local SDF-1α concentration after AMI is strikingly correlated to the neovascularization response (J. Yamaguchi et al., 2003). Interestingly, VEGF-mediated SDF-1α release by perivascular myofibroblasts can act as a potent chemoattractant to both EPCs (Kalka, Masuda, Takahashi, Gordon, et al., 2000) and PACs (Grunewald et al., 2006), suggesting that the same cytokines may cooperate during homing of different BM cell types.

Importantly, retention of PACs near damaged vessels enhances chemoattraction of EPCs via secretion of more recruiting factors. Moreover, it seems that EPCs and PACs also share common adhesion molecules which enable them to adhere to the damaged tissues (Z. J. Liu et al., 2010). SDF-1α specifically upregulates the expression of E-selectin, an adhesion molecule, on the luminal surface of murine and human mature ECs (Z. J. Liu et al., 2010), otherwise minimally expressed constitutively, thus enhancing rolling of EPCs and PACs over EC monolayers (Peled et al., 1999; Vajkoczy et al., 2003).

*Rolling* consists of the brief low-affinity contact of circulating EPCs with the activated EC monolayer, platelets and exposed ECM, through a landing mechanism, determining a drastic velocity reduction from the hydrodynamic velocity just before their subsequent integrin-mediated arrest. Adhesion is initiated by this first tethering event through tissue-specific selectins and their carbohydrate ligands. Expression of E-selectin is restricted to ECs previously activated by inflammatory cytokines, while P-selectin can be expressed both on ECs and platelets (Chavakis, Urbich, & Dimmeler, 2008). Therefore, EPCs, which bear selectins´ ligands P-selectin-glycoprotein ligand-1 (PSGL-1), CD162 and CD44 at the surface can roll slowly along the vessel wall (Z. J. Liu et al., 2010; Peled et al., 1999; Vajkoczy et al., 2003) before firm adhesion, which is confirmed using intravital microscopy (H. Jin et al., 2006). EphB4 mediated EPC activation leads to overexpression of PGSL-1 (Zampetaki et al., 2008), which subsequently enhances adhesion to P-selectin and E-selectin. Remarkably, E-selectin-deficient mice have an impaired homing and recovery after ischemia (Nishiwaki et al., 2007; Oh et al., 2007), while HUVECs transfected with E-selectin small interference RNA (siRNA) significantly capture fewer EPCs under flow than HUVECs treated with control siRNA (Sharma, 2010), further supporting the role of E-selectin for EPC rolling. Additionally, activation of P-selectin also seems to improve EPC-mediated neovascularization (Foubert et al., 2007). On the other hand, the siRNA-mediated inhibition of PSGL-1 impairs the adhesive properties of EPCs (Foubert et al., 2007). Still, some studies suggest that the adhesion force between EPCs and ECs by PSGL-1/selectins only may not be sufficient unless contributions of other bonds are considered (Peled et al., 1999). Concordantly, in addition to E-selectin, adhesion molecules such as VCAM-1, ICAM-1 and integrin α4 are also upregulated in vascular ECs upon SDF-1α stimulation (Z. J. Liu et al., 2010).

The process of rolling is reversible. Many EPCs that roll will not stop, but dissociate from the vessel surface and re-enter the bloodstream. Molecular adhesive bonding must form rapidly for cells to tether, and the bonding must break rapidly for cells to roll ("docking stage"). For the EPC to stop, the low affinity rolling interactions must be replaced by high-affinity bonds. Mechanistically, shear flow and rolling triggers specific EPC intracellular signalling that induce the upregulation of integrins and their activation into high-affinity states for ECM ligands, promoting the subsequent integrin-dependent arrest of the activated EPCs at the site of vascular remodelling ("locking stage") (Green, Pearson, Camphausen, Staunton, & Simon, 2004; Urbich & Dimmeler, 2004). Integrins are glycosylated heterodimeric proteins which consist of non-covalent linked α- and β-subunits. Both subunits are considered type I transmembrane proteins, containing large extracellular domains and short cytoplasmic domains (Humphries, Byron, & Humphries, 2006). Mammalian genomes comprise 18 α subunit and 8 β subunit genes, and so far 24 different αβ combinations have been recognized at the protein level (Humphries et al., 2006). Being a transmembrane protein, integrins on the cytoplasmic face of the plasma membrane coordinate the assembly of the cell cytoskeleton and signalling complexes which may determine cell fate. On the extracellular face, integrins engage both ECM macromolecules or counter-receptors on contiguous cell surfaces. A specific integrin can bind multiple counter-receptors (Humphries et al., 2006) **(Figure 10)**. Likewise, most ECM and cell surface adhesion proteins can bind to different integrin receptors (Plow, Haas, Zhang, Loftus, & Smith, 2000). EPCs can express distinct integrin subunits ($\alpha_1$–$\alpha_6$, $\alpha_9$, $\alpha_v$, $\beta_1$–$\beta_3$, $\beta_5$, $\beta_7$) (Balaji et al., 2013). Integrins families are named after their β component, irrespective of their α dimer. Despite their extensive variety, integrin-ligand combinations are typically clustered into four main classes, reflecting the structural basis of the molecular interaction: RGD- and LDV-binding integrins, or αA-domain-containing β1 integrins and non-αA-domain -containing laminin-binding integrins (Humphries et al., 2006).

β1-Integrins are recognised as one of the other major integrin families implicated in EPC adhesion to activated ECs or directly to the exposed ECM components in denuded vessels, namely, VCAM-I and FN (Balaji et al., 2013). In particular, the α5β1 integrin, which is highly expressed in EPCs (Balaji et al., 2013), combines with exposed FN to form a ligand-receptor complex that not only mediates cell adhesion via focal adhesion

complexes formation (Shyy & Chien, 2002) but can also promote cell proliferation, survival and even differentiation (Pagan, Khosla, Li, & Sannes, 2002). Other integrins such as the α4β1-integrins also play an important part in EPC adhesion to ECM, via interaction with vascular cell adhesion molecule I (VCAM-I) (H. Jin et al., 2006). The laminin-binding α6β1 integrin also promotes EPC engraftment to the sites of vascular repair (Bouvard et al., 2010). β2-Integrins also have an essential role in the *retention* of EPCs by binding to multiple members of the intercellular adhesion molecule family, fibrinogen, and polysaccharides (Chavakis et al., 2005).

**Figure 10 | Integrin ligands.**
This scheme illustrates the major integrins and their ligands' molecular interactions. Adapted from (Humphries et al., 2006). BSP - bone sialoprotein; Del-1 - developmental endothelial locus-1; EGF - epidermal growth factor; ICAM - intercellular cell adhesion molecule; iC3b - inactivated complement component C3b; LAP-TGF – latency associated peptide transforming growth factor; MAdCAM-1 - mucosal addressin cell adhesion molecule 1; MFG-E8 - milk fat globule EGF factor 8; PECAM-1 - platelet endothelial cell adhesion molecule 1 (CD31); PSI - plexin/semaphorin/integrin homology; VCAM-1 - vascular cell adhesion molecule 1; vWF - von Willebrand factor.

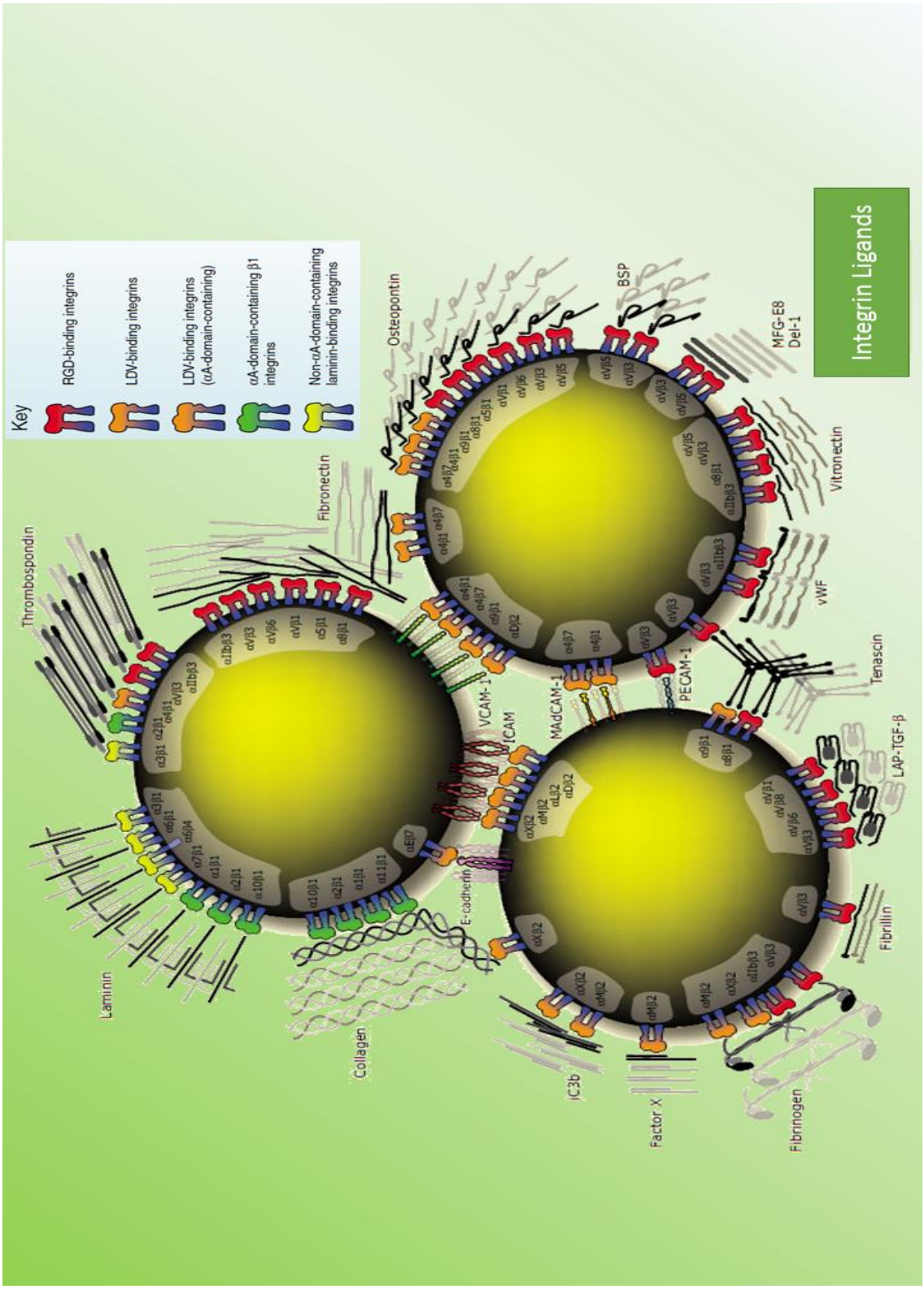


Noticeably, necrotic ECs express high mobility group box 1 (HMGB1) which further reinforces the interaction of β1 and β2 integrins with their ligands, enhancing EPC adhesion and homing to ischemic areas *in vivo* (Chavakis et al., 2007). Additionally, adhesion of EPCs to denuded vessels and faster reendothelialization of injured carotid arteries *in vivo* can also be mediated by αvβ3- and αvβ5-integrins, which bind to FN and

vitronectin (Walter et al., 2002), while inhibition of these integrins with specific cyclic RGD peptides impairs this effect. However, is there an integrin participation sequence?

Blocking studies suggest that α5β1 is the primary integrin involved in the initial cell arrest (Angelos et al., 2010). α5β1 recognises the RGD sequence (Arg-Gly-Asp-Xaa) found in a variety of ECM components, particularly in FN and osteopontin. In fact, this interaction can be quite strong, with single molecule studies revealing that α5β1 can form catch bonds with FN with a maximum bond lifetime at 40 pN per bond (F. Kong, Garcia, Mould, Humphries, & Zhu, 2009). Nevertheless, while high matrix forces are primarily supported by clustered α5β1 integrins bond with FN, less stable links to αVβ3 seem equally important to complement mechanotransduction, resulting in reinforcement of integrin-cytoskeleton linkages through talin-dependent bonds (Roca-Cusachs, Gauthier, Del Rio, & Sheetz, 2009).

Then, once EPCs become adherent at specific homing sites, they need to migrate through the endothelial monolayer and invade through the interstitial ECM to arrive at tissue repair sites, where they will exert their purpose. The process of *trans-endothelial migration* is partly mediated by β2-integrins, MCP-1, CD99 and VEGF (Balaji et al., 2013; Imbert et al., 2006). Moreover, EPC invasion via proteolytic matrix degradation depends on the activity of extracellular proteases, mainly MMP-9 and cathepsin L, and also the serine protease urokinase-type plasminogen activator and tissue-type plasminogen activator, that break down and remodel the matrix components to allow for EPC migration (Basire et al., 2006; Chavakis et al., 2008; Urbich, Heeschen, et al., 2005). In particular, the role of cathepsin L, a highly-expressed protease in EPCs, is essential for matrix degradation and invasion. Cathepsin L knockout mice exhibited impaired recovery after hindlimb ischaemia and cathepsin L knockout EPCs neither homed to sites of ischemia nor participated in neovascularization (Urbich, Heeschen, et al., 2005). MMP-2 is also intrinsically linked to EPCs' invasive properties, since EPCs from $MMP2^{-/-}$ mice exhibit reduced ECM degradation and as a result, these animals respond poorly to hind limb ischaemia because of reduced neoangiogenesis, a phenotype that can be rescued upon transplantation of $MMP2^{+/+}$ wt BM cells (X. W. Cheng et al., 2007).

When engrafted at the site of tissue repair, the process of *differentiation/maturation* into EC phenotype and functional integration into vessels comprises VEGF-induced differentiation and subsequent proliferation (Caiado, Real, Carvalho, & Dias, 2008; Dimmeler et al., 2001). The first step for differentiation depends on integrin-mediated adhesion to ECM components (Caiado & Dias, 2012), in particular, it seems triggered by the interaction between integrin α5β1 and FN (Balaji et al., 2013; Wijelath et al., 2004). Accordingly, the FN-binding integrin subunits αv, α4 and α5 integrins are all expressed throughout EPC differentiation, further reinforcing that the interaction of EPCs with FN is essential for the differentiation process (Qin et al., 2006). Once activated, the maturation and acquisition of an endothelial phenotype is the subsequent step and depends mainly on the regulation of the transcription factor HoxA, which is regulated by histone deacetylases (Urbich & Dimmeler, 2004). Not surprisingly HoxA9 has been linked to the regulation of eNOS, KDR and vascular endothelial cadherin expression (Rossig et al., 2005). Moreover, the final step, EPC survival and proliferation, is regulated by angiopoietin- tyrosine kinase with immunoglobulin-like, EGF-like domains receptor pathways and VEGF (Hildbrand et al., 2004).

VEGF, in particular, has a an essential role in the entire "EPC cycle" (mobilization, homing, differentiation and proliferation) enhancing its functional angiogenesis phenotype (L. Li et al., 2017) , thus, leading to enhanced vascular repair *in vitro* and *in vivo* (Aicher, Heeschen, et al., 2003; J. Chen et al., 2016; Hutter et al., 2004), via multiple signalling pathways including mitogen-activated protein kinase/extracellular signal-related kinase (MAPK/ERK)(Kawasaki et al., 2008; J. Xu et al., 2008). EPCs transfected with adenovirus encoding for VEGF are more capable of homing to denuded areas and differentiating into ECs (Iwaguro et al., 2002). In mammals, the VEGF family consists of five members, VEGF-A, VEGF-B, VEGF-C, VEGF-D and placenta growth factor (PLGF)(Holmes et al., 2007). The biological importance of VEGF-A is highlighted by the fact that VEGF-$A^{-/-}$ mice exhibit severe defects in vascular development and ultimately die at E9.5–10.5 (Carmeliet et al., 1996). VEGF-A binds to both VEGFR-1 and VEGFR-2. In humans, six VEGF-A splice variants have been detected following alternative splicing of a single precursor mRNA(Robinson & Stringer, 2001). VEGF-A165 is the most abundantly expressed and biologically active form (Robinson & Stringer, 2001).

## EPC-mediated endothelial regeneration

Disruption of normal coagulation, fibrinolysis, vascular tone and permeability (Iaconetti et al., 2012), are common features related to the removal of the homeostatic regulation of the endothelium. Moreover, the depletion of the endothelial source of NO generation paves the way for the inducible form of NOS (iNOS), abundantly expressed by infiltrating immune cells, to enhance ROS generation, with subsequent activation of oxidant-sensitive transcriptional pathways that increase VSMC proliferation and migration (Cooke, 2003) leading to neointima formation. Re-endothelialisation after vascular injury is the compensatory response that counteracts this proliferative cascade. Regeneration potential due to the migration and proliferation of the injury adjacent mature ECs is now known to be low (Urbich & Dimmeler, 2004). On the contrary, the contribution of circulating EPCs to support the re-endothelialisation of injured arteries is well established. Besides preventing the contact of VSMC with pro-synthetic circulating products, EPCs prevent neointima formation by directly blocking VSMC proliferation and migration in a paracrine manner (S. Q. Liu et al., 2011), although many of the involved substances are yet to be identified.

Following acute vascular insults such as angioplastly (Gill et al., 2001) or stenting (Garg et al., 2008) a rapid increase in circulating EPCs is observed. Importantly, EPC levels remain unchanged in diagnostic angiography alone (Egan et al., 2009; N. L. Mills et al., 2009), implying that the endothelial injury and ensuing inflammation (Garg et al., 2008) characterised by a robust rise in high sensitivity c-reactive protein (hs-CRP) levels, are warranted for the mobilisation of EPCs from the BM (Werner et al., 2002). Indeed, an 8-fold increase in blood G-CSF concentrations, along with milder elevations in SCF, SDF-1α and VEGF, have been reported following vascular injury (C. H. Wang et al., 2008). The more severe the endothelial injury, the higher the change magnitude of EPCs in circulation (M. Gao et al., 2015). Consistently, the therapeutic transplantation of EPCs forces an inhibitory feedback reducing hs-CRP, tumor necrosis factor (TNF)-α and SDF-1α levels early after arterial injury (S. Q. Liu et al., 2011).

EPC recruitment is preceded by a peak 2.6-fold increase in circulating PACs only 6 hours post-injury (Bonello, Basire, Sabatier, Paganelli, & Dignat-George, 2006), suggesting an

important role for these cells in the immediate response to vascular injury, as opposed to the same fold increase in circulating EPCs occurring simply at 24h (Bonello et al., 2006; Marboeuf et al., 2008). Interestingly, the magnitude of $CD34^{+}CD45^{+}$ PACs mobilisation independently predicts subsequent in-stent restenosis (Inoue et al., 2007). It is possible that an exaggerated response by the hematopoietic precursors ($CD45^{+}$) over endothelial precursors ($CD45^{-}$) may favour a maladaptive response to vascular injury, therefore leading to restenosis.

The proposed timing of events for the EPC-mediated re-endothelialisation is displayed in **Figure 11** and **Figure 12**. PACs are mobilised early after vascular injury, and then avidly secrete angiogenic factors encouraging resident EC proliferation and migration. Over a period of days to months, BM and vessel -derived EPCs home, proliferate and contribute to effective reendothelialization and the restoration of vascular homoeostasis.

**Figure 11 | Hypothetical role of various cellular players in endothelial denudation injury.**
Following endothelial cell denudation injury, loss, or turnover, EPCs migrate and proliferate to repair the middle section of the injured area. There is a minimal adjacent ECs' regenerative contribution at the ends. This follows a series of events where platelets and proangiogenic hematopoietic cells are first drawn to the site of injury to facilitate repair by further recruiting EPCs. Adapted from (Richardson & Yoder, 2011). CD- cluster differentiation; EC – endothelial cell; EPC – endothelial precursor cell; KDR – kinase domain receptor; PAC – proangiogenic cell.

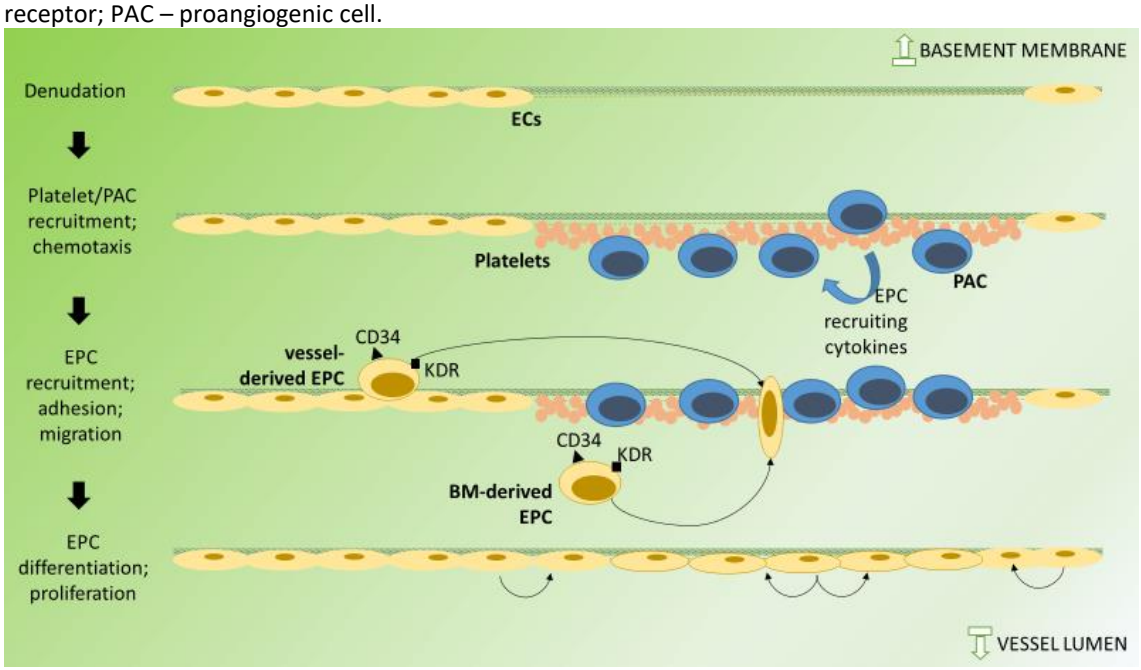


Another interesting model used to study neointima formation is vascular allograft transplantation. ECs of vascular allografts are damaged at an early stage by the immune-mediated reaction and regenerated after that. The paradigm that this type of re-

endothelialisation is dependent on the remaining ECs of donor's vessels has been challenged by recent findings that establish circulating EPCs as sources of neointimal lesions of allografts (Hu, Davison, Zhang, & Xu, 2003). Hu and colleagues, using chimeric mice (wild-type/TIE2-LacZ BM and TIE2-LacZ/wild-type BM), provided solid evidence that regenerated ECs at arterial allografts originate from β-gal expressing recipient circulating EPCs, and not from remaining ECs of donor vessels nor from adjacent recipient ECs from carotid arteries where allografts were anastomosed. Another pertaining observation from Hu *et al.* is that circulating EPCs were also involved in neovascularization of the neointima, thereby modulating its formation. Usually, nourishment of the intima is accomplished by oxygen diffusion from the lumen of the vessel, whereas the media and the adventitia are nurtured by *vasa vasorum*, the vasculature microvessels. When vessel wall thickness exceeds the effective diffusion distance of oxygen (e.g. ruptured plaque or post-angioplasty neointima), *vasa vasorum* then proliferate in the inner layers of the vessel wall (Fuster, Moreno, Fayad, Corti, & Badimon, 2005), where they are usually absent. There is evidence that *de novo vasa vasorum* within allografted vessels are derived from the recipient BM-derived β-gal-expressing EPCs (Hu et al., 2003). The fact that EPCs may modulate the neointima formation is interesting from the therapeutical standpoint, although the purpose of angiogenesis in neointimal lesions remains poorly understood. *Vasa vasorum* coverage and neointima growth (Mulligan-Kehoe & Simons, 2014) seem to be associated, possibly fuelled by facilitated blood and oxygen delivery and trafficking of resident inflammatory cells to the vessel wall, yet, emerging studies provide a different interpretation angle. EPC-derived *vasa vasorum*, rather than being restenosis contributors, may well be a biomarker of endogenous vascular repair (Leor & Marber, 2006) and serve as functional pathways for reverse lipid transport (Moreno, Sanz, & Fuster, 2009) and as stem cell reservoirs (Blum A, 2014), therefore contributing to plaque stabilisation and neointima inhibition (Moreno et al., 2009).

One more possible mechanism by which EPCs can reduce neointima formation is worthy of discussion. BM-derived MSCs are also mobilised after vascular injury and participate in the remodelling process (C. H. Wang et al., 2008). According to Wang and colleagues, on adhesion to the wire injured vessel wall, seeded MSCs proliferate in patches and can differentiate into both smooth muscle cell (SMC) and mesoderm-derived ECs. The same

study revealed that by co-culturing with late-outgrowth EPCs, helped MSCs differentiate towards an EC phenotype, through a paracrine effect. Remarkably, co-transplantation of MSCs plus late-outgrowth EPCs *in vivo* modulated the differentiation of the former mostly into an endothelial-like lineage, leading to early re-endothelialisation and attenuation of intimal hyperplasia.

Irrespective of the EPC-mediated mechanisms supporting re-endothelialisation, the current scientific belief is that the earlier re-endothelialisation is achieved, the less neointima will form (Hristov, Zernecke, Liehn, & Weber, 2007; Larsen et al., 2012) **(Figure 12)**. On the contrary, an inadequate PAC/EPC ratio after injury may result in persistent inflammation and delayed re-endothelialisation, thus potentiating VSMC hypertrophy and ECM deposition, leading to restenosis. Concordantly, the numbers of $CD14^{+}CD45^{+}$ cells are higher in patients with subsequent restenosis, which is in line with the hypothesis that excessive circulating angiogenic cells contribute to the neointima formation (Pelliccia et al., 2010).

**Figure 12 | Hypothetical role of circulating EPCs after iatrogenic injury.**
The endothelial monolayer acts as a non-adhesive surface for platelets and leukocytes and regulates fibrinolysis and vascular tone. **(A)** Under resting conditions, circulating concentrations of the proangiogenic cells (EC-CFUs) and circulating EPCs are low, particularly in patients with atherosclerotic disease. **(B)** Angioplasty and stent placement causes damage to the endothelium exposing collagen and tissue factor, activating platelets and the coagulation cascade, which may result in acute or sub-acute thrombosis. In the absence of an intact endothelium, local platelet/platelet and platelet/leukocyte complexes form, and intense local inflammatory infiltrate ensues with detectable systemic inflammation. A biphasic response to vascular injury caused by percutaneous coronary intervention is hypothesised. **(C)** The early response consists of mobilisation of the precursors of PACs/EC-CFUs involving angiogenic monocytes and lymphocytes. PACs home to the site of injury and avidly secrete angiogenic factors, encouraging resident endothelial cell proliferation and migration and the mobilisation and homing of bone marrow-derived and local EPCs to the site of vascular injury. **(D)** Over a period of days to months, EPCs proliferate, contributing to effective re-endothelialisation and the restoration vascular homoeostasis. **(E, F)** An inadequate PAC/EPC response after percutaneous coronary intervention, due to low progenitor engraftment and activity, may lead to delayed re-endothelialisation and persistent inflammation, thus potentiating smooth muscle hypertrophy and extracellular matrix deposition, leading to restenosis and symptoms of myocardial ischemia. Adapted from (Padfield et al., 2010). CFU - colony-forming unit; EC – endothelial cell; EPC – endothelial progenitor cell; G-CSF - granulocyte-colony stimulating factor; GM-CSF - granulocyte-macrophage- colony stimulating factor; HGF - hepatocyte-like growth factor; IL - interleukin; MMP - matrix metalloproteinase; VEGF - vascular endothelial growth factor; VEGFR2 - vascular endothelial growth factor receptor-2.

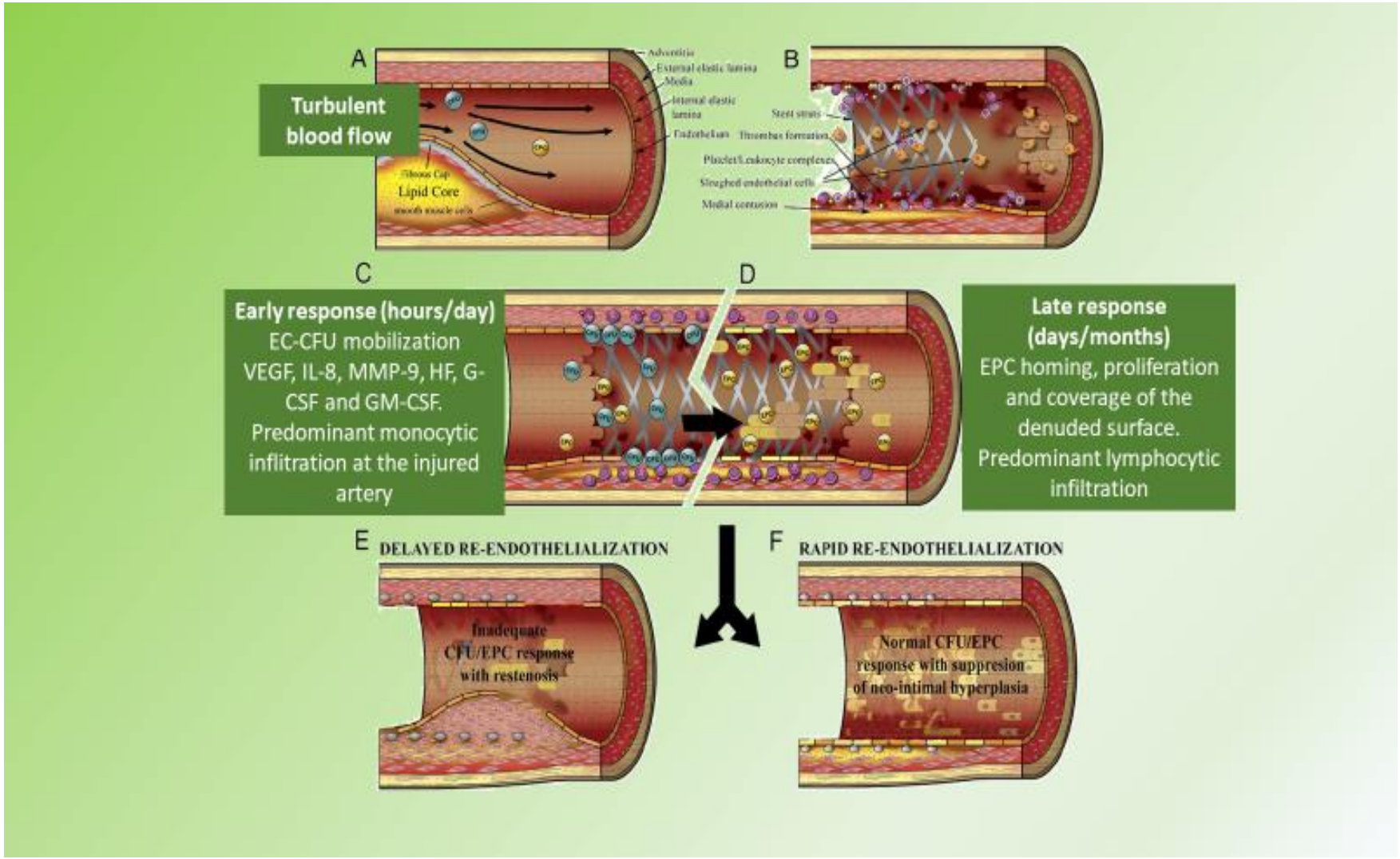
A
Turbulent blood flow
Lipid Core
B
Stent struts
Thrombus formation
Platelet/Leukocyte complexes
Sloughed endothelial cells
Medial contusion
C
Early response (hours/day)
EC-CFU mobilization
VEGF, IL-8, MMP-9, HF, G-CSF and GM-CSF.
Predominant monocytic infiltration at the injured artery
D
Late response (days/months)
EPC homing, proliferation and coverage of the denuded surface.
Predominant lymphocytic infiltration
E
DELAYED RE-ENDOTHELIALIZATION
Inadequate CFU/EPC response with restenosis
F
RAPID RE-ENDOTHELIALIZATION
Normal CFU/EPC response with suppresion of neo-intimal hyperplasia

The “faster EPC-mediated re-endothelialisation the more suppressed neointima” hypothesis has been addressed in several pre-clinical models of arterial injury, providing strong supporting evidence **(Table 2)**.

**Table 2 | Pre-clinical studies addressing EPC-mediated re-endothelialisation after vascular injury.**
BM – bone marrow; CD – cluster of differentiation; CXCR2 - C-X-C chemokine receptor type 2; CXCR4 - C-X-C chemokine receptor type 4; eNOS – endothelial nitric oxide synthase; EPC – endothelial precursor cell; G-CSF - Granulocyte colony-stimulating factor; GFP - Green fluorescent protein; HO1 - Heme oxygenase 1; HPB – peripheral blood from healthy volunteers; LDL – low density lipoprotein; KDR – kinase domain receptor; MCP1 - Monocyte Chemoattractant Protein-1 ; MNC – mononuclear cell; PB – peripheral blood; PPB – peripheral blood from patients; Sca1 - Stem cells antigen-1; UCB – umbilical cord blood; UEA - Ulex Europaeus Agglutinin I; VECAD - vascular endothelial cadherin; vWF - Von Willebrand factor

| Author Year | Model | Subjects | Cell type used | Effect |
|---|---|---|---|---|
| (Walter et al., 2002) | Murine Tie-2/lacZ BM transplant recipients subjected to balloon mediated arterial injury and pre-treatment with simvastatin or placebo | 18 placebo, 34 simvastatin | Di-Ac-LDL$^{+}$lectin$^{+}$ MNCs | Simvastatin enhanced EPC mobilisation after vascular injury and increased their adhesive capacity; re-endothelialisation was accelerated by BM-derived cells and neointimal hyperplasia was reduced |
| (Werner et al., 2002) | Murine GFP BM transfection followed by wire arterial injury and pre-treatment with rosuvastatin or placebo | 5 placebo, 4 rosuvastatin | Sca 1$^{+}$KDR$^{+}$ cells of BM origin | Rosuvastatin enhanced BM-derived EPC mobilisation after vascular injury; reendothelialization was accelerated by BM-derived cells and neointimal hyperplasia was reduced |
| (Werner et al., 2003) | Intravenous cell therapy after wire mediated murine arterial injury | 6 vascular injury | Spleen-derived Di-Ac-LDL-lectin$^{+}$ MNCs with (EPC) or without (MNC) a period of culture in endothelial growth medium | Cell therapy enhanced re-endothelialisation in splenectomized animals and was associated with a reduction of neointima formation, but MNCs were more effective than EPCs |

| | | | | |
|---|---|---|---|---|
| (Fujiyama et al., 2003) | Intravenous cell therapy versus saline after balloon-mediated murine arterial injury | 12 vascular injury, 12 controls | BM: $CD14^+CD34^-$; $CD14^-CD34^+$ PB: $CD14^+CD34^-$ | Compared with saline placebo, BM-derived $CD34^+$ cells and both PB- and BM-derived $CD14^+$ cells up-regulated endothelial markers, accelerated re-endothelialisation. and inhibited neointimal hyperplasia after activation with MCP-1 |
| (Griese et al., 2003) | Transplantation of LacZ transduced EPCs into balloon-injured carotid arteries and bioprosthetic grafts in rabbits | 6-8 EPC, 6-8 saline (morphometric analysis) | PB Dil-Ac-$LDL^+$ $CD34^+$ MNCs differentiated in culture | Transplantation of EPCs led to rapid re-endothelialisation of the denuded vessels and graft segments, resulting in significant reduction in neointima deposition |
| (D. Kong, Melo, Gnecchi, et al., 2004) | G-CSF versus control before balloon mediated murine arterial injury | 5 G-CSF, 5 controls | $CD34^+KDR^+$ | G-CSF enhanced EPC mobilisation after vascular injury; re-endothelialisation was accelerated by BM-derived cells and neointimal hyperplasia was reduced |
| (D. Kong, Melo, Mangi, et al., 2004) | EPCs transduced with specific retroviral vectors were transplanted following balloon angioplasty of the common carotid artery in rabbits | 6 eNOS-EPCs, 6 HO1-EPCs, 6 GFP-EPCs, 6 saline | PB Dil-Ac-$LDL^+$ $CD34^+$ $vWF^+eNOS^+$ $VECAD^+$ MNCs differentiated in culture | EPC transplantation prevented thrombosis and reduced neointimal hyperplasia in denuded carotid arteries by promoting re-endothelialisation; genetic engineering further enhanced this effect with eNOS |

| | | | | |
|---|---|---|---|---|
| (Yoshioka et al., 2006) | G-CSF after wire-mediated arterial injury in mice; treatment pre- and post-arterial injury versus post-arterial injury alone | 22 G-CSF, 20 controls | $CD34^+KDR^+$ | G-CSF reduced neointimal hyperplasia in association with the mobilisation of BM-derived EPCs and accelerated reendothelialization compared with control; the effect was enhanced if administered before the injury |
| (Takamiya et al., 2006) | 1. G-CSF before balloon-mediated arterial injury in rats<br>2. GFP BM-transfected mice subjected to balloon-mediated arterial injury | 10 G-CSF, 5 placebo | $CD117^+KDR^+$ | 1. G-CSF enhanced EPC mobilisation after vascular injury; re-endothelialisation was accelerated, and neointimal hyperplasia was reduced<br>2. GFP-expressing BM-derived cells contribute to neo-endothelialisation |

| | | | | |
|---|---|---|---|---|
| (Hristov, Zernecke, Bidzhekov, et al., 2007) | Wire induced arterial injury in Apo $E^{-/-}$ athymic nude mice followed 24h after by *ex vivo* perfusion of human ester–labelled EPCs pre-treated with mAbs to CXCR2, CXCR4, or IgG2a isotype control<br><br>EPCs labelled with CM-DiI were pre-treated with blocking CXCR2 mAb or isotype and injected *in vivo* intracardially into athymic NMRI nude mice; recruitment to injured carotid arteries was analysed after 7 days | 3-6 treated,<br>3-6 controls<br><br>3 treated,<br>3 controls | BM Di-Ac-$LDL^+$lectin$^+$ $CD31^+KDR^+VECAD^+$ $CXCR2^+CXCR4^+$ MNCs differentiated in culture | Blocking CXCR2 *in vivo* and *ex vivo* inhibited the incorporation of human EPCs expressing CXCR2 at sites of arterial injury in athymic nude mice and reduced re-endothelialisation |
| (X. Zhao, Huang, Yin, Fang, & Zhou, 2007) | 4-,6-Diamidino-2-phenylindole-labelled EPCs or saline were injected through tail vein after wire injury in splenectomized rats | 6 EPCs,<br>6 saline | Spleen-derived Di-Ac-$LDL^+UEA^+$ $CD31^+eNOS^+$ MNCs differentiated in culture | Administration of EPCs enhanced reendothelialization and inhibition of neointima formation at 3 weeks compared with that of saline |
| (Z. L. Ma et al., 2009) | Transplantation of autologous superparamagnetic iron oxide labelled EPCs following carotid artery balloon injury in rabbits | 14 EPCs,<br>6 control | PB $CD34^+$ $CD106^+CD146^+KDR^+$ MNCs differentiated in culture | MRI showed reduced stenosis in EPC-treated rabbits compared moderate to severe stenosis in controls; Histology revealed significantly thinner wall, greater internal diameter and smaller plaque |
| (S. H. Wang et al., 2009) | Transplantation EPC following mice femoral arteries wire-injury | 15 EPCs,<br>15 saline | Wharton jelly in human umbilical cord-derived Di-Ac-$LDL^+CD34^+CD31^+vWF^+$ cells differentiated in culture | EPCs transplantation lead to rapid re-endothelialisation, thereby inhibiting neointimal hyperplasia at 4 weeks |

| | | | | |
|---|---|---|---|---|
| (S. Q. Liu et al., 2011) | Transplantation of autologous EPCs following rabbit ear central artery | 5 EPCs,<br>5 saline | BM Di-Ac-LDL$^+$lectin$^+$ CD144$^+$ eNOS$^+$ caveolin-1$^+$ MNCs differentiated in culture | EPCs participated in re-endothelialisation directly and reduced the increase in intima area at days 14 and 28 |
| (B. Cui et al., 2011) | Transplantation of recombinant retrovirus vector expressing eNOS or GFP infected EPCs after carotid balloon angioplasty in rats | 6 eNOS,<br>6 GFP,<br>6 saline | BM Di-Ac-LDL$^+$UEA$^+$ eNOS$^+$vWF$^+$ MNCs differentiated in culture | Transplantation of both eNOS-EPCs and GFP-EPCs inhibited neointimal hyperplasia compared with saline injection. The antiproliferative effect of EPCs was further enhanced by overexpression of eNOS |
| (Y. Yin et al., 2015) | Balloon angioplasty carotid artery injury in nude rats followed by intraluminal human EPC transplantation | 4 UCB-EPCs,<br>4 PPB-EPCs,<br>4 HPB-EPCs,<br>4 saline | BM Di-Ac-LDL$^+$ CD31$^+$CD34$^+$ KDR$^+$ MNCs differentiated in culture | 2 weeks after transplantation, more labelled UCB-EPCs and HPB-EPCs than PPB-EPCs were found by cell tracking in the injury zone. Administration of PPB-EPCs, HPB-EPCs and UCB-EPCs enhanced re-endothelialisation and inhibited neointima formation compared to the saline control |
| (Ikutomi et al., 2015) | Wire-mediated endovascular injury in rat femoral artery followed by six sequential cell injections ($1 \times 10^6$ per time at 0, 1, 3, 5, 7 and 9 days after the injury). | 8 sham,<br>8 vehicle,<br>8 PACs,<br>8 EPC,<br>8 mature ECs | BM Di-Ac-LDL$^+$lectin$^+$ CD34$^+$CD31$^+$KDR$^+$ MNCs differentiated in culture | After 4 weeks, transplanted EPCs, but not PACs or ECs, significantly attenuated neointimal lesion formation in injured arteries |
| (N. M. Liu et al., 2016) | Intravenous cell therapy versus no therapy after balloon-mediated murine femoral wire arterial injury | 3 treated,<br>3 controls | BM CD31$^+$CD34$^+$ CD133$^+$Flk1$^+$wWF$^+$ MNCs differentiated in culture | Infusion of netrin-1 preconditioned wild type EPCs substantially attenuated neointimal formation |

| | | | | |
|---|---|---|---|---|
| (H. Wang et al., 2016) | Intracarotid transplantation of genetically modified GFP-EPCs overexpressing PDGFR-β into a mouse model of carotid artery injury after splenectomy | 12 pEGFP-N2-PDGFR- β EPCs, 12 pEGFP EPCs, 12 saline | Spleen-derived Di-Ac-LDL$^+$lectin$^+$KDR$^+$ MNCs differentiated in culture | EPCs overexpressing PDGFR-β accelerate re-endothelialsation and mitigate neointimal formation |

Given the observed translational potential of EPCs, therapeutic re-endothelialisation strategies to mitigate restenosis after PCI are being pursued in **clinical studies**. These include 1) EPC pharmacological mobilisation, 2) EPC intravenous transplantation and/or 3) stent-based EPC therapies.

## EPC pharmacological mobilisation

Statins administred for 4 weeks to CAD patients can increase peripheral EPC numbers up to three times (Vasa, Fichtlscherer, Adler, et al., 2001), which occurs in a dose-dependent manner (Leone et al., 2008), via augmentation of Akt phosphorylation within minutes, which yields an increase inmobilization, migration, proliferation, and survival of EPCs (Llevadot et al., 2001). In culture, statins induce differentiation of CD34$^+$ cells toward ECs (Dimmeler et al., 2001) and enhance their adhesive capacity (Walter et al., 2002). Together these observations may help to explain the reduced rate of post-PCI restenosis in patients treated with statins (Walter et al., 2000), although there are no published human statin trials which specifically output EPC-mediated re-endothelialisation in the context of vascular injury. Similarly, angiotensin converting enzyme inhibitors, like ramipril and enalapril, were shown to increase EPC levels both in the experimental model and in patients (C. H. Wang et al., 2006), probably by preventing the membrane-bound extracellular CD26/dipeptidylpeptidase from cleaving the EPC mobilizer/chemoattractant SDF-1a/ CXCL12. The same effect was reported for valsartan, an angiotensin II inhibitor (Bahlmann et al., 2005). The EPC mobilising effect of endogenous G-CSF release after AMI is also well established (Leone et al., 2006). Unfortunately, despite enhanced endothelialisation, intracoronary G-CSF administration in clinical trials has been associated with an increased incidence of in-

stent restenosis, despite improvement in left ventricular ejection fraction (S. Kang, Yang, Li, & Gao, 2008). It is possible that this effect may be mediated by non-specific pro-inflammatory actions of G-CSF leading to SMC mobilisation from the BM instead (Padfield et al., 2010), thus, hampering its translation into clinics. Erythropoietin administered following vascular injury, in spite of also enhancing re-endothelialisation (possibly through eNOS-dependent mobilisation from BM (Urao et al., 2006)), is associated with an increased incidence of neointimal proliferation in animal models, again, perhaps because of the non-specific mobilisation of SMC (Reddy, Vasir, Hegde, Joshi, & Labhasetwar, 2007). Clinical trials which have considered EPO use in PCI-treated AMI patients have confirmed that this strategy is not beneficial for prevention of neointimal hyperplasia (Stein et al., 2012; Taniguchi et al., 2010).

## EPC intravenous transplantation

According to the results in mouse (Werner et al., 2003) and rabbit (Griese et al., 2003; Z. L. Ma et al., 2009) models of endovascular injury, the intraluminal administration of EPCs should, theoretically, accelerate vascular healing by quickly populating denuded parts of the vessel wall. Nevertheless, data regarding the transfusion of progenitor cells into humans are derived from trials using heterogeneous subsets of autologous BM-derived progenitor populations, and not EPCs differentiated in culture (since the safety of phenotypically modified cells in humans is not established yet). BM contains a complex assortment of progenitor cells, including HSCs, SP cells, MSCs and multipotential adult progenitor cells (MAPCs), a subset of MSCs (Dimmeler, Burchfield, & Zeiher, 2008). The potential risk that infusion of BM-derived progenitors may increase post-PCI inflammatory signalling and promote differentiation into VSMCs, thus aggravating the severity of restenosis, has been raised (Inoue et al., 2007). However, only one trial by Bartunek *et al.* in 2005 reported an increased incidence of restenosis after infusion of BM $CD133^{+}$ progenitor cells (despite improved left ventricular performance, increased myocardial perfusion and viability)(Bartunek et al., 2005).

On the contrary, a meta-analysis of 18 randomised controlled trials on the therapeutic effects of adult progenitor cells for acute myocardial infarction (AMI) did not reveal an augmented risk for restenosis (M. Jiang et al., 2010). One of the RCTs included was the

research by Assmus *et al.* that refutes an adverse effect of BM-derived progenitor therapy on restenosis development in the setting of AMI. If anything, revascularization rates were significantly reduced in the BM-derived progenitor group at 2 years' follow-up (Assmus et al., 2010). In contrast, a substudy of REPAIR-AMI assessing the effect of intracoronary BM-derived MNCs transplantation on coronary flow dynamics by intracoronary Doppler flow velocity measurements, indicated a significantly greater recovery of coronary blood flow reserve in the MNC-treated arm compared with control placebo infusion (Erbs et al., 2007). However, a definitive answer to the question whether infusion of BM-derived progenitor cells may alter the process of restenosis development (either adversely by incorporation of inflammatory progenitor cells into the vascular wall, or beneficially via enhanced re-endothelialisation) is still awaited, because the referenced trials used heterogeneous samples of "EPCs" (and none of them studied restenosis as a primary endpoint)(Fisher, Zhang, Doree, Mathur, & Martin-Rendon, 2015).

## EPC stent-based therapy

Recently, the concept of *in vivo/in situ* endothelialisation of stents has been pursued with the rationale that accelerated establishment of the endothelial layer covering the stent struts would reduce the risk of neointimal hyperplasia and, simultaneously thrombosis (which is an adverse effect of drug-eluting stents)(Chong et al., 2016; Simard et al., 2017). Capture stents, using a proprietary coating that contains anti-CD34 antibodies were developed to test this hypothesis. EPCs are proposed to bind to the endoluminal face of the bioengineered struts, proliferate and migrate to fill the intra strut spaces establishing a confluent, functional monolayer of ECs on the stented arterial segment. In HEALING-I, the first human trial using the Genous® stent, CAD patients successfully underwent implantation of the capture stent in a single primary target lesion in a native coronary artery, which was considered safe and feasible. After 6 months, coronary angiography and intravascular ultrasound were performed revealing negligible late luminal loss and safety (Szmitko et al., 2006). Since then, Genous® stents have progressed to phase III clinical trials and have been deployed in over 5,000 patients (J. Aoki et al., 2005; Silber et al., 2011). The clinical trials revealed a binary restenosis

rate for the EPC stent that was 13 percent compared to 26.6 percent for bare metal stents at 6 months (Wojakowski et al., 2013). Among the 4,939 patients included in the e-HEALING registry, the 12-month cumulative event rate for target lesion revascularization was 5.7%, which is similar to that of drug-eluting stents (Lasala et al., 2008), with minimal incidence of late stent thrombosis (0.2%)(Silber et al., 2011).

It is important to understand that the long-term results of the capture stents are not yet available, and until then, no definitive conclusions about long-term safety or effectiveness can be made. A recent study in pigs found that the EPC capture stent improved re-endothelialisation at an early stage but ultimately conferred no effect on neointimal thickness compared with control stents over long-term observation (van Beusekom, Ertas, Sorop, Serruys, & van der Giessen, 2012). On a cautionary note, CD34 alone is not distinctive of EPCs, and it is shared by several progenitors, including smooth muscle progenitor cells (Padfield et al., 2010). Therefore, restenosis with anti-CD34 coated stents may occur because of the non-specific capture of non-EPC cells, posing the theoretical risk of neointima development. This indiscriminate binding effect could be particularly striking in individuals susceptible to in-stent restenosis, such as patients with CVD RF, where SMP are relatively more abundant in circulation than EPCs (Duckers et al., 2007), which could be worsened by low engraftment capability of senescent EPCs.

## EPC consumption, senescence and prognosis

Overall regenerative EPC activity has significant prognosis impact and is dependent on two factors: circulating EPC levels and EPC activity status.

### EPC consumption

A competent BM can translate vascular injury into productive EPC recruitment, restoring normal endothelial function. However, a high CVD RF profile can perpetuate injury by impairing EPC production and mobilisation beyond EPC consumption. The BM then becomes incompetent and the repairing EPCs numbers insufficient. Remarkably, the HEALING II registry reported that patients with normal $CD34^{+}KDR^{+}$ EPC titters had lower rates of in-stent restenosis than patients with reduced circulating EPCs (Duckers et al.,

2007). Moreover, circulating EPC numbers remain significantly lower in patients who developed restenosis after 6 months (Lei et al., 2007; Wojakowski et al., 2013).

There are several important physiological and pathological stimuli for EPC mobilisation. Physical activity and oestrogen levels are included among the physiological factors reported to enhance EPC mobilisation from the BM by acting through eNOS-, -MMP9 (Matrix metalloproteinase-9) and VEGF-mediated mechanisms (Laufs et al., 2004; Strehlow et al., 2003). Growth hormone (GH) and insulin growth factor-1 (IGF-1) are among hormones that increase NO bioavailability, therefore raising EPC mobilization (Thum, Fleissner, et al., 2007). Any reduction in the previous mobilizers could mean decreased EPC levels. Else more, ageing has an adverse impact on EPC levels (Scheubel et al., 2003) via a reduction in IGF-1 and VEGF circulating levels. Smoking is included among the suppressive factors via increased oxidative stress and reduced NO bioavailability, resulting in depletion of EPCs for vascular repair in a dose-dependent manner (Michaud, Dussault, Haddad, Groleau, & Rivard, 2006) and with a rapid amelioration after smoking cessation (Kondo et al., 2004). Diabetes mellitus and glycaemia control also negatively influence EPC levels (Fadini et al., 2005). In particular, the presence of vascular complications seems strictly correlated with reduced peripheral number of EPCs (Fadini et al., 2005), thus suggesting that EPC depletion can be involved in its pathogenesis. In fact, in diabetic patients with carotid disease, the lowest levels of EPCs are observed in patients with over 70% stenosis (Fadini et al., 2006). Diabetics with simultaneous CAD show even lower numbers of circulating EPCs (Kunz et al., 2006). The abnormality in EPC mobilization in diabetes is presumably due to the impairment of eNOS-NO cascade in BM (Z. J. Liu & Velazquez, 2008). Chronic renal failure is similarly associated with lower EPC levels, which occurs with reduced Erythropoietin production, an established EPC mobilisation trigger in humans (Bahlmann et al., 2004). In the setting of severe CAD, higher levels of substances like asymmetric dimethylarginine (ADMA), a potent endogenous inhibitor of eNOS, have been described and are associated with lower levels of EPCs (Thum et al., 2005). Similarly, TNF-α a common CVD inflammation mediator, with its well-known myelosuppressive effect, could be responsible for the reduction of EPC-poiesis and mobilisation levels observed in the late phases of heart failure (Valgimigli et al., 2004).

## EPC senescence

In 2015, Ying and colleagues reported that the transplantation of EPCs from UCB and PB from CVD patients or healthy volunteers, all increased re-endothelialisation and reduced neointima formation in a rat carotid injury model (Y. Yin et al., 2015). However, compared with the patient group, more homing EPCs were observed in the cryopreserved UCB and PB from healthy controls, and these presented a significantly faster re-endothelialisation and reduced neointima. *In vitro* studies then showed that patient-derived PB EPCs displayed decreased migration, proliferation, adhesion, and survival activities as compared to PB-EPCs from healthy volunteers and cryopreserved UCB-EPCs. The same observations were derived in groups of human patients with in-stent restenosis, given that their EPCs also exhibit lower migration and proliferation capacity *in vitro* (Lei et al., 2007).

Thus, it seems that impaired quality of EPCs is also intrinsically associated with CVD and/or CVD RFs (Chong et al., 2016; Urbich & Dimmeler, 2004; Vasa, Fichtlscherer, Aicher, et al., 2001), including diabetes, smoking, hypertension, hyperlipidemia, atherosclerosis, smoking, and obesity, which account for the deterioration of endothelial regeneration. In the elderly, the migration and proliferation capacity of BM-EPCs are decreased (Dimmeler & Zeiher, 2004), and flow-mediated brachial artery reactivity correlates negatively with this impairment (Heiss et al., 2005). Circulating EPCs from healthy smokers also exhibit impaired functional activities (Michaud et al., 2006). Enhanced angiotensin II levels present in hypertensive disease induce oxidative stress, which in turn accelerates EPC senescence by reducing telomerase activity (Imanishi, Moriwaki, Hano, & Nishio, 2005). Hypercholesterolaemia *per se* determines a reduction in EPCs' migratory, proliferative, adhesive and angiogenesis potential secondary to an increase in senescence, as demonstrated after EPC incubation with LDL-oxidized, whereas HDL-cholesterol has the opposite effect (J. Z. Chen et al., 2004; X. Wang, Chen, Tao, Zhu, & Shang, 2004). Similarly, a severe delay of re-endothelialisation after vascular injury is seen in diabetic patients, mostly, due to impaired EPC adhesion, proliferation, integrin profile, engraftment and differention (Balaji et al., 2013; Callaghan, Ceradini, & Gurtner, 2005). High glucose exposure has been shown to promote EPC senescence and

endothelial dysfunction by modifying NO-mediated mechanisms (Y. H. Chen et al., 2007). Further reinforcing the EPC senescence contribution to delayed re-endothelialisation, Ii and colleagues injected diabetic and nondiabetic EPCs intravenously after arterial injury in diabetic and nondiabetic mice (Ii et al., 2006). Notably, diabetic EPCs homing to the denuded vessel were significantly reduced, regardless of the diabetic status of the recipient mice. The underlying EPC functional diabetic impairment might be due, at least in part, to increased NADPH oxidase-dependent processes (Sorrentino et al., 2007) and uncoupling of the eNOS (Thum, Fraccarollo, et al., 2007), both resulting in excessive superoxide anion formation instead of NO, reducing the bioavailability of the latter. CRP, a well-known inflammatory mediator present in CVD, has a direct inhibitory effect on EPC activity, influencing adhesion through a transcriptional reduction of chemoattractant factors such as monocyte chemoattractant protein-1 and -2, macrophage inflammatory protein-1a, colony-stimulating factor, and IFN-gamma inducible protein-10 and inducing early EPC apoptosis (Fujii, Li, Szmitko, Fedak, & Verma, 2006; Verma et al., 2004). Also, the proliferative capacity of EPCs and their ability to support *in vitro* tube formation were reported to be significantly impaired in patients with Cardiac Syndrome X (P. H. Huang et al., 2007).

## Prognosis

To date, one's risk for vascular events has focused exclusively on assessing propensity for vascular damage, either by evaluating conventional RFs, or more recently by evaluating markers of inflammation and other circulating markers related to subclinical target organ injury. Nevertheless, vascular health is better represented as a balance between ongoing injury and resultant vascular repair. EPC enumeration and functional characterization represent the only available assessment of the reparative side of that balance. Therefore, the role of EPCs as biomarkers has recently been considered (Aragona et al., 2016; Leone et al., 2009). The evidence is there that EPC levels decrease in parallel with the presence of RFs. The extent of the EPC pool negatively correlates with cumulative indices of cardiovascular event risk, such as the Framingham risk score (Fadini, Agostini, Sartore, & Avogaro, 2007; Werner & Nickenig, 2006). The ratio

between EPCs and CECs has been proposed as a comprehensive vascular health measure, because EPCs inform on the endothelial repair capacity, whereas CECs are indicators of ongoing endothelial shedding (Cappellari et al., 2016). At the bedside, EPC counts following coronary stenting may potentially serve as a predictor for the risk stratification of therapeutic coronary interventions (M. Gao et al., 2015). Mobilization of EPCs by acute ischemia was also found to be significantly lower in the patients who developed restenosis after 6 months (Wojakowski et al., 2013). These findings correlate nicely with the current view of the EPC pool as an indicator of vascular regenerative capacity, based on the observation that serum EPC levels are markedly decreased in patients with overt atherosclerotic disease (Aragona et al., 2016; Fadini et al., 2007). However, more importantly, EPC may not be simply a marker of vascular fitness. An inverse relationship between circulating EPCs and CAD severity, independent of traditional RFs, has recently been described (Kunz et al., 2006). For every 10-colony forming unit increase in EPCs, the likelihood of multivessel CAD declines by 20% (Kunz et al., 2006), revealing a prognostic contribution. To further characterise the independent prognostic value of circulating EPCs, Werner and colleagues led the EPCAD study. In patients with angiographically documented CAD, the cardiovascular event rate at 1 year increased in parallel with the reduction in baseline EPC levels, after adjustment for known confounders, such as age, gender, vascular RFs, drug therapy, PCI, etc (Werner et al., 2005). Schmidt-Lucke *et al.* later confirmed that reduced numbers of EPCs independently predicted progression of atherosclerotic disease in a mixed population of coronary patients and healthy controls (Schmidt-Lucke et al., 2005). These data revealed that EPCs are not innocent bystanders but active players in maintaining a healthy vascular tree (Leone et al., 2009). In fact, EPC levels are kept in a steady state during the inaugural asymptomatic years of CVD RFs (Fadini et al., 2007), suggesting that EPCs can efficiently counteract the detrimental effect of RFs on vascular function until their pool gets exhausted (Hill et al., 2003), at which point EPC numbers become inversely related to the number of CVD RFs present (Vasa, Fichtlscherer, Aicher, et al., 2001). Following angioplasty, in particular, the individual susceptibility to neointima formation could be determined not only by the extent of the endothelial injury, exposure to simultaneous RFs but also by the capability to mobilise promptly functional, viable EPCs and repair the endothelial damage.

# 1.3 miR-92a inhibitor for EPC priming

EPCs have been used for non-thrombogenic re-endothelialisation of vascular grafts, heart valve replacements, and intravascular stent devices (Balaji et al., 2013). A crucial aspect concerning EPC therapies is the magnitude of engraftment of transplanted or mobilised EPCs into the remodelling vessels as assessed by single-photon emission computed tomography, positron emission tomography or magnetic resonance. Although studies evaluating the biodistribution of the cells by non-invasive imaging cannot give insights into the morphological integration and the cell fate after prolonged time (Chavakis et al., 2008), research thus far has documented only limited engraftment of EPCs (anywhere between 1 and 50%)(Balaji et al., 2013; Haider et al., 2017). The amount of radioactivity detected in the rat ischemic heart was only about 2% after 24 to 96h following infusion of *ex vivo* cultured EPCs, indicating that only a minor percentage of cells home/are retained at the ischemic site (Aicher, Brenner, et al., 2003). Similar results were reported after infusion of uncultured labelled PB MNCs (Hou et al., 2005) or purified $CD34^+$ cells (Brenner et al., 2004), while most of the radioactivity was rather found in the spleen and the liver (Aicher, Heeschen, et al., 2003; Hou et al., 2005). The extent of engraftment indicated in clinical trials, in which labelled BM $CD34^+$ or $CD133^+$ cells were infused directly into the coronary artery of patients with AMI or chronic myocardial infarction, was no different (Caveliers et al., 2007; Goussetis et al., 2006; Kurpisz et al., 2007). Following infusion, only 2.6 to 11% of the radioactivity was sensed in the heart, after that declining to 1 to 7%. Of course, the variation reported so far may be due to differences in the target tissues studied, heterogeneity of EPC subsets used, genetic differences in the chosen clinical models, and lack of standardised tracking techniques (Balaji et al., 2013). However, worryingly there is no question that the paucity of EPC levels among PCI patients, combined with the fact that traditional CVD RFs impair normal survival, differentiation, proliferation, migration (Fadini et al., 2007) and engraftment (Chavakis et al., 2008) of the few EPCs remaining, negatively impacts upon PCI outcomes. Paradoxically, it is those patients who undergo vascular interventions that have both reduced EPC numbers and function, despite having the greatest need for these cells to repair the injured vessels. Thus, the functional impairment identified in EPCs from high-risk CVD patients poses itself an additional

hurdle for mobilisation strategies or for using autologous cell sources for transplantation. At present, there is no pharmacological treatment available to increase arterial endothelialisation established as such. Recently, one of the key breakthroughs for the study of gene expression regulation has been the discovery of micro ribonucleic acids (miRNAs), which may directly regulate 30% (C. Zhang, 2010) to 90% (R. A. Ambros, 2000) of the genes in a cell. The expression of miRNAs can regulate various aspects of stem/progenitor cell functions (Heinrich & Dimmeler, 2012). A priming/regeneration therapy utilising miRNAs, designed to increase EPC adhesion, survival and proliferation at the site of injury in elderly patients with chronic disease, could considerably facilitate vascular repair.

## miRNAs as potent transcriptional regulators

microRNAs are a type of regulatory non coding RNAs (ncRNAs) which have been recently shown to govern fundamental processes during vascular disease (Iaconetti, Gareri, Polimeni, & Indolfi, 2013). Unlike structural ncRNAs, which include ribosomal and transfer RNAs, regulatory ncRNAs can further be classified according to their transcript size (Iaconetti et al., 2013; X. Liu, Hao, Li, Zhu, & Hu, 2015) **(Table 3).**

**Table 3 | Classification of non-coding regulatory RNAs.**

| Noncoding regulatory RNAs | Abbreviation | Functions |
|---|---|---|
| **Small (<50 nucleotide)** | | |
| microRNAs | miRNA | post-transcriptional regulators |
| PIWI-interacting RNA | piRNA | DNA methylation, transposon repression |
| short interfering RNA | siRNA | RNA interference |
| **Medium (50-200 nucleotide)** | | |
| small nucleolar RNAs | snoRNA | RNA modification, rRNA processing |
| promoter upstream transcripts | PROMPTs | Associated with chromatin changes |
| transcription initiation RNAs | tiRNAs | Epigenetic regulation |
| **Long (>200 nucleotide)** | | |
| long intergenic ncRNA | lincRNAs | Epigenetic regulators of transcription |
| enhancer-like ncRNA | eRNA | Transcriptional gene activation |
| transcribed ultraconserved regions | T-UCRs | Regulation of miRNA and mRNA levels |
| natural antisense transcripts | NATs | mRNA stability |
| promoter-associated long RNAs | PALRs | chromatin changes |
| pseudogenes | None | microRNA decoys |

The first miRNA was identified in C. Elegans in 1993 (R. C. Lee, Feinbaum, & Ambros, 1993). Back then lin-4 was thought to be a worm-specific curiosity, but with the subsequent identification of the phylogenetically conserved let-7 (Pasquinelli et al., 2000), scientists took greater notice and began looking for other similar small non-coding RNAs. Since then, thousands of miRNAs have been identified, and it is evident now that they have a considerable impact on shaping transcriptomes and proteomes of eukaryotic organisms (Lim et al., 2005). In fact, miRNA have been shown to control EC and VSMC biology and thereby can regulate the progression of vascular diseases, such as restenosis (Iaconetti et al., 2013).

## Biological definition and function of miRNAs

miRNAs are a class of approximately 22-nucleotide long regulatory noncoding RNAs, which work at a post-transcriptional level, i.e. between the transcription and the translation of a gene at the RNA level. They are now known to be critical regulators of signalling pathways in multiple cell types including ECs, EPCs and perivascular cells (Garcia de la Torre et al., 2015). miRNAs are assembled into RNA-induced silencing complexes (RISC) resulting (mostly) in gene silencing, either by transcript destabilisation, translational inhibition, or both (Filipowicz, Bhattacharyya, & Sonenberg, 2008) **(Figure 13)**. The current notion is that translational inhibition alone seems to be the exception rather than the rule, at least for mammalian miRNAs (Siomi & Siomi, 2010). The specificity of miRNAs to their target messenger ribonucleic acids (mRNAs) is canonically determined by base-pairing of a 6–8-nucleotide seed sequence in the 5′ end of the mature miRNA to a perfectly or imperfectly complementary match sequence in the 3′ UTR end of the target mRNA (Bartel, 2004; Hausser & Zavolan, 2014). More than 60% of human protein-coding genes are predicted to contain miRNA-binding sites within their 3´UTRs (Friedman, Farh, Burge, & Bartel, 2009). The nature of the miRNA:mRNA interaction means that a single miR can target sequentially, on average, hundreds of distinct mRNA molecules with related biological functions (Lim et al., 2005; Siomi & Siomi, 2010; Urbich, Kuehbacher, & Dimmeler, 2008). Moreover, conversely, individual mRNAs can be targeted by multiple miRs which appear to act cooperatively, since

mRNAs frequently possess multiple miRNA-binding sites. Hence, it has become evident that complementary miRNAs often function by acting in concert, resulting in a highly complex miR regulatory potential. Additionally, several miRNAs exhibit tissue-specific expression patterning, suggesting a cell type-specific function (W. J. Yang et al., 2005).

## Biogenesis and maturation of miRNAs

The transcription of miRNAs depends on their localisation within the genome. Primary miRNA transcripts (pri-miRNA) are generated individually or in clusters after the transcription of specific sequences by RNA polymerase II and III located either in exons or introns of coding genes or non-coding genes (Issler & Chen, 2015; Urbich et al., 2008). miRNAs that have their promoters are independently expressed, while miRNAs organised in clusters share similar transcriptional modulation (Urbich et al., 2008). Pri-miRNAs form unique secondary hairpin structures (one or more), each composed of a stem and a terminal loop **(Figure 13)**. Pri-miRNAs are 5'-capped, spliced, and polyadenylated, and they can produce more than one functional miRNA (Siomi & Siomi, 2010).

The pri-miRNA nuclear processing into stem–loop precursors is mediated by a complex containing Drosha and the microprocessor complex subunit DiGeorge syndrome critical region 8 (DGCR8). The Microprocessor complex includes several other cofactors such as the DEAD-box RNA helicases p68 (DDX5) and p72 (DDX17), as well as heterogeneous nuclear ribonucleoproteins (hnRNPs)(Gregory et al., 2004), which may function to promote the specificity and activity of Drosha cleavage (Siomi & Siomi, 2010). Following cleavage, the RNA molecule is reduced to 70–110 nucleotides in length, and it is referred to as precursor miRNA (pre-miRNA). Nuclear processing generates a product with a 2 nucleotide 30 overhang (Siomi & Siomi, 2010), characteristic of RNase III-mediated cleavage. The pre-miRNA is then exported to the cytoplasm through exportin 5 (XPO5) which recognises the overhang, in a complex with RAS-related nuclear protein (RAN)–GTP (Issler & Chen, 2015).

**Figure 13 | miRNA biogenesis, maturation pathway and mode of action.**
The miRNA biogenesis pathway is a series of biochemical steps that converts the primary miRNA transcript (pri-miRNA) to the biologically active, mature miRNA. MiRNAs are transcribed from intergenic or intronic genomic sequences as mono- or polycistronic, long, primary precursor transcripts (pri-miRNAs). These are cleaved into precursor hairpins (pre-miRNAs) by the nuclear RNase III-like enzyme Drosha. Drosha cleaves the 5′ and 3′ arms of the pri-miRNA hairpin, whereas DGCR8 stabilises the complex and determines the precise cleavage site. Pre-miRNAs hairpins are then exported to the cytoplasm by Exportin-5 in a Ran-GTP–dependent manner and are further cleaved by a complex containing the endonuclease Dicer to mature miRs of 18 to 25 nucleotide length. Following Dicer-mediated cleavage, Dicer and its interaction-domain protein TAR RNA binding protein (TRBP) dissociate from the miRNA duplex to form the active RNA-induced silencing complex (RISC) that becomes functional upon assembly of one of the two strands. The RNA-induced silencing complex directs the miRNA to the target mRNA, which leads either to translational repression or degradation of the target mRNA. The re-import of miRNAs into the nucleus or its export through exosomes are alternative options. Adapted from (Issler & Chen, 2015), (Kuehbacher, Urbich, & Dimmeler, 2008), (Urbich et al., 2008) and (Bauersachs & Thum, 2011). AGO2 – argonaute 2; ATP – adenosine triphosphate; DGCR8 -DiGeorge syndrome critical region 8; GTP – guanosine triphosphate; mRNA – messenger RNA; miRNA – microRNA; miRISC – miRNA-loaded into RNA-induced silencing complex; XPO5 – exportin 5.

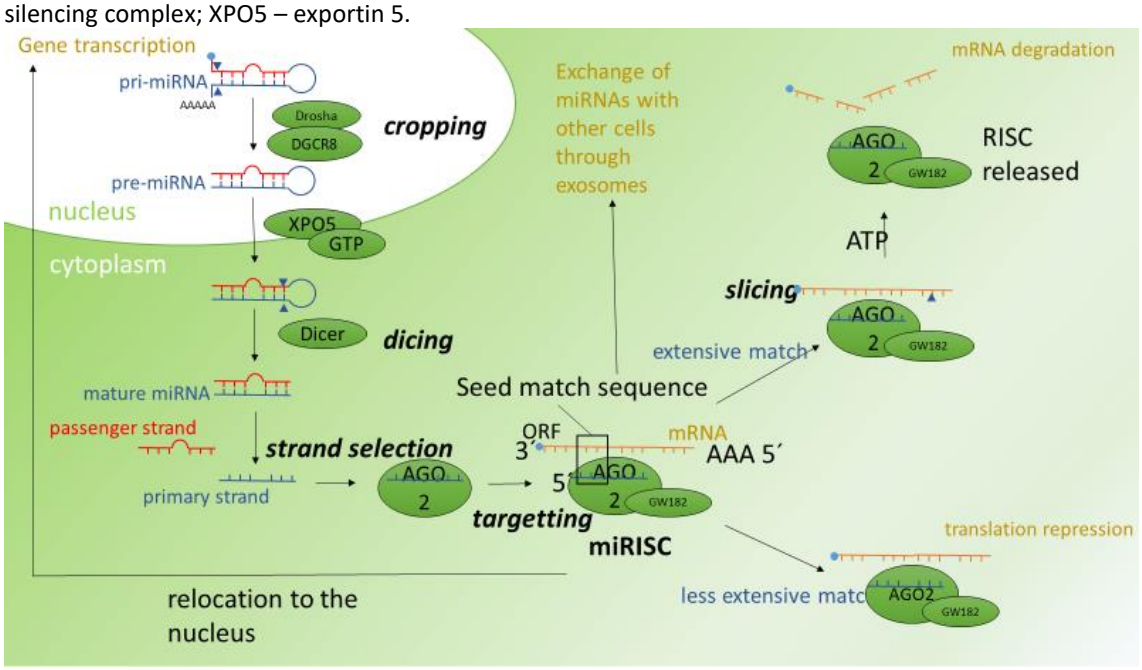


The pre-miRNA is then cleaved by Dicer to generate a mature ~22-nucleotide miRNA duplex. While most miRNAs are produced by this canonical pathway, in certain circumstances, splicing can replace Drosha-mediated processing of pri-miRNAs into pre-miRNAs. The less abundant miRNAs which circumnavigate Drosha processing are called mirtrons, and consist of pre-miRNA- like hairpins that are made by splicing and debranching of short hairpin introns. If the intron-derived miRNAs resulting from splicing from their host transcripts and the debranching lariat enzyme has the appropriate size to form a hairpin resembling a pre-miRNA, it then bypasses Drosha cleavage (Winter, Jung, Keller, Gregory, & Diederichs, 2009).

The double-stranded duplex must be separated into the primary strand (which is complementary to the target mRNA) and the passenger strand (which is subsequently degraded). Selection of the miRNA strand which will be incorporated into the RISC is regulated in a cell type-specific manner, but one important parameter for strand selection is the thermodynamic asymmetry of the miRNA duplex (Khvorova, Reynolds, & Jayasena, 2003). Typically, the miRNA strand whose 5' end is less stably base-paired will be more frequently sorted as the functional guide (Siomi & Siomi, 2010). Nevertheless, recent deep-sequencing studies revealed that pre-miRNAs could be bifunctional with individual passenger strands sometimes not being degraded, but rather associate with Argonaute2 (AGO2) dependent on specific mismatches (Siomi & Siomi, 2010). The strand of the mature miRNA is then loaded into the RISC complex together with two major class of proteins (AGO2 and GW182)(Issler & Chen, 2015), guiding the complex to target the 3' untranslated region (3' UTR) of the mRNAs to promote their degradation or simply inhibit their translation. Although the entire sequence of miRNA can bind to the target, it is usually nucleotides at position 2-7 that compose the seed sequence that determines target specificity (Lai, 2002). Whereas mRNA degradation needs a high miRNA-target complementarity, the translational repression only requires low miRNA-target complementarity (Lewis, Shih, Jones-Rhoades, Bartel, & Burge, 2003). The GW182 proteins have been shown to interact with the cytoplasmic poly(A)-binding protein (PABP) and together might function as a scaffold for the assembly of the multiprotein deadenylation complex that silences miRNA targets, including the PAN2-PAN3 and CCR4-NOT (Bauersachs & Thum, 2011). Additionally, human AGO2 can endonucleolytically cleave target mRNA (via Rnase H recruitment) which is perfectly complementary to the miRNA (Dias & Stein, 2002; D. Gibbings & Voinnet, 2010). Of note, miRNAs in the cell are present as miRISC complexes, in which both the 5' and 3' ends are thought to be bound directly by AGO2, thus being protected from instantaneous exonuclease-mediated degradation (Y. Wang, Sheng, Juranek, Tuschl, & Patel, 2008). Re-importation of miRNAs into the nucleus is an alternative pathway and is especially relevant because there is accumulating evidence that miRNAs can regulate gene expression at the transcriptional level (Kim, Saetrom, Snove, & Rossi, 2008).

## Location of the miRNA machinery

There appears to be a link between miRNA -mediated silencing and membrane trafficking since formation and turnover of the RISC complex occur at the endosomal membrane (Siomi & Siomi, 2009) **(Figure 14)**. Endosome maturation requires gradual accumulation of inwardly budding vesicles termed multivesicular bodies (MVB), using the Endosomal Sorting Complex Required for Transport (ESCRT). Depleting ESCRT will block MVB formation, which results in impaired miRNA silencing (Piper & Katzmann, 2007). GW182 and AGO2, mutually associated with miRNA gene silencing, are enriched in the endosomal MVB fraction in particular foci called GW-bodies (D. J. Gibbings, Ciaudo, Erhardt, & Voinnet, 2009), which are GW182-rich and DCP1-poor. In fact, MVBs seem to be the site where miRNA biogenesis and RISC-assembly pathways intersect, with continuous removal of GW182 being required for the efficient passage of miRNA strand duplex from DICER to AGO2 (Siomi & Siomi, 2009). AGO2 is an essential component of the RISC complex that can directly degrade mRNA by slicing (Meister, 2013). A second AGO2 pool distinct from GW-bodies has been identified. These GW182-poor cytoplasmic foci are called cytoplasmic processing bodies (P-bodies). Inside the P-body, miRNA targets are sequestered from the translational machinery and are subjected to mRNA degradation, at least partially, through deadenylation. There, enzymes involved in mRNA decapping (DCP1 and DCP2) are usually concentrated and promote translational inhibition and mRNA decay (Meister, 2013). RISC complex and P-bodies seem to interact physically (Siomi & Siomi, 2009) with targeted mRNAs being pushed away from the translational machinery into the latter. The miRNA-mediated silencing occurs by fusion with lysosomes and consequential release of the miR-RISC to another repression cycle. Concordantly, blocking the maturation of MVBs into lysosomes by the loss of the tethering factor HPS4 enhances miRNA-mediated silencing and leads to overaccumulation of GW-bodies (Y. S. Lee et al., 2009). KRAS-MEK-ERK (Extracellular signal–regulated kinase) signalling was shown to occur on late endosomes (McKenzie et al., 2016), and in fact, MEK-ERK signalling downstream of mutant KRAS suppresses AGO2 (via phosphorylation) and its association with MVBs, thereby inhibiting release of AGO2 and several miRNAs in exosomes, favouring their transfer into P-bodies (McKenzie et al., 2016). Alternatively, if AGO2 is not phosphorylated, miRNAs

can be packaged inside 50- to 90-nm membrane-derived particles called exosomes, which are generated from MVBs and are secreted from the cells after fusion with the plasma membrane, into plasma or other cells (Y. S. Lee et al., 2009; Valadi et al., 2007). Not to be confused with microvesicles which are directly shed from the cell membrane. Of note, there seems to be a protection via association with other molecules (e.g., the miRNA– AGO2 complex (Melo et al., 2014)) or modifications of the miRNAs that make them resistant to RNase activity when being transported or when unloaded from the exosomes.

**Figure 14 | miRNA-RISC assembly & turn-over and corresponding cellular compartments**
MVBs are late endosomal compartments, between early endosomes and lysosomes. MVBs can also release internal vesicles, called exosomes, into the extracellular space. RISC formation and turnover appear to occur in MVBs, specifically at GW bodies. Briefly, PABP binds the CBC, as well as the 3' polyA-tail of a 5' m7G capped mRNA, thereby circularising the mRNA allowing it to be translated by ribosomes. Recognition of an mRNA by a miRNA bound to AGO2 which favours the release of CBC from mRNA. Upon CBC release, new translation initiation cannot occur, and ribosomes are eventually released from the repressed mRNA. Repressed mRNA is no longer circularised by PABP linking the 5' cap and polyA tail. PABP is presumably released at this stage from repressed mRNA since PABP is not enriched in P-bodies. P-bodies are enriched in mRNA decapping and deadenylation complexes (DCP1A/DCP2 and CAF1/CCR4-NOT, respectively). Cap and polyA tail are removed from repressed mRNA. AGO is released from miRNA and repressed mRNA. Then, HSP90 stabilises empty AGO, which is presumably retained on the membrane. AGO binds Dicer and acquires the duplex miRNA. On the other hand, phosphorylation of AGO2 specifically inhibits AGO2 association with MVBs (reduced slicing activity), diminishes secretion into exosomes, and increases association with P-bodies (therefore promoting translational repression). Adapted from (D. Gibbings & Voinnet, 2010) and (McKenzie et al., 2016). AGO2 – argonaute 2; CBC - Cap-Binding Complex; CAF1 - chromatin assembly factor-1; DCP1 - mRNA-decapping enzyme 1; DCP2- mRNA-decapping enzyme 2; ESCRT - endosomal sorting complexes required for transport; HPS4 - Hermansky-Pudlak syndrome 4 protein; HSP90 – heat shock protein 90; MEK – mitogen-activated protein kinase; mRNA – messenger RNA; miRNA – microRNA; MVB - multivesicular bodies; PABP - Poly(A)-binding protein; RISC – RNA-induced silencing complex.

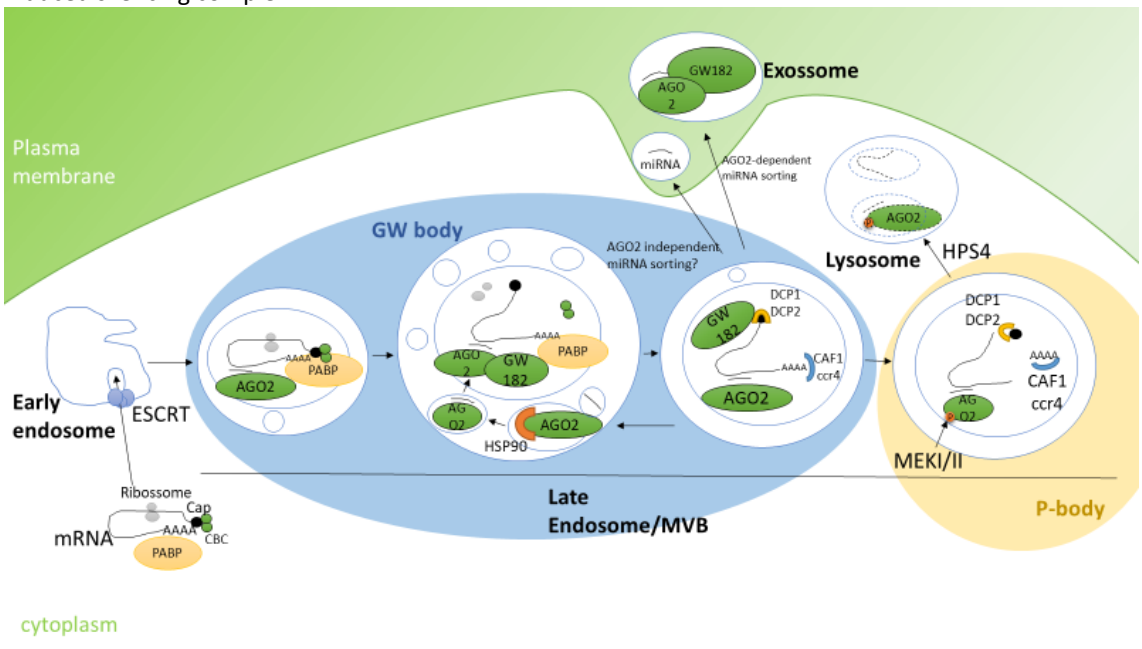

## miRNA regulation

Importantly, most miRNAs exhibit strict developmental stage-specific and tissue-specific expression patterns, and moreover, their levels can become altered during disease (Siomi & Siomi, 2010). In contrast to the linear miRNA processing pathway that was initially thought to be universal for the biogenesis of all mature miRNAs, multiple studies led to the understanding that there are several regulatory options to express and process individual miRNAs differentially. Many steps can be performed in multiple ways, omitted or replaced, and are affected by different mechanisms for individual miRNAs. miRNA expression is mainly controlled at the transcriptional level, through feedback regulation. For instance, some miRNAs regulate transcription factors that, in turn, regulate expression of the miRNA, forming a negative feedback loop (Siomi & Siomi, 2010). Moreover, host genes harbouring miRNA sequences in their intronic sites impose their pattern of expression to the respective miRNAs (Kuchen et al., 2010). Remarkably, several miRNAs exhibit a promoter structure similar to that of protein-coding genes (i.e., TATA box, initiator elements, frequencies of CpG islands, transcriptions factor bindings sites), making them amenable to transcriptional regulation **(Figure 15)** (Ozsolak et al., 2008). Particularly, regulatory sequences present in their promoters can lead to tissue and development-specific miRNA expression (Obernosterer, Leuschner, Alenius, & Martinez, 2006). miRNA editing can be another biogenesis regulation step. Editing corresponds to the post-transcriptional change of RNA sequences by deamination of adenosine (A) to inosine (I), altering the base pairing and structural properties of the transcript. Editing of miRNA transcripts by ADAR1 and ADAR2 inhibits its cleavage by the endonuclease Drosha and leads to the degradation by the ribonuclease Tudor-SN, which preferentially cleaves double-stranded RNA containing inosine–uracil pairs (W. Yang et al., 2006). Editing can also impact further downstream processing steps such as cleavage by Dicer in the cytoplasm (Winter et al., 2009). Additionally, miRNAs' maturation can be suppressed as a consequence of the Drosha or Dicer -processing steps (Obernosterer et al., 2006; Thomson et al., 2006).

**Figure 15 | Transcriptional regulation of miRNAs.**
Most miRNAs are processed by RNA polymerase II from independent genes or introns of protein-coding genes. Usually, miRNAs have their promoter region, regulated by numerous transcription factors. In a main canonical pathway, primary miRNA precursors (pri-miRNA) are first processed by Drosha and then exported to the cytoplasm. Few pre-miRNAs are produced independently (thus bypassing Drosha-mediated processing) from very short introns of genes (mirtrons) by splicing actions. Drosha associates with DGCR8 and many other cofactors to form the Drosha-DGCR8 complex. Many factors associate with the Drosha/DGCR8 complex, thereby regulating its stability and activity. The p68 forms heterodimers with p72, p53, and Smad factors, whereas further editing of pri-miRNAs occurs by ADARs that affect miRNA accumulation and miRNA target specificity. After export to the cytoplasm, pre-miRNAs associate with the endonuclease Dicer and several other regulatory proteins, such as TRBP and Argonaute 2. AGO2 and PABP can interact with the deadenylases CAF1/CCR4 or with DCP1/2, facilitating mRNA deadenylation and uncapping respectively, thus contributing towards mRNA degradation. Additionally, human AGO2 can endonucleolytically cleave target mRNA which is perfectly complementary to the miRNA. Adapted from (Siomi & Siomi, 2010). ADAR - adenosine deaminases acting on RNA; CAF1 - chromatin assembly factor-1; DCP1 - mRNA-decapping enzyme 1; DCP2- mRNA-decapping enzyme 2; hnRNP - heterogeneous nuclear ribonucleoprotein; PABP - Poly(A)-binding protein; NF - nuclear factor; KSRP - KH-type splicing regulatory protein; SMAD - mothers against decapentaplegic homolog; SNIP1- Smad nuclear interacting protein 1; TF – transcription factors; TRBP - transactivation-response RNA-binding protein.

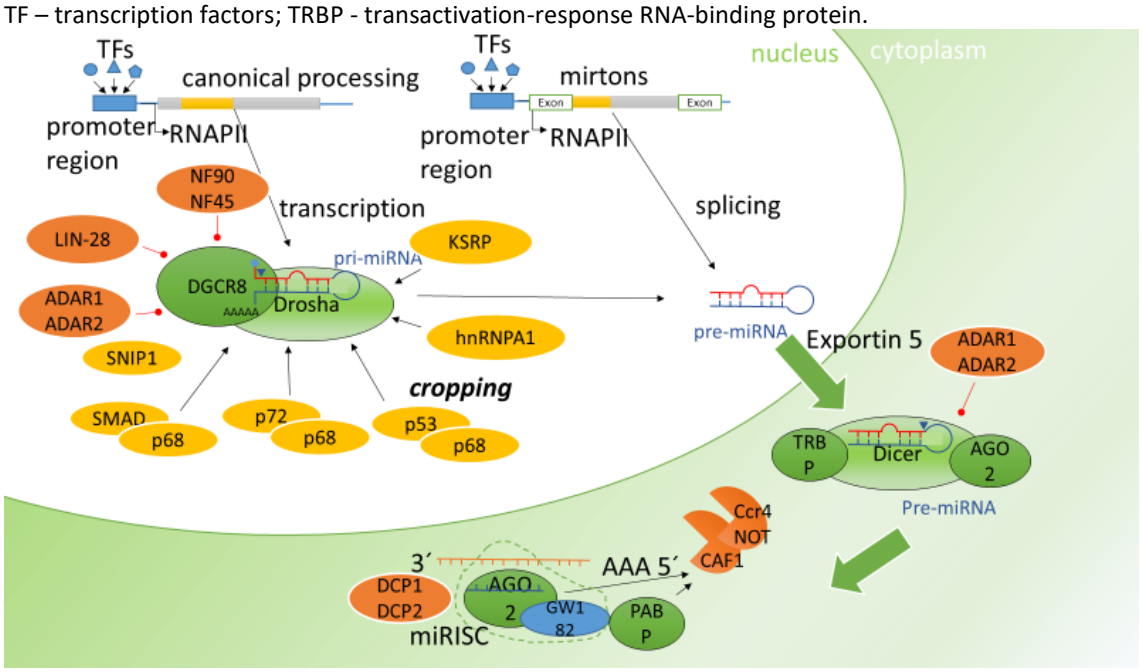


Other layers of biogenesis modulation have been described such as epigenetic (e.g. methylation inactivation) or during export of pre-miRNA from the nucleus to the cytoplasm (which may be differentially regulated). Interestingly, many miRNAs are encoded in the genome as clusters and are transcribed as polycistronic primary transcripts. However, there is evidence that miRNAs located in those clusters can be independently regulated (Guil & Caceres, 2007), suggesting that individual miRNAs can be regulated post-transcriptionally by factors that confer them specificity. Other post-transcriptional regulatory mechanisms during miRNA maturation include strand selection mechanisms and stabilisation of the transcripts through terminal adenylation (Katoh et al., 2009). Also, it seems that miRNA degradation by exonuclease XRN-2 can

be blocked by the binding of miRNA-target RNA, suggesting that targets can modulate the stability of specific mature miRNAs and help to prevent detrimental overexpression of miRNAs when target abundance is low. In summary, it is conceivable that that miRNA processing pathways are more complex than currently recognised.

### miRNA terminology

Several thousands of miRNAs across different species have been identified. Thus, an intuitive annotation system had to be adopted (V. Ambros et al., 2003). Newly identified miRNA genes are numbered sequentially and prefixed by 'mir' followed by a dash (e.g., mir-92). The uncapitalized 'mir' refers to the pre-miRNAs while the capitalised 'miR' refers to the mature forms. miRNAs with similar mature sequences are annotated in lower case letters to show their similar structure (e.g., miR-92a and miR-92b). Distinct precursor sequences that express equal mature sequences are indicated with an additional number (e.g., miR-92a-1 and miR-92a-2). Annotation for the species they are identified in should come first (e.g., hsa-miR-92a in *Homo sapiens*). miRNAs originating from the 3’ end or 5’ end are denoted with a '-3p' or '-5p' suffix, respectively (e.g., miR-92a-1-3p and miR-92a-1-5p).

## Upregulation of miR-92a following vascular injury

Over the last few years, several miRNAs have been recognised as emerging gene regulators in the pathogenesis of vascular remodelling (L. J. Chen, Lim, Yeh, Lien, & Chiu, 2012). EPCs, ECs, VSMCs and inflammatory cells, all have specific roles in restenosis and vascular remodelling after angioplasty and stenting. MiRNAs are ubiquitous and have been shown to modulate the stress response of ECs to injury, to drive VSMC phenotype switch, and to control macrophage function involved in arterial remodelling (L. J. Chen et al., 2012). Evidence of changes in miRNA expression profiles after angioplasty in animal models is growing, and a few expression signatures have now been correlated with restenosis (Small & Olson, 2011). Compared with uninjured arteries, microarray analysis demonstrated that 7 days after balloon angioplasty 113 out of 140 miRNAs were differentially expressed: 60 were up-regulated, and 53 were down regulated (Ji et al.,

2007). At 14 days after injury, 63 were upregulated, and 47 were downregulated out of 140 artery miRNAs, whereas 102 of the 140 artery miRNAs were aberrantly expressed (55 overexpressed and 47 downregulated) at 28 days after angioplasty. A large number of miRNAs that were found to be upregulated both in VSMCs and in ECs after or during vascular injury further highlights their importance in the pathophysiology of arterial restenosis after injury (Gareri, De Rosa, & Indolfi, 2016). Using this microarray approach, Ji and colleagues noticed that miR-21 was upregulated 5-fold in neointimal lesions, which was confirmed by qPCR. This miRNA is particularly interesting because it highlights an orchestrated action targeting different molecules in the EPC, EC, VSMC or macrophage, leading to various stress-specific responses, but exerting their function in a combined mode, across interacting cell types. MiR-21 simultaneously induces EPC senescence through High motility group AT-hook 2 (HMGA2) (Zhu et al., 2013), reduces EC-mediated angiogenesis and migration by targeting RhoB (Sabatel et al., 2011), promotes proliferation and inhibits apoptosis of VSMC via suppression of the phosphatase (PTEN) and up-regulation of Bcl-2 (Ji et al., 2007), and enhances VCAM-1– and CCL2-dependent monocyte adhesion via suppression of PPAR-gamma (Zhou et al., 2011).

Given the miR-21 example, the scientific community became convinced that the identification of miRNAs that might have specific functions in vascular remodelling by advanced high-throughput analyses at the transcriptome levels in injured vessels could unveil a new class of potential therapeutic targets for restenosis. Revisiting the microarray data, I searched for another miRNA aberrantly expressed after vascular injury which could theoretically have a differential effect on ECs and SMCs **(Table 4)**. Such miRNA aimed to selectively accelerate the formation of novel endothelium on injured segments (and simultaneously inhibit smooth muscle) could putatively be an attractive strategy to prevent post-injury restenosis.

**Table 4 | miRNAs possibly involved in the vascular response to injury.**
(+) or (−), respectively, indicate induction or inhibition of a specific phenotype/biological effect. Adapted from (Polimeni, De Rosa, & Indolfi, 2013), (Forte et al., 2014) and (Gareri et al., 2016). BMPR2 - bone morphogenetic protein receptor type II; Cdc-42 - cell division control protein 42; EC – endothelial cell; FGF1 – fibroblast growth factor 1; FOXO4 - Forkhead box protein O4; HMGA2 - High-mobility group AT-hook 2; ITGA5 – integrin alpha 5 subunit; KDR – kinase insert domain receptor; KLF-2 - Krüppel-like factor 2; KLF-4 - Krüppel-like factor 4; KLF-5 - Krüppel-like factor 5; miR – microRNA; MKK4 - mitogen-activated protein kinase kinase 4; PTEN - phosphatase and tensin homolog; RhoB - Ras homolog gene family; member B; SDF1 – stromal derived factor 1; SMAD3 - small mother against decapentaplegic; SMC – smooth muscle cell; Spred1 - Sprouty-related; EVH1 domain-containing protein 1; STIM - stromal interaction molecule; uPA - urokinase-type plasminogen activator - VCAM-1; vascular cell adhesion molecule 1; WWP1 - NEDD4-like E3 ubiquitin-protein ligase.

| **miRNAs** | ***In vitro* effect in ECs** | **Modulation after injury** | **Validated targets** |
|---|---|---|---|
| miR-21 | Apoptosis and proliferation (-) | ↑ | HMGA2, RhoB |
| miR-92a | Angiogenesis, proliferation and migration (-) | ↑ | ITGA5, KLF-4, MKK4 |
| miR-126 | Vascular integrity and angiogenesis (-) | ↑ | Spred-1, VCAM-1, KDR, SDF1 |
| miR221/222 | Proliferation and migration (-) | ↑ | c-kit, eNOS |
| **miRNAs** | ***In vitro* effect in SMCs** | **Modulation after injury** | **Validated targets** |
| miR-17~92 | Differentiation, migration and proliferation (+) | ↑ | BMPR2 |
| miR-21 | Apoptosis and proliferation (+) | ↑ | PTEN, BMPR2, BCl2, WWP1 YOD1, SATB1 |
| miR-23b | Differentiation, migration and proliferation (-) | ↓ | FOXO4, uPA, SMAD3 |
| miR-31 | Pro-synthetic (+) | ↑ | LATS2 |
| miR-133a | Differentiation and proliferation (-) | ↓ | Sp-1 |
| miR-125 | Differentiation, migration and proliferation (-) | ↓ | Ets-1 |
| miR-145 | Differentiation, migration and proliferation (+) | ↓ | KLF-5, KLF-4, calmodulin kinase IIδ |
| miR-143 | Proliferation and migration (-) | ↓ | KLF-5, Elk-1 |
| miR-146 | Proliferation and migration (+) | ↑ | KLF-4 |
| miR-195 | Proliferation and migration (-) | ↓ | Cdc-42, FGF1, Cyclin D1 |
| miR-221/222 | Proliferation and migration (+) | ↑ | p27, p57 |
| miR-424 | Differentiation, migration and proliferation (+) | ↑ | Cyclin D1, STIM, Calumenin |

miR-92a, which was overexpressed at 1.57 in a log2ratio compared to normal arteries after 28 days (Ji et al., 2007), seemed to be a match, given that its overexpression results in a significant reduction in EC proliferation and migration *in vitro*, while the same does not apply to SMCs when subject to the same treatment (Daniel et al., 2014). These findings suggest that the functional impact of miR-92a is predominantly restricted to ECs. Vice versa, inhibition of miR-92a produces differential effects on ECs and VSMC, reducing proliferation of the latter (Iaconetti et al., 2012). Already during my PhD, miR-92a was confirmed by qPCR to be significantly up-regulated in ECs adjacent to the vascular injury site following wire-induced manipulation of the femoral artery in mice (Daniel et al., 2014). This is particularly interesting for EPC priming since there are reasons to believe that EPCs, besides sharing some functional features with ECs, also have a similar miRNA signature, which includes miR-92a, miR-126, miR-130a and miR-221/222 (Q. Zhang, Kandic, & Kutryk, 2011).

## Circulating miR-92a as biomarker

Interestingly, although miR-92a levels rise locally after vascular injury (Daniel et al., 2014), circulating miR-92a levels in CAD patients are significantly downregulated (Fichtlscherer et al., 2010). The exact mechanisms leading to this reduction remain unclear. Possible reasons put forward include exhaustion of miRNAs storage and production in vascular cells after bout release and activation of the vasculature, or, alternatively, enhanced uptake by blood cells or cells at the atherosclerotic/injury lesions. When these patients are treated with statins a trend towards a further reduction in the levels of circulating miR-92a is observed (Fichtlscherer et al., 2010; Y. Jiang et al., 2015), suggesting that low circulatory levels of miR-92a likely represent a global compensatory protective mechanism that might be boosted in response to statin therapy, while miR-92a overexpression following injury is part of a stress and harmful response. This phenomenon reinforces the potential role of circulating miRs as biomarkers for diagnosis of CVD. In fact, circulating miR-21, miR-143, miR-145, and miR-100, which are found to be dysregulated in patients with intra-sent restenosis compared to controls, have already been studied as biomarkers for intra-stent restenosis (He et

al., 2014), which could easily be exploited to risk stratify patients after PCI non-invasively and to assess possible intervention failure (He et al., 2014).

## The importance of miR-92a in vascular biology

The modulation of vascular-specific processes by some miRNAs which control cell growth, migration, apoptosis, capillary tube formation has been extensively studied to date (Bonauer, Boon, & Dimmeler, 2010). In the next section, I focus on the specific role of miR-92a in vascular biology.

### miR-92a-1 is encoded in the mir-17~92 cluster

The polycistronic mir-17~92 cluster maps to human chromosome 13 and encodes 6 mature miRNAs (miR-17, miR-18a, miR-19a, miR-19b, miR-20a and miR-92a-1) transcribed as one common primary transcript (Concepcion, Bonetti, & Ventura, 2012; Venturini et al., 2007). The sequence of the mir-17~92 cluster is highly conserved among vertebrates, and evolutionary gene duplications followed by subsequent loss of individual miRNA components have resulted only in two mammalian paralogs: the miR-106a~363 cluster and the miR-106b~25 cluster **(Figure 16)**. These are located on different chromosomes and contain individual miRNAs that are highly similar to those encoded by the mir-17-92 cluster. The miR-106a~363 is located on chromosome X, while the miR-106b~25 cluster is located on human chromosome 7. It is curious to note that not only the sequence of each miRNA component is highly conserved across species among all 3 paralogs, the entire organisation of these miRNAs within the family also exhibits a high level of conservation. Curiously, ablation of miR-106b~25 or miR-106a~363 causes no obvious phenotype (Ventura et al., 2008). The functional significance of this conservation remains still unclear (Olive, Jiang, & He, 2010). Another important concept is that of "seed family". miRNAs with similar seed sequences are predicted *in silico* to target highly overlapping sets of genes and are usually grouped functionally in the same "seed family".

**Figure 16 | Schematic representation of the gene of miR17~92 cluster and its paralogs.**
miRNAs sharing the same seed sequence are represented by boxes of the same colour. The miRNAs encoded by the 3 clusters can be categorized into four separate miRNA families according to their seed sequences, including the miR-17 family (miR-17, miR-20a, miR-20b, miR-106a, miR-106b and miR-93), the miR-18 family (miR-18a and miR-18b), the miR-19 family (miR-19a, miR-19b-1 and miR-19b-2) and the miR-92 family (miR-92a-1, miR-92a-2, miR-363 and miR-25). Black bands represent future mature strand regions. Adapted from (Concepcion et al., 2012). chr – chromosome; miR – miRNA.

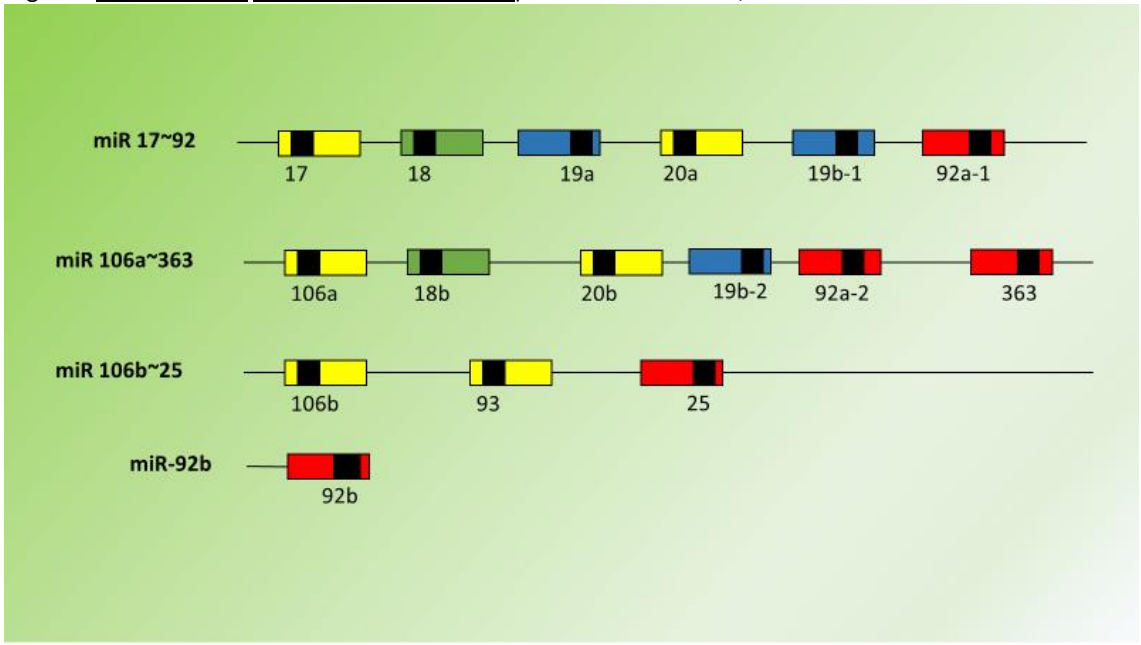


The miR 17~92 polycistron first raised awareness after several studies revealed its upregulation in different hematologic (Venturini et al., 2007) and solid (Hayashita et al., 2005; Volinia et al., 2006) malignancies and that there was an association with cancer-related angiogenesis (Kuehbacher et al., 2008). Nevertheless, opposing studies showed that the DNA region encoding the cluster is deleted in patients with ovarian, breast and melanoma cancers (L. Zhang et al., 2006). Moreover, enforced expression of miR-17 in breast cancer cell lines reduces the proliferation of the cancer cells, likely via repression of AIB1, a transcriptional co-activator of E2F1 and the oestrogen receptors (Hossain, Kuo, & Saunders, 2006). Further adding to the complexity of this cluster's signature, there is considerable evidence suggesting that its various members differ in their oncogenic potential (Concepcion et al., 2012). Therefore, one might speculate that the mir-17~92 cluster tumorigenicity is context, cell and miR product-dependent, although it is also possible that its multiple members can act synergistically, either by converging on the same targets or by targeting multiple nodes from a common pathway or biological output. Theoretically, depending on cell type and physiological context, there is an enormous plasticity potential for gene regulation here, as different target mRNAs

may be repressed by a combination of cluster components. Additional roles for the mir-17~92 cluster have been identified. These include the regulation of essential immune and hematopoietic processes, and of the lung, heart and skeletal development (Bonauer & Dimmeler, 2009; Xiao et al., 2008). In fact, the developmental defects can be severe enough to cause death shortly after the birth of mir-17~92 homozygotes null mice, with lung hypoplasia and a ventricular septal defect (Ventura et al., 2008). Remarkably, there is a lack of an obvious vascular phenotype in mir-17~92–deficient mice, hinting that the cluster may not be essential for endothelial differentiation during embryonic development (Jevnaker, Khuu, Kjole, Bryne, & Osmundsen, 2011). Although the mir-17~92 cluster has been associated with fundamental aspects of EC biology, namely, the regulation of cell cycle and sprouting angiogenesis, curiously, neither the cluster nor its individual members seem to be essential for endothelial differentiation (Treguer, Heinrich, Ohtani, Bonauer, & Dimmeler, 2012). Individual and combined inhibition of the members of the miR-17–92 cluster during differentiation from ESC or iPS cells did not affect the expression of well-established endothelial markers.

Recently, a hemizygous germline deletion involving the mir-17~92 locus has been identified as the genetic determinant of the rare autosomal dominant condition known as Feingold syndrome (Marcelis et al., 2008). Patients with this condition present a broad range of skeletal defects, including short stature, brachymesophalangy and microcephaly. Affected individuals may also present mental retardation and gastrointestinal atresia, albeit with lower penetrance (Marcelis et al., 2008).

This syndrome with peculiar phenotype abnormalities highlights the importance of miRNA in fine-tuning gene expression in a timely, spatially and coordinated manner. Given the functional specificity of different mir-17~92 components, it is evident now that the polycistronic cluster is subjected to complex transcriptional regulation. The cluster regulation at transcriptional level relies on its promoter **(Figure 17)**. ChIP assay has shown the binding of c-Myc, E2F, and cyclin D1 to the upstream promoter region of the miR-17–92 cluster (O'Donnell, Wentzel, Zeller, Dang, & Mendell, 2005). Also, an STAT3 binding site is present in this promoter (Brock et al., 2009).

Inhibition of their transcriptional activity or targeting the respective downstream signalling pathways have been shown to prevent neointima formation. Venturini and

O'Donnell were the first to show that c-Myc stimulated the transcription of the miR-17~92 cluster in human B-cells and chronic myeloid leukaemia cells (O'Donnell et al., 2005; Venturini et al., 2007). Remarkably, the cluster can be directly activated by c-Myc proto-oncogene alone or in association with RAS (Dews et al., 2006; O'Donnell et al., 2005). Not surprisingly, the cluster is also documented to be transcriptionally activated by c-myc homolog MYCN in neuroblastoma cells (Haug et al., 2011). In fact, the observations that either MYCN loss-of-function mutations or miR-17~92 haploinsufficiency can lead to the very same defective Feingold phenotype are in agreement (Marcelis et al., 2008). These findings are consistent with the functions of mir-17~92 in promoting proliferation in a diversity of cell types, including cells of epithelial, lymphoid and neural origin. An interesting aspect is that, in contrast to the expression of the mir17~92 cluster promoter transcription factors, miR-92a alone seems to be mainly expressed in ECs (Iaconetti et al., 2012), so that clinical inhibition of miR-92a might result in higher cell specificity than inhibition of the corresponding transcription factors. Further transcriptional activators found to directly bind to the promoter of miR-17~92 include E2Fs (chromatin immunoprecipitation reveals that E2F3 is the major E2F family member that binds to the promoter region according to (Sylvestre et al., 2007)), Smad3 and Cyclin D1, which are regulated by miR-17 and miR-20a, which in turn can regulate the cluster promoter through a negative feedback loop (Bonauer & Dimmeler, 2009; T. Luo, Cui, Bian, & Yu, 2014; Sylvestre et al., 2007; Woods, Thomson, & Hammond, 2007; Yu et al., 2008). E2Fs are vital for the progression of the cell cycle, as they trigger a large number of S phase genes, including Cyclins E and A, thymidine kinase and DNA polymerase. As a consequence, theoretically, cycling cells are likely to have elevated mir-17~92 levels due to the periodic surge of E2F activity during S phase, while quiescent cells would present reduced cluster levels. This is consistent with the high level of mir-17~92 polycistron expression in transformed cell lines, but not in the primary cell culture or fully differentiated cell types (Olive et al., 2010). Additionally, stimulation of mir-17~92 expression by pro-inflammatory cytokines such as IL-6 (Brock et al., 2009) or VEGF (Suarez et al., 2008) may occur, although it was recently identified that VEGF-mediated up-regulation of mir-17~92 only elevates the expression level of three individual miRNAs of the entire cluster (miR-17, miR-18 and miR-20) (Suarez et al., 2008) while reducing miR-92a (Iaconetti et al., 2012), to

contribute to the control of angiogenic phenotypes. In summary, there seems to be a selective mir-17~92 biogenesis under specific biological contexts.

**Figure 17 | Known mechanisms accounting for transcriptional and post-transcriptional regulation of the miR-17~92 cluster.**
Adapted from (Bonauer & Dimmeler, 2009). IL-6 – interleukin 6; miR – microRNA; MYCN - N-Myc proto-oncogene protein; Smad3 - mothers against decapentaplegic homolog 3; STAT3 - signal transducers and activators of transcription 3; VEGF – vascular endothelial growth factor.

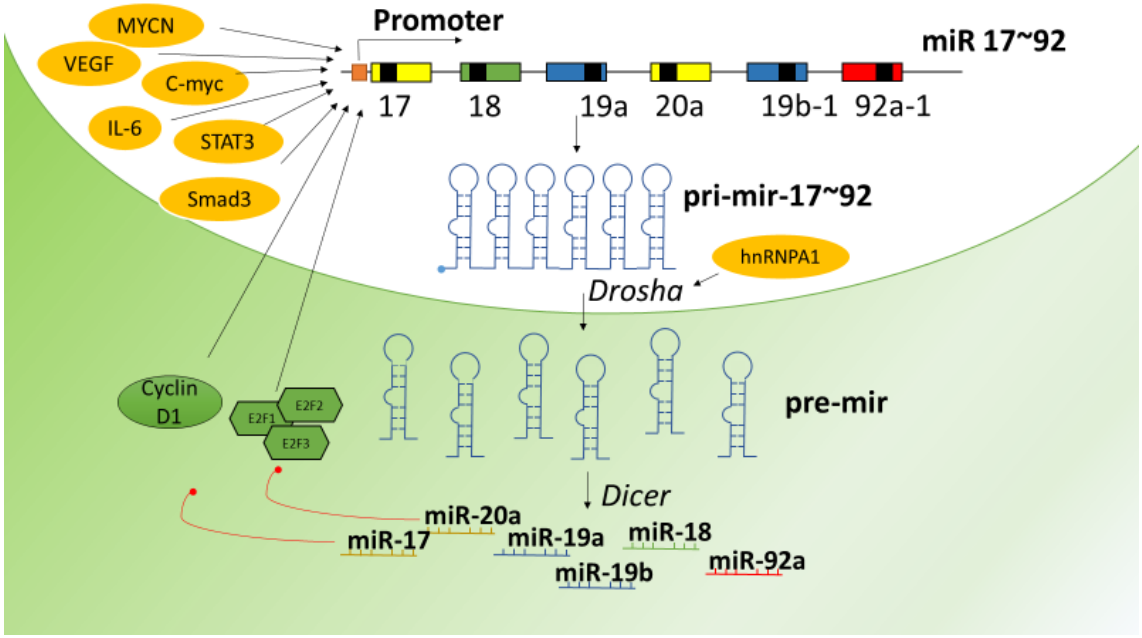


Although initial studies focused only on the transcriptional regulation of mir-17~92, more current research has begun to shed light on how members of the cluster are individually and uniquely regulated beyond transcription. In fact, the six miRNAs encoded by the mir-17~92 cluster are often expressed at different levels, suggesting that they are either processed at varying rates or that their stability can be modulated (Concepcion et al., 2012). For instance, the RNA-binding protein hnRNPA1 binds to the loop structure of miR-18a and facilitate its processing by Drosha, without affecting the processing of the remaining mir-17~92 cluster members (Guil & Caceres, 2007).

Cluster members, if differentially triggered, may be capable of regulating distinct pathophysiological components of vascular regeneration, our main focus. The redundancy in miRNA function and the occurrence of compensatory mechanisms has been emphasised. For instance, overexpressing the entire mir-17~92 cluster in c-Myc-induced tumours increases angiogenesis (Dews et al., 2006), which is thought to the

result of the dominant downregulation of the antiangiogenic molecules thrombospondin-1 (TSP-1) and connective tissue growth factor (CTGF) by miR-18 and miR-19, respectively (Dews et al., 2006). Similarly, miR-17 has been described to repress the anti-angiogenic factor tissue inhibitor of metalloproteinase 1 (TIMP1) (Otsuka et al., 2008). On the contrary, the overexpression of miR-17 and miR-20a *per se* blocks angiogenic sprouting and migration (via Jak-1 downregulation?)(Doebele et al., 2010; Shan et al., 2009), and overexpression of miR-92a interferes with intersegmental vessel development in zebrafish (Bonauer et al., 2009). Based on the reported studies it appears that the mir-17~92 cluster members may exhibit distinct specific vasculogenic effects depending on the cell type, miRNA abundance and context. Therefore, the effect of miRNAs from the cluster differs for ischaemia and tumour-associated angiogenesis, which is fundamental if one considers these miRNAs as potential therapeutic targets. However, surprisingly, in ECs, the response seems to be highly consistent. All cluster members appear to behave as negative angiogenic regulators. Recently Doebele et al. revealed that overexpression of the individual members miR-17, miR-18, miR-19a, and miR-20a specifically in ECs, reduced angiogenic sprouting *in vitro*, whereas inhibitors of these miRNAs rescued the effect (Doebele et al., 2010). Overexpression of miR-92a in HUVECs also suppresses angiogenic sprout formation *in vitro*, and vice versa, while the inhibition of miR-92a *in vivo* promotes neovascularization and the functional recovery after hindlimb ischemia in mice (Bonauer et al., 2009).

## miR-92a exerts anti-angiogenic actions in ECs

Several members of the miR-17~92 cluster have been shown to control angiogenesis. miR-92a too is considered an endogenous repressor of the angiogenic program in ECs and a potent regulator of angiogenesis *in vivo* (Zampetaki & Mayr, 2012). Moreover, miR-92a is reported to inhibit EC proliferation, migration, adhesion and vascular sprouting *in vitro* by downregulating the expression of validated target genes, which include the class III histone deacetylase sirtuin 1 (SIRT1), integrin subunit α5 (ITGA5) and αv (ITGAV), sphingosine-1-phosphate receptor-1 (SIP-1), Suppressor of cytokine signalling 5 (SOCS5)(Loyer et al., 2014), mitogen activated protein kinase kinase-4 (MKK-4) and the flow-induced atheroprotective transcription Krüppel-like factor 2 and 4 (KLF2

and KLF4)(Bonauer et al., 2009; Doebele et al., 2010; Y. Fang & Davies, 2012; Wu et al., 2011). These genes are all known to contribute to the cell-matrix interaction, cell migration, apoptosis and angiogenesis in ECs (Seeger, Zeiher, & Dimmeler, 2013). Remarkably, miR-92a is also involved in the modulation of eNOS in ECs (Bonauer et al., 2009). Namely, its inhibition leads to an increase in NO production, which is paramount in fostering endothelial regeneration besides inhibiting VSMCs proliferation, thus preventing neointimal hyperplasia (Indolfi et al., 2002). Consistently, the functional inhibition of miR-92a enhances EC proliferation and migration (Iaconetti et al., 2012). *In vivo*, miR-92a expression is increased in ischemic tissues within the first days after infarction (Bonauer et al., 2009; Hinkel et al., 2013) and the respective antagomir-based silencing increases infarct border zone neovascularization and improves heart function after AMI (Bonauer et al., 2009). Loyer *et al.* reported that miR-92a also acts as a proinflammatory regulator in ECs by activating inflammatory cytokines, thus promoting monocyte adhesion (Loyer et al., 2014). Systemic administration of miR-92a inhibitor rescued this effect after AMI and limb ischemia by enhancing blood vessel growth (Bonauer et al., 2009). Similarly, systemic administration of miR-92a inhibitor enhanced re-endothelialisation and reduced neointima formation after balloon injury (Iaconetti et al., 2012).

Besides being involved in neointima formation, miR-92a is also known to promote atherosclerosis under disturbed flow (Iaconetti et al., 2012; Loyer et al., 2014), through the suppression of KLF2 and its key targets eNOS and thrombomodulin (Cowan et al., 2010; Salameh, Galvagni, Bardelli, Bussolino, & Oliviero, 2005). The miR-92a induced increase in IL-6 and MCP-1 secretion, which are proinflammatory EC cytokines, besides promoting monocyte adhesion to ECs via increased ICAM-1 expression are also likely contributors (Loyer et al., 2014). Proatherogenic oxidised LDLs strongly activate miR-92a expression in ECs in atheroprone areas with low shear stress (oscillatory flow)(Loyer et al., 2014). On the contrary, high shear stress (laminar flow) protects ECs cells from miR-92a induction by oxLDL (Loyer et al., 2014). The *in vivo* evidence corroborates that miR-92a is highly expressed in ECs isolated from the atheroprone aortic arch, in contrast to non-susceptible regions (Y. Fang & Davies, 2012). Concordantly, a reduction in circulating endothelial microparticles (a marker of EC dysfunction)(Rautou et al., 2011)

and a reduction of ICAM-1 expression in atherosclerotic lesions is seen following miR-92a inhibitor treatment *in vivo*. Also, eNOS expression is restored by miR-92a inhibition *in vitro* (Loyer et al., 2014). Moreover, by specifically blocking miR-92a in hypercholesteremic $LDLR^{-/-}$ mice, Loyer et al. managed to reduce endothelial inflammation, decrease atherosclerotic plaque burden and promote a more stable lesion phenotype (Loyer et al., 2014).

## miR-92a inhibition for EPC priming

miR-92a seems to be associated with EC senescence. miR-92a expression is upregulated in ECs upon aging (X. Lin et al., 2016), which inhibits cell proliferation by targeting SIRT1 (Iaconetti et al., 2012). Moreover, miR-92a expression is upregulated by ischemia (Bonauer et al., 2009; Hinkel et al., 2013) and in ECs and EPCs of CAD patients (Fichtlscherer et al., 2010; Q. Zhang et al., 2011). A TNF-α-induced inflammatory response also upregulates miR-92a in ECs (Iaconetti et al., 2012). On the other hand, miR-92a is decreased during EC differentiation (Kane et al., 2010; Treguer et al., 2012) and VEGF stimulation (Iaconetti et al., 2012) (which is needed for differentiation), whereas miR-17, miR-18 and miR-19 are upregulated upon induction of differentiation. The differential expression pattern is consistent with the observation that after induction of hindlimb ischemia only miR-92a from the cluster is significantly upregulated (Bonauer et al., 2009). One can, therefore, hypothesise that miR-92a is in a quiescent state in active, healthy cells and is only upregulated upon pathophysiological conditions **(Table 5)**.

**Table 5 | miR-92a local expression levels in specific settings.**
(↑) or (↓), respectively, indicate downregulation or upregulation of miR-92a levels. CAD – coronary artery disease; EC – endothelial cell; EPC – endothelial precursor cell; miR – microRNA; oxLDL – oxidated low density lipoprotein; TNF – tumour necrosis factor; VSMC – vascular smooth muscle cell.

| **↓miR-92a (species)** | **Studies** |
|---|---|
| EC after atorvastatin (human) | (Fichtlscherer et al., 2010) |
| Laminar blood flow (human) | (Wu et al., 2011) |
| VEGF stimulation (rat) | (Iaconetti et al., 2012) |
| **↑miR-92a (species)** | **Studies** |
| EC from CAD patients (human) | (Q. Zhang et al., 2011) |
| EPCs from CAD patients (human) | (Q. Zhang et al., 2011) |
| ECs/VSMCs in vascular injury site (rat, human) | (Daniel et al., 2014), (T. Luo et al., 2014) |
| Ischemic injury (rat, pig, rat) | (Bonauer et al., 2009), (Hinkel et al., 2013), (H. Liu, Li, Zhao, & Hu, 2016) |
| Inflammation (stimulation with TNFα) (rat) | (Iaconetti et al., 2012) |
| Oscillatory blood flow (mice) | (Loyer et al., 2014) |
| Hypercholesterolemia/Atherogenic oxLDL (mice) | (Loyer et al., 2014) |

Up-regulation of anti-angiogenic miR-92a in high CVD risk patients is likely to contribute to the dysfunction of their EPCs and reduced regenerative capacity. Everything considered, inhibition of miR-92a expression could be exploited to increase endothelial regeneration via EPC priming and inhibit neointimal proliferation after vascular injury. To inhibit endogenous miRNAs, chemically engineered oligonucleotides assembled as single-stranded RNA analogues designed to bind and silence complementary miRNAs have been tried (Krutzfeldt et al., 2005).

## miRNA inhibition

The use of miRNAs inhibitors offers exceptional **advantages** over other regulatory mechanisms that also control gene expression, such as transcriptional regulators, epigenetic modifications or viral vectors. Firstly, miRNAs do not integrate into the

genome. Therefore insertional mutagenesis concerns are averted. Secondly, inhibitors, by repressing endogenous miRNAs with the ability to concurrently target many mRNAs of integrated pathways, result in a more efficient upregulation of combined effectors in specific settings. This aspect may also be an advantage, since targeting multiple genes simultaneously with a single inhibitor could modulate complex networks such as restenosis. In fact, *in silico* simulations indicate that miRNA -mediated feed-forward loops are more effective than transcriptional repressors in buffering gene expression under perturbed conditions (Osella, Bosia, Cora, & Caselle, 2011). Given the functional network redundancy, miRNAs are known to exert mild effects at baseline but pronounced biological functions under stress/pathology (N. Liu & Olson, 2010), which is the case in post-angioplasty restenosis. Moreover, by acting post-transcriptionally at the cytoplasm level, miRNAs inhibitors can have an immediate effect on protein synthesis, thereby achieving greater potency than otherwise possible in a short period. The latter seems particularly adequate for a circulating EPC rolling at a denuded vessel. Lastly, miRNA inhibition results in a transient expression of the target effectors for a short period of days only. miR-92a repression during the first steps of EPC adhesion, migration and proliferation is most useful before EPCs already incorporated in the vascular wall can return to a wild-type phenotype. This strategy may be of interest to avoid the possibility of long-term functional cell modification in vessels, as uncontrolled cell proliferation or low differentiation state.

Altogether, these are exciting times for the application of miR-92a inhibitors. However, there are certain **limitations** to therapeutic targeting of miRNAs. This modality carries the inherent risk of affecting RNA species other than the intended miRNA target. Hence, the specificity of these constructs is among the issues that still need addressing (Thum, 2012). There are cell type-specific effects, discrepancies between prediction algorithms and experimental observations, not to mention differences in targets between humans and other species (Anand, 2013). Ideally, inhibitors must be designed to target the seed sequence, since targeting other regions of the mature miRNA may have no or limited effect on miRNA activity (Stenvang, Petri, Lindow, Obad, & Kauppinen, 2012). Interactions are likely to occur through imperfect base pairing, but the recent development of chemical modifications have improved the miR antagonism field by

reducing mismatch discrimination (Beavers, Nelson, & Duvall, 2015). However, the latter have increased complexity versus the simple Watson-Crick base pairing rules making it harder to predict interaction sites for fully complementary miRNA inhibitors accurately. Another potential miRNA inhibitor -mediated off-target effect is determined by miRISC oversaturation (Khan et al., 2009). The exogenous miRNA inhibitor competes for RISCs, thereby rendering it unavailable to other endogenous miRNAs (Stenvang et al., 2012). The resulting loss of available RISC complexes leads to a global abrogation of endogenous miRNA-mediated regulation.

Another issue still pending is safety. More evidence from large animal studies is warranted before therapeutic inhibition of miR-92a can enter human trials for CVD. Even though miR-92a has also been implicated in non-cancerous settings, there are reports that aberrant expression of miR-92a can be a feature in neoplastic transformation and is sometimes associated with enhanced tumour proliferation, survival, invasion and metastasis (M. Li et al., 2014). Plasma miR-92a levels have been used to successfully distinguish between acute leukaemia or colorectal cancer patients and healthy controls (Z. Huang et al., 2010; Tanaka et al., 2009). Remarkably, inhibition of mir-92a in a cell line reproducing acute promyelocytic leukaemia prevented cellular proliferation (Sharifi, Salehi, Gheisari, & Kazemi, 2013). Hepatocellular carcinoma patients present elevated miR-92a levels in the cancerous tissue, albeit they have reduced levels of miRNA in plasma compared to healthy donors (Shigoka et al., 2010). The role of miR-92a in breast cancer has not been fully clarified. Zhang *et al.* showed that the miR-17∼92a cluster was deleted in 21.9% of analysed breast cancer tissue samples (L. Zhang et al., 2006). More recently, Nilsson *et al.* reported that downregulation of miR-92a in breast cancer cells resulted in increased cell migration, possibly through miR-92a affected genes that are involved in the regulation of the actin cytoskeleton and Mitogen-activated protein kinase (MAPK) signalling pathway. Altogether, evidence indicates that miR-92a expression status can differ depending on cancer type and have diverging functional implications. It is likely that miR-92a is involved in some cancer hallmarks, tumor-associated angiogenesis being one. If miR-92a can behave as an oncomir or its modulation influence tumour suppressors, then its modulation should be used with extreme caution, but this is extensible to every miRNA in study.

miRNAs inhibitors can be divided into four **type** classes: antagomiR oligonucleotides, miR sponges (oligos with multiple miR binding sites), miR-masks (oligos with gene specific sequences complementary to miR binding sites to act as competitive inhibitors) and small-molecule miR inhibitors (molecules that can unspecifically inhibit the miRNA pathway). AntagomiRs are the most common class of miRNA inhibitors. They are synthetic oligos that bind to and sterically inhibit the binding of the RISC-loaded miRNA guide strand to target mRNAs. The first antagomiRs were DNA oligos of complementary sequence and equal length to the full target mature miRNAs. Normally, nucleic acids are quickly degraded in biological compartments (Thum, 2012). Unmodified DNA oligos were very unstable (Hutvagner, Simard, Mello, & Zamore, 2004). Therefore, subsequent antagomiR designs have focused on increasing stability and endonuclease resistance, in addition to improving binding affinity to miRNA. The earliest modifications included methylation of nucleoside ribose 2' hydroxyl groups ("OMe"), which improved RNA binding affinity compared to unmodified sequences, but did little towards increasing oligo stability and nuclease resistance (Beavers et al., 2015; Lennox & Behlke, 2011). Cholesterol modified antisense oligos were later developed with a 3' end conjugation to cholesterol which imparts nuclease resistance (Krutzfeldt et al., 2007) and improves cellular uptake and the biostability (Krutzfeldt et al., 2005). Additionally, the hydrophobic cholesterol moiety enables these antagomiRs to better traverse the cell membrane and enter cells without the aid of a delivery vector (Krutzfeldt et al., 2005). However, clinical translation of this strategy has been limited by the relatively high doses to achieve miRNA inhibition (up to 80 mg/kg in a mouse model)(Krutzfeldt et al., 2005), and the concerning off-target effects demonstrated *in vivo* (Krutzfeldt et al., 2005). A recently designed, highly efficient, antagomiR by Exiqon™ relies on highly-modified locked nucleic acids (LNA). LNAs contain a methylene bridge between the 2'-O and 4'C of ribose to "lock" it into an optimal C-3'-endo conformation which results in a thermodynamically very strong duplex hybridization with the complementary miRNA (Beavers et al., 2015). Consequently, LNA-modified chemistries show higher anti-miRNA affinity at lower doses compared with the equivalent antagomiR (Fabani & Gait, 2008). LNA nucleotides can be mixed with RNA residues in the oligonucleotide whenever desired and hybridize with RNA according to Watson-Crick base-pairing rules. Also, full or mixed LNA oligos show a 10-fold increase in serum stability compared with

unmodified oligonucleotides (Rapozzi, Cogoi, & Xodo, 2006). Recently, very short 8-mer fully modified LNA oligomers only directed against the seed region of a miRNA were introduced (Obad et al., 2011). This strategy is useful for targeting multiple miRNA from seed families, but can also result in significant off-target effects given the small oligonucleotide sequence (Thum, 2012).

mirVana® miRNA inhibitor from Ambion™ (used in this study to achieve miR-92a repression) are the latest generation of commercially available chemically -modified antagomiRs at the time. They are single-stranded oligonucleotides with proprietary chemical modifications (3rd generation), that irreversibly bind and inactivate the natural miRNAs when transfected into cells, resulting in artificial up-regulation of target mRNA translation. According to the manufacturer, these inhibitors have the highest-potency inhibition at the lowest miRNA inhibitor concentration *in vitro*, when compared with other two leading competitors (Exiqon or Dharmacon)(Lam, 2012; LifeTecnhologies, 2012). They are allegedly highly specific, stable and previously validated for *in vivo* use, given their purity and non-toxicity (Lam, 2012). Non-specific off-target effects are therefore unlikely. Importantly, the use of miR-92a miRvana mimic and inhibitor has been validated in ECs (H. Liu et al., 2016).

# 1.4 Aims of this thesis

Restenosis remains a cause of failure in a significant number of coronary interventions, requiring innovative solutions. Current strategies to reduce the incidence of restenosis are mainly based on suppressing VSMC proliferation (e.g. drug eluting stents) rather than increasing endothelial healing. In fact, antiproliferative therapies may even interfere with arterial endothelialisation. The contribution of circulating EPCs homing to injured vessels is considered essential to selectively promote re-endothelialisation and therefore prevent neointima formation (Curcio, Torella, & Indolfi, 2011). However, EPC regeneration potential depends greatly on the extent of their engraftment and activity at the target site. Often, EPC numbers and function among CVD patients are intrinsically impaired leading to low engraftment, which could limit re-endothelialisation. Therefore, EPC-priming therapies designed to increase their ability to engraft at the site of vascular injury are attractive and have the potential to improve clinical outcomes after PCI. miRNAs have emerged as gene network regulators, engaging several distinct mRNAs in an orchestrated manner across different interacting cell types. In previous work, miR-92a was shown *in vitro* to reduce angiogenesis, proliferation, migration and adhesion to ECM in ECs (Bonauer et al., 2009). Since the anti-angiogenic miR-92a was also shown to be upregulated in vessels after injury (Ji et al., 2007) and in EPCs from CAD patients (Q. Zhang et al., 2011), we hypothesized that miR-92a antagonism in $CD34^+$-derived EPCs could result in a more favourable angiogenesis profile *in vitro* similarly to ECs, with the rationale of developing a future functional priming strategy before cell transplantation which could lead to increased engrafting/thriving and accelerated re-endothelialisation on injured segments, hence, contributing towards post-PCI restenosis prevention.

The specific aims of my research are as follows:

1. Differentiate and characterise $CD34^+$-derived late-outgrowth EPCs from an enriched human source;

2. Characterise gene expression and demonstrate the functional priming following miR-92a inhibitor treatment on $CD34^+$-derived late-outgrowth EPCs *in vitro*, and relate it to the target ITGA5 expression

# Chapter 2: Materials and Methods

## 2.1 Reagents

- Accustain Solution ADR-1000, NanoEnTek, Pleasanton, USA
- ABC solution, Vecastain Elite ABC Kit, PK 6100, Vector Laboratories, Peterborough, UK
- Alexafluor488 AcLDL, L-23380, Biomedical Technologies, Stoughton, USA
- Anti-biotin microbeads, 130-090-485, Milteny Biotec, Bergisch Gladbach, Germany
- Antibody one step biotinylation kit, 130-093-385, Milteny Biotec, Bergisch Gladbach, Germany
- Avidin/Biotin Blocking Kit, SP-2001, Vector Laboratories, Peterborough, UK
- Bio-Rad Protein Assay Kit, 500-0112, Bio-Rad, Herts, UK
- Blocker Casein, 37528, ThermoFisher Scientific, Surrey, UK
- Bovine serum albumin (BSA), 23209, Thermo Fisher Scientific, Surrey, UK
- Brilliant II SYBR Green qPCR Master Mix, 600828, Agilent, CA, USA
- Bupivacaine 0.5% with epinephrine 1:200,000, Cook-Waite Marcaine 0.5% with epinephrine, 185-2557, Carestream dental, Hertfordshire, UK
- DAB substrate solution, D4168, SigmaFast DAB tablets, Sigma Aldrich, Dorset, UK
- CD133 Microbead kit, 130-097-049, Milteny Biotec, Bergisch Gladbach, Germany
- CD34 Microbead Kit, 130-046-702, Milteny Biotec, Bergisch Gladbach, Germany
- Cell Titer Glo, G7571, Promega, Southampton, UK
- CellTracker CM-DiI, C7001, Invitrogen, Paisley, UK
- Collagen type I rat tail, 08-115, Milipore, Temecula, USA
- Complete Protease Inhibitor Cocktail, 11873580001, Roche, Mannheim, Germany
- DMEM 10x, 12800-017, Gibco Thermo Fisher Scientific, Surrey, UK
- DNAse I, 11284932001, Roche Diagnostics, Mannheim, Germany
- DPX Mountant for histology, slide mounting medium, 06522, Sigma Aldrich, Dorset, UK
- EDTA (Ethylenediaminetetraacetic acid), 17892, Thermo Scientific, Surrey, UK
- E-gel precast agarose gel 1.2%, ThermoFisher Scientific, Surrey, UK
- Endothelial Basal media (EBM), CC-3121, Lonza, Gaithersburg, USA
- Endothelial Growth Media bullet kit (EGM), CC-3124, Lonza, Gaithersburg, MD, USA
- Enhanced Chemiluminescence (ECL) Plus Reagent Detection system, PI80196, Thermo Scientific, Surrey, UK
- Ethanol, 20816.298, VWR BDH Prolabo, Leuven, Germany
- Ethidium bromide, 15585011, Thermo Scientific, Surrey, UK
- FcR blocking reagent, human, 130-059-901, Miltenyi Biotec, Bergisch Gladbach, Germany
- Fentanyl/fluanisone (40µg/100g), Hypnorm, Vm21757/4000, Vetapharma, Leeds, UL

- Fetal bovine serum (FBS), 10437028, Gibco Thermo Fisher Scientific, Surrey, UK
- Fibronectin from human plasma, 0,1% solution, F0895, Sigma Aldrich, Dorset, UK
- Fluoresceinamine, 46930, Sigma Aldrich, Dorset, UK
- Fms-related tyrosine kinase 3 (Flt3) ligand, 300-19-100, PrepoTech Inc, Rocky Hill, USA
- Formalin, HT501128-4L, Sigma Aldrich, Dorset, UK
- Gel, Nu-PAGE Novex 4-12% Bis-Tris gels, NP0321BOX, ThermoFisher Scientific, Surrey, UK
- Gelatin from porcine, G1890, Sigma Aldrich, Dorset, UK
- Haematoxylin solution, 51275, Fluka, USA
- Heparin sodium salt from porcine intestinal mucosa, H3393, Sigma Aldrich, Dorset, UK
- Histopaque-1077 HybriMax, 10771, Sigma-Aldrich, Dorset, UK
- Human serum lyophilized albumin (HSA) powder, A9511, Sigma-Aldrich, Dorset, UK
- Hydrogen peroxide, 216763, Sigma Aldrich, Dorset, UK
- Hyperfilm, 28-9068-40, GE Healthcare, Buckinghamshire, UK
- Isoflurane, Isoflo B506, Abbott, MaidenHead Berkshire, UK
- Krebs solution, K4002, Sigma Aldrich, Dorset, UK
- LDS Sample Buffer (4x), NuPAGE, NP0007, ThermoFisher Scientific, Surrey, the UK
- Matrigel Matrix Growth Factor Reduced, 356230, BD Biosciences, Erembodegem, Belgium
- Midazolam, Versed, Roche, Mannheim, Germany
- Molecular Weight Marker, Spectra Multicolor Broad range protein ladder, 26634, ThermoFisher Scientific, Surrey, UK
- MOPS SDS Running Buffer (20X), NuPAGE, NP0001, ThermoFisher Scientific, Surrey, UK
- Opti-MEM and GlutaMAX-I, 51985-026, ThermoFisher Scientific, Surrey, UK
- Oligofectamine (OF) transfection reagent, 12252-011, ThermoFisher Scientific, Surrey, UK
- Paraformaldehyde (PFA), P6148, Sigma Aldrich, Munich, Germany
- Penicillin 100U/ml + Streptomycin 100µg/ml, 15070-063, Life Technologies, Paisley, UK
- Pentobarbitone sodium 20% (w/v), Pentojet, 05055037400045, Animal Care, York, UK
- Perfluoro-1,5-crown ether (PFCE), 9312, Fluorochem, Derbyshire, UK
- Phosphate buffered saline (PBS), 4417, Sigma Aldrich, Dorset, UK
- Phosphate buffered saline (PBS) with $CaCl_2$ and $MgCl_2$, 14080-048, Gibco ThermoFisher Scientific, Surrey, UK
- Polylactic-co-glycolic acid (PLGA), Resomers 502 H; 50:50 lactic acid: glycolic acid, Boehringer Ingelheim, Ingelheim am Rhein, Germany
- PLGA-PEG Ak12k24 (for the gel), Akina, Inc, IN, USA
- Pluronic F-127, powder, P2443, Sigma Aldrich, Dorset, UK
- Polyvinyl alcohol, 363146, Sigma Aldrich, Dorset, UK
- Prolong Gold anti-fade reagent with DAPI (4',6-diamidino-2-phenylindole); P36931, ThermoFisher Scientific, Surrey, UK
- Pronase, 10165921001, Roche Diagnostics, Mannheim, Germany

- Propylene carbonate, 310328, Sigma Aldrich, Dorset, UK
- Protamine sulphate, P3369, Sigma Aldrich, Dorset, UK
- QuantiTect Reverse Transcription Kit, +205311, Qiagen, Dusseldorf, Germany
- Quantum Simply Cellular anti-Mouse IgG Kit, 815A, Bangs Laboratories, Indiana, USA
- Radio-Immunoprecipitation Assay (RIPA), R0278, Sigma Aldrich, Dorset, UK
- Reastain Quick Diff Kit, 102164, Gentaur, Kampenhout, Belgium
- ReBlot Plus Strong antibody stripping solution, 2504, Millipore, CA, USA
- RPMI 1640 medium, 11875-093, ThermoFisher Scientific, Surrey, UK
- Sample reducing buffer (10x), NuPAGE, NP009, ThermoFisher Scientific, Surrey, UK
- Serum donkey, D9663, Sigma Aldrich, Dorset, UK
- Serum goat, X0907, Dako, Glostrup, Denmark
- Serum human, AB, 14-490E, Lonza, Gaithersburg, USA
- Serum porcine, 26250084, Thermo Scientific, Paisley, UK
- Skin moisturiser, Opsite 66004978, Smith&Nephew, UK
- Sodium citrate tribasic dehydrate, 54641, Sigma Aldrich, Dorset, UK
- Stem cell factor (SCF), 300-07-100, PrepoTech Inc, Rocky Hill, USA
- Transfer buffer (1x), NuPAGE, NP00061, ThermoFisher Scientific, Surrey, UK
- Trifluoroethanol, T63002, Sigma Aldrich, Dorset, the UK
- Triton X-100, X100-1L, Sigma Aldrich, Dorset, UK
- Trypan Blue, 17-942E, Lonza, Gaithersburg, MD, USA
- Trypsin, 15090-046, Invitrogen, Paisley, UK
- Tween 20, 23360010, Acros Organics, NJ, USA
- Vascular endothelial growth factor (VEGF165), 100-20, PrepoTech Inc, Rocky Hill, USA
- X-VIVO 15, serum free hematopoietic cell medium, 04-744Q, Lonza, Gaithersburg, MD, USA
- Xylene, 28975.360, VWR BDH Prolabo, Leuven, Germany

# 2.2 Equipment

- Accuchip2x Kit AD2K-200, NanoEnTek, Pleasanton, USA
- Adam-MC, Cell Counter, NanoEnTek, Pleasanton, USA
- Angiogenesis 96 Well ibiTreat µ-Plate, 89646, Ibidi, Munich, Germany
- Axio Observer, Carl Zeiss International, Germany
- Axiovert A1, fluorescence microscope, Carl Zeiss International, Germany
- Axiovert 40 C, inverted optical microscope, Carl Zeiss International, Germany
- BD FACScalibur, Flow cytometer, Becton Dickinson, CA, USA
- BD FACS Verse, Flow cytometer, Becton Dickinson, CA, USA
- BD 115 Model, incubator, Binder Gmbh, Tuttlingen, Germany
- Branson 2510, Ultrasonic Cleaner, Brandson, Danbury, CT, USA
- Catheter 2Fogarty embolectomy, #120602F, Edwards Lifesciences, Nyon, Switzerland
- Cell Strainer 100 µm mesh, 352360, Falcon, Corning, Corning, USA)
- CellTrics 30, separation filters, 04-0042-2316, Sysmex Partec, Görlitz, Germany
- Ceramic beads pre-filled 0.5 mL tubes, Precellys soft tissue homogenising kits, CK14-KT03961-1-203.05, Bertin Technologies, France
- Coverslips, CB00140RA1, 14 mm Menzel-Glaser, Braunschweig, Germany
- Deskscan, scanner, Hewlett-Packard, London, UK
- Dialysis membrane (50 kDa), 132 544, Spectrum Labs, Rancho Dominguez, CA, USA
- Dialysis membrane (12-14 kDa), 132 706, Spectrum Labs, Rancho Dominguez, CA, USA
- E-Gel® iBase™ Power System, Thermo Scientific, Surrey, UK
- GENios, Fluorescence, Absorbance and Luminescence Reader, TECAN, Mannendorf, Switzerland
- Heating mat, 75404, Magnetic heat pad, morphy Richards, the UK
- ImageLock 96-well Plates, 4379, Essen Bioscience, Herts, UK
- IncuCyte Cell Migration Kit, 4493, Essen Bioscience, Herts, UK
- Incucyte Zoom live-cell analysis system, microscope, Essen Bioscience, Herts, UK
- Jamshidi T-handle, 13 G x 3", TJC3513, Carefusion, Vernon Hils, USA
- Lab-Tek II, chamber slides, 154534; Nalge Nunc International, IL, USA
- Leica M80, stereomicroscope, Leica Microsystems, Milton Keynes, United Kingdom
- Leica Macrofluo, macroscope, Leica Microsystems, Milton Keynes, the UK
- Minilys, tissue homogenizer, Bertin Technologies, France
- Mini&MidiMACS, Immunomagnetic sorting system, 130-042-501, Miltenyi Biotec, Bergisch Gladbach, Germany
- Mx3000P qPCR System, Stratagene, CA, USA
- Nanodrop 3300 spectrophotometer, Thermo Scientific, Surrey, UK
- NDP Nanozoomer Digital Pathology, Slide scanner microscope, Hamamatsu, Tokyo, Japan

- Pap pen for IHC, delimiting pen, S2002, Dako, Glostrup, Denmark
- PVDF/Filter Paper Sandwich, 0.45 µm pore size, Invitrolon, LC2005, ThermoFisher Scientific, Surrey, UK
- QIAshredder, Tissue and Cell Homogenizer, 79654, Qiagen, Dusseldorf, Germany
- RNeasy Mini kit, RNA isolation kit, 74104, Qiagen, Dusseldorf, Germany
- Slide, microscope slide, 6310098, Menzel-Glaser, Braunschweig, Germany
- Snijders Scientific, Lyophilisator, Tiburg, Holland
- Surgical micro-clips, S&T B-2 Vascular Clamp, 00398-02, Finescience tools, Heidelberg, Germany
- Surgical micro-scissors, Vannas Spring Scissors, 15000-00, Finescience tools, Heidelberg, Germany
- Surgical vessel dilating forceps, S&T D-5a, 00125-11, Finescience tools, Heidelberg, Germany
- Suture 3-0 mersilk, W587, Johnson & Johnson Intl, St. Stevens-Woluwe, Belgium
- Suture 3-0 sofsilk, S-304, Covidien Syneture, Dublin, Ireland
- Suture 4-0 vycril, W9570, Johnson & Johnson Intl, St. Stevens-Woluwe, Belgium
- Thermo Denley Spiramax 5, roller, ST124080, Thermo Scientific, Paisley, UK
- Thermomix comfort; Eppendorf mixer, Hamburg, Germany
- Transwell 8 µm membrane pore size, 353097, Falcon, Becton Dickinson
- VibraCell, Sonicator, Sonics, CT, USA
- Zeiss LSM 510 Meta, confocal microscope, Carl Zeiss International, Germany
- Zeta Pals light scattering analysis, Brookhaven Instruments Corporation, NY, USA

Unless otherwise stated, tissue culture plasticware was from BD Biosciences

## 2.3 Software

- Axiovision 4.5, Carl Zeiss International, Germany
- Cell Quest Pro, Becton Dickinson, California, USA
- FlowJo, Ashland, USA
- Image J, National Institute of Health, rsb.info.nih.gov/ij
- Incucyte Zoom software, Essen Bioscience, Herts, UK
- Simple PCI, HCImage, PA, USA
- QuickCal, Bangs Laboratories, Indiana, USA
- Zeta Plus Particle Sizing v. 2.27, Brookhaven Instruments Corporation, NY, USA

## 2.4 Animals

Animal experiments were conducted by the Animal Care and Ethics Guidelines of UCL, Royal Veterinary College, University of London, and the United Kingdom Home Office Animals (Scientific Procedures) Act (1986).

*Pigs:* Bone marrow (BM) samples were obtained from a total of 35 healthy 2-3-month-old Yorkshire pigs (25 to 35 kg) immediately after they were euthanised by penetrating captive bolt shot to the brainstem. The pigs were being used for a dermal toxicology study at the University of Hertfordshire but were not subject to any prior treatment/surgery. Pigs were kept at 20º-25ºC all the time with daylight and free access to tap water and regular daily food.

*Mice:* Mouse aortic rings were obtained from C57BL/6 mice housed at UCL Biological Service Unit services, which were culled by schedule 1 procedure. Mice were kept at 20ºC to 25ºC all the time with free access to tap water and regular daily food.

*Rats:* Male Sprague-Dawley rats (Charles River UK) 350-400g (2-3 months old) were used for the carotid artery balloon angioplasty experiments. Specimen retrieval was done following perfusion under terminal anaesthesia using pentobarbitone via intraperitoneal injection (50 mg/kg), according to the UCL Biological Services Unit protocol. Rapid euthanasia was accomplished by exsanguination (liver tear), while simultaneously perfusing the arterial tree via an intra-cardiac 200 mL continuous injection of 0.9 % saline solution at a physiological pressure.

## 2.5 Umbilical coord blood collection

Fresh, non-cryopreserved, red blood cell (RBC)-replete umbilical cord blood (UCB) units were provided by Anthony Nolan's Research Institute for Laboratory Research after normal delivery from full-term births (≥36 weeks gestational age) using standard collection procedures. The collection was approved by the Anthony Nolan Cell Therapy Center's generic research tissue bank ethics approval extendable to external applicants for material. Written informed consent from subject mothers was obtained before donation. The samples were stored in 100 mL sterile bags containing 35 mL of citrate-

phosphate-dextrose anticoagulant solution and processed within 24h after collection from parturient. All units were transported and stored at room temperature (RT).

## 2.6 Bone marrow blood collection

Pigs were placed ventrally, and 50 mL of BM were aspirated from the iliac crest using a Jamshidi T-handle biopsy needle and syringe **(Figure 18)**, and then transferred to a 50 mL tube, previously heparinized (final concentration 25 international units/ml) and supplemented with 1% (v/v) Penicillin/Streptomycin. The samples were then filtered through a Falcon 100 µm cell strainer and kept overnight on a roller at RT for next day processing.

**Figure 18 | Pig bone marrow blood aspiration performed in the iliac crest (white arrows) with specific biopsy apparatus.**

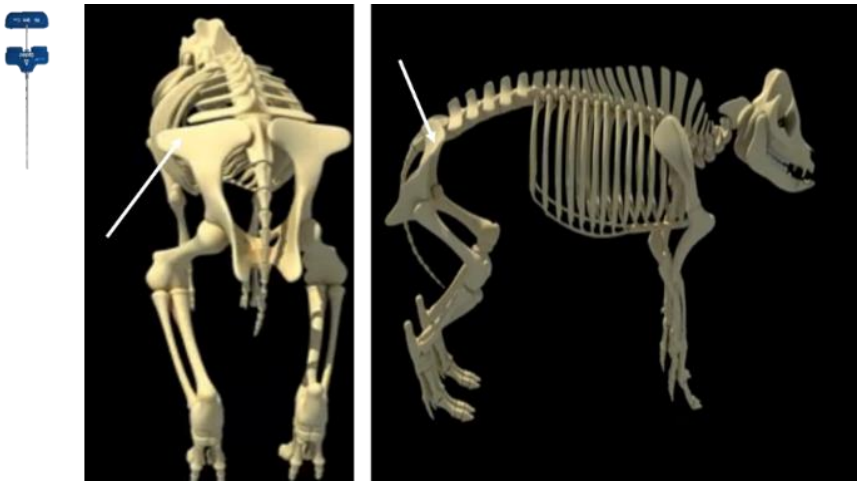

## 2.7 Immunomagnetic sorting of progenitor cells

Enrichment of progenitor cells in suspension is usually performed by fluorescent activated (FACS) (Bonner, Hulett, Sweet, & Herzenberg, 1972) or immunomagnetic (MACS) (Miltenyi, Muller, Weichel, & Radbruch, 1990) selection systems. Both techniques take advantage of the expression of known surface antigens for cellular separation, using specific antibody binding. FACS separation depends on the conjugation of fluorescent tags to these antibodies, while MACS uses conjugation to superparamagnetic iron-dextran containing microbeads. Unlike FACS which requires single-cell analysis (excitation above a threshold level signals the corresponding tagged

cell to be separated), MACS is more of a bulk method, where unlabelled cells are eluted, and labelled cells are retained in the magnetic field, giving the separated populations. An obvious consequence is that while FACS can be more accurate (especially if using multiple antibodies), it is significantly slower than MACS (Tomlinson, Tomlinson, Yang, & Kirkham, 2013), thus negatively impacting on viability (Q. Li et al., 2013). CliniMACS (the automated isolation system from the same company) enjoys FDA approval for clinical applications and is currently the only Good Manufacturing Practices compliant cell separation system available for immunomagnetic separation of progenitor cells from blood products (Blake et al., 2012).

For these reasons, I opted for the MACS system from Miltenyi Biotec to isolate progenitor cells from mononuclear cells (MNCs) for its ease of use and reliability (Kekarainen, Mannelin, Laine, & Jaatinen, 2006). The mini- and midi-MACS column matrix provides a strong magnetic field, allowing the positive selection of cells carrying specific antigens on their surface, previously incubated with corresponding superparamagnetic microbead-conjugated antibodies. Unlabeled cells pass through the column, while the retained labelled cells can then be eluted from the column after removal from the magnet.

### 2.7.1 Isolating human $CD34^+$ or $CD133^+$ cells from UCB

Labelled human CD34 and CD133 progenitor cells were isolated from MNCs using MACS immunomagnetic separation system (Mini&MidiMACS) **(Figure 19)**, overall as described elsewhere (Jaatinen & Laine, 2007), but with significant optimisation steps introduced resulting in higher purity and viability of selected population. Briefly, buffy coats were obtained after centrifugation of ~100 mL UCB samples for 45 min at 500g at 20ºC (brake 0) and diluted 1:3 in RPMI medium. Buffy coat is the white coloured leukocyte layer that resides directly above the RBC/granulocyte layer after crude centrifugation of whole blood. MNCs were then obtained after buffy coat density gradient separation using Histopaque reagent (40% reagent:60% sample per Falcon). Upon centrifugation, the relatively lower density MNCs migrate into a layer that floats on top of the histopaque reagent layer, while higher density RBCs contaminants rest below. MNCs were resuspended in 300 µl of DNAse (filtered; 1mg/mL in PBS) to prevent unwanted cell

clumping (Hering et al., 1989), pooled together and then 10 mL of manufacturer's labelling buffer at 4ºC was added, so that the total yield of MNCs could be estimated using a 50-fold dilution in PBS. The sample was then centrifuged for 10 min, 20ºC, 300 G, accelerator 9/ brake 9 and the cells re-suspended again in 200 µl of DNAse 1mg/mL and 1 mL of pre-cooled MACS buffer (BSA 0,5% w/v in PBS with EDTA 2 mM). This was followed by a 30-minute incubation at 4ºC of MNCs with paramagnetic microbeads conjugated to mouse monoclonal anti-human CD34 or CD133 antibodies (100 µl FcR blocking reagent and 100 µl microbeads per $10^8$ cells), in manufacturer's labelling buffer enriched with 20% (v/v) human serum (300 µl per $10^8$ cells). Cells were washed once and resuspended in 500 µl DNAse 1mg/mL and MACS buffer (500 µl per $10^8$ cells). After application through pre-primed 30µm CellTrics separation filters, labelled cells were enriched on a LS column placed in a magnetic field. Eluted cells were labelled a second turn with 25 µl FcR blocking reagent plus 25 µl micro beads in 300 µl of MACS buffer for 15 minutes at 4ºC. After one wash, cells were resuspended in 2 mL of MACS buffer and placed in a MS column in the magnetic field for the final elution. After centrifugation at 1000 rpm for 8 min at RT, cells are then resuspended in the appropriate medium according to laboratory assay to be conducted, counted and plated at the desired cell density.

**Figure 19 | MACS direct labelling system.**
Column-based separation implies the injection of magnetically labelled cell suspension into a column held within a magnet. Cells then flow through the column and those who are labelled will be retained, whereas unlabeled cells are washed out. Finally, the column is removed from the magnet stand, and the suspension buffer is forced through the column by plunger giving labelled target cells in suspension. Adapted from MACS manual.

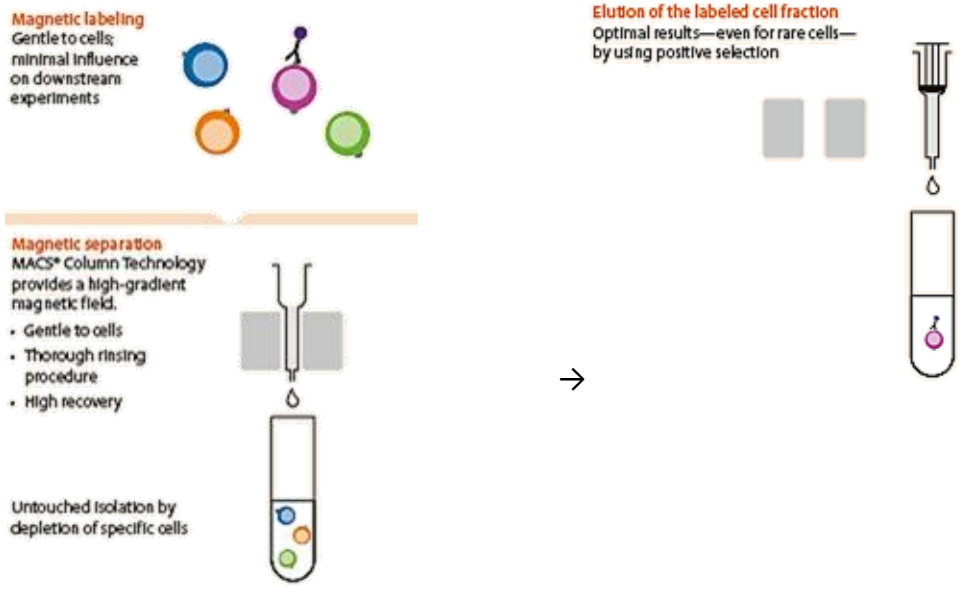

## 2.7.2 Isolating porcine CD34$^+$ cells from pig BMB

CD34$^+$ progenitor cells were isolated from pig BM blood MNCs using MACS immunomagnetic separation system, overall according to the human UCB isolation protocol, but with relevant, original, modifications since no anti-pig CD34 microbeads were available. An indirect labelling method was performed instead, where cells were labelled with a primary antibody that was biotinylated **(Figure 20)**. In a second step, magnetic labelling was carried out by using anti-biotin microbeads. Briefly, following buffy coat separation, MNCs were labelled with 50 µl of the biotinylated goat anti-pig CD34 antibody (Anti-CD34 Antibody (Extracellular Domain) LS-C35556, LSBio, Seattle, USA) for 5 minutes at RT, for a final concentration of 1:20. The anti-porcine antibody needed to be biotinylated the day before as per Miltenyi Biotec's instructions. Cells were then washed in 10 mL MACS buffer twice (centrifugation for 10 min, 20º C, 300 g, accelerator 9/ brake 9), and re-suspended in 80 µl MACS buffer enriched with 20% (v/v) porcine serum per $10^8$ mononuclear cells. The MNC fraction mixture was after that incubated with Miltenyi Biotec's anti-biotin microbeads for 15 minutes at 4ºC, following a 20 µl per $10^7$ cells ratio. Again, cells were washed with 10 mL MACS buffer and centrifuged for 10 min, 20º C, 300 g, accelerator 9/ brake 9. After pellet resuspension in buffer (500 µl per $10^8$ cells), labelled cells were primed with a CellTrics 30 µm meshwork and enriched once on a LS column placed in a magnetic field. The sample was eluted twice using 5 mL MACS buffer, and, after a final centrifugation at 1000 rpm for 8 min at RT, cells were resuspended in medium and plated at the desired cell density.

**Figure 20 | MACS indirect labelling schematics.**
Adapted from MACS manufacturer manual.

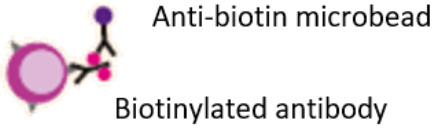

## 2.8 Automatic cell counting and viability determination

Quantification of total cell number and mean cell viability was achieved by using Accuchip slides and an Adam-MC haemocytometer-based automated cell counter, according to manufacturer's protocol. Briefly, this technology identifies propidium iodide stained cells, by using integrated microfluidic chip technology, LED-based fluorescence microscopy and charged coupled device detection.

## 2.9 Flow cytometry

Flow cytometry captures information about the properties of individual cells, including size, intracellular organelle density (forward scatter – side scatter FSC-SSC dot plot) and the presence of specific fluorescently labelled antibodies bound to or inside cells. Fluorescent activated cell sorting (FACS) can be used to sort cells into populations defined by these parameters. A beam of light of a single wavelength generated by a laser is directed onto a hydrodynamically focused stream of fluid containing cells conjugated with specific fluorophores, allowing the determination of the proportion of cells containing that specific antigen, and the degree of expression (intensity). The antibodies used for FACS, and corresponding dilutions, are described in **Table 6**. The excitation and emission maxima of the fluorophores used are given in **Table 7**.

**Table 6 | Antibodies used for flow cytometry.**
BMB - bone marrow blood; CD – cluster of differentiation; FITC - Fluorescein isothiocyanate; Ig – immunoglobulin; PE – Phycoerythrin; UCB – umbilical cord blood; VEGFR2 – vascular endothelial growth factor receptor 2.

| Target antigen | Cell type | Primary and secondary antibodies |
|---|---|---|
| **CD34** | human UCB progenitor cells and human late-outgrowth EPCs | 1° = mouse monoclonal anti-human CD34-PE conjugated (1:11, 130-081-002, Milteny Biotec, Bergisch Gladbach, Germany)<br>Isotype control = mouse monoclonal IgG2a-PE conjugated (1:11, 130-091-835, Miltenyi Biotec, Bergisch Gladbach, Germany) |
| **CD34** | pig BMB $CD34^+$ cells | 1° = goat anti-pig CD34 (1:11, LS-C35556, LSBio, Seattle, USA)<br>2° = donkey anti-goat IgG-FITC (1:100, A11055, Life technologies, Paisley, UK)<br>Isotype control = normal goat IgG (sc-2028, Santa Cruz Biotechnology, Heidelberg, Germany) |
| **CD133** | human UCB progenitor cells and human late-outgrowth EPCs | 1° = mouse monoclonal anti-human CD133/1(AC133)-PE (1:11,130-080-801, Milteny Biotec,Bergisch Gladbach, Germany)<br>Isotype control = mouse monoclonal IgG1-PE (1:11, 130-098-106, Miltenyi Biotec, Bergisch Gladbach, Germany) |
| **VEGFR2/KDR** | human UCB progenitor cells and human late-outgrowth EPCs | 1° = mouse monoclonal anti-human VEGFR2-PE conjugated (1:11, 130-093-598, Milteny Biotec, Bergisch Gladbach, Germany)<br>Isotype control = mouse monoclonal IgG1-PE (1:11, 130-098-106, Miltenyi Biotec, Bergisch Gladbach, Germany) |
| **VEGFR2/KDR** | pig BMB late-outgrowth EPCs | 1° = rabbit anti-pig VEGFR2-FITC conjugated (aa8-290) (1:11, LS-C420389, LSBio, Seattle, USA)<br>Isotype control = normal rabbit IgG-FITC conjugated (1:11, sc-3870, Santa Cruz Biotechnology, Heidelberg, Germany) |

**Table 7 | Fluorophores used in flow cytometry**
Approximate fluorescence excitation and emission maxima are indicated (solvent-dependent) from corresponding manufacturers' online resources. FITC - Fluorescein isothiocyanate; miRNA – microRNA; NP – nanoparticle; PE – Phycoerythrin.

| Probe | Fluorophore | Excitation (nm) | Emission (nm) |
|---|---|---|---|
| Conjugated miRNA | FITC | 494 | 521 |
| Conjugated antibody | FITC | 495 | 519 |
| Conjugated NP | Fluoresceinamine | 495 | 519 |
| Conjugated antibody | PE | 565 | 573 |

## 2.9.1 Determination of the proportion of cells containing a specific fluorophore

FACS was used with different cell types and in different experimental settings:

1) To determine the purity of the populations enriched by immunomagnetic sorting for CD34 or CD133, cells freshly isolated from blood samples were left to recover 48h in a 5% carbon dioxide ($CO_2$) incubator at 37ºC (200,000 cells/96 well plate) in 200 uL of X-VIVO serum-free medium supplemented with Flt3-ligand and SCF at 50 ng/mL, to allow the magnetic microbeads used for cell isolation to disintegrate from the cell surface, before carrying out the protocol. This was particularly important because the antibodies used for flow cytometry were chosen precisely to tag the same epitopes than the microbeads antibodies, to increase specificity.

2) To quantify the presence of specific fluorescently-labelled surface antigens, adherent cells in culture were harvested by trypsinization (trypsin 0.1% v/v in PBS) and pelleted with one centrifugation step, before carrying out the protocol.

3) For confirmation of cellular internalisation of nanoparticles(NP):miRNA complexes using FACS analysis, late-outgrowth EPCs were transfected for 4h with fluoresceinamine-labelled NPs (500 µg/mL) or NPs conjugated with 5'-fluorescein labelled miR-92a (250µg/ml and 100nM respectively). The miRNA used was 5' fluorescein-labelled hsa-miR-92a-1 miRCURY LNA inhibitor, 410456-04, Exiqon,

Vedbaek, Denmark. After treatment with particles or complexes, cells were washed twice with PBS 1% (w/v) BSA, incubated in a solution of 600 µg/mL Trypan blue for 2 minutes, at RT, and washed twice with PBS before being trypsinized (trypsin 0.1% v/v in PBS) and carrying out the protocol. Trypan blue is used to quench externally attached particles/miRNA to differentiate between the signal from membrane-associated (external) and internalised fluorochromes (internal)(McNeer et al., 2011). The omission of NPs treatment (with or without quenching with trypan blue), and NP-fluoresceinamine treatment without quenching, were used as controls in the confirmation of NP-fluoresceinamine internalisation experiments. Omission of NPs treatment (with or without quenching with trypan blue), miRNA- fluorescein labelled treatment (with or without quenching with trypan blue), NPs non-fluoresceinamine labelled treatment (with or without quenching with trypan blue), and NP:miRNAs-fluorescein labelled treatment without quenching, were used as controls in the confirmation of NP:miRNAs-fluorescein internalization experiments.

4) For confirmation of cellular internalisation of miRNA using FACS analysis, $CD34^{+}$-derived late-outgrowth EPCs were transfected with hsa-miR-92a-1 inhibitor-FITC (410456-04, Exiqon, Vedbaek, Denmark) at 30nM for 4h using OF, and cells allowed to rest 24h in the transfection mixture supplemented with 10% FBS before carrying out the protocol. Treatment with OF only was used as control.

Cells from experimental layouts (1-2) were then transferred into a 1.5 mL Eppendorf tube, and centrifuged for 10 minutes at 300g at RT. Cells were then resuspended in 80 µL of PBS 1% (w/v) BSA with 20 µL of human FcR blocking reagent (or 100 µl PBS/BSA 1% for non-human samples), after which 10 µL of primary antibody were added, according to the manufacturer's recommendations. In the case of CD34 and CD133, the chosen antibodies bound an epitope different from that recognised by the CD34 and CD133 monoclonal antibodies used for sorting. The corresponding IgGs were used at the same concentration as isotype controls. Samples were kept 10 minutes at 4ºC, before adding 1 mL PBS 1% (w/v) BSA and centrifuging for 10 minutes at 300 g. If the primary antibody was not conjugated to a fluorophore, then a further incubation step with a

fluorescently-labeled secondary antibody was needed, for 10 minutes at RT, covered from light before carrying out the protocol.

Then, cells from experimental layouts (1-4), were washed with PBS 1% (w/v) BSA and fixed in PFA 2% (v/v) in PBS for 10 min at RT, again protected from light. The PFA was then washed off, and the cells resuspended in 400 µL PBS 1% (w/v) BSA, and the cells transferred to FACS tubes before running them on FACS cytometer.

For time course experiments with a total duration of several days, a small adaptation of the protocol was assumed. Cells were harvested at designated time points, fixed with PFA 2%, stored in PBS 1% (w/v) BSA at 4ºC and only batch stained on the day of running the samples instead.

A total of 10,000 gated events were recorded per measurement, and each condition was measured in duplicate in the corresponding fluorescent channel. Data acquisition and analysis were performed using specific software (Cell Quest Pro software for human cells or FlowJo for porcine cells).

### 2.9.2 Antigen surface density quantification

$CD34^+$ progenitor cell and late outgrowth EPC characterization also included determining the fluctuation of stem and endothelial lineage surface markers throughout the cellular differentiation process. Antigen quantitative analysis was performed as described before (Scolnik, Morilla, de Bracco, Catovsky, & Matutes, 2002). Briefly, the measurement of CD34, CD133 or KDR antigen surface densities was performed using Quantum Simply Cellular anti-Mouse IgG Kit. This kit contains a mixture of four types of polystyrene beads coated with anti-mouse IgG, with known antibody binding capacities, and one blank population with no specific binding capacity for mouse IgG. The beads bind to the fluorochrome-conjugated monoclonal antibodies and act as a set of standards to calibrate the fluorescence scale of the flow cytometer. The beads and the human cells were incubated individually with mouse monoclonal anti-human CD34-PE, CD133-PE or KDR-PE antibody at the same concentration as experimental conditions, according to manufacturer's protocol. Pig cells were stained with rabbit anti-porcine CD34 (FITC conjugated secondary) or KDR-FITC primary antibodies. Cells were then fixed with PFA 2% (w/v) in PBS, washed and run in the flow cytometer, using identical intensity

parameter settings for the samples and the quantitative beads. For time course experiments with a total duration of several days, a small adaptation of the protocol was assumed. Cells were harvested at designated time points, fixed with PFA 2% (w/v) in PBS, stored in PBS 1% (w/v) BSA at 4ºC and only batch stained on the day of running the samples instead. A total of 1,000 or 10,000 gated events were recorded per measurement for beads or cells populations, respectively. Host specific isotype immunoglobulins conjugated with PE served as negative control, allowing for auto-fluorescence compensation. The geometric mean fluorescence intensities of the beads and cells were entered into the QuickCal software included in the kit, which extrapolates, after subtraction of isotype negative control auto-fluorescence, the antibody binding capacities of the cells from the standard curve. If monovalent antibody-to-surface receptor binding is presumed, then the antibody binding capacity is equal to the number of surface receptors. Each condition was measured in duplicate in the corresponding fluorescent channel.

## 2.10 Differentiation of $CD34^+$ cells into late-outgrowth EPCs

Freshly isolated $CD34^+$ cells were differentiated into EPCs using a published in-house protocol (Pedroso et al., 2011). Briefly, cells were plated onto 1% (w/v) gelatin coated 24-well plates ($2x10^5$ cells/well). Gelatin was prepared at the desired concentration in milQ and allowed full dissolution at autoclaving temperature for at least 1 hour. Then cells were incubated in Endothelial Growth medium (EGM) with 20% (v/v) FBS and 50 ng/mL VEGF, at 5% $CO_2$, 37ºC. After 5 days and then every other day, half of the volume of the medium was replaced with fresh one, until the 3$^{rd}$ passage of a nascent adherent cell population was reached, at which point, EGM 10% (v/v) FBS medium was used for nurturing instead. Bright-field images during differentiation were captured using an inverted Axiovert 40 C optical microscope.

## 2.11 EPC culture

Human late-outgrowth EPCs were cultured in the same fashion than HUVECs usually are, i.e., they needed to be seeded in 1% (w/v) gelatin coated vessels and incubated in EGM 10% (v/v) FBS medium at 37ºC and 5% $CO_2$ (see gelatin preparation method in section 2.10). Expanding EPCs were split into new vessels by trypsinization (trypsin 0.1% v/v in PBS) when 80% confluency was reached, until passage 6, at which time they were discarded. Unless stated otherwise, experiments were performed on cells at approximately 80% confluency.

## 2.12 Matrigel angiogenesis assay

A tube formation assay using Matrigel is well established to demonstrate the angiogenic activity of vascular endothelial cells *in vitro* (Shao et al., 2004). This is a short-term culture assay in a gelatinous protein mixture obtained from Engelbreth-Holm-Swarm mouse sarcoma, which stimulates vascular phenotype cells to form capillary-like hexagonal structures within just a few hours **(Figure 21)**. The assay was performed using matrigel overall according to manufacturer's instructions, on 96 µ-Plates specifically designed for the angiogenesis assay. The latter uses the validated "well-in-a-well" feature to avoid meniscus formation in individual wells and allowing more efficient imaging as all cells are in one focal plane while requiring 90 % less Matrigel than compared to standard 96-well plate.

**Figure 21 | Matrigel angiogenesis assay performed in the µ-slide plate.**
Adapted from IBIDI online resources.

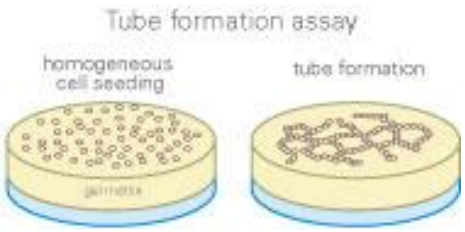

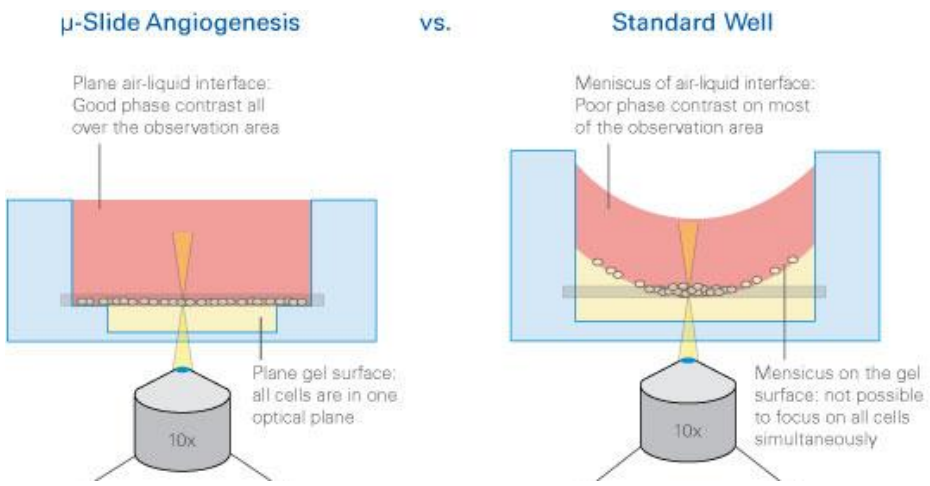


Briefly, the growth factor reduced Matrigel solution was thawed at 4ºC overnight and 10 µL dispensed into each well of a pre-cooled 96 µ-Plate Angiogenesis well plate. The plate was then placed in humidified chamber at 37°C for 1 h to allow for jellification. Cells were dissociated with 0.1% (v/v) trypsin solution, re-suspended at $1x10^5$ cells/mL in serum-free medium EBM, and 50 µL dispensed on top of the matrigel and left undisturbed in the incubator. For the purpose of EPC characterization, samples were left for 6 hours in an Incucyte Zoom incubator microscope, that allows time-lapse live cell and tubule-like formation imaging always at the same gridlock position. Five replicates were used for each experimental condition.

## 2.13 VEGF activation of p-ERK and p-Akt signalling

Pig $CD34^+$-derived EPCs (~80% confluency) from day 21 of differentiation were starved in SFM for 2 hours at 37ºC, before being challenged for 10 mins with either 25 ng/mL VEGF, PDGF or SFM. The reactions were terminated by adding 2 ml of ice-cold PBS.

## 2.14 miRNA and siRNA transfection

miRNAs and siRNAs can silence gene expression via interaction with RISC complex. miRNAs are short, noncoding RNAs, that are assembled into miRNA-induced silencing complexes that localise to miRNA seed sites (usually in the 3'- untranslated region) of specific mRNAs with perfect and imperfect strand complementarity, resulting (mostly)

in post-translational cleavage or repression (Filipowicz et al., 2008). siRNA-induced silencing of gene expression after complementary mRNA base pairing is a result of the action of the RNaseH enzyme argonaute /slicer, which initiates nucleolytic degradation of the target cellular mRNA (Hammond, 2005). miRNAs and siRNAs are negatively charged and are, thus, not readily taken up by most cells. Liposome-like reagents such as Oligofectamine (OF) or cationic NPs can be used to introduce miRNAs/siRNAs into the cell, given their solubility in the cell membrane. **Table 8** lists the used oligonucleotides in the transfections.

**Table 8 | miRNAs and siRNAs used.**
EPC – endothelial precursor cell; hsa – *homo sapiens*; miR- microRNA; si – siRNA.

| Oligonucleotide | Specificities | Concentration |
|---|---|---|
| hsa-miR-92a-1-5p | mirVana mimic, MC12696, 4464066 Thermofisher Scientific, Paisley, UK | EPCs (30 nM), Arteries (1 µM) |
| hsa-miR-92a-1-3p | mirVana mimic, MC10916, 4464066 Thermofisher Scientific, Paisley, UK | EPCs (30 nM) |
| hsa-miR-92a-1-5p | mirVana inhibitor, MC12696, 4464084, Thermofisher Scientific, Paisley, UK | EPCs (30 nM), Arteries (1 µM) |
| hsa-miR-92a-1-3p | mirVana inhibitor, MC109166, 4464084, Thermofisher Scientific, Paisley, UK | EPCs (30 nM) |
| miR scrambled | mirVana inhibitor, negative control 1, 4464076, Thermofisher Scientific, Paisley, UK | EPCs (30 nM), Arteries (1 µM) |
| si ITGA5 | ON-TARGET Plus human ITGA5 SMARTpool, 3678, | EPCs (30 nM) |
| si scrambled | ON-TARGET Plus non-targeting siRNA #1, D-001810-01-05, Dharmacon, UK | EPCs (30 nM) |

## 2.14.1 Oligofectamine EPC transfection

OF reagent is a proprietary formulation for transfecting oligonucleotides into eukaryotic cells, used in this case for EPC and HUVECs transfection. For each transfection sample (1 well of a 6-well plate with 80% confluent adherent cells), complexes were prepared as follows. First, a dilution of oligonucleotide in warm basal media Opti-MEM I was prepared by mixing 1,5 µL oligonucleotide (20 µM stock) with 176 µl of basal media and

allowed to rest for 10 minutes at RT. Simultaneously, a second dilution of transfection reagent in basal media was set by mixing 10 µL OF with 10 µl of Opti-MEM I and incubated for 10 minutes at RT. The diluted oligonucleotide with the diluted OF was combined for a total volume of 200 µL and incubated for 25 minutes at RT with occasional mixing. While the complexes were forming, cells were washed once and then 800 µL of Opti-MEM I per well were added. The complexed oligonucleotides solution (200 µL) was gently added to the cells (for a total volume of 1 mL and 30nM oligonucleotide transfection concentration), and incubated for 4h at 37ºC. After this period, 500 µL of Opti-MEM I 30% (v/v) FBS were added to the well (for a final concentration of 10% serum), and cells allowed to rest overnight with transfection mixture for 24h at 37ºC. The following day, cells were washed once with EBM before 2mL of complete medium EGM 10% (v/v) FBS were added. Cells were incubated for a further 24h if doing a 48h knockdown. For 96 well plate format, the transfection was scaled down proportionally, assuming 100 µL transfection volume per well.

### 2.14.2 Nanoparticle-mediated EPC transfection

For cell culture transfection, a total of $2\times10^5$ adherent human late-outgrowth EPCs plated in gelatin 1% pre-coated wells (see gelatin preparation method in section 2.10) were washed twice with PBS to remove any excess FBS which might adsorb and sequester NPs and miRNAs. Cells were incubated for 4h(Duinhouwer et al., 2015) at 37ºC with serum free EBM containing NPs or NP:miRNA complexes at a final NP and miRNA concentration of 125 µg/mL and 200 nM, respectively. Different well sizes and cell densities were used according to prospective assay, always keeping the same NP mass (:miRNA molecules):cell number ratio **(Table 9)**. Following the incubation, cells were gently washed 2 times with serum-free medium and left in EGM 10% (v/v) FBS overnight before conducting any assay. miR knockdown occurred during the assay itself.

**Table 9 | EPC transfection protocol using nanoparticles.**
Transfection numbers used to keep same NP(:miRNA):cells ratio, irrespective of the assay; Final NP and miRNA (when applicable) concentration of 125 µg/mL and 200nM, respectively. IF – immunofluorescence; rt-PCR – real-time polymerase chain reaction.

| Well number | Cell density/well | Transfection medium | Assay |
|---|---|---|---|
| 1 well (6 well plate) | 200.000 cells | 1 mL | rt-PCR |
| 4 wells (24 well plate) | 50.000 cells | 250 µL | Confocal microscopy, IF, wound healing |
| 10 wells (96 well | 20.000 cells | 100 µL | Survival |

## 2.14.3 Nanoparticle-mediated arterial wall transfection

In the *in vivo* setting, an intravascular delivery of the NPs or NP:miRNAs was carried out by exposing the external carotid artery (ECA) and performing the arteriotomy, before infusing intra-luminally 200 µl of a 5mg/mL NP-fluoresceinamine or 5mg/mL:1µM NP:miR-92a inhibitor-FITC solution in Opti-MEM I at an infusion rate of 10 µL/min. After a total of 20 min of occlusion time the artery was finally flushed with PBS, before excluding the ECA proximally and resuming blood flow.

Rat carotid ring segments were used for *ex vivo* transfection with NPs or NP:miRNAs. Each ring was incubated with 200 µl of NP- fluoresceinamine (5 mg/mL) or NP:miR-92a inhibitor-FITC solution (5 mg/mL; 1 µM respectively) in Opti-MEM I in 96 well plates for 4 h, at 37ºC.

## 2.14.4 Pluronic mediated arterial wall transfection

In the *in vivo* setting, a 30% (w/v) Pluronic F-127 solution was prepared the day before surgery by dissolving the powder in cold double-distilled deionized water and allw. The solution was placed on a windmill rotating platform overnight at 4°C to ensure the polymer was homogenously mixed. The common carotid artery (CCA) was separated from the surrounding tissue using blunt tissue scissors, and a total volume of 300 µL ice cold pluronic solution containing NP (5 mg/mL), NP:miRNAs (5 mg/mL:1 µM) or 1 µM miRNA was applied externally to the adventitial surface of the exposed carotid artery

with a 100 µL micropipette, overall as described elsewhere (Kee et al., 2011). The solution jellified as soon as it came in contact with the rat tissue. Depending on the experimental layout, the administration was done on uninjured arteries or immediately after balloon angioplasty.

For *ex vivo* assays, NP-fluoresceinamine (5 mg/mL) or NP:miR-92a inhibitor-FITC solution (5 mg/mL; 1 µM respectively) was resuspended in Pluronic or Poly(lactic-co-glycolic acid) (PLGA) gel, before being applied to the rings for 24h.

## 2.15 Mouse aortic ring angiogenesis

The mouse aortic ring assay to study angiogenesis was generally performed as described previously (Baker et al., 2012). C57BL/6 mice were culled by schedule 1 procedure, after which the aortas were harvested and transferred into Opti-MEM I supplemented with Penicillin 100 U/mL + Streptomycin 100 µg/mL. Under a Leica M80 dissection microscope, fat tissue and branching vessels were removed using forceps and microdissection scissors. The vessel was cut into 0.5 mm thick rings with a scalpel, with 6-12 rings being placed per well in a 24 well plate. Rings were then transfected overnight using OF with the miRNA of interest (at a final concentration of 30 nM and a total volume of 1 mL/well), at 37 ºC and 5% $CO_2$ in Opti-MEM I supplemented with Penicillin 100 U/mL + Streptomycin 100 µg/mL. On the following day, rings were transferred into a 96 well plate (1 ring/well) to be embedded in 50µl of a collagen matrix, obtained by adding on ice 0.5 mL 10X DMEM, 3.13 mL $dH_2O$, 1.37ml collagen type I (rat tail) and 10 µL 5 N NaOH (measures needed per 96 well plate). After 1-hour incubation at 37 ºC, the embedded rings were fed with 150 µl Opti-MEM I supplemented with 2.5% (v/v) FBS, 30 ng/mL VEGF and Penicillin 100 U/ml + Streptomycin 100 µg/ml, again to be placed in the incubator **(Figure 22)**. In each experimental condition, a non-VEGF supplemented well was tested as a negative control. Rings were fed on day 5 by removing 130 µL and adding 150 µL of fresh medium, and the protocol was stopped on day 7. At this point, bright field pictures were captured using an Axiovert 40 C inverted optical microscope before culture media was removed and rings washed with PBS with $CaCl_2$ and $MgCl_2$. Rings were then processed for IF (as described in Section 2.18.3) and the concentric peripheral

angiogenesis network coverage area estimated (in triplicates in the red channel), using Image J imaging software (after digital subtraction of the ring area itself).

**Figure 22 | Aortic ring setup.**

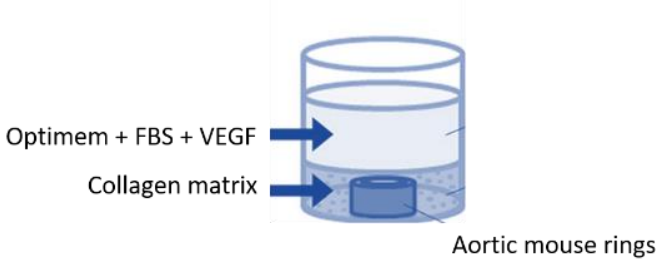


## 2.16 Time-lapse microscopy

The Incucyte Zoom (Essen Biosciences) comprises a microscope inside a tissue culture incubator, capable of recording live cell imaging experiments over several days while providing consistent standard tissue culture conditions for the growing cells (37°C, 95% air, 5% $CO_2$). Bright field and fluorescent images and videos of cells were captured and analysed using the proprietary software.

## 2.17 Long-term fluorescence cell labelling

For certain assays, EPCs were stained using CellTracker CM-DiI lipophilic, photostable fluorescence compound (excitation 553 nm, emission 570 nm), according to the manufacturer's protocol. Briefly, the probe was resuspended in PBS to 2 µM and incubated with pre-washed adherent cells in culture for 5 minutes or less at 37°C, and then for an additional 15 minutes at 4°C. Incubation at this lower temperature appears to allow the dye to label the plasma membrane but slows down endocytosis, thus reducing dye localisation into cytoplasmic vesicles.

## 2.18 Fluorescence microscopy

Fluorescence is a type of luminescence. When molecules with luminescent properties absorb light, they emit light of a different wavelength. With fluorescence, the emission

of light occurs extremely rapidly after the absorption of excitation light. Fluorescent materials give off light because of their atomic structure. Electrons are arranged in discrete energy levels surrounding the atom's nucleus with each level having a predetermined amount of energy. When an electron absorbs the energy from a photon of light, it becomes "excited" and jumps to a higher, less stable energy level. The half-life of the excited state is generally less than 10 seconds. The electron loses a small amount of energy as heat, and the remainder of the extra energy is given off in the form of a photon. The emitted fluorescence has a lower energy than the absorbed light, so the wavelength of the emitted light is longer than that of the excitation light. A range of wavelengths of light can excite the electrons of a fluorochrome. **Table 10** lists the fluorochromes used and corresponding excitation/emission spectra.

**Table 10 | Fluorochromes used in fluorescence microscopy.**
Approximate fluorescence excitation and emission maxima are indicated (solvent-dependent) from corresponding manufacturers' online resources. DAPI - 4',6-diamidino-2-phenylindole; FITC - fluorescein isothiocyanate; LDL – low density lipoprotein; miRNA – microRNA; NP – nanoparticle.

| Probe | Fluorochrome | Excitation (nm) | Emission (nm) |
|---|---|---|---|
| Prolong Gold anti-fade | DAPI | 350 | 461 |
| Conjugated Acetylated LDL | Alexafluor-488 | 495 | 519 |
| Conjugated miRNA | FITC | 494 | 521 |
| Conjugated antibody | FITC | 495 | 519 |
| Conjugated NP | Fluoresceinamine | 495 | 519 |
| Conjugated antibody | Alexafluor-488 | 519 | 495 |
| Lipophilic carbocyanine | CM-DiI | 553 | 570 |
| Conjugated antibody | Alexafluor-555 | 555 | 568 |
| Conjugated miRNA | DyLight 547 | 557 | 570 |
| Conjugated antibody | PE | 565 | 573 |
| Conjugated isolectin B4 | DyLight 594 | 592 | 617 |
| Conjugated antibody | Alexafluor-594 | 617 | 590 |
| Conjugated antibody | DyLight 649 | 652 | 647 |

## 2.18.1 Acetylated LDL internalisation

The endothelial commitment of EPCs was evaluated by incubating cells with acLDL conjugated to Alexafluor-488 and determining its uptake by fluorescent microscopy, a feature typical of ECs and microglial cells in primary cell culture (Sunada, Masuda, & Fujiwara, 1993). If the lysine residues of LDL's apoprotein have been acetylated, the LDL complex no longer binds to the LDL receptor, but rather is taken up by macrophage and endothelial cells that possess "scavenger" receptors specific for the modified LDL (Voyta, Via, Butterfield, & Zetter, 1984). Once the acetylated LDL complexes accumulate within these cells, they assume an appearance similar to that of foam cells found in atherosclerotic plaques. Briefly, AlexaFluor488 conjugated Ac-LDL was added directly to cells growing in culture in 1 mL serum-free media EBM to yield a final concentration of 10 µg/ml and left to incubate for 4 h at 37ºC. The medium was then aspirated, and the cells washed twice with PBS, before analysis. Imaging was captured using Axio Vert A1 fluorescence (human EPCs) or Incucyte Zoom microscopes (pig EPCs) in the bright-field and green channels, before being processed in Simple PCI or Incucyte Zoom softwares, respectively.

## 2.18.2 Fluoresceinamine internalisation

Rat carotid artery rings were incubated at 37ºC with either NPs-fluoresceinamine labelled or NPs conjugated with hsa-miR-92a-1-fluorescein labelled (410456-04 Exiqon, Vedbaek, Denmark) at increasing concentrations of NPs (0-5mg/mL) and miRNAs (0-1µM) in Opti-MEM I medium (for 4h) or gel (for 24h). Treatment with non-labelled NPs and omission of any treatment were used as negative controls. The samples were observed and photographed under Leica Macrofluo fluorescent macroscope.

## 2.18.3 Immunofluorescence

IF is the visualisation of antigens in cells/tissues specifically using antibodies as fluorescent probes. In IF techniques, antibodies are chemically conjugated to fluorescent dyes, which bind (directly or indirectly) to the antigen of interest allowing

for antigen detection through fluorescence or confocal microscopy. The specific antibodies used for these assays are listed in **Table 11**. Advantages of direct IF include shorter sample staining times and simpler dual and triple labelling procedures. Disadvantages of direct IF include lower signal, higher cost, less flexibility and difficulties with the labelling procedure when commercially labelled direct conjugates are unavailable. Advantages of indirect IF include greater sensitivity than direct IF. There is an amplification of the signal in indirect IF because more than one secondary antibody can attach to each primary. Commercially produced secondary antibodies are available in an array of colours. Disadvantages of indirect IF include the potential for cross-reactivity and the need to find primary antibodies that are not raised in the same species or of different isotypes when performing multiple labelling experiments.

**Table 11 | Antibodies used for immunofluorescent staining.**
CD – cluster of differentiation; EPCs – endothelial precursor cells; FITC - Fluorescein isothiocyanate; Ig – immunoglobulin; PE – Phycoerythrin; VEGFR2 – vascular endothelial growth factor receptor 2; vWF – von Willebrand factor.

| Target antigen | Cell type | Primary and secondary antibodies |
|---|---|---|
| CD31 | human EPCs | 1° = mouse monoclonal anti-human CD31 (JC70A) (1:20, M0823, Dako, Glostrup, Germany)<br>2° = Dylight 649 donkey anti-mouse IgG (1:400, AP192SD, Milipore, Temecula, USA)<br>Isotype control = mouse monoclonal IgG1 (NCG01, abcam, Cambridge, UK) |
| CD34 | human EPCs | 1° = mouse monoclonal anti-human CD34-PE (1:11, 130-081-002, Milteny Biotec)<br>2° = Alexafluor-594 goat anti-mouse IgG (1:500, A11005, ThermoFisher Scientific, Paisley,UK)<br>Isotype control = mouse monoclonal IgG2a-PE (130-091-835, Miltenyi Biotec, Bergisch Gladbach, Germany) |
| FITC | human EPCs | 1° = polyclonal rabbit anti-FITC (1:50, 71-1900, Invitrogen ThermoFisher Scientific, Paisley,UK)<br>2° = Alexafluor-555 donkey anti-rabbit IgG (1:500, A31572, ThermoFisher Scientific, Paisley,UK)<br>2° = Alexafluor-488 donkey anti-rabbit IgG (1:500, A21206, ThermoFisher Scientific, Paisley,UK)<br>Isotype control = normal rabbit IgG (sc2027, Santa Cruz Biotechnology, Heidelberg, Germany) |
| FITC | rat arteries | 1° = polyclonal rabbit anti-FITC (1:50, 71-1900, ThermoFisher Scientific, Paisley,UK)<br>2º = Alexafluor-555 donkey anti-rabbit IgG (1:500, A31572, ThermoFisher Scientific, Paisley,UK)<br>Isotype control = normal rabbit IgG (sc2027, Santa Cruz Biotechnology, Heidelberg, Germany) |

| | | |
|---|---|---|
| SMA | human EPCs | 1° = rabbit polyclonal anti-human SMA (1:100, ab5694, Abcam, Cambridge, UK)<br>2° = Alexafluor-488 donkey anti-rabbit IgG (1:500, A21206, ThermoFisher Scientific, Paisley,UK)<br>Isotype control = normal rabbit IgG (sc2027, Santa Cruz Biotechnology, Heidelberg, Germany) |
| SMA | mouse aortic rings | 1° conjugated = mouse monoclonal Anti-Actin, α-Smooth Muscle – FITC, clone 1A4 (1:100, F3777, Sigma-Aldrich, Dorset, UK)<br>Isotype control = mouse monoclonal IgG2a-PE (130-091-835, Miltenyi Biotec, Bergisch Gladbach, Germany) |
| VECAD | human EPCs<br>pig EPCs | 1° = mouse monoclonal anti-human/pig VE-cadherin (1:50, sc9989, Santa Cruz Biotechnology, Heidelberg, Germany)<br>2° = Alexafluor-488 goat anti-mouse IgG (1:500, A11001, ThermoFisher Scientific, Paisley, UK)<br>Isotype control = mouse monoclonal IgG1 (NCG01, Abcam, Cambridge, UK) |
| VEGFR2/ KDR | human EPCs | 1° = mouse monoclonal anti-human VEGFR2-PE (1:50,130-093-598, Milteny Biotec, Bergisch Gladbach, Germany)<br>2° = Alexafluor-594 goat anti-mouse IgG (1:500, A11005, ThermoFisher Scientific, Paisley, UK)<br>Isotype control = mouse monoclonal IgG1-PE (130-093-188, Miltenyi Biotec, Bergisch Gladbach, Germany) |
| vWF | human EPCs | 1° = polyclonal rabbit anti-human vWF (1:100, A0082, Dako, Glostrup,Germany)<br>2° = Alexafluor-488 donkey anti-rabbit IgG (1:500, A21206, ThermoFisher Scientific, Paisley, UK)<br>2º = Alexafluor-488 goat anti-rabbit IgG (1:2000, A11034, ThermoFisher Scientific, Paisley, UK)<br>Isotype control = normal rabbit IgG (sc2027, Santa Cruz Biotechnology, Heidelberg, Germany) |

## IF for EPC surface epitope characterization

At the end of the differentiation, expression of EC markers was evaluated by IF staining. Briefly, $6x10^4$ EPCs (from human or pig origin) were plated in 1% gelatin coated Lab-Tek II chamber slides and left to rest overnight in 500 µl EGM 20% (v/v) FBS (see gelatin preparation method in section 2.10). The cells were fixed with PFA 4% (w/v) in PBS for 15 min at RT and washed twice with PBS 1% (w/v) BSA. Then, PBS/0.1% (v/v) Triton X-100 was added to each chamber well to permeabilize the cell membrane. The solution was aspirated after 10 minutes at RT, and the cells were washed twice with PBS. CD34, KDR, vWF, VE-cadherin and SMA primary antibodies were prepared in PBS/0.1% (v/v) Tween-20/ 1% (w/v) BSA. After the addition of the primary antibody, the chamber slide was left overnight at 4°C on a shaking platform. Negative controls were obtained by using isotype-matched IgG control. Next morning, cells were washed 3 times with PBS.

The appropriate secondary antibodies were prepared in the same solution as before and added to the cells for 1 h at RT, protected from light. The wells were again washed 3 times with PBS. The nuclei of the cells were counter-stained with 4',6-diamidino-2-phenylindole (DAPI) for 5 minutes at RT, protected from light, which also functioned as a mounting reagent (DAPI propriatery concentration). The cells were examined and photographed under a Carl Zeiss Axio Vert.A1 fluorescence microscope.

## IF for confirmation of cellular internalisation of miRNA

After miR transfection using OF or NPs, confirmation of internalisation was done by IF staining. Briefly, $4x10^5$ human EPCs were seeded in coverslips pre-coated with 1% gelatin (see gelatin preparation method in section 2.10) inserted in 6 well plates and incubated overnight in EGM 30% (v/v) FBS. The following day cells were transfected with 30nM hsa-miR-92a-1 inhibitor-FITC (410456-04, Exiqon, Vedbaek, Denmark) using OF protocol. The omission of OF or incubation with the miR only were the negative controls. Alternatively, for NP assays, NPs-fluoresceinamine labelled (250 μg/ml) or NPs conjugated with miRNA-fluorescein labelled (250 μg/ml and 100nM) were the transfection vectors. Treatment with non-labelled NPs, treatment only with labelled NPs and omission of treatment were used as negative controls for NP transfections. After 24h, cells were fixed in PFA 2% (w/v) in PBS for 15 min at RT and washed twice with PBS 2% (w/v) BSA. Then, PBS/0.1% (v/v) Triton X-100 was added to the well to permeabilize the cell membrane. The solution was aspirated after 10 minutes at RT, and the cells were washed twice with PBS 2% (w/v) BSA. Primary anti-FITC antibody was prepared in PBS/0.1% (v/v) Tween-20/ 1% (w/v) BSA. After the addition of the primary antibody at 1:50, the 6 well plate was left overnight at 4°C on a shaking platform. Negative controls were obtained by omission of primary antibody. Next morning, cells were washed 3 times with PBS 0.1% (v/v) BSA. The appropriate secondary antibodies were prepared in the same solution as before and added to the cells for 1 h at RT, protected from light. The wells were again washed 3 times with PBS 0.1% (v/v) BSA. The nuclei of the cells were counter-stained with DAPI (proprietary concentration) for 5 minutes at RT, protected from light, which also functioned as a mounting reagent. The cells were photographed under a Carl Zeiss Axio Vert.A1 fluorescence microscope.

## IF for confirmation of arterial wall internalisation of NP and miRNAs

Carotid arteries once harvested and cleaned from the exceeding surrounding connective tissue were left to fix overnight in 4% PFA (w/v) in PBS at 4°C. They were then transferred to 70% ethanol until they were embedded in paraffin and cut perpendicularly to their longitudinal axis at Barts Cancer Institute pathology services, London, UK. 7µm cuts were performed along the arteries at 6 different levels (approximately every 1.5 mm along the average 1-1.2 cm total length of the artery). For rat carotid rings one cross-section per sample was performed at the midpoint level. Retrieved 5 µm-thick paraffin cross-sections were dewaxed and hydrated, by sequentially passing the slides through the following steps: Xylene 5 min, Xylene 5 min, Xylene 5 min, absolute ethanol 5 min, absolute ethanol 5 min, 95% ethanol 3 min, 80% ethanol 2 min, distilled water 5 min. Antigen retrieval was performed by boiling in Citrate buffer pH 6.0 for 10 minutes. Citrate buffer was prepared by dissolving 2.94g of Trisodium citrate in 5.4 mL 1M HCl, topped up to 1L of milQ water. The sections were washed 3 times with PBS-Tween 20 (PBS-T). PBS-T was prepared by dissolving 4 tablets of PBD in 2 mL of Tween 20 and 2 mL of milQ water. A boundary was made around the tissue section using a DAKO pen. Non-specific antibody binding to proteins in tissue preparations was prevented by applying 5% donkey serum/0.5%Triton X100/PBS-T to each slide for 30 minutes at RT, the serum being from the species which provided the second layer antibody. The primary antibody rabbit anti-FITC was diluted in the same solution at 1:50 and pipetted on the tissue sections within the boundary (~100 µl). The slides were then placed at 4ºC overnight in a humidified chamber. Negative controls were obtained by omitting the incubation with primary antibody. Next morning, the slides were washed 3 times with PBS-T and the Alexafluor-555 donkey anti-rabbit IgG secondary antibody diluted 1:500 in the same buffer was applied for 1h30m at RT, protected from light in a humidified chamber. Following 3 more PBS-T washes the tissue sections were counterstained and mounted with DAPI reagent (proprietary concentration) for 5 minutes at RT, protected from light. The slides were examined and photographed under a fluorescence microscope.

## IF for quantification of mouse aortic ring angiogenesis

After a 4% formalin fixation step for 30 minutes at RT, rings were permeabilized with PBS with $CaCl_2$ and $MgCl_2$ and 0.25% Triton X-100 for 15 minutes at RT twice and then blocked using 1 drop of 2x casein buffer per well for 30 minutes at RT. Overnight incubation at 4ºC with DyLight 594 Labelled GSL I - isolectin B4 (1:100 dilution in PBLEC; DL-1207, Vector Labs, Burlingame, USA) and monoclonal anti-actin alpha-Smooth Muscle-FITC (1:100 dilution in PBLEC) then followed. PBLEC was constituted by diluting 10X PBS with $CaCl_2$ and $MgCl_2$ in $dH_2O$ and add 0.1ml of 1M $MnCl_2$ and 1% Tween 20. Next day, each well was washed three times in PBS and 0.1% Triton X-100 for 15 minutes and then wash once more with distilled water. The gel was detached from the walls of the well using curved thin forceps before being carefully transferred to a slide (6 embedded rings per slide). Fluorescence mounting medium with DAPI (proprietary concentration) was added, before placing a coverslip over (avoiding air bubble formation). The slides were examined and photographed under a Carl Zeiss AxioVert A1 fluorescence microscope.

## IF for quantification of co-culture angiogenesis

Co-culture samples were fixed in ethanol 100% for 2 hours at RT. After one PBS-T wash, cells were blocked in dry milk 5% (w/v) in PBS-T for 1h at RT on an orbital shaker. Then, the coculture was incubated overnight at 4ºC on an orbital shaker with 200 µl of primary vWF antibody (1:1000) in 5% (w/v) dry milk in PBS-T. The next day, cells were washed twice with PBS-T, before secondary goat anti-rabbit Alexafluor 488 conjugated antibody diluted in PBS-T (1:2000) was added for 60 minutes at RT, on the shaker and protected from light. After 2 more washes with PBS-T, samples were stored in MilQ water and images of the wells captured on demand using Incucyte Zoom fluorescent microscope at 10x magnification.

### 2.18.4 Confocal

The joint application of immunofluorescent staining with confocal microscopy allows the visualisation of protein localisation within the cell in a single plane. For confirmation of cellular internalisation of miRNA, 50 000 human late-outgrowth EPCs were plated in gelatin 1% pre-coated coverslips (see gelatin preparation method in section 2.10) placed in a 24 well plate, and incubated overnight with EGM/20% (v/v) FBS at 37ºC. In the following day, after 2 washes with PBS, cells were transfected with dual labelled NPs-fluoresceinamine conjugated with sham miRNA-Dy547 (CP-004500-01-05, miRIDIAN microRNA Mimic Transfection Control Dy547, Thermo Scientific, Surrey, UK) at 125 µg/mL and 100 nM respectively. Exclusive NP, miRNA or no treatment were used as used as control conditions. Following the 4 h of treatment, cells were washed twice with PBS 1% (w/v) BSA for 2 mins, before fixation in situ with PFA 4% (w/v) in PBS for 15 min at RT. Cells were gently washed twice with the coverslip inverted on top of a PBS drop, followed by anti-CD31 incubation for 2 h at RT and protected from light. The antibody predominantly displays staining of the cell membrane, with weaker cytoplasmic staining, according to the manufacturer. Cells were gently washed twice with the coverslip inverted on top of a PBS drop, before staining with the secondary antibody for 1h at RT, protected from light. Again, cells were washed twice on a PBS drop, before counterstaining with DAPI mounting media (proprietary concentration) for 5 min at RT in the same fashion, and then placed on a microscope slide. Digital micrographs and z-stack videos were taken on a Zeiss LSM 510 Meta confocal laser microscope using an oil immersion 63x objective.

## 2.19 Immunohistochemistry

Carotid arteries and rings were processed as in page 130 until the antigen retrieval step. Then, antigen retrieval was performed by treating the tissue sections with Pronase for 15 minutes at RT. After 3 washes in PBS-T and 1 wash with distilled water, the sections were then treated with 3% (v/v) Hydrogen peroxide in milQ water for 15 minutes to block endogenous peroxidases. The sections were washed once with distilled water and twice with PBS-T before a boundary was made around the tissue section using a

hydrophobic PAP pen. The Avidin/Biotin Blocking Kit was used, according to manufacturer's instruction, to block all endogenous biotin, biotin receptors, and avidin binding sites present in tissues. The slides were washed 3 times with PBS-T and blocked in 5% goat serum/0.5%Triton X100/PBS for 30 minutes at RT. The primary rabbit anti-FITC antibody (71-1900, ThermoFisher Scientific, Paisley, UK) was applied at 1:50 dilution and samples left overnight in a humidified chamber at 4ºC. Negative controls were obtained by omitting the incubation with primary antibody. Next morning, the slides were washed 3 times with PBS-T before adding secondary goat anti-rabbit biotinylated IgG (E0432, Dako, Glostrup, Denmark), at 1:100 in 5% goat serum/0.5%Triton X100/PBS. The slides were kept at RT for one hour. During the last half hour of incubation, the ABC solution was prepared as per manufacturer's protocol and allowed to stand at RT for at least 30 minutes. The slides were then washed with PBS-T (1 wash). The ABC solution was added to the tissue sections after gently drying off the excess buffer. The slides were further incubated at RT for 30 min. Towards the end of incubation, the 3-3'diaminobenzidine (DAB) substrate solution was prepared. Briefly, 1 golden and 1 silver tablets were dissolved in 1 ml of PBS (vortex). The slides were washed with PBS-T, before adding the DAB solution dropwise. The slides were allowed to stain for about 15 minutes under the microscope before the reaction was stopped by transferring the slides to PBS-T. The stained sections were counterstained for 10 seconds with Mayer's haematoxylin solution (solution previously filtered) and differentiated in tap water. The slides were then washed one final time in PBS-T and dehydrated by passing through an ascending alcohol gradient, followed by 2 changes in xylene. They were finally mounted in DPX - a mixture of distyrene + plasticiser (tricresyl phosphate) +xylene -, and covered with a slip. The slides were examined under an inverted optical microscope, and the appropriate primary antibody concentration was determined, after which all remaining slides were stained using this concentration. The slides were photographed for analysis in a Nanozoomer slide scanner microscope.

## 2.20 rt-PCR

The gene expression profile of specific targets of hsa-mir-92a-1-5p mirvana mimic and hsa-mir-92a-1-5p mirvana inhibitor were evaluated in EPCs transfected with NPs

complexed with miRNA at 250 µg/mL and 200 nM respectively in 6 well plates. EPCs transfected with NP:Dy547 (CP-004500-01-05, miRIDIAN microRNA Mimic Transfection Control Dy547, Thermo Scientific, Surrey, UK) served as negative transfection controls. Cell lysates were homogenised with QIAshredder, and total RNA was extracted with RNeasy Mini kit, according to the instructions of the manufacturer. Total RNA was quantified using Nanodrop 3300 spectrophotometer, and cDNA was prepared from 1 µg total RNA using QuantiTect Reverse Transcription Kit. Real-time PCR was carried out with the Brilliant II SYBR Green QPCR Master Mix on a Mx3000P qPCR System, following the manufacturer's instructions. Each cDNA was analysed with the target gene and housekeeping gene primer sets that approached 100% amplification efficiency, allowing direct comparison of threshold cycle (Ct) values to determine relative gene expression. The target gene signal was first normalised to b-actin and then expressed relative to the value obtained with control EPCs by using the formula $2^{-\Delta\Delta Ct}$, as described elsewhere (X. Yang et al., 2005). The mean minimal Ct were calculated from triplicate reactions. Primer sequences, reaction conditions, and optimal cycle numbers are outlined in **Table 12**. Quality control checking included melting curve analysis after amplification of original template (95°C, 1min; melt ramp 30 sec from 65ºC to 95° rising by 1°C per step; 95°C, 30 sec), and running a 1.2% pre-cast agarose gel electrophoresis of PCR products stained with 0.01% Ethidium bromide in E-gel iBase powersystem (Thermofisher Scientific).

**Table 12 | Primers for rt-PCR**
rt-PCR conditions: Initial denaturation step at 95ºC, 3min; 40 cycles of denaturation at 95ºC for 5 sec, primer annealing/elongation at 60ºC for 20 sec. ACTB – β actin; ITGA5 – integrin α5 subunit; rt-PCR – real-time polymerase chain reaction.

| Target gene | Sense primer sequence (5'->3') | Anti-sense primer sequence (5'->3') | Concentration (nM) |
|---|---|---|---|
| ACTB | TGTCCCCCAACTTGAGATGT | TGTGCACTTTTATTCAACTGGTC | 500 |
| ITGA5 | TCTTCCCCGCCATGTTCAACCC | AAGGTTGATGCAGGCCACAGGG | 500 |

# 2.21 Western blotting

Cell lysate samples are prepared with a denaturing buffer, containing an anionic surfactant such as sodium dodecyl sulphate (SDS) or lithium dodecyl sulphate (LDS), and a reducing agent such as beta-mercaptoethanol, dithiothreitol (DTT) or Tris(2-

carboxyethyl)phosphine (TCEP). This denaturing buffer causes the loss of native protein conformation by disrupting non-covalent intra- and inter-molecular protein bonds. Denatured cell lysate samples are run by electrophoresis through a polyacrylamide gel. Proteins are separated by size, as larger proteins migrate more slowly through the pores of the gel than smaller proteins. Proteins separated on the gel are then transferred via electrophoretic blotting to a protein-binding polyvinylidene fluoride (PVDF) membrane. After electrophoretic transfer, the membrane can be cut into strips based on the known molecular weight of the proteins of interest. Membranes are initially incubated in a protein solution such as BSA or milk to block non-specific binding sites. The specific protein of interest is detected by incubation with an antibody to that protein. This antibody is then visualised via incubation with a secondary antibody conjugated to an enzyme such as Horse-radish peroxidase (HRP). Upon addition of a substrate solution, the conjugated antibody catalyses a reaction to produce a tightly localised chemiluminescent product, which is then detected using a photographic film.

Western blotting can be considered a semi-quantitative technique, as the amount of protein present in the cell lysate, is proportionally represented by the amount of bound antibody on the membrane. This, in turn, is represented by the amount of light produced by the chemiluminescent reaction which is detected by the photographic film. The intensity of the band produced is the representation of the level of the specific protein in the sample and can be quantified by densitometry after scanning, using software such as ImageJ.

### 2.21.1 Protein extraction from EPC cultures

Cells cultured in 6 well plates were washed twice with cold PBS on ice and lysed in RIPA buffer (50 µl per well) including complete protease inhibitor cocktail (working concentration 1x). The cells were scraped off the plate and the lysates transferred to 1.5 mL tubes. The samples were centrifuged for 15 minutes at 13 000 x *g* at 4 °C to pellet the insoluble material. The supernatant containing the protein lysate was removed and kept on ice, or at -20 °C for longer-term storage.

## 2.21.2 Protein extraction from rat arteries

Rat carotid arteries were harvested, incubated in Krebs solution (10x solution reconstituted in milQ water), cleared out of extraneous tissues under a stereomicroscope and snap frozen in liquid nitrogen. Protein extraction involved the sample lysis, bead-beating homogenization and retrieval of the protein lysate. Briefly, a solution of RIPA buffer containing Complete Protease Inhibitor Cocktail was prepared at 4° C as per manufacturers' recommended dosages, and 100 µl dispensed into Precellys ceramic beads pre-filled 0.5 mL tubes. The frozen artery was inserted into the tube, and the samples homogenised for 3 x 60 seconds at full speed in a Minilys tissue homogenizer. The tubes were kept at 4 °C for 60 seconds in between the homogenizer runs. The uniform sample was transferred to a 1.5 mL Eppendorf and centrifuged at 13 000 rpm for 15 minutes at 4 °C. The supernatant was then transferred to a clean tube and stored at -20 °C.

## 2.21.3 Determination of protein concentration and normalisation

The Bradford protein assay allows the determination of protein concentration in tissue and cell lysate samples as essentially described elsewhere (Ramagli, 1999). There are commercially available kits for this assay. Therefore the Bio-Rad Protein Assay Kit was used. It is a colorimetric test based on the absorbance shift of the dye Coomassie Brilliant Blue G-250 under acid conditions when a redder form of the dye is converted into a bluer form on binding to the protein. The characteristic blue colour produced by the reaction has a maximum absorbance at 750 nm and the minimum absorbance at 405 nm due to the amino acids tyrosine and tryptophan and to a lesser extent cysteine and histidine (from the Bio-Rad instruction manual). The amount of the blue-coloured complex in solution is a measure of protein concentration and can be quantified using absorbance reading to determine the protein concentration.

Protein standards were prepared using BSA diluted in the same buffer in which protein extraction had been performed. The following dilutions of BSA were prepared – 2.0, 1.5, 1.0, 0.5, 0.25, 0.125, 0.0625, 0.03125 and 0 mg/mL protein. Protein concentration was measured by taking 5 µL of cell lysate sample or standard and adding to 25 µl of the Bio-

Rad A' solution (alkaline copper tartrate solution) and mixing in a 96-well plate with 200ul of the B solution (a dilute Folin reagent). The mixture was incubated at RT for 15 minutes, shaking, protected from light. The absorbance of each well was measured at 595 nm using a Tecan Genios plate reader. Every serial dilution or tissue sample was tested on two wells and the final result taken as the average. The absorbance values for the calibration dilutions were plotted against the standard concentrations of BSA to produce a linear calibration curve **(Figure 23)**, and the protein concentration of the tissue samples was determined against it. Tissue samples that gave a higher absorbance reading than that of the highest standard (2.0 mg/mL) were re-diluted so that their absorbance fell within the linear range of the assay.

**Figure 23 | Bradford assay standard curve.**
A representative standard curve generated with BSA used to determine the concentration of protein extracts from EPCs and rat carotid arteries.

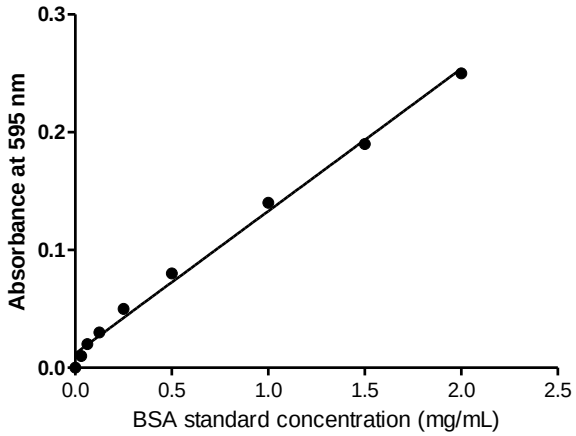


## 3.21.4 SDS-PAGE and immunoblotting

Different volumes of protein samples normalised to the same lowest concentration, were added to 4x loading buffer and 10x reducing buffer and topped up with RIPA+PIC buffer to make up 25 µl final volume, which was then reduced by boiling at 80 °C for 4 minutes and vortexed for 2 seconds prior to loading. The reduced samples were separated using SDS-polyacrylamide gel electrophoresis (SDS-PAGE), by running them on a 4-12% Bis-Tris Gel in 5% MOPS-SDS Running buffer alongside a molecular weight marker. The protein was then transferred to a 0.45-µm pore size protein-binding polyvinylidene fluoride (PVDF) membrane using a wet transfer apparatus in 1x NuPAGE transfer buffer containing 20% methanol. The transfer was carried out at 35V for 90

minutes. Membranes were blocked in 5% (w/v) non-fat milk made up in PBS + 0.1% (v/v) Tween20 (PBS-T) for an hour at RT. Membranes were incubated with appropriate primary antibody diluted in the 5% milk-PBST solution overnight on a rocker at 4°C. A list of used antibodies and corresponding titrations can be seen in **Table 13**. Next morning, membranes were given three rounds of 5-minute washes with PBST (on a rocker), prior to addition of the HRP conjugated secondary antibody of the appropriate species, in 5% milk-PBST solution. This was incubated for 1 hour with rocking at RT and was then subjected to three 5 minute rounds of washing in PBST (with rocking). Protein bands were visualised using ECL-plus western blotting detection system on Hyperfilm ECL. The hyper film was scanned using the HP Deskscan system. β-actin (ACTB) was usually probed for as a loading control in Western blotting. As this is considered a house-keeping gene, its level can be used to determine the relative amounts of protein loaded in each well. Accordingly, protein expression results were then quantified by scanning densitometry using Image J software.

**Table 13 | Antibodies used for western blotting.**
ACTB – β actin; Akt – protein kinase B; CD – cluster of differentiation; eNOS – endothelial nitric oxide synthase; EPCs – endothelial precursor cell; ERK1/2 - Extracellular signal–regulated kinase 1/2; FITC - Fluorescein isothiocyanate; GAPDH - Glyceraldehyde 3-phosphate dehydrogenase; HRP – horse-radish peroxidase; Ig – immunoglobulin; ITGA5 – integrin α5 subunit; ITGAV – integrin αv subunit; kDa – kilodaltons; MKK4 - Mitogen-activated protein kinase kinase 4; PE – Phycoerythrin; SIRT1 – sirtuin 1; VECAD – vascular endothelial cadherin; VEGFR2 – vascular endothelial growth factor receptor 2; vWF – von Willebrand factor.

| Target | Cell type | Primary and secondary antibodies |
|---|---|---|
| ACTB<br>42 kDa | rat<br>arteries | 1° = monoclonal mouse anti-rat ACTB, Clone AC-15 (1:20,000, A5441, Sigma Aldrich, Dorset, UK)<br>2° = goat anti-mouse IgG-HRP (1:10000, SC2005, Santa Cruz Biotechnology, Heidelberg, Germany) |
| ACTB<br>42 kDa | human<br>EPCs<br>pig EPCs | 1° = monoclonal mouse anti-human/pig, Clone AC-15 (1:$10^6$, A5441, Sigma Aldrich, Dorset, UK)<br>2° = goat anti-mouse IgG-HRP (1:10000, SC2005, Santa Cruz Biotechnology, Heidelberg, Germany) |
| Akt-p<br>60 kDa | pig EPCs | 1° = rabbit anti-pig (Ser 473) (1:1000, 9271, Cell signalling, Massachusetts, USA)<br>2° = goat anti-rabbit IgG-HRP (1:10000, SC2030, Santa Cruz Biotechnology, Heidelberg, Germany) |

| | | |
|---|---|---|
| Akt-t<br>60 kDa | pig EPCs | 1° = rabbit anti-pig (C73H10) (1:1000, 2938, Cell signalling, Massachusetts, USA)<br>2° = goat anti-rabbit IgG-HRP (1:10000, SC2030, Santa Cruz Biotechnology, Heidelberg, Germany) |
| eNOS-p<br>140 kDa | human EPCs | 1° = rabbit anti-human/rat (Ser 1177) (C9C3) (1:000, 9570, Cell signalling, Massachusetts, USA)<br>2° = goat anti-rabbit IgG-HRP (1:10000, SC2030, Santa Cruz Biotechnology, Heidelberg, Germany) |
| eNOS-t<br>140 kDa | human EPCs<br>rat | 1° = mouse anti-human/pig (1:3000, 610296, BD Biosciences, USA)<br>2° = goat anti-mouse IgG-HRP (1:10000, SC2005, Santa Cruz Biotechnology, Heidelberg, Germany) |
| ERK1/2-p<br>42,44 kDa | pig EPCs | 1° = rabbit anti-pig (Thr202/Tyr204) (D13.14.4E) (1:000, 4370, Cell signalling, Massachusetts, USA)<br>2° = goat anti-rabbit IgG-HRP (1:10000, SC2030, Santa Cruz Biotechnology, Heidelberg, Germany) |
| ERK1/2-t<br>42,44 kDa | pig EPCs | 1° = rabbit anti-pig (1:1000, 9102, Cell signalling, Massachusetts, USA)<br>2° = goat anti-rabbit IgG-HRP (1:10000, SC2030, Santa Cruz Biotechnology, Heidelberg, Germany) |
| GAPDH<br>37 kDa | Human EPCs | 1° = polyclonal goat anti-human/rat/mouse, V-18, HRP conjugate (1:2000, SC20357 Santa Cruz Biotechnology, Heidelberg, Germany) |
| ITGA5<br>95 kDa | rat arteries | 1° = mouse monoclonal anti-human ITGA5, Clone IgG2A (2ug/mL, MAB18642, R&D systems, MN, USA)<br>2° = goat anti-mouse IgG-HRP(1:10000, SC2005, Santa Cruz Biotechnology, Heidelberg, Germany) |
| ITGA5<br>114 kDa | human EPCs | 1° = rabbit anti-human ITGA5, c-terminus, intracelular (1:1000, AB1928, Milipore, Temecula, USA)<br>2° = goat anti-rabbit IgG-HRP (1:10000, SC2030, Santa Cruz Biotechnology, Heidelberg, Germany) |
| ITGAV<br>135,140 kDa | human EPCs | 1° = rabbit anti-human (1:000, 4711, Cell signalling, Massachusetts, USA)<br>2° = goat anti-rabbit IgG-HRP (1:10000, SC2030, Santa Cruz Biotechnology, Heidelberg, Germany) |
| MKK4<br>44 kDa | human EPCs | 1° = rabbit anti-human (1:000, 9152, Cell signalling, Massachusetts, USA)<br>2° = goat anti-rabbit IgG-HRP (1:10000, SC2030, Santa Cruz Biotechnology, Heidelberg, Germany) |
| SIRT1<br>120 kDa | human EPCs | 1° = rabbit anti-human (1:1000, C14H4 Cell signalling, Massachusetts, USA)<br>2° = goat anti-rabbit IgG-HRP (1:10000, SC2030, Santa Cruz Biotechnology, Heidelberg, Germany) |
| VECAD<br>130 KDa | pig EPCs | 1° = mouse monoclonal anti-human/pig VE-cadherin (1:50, sc9989, Santa Cruz Biotechnology, Heidelberg, Germany)<br>2° = goat anti-mouse IgG-HRP (1:10000, SC2005, Santa Cruz Biotechnology, Heidelberg, Germany) |

### 2.21.5 Stripping and reprobing western blot membranes

Membranes were occasionally stripped of the bound antibodies following the development of the western blot. Reblot Plus Strong stripping solution was used according to the manufacturer's instructions to remove bound antibodies. Briefly after 2 washes with PBS-T, the membrane was incubated with the stripping solution for 15 minutes at room temperature in the roller (1mL of 10x Milipore solution + 9 mL of molecular biology grade water). Then, the membrane was washed in running milQ water for 1 minute. The stripped membranes were then blocked in 5% milk (w/v)-PBS-T solution and incubated with the relevant primary and then secondary antibodies, and Western blots were then developed as previously described.

## 2.22 EPC functional assays

### 2.22.1 Luminescence-based survival

Following the miRNA transfection procedure with OF in two white-walled multiwell 96 well plates (30,000 cells/well), human EPCs were incubated for 48 h in EGM 10% (v/v) FBS to allow miRNA knockdown. Survival in serum-free medium after 6h was assessed using a Luminescent cell viability Adenosine triphosphate (ATP)-based assay (Cell Titer Glo), following the manufacturer's instructions. This assay is a homogeneous method of determining the number of viable cells in culture based on quantitation of the ATP present, an indicator of metabolically active cells. The assay system utilises the properties of a thermostable luciferase to enable reaction conditions that generate a stable luminescent signal while simultaneously inhibiting endogenous enzymes released during cell lysis (e.g., ATPases). The ATP-based detection of cells has been shown to be more sensitive than other methods (Maehara, Anai, Tamada, & Sugimachi, 1987; Petty, Sutherland, Hunter, & Cree, 1995) and has already been used to assess endothelial cell viability (Logie et al., 2010).

Briefly, one of the 96 well plates was used for the baseline reading. Cells were washed once, before equilibrating in 50 µl in EBM for 15 mins at 37°C, following the manufacturer's instructions. Then an equal volume of Cell Titer Glo reagent was added

per well and the plate inserted on an orbital shaker (to induce cell lysis) for 2 mins at RT. The mixture was allowed to rest for 15 minutes, covered with a lid in the dark, before being read in a Genios Tecan luminometer (firefly luciferase peak emission 560 nm). Replicates of 6 were used for each experimental condition. The medium without cells was used as a blank control and deducted from the values in experimental wells. As for the second well plate, cells were washed once and incubated in EBM serum free medium for 6h, before executing the luminescence assay.

If NPs were used as the transfection vector in 96 well plates (20,000 cells/well), then EPCs would be incubated in EBM under normal $FiO_2$ (21%) and the assay conducted using Cell Titer Glo, as described previously but using a 48h endpoint instead. The medium without cells was used as a blank control and deducted from the values in experimental wells, and treatment with only NPs was used as an internal control when evaluating NP:miRNA effect. Replicates of 5 were used for each experimental condition. An interference assay demonstrating that NPs do not block the luciferase reporter was conducted with the following experimental conditions: NP 125 µg/mL + ATP 50 µM in PBS; ATP 50 µM in PBS as a positive control and only medium as a negative control **(Figure 24)**.

**Figure 24 | Nanoparticles were incubated with ATP revealing no luciferase reporter interference.**

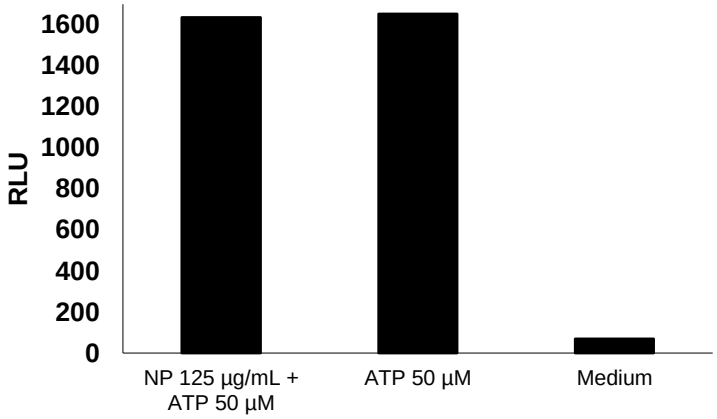


## 2.22.2 Co-culture angiogenesis

Late outgrowth EPCs were transfected using OF in 6 well plates for 4 hours with miRNA of interest (30nM), as described previously. After overnight rest in EGM 10% (v/v) FBS,

20,000 transfected EPCs in 100 µl of EGM 5% (v/v) (i.e. $2x10^5$ cells/mL) were added to confluent fibroblast monolayers already in 400 µl of the same medium. The fibroblasts had been previously seeded in 24 well plates 3 days before at a density of $1x10^5$ cells/mL and allowed to expand on DMEM 10% (v/v) FBS. Next day, medium was replaced to EGM 1% (v/v) FBS + VEGF 25 ng/mL, and co-cultures grown for 96h. Replacement of medium occurred at 48h. The omission of VEGF treatment was the negative control condition. At the end of the assay, brightfield pictures of the coculture taken with Incucyte Zoom microscope, while the effects of angiogenic stimuli were assessed by IF (as described in section 2.18.3). Images of the wells were captured on demand using Incucyte Zoom fluorescent microscope. All experimental conditions were measured in triplicate. Angiogenesis network length, area and number of branch points based on fluorescence signal were automatically calculated using proprietary Incucyte Zoom software algorithm **(Figure 25)**.

**Figure 25 | Co-culture angiogenesis network analysis algorithm run by Incucyte Zoom software.**
wWF – von Willebrand factor

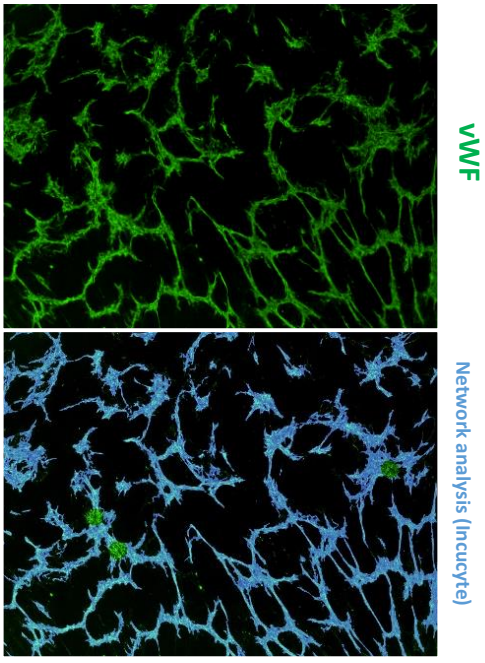


## 2.22.3 Luminescence-based proliferation

The proliferation assay consisted in a luminescent method using Cell Titer Glo reagent to determine the number of viable cells in culture based on quantitation of the ATP present, an indicator of metabolically active cells. Following oligonucleotide transfection

using OF in two white opaque 96 well plates, EPCs (30 000 cells/well) were incubated overnight in Opti-MEM I 30% (v/v) FBS, before starting the proliferation assay itself. The next day, one of the 96 well plates was used for the baseline reading. Following the manufacturer's instructions, cells were washed once, before equilibrating in 50 µl in EBM for 15 mins at 37ºC. Then 50 µl of Cell Glo Titer reagent was added per well (1:1 ratio) and the plate inserted on an orbital shaker (to induce cell lysis) for 2 mins at RT. The mixture was allowed to rest for 15 minutes, covered with a lid in the dark, before being read in a Genios Tecan luminometer (firefly luciferase peak emission 560 nm). Replicates of 4 were used for each experimental condition. The medium without cells was used as a blank control and deducted from the values in experimental wells. As for the second well plate, cells were washed once and incubated in EGM 10% plus or minus VEGF 25 ng/mL for 48 h, i.e. during oligonucleotide knockdown, before executing the luminescence assay.

### 2.22.4 Cell-matrix adhesion

Cell population adhesion studies, as opposed to single cell studies, involve the analysis of attachment events for a group of cells. In a wash assay as the one used, cells are cultured in static 96 multiwell plates for the cell attachment events, followed by cell washing, providing basic quantitative adhesion data by determining the fraction of cells which remains attached. Briefly, the day before running the assay, black walled 96 well plates were coated overnight at 4°C with 1 µg/mL FN (7 replicates per condition) or 3% (w/v) BSA to control for unspecific binding (3 replicates per condition). The coating was then blocked for one hour at RT with 3% (w/v) BSA. 72h after vital fluorescence labelling with CellTracker CM-DiI and 48h after oligonucleotide transfection in 6 well plates, EPCs were detached with trypsin (trypsin 0.1% v/v in PBS), resuspended in EBM with 0.05% HSA, and immediately seeded at 10 000 cells/100 µL/coated well. Cells not stained with DIi served as internal controls. Cells at baseline were captured using Incucyte Zoom at 10x magnification, focused to the centre of the well, benefiting from gridlocked immunofluorescent imaging. After 20 mins at 37°C, nonadherent cells were washed away with warm EBM, and adherent cells were then photographed already in EGM 10% (v/v) FBS at the same gridlocked focus point. Baseline and final red object count were quantified using Incucyte zoom software **(Figure 26)**, and data are expressed as mean

adhesion on FN minus mean unspecific adhesion on HSA. The excitation and emission maxima of the fluorophore used are given in **Table 10**.

**Figure 26 | Incucyte red object count algorithm.**

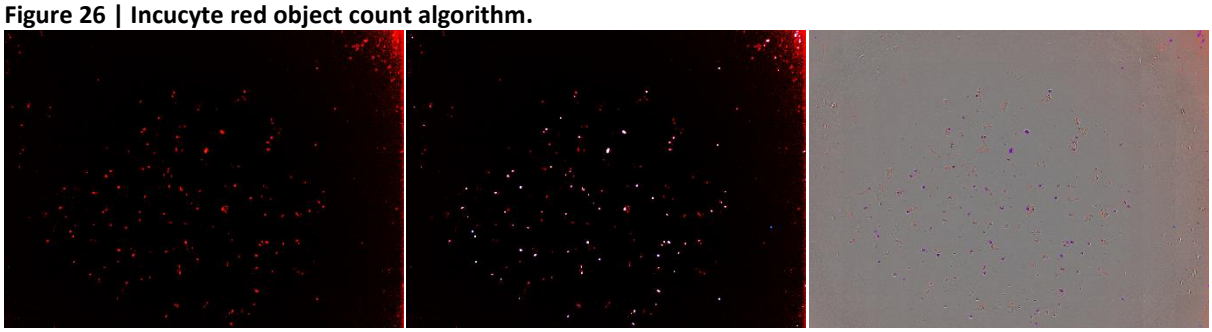

Red channel (Dii+ cells) | Incucyte algorithm mask | Merge (red channel + mask + phase)

## 2.22.5 Wound healing migration

This method is based on the observation that, upon creation of a new artificial gap, so-called ‘‘scratch’’, on a confluent cell monolayer, the cells on the edge of the newly created gap will move toward the opening to close the ‘‘scratch’’ until new cell–cell contacts are established again. Compared to other methods, the in vitro scratch assay is particularly suitable for studies on the effects of cell-matrix and cell-cell interactions on cell migration (Liang, Park, & Guan, 2007). EPCs grew to an 80% confluent monolayer in gelatin 1% coated ImageLock 96-well plates (see gelatin preparation method in section 2.10) were transfected with 30 nM miRNA using OF (as described in section 2.14.1). After 48h knockdown in EGM 10% (v/v) FBS cells were washed once with PBS and subject to 2h incubation in serum-free medium (EBM). Then, an identical wound was made in the monolayer of each well using IncuCyte woundmaker. After washing once with warm PBS, the medium was replaced with EBM 0.5% (v/v) FBS (200 µL/well) ± VEGF at 25 ng/mL. Cells were placed in Incucyte Zoom incubator time-lapse microscope, and images were captured every 2h at the desired magnification for a total duration of 48h. Each experimental condition was repeated in 6 replicates. The rate of wound closure was calculated using the Incucyte Zoom software and expressed as relative wound density. **Figure 27** represents brightfield images of assay baseline and endpoint and corresponding masks automatically defined and used by Incucyte Zoom software to calculate the rate of wound closure.

**Figure 27 | Scratch assay Incucyte algorithm.**

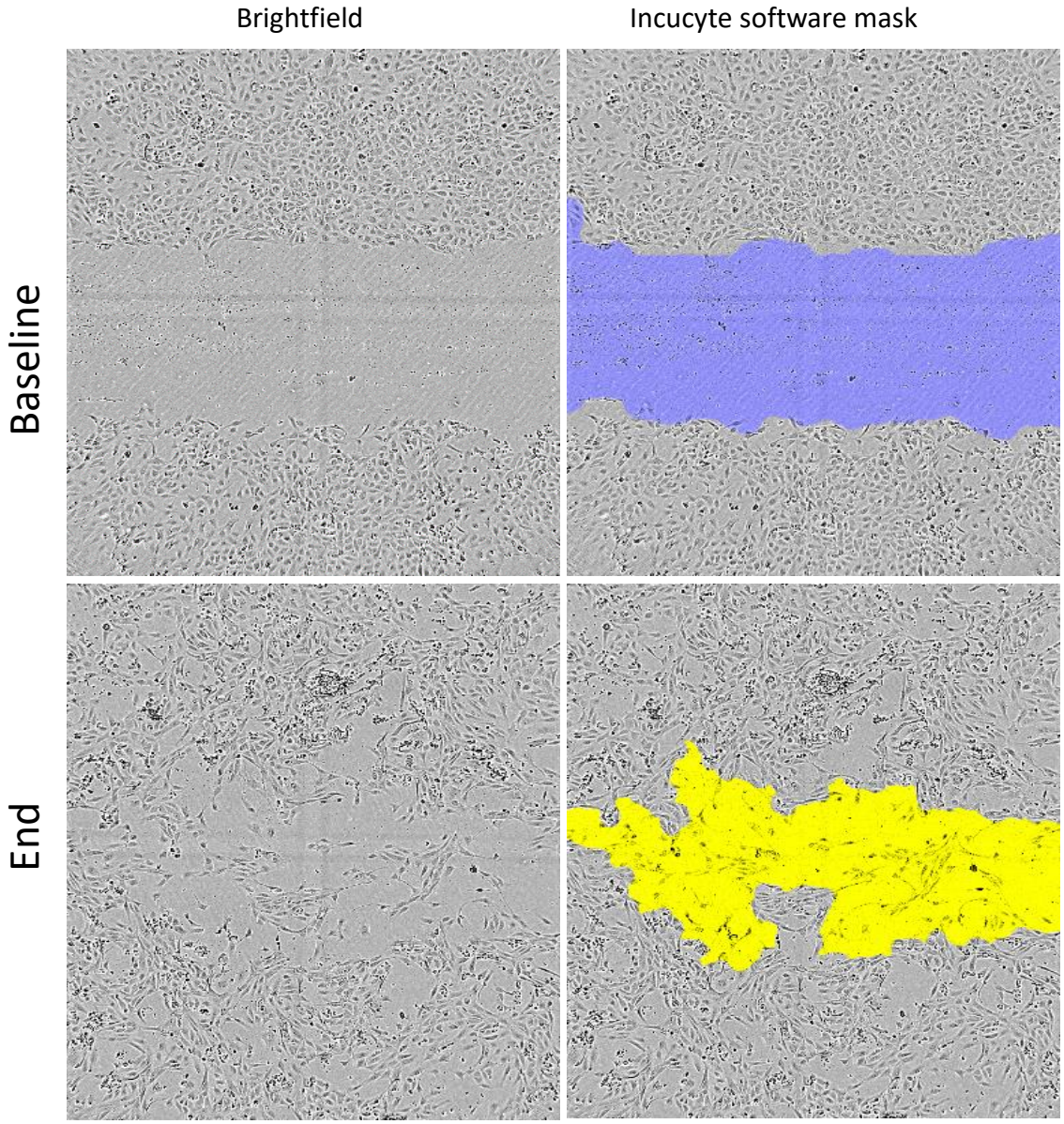


For EPCs that were transfected with NP:mir-92a inhibitor in 24 well plates, a manually performed scratch was performed as reported elsewhere (Liang et al., 2007). The day following transfection, the cell monolayer was scraped in a straight line to create a ‘‘scratch’’ with a P200 pipet tip. The debris were removed by aspirating the medium. The remaining cells were washed with EBM and incubated without serum and VEGF over 48 hours, under normal $FiO_2$ (21%) content. Cells were photographed at 5x using an Axio Observer inverted optical microscope and the denuded area ($\mu m^2$) at the end of the follow-up period was quantified with Axiovision 4.5 digital image analysis software. Duplicates were used for each experimental condition.

## 2.22.6 Chemotaxis migration

A transwell assay was used to assess cellular migration through a porous membrane towards the chemoattractant in the lower chamber as described before (Pellet-Many et al., 2011; Sadahira, Ruan, Hakomori, & Igarashi, 1992). The principle of the transwell assay was initially developed for the study of leukocyte chemotaxis by S.V. Boyden in 1962 and is thus also known as the modified Boyden chamber assay. Briefly, 48h prior to the migration assay, EPCs were transfected with different miRNAs at 30nM using OF in a 6 well plate. Transwell inserts with 8 µm membrane pore size were coated with FN 2.5 µg/mL at RT for 1h, before being inserted into 24-well plate with 700 µl EBM ± 50 ng/mL VEGF in the lower chamber **(Figure 28)**. Cell suspensions in serum-free medium were then added to the upper chamber (at a density of $5x10^5$ cells/well in 500 µl) and incubated at 37ºC for 5 h. Each treatment was performed in duplicate. Unmigrated cells were removed by scraping the upper side of the membrane with a cotton bud, and the migrated cells were fixed, stained with the Reastain Quick Diff and mounted onto glass slides. The inserts were seen and photographed under a Leica Macrofluo macroscope (×8 magnification). A total number of nuclei of migrated cells per insert were counted digitally using Image J imaging software. No VEGF was used as internal migration negative control, 10% FBS as positive internal control, and miRNA scrambled was used as transfection control.

**Figure 28 | Chemotaxis migration assay setup.**
EBM – endothelial basal medium; EPC – endothelial precursor cell; VEGF – vascular endotelial growth factor.

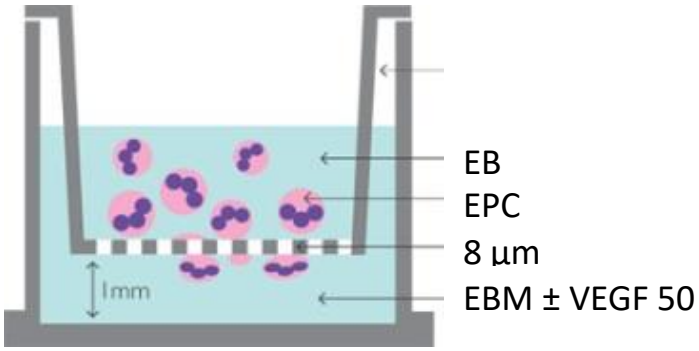

# 2.23 Rat Carotid Artery Balloon Angioplasty

Male Sprague-Dawley rats (Charles River, UK) 350-400g (2-3 months) were used for the arterial injury, following the surgical recommendations described elsewhere (Tulis, 2007). Male rats were preferred due to the potential impact of hormone levels on various cellular functions that have been identified in females (Tulis, 2007). It was important to use fully grown animals as vessel calibre will directly impact the severity of the injury from use of a standard-sized (2 French) inflated balloon catheter. Briefly, animals were induced by anesthesia using a combination of intraperitoneal midazolam (625 µg/100g animal weight) and intramuscular Fentanyl/fluanisone (40 µg/100g animal weight) and supported by Isoflurane 0.5-2% at 2 L/min $O_2$ flow, following the UCL Cruciform Biological service unit (BSU) protocol. Other pre-operative procedures included placement of the animal in heating, clipping of the neck hair, topical disinfection of the surgical field with an antiseptic solution followed by 70% alcohol, and the subcutaneous + topical administration of 1:10 Bupivacaine 0.5% with epinephrine 1:200 000 at the site of the incision. The local anaesthetic lasts up to 6 hours, has prolonged soft-tissue pain control for up to 7 hours, decreases the incidence of muscular spasm of the carotid vasculature, and offers a moderate degree of vasodilation to simplify insertion of the catheter through the arteriotomy incision. Following a midline neck skin incision, the left CCA was exposed at the bifurcation to the ECA and internal carotid artery (ICA) via blunt tissue dissection and the use of 3-0 mersilk sutures to retract the subcutaneous tissue **(Figure 29)**. The superior thyroid artery, the first branch of the ECA, was identified and ligated to ensure a bloodless operating field. The ECA was permanently ligated cranially. Surgical micro-clips were placed on the ICA and proximal CCA for temporary exclusion of the ECA, followed by a transverse arteriotomy in the ECA 3mm distally from the bifurcation produced with micro-scissors. A 2F Fogarty embolectomy catheter was inserted via the arteriotomy with the aid of vessel dilating, and the catheter advanced proximally into the CCA down to just above the aortic arch. The catheter was then inflated using 100 µL of air and then rotated while retracting. This manoeuvre was repeated three times ensuring complete endothelial denudation and exposure of the subendothelial ECM consisting of the internal elastic lamina. The length of the injured segment was similarly defined proximally by the carotid bifurcation and

distally by the edge of the omohyoid muscle. The balloon was removed from the vessel, and a proximal 3-0 sofsilk suture placed previously was tied to ligate the arteriotomy hole. The clips at the CCA and ICA were released, and the blood flow was restored. The subcutaneous tissue and skin were closed with continuous 4-0 vycril. The mean total duration of the surgery was 30 minutes. Post-operative procedures leading to swift animal recovery included top up of local anaesthesia/analgesia, the application of a topical antiseptic, spraying of the wound with skin moisturiser and the administration of supplemental fluids.

**Figure 29 | Rat carotid balloon angioplasty model.**
CCA – common carotid artery; ECA – external carotid artery; ICA – internal carotid artery.

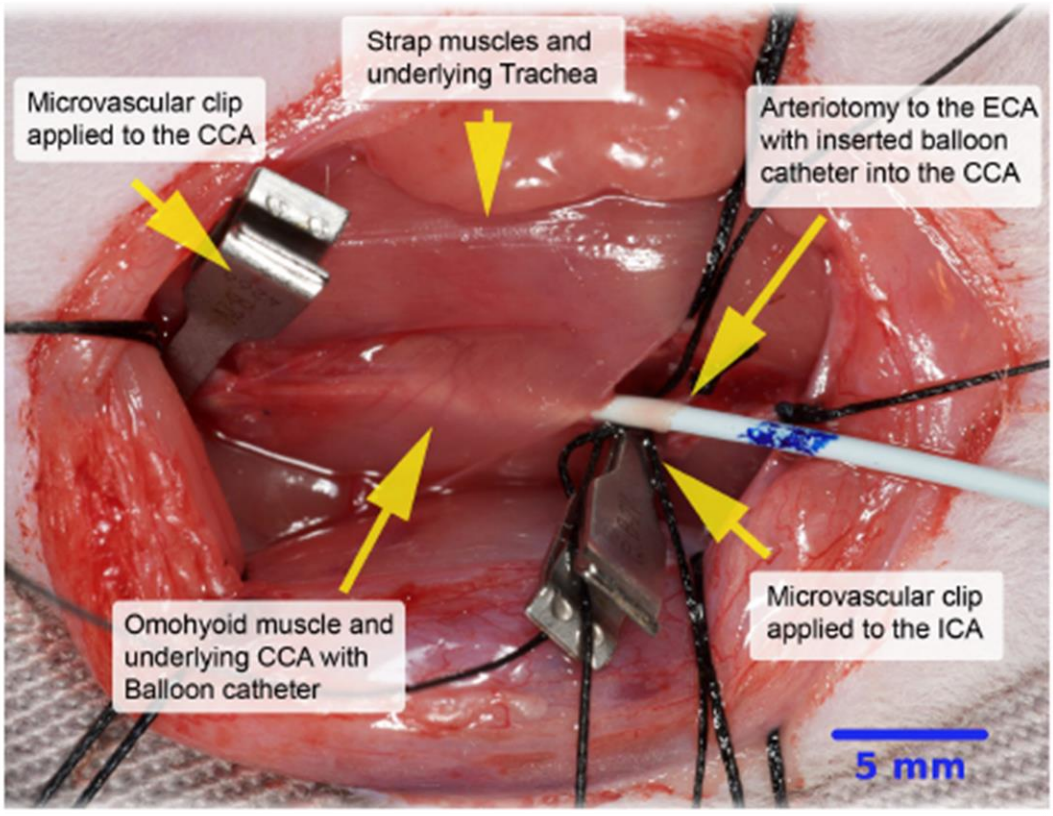

# 2.24 Intravascular transplantation of EPCs

In order to study the engraftment capacity of transfected EPCs at the angioplasty site, human late-outgrowth EPCs were previously labelled with CellTracker CM-DiI lipophilic, photostable fluorescence compound. The day after labelling, EPCs were transfected in 6 well plates with the selected miRNAs using OF. After 48h of knockdown and immediately before rat carotid artery injury, $5x10^5$ cells were resuspended in 300 µL of EBM in 1.5 mL Eppendorf. After retraction of the balloon catheter, a 26G needle catheter was inserted into the site of the arteriotomy. The cell suspension was gently infused into the clamped carotid artery over a total 10 min occlusion period. A PBS flush through the needle was then performed before ligating the artery. Rats were sacrificed 24h post-transplantation of DIi-labelled EPCs, perfused with PBS and their carotid arteries harvested and incubated in Krebs solution. In order to quantify the number of EPC transplanted at the injury site, arteries were then opened longitudinally and examined "*en face*" on a fluorescent Leica macroscope (red channel), following anatomical references (S1- distal CCA, S2 – middle CCA, S3 – proximal CCA as displayed in **Figure 30**. Engrafted cellular area was quantified using freehand selection tool in Image J.

**Figure 30 | Carotid artery normal anatomy.**
Adapted from Netter atlas.

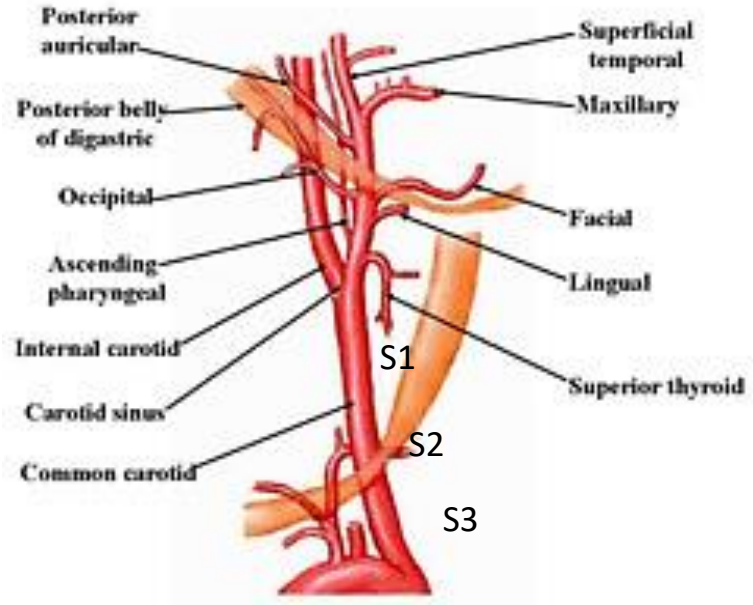

## 2.25 Harvesting of the arteries for post-mortem analysis

Following left carotid artery exposure using forceps and small scissors, the distal end of the CCA at the bifurcation suture was cut, gently lifted, and the entire length of the artery separated from extraneous tissues in a caudal direction to the aorta. Extraneous tissues still attached to the vessel were gently clean, and the lumen was freed of blood clots, if any, gently flushing the lumen with Krebs. The suture knot allowed to maintain proper orientation of the vessel. The sample was placed in 1:10 Krebs Solution for protein, fluorescence and histomorphometric assays. Alternatively, for *ex vivo* transfection assays, the samples were placed in Opti-MEM I medium supplemented with Penicillin 100 U/ml + Streptomycin 100 µg/ml, before being sliced into smaller 2-5 mm thick rings under a Leica M80 stereomicroscope. The uninjured right carotid arteries were also excised as controls.

## 2.26 Histomorphometric analysis to quantify intima/media ratio

Four serial cross-sections (5 µm thick) of hsa-mir-92a (5p) inhibitor transfected arteries (using pluronic gel), were sectioned at equally spaced intervals, and stained with hematoxylin and eosin at Barts Cancer Institute pathology services, to quantify the intima/media ratios 7 days after injury. Arteries transfected with scrambled miRNA were used as controls. The analysis was done at UCL by examining 4 cross-sectional photomicrographs (NDP Nanozoomer Digital Pathology) of each carotid artery segment in Image J software to obtain the mean relative areas of the intimal and medial layers and their respective ratios. Briefly, the medial area was calculated by subtracting the area defined by the internal elastic lamina (IEL) from the area defined by the external elastic lamina (EEL), and the intimal area was determined by subtracting the lumen area from the area defined by the IEL. Finally, the intima to media area ratio (I/M) of each section was calculated. The average I/M of the six sections was used as the I/M of this

animal. All measurements were performed twice by the same observer, who was blinded to the treatment applied to the carotid artery.

## 2.27 Double emulsion-solvent evaporation synthesis of NPs

PLGA NPs can be synthesized using different techniques, which yield different size and structural characteristics accordingly. Emulsion–solvent evaporation is a common synthesis method, and two types of this technique can be used depending on the hydrophilicity of the drug to be encapsulated: the single and double emulsion. The emulsion is defined as the mixture of two or more entirely or partially immiscible liquids obtained in the presence or absence of a surface active agent. In the single emulsion–solvent evaporation strategy, both drug (hydrophobic) and polymer are first dissolved in a water immiscible organic solvent, to form a single-phase oil solution. A suitable solvent should be able to dissolve the polymer, be poorly soluble in the continuous phase, and exhibit high volatility and low toxicity. Then, the organic oil phase is emulsified in water containing an appropriate emulsifier (O/W emulsion). This surfactant should promote a considerable reduction of the interfacial free energy, thus, avoiding the coalescence and agglomeration of drops, leading to a stabilised emulsion. If the molecule to encapsulate is hydrophilic (such as Perfluoro-1,5-crown ether - PFCE), it is necessary to prepare two emulsions instead. The drug is first dissolved in an aqueous phase (Trifluoroethanol - TFE), then added to the oil phase (water-on-oil emulsion). Then sonication allows breaking up the primary droplets of dispersed oil into nanosized droplets before the solution is again added to an aqueous solution (water-oil-water emulsion). The subsequent removal of the organic solvent transforms droplets of dispersed phase into solid particles. An extra dialysis step allows selecting NPs according to size. If needed certain electrostatic linkers can be added to the surface of the NP to modify its surface charge.

## NP synthesis

Briefly, our NPs were prepared by dissolving 100 mg PLGA in a 5 mL solution of propylene carbonate (water immiscible organic solvent). Where required, PLGA was covalently conjugated to fluoresceinamine according to a protocol reported elsewhere(Horisawa et al., 2002). The PLGA solution was mixed with 100 mg PFCE dissolved in 1 mL TFE (aqueous solvent). This solution was then added dropwise to 10 mL of an organic stabiliser Polyvinyl alcohol solution (PVA) 1% (w/v) in milQ water, sonicated for 90 seconds (50% amplitude, 0% pulse), diluted 1:6 in milQ water, and stirred for 3h at RT. The NPs were then transferred to a dialysis membrane and dialysed (Molecular weight cut off or MWCO of 50 kDa) against distilled water consecutively for 2 days. Then, NPs were coated with protamine sulphate by means of a 15-minute incubation with a 1 mg/mL (in PBS) at a 1:1 concentration ratio under agitation, at RT. After the incubation period, the NPs were dialysed (MWCO of 12-14 kDa) against distilled water for 2 days, freeze-dried and lyophilized **(Figure 31)**.

**Figure 31 | Synthesis of PLGA NP containing a fluorine compound.**
O – oil: PC – polycarbonate; PFCE - perfluoro-1,5-crown ether; PLGA - poly(lactic-co-glycolic acid); PS – protamine sulphate; PVA - Polyvinyl alcohol solution; W – water; TFE – trifluoroethanol.

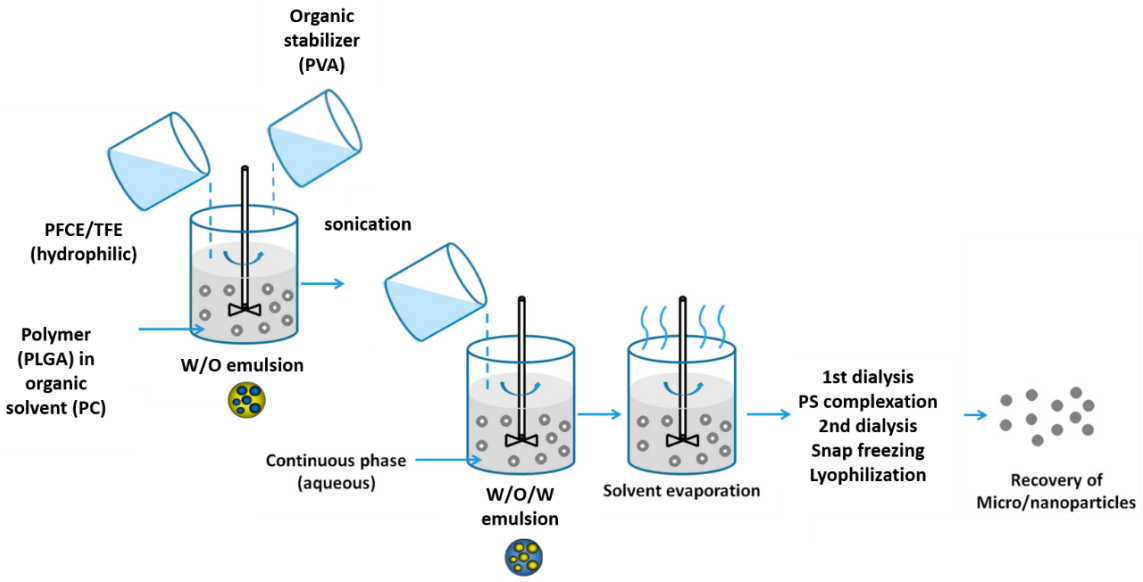

# 2.28 Complexation of miRNAs with NPs

The complexation of miRNA to the NP surface was achieved by modifying the surface chemistry of the NP since the NP are overall negatively charged. Thus, NPs were coated with protamine sulphate (PS), a polycationic peptide that makes the overall charge of the particle positive **(Figure 32)**, permitting miRNA electrostatic adsorption and also facilitating cell internalisation.

## Complexation

Briefly, for cell transfection, NPs were weighed, sterilised under ultraviolet light for 30 min and resuspended in EBM serum-free medium to a final concentration of 500 µg/mL. The suspension of NPs was vortexed and dispersed by ultrasound twice for 10 seconds. MicroRNAs were added at 400 nM and allowed to complex electrostatically with the NPs for 1 hour at 37ºC, with intermittent agitation. The resulting complexes were diluted 1:4 in the same medium. For tissue transfection, complexation was accomplished the same way in Opti-MEM I *(ex vivo* applications*)* or in PBS *(in vivo* applications*)* at 30 mg/mL, and miRNAs added at 6 µM. The resulting complexes were further diluted 1:6 in Opti-mem for *ex vivo* applications, and in either PBS or a thermoreversible gel for *in vivo* applications.

**Figure 32 | Adsorbing miRNA to the surface of PFCE encapsulating NPs is possible using a cationic peptide linker.**
Overall NP charge in brackets. miR – microRNA; PFCE - perfluoro-1,5-crown ether; PLGA - poly(lactic-co-glycolic acid); PS – protamine sulphate.

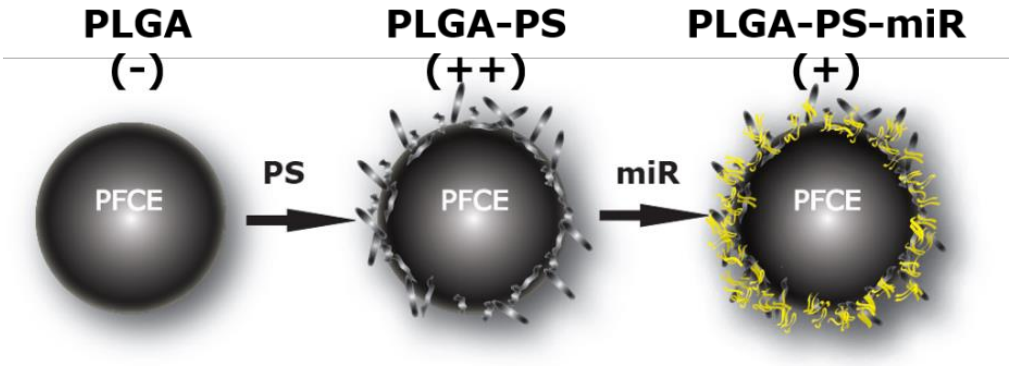

# 2.29 NP characterization by dynamic light scattering

Dynamic light scattering (DLS) is a well-established method to determine the size of NP in solution and Polydispersity index (PdI), an indicative of the heterogeneity of NPs sizes in a suspension. PdI is obtained from the photon correlation spectroscopic analysis. It is a dimensionless number extrapolated from the autocorrelation function. A PdI of <0.1 is expected for a near-monodisperse sample (Nobbmann et al., 2007). In the presence of aggregates the equipment analyses them as a large size single particle, resulting in higher PdI results. Additionally, DLS also allows the determination of the surface charge density by zeta potential. When a particle is immersed in a fluid, a range of processes causes the interface to become electrically charged. Some of the most commonly found charging mechanisms include adsorption of charged surfactants to the particle, loss of ions from the solid crystal lattice and ionisation of surface groups. These processes lead to the production of a surface charge density. The charge cannot be measured directly, but only via the electrical field it creates around the NP. Thus, the surface charge is usually characterised in terms of a voltage at the particle surface, the surface potential, rather than a charge density. The zeta potential occurs at a distance from the surface, and this will be different to the surface potential. In the simplest approximation, the potential decays exponentially with distance from the surface of the particle. The rate of decay is dependent on the electrolyte content of the fluid.

## Estimation of NP diameter

NP size was determined by Zeta Pals light scattering analysis using Zeta Plus Particle Sizing Software, as described previously (Maia et al., 2011). Briefly, NPs or NP:miR complexes were resuspended at 125 µg/mL in 1 mM KCl pH 5.5 solution and then dispersed by Branson 2510 ultrasound and vortexed twice for 30 s each time. All size measurements were performed at 90° angle after an equilibration time of 5 min at 25°C, and all data was recorded following individual run times of 60 seconds (3 runs per measurement).

### Estimation of NP charge

The zeta-potential of NPs was determined using a Zeta PALS Zeta Potential Analyser software. All data were recorded with at least five runs with a relative residual value of 0.03 (a measure of data fit quality).

## 2.30 Statistical analysis

All the experiments were performed independently at least 3 times, i.e. the definitive quantitative results were obtained from at least 3 different biological samples. Each sample generated an averaged result ± standard error of deviation following the reading of experimental replicates (the exact number of replicates per protocol are indicated in the corresponding figure legend). All data are presented as mean ± standard error of mean (SEM).

Normality was checked using Shapiro-wilk test or assumed when the n number was insufficient to test. Multiple group comparisons (for more than two groups) on normally distributed data were done by 1-way (1 independent variable) or 2-way ANOVA (>1 independent variable), using the Bonferroni's test (post-hoc) for multiple comparisons to locate statistical differences between conditions. Within subject or repetead measures analysis used when appropriate. For only two groups, these were compared by two-tailed student´s *t*-test (paired when necessary). $P \leq 0.05$ was considered statistically significant. The specifics of each statistical analysis performed are indicated in the appropriate figure legend, with the adjusted p values. Data statistical analysis was performed using GraphPad 5.0 from Prism software.

# Chapter 3: Establishment of a primary cell culture of CD34$^+$ - derived late-outgrowth EPCs

**Aims:** This chapter describes the results of a stepwise process to establish a human primary CD34$^+$-derived endothelial precursor cells (EPC) culture in which I could study the *in vitro* effects following miR-92a inhibitor treatment.

**Objectives:**

- Isolation of CD34$^+$ progenitor cells from human umbilical cord blood (UCB)
- Differention in culture of the former into vascular progeny (late-outgrowth EPCs)
- Characterization of the resulting EPCs both phenotypically and functionally to ascertain about the simultaneous presence of stem features and endothelial commitment.

**What is new:** Optimization of a CD34$^+$ MACS enrichment method; an original indirect labelling enrichment method for pig BM CD34$^+$ progenitor cells (appendix I).

# 3.1 Enrichment of $CD34^+$ and $CD133^+$ cells from human UCB

As discussed in the Introduction, $CD34^+$ (and arguably $CD133^+$) populations are likely enriched in cells with endothelial progenitor capacity. On average, using MACS microbeads system after technical optimization, I was successful in isolating 1.05 ± 0.12 $x10^6$ cells from each UCB unit sorted for CD34 **(Table 14)**. Recovered cells were present at a frequency of 0.38 ± 0.07 % of total mononuclear cells (MNCs), and their mean viability, as determined by an automated cell counter, was 78.33 % ± 1.03. As for $CD133^+$ selection, an average of 5.10 ± 1.10 $x10^5$ cells were recovered from each unit, corresponding to 0.16 % ± 0.02 from the total MNC fraction. Cell viability after the selection was maintained at a mean 76.66 % ± 5.48.

**Table 14 | Quantification of $CD34^+$ and $CD133^+$ cells obtained from human UCB.**
$CD34^+$ and $CD133^+$ cells were isolated from human UCB MNCs using MACS immunomagnetic separation system and then counted following staining with propidium iodide. Data from 9 independent ($CD34^+$) and 3 independent ($CD133^+$) isolations is presented as mean values ± SEM. CD – cluster of differentiation; MNC – mononuclear cell; SEM - standard error of the mean; UCB – umbilical cord blood

| Enriched population | MNCs ($x10^8$) | Recovered cells ($x10^5$) | Recovered cells (% of MNCs) | Viability of recovered cells (% total cells) |
|---|---|---|---|---|
| **UCB $CD34^+$ cells** | 3.31 ± 0.4 | 1.05 ± 0.12 | 0.38 ± 0.07 | 78.33 ± 1.03 |
| **UCB $CD133^+$ cells** | 3.43 ± 1.13 | 0.51 ± 0.11 | 0.16 ± 0.02 | 76.66 ± 5.48 |

Viable and functionally active $CD34^+$ and $CD133^+$ cells can be used in various downstream applications, such as flow cytometry and cell culture, but highly pure cell fractions are required. After using the optimised immunomagnetic sorting protocol with two successive column separations, the retrieved $CD34^+$ and $CD133^+$ labelled cell populations revealed a high degree of purity (99.53 % ± 0.14 and 98.27 % ± 0.21, respectively) as determined by FACS using antibodies for the same epitope **(Figure 33)**. When sampling flow through cells, I specifically focused on the gate region R3, containing cells with low granularity which included MNCs as well as progenitor cells, and examined the expression of CD34 and CD133. The R1 gate (used for enriched cells) was similar to R3 for homogeneity of results.

**Figure 33 | CD34⁺ and CD133⁺ cell fractions isolated from human UCB were highly pure.**
To determine the purity of the populations enriched for CD34⁺ or CD133⁺ by immunomagnetic sorting, cells were stained with anti-CD34 or anti-CD133 antibody conjugated with PE, before being processed by flow cytometry. Mouse immunoglobulins of the relevant IgG subclass conjugated with PE served as negative controls. **(A)** Representative FSC-SSC dot plots (R1=R3 gate) and histograms are presented. (**B)** Enriched cells exceeding a threshold fluorescence defined by the IgG control were considered positive for the corresponding CD and quantified. Results are presented in a tabular format as mean antigen positive cells percentage ± SEM from 3 independent experiments (each condition measured in duplicate). CD – cluster of differentiation; FSC – forward scatter; IgG – Immunoglobulin; PE – phycoerythrin; SEM - standard error of the mean; SSC – side scatter; UCB – umbilical cord blood.

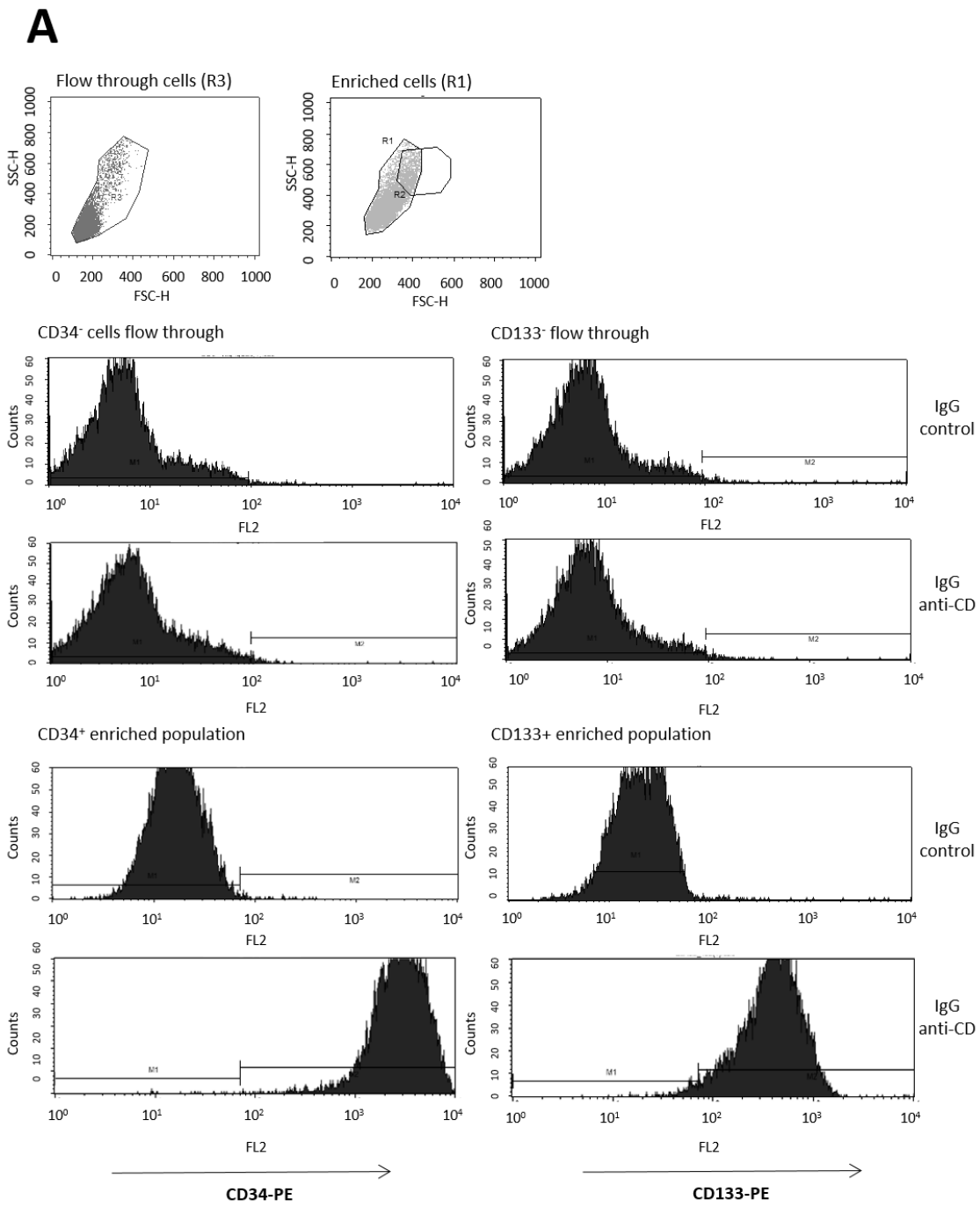

**B**

| Enriched population | Antigen | Positive cells (%) |
|---|---|---|
| **UCB CD34$^+$ cells** | CD34 | 99.53 ± 0.14 |
| **UCB CD133$^+$ cells** | CD133 | 98.27 ± 0.21 |

FACS analysis revealed that most cells enriched for CD34$^+$ (86.62 % ± 2.03) also co-expressed CD133 **(Table 15)**. Remarkably, nearly all CD133$^+$ cells were positive for surface CD34 (98.28 % ± 0.15).

**Table 15 | Most human UCB cells enriched for CD34$^+$ also co-expressed CD133 and vice-versa.**
To quantify the specific CD133 and CD34 antigen in the populations enriched for CD34$^+$ or CD133$^+$ cells by immunomagnetic sorting, respectively, cells were stained with anti-CD34 or anti-CD133 antibody conjugated with PE, before being processed by flow cytometry. Mouse immunoglobulins of the relevant IgG subclass conjugated with PE served as negative controls. Enriched cells exceeding a threshold fluorescence defined by the IgG control were considered positive for the corresponding CD and quantified. Results are presented in a tabular format as mean antigen positive cells percentage ± SEM from 3 independent experiments (each condition measured in duplicate). CD – cluster of differentiation; PE – phycoerythrin; SEM - standard error of the mean; UCB – umbilical cord blood.

| Enriched population | Antigen | Positive cells (%) |
|---|---|---|
| **UCB CD34$^+$ cells** | CD133 | 86.62 ± 2.03 |
| **UCB CD133$^+$ cells** | CD34 | 98.28 ± 0.15 |

To further characterise the levels of expression of cell surface CD34 and CD133 on enriched populations, I used flow cytometry and commercially available microbeads with known antibody binding capacity **(Figure 34)**. Assuming monovalent antibody-receptor binding, I was able to estimate the cell surface receptor density using an antibody binding capacity standard curve derived from microbeads fluorescence analysis. The isolated CD34$^+$ population expressed over 200,000 CD34 receptors per cell and only a residual density of CD133 surface molecules. On the other hand, CD133 enriched population exhibited a higher density of CD34 membrane receptors (> 300,000/cell).

**Figure 34 | Antigen surface density quantification in CD34$^+$ and CD133$^+$ cells isolated from human UCB.**
CD34 and CD133 antigen surface density quantification were performed in human UCB CD34$^+$ and CD133$^+$ cells by flow cytometry using Quantum Simply Cellular Kit. **(A)** A representative beads FSC-SSC dot plot and a fluorescence histogram of the distinct beads population with increasing avidity towards anti-CD34-PE is presented. The beads fluorescence intensities were entered in QuickCal software, which extrapolated the CD34 antibody binding capacity standard curve. **(B)** A representative FSC-SSC dot plot,

plus CD34-PE and CD133-PE histograms of CD34⁺ cells are presented. **(C)** Box plot exhibiting the quantification of CD34, CD133 surface antigen density in CD34⁺ and CD133⁺ cells (mean values ± SEM, n=3, samples run in duplicate). CD – cluster of differentiation; FSC – forward scatter; MESF/ABC - Molecules of Equivalent Soluble Fluorochrome/Antibody binding capacity; SEM – standard error mean; SSC – side scatter; PE – phycoerythrin.

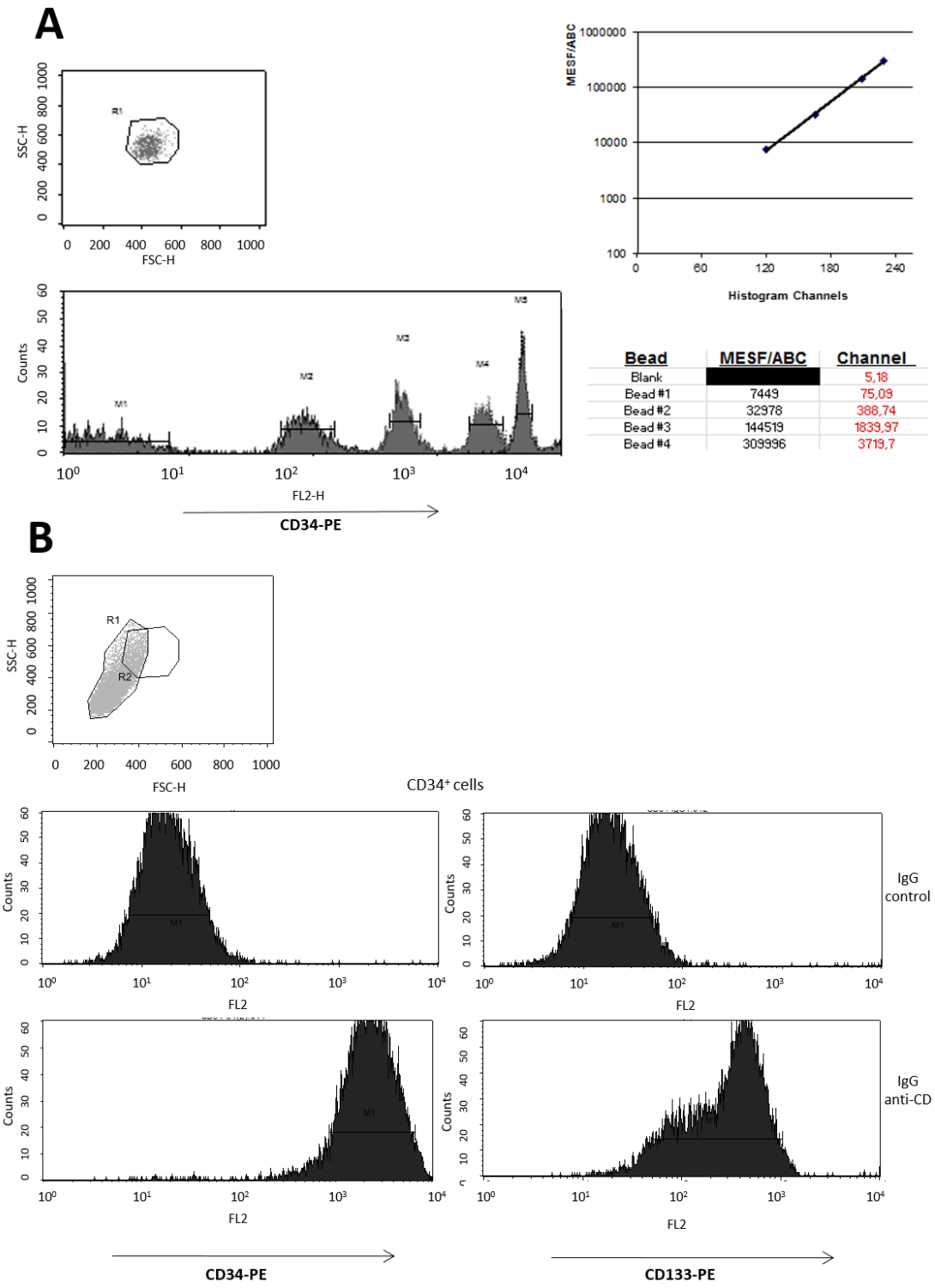


| Bead | MESF/ABC | Channel |
|---|---|---|
| Blank | | 5,18 |
| Bead #1 | 7449 | 75,09 |
| Bead #2 | 32978 | 388,74 |
| Bead #3 | 144519 | 1839,97 |
| Bead #4 | 309996 | 3719,7 |

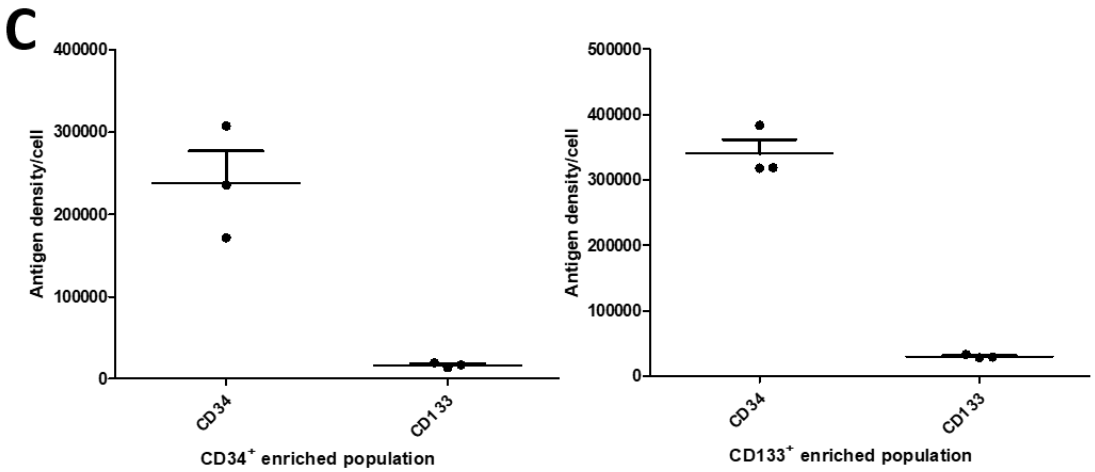


There is substantial evidence that progenitors expressing CD34 or CD133 include a population of proangiogenic cells (PACs) with a specific role in regenerative angiogenesis (Fadini et al., 2008). Since these cells can be harvested from a donor and transplanted within a few hours with minimal tissue culture-associated risks (infection, mutations), which contributes towards their clinical applicability, it would have been interesting to test these cells for miR-92a inhibitor modulation. Nevertheless, using them would pose significant technical problems, as their isolation is time-consuming and expensive. Blood donations would be needed daily. Moreover, absolute cell numbers isolated from each sample are heterogeneous from donor to donor and usually low (Janic et al., 2010), thus, it would be challenging to meet the count requirements per experimental setup. Moreover, MNCs have a very scarce cytoplasm, making them less ameneable to transfection, even with electroporation, which may result in varying efficiencies, with several cell lines and primary cells showing poor transfection rates and cell death (H. Yin et al., 2014). Adittionaly, PACs should be used with caution because of their monocytic nature and possible role in enhancing tissue inflammation (Medina et al., 2010), which could exacerbate a pre-existing pathology such as diabetic vasculopathy (Awad, Jiao, Ma, Dunnwald, & Schatteman, 2005). Moreover, CD34 and/or CD133 positivity is not a synonym of PACs. The CD34 marker can also be present in mesenchymal stem cells (MSCs) and other nonhematopoietic cell types including muscle satellite cells, epithelial progenitors, corneal keratinocytes, interstitial cells, and vascular endothelial progenitors (Sidney et al., 2014). In the blood, CD133 is a marker of both immature haematopoietic and progenitor cells (A. H. Yin et al., 1997). In other words, studying miR-

92a inhibitor biological effects in this miscellaneous population of circulating cells would possibly not be very informative.

Remarkably, among $CD34^+$ progenitor cells a small minority are known to have true endothelial differentiation potential (Medina et al., 2010) and display postnatal vasculogenic activity (Yoder et al., 2007), unlike primary PACs promoting angiogenesis via paracrine effects. Therefore, as an alternative to using monocyte-committed PACs ("early EPCs"), having optimized the protocol for isolation of highly pure fractions of $CD34^+$ cells from human UCB, I attempted to demonstrate that these progenitor cells comprehend/can be differentiated into functional late-outgrowth EPCs by culture assay. The rationale was that EPCs are equally fundamental (compared to PACs) in the re-endothelialisation process, but at a later stage (Fadini et al., 2008). The ability to amplify EPCs by *in vitro* expansion, while preserving their angiogenic potential, was considered the single most important technical advantage of using the late-outgrowth progenitors instead. Other advantages included higher transfectability and more robustness under tissue culture conditions compared to "early EPCs", and a predictable EC-like phenotype which could be evaluated by well-established functional assays (Medina et al., 2017; Timmermans et al., 2007).

## 3.2 Differentiation of late-outgrowth human EPCs from $CD34^+$ cells

Culturing UCB $CD34^+$ cells, using a protocol established during my collaboration with Biocant Institute in Portugal during my first PhD year, reproducibly generated $CD34^+$-derived late-outgrowth EPCs. Initially, freshly purified $CD34^+$ cells were small and round. After 2-6 days of tissue culture, non-adherent cells started clumping in the middle of the well, while showing a more elongated morphology with some spindle-shaped extensions **(Figure 35, A)**, which correspond to PACs/"early EPCs". By day 14, the cells in suspension were more elongated **(Figure 35, B)** and Endothelial cell – colony forming units (EC-CFUs) could be seen **(Figure 35, C)**. CFU is defined as a cell mass composed of a central cord of round cells that sits on top of elongated spindle–shaped cells sprouting at the periphery

of the colony. These cellular clusters were first described by Asahara (Asahara et al., 1997). Over time the clusters disappeared, revealing beneath a uniform adherent cell population that displayed features characteristic of more mature endothelial cells (ECs) **(Figure 35, B)**. Namely, these possessed large nuclei that were deeply indented one or several-fold. Typically, after 14–20 days of culture, these adherent $CD34^+$-derived EPCs had formed a confluent monolayer with cobblestone appearance **(Figure 35, C)** and could be expanded by tissue culture.

**Figure 35 | Late-outgrowth EPCs were successfully differentiated from human UCB $CD34^+$ cells.**
UCB human $CD34^+$ cells were differentiated into late-outgrowth EPCs. Bright-field images during differentiation were captured. **(A)** $CD34^+$ cells 2-4 days after isolation tend to accumulate in the centre of the culture well as seen at 20x; **(B)** At 14-16 days post-isolation, some of the differentiating cells assume a cobblestone-like morphology (see arrowed, 20x). **(C)** Occasionally, colony forming units from which elongated spindle-like cells radiate in all directions were also observed at 5x. **(D)** After 20 days of culture, internalisation of Ac-LDL was confirmed by IF at 20x. **(E-I)** After 20 days of culture, the presence of endothelial lineage markers was evaluated by IF. $CD34^+$-derived EPCs stained positive for **(E)** vWF (40x), **(F)** VE-cadherin (60x) and **(G)** KDR (60x), and negative for **(H)** SMA (20x). **(I)** Negative controls were obtained by using isotype-matched IgGs (20x). CD – cluster of differentiation; DAPI - 4',6-diamidino-2-phenylindole; EPC – endothelial precursor cell; IF – immunofluorescence; IgG – immunoglobulin; KDR – kinase insert domain receptor; LDL - low-density lipoprotein; SMA – smooth muscle α- actin; VE – vascular endothelial; vWF – von Willebrand factor.

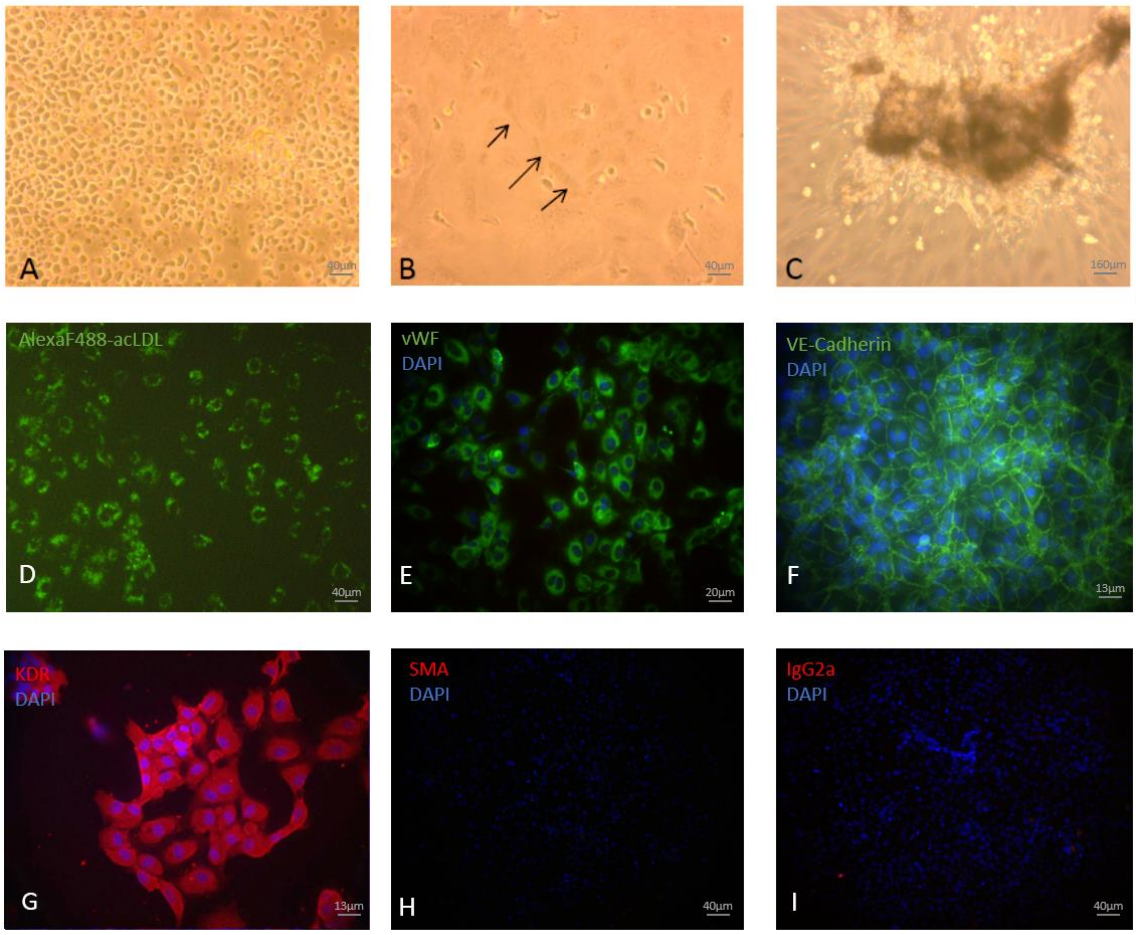

After having established EPC differentiation, I attempted different adaptations to the protocol to have a better understanding and to narrow down the source of the late-outgrowth $CD34^+$-derived EPCs. Starting from the observation that within 24 hours in culture a limited number of $CD34^+$ cells had promptly attached to the gelatin-coated flasks, I transferred non-adherent $CD34^+$ cells to fresh gelatin-coated flasks at first medium change. These cells did not become adherent and eventually died. It was also noteworthy that in the absence of the non-adherent cells, and despite the continuation of VEGF supplementation, the sparsely attached cells that were left in original flask also ultimately died. Culturing freshly isolated $CD34^+$ cells in uncoated flasks also prevented cell attachment and successful differentiation. Likewise, in the absence of VEGF, all $CD34^+$ cells failed to attach or proliferate and at that point died, indicating their dependence on exogenous vascular growth factors.

The next step was to confirm the endothelial commitment of the $CD34^+$-derived EPCs with IF, flow cytometry and functional assays, as other have done previously following their differentiation protocols (Melero-Martin et al., 2007). To do so, I initially performed IF analysis using a selected set of endothelial specific markers (Medina et al., 2017; Nguyen et al., 2009). The late-outgrowth EPCs stained positively for vascular endothelial cadherin (VE-cad), von Willebrand factor (vWF) and kinase insert domain receptor (KDR) and did not stain for Smooth muscle cell (SMC)-specific α-actin, the negative control, as expected **(Figure 35, E, F and G)**. Furthermore, EPCs efficiently incorporated Alexafluor488-conjugated ac-LDL **(Figure 35, D)**, which is another important function of mature ECs (Nguyen et al., 2009), and previously described for BM-derived EPCs (Rafii et al., 1994). Most interestingly, $CD34^+$-derived EPCs continued exhibiting the immature marker CD34 **(Figure 36)**, suggesting a likely maintenance of specific progenitor cell activity, despite the acquisition of many features from terminally differentiated ECs during differentiation.

**Figure 36 | Late-outgrowth human EPCs maintained CD34 expression.**
After 20 days of culture, the presence of stem markers was evaluated by IF at 40x magnification. Negative controls were obtained by using isotype-matched IgGs (20x). The arrows represent human $CD34^+$-derived EPCs which were still positive for CD34. They revealed an elongated morphology with extending filopodia. CD – cluster of differentiation; DAPI - 4',6-diamidino-2-phenylindole; EPC – endothelial precursor cell. IF – immunofluorescence; IgG – immunoglobulin.

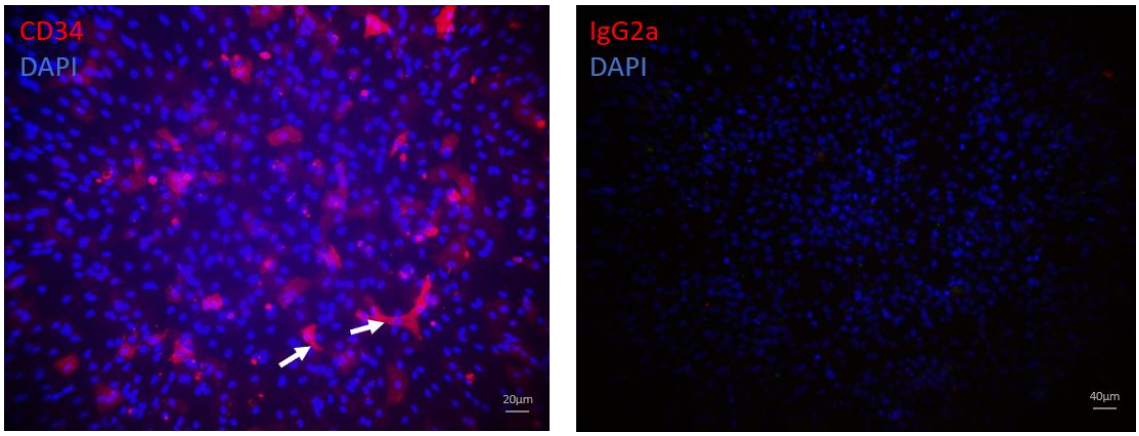


The observation that cultured cells preserved progenitor features, was further investigated by quantifying the changes in stem-like and endothelial lineage surface markers throughout the cellular differentiation process, using flow cytometry. Freshly isolated $CD34^+$ primary cells expressed approximately 10-fold more surface CD34 molecules than CD133 and expressed virtually no KDR at the surface, an EC lineage commitment marker (Eichmann et al., 1997) **(Figure 37)**. During the differentiation process CD34 antigen density decreased significantly but never ceased to be expressed at the surface, unlike CD133, another progenitor immaturity marker, which was absent by day 40 in culture. On the contrary, there was a KDR upregulation trend observed in $CD34^+$-derived EPCs.

**Figure 37 | Late-outgrowth human EPCs maintain stemness marker CD34 while acquiring vascular marker KDR.**
Quantification of CD34, CD133 and KDR surface antigen density was performed in primary human UCB $CD34^+$ cells and corresponding derived late-outgrowth EPCs ($3^{rd}$ passage) by flow cytometry, using Quantum Simply Cellular kit. **(A)** Representative FSC-SSC dot plots of cells are displayed, as well as the corresponding CD34, CD133 and KDR conjugated PE intensities' histograms. **(B)** Box plot displaying quantification of surface antigen density for $CD34^+$ primary cells vs. $CD34^+$-derived late-outgrowth EPCs (mean values ± SEM; all conditions were measured in duplicate; results in this graphic are representative of 1-3 experiments cells, depending on cell type and markers used, and therefore preliminary except for CD34 surface characterization). **(C)** Bright-field images of $CD34^+$ cells **(top)** and $CD34^+$-derived EPCs **(bottom)** were captured at 20x. CD – cluster of differentiation; EPC – endothelial precursor cell; FSC – forward scatter; KDR – kinase insert domain receptor; SEM – standard error mean; SSC – side scatter; PE – phycoerythrin; UCB – umbilical cord blood.

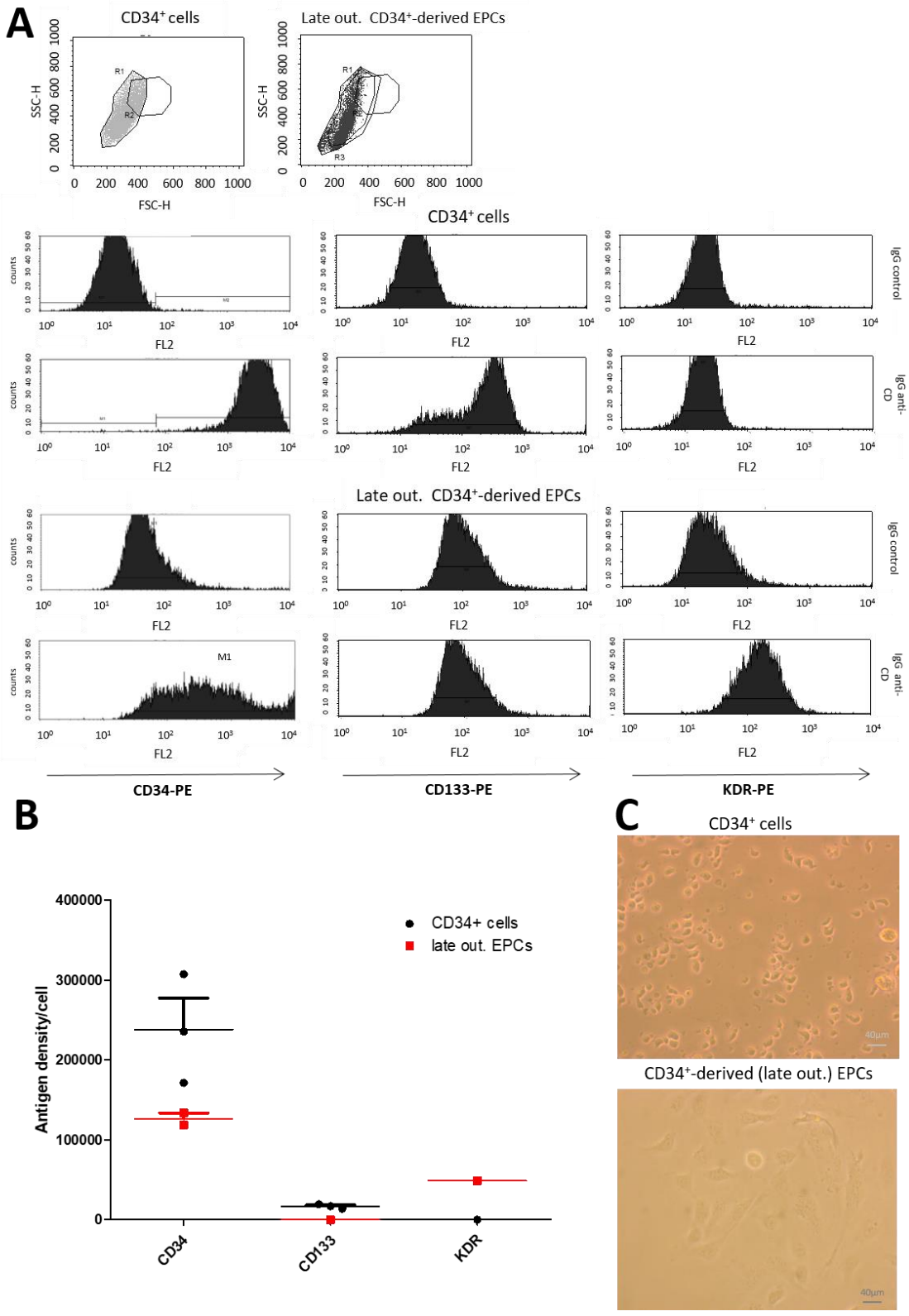


KDR upregulation in CD34$^+$-derived EPCs was further characterised by time course analysis **(Figure 38)**. Interestingly, KDR levels rose progressively to become higher than mature HUVECs by the end of differentiation, a finding also reported by others (Lavergne et al., 2011). The increase in KDR expression was sustained despite termination of FBS

and VEGF supplementation by day 25, according to the protocol, suggesting definitive commitment.

**Figure 38 | CD34⁺-derived late-outgrowth EPCs acquire KDR expression during their differentiation.** Quantification of KDR density was performed in human UCB CD34⁺ cells (non-adherent), CD34⁺-derived late-outgrowth EPCs (adherent) and mature endothelial cells (HUVECs) by flow cytometry, using Quantum Simply Cellular. **(A)** Representative FSC-SSC dot plots of cell subtypes are presented, as well as corresponding KDR conjugated PE intensity histograms. **(B)** The graphic presents the mean KDR density per cell for CD34⁺ cells versus CD34⁺-derived EPCs. The dashed line represents the mean surface KDR density expressed in HUVECs. Results in this graphic are representative of 1 (CD34⁺ cells and HUVECs) to 3 (late-outgrowth EPCs) experiments (mean values ± SEM; all conditions were measured in duplicate). CD – cluster of differentiation; EPC – endothelial precursor cell; FSC – forward scatter; HUVEC - Human Umbilical Vein Endothelial Cell; KDR – kinase insert domain receptor; PBS - phosphate-buffered saline; SEM – standard error mean; SSC – side scatter; PE – phycoerythrin.

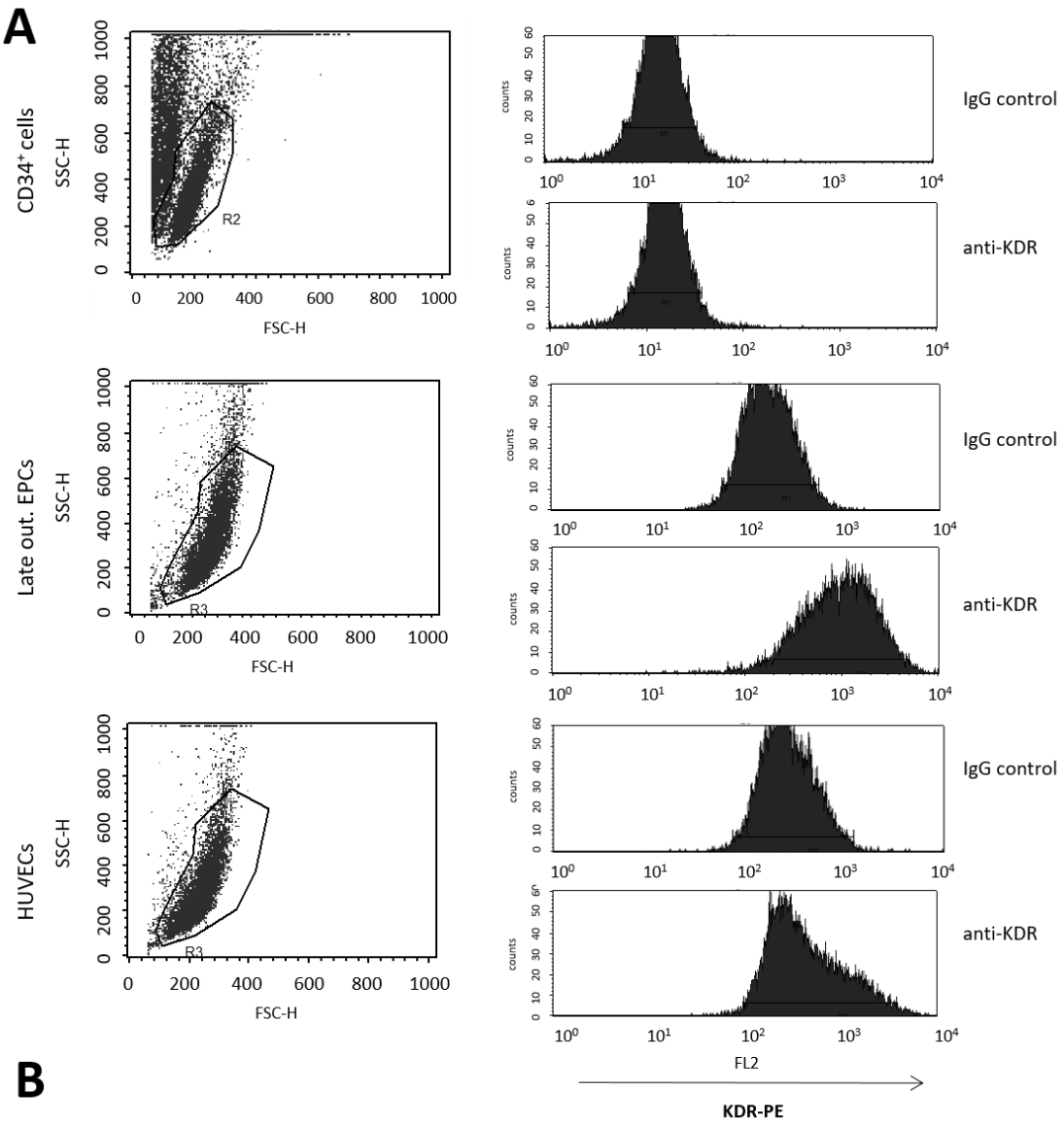

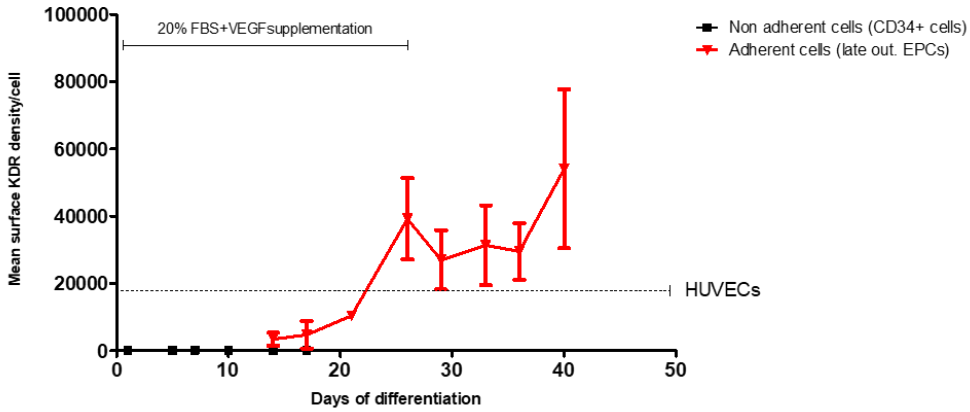


Finally, the generated CD34$^+$-derived EPCs were able to form tube networks on Matrigel **(Figure 39)**, a typical feature of endothelial commitment (Nguyen et al., 2009). Within just 6 hours of incubation, EPCs assembled into a capillary-like network on a Matrigel-coated surface, indistinguishable from those formed by HUVEC under the same conditions.

**Figure 39 | UCB CD34$^+$-derived late-outgrowth EPCs exhibit angiogenic potential.**
The angiogenesis assay was performed using a Matrigel matrix with reduced growth factor content. A set of representative brightfield images (10x magnification) taken at 15 min, 2h and 6h post incubation is presented for EPCs, revealing tubule-like formation ability. HUVECs were used as positive controls and rat colonic SMC as negative controls. CD – cluster of differentiation; EPC – endothelial precursor cell; HUVEC - Human Umbilical Vein Endothelial Cell; SMC – smooth muscle cell; UCB – umbilical cord blood.

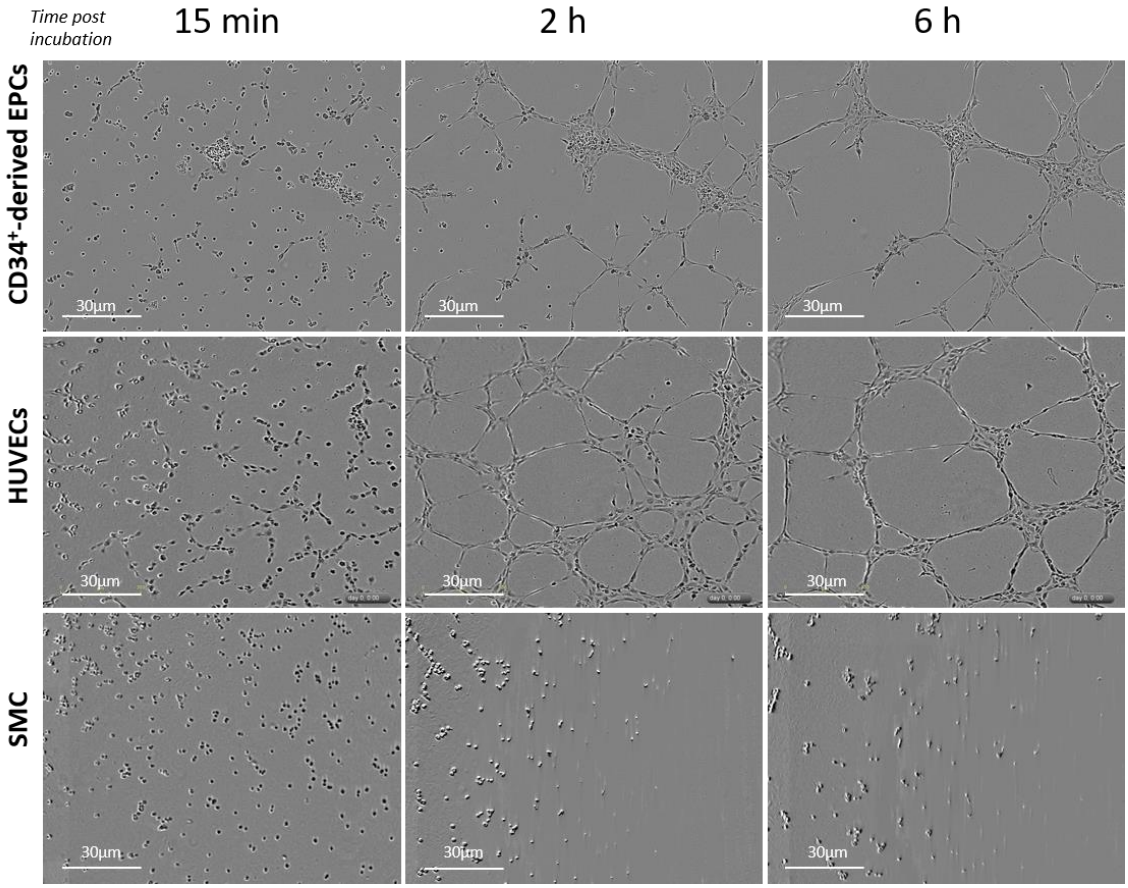

Later, I replicated the strategy with a porcine BM source generating $CD34^+$derived late-outgrowth pig EPCs, to pave the way for future autologous transplantation pre-clinical experiments with miR-92a inhibitor transfected EPCs **(Appendix I)**.

## 3.3 Differentiation of late-outgrowth human EPCs from $CD133^+$ cells was unsuccessful

Peichev and colleagues postulated that a small subset of $CD34^+$ cells from UCB, G-CSF–mobilized peripheral blood (PB) and human fetal liver, co-expressing CD133 and KDR had EPC -potential (Peichev et al., 2000). But, in fact, triple positive $CD34^+CD133^+KDR^+$ cells despite being proangiongenic, have an haematopoietic origin ($CD45^+$) and do not represent true EPCs (Case et al., 2007) since they do not possess the postnatal vasculogenic profile that was originally proposed for a cell with endothelial progenitor properties (Estes et al., 2010). Nevertheless, some groups still reported that $CD133^+$ cells can differentiate into endothelial progeny (Friedrich, Walenta, Scharlau, Nickenig, & Werner, 2006; Gehling et al., 2000; Nguyen et al., 2009). With the hypothesis that another subset of $CD133^+$ cells could comprehend a possible EPC source, I applied the same culture differentiation protocol used for $CD34^+$ cells in UCB $CD133^+$ cells. However, I was unable to generate cells with endothelial phenotype, i.e. cells did not adhere and form cobblestone shaped cell clusters, despite VEGF supplementation and 3 weeks in culture **(Appendix II)**. Hence, I studied the effects of miR-92a inhibitor in $CD34^+$-derived late-outgrowth EPCs only for the entire research project.

# 3.5 Discussion

## Human UCB were the preferred EPC source

$CD34^+$ progenitor cells are present in different blood sources. Their collection is possible from mobilised PB, bone marrow blood (BMB) and UCB. The latter has been emerging as a valuable source (Kekarainen et al., 2006), due to some unique advantages compared to the counterparts. Cord blood stem cells are immunologically naïve (Slovinska et al., 2011), present enhanced human leukocyte antigen (HLA) mismatch tolerance (Riordan, Chan, Marleau, & Ichim, 2007), and thus contribute to a reduced risk of graft-versus-host disease compared to transplantation from other sources (Grewal, Barker, Davies, & Wagner, 2003). UCB is readily available from public/private tissue banks, which are on the increase, and can safely be cryopreserved without loss of cell viability (Liao, Geyer, Yang, & Cairo, 2011; R. Z. Lin, Dreyzin, Aamodt, Dudley, & Melero-Martin, 2011). Reassuringly, outgrowth EPCs obtained from culturing UCB cryopreserved MNCs are described to be phenotypically and functionally indistinguishable from those arising from freshly isolated MNCs like the ones used in this study (R. Z. Lin et al., 2011), including their ability to generate blood capillaries *in vivo*. UCB donation is painless in contrast to that of BM or PB. Moreover, there is a lesser risk of transmitting viral infections or somatic mutations compared with using adult tissues (Roura, Pujal, Galvez-Monton, & Bayes-Genis, 2015). Strikingly, the acquisition of phenotypic and functional characteristics of the endothelial lineage has also already been reported for progenitor cells isolated from UCB (Janic et al., 2010; Pedroso et al., 2011). Compared to PB or BM, UCB-isolated $CD34^+$ cells' enhanced engraftment potential (Vormoor et al., 1994) allied with a faster proliferation rate in response to cytokine stimulation (Hao, Shah, Thiemann, Smogorzewska, & Crooks, 1995), and the generation of sevenfold more progeny under culture conditions (Hao et al., 1995), make the use of this progenitor source very promising for vascular therapy (Janic & Arbab, 2012). UCB-derived late EPCs are at a higher frequency (Yoder et al., 2007), display greater telomerase activity (Ingram et al., 2004) and are more efficient in actively forming vascular structures within ischaemic tissues than those derived from adult PB (Ingram et al., 2004). In fact, a longer stability of the vascular networks formed *in vivo* was described (Au et al., 2008). EPC

colonies from CB-MNCs emerge 5-7days earlier, were 3-fold higher in number, and consistently larger in size than in PB-MNCs(X. Gao, Yourick, & Sprando, 2017). Colonies originated from UCB progenitors can give rise to secondary and tertiary colonies, a property not shared by PB progenitors (Ingram et al., 2004), suggesting that these cells despite having undergone some degree of differentiation maintain more immature features, which may confer upon them greater tissue repair capacity. Indeed, the transcriptomic analysis shows that expression levels of progenitor markers CD34 are higher in UCB-derived late-outgrowth EPCs than their PB counterparts, confirming the apparent cell immaturity which would be consistent with their more primitive developmental stage (van Beem et al., 2009).

This might explain the fact that iPSC colonies generated from CB-EPCs are 2.5-fold higher in number than from PB-EPCs, indicating CB-EPCs have a higher reprogramming efficiency than PB-EPCs (X. Gao et al., 2017). The differences in the gene expression pattern between CB-EPCs and PB-EPCs as revealed by the transcriptomic study by Gao *et al.* using microarrays, especially those involved in the human embryonic stemcell pluripotency pathway, may result in increased endogenous expression in CB-EPCs of someof the key transcription factors such as SOX2 and OCT4, thus promote the reprogramming process and ultimately lead to an increased reprograming efficiency in these cells compared to PB-EPCs(X. Gao et al., 2017).

Consistingly, generation of EPC colonies from PB sometimes cannot be obtained from all donors, especially in relation to age and the presence of CVD (Meneveau et al., 2011). Even though the use of PB from CVD subjects would better portray EPC clonogenic and biological activity in patients with real restenosis risk, given the invasive nature of its collection, reduced circulating progenitor numbers and heterogeneous success of differentiation from patient to patient, I chose to pursue the isolation of $CD34^{+}$ progenitors from UCB instead for *in vitro* miR-92a inhibitor proof-of-principle studies. Indeed, the use of cryopreserved CB products for autologous use in the presence of adulthood CVD might be a promising strategy for cellular angiogenic therapies in the future.

## The advantage of using a mixed methodology for isolation of $CD34^+$-derived EPCs

If the identification of putative EPCs has been most controversial (Hristov et al., 2003; Medina et al., 2017), their isolation has not been any less challenging. Generally speaking, two primary isolation methods from MNCs are used (Fadini et al., 2012):

(1) Cell sorting according to surface phenotype, i.e. enriching a progeny population (Casamassimi et al., 2007; Ott et al., 2005)
(2) Colony assays, i.e., selecting EPCs by their ability to form endothelial-cell like clusters in culture, in the presence of specific differentiation growth factors (Fadini et al., 2012; Hill et al., 2003)

The direct isolation of cell populations using surface antigen markers has the advantage to specifically select defined enriched populations of cells without the need for *ex vivo* manipulation, which may induce cellular senescence and impair their regenerative function. However, a low isolation yield and the fact that it can take some time to reach a minimum cell number suitable for clinic applications are possible limitations of this technique. Moreover, given the absence of a unique cell signature that exclusively defines EPCs, a sorted population at an early state of differentiation may not reflect the putative EPCs (R. Z. Lin et al., 2011) exclusively. Indeed, comparing six flow cytometric methodologies for EPC identification using anti-CD34 and KDR markers revealed only poor to a reasonable agreement among strategies (Van Craenenbroeck et al., 2008). On the other hand, MNC culture assays have the advantage that they generate and expand late-outgrowth EPCs depending on protocol used (Fadini et al., 2012). However, it remains unclear when starting with a preparation of total unselected MNCs, how the interaction/plasticity of the different cells present in varying percentages (hematopoietic stem cells, mesenchymal stem cells, side population cells) may influence EPC phenotype (Rehman et al., 2003). Unselected MNCs can be stimulated by a variety of host growth factors that promote expression of numerous proteins, and such may lead to differential pathways of alternative macrophage activation. Thus, use of culture methods for putative EPC isolation from MNCs is fraught with complexities in identifying which cell may be playing a functional role. Additionally, most culture protocols used so far differ regarding the culture time, the type of substrate, and the positive or negative

selection of cellular subtypes during the assay. Particularly, to what extent the use of different growth factors/substrates/conditions and how the *in vitro* environment can reprogram the cells and generate an artificial phenotype, is still debatable (Muscari et al., 2010; Simard et al., 2017; Timmermans et al., 2009).

In summary, both surface phenotype sorting and MNC adherent culture methods have considerable limitations. In fact, we should keep in mind that flow cytometrically isolated EPCs probably have little in common with EPCs derived from cultured MNCs. Two profoundly different techniques may yield profoundly different biological information. Exactly to circumvent these shortcomings, I used a more reliable strategy, combining cell sorting technology with subsequent differential attachment. By first enriching a primary cell population of $CD34^+$ cells before culturing them (instead of using MNCs as the starting material), I reduced the complexity of cell composition and narrowed down possible sources for EPC generation via differential attachment, speeding up the process of expanding a pure cell population after two to three weeks in culture.

## Recovery

The $CD34^+$ cells recovery yields obtained using MACS system are in concordance with the literature, with progenitor recovery from human UCB for CD34 usually ranging from 0.1 to 0.5% of total MNCs (Chaisiripoomkere et al., 1999; D'Arena et al., 1996; Kekarainen et al., 2006). The $CD133^+$ cells recovery numbers are lower than the 0.5 to 1 % published retrieval rates using MACS system, which follow single tagging/two-step enrichment and single tagging/single column enrichment (Pelagiadis, Relakis, Kalmanti, & Dimitriou, 2012; Slovinska et al., 2011). Instead, my methodology included an extra labelling step with CD133 microbeads before the second column enrichment, which could account for the reduced recovery. Also, a wide donor heterogeneity of progenitor numbers could be suspected, as other groups also reported the different percentage of $CD133^+$ cells, often beyond the accepted range, resulting from each isolation procedure (Pelagiadis et al., 2012).

## Viability

In an attempt to optimise cell viability 20% AB human supplemented MACS buffer was used during the prolonged incubation with microbeads at 4ºC instead of plain buffer. The mean viability of recovered human $CD34^+$ progenitors (78.33 % ± 1.03) from UCB is in keeping with published post-selection results obtained by others (74 % ± 4.1)(Blake et al., 2012). The mean human UCB CD133 progenitor viability was maintained at 76.66% ± 5.48 after selection, which is similar to what is found in the literature (70-80%)(Slovinska et al., 2011). The assessment of cell viability at the end of the isolation is essential since the downstream applications required live cells. However, the fact that cells are alive may not necessarily mean they will exhibit differentiation capacity. Live cell assays, like the propidium iodide method used, miss out on cells that are pre-apoptotic or senescent due to the harsh separation. The colony forming assay is reportedly the best one to give a more relevant assessment of the ability of the progenitor cells to be used in downstream applications, taking into consideration additional factors other than whether the cells are merely alive (Tomlinson et al., 2013). Apparently, given the results of $CD34^+$ cells differentiation, one would assume cell were alive and metabolically fit.

## Purity

Purity is linked with the enrichment of cells of interest from a heterogeneous population based on defined features known to be present, such as surface markers. In the separated fraction, the percentage of target cells compared to isolated non-target cells can be calculated. According to the literature, producing highly pure progenitor fractions from UCB with good recovery has revealed to be a challenging task so far. Wynter and colleagues tested the purity after enrichment of $CD34^+$ cells from different blood sources using MACS and described outputs of 73.8% from UCB (de Wynter et al., 1995). Other groups described even lower average purities around 60% (Melnik et al., 2001). Belvedere and colleagues tested a two-step enrichment, and they reported mean $CD34^+$ cell purities of 41% and 85% after first and second passage through the MACS columns, respectively (Belvedere et al., 1999). Lately, optimised protocols have been published where purities after $CD34^+$ enrichment achieved have been boosted considerably.

Nguyen and Kekarainen groups reported > 90% purity (Kekarainen et al., 2006; Nguyen et al., 2009), while Pelagiadis *et al.* obtained 93% (Pelagiadis et al., 2012). Regarding CD133 enrichment, Ma *et al.* also used two cell separation cycles with Mini-MACS columns for CD133 selection, and they reported average purity of 91% of the CD133-enriched UCB cell products (N. Ma et al., 2006), results which are consentaneous with mine (98%). Other groups acknowledged wider variation in their purity results following their protocol, which ranged from 10% to 85% (median 60%)(Pelagiadis et al., 2012).

To my knowledge, the purity reported in this chapter is the highest (98-99%) ever reported for both progenitor types. This may be attributed to specific modifications (to the manufacturer protocol) introduced to increase the output target cell purity. The handling of UCB can be challenging due to the relatively high content of nucleated erythroid precursors and granulocytes, which may have a similar density to MNCs, thus negatively influencing their isolation (Kekarainen et al., 2006). Separation of MNCs, the initial step of progenitor isolation, was performed from diluted buffy coats using a histopaque density centrifugation method. However, there are even problems with specificity at this stage, as the differing densities of MNCs and granulocytes are, in some instances, not large enough to be separated by the histopaque. Therefore, to prevent unwanted cell clumping (Hering et al., 1989) and maximise single cell labelling I incubated the cell solution with DNAse after each following centrifugation. Plus, 30 µm pre-separation filters were used before injecting the cell solution into the magnetic column with the objective of promoting individual cell retention. Additionally, to increase the purity of the isolated human progenitor cells, the eluted fraction was labelled and enriched once more over a second magnetic column, to take further advantage of the antibody–antigen specificity, a methodology also applied by others (Kekarainen et al., 2006). Single column separation of $CD34^+$ cells may result in low purity (typically <50%), yet a relatively large number of cells can be obtained. Two successive column separations with the additional labelling step increased the purity to >90%, without significantly lowering the yield recovery. It is worth mentioning that the choice to use QBEnd10 microbead-conjugated antibodies for human CD34 isolation was deemed appropriate according to literary evidence. There are over 30 monoclonal antibodies against CD34 selecting for different epitopes which may be sensitive to cleavage with neuraminidases (sialidase) and glycoproteases (Lanza, Healy, &

Sutherland, 2001). Their binding is dependent on sialic acid residues remaining on the antigen. QBEnd10 is one of the most frequently used antibodies since it has been shown to detect both sialylated and desialylated CD34 successfully and as the epitope is at the N-terminus, it is ideally suited to selection protocols such as MACS (Sidney et al., 2014). Also of particular note, cells were left to recover 48h in serum free medium supplemented with Flt3 ligand and SCF before flow cytometry phenotyping. This technicality was particularly important because the antibodies used for flow cytometry were chosen precisely to tag the same epitopes than the microbeads antibodies, to increase analysis specificity. The selected period was sufficient to allow the magnetic microbeads used for cell isolation to disintegrate from the cell surface, according to Miltenyi Biotec reply to my questions.

Even after all the pursued modifications, in the end, there will always be a residual pool of contaminating granulocytes, but the evidence is that they do not adhere to culture dishes during the differentiation of EPCs in culture (M. Aoki, Yasutake, & Murohara, 2004), and thus are easily removed for the first replacement of culture medium.

## The origin of $CD34^+$-derived late-outgrowth EPCs

The baseline levels of the immature marker CD133 expression (86.62 % ± 2.03) observed in freshly isolated UCB $CD34^+$ cells are in keeping with the literature, as some groups have also highlighted that most $CD34^+$ cells (anywhere over 80%) also expressed CD133 (Nguyen et al., 2009; C. Zhang et al., 2014). Baseline flow cytometry also revealed that nearly all retrieved UCB $CD133^+$ cells (98.28 % ± 0.15) co-expressed CD34 surface marker, a result also witnessed by others (Gehling et al., 2000; Herrmann et al., 2014). In fact, in the hematopoietic system, CD133 expression seems to be narrowed to a subset of $CD34^{bright}$ progenitor cells in human fetal liver, BM, UCB and PB (Buhring et al., 1999; A. H. Yin et al., 1997), and the double positive cells should not be regarded as EPCs because they lack endothelial markers and mostly represent HPCs which are also CD45-positive (Case et al., 2007; Gehling et al., 2000; Medina et al., 2017; Timmermans et al., 2007).

I believe that the relatively small number of putative EPCs that became adherent in culture were not simultaneously $CD34^+$ and $CD133^+$ **(Figure 40)**. According to the flow cytometry results, $CD34^+CD133^+$ cells were confined to the cellular suspension which was discarded after the first medium change. Transfering those non-adherent $CD34^+$ cells to gelatin-coated flasks cells did not generate adherent EPCs, therefore possibly narrowing the EPC source to the originally attached $CD34^+$ cells within the first hours in culture. I envision that these adherent cells were $CD34^+CD45^-KDR^+$, as suggested by others (Timmermans et al., 2009). By attaching to the matrix within 24 hours in culture, the $KDR^+$ (VEGF receptor) cells were then able to complete their differentiation driven by VEGF, while further benefiting from the paracrine provision of PACs in suspension. In fact, the supporting role of PACs cells in suspension was highlighted by the fact that their removal early in the differentiation protocol (despite VEGF supplementation), conditioned the sparsely attached cells to senesce and die. If not for the supporting role of PACs in the differentiation, I believe that adding CD45 (negative selection) or KDR (positive selection) MACS step to $CD34^+$ enriched cells would contribute to narrow down even further the EPC source to $CD34^+KDR^+$ precursors.

Alternatively, the possibility that late EPCs originate from a rare population of cells within the PACs must be acknowledged. The environment may influence the cultured cells' fate and function. It is possible that a particular subset of $CD34^+(CD45^+CD133^{+/-}?)$ PACs might have lost CD45 positivity and gained KDR expression in culture, allowing them to become VEGF-responsive **(Figure 40)**. KDR positivity then would grant the progenitor cells the ability to respond to the external VEGF stimuli driving further maturation and expansion. Remarkably, regardless of the true EPC origin, in the absence of VEGF, all $CD34^+$ cells failed to attach or proliferate and at that point died, indicating their dependence on exogenous vascular growth factors.

**Figure 40 | Hypothetical origin of $CD34^+$-derived late-outgrowth EPCs.**
KDR positivity grants the progenitor cells the ability to respond to the external VEGF stimuli driving differentiation and expansion. Therefore, $CD34^+$-derived EPCs might have originated from a minuscule and outnumbered subset of $CD34^+$ cells (likely $CD45^-KDR^+$) which adhere to the gelatin coating within the first days. Alternatively, a particular subset of $CD34^+CD45^+$ PACs might have lost CD45 positivity and gained KDR expression in culture, allowing them to respond to VEGF. In both pathways, adherent $CD34^+$ cells were supported paracrinally by the PACs in suspension, allowing for the acquisition of terminally mature EC markers and expansion of the former. CD – cluster of differentiation; KDR – kinase insert domain receptor; PAC – proangiogenic cells; VEGF – vascular endothelial growth factor.

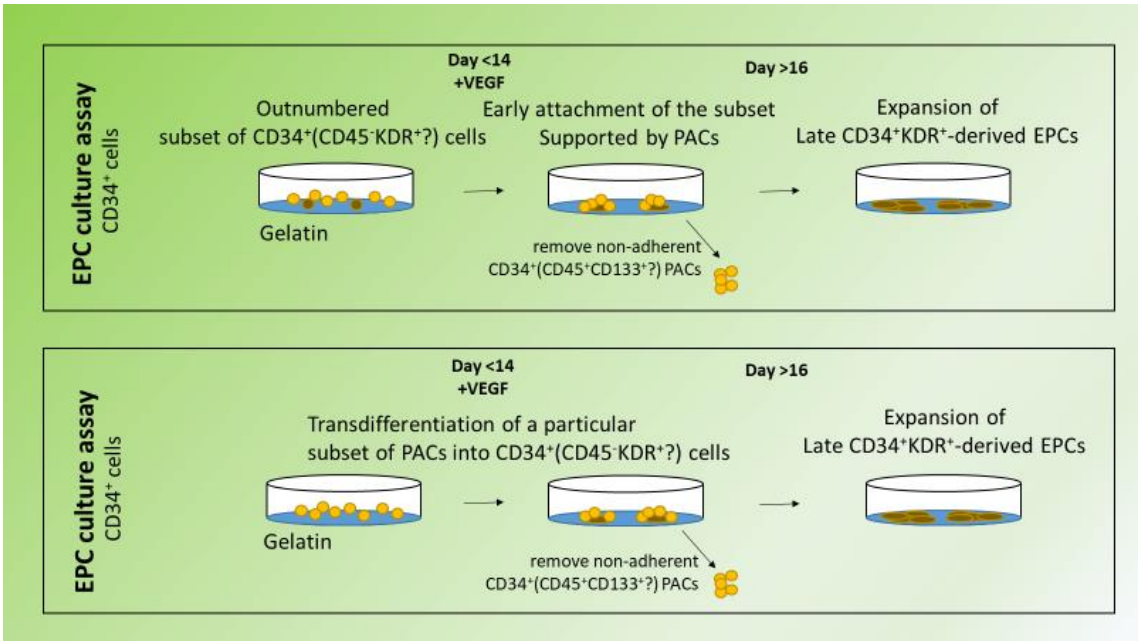


This theory is plausible also when interpreting the unsuccessful differentiation of $CD133^+$ cells into EPCs. To understand this result, we need to go back to Timmermans's experiments (Timmermans et al., 2007). He did not detect CD133 expression in $CD34^+CD45^-KDR^+$ cells (best late-outgrowth EPC candidate to date), seconding Delorme's findings (Delorme et al., 2005). He then examined whether highly purified $CD133^+$ cells were able to generate cells with endothelial phenotype, but he failed to show endothelial commitment. Unlike $CD34^+$ enriched cells, no $CD45^-$ cells could be demonstrated in the MACS-purified $CD133^+$ population given that all $CD133^+$ cells were limited to $CD45^+$ cells (i.e PACs). Contrastingly, Gehling and Quirici reported having generated EPCs from $CD133^+$ cells (Gehling et al., 2000; Quirici et al., 2001). The contradictory results from Gehling and Quirici may be because progenitor populations used in these studies were selected by highly variable protocols yielding suboptimal enrichment purities: 72% (range 62%-98%) and 90% ± 5, respectively. It is possible that contaminating $CD34^+CD133^-KDR^+$ cells within the heterogeneous $CD133^+$ enriched fraction might have originated the derived late-outgrowth EPCs. Alternatively, since the cells generated were not extensively phenotyped (using morphology, proliferative capacity, surface markers FACS, in vitro functionality tests), they might not be late-outgrowth EPCs, but rather $CD45^+$ PACs, just like the ones generated by others from $CD34^+CD45^+$ cells (Timmermans et al., 2007), $CD14^+$ monocytes (Yoon et al., 2005), $CD34^-$ cells (Harraz, Jiao, Hanlon, Hartley, & Schatteman, 2001) and total $CD45^+$ cells

(Timmermans et al., 2007). In summary, the use of higher cell purities, such as described in this chapter, appears to mitigate against effects of population heterogeneity and points to the true EPC source being a very small subset of $CD34^+CD45^-KDR^+$ cells. However, to validate the EPC differentiation capacity of a candidate $CD34^+$ progenitor cell, a single cell type study would offer the most rigorous approach. However, several biological and technical obstacles need to be overcome in performing such a clonal assay. For instance, an isolated single cell population may behave differently in the absence of other cells, as revealed when non-adherent cells were removed from the culture. Hence, culturing a single cell may not be an appropriate EPC culture assay, but may require the presence of supporting cells with a different phenotype or function.

## The phenotype of $CD34^+$-derived late-outgrowth EPCs

The culture of UCB and BM $CD34^+$ cells yielded two cell types, as previously described for whole MNC assays (Fadini et al., 2012). Initially, non-adherent spindle-shaped PACs developed after 4–7 days in culture **(Figure 35)**. At a later stage in culture (14-16 days post-isolation), $CD34^+$-derived late-outgrowth cells appeared, fully matching the described EPC-defining criteria, based on morphology (monolayer with cobblestone pattern as seen in **Figure 35**) and the presence of surface markers detected by IF and FACS. EPCs are characterised by including hematopoietic stemness and endothelial commitment markers in combination (Medina et al., 2017). Hence, the expression of the stemness marker, CD34, was followed during the culture protocol. Research indicates a correlation between CD34 expression and cell plasticity, with the loss of CD34 suggestive of lineage commitment (J. H. Jang et al., 2007; Sidney et al., 2014). Accordingly, CD34 antigen density was highest on early progenitors and gradually reduced as the cells attached and matured, but it was still detectable at the end of differentiation in contrast to most cultured ECs (Siemerink et al., 2012). This was demonstrated in the $CD34^+$-derived late-outgrowth EPCs both by IF and flow cytometry. Remarkably, most ECs are also negative for CD34 *in vivo*, particularly in larger veins and arteries (Fina et al., 1990). However, there is a subset of adult ECs that do express CD34, and these are more prevalent in smaller blood vessels (Siemerink et al., 2012). These specialised vessel $CD34^+$-ECs seem to be quiescent (Siemerink et al., 2012) and when activated become

involved in migration and adhesion at the tip of vascular sprouts (Fina et al., 1990). They are more elongated, lack tight junctions, and extend filopodia (Siemerink et al., 2012), in contrast to the typical cobblestone ECs. The sialomucin CD34 is largely expressed on the *filopodia* at the luminal membrane of these tip cells, and evidence underlines the critical role of CD34 in sites of active angiogenesis (Schlingemann et al., 1990). CD34 is proposed to act as an anti-adhesive molecule during lumen formation in developing blood vessels, by maintaining or promoting the separation between contralateral apical endothelial cell surfaces in a luminal tube, while allowing the migration of tip cells and the movement and probing of their filopodia through the tissue matrix (Nielsen & McNagny, 2009). According to my CD34 IF images, some of the $CD34^{+}$-derived late-outgrowth EPCs seem remarkably similar to these tip cells. Thus, it is fair to assume that after differentiation we might end up with a mixed population of $CD34^{bright}$ EPCs which are more associated with migration/adhesion, and $CD34^{dim\ to\ neg}$ EPCs with more of a proliferative phenotype. The corresponding flow cytometry histogram in **Figure 37** seems to confirm exactly the existence of that mixed CD34 population corresponding to two distinct spikes. Importantly, and in agreement with others (Medina et al., 2017), the EPCs did not express the leukocyte markers CD133 as shown by flow cytometry **(Figure 37)**. Unlike cells in suspension identified as $CD34^{+}CD133^{+}$, adherent cells did not exhibit surface CD133. Either all $CD133^{+}$ cells were confined to cells in suspension corresponding to PACs (a possibility already addressed) or differentiating adherent $CD34^{+}$ cells abolished the expression of CD133 on their surface, a phenomenon similarly seen in the maturation of $CD133^{+}$ HSCs (Miraglia et al., 1997; Quirici et al., 2001; A. H. Yin et al., 1997). Regarding commitment markers, KDR is known to be involved in the early stages of vasculogenesis (T. P. Yamaguchi, Dumont, Conlon, Breitman, & Rossant, 1993). The expression of cell surface KDR is inducible by VEGF (Tang et al., 2008) and considered to be mostly EC-specific (J. H. Jang et al., 2007). I have noted that as soon as the $CD34^{+}$-derived EPC colonies were formed (day 14), the cells started showing (as expected) a progressive upregulation of KDR, which persisted beyond the withdrawal of VEGF supplementation, demonstrating definitive EC-commitment. Remarkably, $CD34^{+}$derived-EPCs positively incorporated ac-LDL. Contrary to traditional belief the ability to uptake ac-LDL is not unique to committed ECs. Recently, it was demonstrated that monocytes and macrophage could also take up ac-LDL and bind lectin (Ouchi et al.,

2001). That is one of the reasons why a combined characterization of the putative EPCs was sought using additional IF to identify lineage commitment markers and functional assays. The continuous culturing revealed *de novo* expression of mature EC markers. $CD34^+$-derived EPCs stained positive for vWF, VE-cadherin and was negative for SMA, a typical EC-expression profile also obtained with other EPC differentiation attempts (Fujiyama et al., 2003; J. H. Jang et al., 2007). Confirmation of endothelial phenotype came from directly testing for endothelial angiogenesis capacity in a Matrigel assay, which was positive. Although Matrigel has been shown to direct ECs along the differentiation pathway, there is some debate as to whether tubules generated on Matrigel represent functional capillaries, as the presence of lumen has been shown by some groups using electron and light microscopy (Connolly, Simpson, Hewlett, & Hall, 2002) and disputed by others who could not detect a lumen(Bikfalvi, Cramer, Tenza, & Tobelem, 1991). Moreover, it should also be noted that some non-EC types including primary human fibroblasts, glioblastoma cells and human prostate carcinoma cell line have been shown to also form 'tubules' on Matrigel (Donovan, Brown, Bishop, & Lewis, 2001), thus, the results should be interpreted with caution. An alternative assay to test angiogenesis capacity is the organotypic co-culture model in which fibroblasts are co-cultured with ECs, which I have used to test the functionality of miR-92a inhibitor in EPCs in the next chapter. The fibroblast secretes matrix components that act as a scaffold and enables the EC to form sprouting tubules that contain lumen, which more closely resemble the capillary bed in vivo (Donovan et al., 2001). However, as this assay is time-consuming (it lasts up to 12–14 days), the results measure proliferation as well as differentiation.

One might speculate that the mere occurrence of outgrowth is insufficient evidence to confirm the presence of EPCs. To make things more complicated, CECs also proliferate in culture (A. Solovey et al., 1997) and are $CD34^+KDR^+$ like EPCs (Cappellari et al., 2016). However, unlike late EPCs (Y. Lin et al., 2000), CECs (or other ECs for that matter) bear low proliferative potential in culture (Blann et al., 2005) (as evidenced by the routine use of vessel segments as sources for endothelial culture in vitro which stop proliferating after a few passages). Despite EPC robustness and endurance to oxidative stress (Rossig, Urbich, & Dimmeler, 2004), I did not use $CD34^+$-derived late-outgrowth EPCs for

experiments beyond their 6$^{th}$ passage in culture. At that point, EPC senescence in culture and transition from endothelial to other lineage cells have (rarely) been described (Ikutomi et al., 2015). Ikutomi and colleagues reported that older EPCs presented *de novo* staining with a fibroblast marker vimentin and CD90 compared to younger EPCs, which likely supports my observation that the cultivated EPCs did progressively lose their proangiogenic potential over time.

In summary the generated CD34$^{+}$-derived EPCs ticked all the the minimum requirements for the definition by Medina et al. of an endothelial cell forming colony (ECFC): unequivocal endothelial cell phenotype (depicted as positive for CD31, VE-Cadherin, von Willebrand factor, and VEGFR2), significant proliferative potential, and possess vascular network forming potential *in vitro* and *in vivo* (Medina et al., 2017), the latter condition not tested for time restraints.

# Results

# Chapter 4: Post-transcriptional modulation of miR-92a inhibitor on CD34$^+$-derived late-outgrowth EPCs

**Aims:** This chapter describes the optimisation of a priming strategy capable of enhancing the capacity of EPCs to promote a faster re-endothelialisation in the post-injury setting.

**Objectives:**

- Transfection of human CD34$^+$-derived late-outgrowth endothelial precursor cells' (EPCs) transfection with miR-92a inhibitor using oligofectamine (OF)
- Testing treatment with both miR-92a inhibitor strands, its optimal concentration and treatment duration for maximal target protein upregulation.
- Demonstration of the post-transcriptional modulation of miR-92a inhibitor on its target proteins, namely Integrin alpha 5 subunit (ITGA5), and the subsequent *in vitro* and *ex vivo* functional repercussions on EPCs.
- Clarification of the mechanistic pathways by which miR-92a inhibition exerts its functions in EPCs by co-transfection studies with si-ITGA5

**What is new:** Demonstration of pro-angiogenic,-migratory,-proliferative, and -adhesive effects of miR-92a inhibitor treatment on CD34$^+$-derived EPCs, which are partially abrogated by ITGA5 knockdown (adhesion).

# 4.1 miR-92a inhibitor is efficiently internalised by EPCs using oligofectamine

Bonauer *et al.* used Lipofectamine RNAiMAX (Invitrogen) to transfect miR-92a mimic and inhibitor into Human Umbilical Vein Endothelial Cell (HUVECs) (Bonauer et al., 2009), whereas Iaconetti *et al.* utilised siPORT NeoFX Transfection Agent (Ambion) in rat aortic ECs (Iaconetti et al., 2012). Moreover, the mirVana™ miRNA manufacturer has validated Lipofectamine® RNAiMAX for transfection of its mimics and inhibitors in cell-based systems. Therefore, I have attempted to use both transfection reagents in $CD34^+$-derived EPCs to facilitate miR-92a (mimic and inhibitor) internalisation, but with no success (**Appendix III).**

Successful transfection of miR-92a and its inhibitor into $CD34^+$-derived EPCs at 30 nM was only accomplished using OF **(Figure 41)**, a liposomal reagent previously used to transfect oligonucleotides into HUVECs, bovine and human aortic endothelial cells (ECs) (Chamorro-Jorganes et al., 2011). The IF staining demonstrated that internalisation of miR-92a inhibitor only occurred when using the liposomal transfection reagent since miRNAs are negatively charged particles unable to transmigrate across the cellular layer by themselves.

**Figure 41 | miR-92a is internalised by CD34$^{+}$-derived EPCs using oligofectamine**
After OF transfection, confirmation of FITC conjugated miR-92a internalisation was evaluated by IF staining at 20x. AB – antibody; DAPI - 4',6-diamidino-2-phenylindole; FITC - Fluorescein isothiocyanate; miR – microRNA; OF – oligofectamine; PFA – paraformaldehyde.

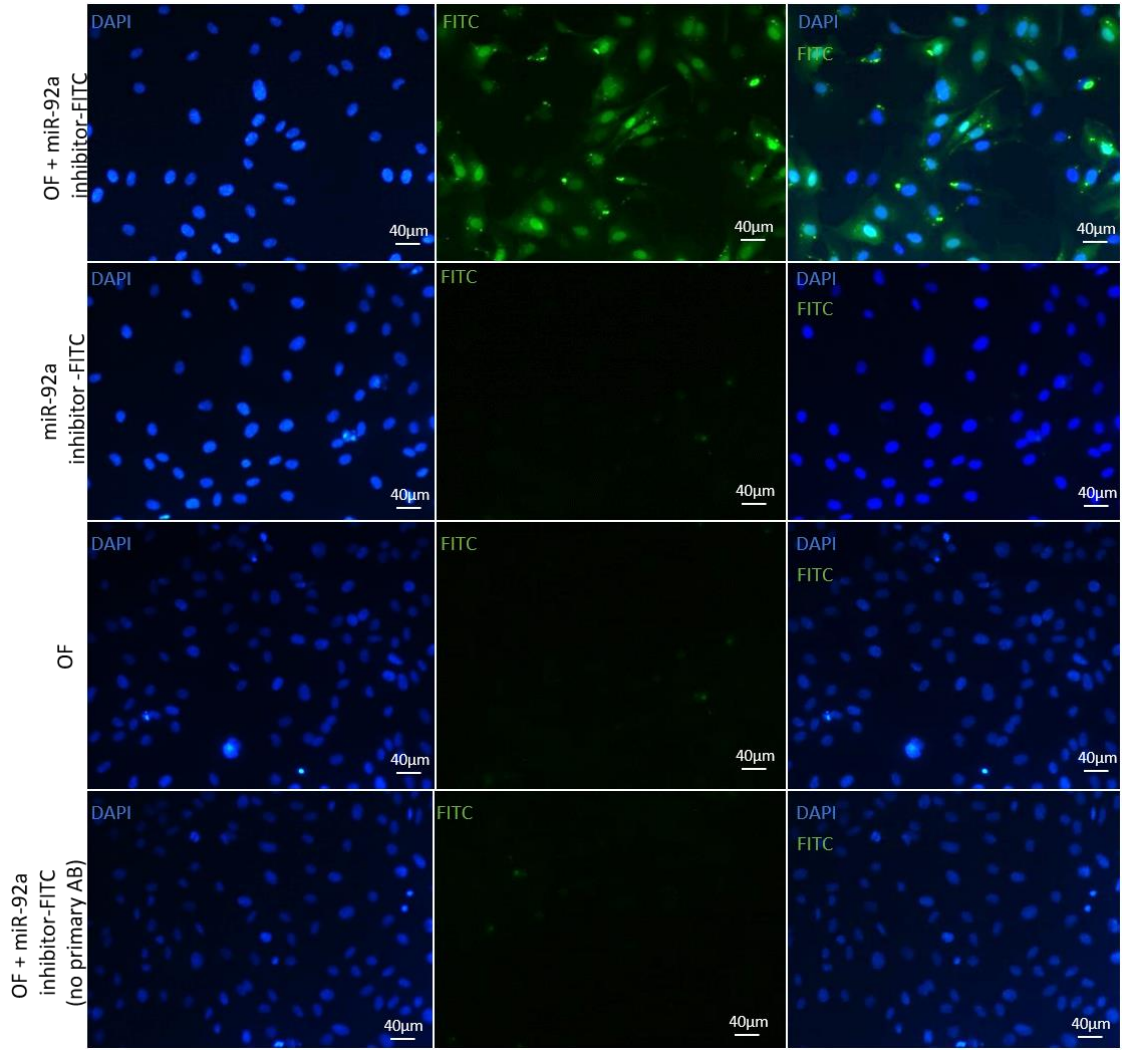


The efficiency of cellular transfection using OF was 93.7 % as assessed by flow cytometry, i.e. almost every cell internalised the miRNA of interest using the proposed protocol **(Figure 42)**.

**Figure 42 | Internalisation of miR-92a inhibitor by CD34$^+$-derived EPCs using oligofectamine is highly efficient.**

The OF transfection of human CD34$^+$-derived late-outgrowth EPCs with miR-92a inhibitor was confirmed by flow cytometry. Cells treated only with OF were used as negative transfection controls. Preliminary results are plotted as mean values ± SD after 1 independent experiment. FITC - Fluorescein isothiocyanate; miR– microRNA; SD – standard deviation.

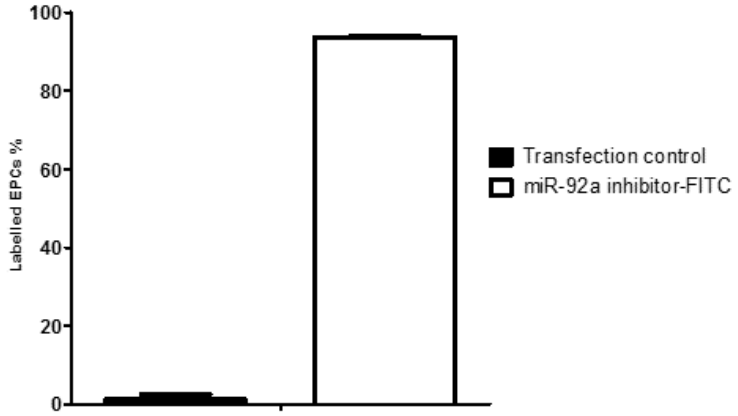


Mature miRNAs after exerting their biological post-transcriptional repression activity are degraded (Y. Lee et al., 2003). However, because there are a plethora of post-transcriptional regulatory options to process individual miRNAs differentially, little is known about the half-life of individual miRNAs in specific cell types (Winter et al., 2009). Bonauer *et al.* in a seminal work published in Science demonstrated the endogenous expression of miR-92a in HUVECs (Bonauer et al., 2009). In their studies where supplemental miR-92a and its inhibitor were transfected into HUVECs to control angiogenesis, they opted for a 48h post-transfection duration in most *in vitro* functional experiments (Bonauer et al., 2009). Given the phenotypic similarities between ECs and CD34$^+$-derived EPCs, I assumed endogenous miR-92a presence in the latter and pursued the ideal post-transfection period to allow for maximal target protein modulation before miRNA decay and normalisation of target protein levels. Therefore, I tested 24h, 48h and 72h with the rationale that CD34$^+$-derived EPCs' RNA-induced silencing comples (RISC) machinery should be similar to that of HUVECs. Since ITGA5 is a validated miR-92a target protein (Abdellatif, 2012; Bonauer et al., 2009), I determined the post-transfection change in endogenous ITGA5 expression. According to the results obtained, 48h was considered the optimal duration for miR-92a knockdown in CD34$^+$-derived EPCs, since there was no further reduction in ITGA5 protein levels past that time point **(Figure 43)**. Regarding miR-92a inhibitor modulation, the maximum target protein levels were also obtained after 48h of processing, although in the optimisation experiment

overexpression was not attained. Verification of the degree of miR-92a overexpression and inhibition by quantitative reverse transcription–polymerase chain reaction would have added valuable information to the time course. In this particular experiment, one can hypothesise that cells could have had low baseline levels of the anti-angiogenic miR-92a. Hence transfection with the antisense miRNA would not capture many endogenous sense strands and impact significantly at the protein level. Nevertheless, because of miRNA biogenesis and maturation complexity, the cellular concentration of mature miRNAs does not always reflect transcriptional changes (Kuchen et al., 2010). One single miRNA molecule can reversibly hybridise with several mRNA molecules before being degraded. Therefore, target protein levels should be regarded as the gold standard endpoint for biological efficacy of miRNA transfection, which is the method I used.

**Figure 43 |48h miR-92a (inhibitor) processing duration seems to generate the maximal target protein modulation in human CD34$^{+}$-derived EPCs.**
Cells were transfected with either 30nM control scrambled miRNA, miR-92a-5p or miR-92a-5p inhibitor using oligofectamine. **(A)** Following a time course incubation, the cells were lysed and its proteins were separated by SDS-PAGE and immunoblotted with the antibodies indicated. **(B)** Levels of ITGA5, a direct miR-92a target protein, were quantified by scanning densitometry and expressed as relative units compared to ACTB. Results in this figure are preliminary and reflective of one experiment. ACTB - β-actin; ITGA5 – Integrin α5 subunit; miR – microRNA; RU – relative units.

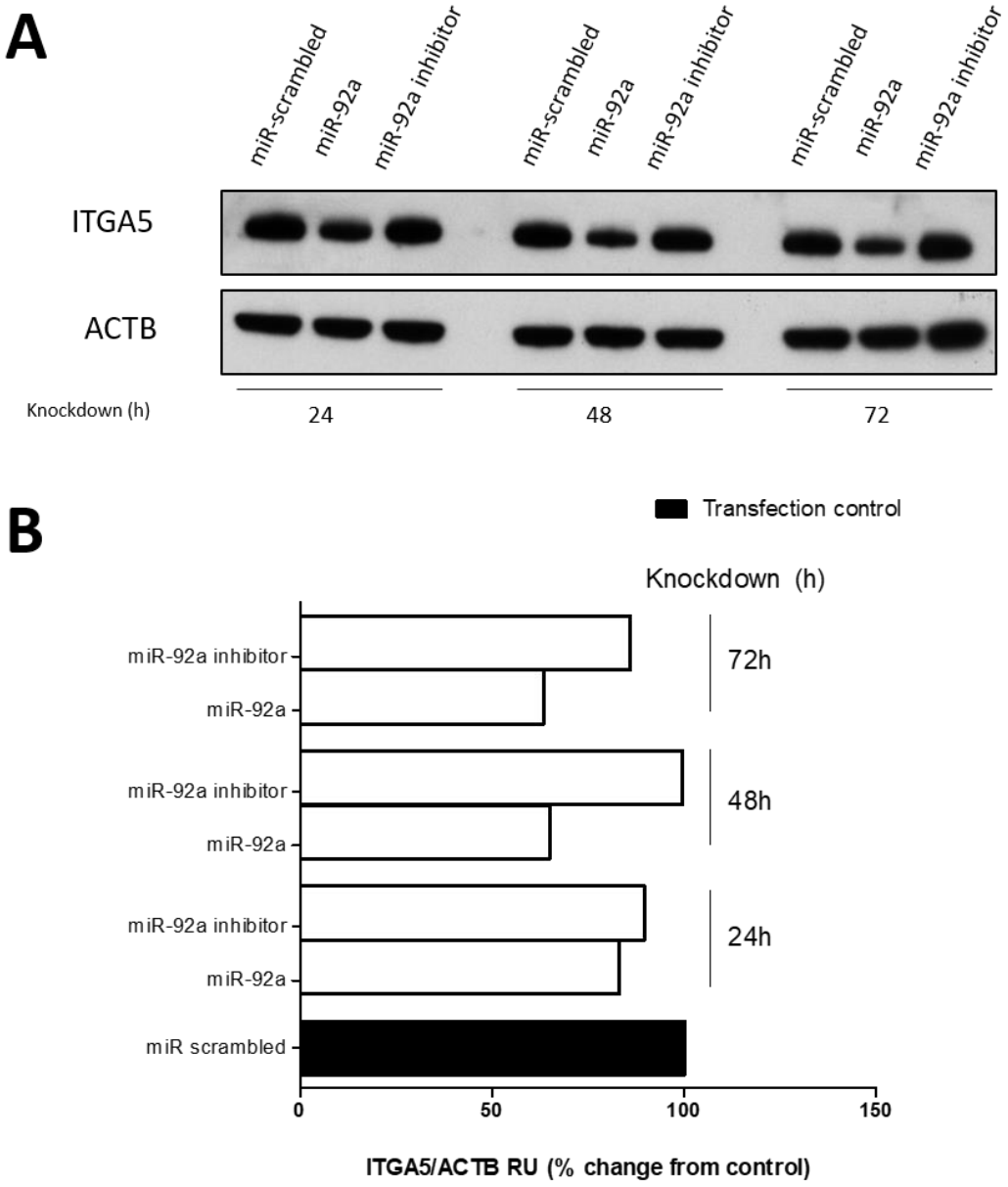


Then, the working concentration of miR-92a mimic and inhibitor was selected based on dose-response experiments **(Figure 44)**. Of note, all experimental control samples were treated with an equal concentration of a non-targeting control mimic sequence to adjust for non-sequence-specific effects in miRNA experiments. Our results suggested that 30 nM was the optimal concentration for miR-92a knockdown in human late-outgrowth EPCs, since there was no added reduction in ITGA5 protein levels at higher concentrations which may result in more detrimental side effects. Also, miR-92a inhibitor processing seemed to yield maximum target protein levels at 30 nM.

**Figure 44 | CD34$^{+}$-derived EPC transfection using oligofectamine seems equally effective at 30 nM or 200 nM concentration of miR-92a (inhibitor).**
Cells were transfected in 6 well plates with 30nM or 200nM control scrambled miRNA, miR-92a-5p or miR-92a-5p inhibitor using oligofectamine. **(A)** Following 48h knockdown in complete medium cells were lysed, proteins were separated by SDS-PAGE, and immunoblotted with the antibodies indicated. **(B)** Levels of ITGA5, a direct miR-92a target protein, were quantified by scanning densitometry and expressed as relative units compared to ACTB. Results in this figure are preliminary and reflective of one experiment. ACTB - β-actin; ITGA5 – Integrin α5 subunit; miR – microRNA; RU – relative units.

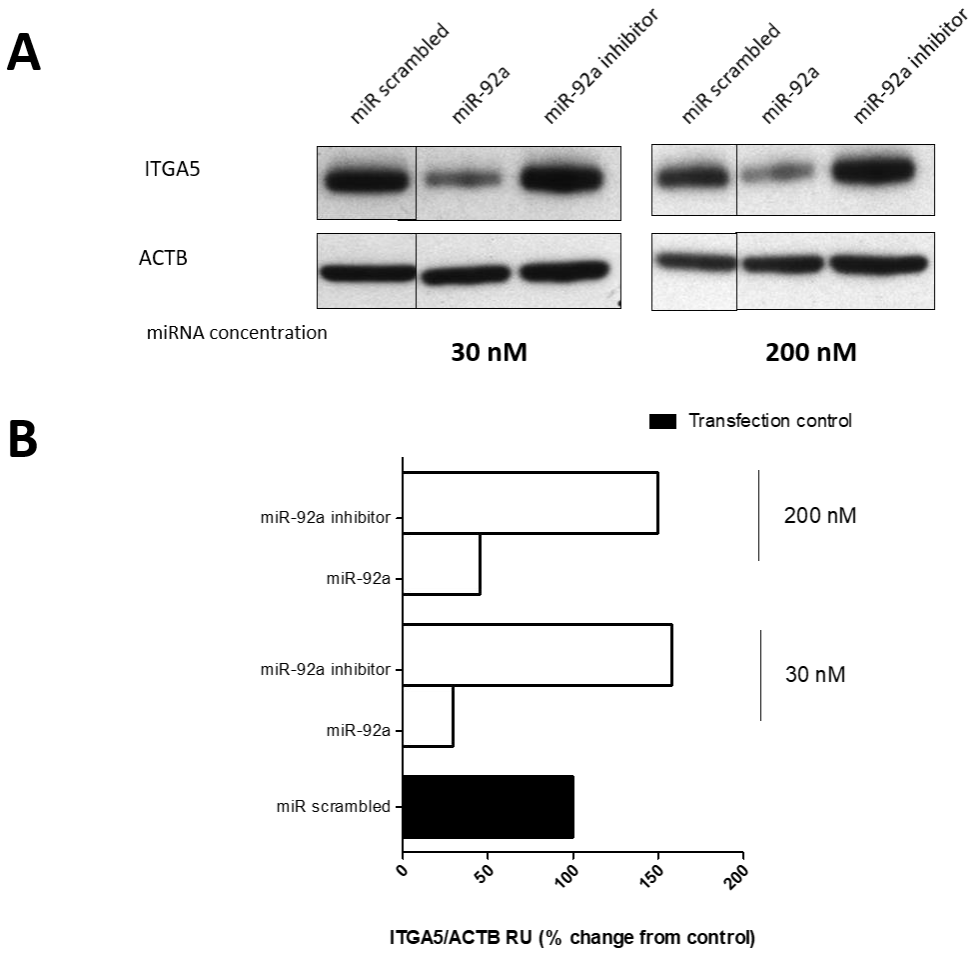


# 4.2 miR-92a inhibitor downregulates angiogenesis-related target proteins in EPCs

In the stem-loop structure of the precursor miRNA, the 5p strand is present in the forward (5'-> 3') position, and the 3p strand (which will be almost complementary to the 5p strand) is located in the reverse position. Following cleavage of the stem-loop by Dicer, two mature strands are produced. The resulting 5p and 3p miRNA molecules are biologically different in terms of stability and functionality, and in general, only the more stable strand will be incorporated into the RISC, and guide the complex to target the 3'

untranslated region (3' UTR) of the imperfectly paired mRNAs to inhibit their translation or promote their degradation. The less stable partner arm, the *-strand (star or passenger strand), accumulates in lower levels and is presumed to be mostly degraded. However, in some cases, both mature strands can be functional. Therefore, to determine which one was the primary and minor miR-92a strands in $CD34^+$-derived EPCs, I tested both synthetic miRs and its inhibitors at 30 nM and allowed 48h processing. The 5p mature form of mir-92a and its corresponding inhibitor had a more potent effect than the 3p strand in $CD34^+$-derived EPCs according to the change in selected target proteins´ levels **(Figure 45)**. The latter included Mitogen-activated protein kinase kinase 4 (MKK4), sirtuin1 (SIRT1), ITGA5, integrin alpha v subunit (ITGAV), all previously used as mir-92a targets by others (Bonauer et al., 2009). EPC transfection with miR-92a-1 (5p) significantly reduced ITGA5, ITAGV and total endothelial nitric oxid synthase (T-eNOS) protein expression, whereas its (5p) inhibitor significantly enhanced ITGA5 and T-eNOS levels, comparing both treatments to miR scrambled.

**Figure 45 | miR-92a (5p) and its inhibitor produce more potent protein levels reduction and rescue in $CD34^+$-derived EPCs than the (3p) forms.**
Cells were transfected with either 30nM control scrambled miRNA, miR-92a-1 or miR-92a-1 inhibitor using oligofectamine. Both 3p or -5p strands of miR-92a and its inhibitor were tested. **(A)** Following 48h incubation in complete medium, cells were lysed, proteins were separated by SDS-PAGE, and immunoblotted with the antibodies indicated. **(B-E)** MKK4, SIRT1, ITGAV, ITGA5 (direct miR-92a targets) and T-eNOS (indirect target) protein levels were quantified by scanning densitometry and expressed as relative units compared to housekeeping protein ACTB or GAPDH. Combined results after up to 8 independent experiments are plotted as means, with errors bars representing ± SEM. **P*<0.05, ***P*<0.01, and ***P<0.001 compared with miR scrambled transfected EPCs (1-way ANOVA, Bonferroni´s test for multiple comparisons). EPC – endothelial precursor cell; ITGA5 – Integrin α5 subunit; ITGAV - Integrin αv subunit; miR – microRNA; MKK4 - Mitogen-activated protein kinase kinase 4; RU – relative units; SEM – standard error of mean; T-eNOS – Total endothelial nitric oxide synthase.

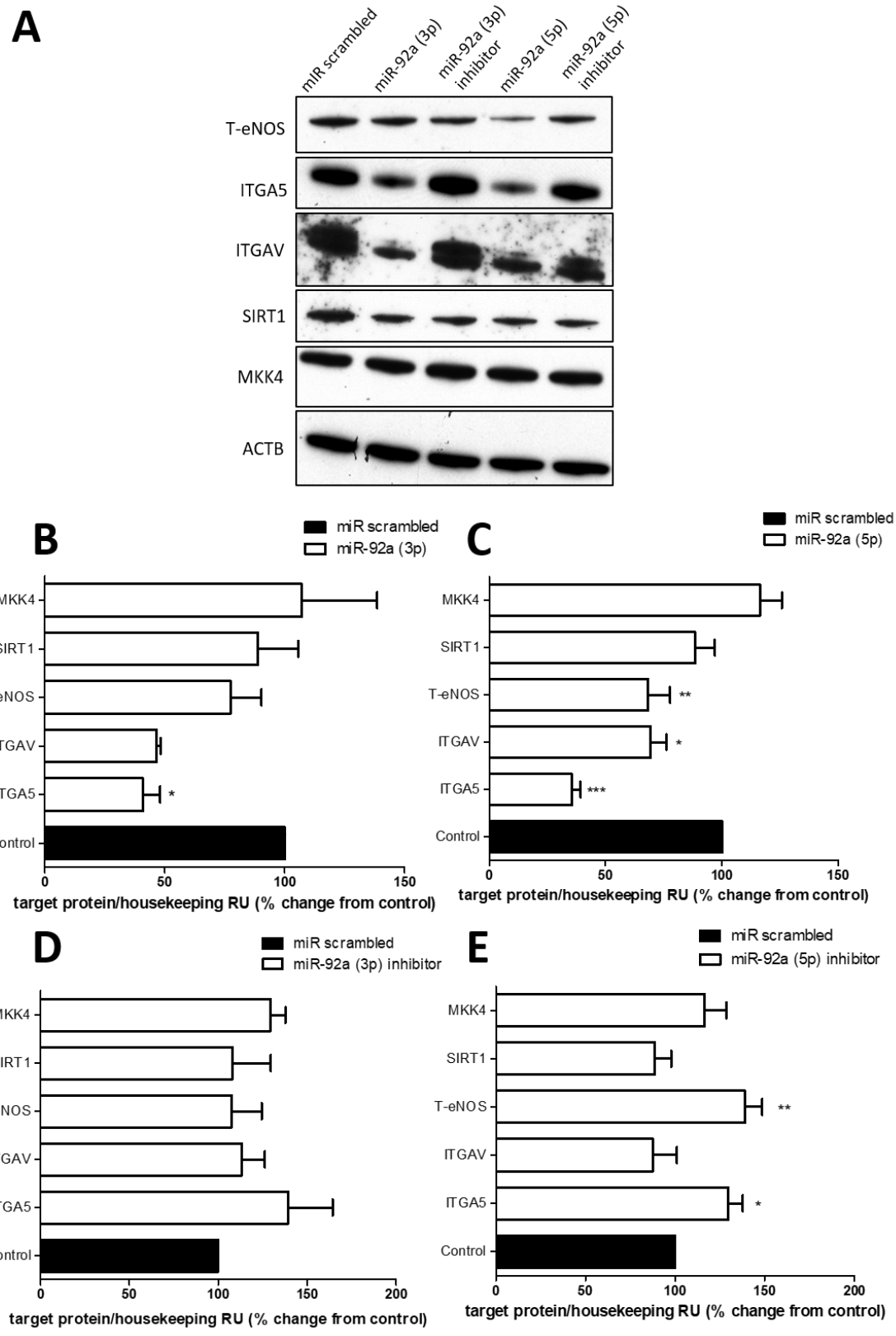


Transfection with 3p strands did not produce a statistically significant change from miR-scrambled treated cells, except for reduced ITGA5 levels with miR-92a-1 (3p) treatment. On the other hand, EPC transfection with miR-92a-1 (5p) significantly reduced ITGA5 and

ITAGV (direct miR-92a targets) protein expression, whereas its (5p) inhibitor significantly enhanced ITGA5 levels, compared to miR scrambled treatment.

MKK4 and SIRT1 both predicted targets in miRbase were not specifically affected by treatment with miR-92a (or its inhibitor) in $CD34^+$-derived EPCs. Curiously, despite miR-92a downregulating ITGAV, its overexpression was not apparent following miR-92a inhibitor treatment. It was interesting as well to note a statistically significant miR-92a-dependent regulation of T-eNOS when $CD34^+$-derived EPCs were treated with the primary strand (5p), although eNOS was not present in miRBase as a predicted miR-92a candidate target. Mechanistically, ITGA5 is a crucial regulator of EC functions and vessel growth by mediating cell-matrix interactions, cell migration and anti-apoptotic signalling (Francis et al., 2002; Urbich et al., 2002; N. Yang et al., 2011). On the other hand, NO is equally important for EC and vessel homeostasis since it controls re-endothelialisation, neovascularization and vascular tone (B. Cui et al., 2011; Murohara et al., 1998; Palmer, Ferrige, & Moncada, 1987; Y. Zhao, Vanhoutte, & Leung, 2015). Given the essential functions of both these targets in ECs, we next sought the functional relevance of miR-92a (5p) inhibitor treatment in $CD34^+$-derived EPCs.

## 4.3 miR-92a inhibitor -treated EPCs exhibits enhanced angiogenesis, migration, proliferation and adhesion

To demonstrate the pro-angiogenic activity of miR-92a (5p) inhibitor, $CD34^+$-derived EPCs were seeded with fibroblasts in a coculture system grown for 96 hours **(Figure 46)**. miR-92a inhibitor exerted a statistically significant proangiogenic effect in EPCs. Cell treatment with miR-92a inhibitor significantly increased vascular network length (133 % ± 3.62 vs. 100%, $p < 0.05$, % of controls), area (126.5 % ± 3.28 vs. 100%, $p < 0.05$, % of controls) and number of branch points (164.5 % ± 0.12 vs. 100%, $p < 0.05$, % of controls) compared to miR scrambled, whereas miR-92a seemed to have the opposite effect regarding the absolute reduction of network length compared to miR scrambled.

**Figure 46 | miR-92a (5p) inhibitor is proangiogenic in $CD34^+$-derived EPCs.**
Suspensions of EPCs previously transfected with 30nM miR scrambled, miR-92a (5p) and miR-92a (5p) inhibitor using oligofectamine, were added to the fibroblast monolayer, so that an EPC-fibroblast co-culture assay (96h) could be pursued in the presence or absence VEGF, before cells were fixed and stained

for vWF using a secondary antibody conjugated to Alexafluor-488. **(A)** Representative brightfield picture of the coculture taken at 4x magnification. **(B)** Representative network sprouting fluorescent images captured at the end of the assay at 10x magnification **(C-E).** Angiogenesis network length, area and number of branch points based on fluorescence signal are represented. All experimental conditions were measured in triplicate. Results after 2 independent experiments are plotted as means, with errors bars representing ± SEM. ***P<0.001 compared with *Null VEGF-treated condition* (1-way ANOVA, Bonferroni's test for multiple comparisons); ^P<0.05, ^^P<0.01 compared with *miR scrambled treated with VEGF* (1-way ANOVA, Bonferroni's test for multiple comparisons). EPC – endothelial precursor cell; FBS – fetal bovine serum; miR – microRNA; SEM – standard error of mean; VEGF – vascular endothelial growth factor; vWF – von Willebrand factor.

**A**

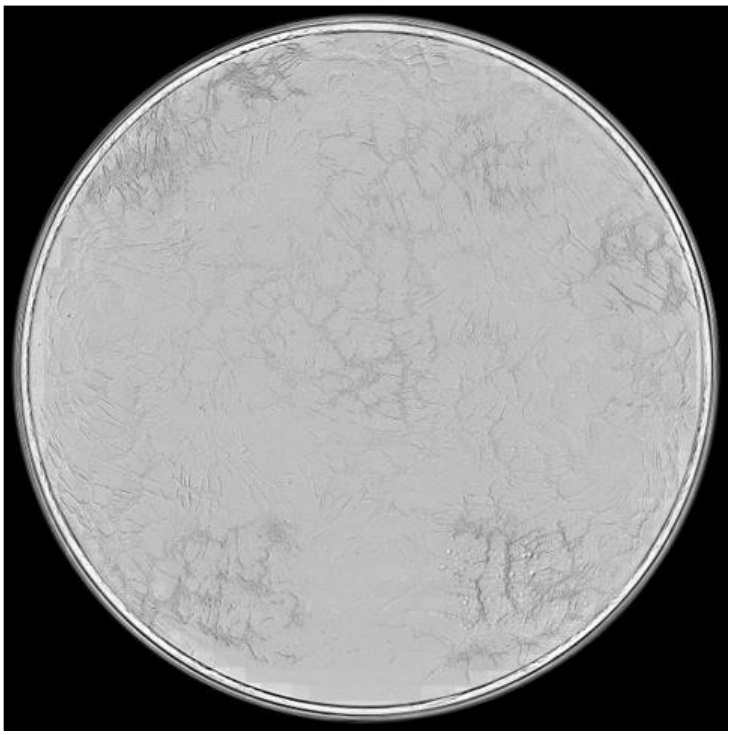

**B**

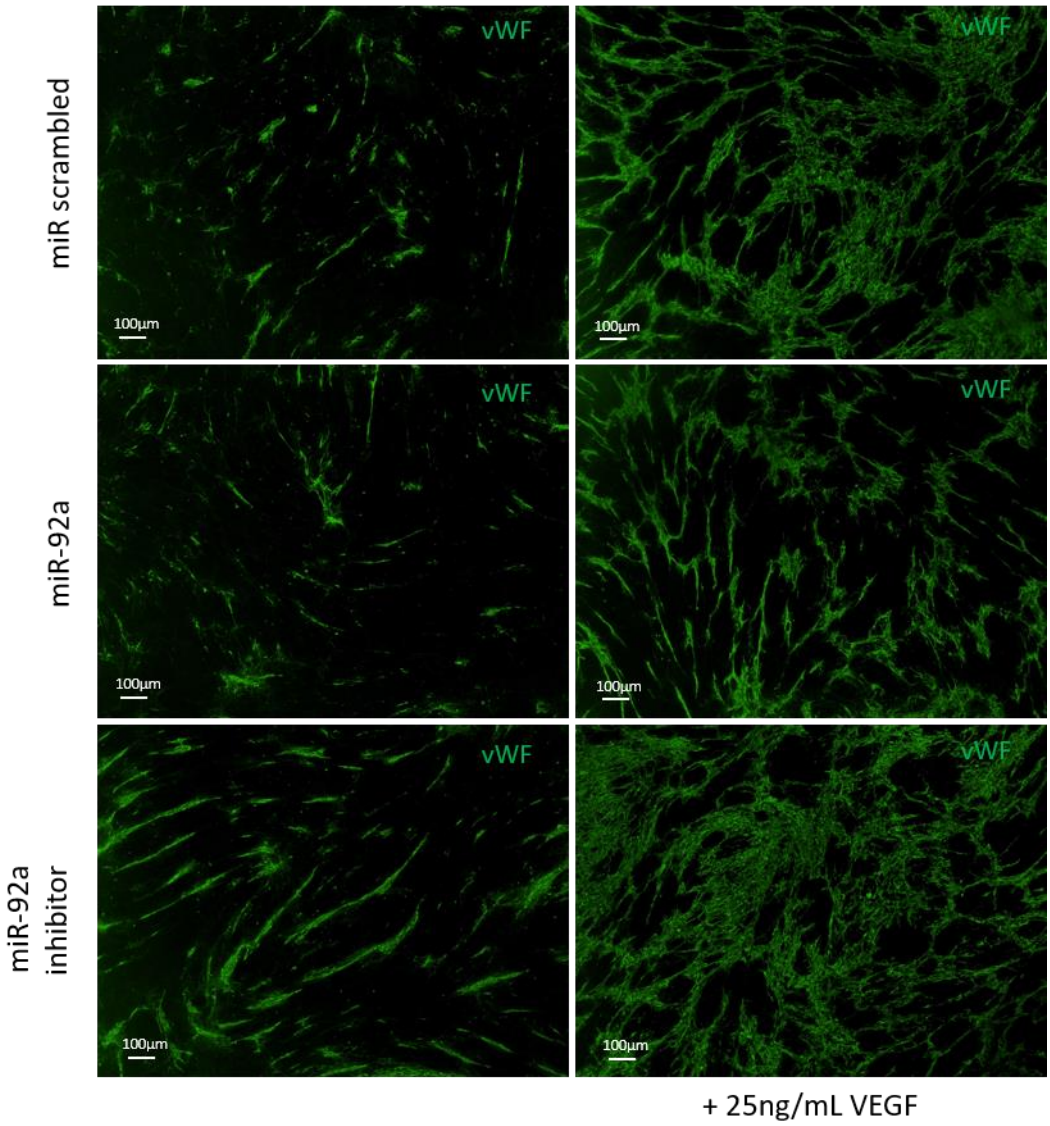
miR scrambled
miR-92a
miR-92a inhibitor
vWF
100µm
+ 25ng/mL VEGF

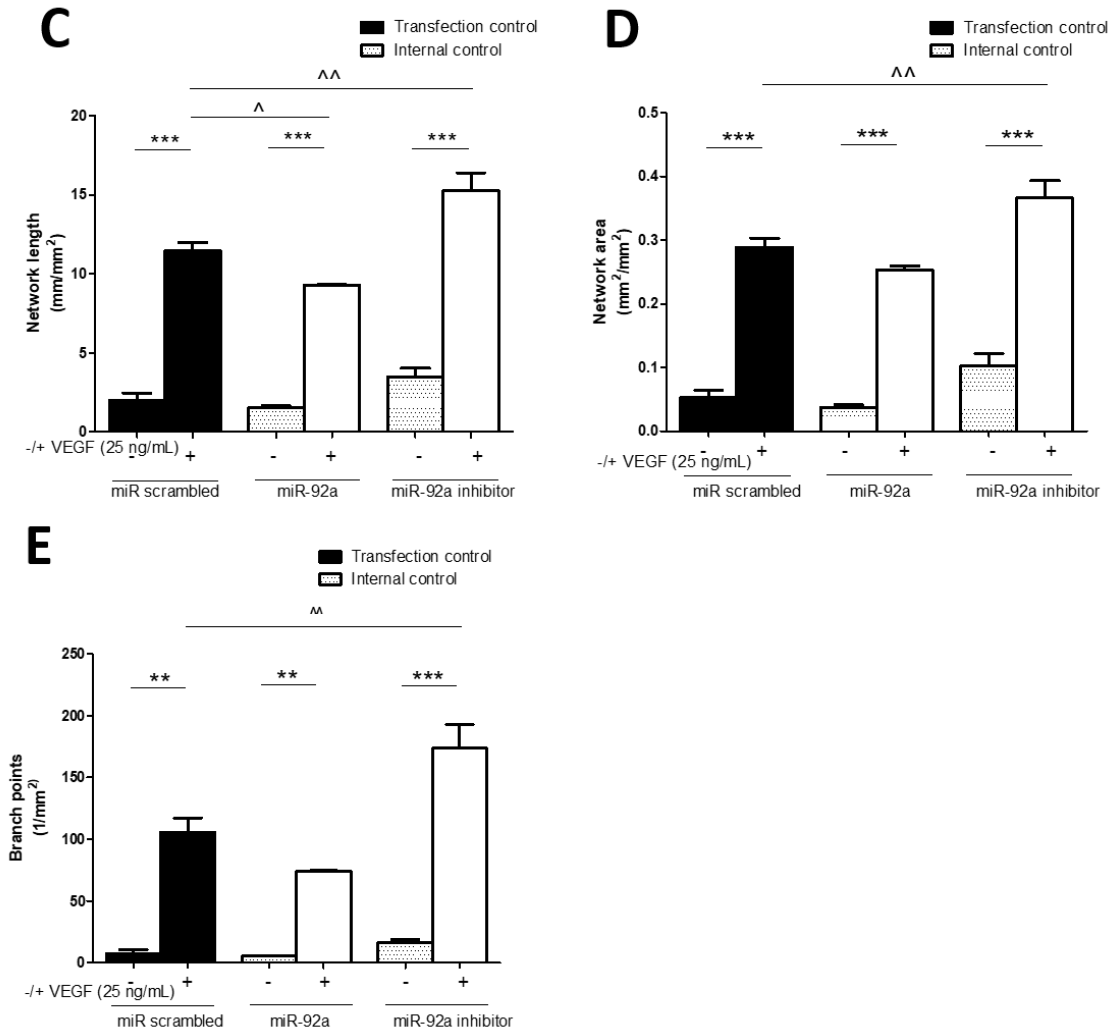


The scratch assay was used to assess the effects of miR-92a inhibitor delivery on EPC wound closure migration **(Figure 47)**. EPCs treated with miR-92a inhibitor managed to narrow the wound gap area significantly more than controls by 48 hours under VEGF deprivation (58.48 % ± 3.41 vs. 45.22 % ± 6.04, $p<0.05$, % of baseline wound area), an effect size which was attenuated upon VEGF co-stimulation (63.94 % ± 4.09 vs. 59.56 % ± 5.86, $p>0.05$, % of baseline wound area). In contrast, miR-92a significantly delayed wound closure at 48h compared with miR scrambled either in the presence (47.65 % ± 6.52 vs. 59.56 % ± 5.86, $p<0.001$, % of baseline wound area) or absence (35.12 % ± 6.31 vs. 45.22 % ± 6.04, $p<0.05$, % of baseline wound area) of VEGF supplementation.

**Figure 47 | miR-92a (5p) inhibitor significantly enhances wound closure migration in CD34⁺-derived EPCs in the absence of VEGF.**

Cells were transfected with either 30 nM miR scrambled (black line), miR-92a (5p) (red line) or miR-92a (5p) inhibitor (green line) using oligofectamine. After a 48h knockdown, wound closure migration in EBM 0.5% FBS was assessed in the presence or absence of 25 ng/mL VEGF by live-cell Imaging. Images were

captured at 10x every 2h for a total duration of 48h. **(A)** Representative brightfield images of wound closure over time in the presence of 25 ng/mL VEGF by EPCs transfected with either miR scrambled, miR-92a or miR-92a inhibitor. **(B)** Relative wound closure quantification results after 9 independent experiments (each condition was repeated in 6 replicates) are plotted as means, with errors bars representing ± SEM. *P<0.05 compared with *miR scrambled/no VEGF supplementation;* ^^^P<0.001 compared with *miR scrambled/VEGF supplementation* (2-way ANOVA, Bonferroni's test to compare multiple means by row). EPC- endothelial precursor cell; FBS – fetal bovine serum; miR – microRNA; SEM – standard error of mean; VEGF – vascular endothelial growth factor.

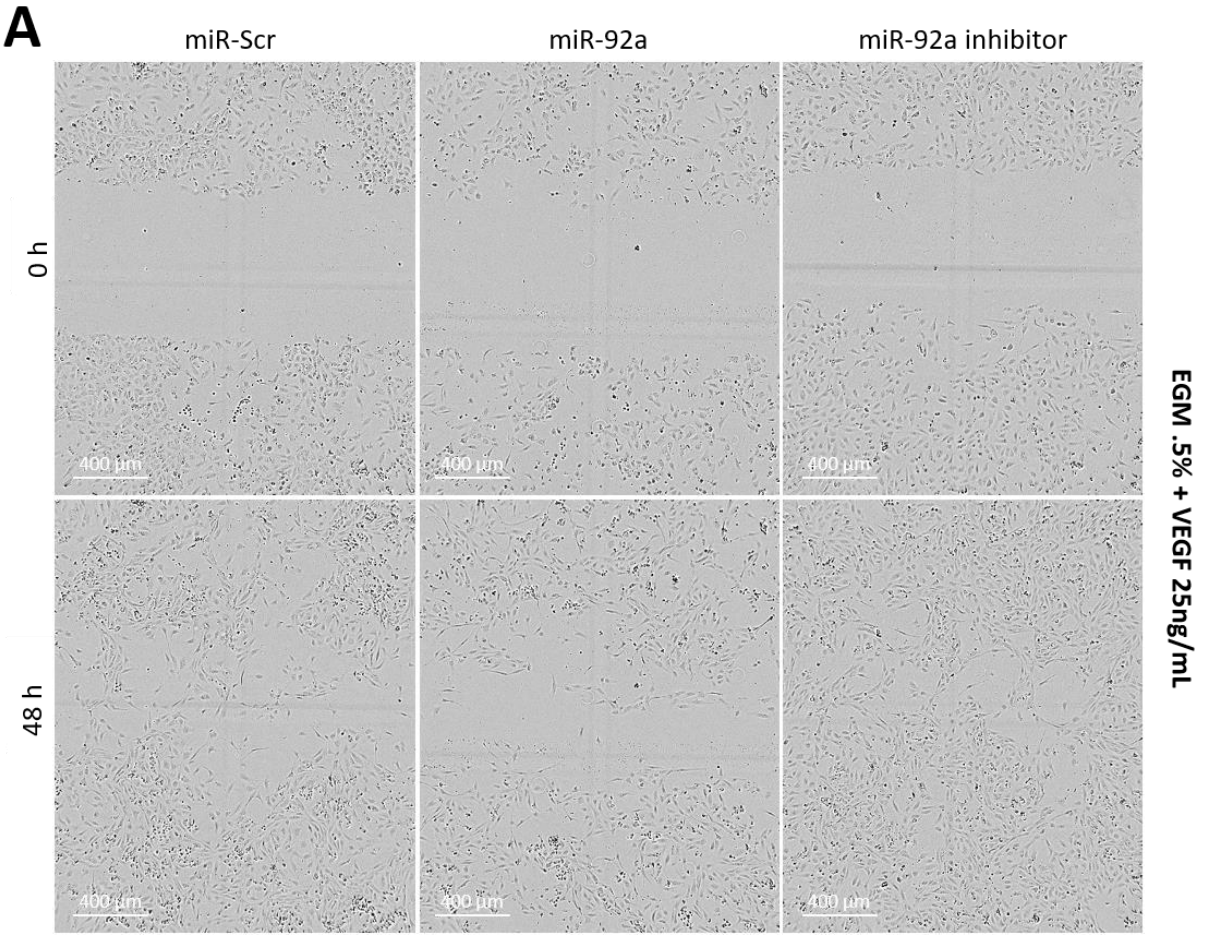

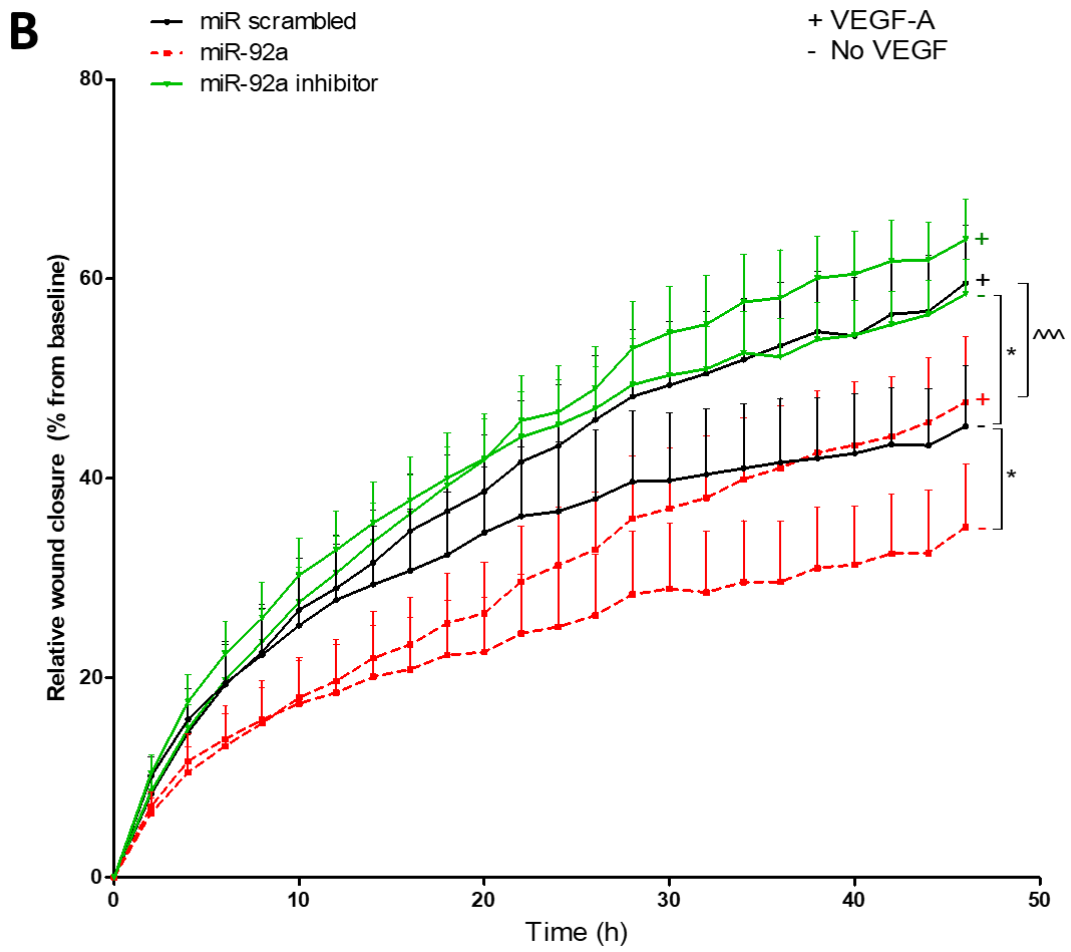


EPC homing and engraftment into an active site of injury is essential for a prompt re-endothelialisation and is mechanistically associated with cytokines/growth factor signalling. Thus, the effect of miR-92a inhibitor treatment on EPC migration towards VEGF was studied using an *in vitro* transwell assay **(Figure 48)**. The results showed that EPCs transfected with miR-92a inhibitor revealed a significantly enhanced migration towards VEGF stimuli compared to miR scrambled-treated controls (63.67 ± 14.72 vs. 5.67 ± 5.67, p<0.001, migrated cells after 5h/well).

**Figure 48 | Inhibition of mir-92a enhances VEGF-induced chemotaxis migration of CD34$^+$-derived EPCs.** Cells were transfected with either 30 nM miR scrambled (transfection control), miR-92a (5p), miR-92a (5p) inhibitor using oligofectamine. After 48h cells were transferred to transwell inserts and chemotaxis migration was determined as the number of migrated cells after 5h in response to 50 ng/mL VEGF or no treatment (internal negative control). Treatment with 10% FBS was tested as a positive internal control. **(A)** Representative images of transwell inserts are shown for each treatment, and illustrative stained cells are arrowed for each condition (8x magnification). **(B)** Quantification of migration is presented as mean ± SEM from 3 independent experiments, and each treatment was performed in duplicates. **P<0.001 compared with *miR scrambled;* ^^^P<0.001 compared with *no VEGF* (1-way ANOVA, Bonferroni's test for multiple comparisons). EPC- endothelial precursor cell; FBS – fetal bovine serum; miR – microRNA; SEM – standard error of mean; VEGF – vascular endothelial growth factor.

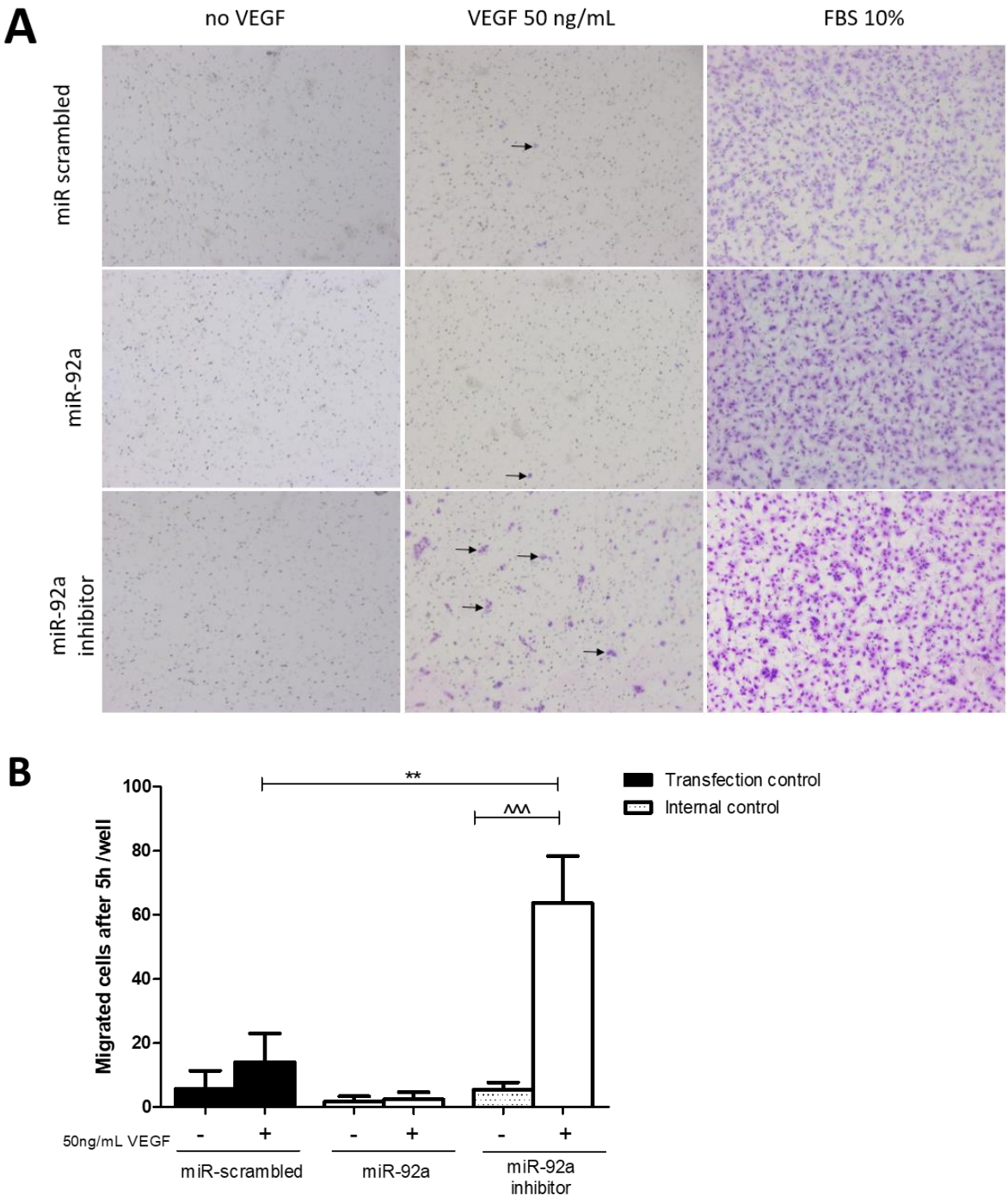


The effect of miR-92a inhibitor on EPC proliferation was determined by an ATP-based luminescence assay **(Figure 49)**. The follow-up at 48h post miRNA treatment indicated that miR-92a inhibitor modestly enhanced VEGF-induced proliferation (168.07 ± 23.61 vs. 162.12 ± 22.84, $p<0.01$, % change from baseline after 48h), while miR-92a had the opposite effect regardless of VEGF supplementation status (without VEGF: 137 ± 11.66 vs. 151.10 ± 19.96, $p<0.05$; with VEGF: 157.87 ± 22.84 vs. 162.12 ± 22.84, $p<0.05$, % change from baseline after 48h).

**Figure 49 | miR-92a (5p) inhibitor enhances VEGF-induced proliferation of CD34$^+$-derived EPCs.**
Cells treated with 30nM miR scrambled, miR-92a (5p) or miR-92a (5p) inhibitor were incubated with an ATP quantifying luciferase reporter at baseline. For the time course, cells in a second well plate were incubated in enriched medium for 48h before performing the luminescence assay. Results in **(A-B)** are plotted as means, with errors bars representing ± SEM after 4 independent experiments (4 replicates for each experimental condition). *P<0.05, ***P<0.001 compared with baseline condition; &P<0.05 compared with miR scrambled processed for 48h with no VEGF; #P<0.05, ##P<0.01 compared with miR scrambled processed for 48h with VEGF (1-way ANOVA, Bonferroni's test for multiple comparisons). ATP - adenosine triphosphate; EGM – endothelial growth medium; EPC – endothelial precursor cells; FBS - fetal bovine serum; miR- microRNA; RLU – relative light units; SEM – standard error mean; VEGF – vascular endothelial growth factor.

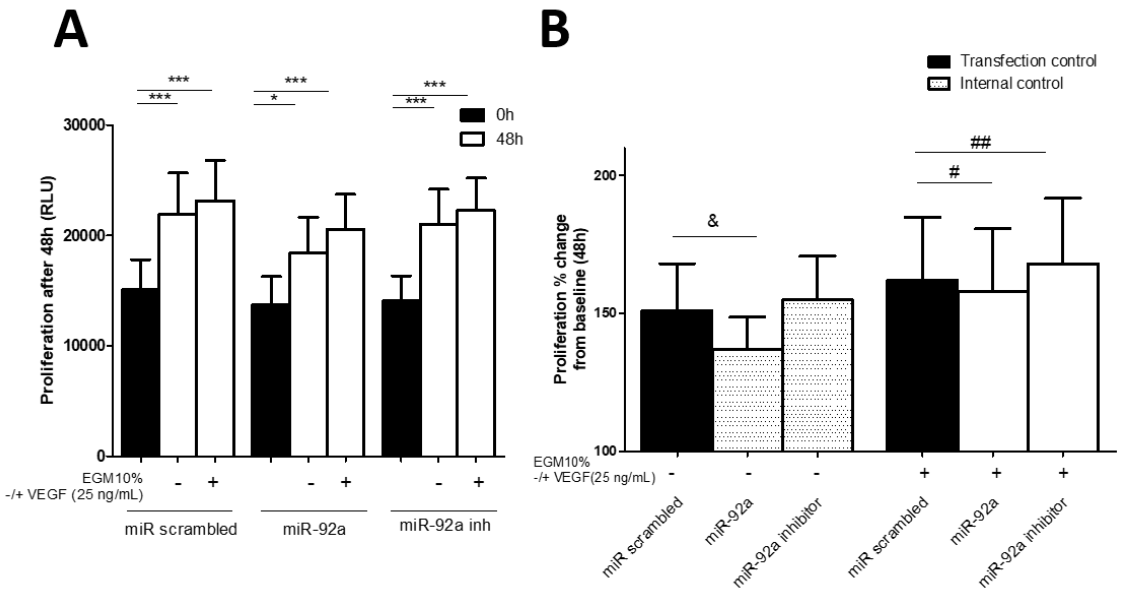


One of the most important properties of EPCs contributing to re-endothelialisation is their ability to adhere to ECM at denuded vascular sites. I used an *in vitro* static culture assay to determine whether mir-92a inhibitor treatment could enhance EPC adherence to FN (a ligand for ITGA5), through upregulation of ITGA5 receptors **(Figure 50)**. The results revealed that, indeed, miR-92a inhibitor significantly enhanced EPC adhesion to FN after 20 minutes compared to miR scrambled control (23.57 % ± 6.43 vs. 14.46 % ± 5.22, p<0.05, specific adhesion to FN, % from baseline). This equated to 87% more cells adhering to the matrix within the designated period than the sham-treated EPCs. Conversely, an EPC reduced adhesion following miR-92a treatment trend was observed (7.47 % ± 3.71 vs. 14.46 % ± 5.22, p>0.05, specific adhesion to FN, % from baseline).

**Figure 50 | mir-92a (5p) inhibitor enhances adhesion of CD34$^+$-derived EPCs to fibronectin.**
FN specific adhesion capacity was determined in fluorescently -labelled cells previously transfected with 30nM miR scrambled, miR-92a (5p) or miR-92a (5p) inhibitor using oligofectamine. **(A)** Representative images of labelled EPCs transfected with indicated miRNAs captured at baseline and after one wash 20 minutes past at 10x. **(B)** Representation of labelled and unlabeled EPCs, the latter used as an internal assay control, seeded on FN. **(C)** Baseline and final red object count were quantified, and data are expressed as mean adhesion on FN (7 replicates per experiment) minus mean unspecific adhesion on HSA (3 replicates per experiment). Results are representative of a total of 4 independent experiments and are plotted as means, with errors bars representing ± SEM. *P<0.05 compared with *miR scrambled* (1-way

ANOVA, Bonferroni's test for multiple comparisons). EPC – endothelial precursor cell; EBM – endothelial basal medium; EGM – endothelial growth medium; FBS – fetal bovine serum; FN – fibronectin; HSA – human serum albumin; miR – microRNA; SEM – standard error mean.

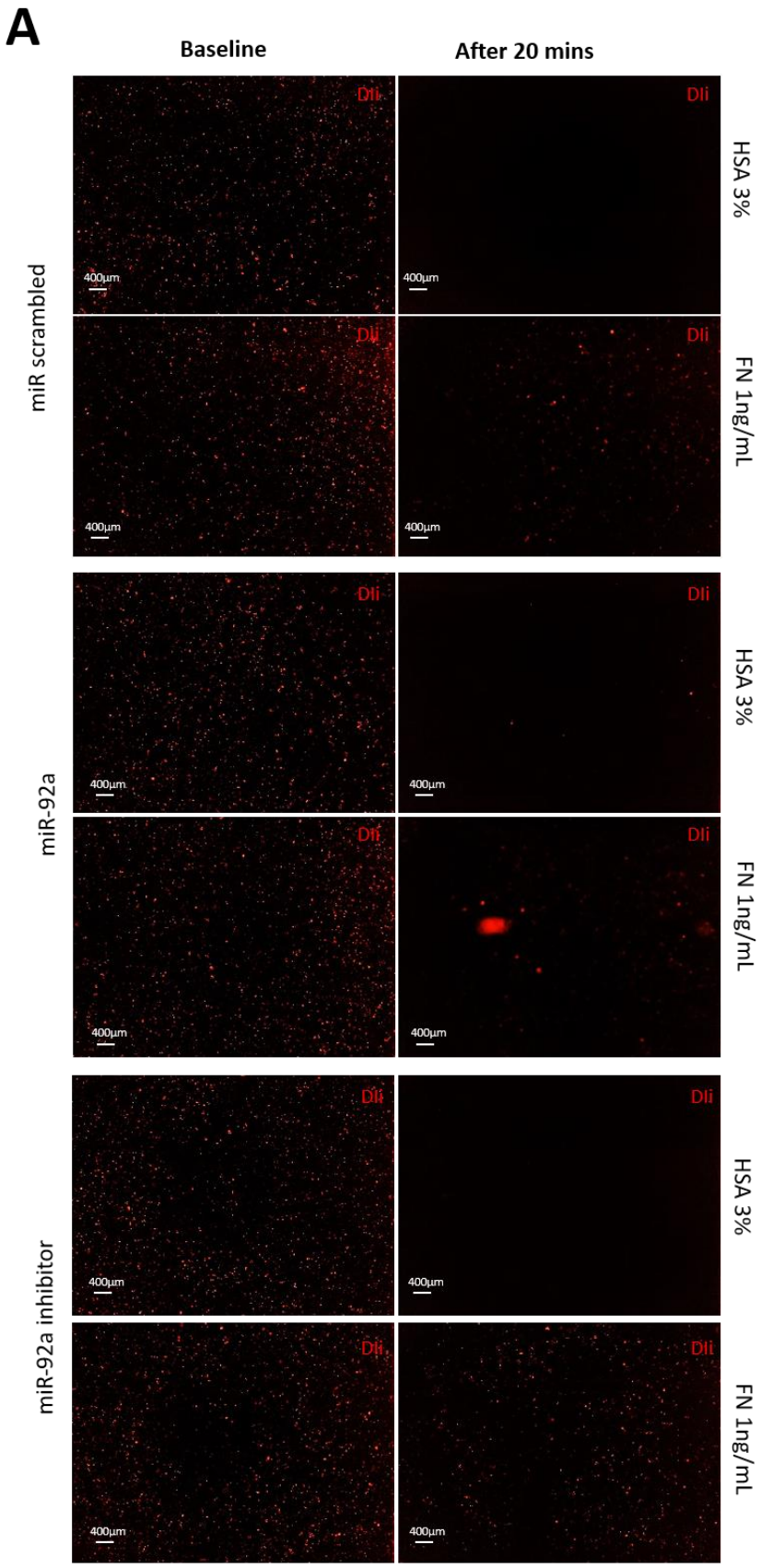

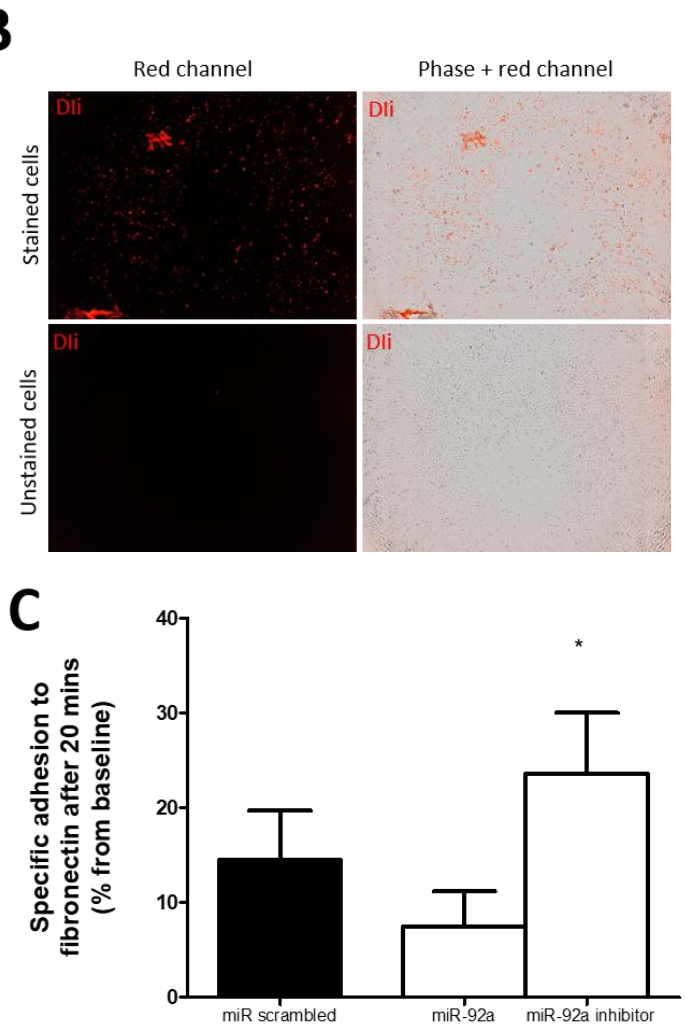


# 4.4 miR-92a inhibitor does not change survival of EPCs under starvation

To investigate the effects of miR-92a inhibitor on the viability of $CD34^{+}$-derived EPC subject to a starvation period (to recapitulate the oxidative stress they might experience on injury sites), cells were transfected with miR-92a, mir-92a inhibitor or miR scrambled for two days, and then starved for 6 hours. No significant relative survival benefit was found when compared to control, as assessed by a luminescent ATP-based assay **(Figure 51)**.

**Figure 51 | miR-92a (5p) inhibitor does not significantly enhance $CD34^{+}$-derived EPC survival in serum-free medium.**

Survival of cells treated with the 30nM miR scrambled, miR-92a (5p), miR-92a (5p) inhibitor in serum-deprived medium after 6h was assessed using a Luminescent cell viability ATP-based assay. Survival from baseline results are representative of a total of 6 independent experiments and are plotted as means, with errors bars representing ± SEM. Replicates of 6 were used for each experimental condition. Results in **(A-B)** are representative of a total of 6 independent experiments and are plotted as means, with errors bars representing ± SEM. ***P<0.0001 compared with baseline condition (1-way ANOVA, Bonferroni's test for multiple comparisons). ATP - Adenosine triphosphate; miR- microRNA; RLU – relative light units; SEM – standard error mean.

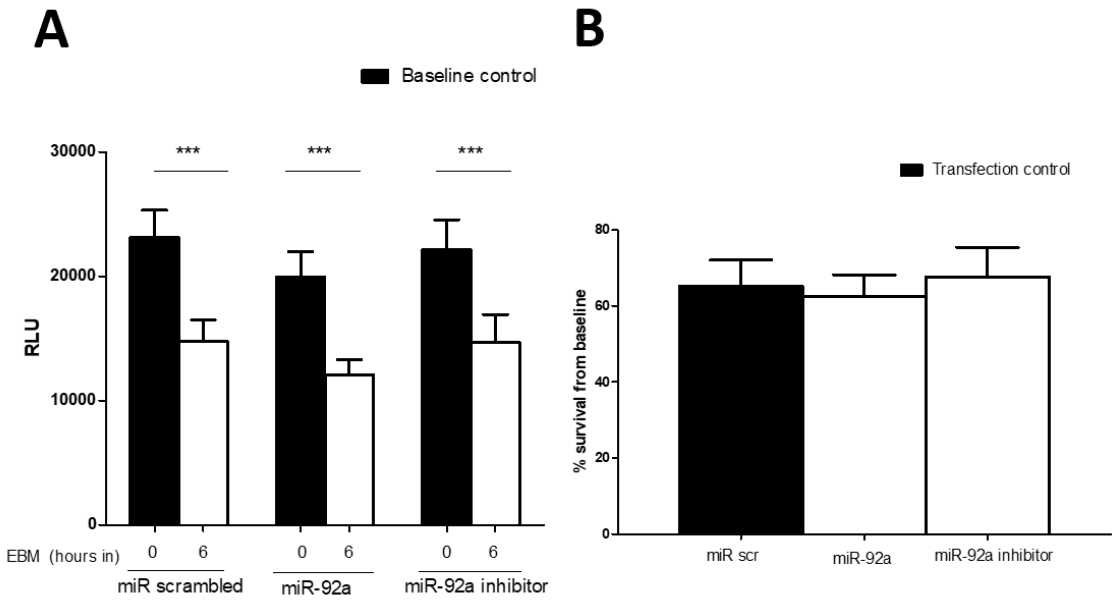


# 4.4 miR-92a inhibitor treated EPCs and post-angioplasty engraftment

To test if the observed effects of mir-92a inhibitor on EPCs could influence their engraftment capacity *in vivo,* I used a rat carotid artery balloon injury model, which typically causes the removal of the endothelium. To follow up transplanted human EPCs at the injury site for a short-term period, cells were labelled with a lipophilic, photostable fluorescence compound. After the injury, a needle catheter was inserted into the arteriotomy, and a suspension of fluorescently labelled EPCs was gently infused into the clamped carotid artery over a 10-minute occlusion period. The potential for mir-92a inhibitor to enhance circulating EPCs' engraftment potential, as initially hypothesised, was then investigated *in vivo* **(Figure 52)**. Following balloon-induced injury, cell engraftment to the denuded intima was evident, as revealed by *en face* fluorescence microscopy, apparently with no discernible complications suggesting host

versus graft rejection by 24h. No intraluminal thrombosis was reported, and the animals' behaviour appeared normal after transplantation.

**Figure 52 | miR-92a (5p) inhibitor seems to enhance CD34$^{+}$-derived EPC engraftment after intravascular transplantation.**
To study the engraftment capacity of transfected human EPCs at a vascular injury site, cells were previously labelled with a vital dye. Cells treated with 30 nM miR scrambled, miR-92a (5p) or miR-92a (5p) inhibitor were transplanted intra-luminally in the rat carotid artery immediately after angioplasty. **(A)** Representative fluorescent macroscopy images of the rat carotid arteries taken 24h following angioplasty at different topographic levels at 3.2x in the red channel. These were opened longitudinally and mounted *en face*, revealing engrafted cells stained with the red cell DIi tracker dye. **(B)** The agglomerate of engrafted miR-92a inhibitor-transfected EPCs seen at higher magnification (8x). **(C)** Preliminary results following quantification of EPC engraftment area per artery after 2 individual experiments (6 rats). EPC – endothelial precursor cell; CCA – common carotid artery; miR – microRNA.

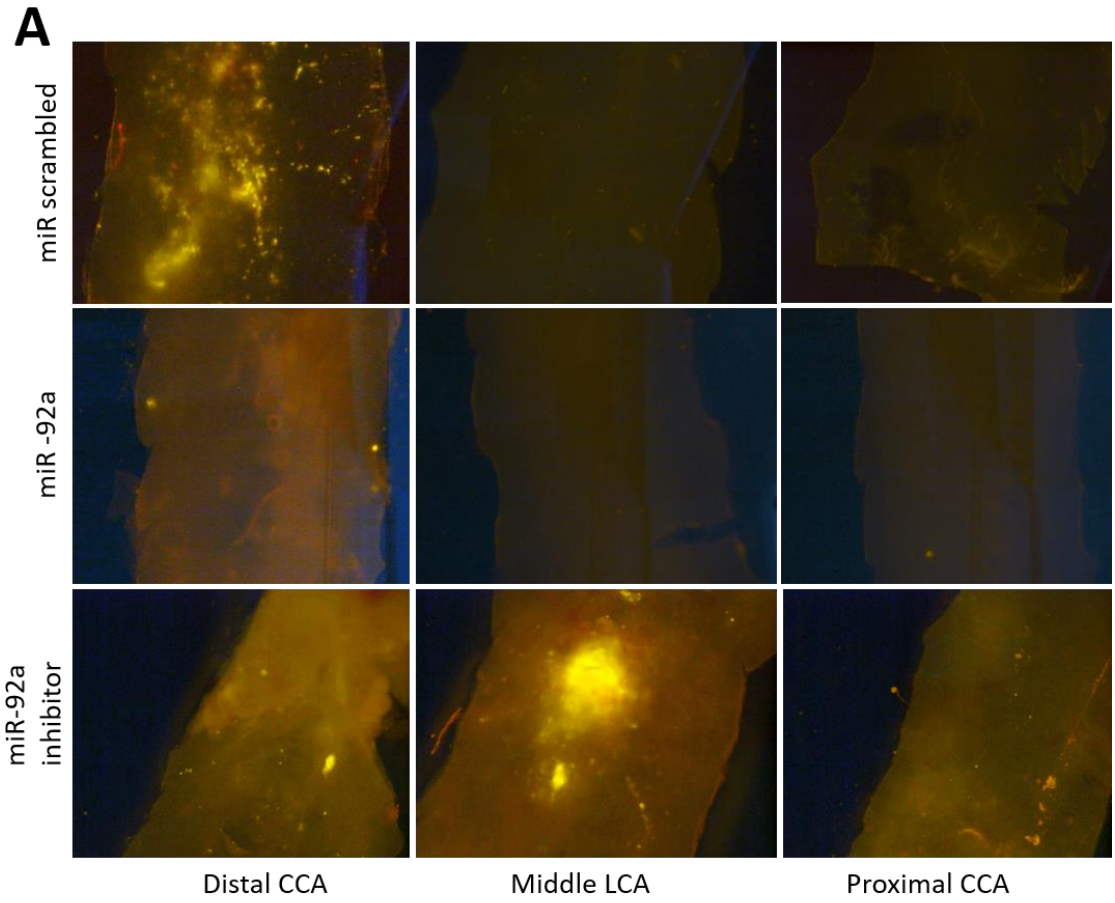

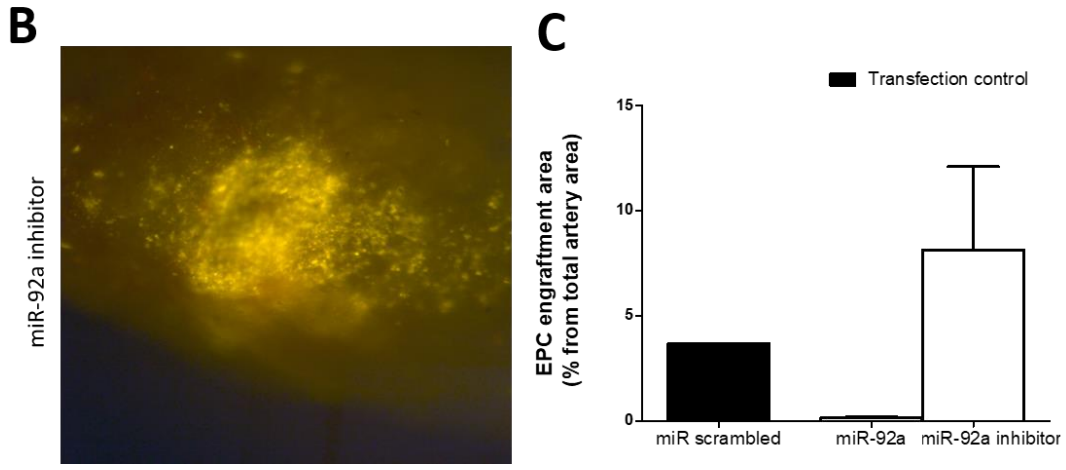


Although the difference between conditions did not reach statistical significance, a trend was noticed in this pilot study. miR-92a inhibitor treated EPCs were observed in higher numbers in the luminal arterial face. miR-92a, on the other hand, seemed to cause decreased EPC engraftment, though the difference was not statistically significant.

## 4.5 ITGA5 knockdown abrogates miR-92a inhibitor adhesion effect in EPCs

To determine whether the overexpression of ITGA5 (direct miR-92a target) contributed to the enhanced proliferation, adhesion to FN and migration exhibited by human $CD34^+$-derived EPCs after miR-92a inhibitor treatment, ITGA5 expression was repressed by co-transfecting cells with the targeted siRNA. Confirmation of successful knockdown by si-ITGA5 was verified by western blot 48h after treatment **(Figure 53)**.

**Figure 53 | si-ITGA5 cancelled miR-92a (5p) inhibitor-mediated ITGA5 and T-eNOS overexpression in $CD34^+$-derived EPCs.**
Cells treated with either miR-scrambled, miR-92a (5p), mir-92a (5p) inhibitor, siTGA5, mir-92a (5p) + si-ITGA5 or miR-92a (5p) inhibitor + si-ITGA5 (all at 30 nM) were lysed, proteins separated by SDS-PAGE and immunoblotted with the indicated antibodies. **(A)** Representative western blot, with (**B**) ITGA5, **(C)** T-eNOS and **(D)** SIRT1 protein expression quantified by scanning densitometry. Protein of interest levels was normalised to levels of the housekeeping gene ACTB. Combined results from 6 independent experiments are plotted as means, with errors bars representing ± SEM. *P<0.05, **P<0.01 and ***P<0.001 compared with *miR scrambled* (1-way ANOVA, Bonferroni's test for multiple comparisons). EPC – endothelial precursor cell; miR – microRNA; Si – small interfering; RU – relative units; SEM – standard error of mean.

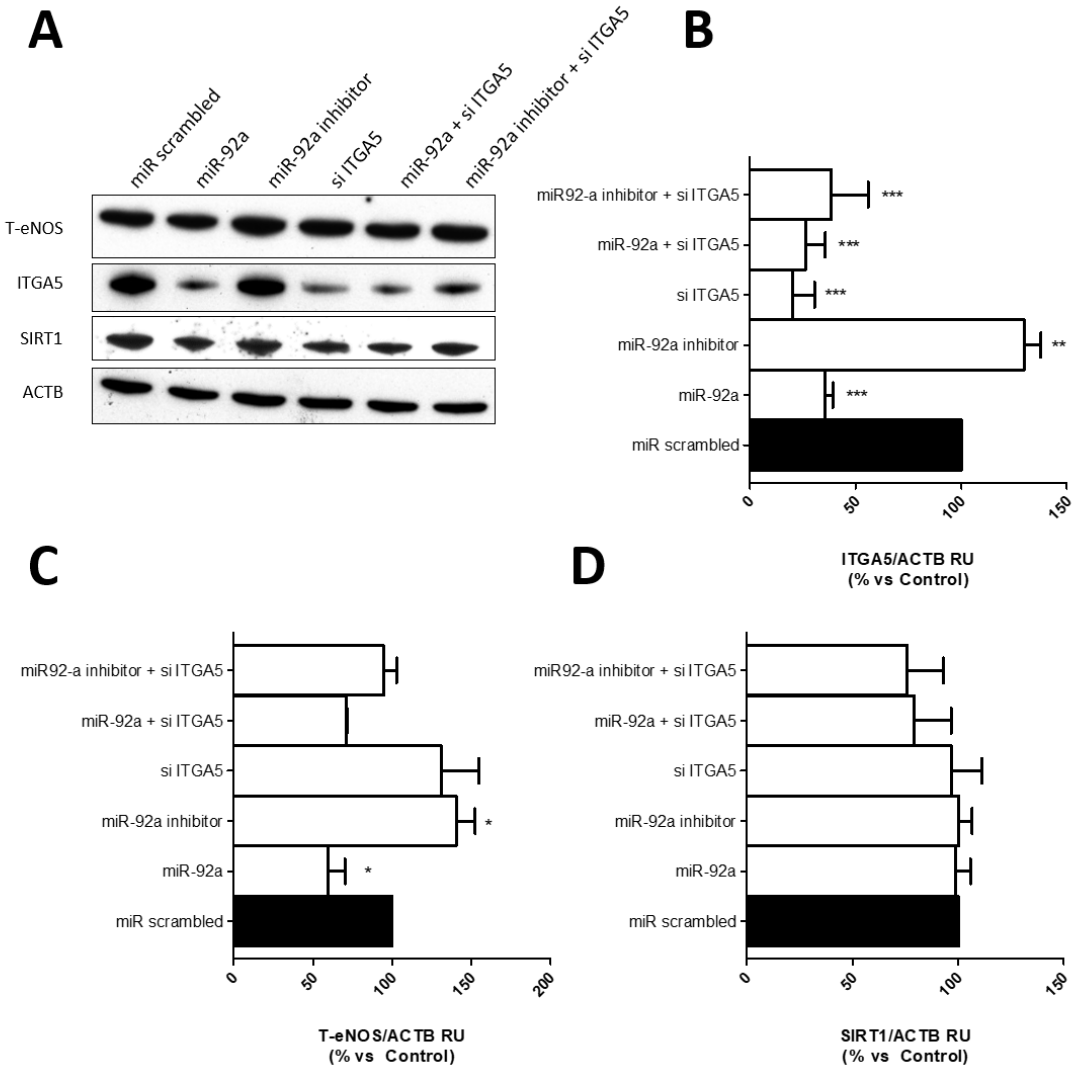


Co-transfection experiments revealed that ITGA5 overexpression as result of miR-92a inhibitor treatment (129.80 % ± 7.91 vs. 100%, ITGA5/ACTB RU, % vs control) was abrogated by si-ITGA5 (38.55 % ± 17.44 vs. 100%, ITGA5/ACTB RU, % vs control). Moreover, T-eNOS overexpression following miR-92a inhibitor treatment (140.04 % ± 11.80 vs. 100%, T-eNOS /ACTB RU, % vs control) was also lost when EPCs were co-transfected with si-ITGA5 (94.75 % ± 8.04 vs. 100%, T-eNOS /ACTB RU, % vs control). Contrastingly, SIRT1 levels remained unchanged in all experimental settings.

Then, to determine the contribution of ITGA5 overexpression to the previously described enhanced adhesive profile of miR-92a inhibitor-treated EPCs, a new cell-matrix assay was performed where I knocked down ITGA5 using the specific siRNA **(Figure 54)**.

After co-transfecting cells with both miR-92a inhibitor and si-ITGA5, there was a significant decrease in adhesion when compared to cells treated with mir-92a inhibitor (41.98 % ± 1.93 vs. 49.61 % ± 0.76, p<0.001, specific adhesion to FN, % from baseline) and also when compared with control EPCs treated with miR scrambled + si scrambled (41.98 % ± 1.93 vs. 46.31 % ± 0.87, p<0.05, specific adhesion to FN, % from baseline). Remarkably, EPCs treated with both miR-92a inhibitor + si-ITGA5 adhered in higher numbers than cells treated with si-ITGA5 (41.98 % ± 1.93 vs. 35.52 % ± 1.50, p<0.05, specific adhesion to FN, % from baseline), revealing a still likely higher ITGA5 relative expression caused by miR-92a inhibitor, or that there are other players besides ITGA5 involved in EPC adhesion which is also upregulated by miR-92a inhibitor.

Oddly, when adding si-scrambled to miR-92a inhibitor, I failed to reproduce the statistically significant enhancement of adhesion caused by miR-92a inhibitor seen before, a topic which will be discussed later.

**Figure 54 | si-ITGA5 abrogated the miR-92a (5p) inhibitor adhesion effect in CD34$^+$-derived EPCs.**
FN specific adhesion capacity was determined in fluorescently -labelled cells previously treated with with a combination of 30nM miR scrambled, miR-92a (5p) inhibitor, si-scrambled and si-ITGA5, as indicated. Baseline and final red object count were quantified, and data are expressed as mean adhesion on FN (7 replicates per experiment) minus mean unspecific adhesion on BSA (3 replicates per experiment). The adhesion results are representative of a total of 3 independent experiments and are plotted as means, with errors bars representing ± SEM. *P<0.05 and **P<0.001 compared with *miR scrambled + si-scrambled;* ^P<0.05 and ^^P<0.01 compared with *miR-92a inhibitor + si-scrambled;* #P<0.05 compared with *miR scrambled + si-ITGA5* (1-way ANOVA, Bonferroni's test for multiple comparisons). BSA – bovine serum albumin; EPC – endothelial precursor cell; FN – fibronectin; ITGA5- integrin alpha 5 subunit; miR – microRNA; si – small interfering; SEM – standard error mean.

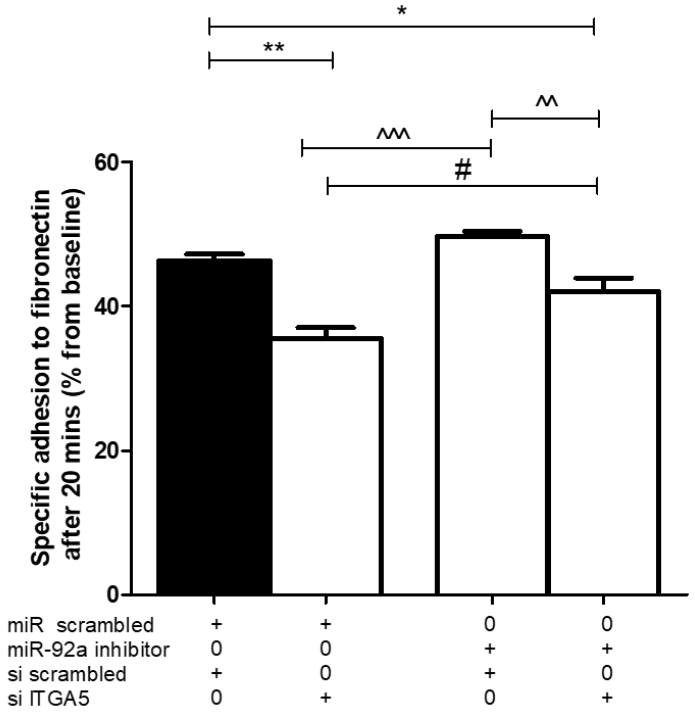

Because we had also witnessed an enhanced EPC proliferation (under VEGF stimulus) resulting from miR-92a inhibitor treatment, and since integrin outside-in signalling has been linked to cell proliferation (Shen, Delaney, & Du, 2012), ITGA5 was downregulated with siRNA in miR-92a inhibitor -treated EPCs and tested as an additional experimental condition in a new proliferation assay **(Figure 55)**. Remarkably, the knockdown of ITGA5 with the siRNA did not influence EPC cumulative proliferation after 48 hours, either in the absence or presence of VEGF, suggesting the implication of alternative miR-92a targets to explain the previously described effects. Oddly enough, when adding si-scrambled to miR-92a inhibitor, I failed to reproduce the miR-92a inhibitor enhancement of proliferation with VEGF seen before, a topic which will be discussed later.

**Figure 55 | si-ITGA5 had no effect on the proliferation of CD34$^{+}$-derived EPCs.**
Cells treated with a combination of 30nM miR scrambled, miR-92a (5p) inhibitor, si-scrambled and si ITGA5, as indicated, were incubated with an ATP quantifying luciferase reporter at baseline. For the time course, cells in a second well plate were incubated in enriched medium plus or minus VEGF 25 ng/mL for 48h before performing the luminescence assay. The results are representative of a total of 4 independent experiments (each condition run in replicates of 4) and are plotted as means, with errors bars representing ± SEM. ***P<0.001 compared with baseline condition; ^^P<0.01 and ^P<0.05 compared with the VEGF-negative condition at 48h (1-way ANOVA, Bonferroni's test for multiple comparisons). Adenosine triphosphate; EPC – endothelial precursor cells; miR- microRNA; SEM – standard error mean; VEGF – vascular endothelial growth factor.

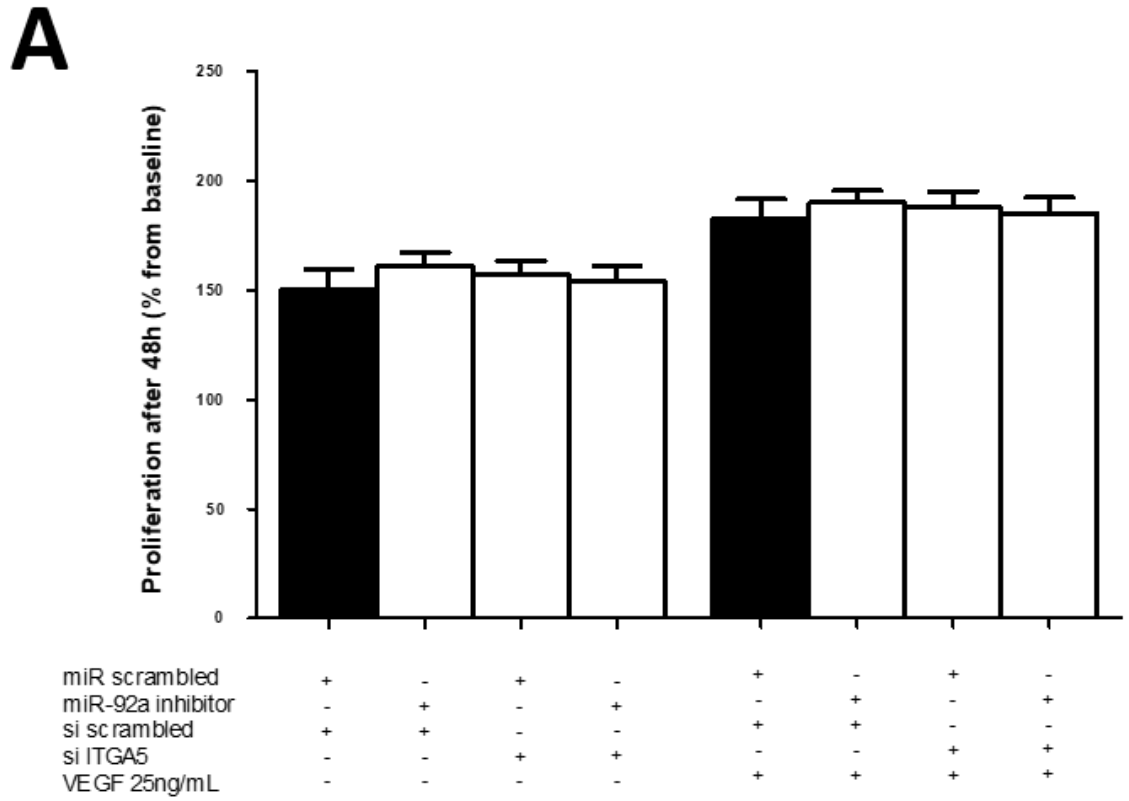

Integrins are mechanistically involved in cell migration(Bokel & Brown, 2002). Therefore, one would expect to see at least a reduction of miR-92a inhibitor-induced enhancement on wound healing migration by si-ITGA5 co-transfection into EPCs. To test the hypothesis that miR-92a target protein ITGA5 is involved in the enhanced EPC wound healing regeneration seen after miR-92a inhibitor treatment, I performed a new scratch assay **(Figure 56)**. The data exhibited represents a single experiment, thus the results are still preliminary, but it seemed to point towards a reduction of EPC wound closure migration in the conditions where si-ITGA5 was applied. When adding si-scrambled to miR-92a inhibitor, I failed to reproduce the miR-92a inhibitor enhancement of wound closure migration, hinting at a possible si-scrambled off-target effect to be discussed later.

**Figure 56 | si-ITGA5 could abrogate the miR-92a (5p) inhibitor effect on CD34$^+$-derived EPC migration.** Cells were treated with either si scramble + miR scrambled (black line), si scramble + miR-92a (5p) inhibitor (green line), si-ITGA5 + miR-92a (5p) inhibitor (red dashed line) and si-ITGA5 + miR scrambled (red line). All oligonucleotides were transfected at 30 nM concentration. After a 48h knockdown, wound closure migration in EBM 0.5% FBS was assessed in the presence or absence of 25 ng/mL VEGF by live-cell Imaging. Images were captured every 2h for a total duration of 48h. The line graphic represents the effect of siITGA5 on EPC migration. Each condition counted 6 replicates and data exhibited represents one single experiment, therefore the results are still preliminary. EPCs – endothelial precursor cell; FBS–fetal bovine serum; ITGA5–integrin alpha 5; Si–small interference; miR–microRNA; VEGF–vascular endothelial growth factor.

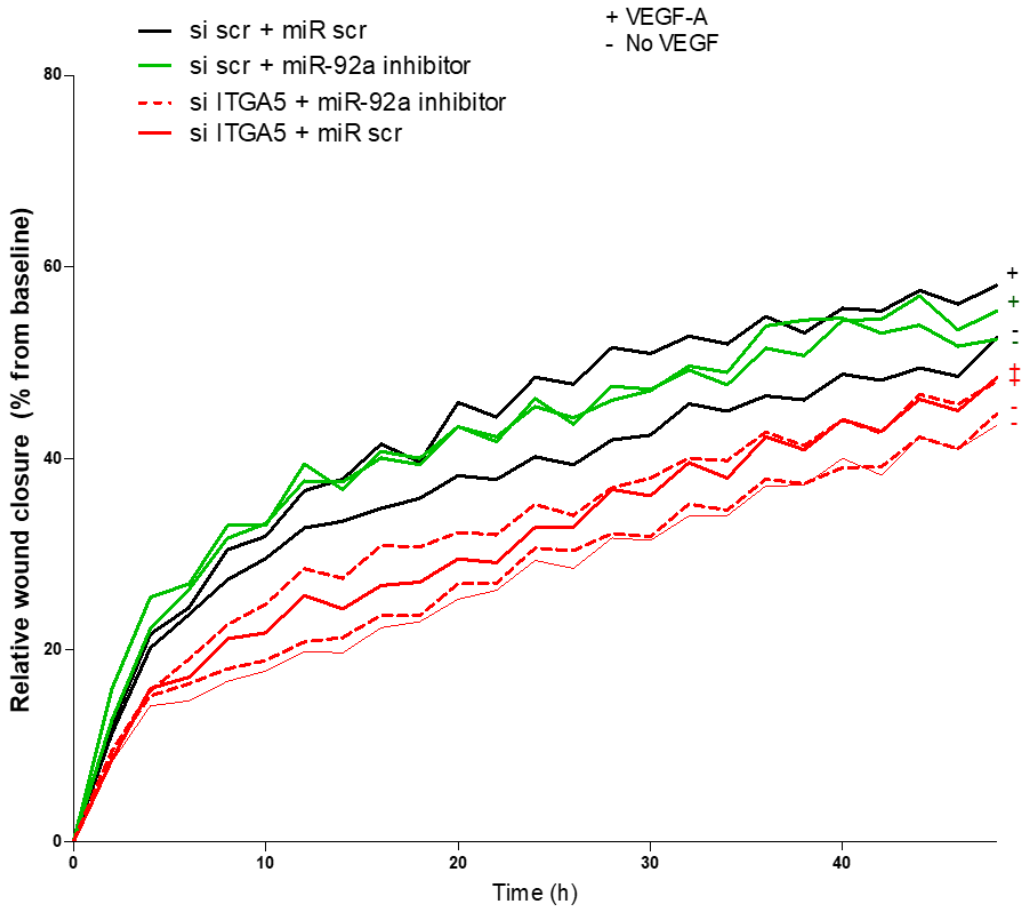

# 4.6 Discussion

## Inhibition of miR-92a for EPC priming: what grounds?

Developing a miRNA priming strategy for EPCs was based on the premise that aberrantly expressed miR-92a contributes towards a dysfunctional EPC phenotype (Q. Zhang et al., 2011), and that antagonising it could provide gain-of-function therapeutic benefit. Using antisense sequences which sequester the mature miRNA in competition with cellular target mRNAs, would lead to the functional inhibition of the endogenous miRNA and derepression of the direct targets.

### The choice of miR-92a-1 inhibitor

miRNAs with similar seed sequences are predicted *in silico* to target highly overlapping sets of genes and are usually grouped functionally in the same "seed family". Together the group of highly conserved miRNAs miR-92a-1, miR-92a-2, miR 363, miR25 and miR-92b (which is generated independently from chromossome1) constitute the miR-92 seed family **(Table 16)**.

**Table 16 | Sequence of the miR-92 seed family.**
The mature miRNA sequences of the miRNAs belonging to the miR-92 seed family are displayed in the table. The predicted seed sequence is shown in bold for both miR strands. Adapted from (Concepcion et al., 2012). Chr – chromosome; miR – miRNA

| 3p strand | miRNA Annotation | Location |
|---|---|---|
| U**AUUGCA**CUUGUCCCGGCCUGU | hsa-miR-92a-1-3p | Chr. 13 |
| U**AUUGCA**CUUGUCCCGGCCUGU | hsa-miR-92a-2-3p | Chr. X |
| A**AUUGCA**CGGUAUCCAUCUGUA | hsa-miR-363-3p | Chr. X |
| C**AUUGCA**CUUGUCUCGGUCUGA | hsa-miR-25-3p | Chr. 7 |
| U**AUUGCA**CUCGUCCCGGCCUCC | hsa-miR-92b-3p | Chr. 1 |
| **5p strand** | **miRNA Annotation** | **Location** |
| A**GGUUGG**GAUCGGUUGCAAUGCU | hsa-miR-92a-1-5p | Chr. 13 |
| G**GGUGGG**GAUUUGUUGCAUUAC | hsa-miR-92a-2-5p | Chr. X |
| C**GGGUGG**AUCACGAUGCAAUUU | hsa-miR-363-5p | Chr. X |
| A**GGCGGA**GACUUGGGCAAUUG | hsa-miR-25-5p | Chr. 7 |
| A**GGGACG**GGACGCGGUGCAGUG | hsa-miR-92b-5p | Chr. 1 |

I have opted to study the modulation of miR-92a-1 on EPCs (and not any other paralogs), since most of the literature published on the effects of miR-92 on angiogenesis, in particular in ECs (Bonauer et al., 2009), comes from studying the mir-17~92 cluster (Bonauer & Dimmeler, 2009; Concepcion et al., 2012). Despite the possibility that miR-92a-1 inhibition can also repress other seed family paralogs being more than theoretical (Hinkel *et al.* used LNA-92a inhibitor and showed miR-25 repression in pig arteries(Hinkel et al., 2013)), I did not test for paralog targeting by qPCR. I have assumed high oligo specificity as described by the manufacturer, an assumption also made by Bonauer (Bonauer et al., 2009), Iaconetti (Iaconetti et al., 2012) and Daniel (Daniel et al., 2014) groups' when inhibiting miR-92a in ECs and VSMCs in their critical research. Then, after testing the potency of both 5p and 3p strands of the mimic and inhibitor of miR-92a-1 regarding target gene expression, I have opted to pursue the functional assays using solely the miR-92a-1 5p strand, which was considered the primary strand, i.e. most efficient and consistent in $CD34^{+}$-derived EPCs.

## Suitability of oligofectamine for internalisation of miR-92a inhibitor

AntagomiR-based therapies must overcome commonly described obstacles to nucleic acid delivery, including cell membrane impermeability, trafficking to the desired intracellular compartment (cytoplasm), recognition by the innate immune system, and nuclease-based degradation reducing the half-life (Sakurai, Kawabata, Sakurai, Nakagawa, & Mizuguchi, 2008). Efficient delivery of miRNAs mimics into cells can bypass the endogenous miRNA biogenesis pathway and alter miRNA abundance instantly, whereas inhibitors can repress the endogenous species. A variety of agents has been tested for non-viral miRNA transient transfection. Examples include nanoparticles (NP), amphiphilic polymer micelles, cell penetrating peptides and liposomes. The latter, also known as lipofection, is a widely used technique to transfect nucleic acids material into a cell using liposomes, which are vesicles that can easily merge with the cell membrane since they are both made of a phospholipid bilayer (Felgner et al., 1987). Lipofection

uses a positively charged (cationic) lipid to form an aggregate with the negatively charged (anionic) miRNA. Lipofection needs no specialised equipment (like electroporation), and it is widely available since several companies have developed commercial kits, with suitable experimental reproducibility. Such lipofection commercial kits have been previously validated for miR-92a transfection into ECs. Bonauer *et al.* used Lipofectamine RNAiMAX (Invitrogen) to transfect miR-92a mimic and inhibitor into HUVECs (Bonauer et al., 2009), whereas Iaconetti *et al.* utilised siPORT NeoFX Transfection Agent (Ambion) in rat aortic ECs (Iaconetti et al., 2012). Therefore, I have attempted to use both transfection reagents in $CD34^+$-derived EPCs to facilitate miR-92a (mimic and inhibitor) internalisation, but with no success. Regarding the transfection results in $CD34^+$-derived EPCs, one can argue that cells were either resistant to some of the miRNA cationic lipid transfection reagents previously validated for ECs due to cell type-specific membrane structural or endocytosis-related differences, or, alternatively, if the miR-92a (mimic or inhibitor) was indeed internalized, then the miRNA was not able to be incorporated in the RISC machinery (compartmentalization issue? liposome sequestration?).

OF was one of the first lipid formulations to be examined for the *in vitro* delivery of siRNA. Since our group had significant experience in using it for siRNA transfection into ECs, and given that OF was previously shown to also be effective for miRNA transfection into ECs (Ye & Steinle, 2015), I attempted to use this methodology for the transfection of miR-92a (mimic and inhibitor) into $CD34^+$-derived EPCs. The commercially available cationic lipid OF is a proprietary formulation able to transfer RNA interference oligonucleotides into eukaryotic cells. The transfection complex is thought to enter the cell through endocytosis, defined as the process where a localised region of the cellular membrane uptakes the complex by forming a membrane bound/intracellular vesicle. Since the RISC machinery is also located in the endosomal compartment, exogenous miRNA can be almost immediately processed. The transfection method is simple to perform and ensures consistently reproducible results. Despite some cationic lipid formulations eliciting inadvertent gene expression (Omidi et al., 2003), OF is reported to have minimal cytotoxicity in EC cells. According to the IF and FACS results, OF was shown to be highly efficient in miR-92a inhibitor transfection into EPCs.

## Assessment of miR-92a inhibition

Several methods can assess the effect of miRNA inhibition by antagomiR oligonucleotides. Approaches that directly measure changes in miRNA levels following antagomiR -mediated inhibition by hybridization techniques (such as qPCR or small RNA Northern blotting) present some limitations and should be analysed with caution due to possible assay interference. Firstly, the antagomiR chemistry may dictate the fate of the targeted miRNA. Chemically modified oligonucleotides like LNAs sequester the targeted miRNA in a heteroduplex (meaning that sometimes they can still be detected in hybridization studies), whereas lower affinity modified oligonucleotides, such as 2'-OMe and cholesterol-conjugated 2'-OMe antagomiRs, promote miRNA degradation (Stenvang et al., 2012). Secondly, the presence of excess miRNA inhibitor in the RNA sample may interfere with the detection step of the assay, for example, primer annealing or extension in miRNA-specific real-time qPCR (Stenvang et al., 2012). The observed readout in some settings may, thus, constitute underestimated reductions in the concentration of the miRNA of interest due to assay interference by the miRNA inhibitor. Therefore, assays that measure a functional readout of miRNA inhibition by antagomiRs should be preferred (Stenvang et al., 2012). These include the assessment of the de-repression of direct targets by real-time qPCR or Western blot analysis. In most cases, there is a striking correlation between mRNA and protein levels following miRNA disturbance (Baek et al., 2008). However, since miRNA-mediated mRNA repression involves both mRNA degradation and translational repression, the cellular concentration of target mRNAs following antagomiR treatment may not always reflect their true "availability to be translated". Translationally -repressed mRNAs captured by miRISCs can contribute to the overestimation of target mRNAs. Hence, assessing target de-repression at the protein level by Western blotting seemed more in line with true effector concentration, which was the methodology used in this study.

After having optimised the transfection conditions of EPCs in what concerns miRNA working concentration and processing duration, I sought proof of miR-92a inhibition at the protein level. According to the obtained results, inhibition of miR-92a-1-5p by the corresponding mirVana inhibitor led to significant upregulation of ITGA5 and T-eNOS

protein levels in EPCs (direct and indirect miR-92a targets, respectively) compared to the transfection control. Bonauer *et al.* in their seminal paper on miR-92a inhibition impact on EC biology described the same results (Bonauer et al., 2009) but using qPCR. Likewise, Ohyagi-Hara *et al.* demonstrated that miR-92a inhibitor upregulated ITGA5 mRNA levels in non-EC cells (Ohyagi-Hara et al., 2013). More recently, Iaconetti *et al.* also confirmed the T-eNOS upregulation at the protein level in ECs following miR-92a inhibitor treatment (Iaconetti et al., 2012). Sadly, ITGA5 levels were not assessed by them. This group also described that protein expression of MKK4 (another validated miR-92a direct target) was up-regulated in ECs following miR-92a inhibitor treatment, a result we failed to see in EPCs. Of note, to the best of our knowledge, our study was the first to report MKK4 expression in late-outgrowth EPCs. The discrepancy regarding MKK4 results in ECs and EPCs might be due to cell type specific variations, or as a consequence of the different protocoled miR inhibitor and transfection reagents used. However, one also needs to be aware that the degree of miRNA target de-repression can often be modest, with some proteomic studies reporting average changes limited to less than two-fold (Baek et al., 2008). In some cases, the upregulation of specific target protein may not be apparent or significant (like MKK4 in EPCs), and still, a cellular phenotypical change occur (like the gain-of-function reported in our work). This phenomenon is likely explained by the combined interplay between targets de-repressed.

On the other hand, treatment with miR-92a-1 (5p) mimic was pursued throughout the thesis as a negative treatment control. Currently in microRNA research, both the microRNA precursor and mimic (the mature form) are commercially available. Theoretically, utilising the miRNA mimic should lead to clearer results, as the effects of the minor strand miRNA are avoided. Hence, I have chosen to use the mirVana™ mimic for validation of target gene repression following transfection with OF in $CD34^{+}$-derived EPCs. The mimic is a double-stranded oligonucleotide (with two nucleotide overhangs) that reproduces the endogenous microRNA. These molecules do not have any loops or additional bases, but some proprietary chemical modifications are often operated, such as nucleotide changes in the passenger strands, to improve mimic stability, to facilitate guide miRNA loading to RISC, and to selectively exclude the passenger strand (H. Y. Jin et al., 2015). The observed downregulation of targets ITGA5 and T-eNOS (which have

been previously described as direct and indirect miR-92a target genes) obtained in $CD34^+$-derived EPCs following miR-92a transfection had been previously observed by others in ECs, both at mRNA (Bonauer et al., 2009; Daniel et al., 2014; Iaconetti et al., 2012) and protein level (Bonauer et al., 2009). However, while we have reported downregulation of ITGAV at the protein level in EPCs, the reduction of this integrin at mRNA level in ECs did not reach statistical significance (Bonauer et al., 2009). In contrast, MKK4 (Bonauer et al., 2009; Iaconetti et al., 2012) and SIRT1 (Daniel et al., 2014) mRNAs were significantly downregulated after miR-92a treatment in ECs, a finding that I could not reproduce at the protein level in EPCs. Altogether, the individual target regulation discrepancies pointed in our work may be cell type specific, or, simply result from the different synthetic miR-92a oligonucleotides and transfection reagents used by the various groups. However, in the overview, it appears that the miR-92a target signature is quite similar in both $CD34^+$-derived late-outgrowth EPCs and mature ECs, with ITGA5 targeting now being established as common ground for the first time, according to our literature review.

## The functional outcome of miR-92a inhibition in $CD34^+$-derived EPCs

Validation of exogenous miR-92a inhibitor activity in $CD34^+$-derived EPCs at the protein level was considered essential before I could test the hypothesised functional outcomes of miR-92a inhibition priming in these cells.

### Angiogenesis

The inhibition of miR-92a in EPCs lead to a significant pro-angiogenesis effect *in vitro* as reported by the co-culture with fibroblasts. A similar result was obtained by other groups after treating ECs with miR-92a inhibitor in a Matrigel model *in vitro* (Bonauer et al., 2009; Doebele et al., 2010; L. Zhang, Zhou, Qin, Weintraub, & Tang, 2014). On the other hand, I have observed a non-significant reduction in the angiogenic potential of EPCs following miR-92a treatment, which is in agreement with the results by Bonauer *et al.* also using a Matrigel assay *in vitro* (Bonauer et al., 2009).

## Migration

Using an automated scratch wound assay, we have noticed that miR-92a inhibitor treatment lead to enhanced wound closure migration in $CD34^+$-derived EPCs (only statistically significant when compared to transfection control in the absence of VEGF stimulus). Previously, Iaconetti *et al.* had also reported that functional inhibition of miR-92a on rat aortic ECs significantly enhanced wound healing migration in a 36h assay (Iaconetti et al., 2012). The wound healing test is well suited for the investigation of cell-cell interactions on cell migration. However, one must recognise that the mechanics of cell movement are difficult to interpret. Cell population assays do not consider single cell locomotion or distinguish between the roles played by cell migration and cell growth. Often, experimental conditions will impact on both proliferative and motile activity. Therefore, a transwell cell culture experiment might be more informative for cell migration, since cells must first digest the artificial ECM before their migration, similarly to the *in vivo* context. In the modified Boyden chamber assay, $CD34^+$-derived EPCs treated with miR-92a inhibitor showed significantly enhanced VEGF-induced chemotaxis migration ability compared to controls.

On the other hand, we witnessed a reduction in EPC migration capacity after miR-92a treatment, albeit not reaching statistical significance. Bonauer *et al.* reported similar results, with the migration of ECs being non-significantly reduced by pre-mir92a treatment (Bonauer et al., 2009). Daniel *et al.* had also tested miR-92a treated ECs in a modified Boyden chamber assay and detected impaired migration compared to controls (Daniel et al., 2014). The results from head-to-head comparison do not necessarily correlate with the cells' ability to traverse the matrix in response to a chemoattractant. Protocol differences, such as cell density and the size of the filter pores, could have influenced the migration/invasion rate significantly (Sieuwerts, Klijn, & Foekens, 1997).

## Proliferation

By using an ATP quantifying luciferase reporter assay, it was possible to document that miR-92a inhibitor enhanced VEGF-induced EPC proliferation at 48h. Iaconetti *et al.* also

reported a similar significant increase in VEGF-induced EC proliferation after functional inhibition of miR-92a, according to a BrdU assay (Iaconetti et al., 2012). Following a different strategy, Liu *et al*. also verified increased relative proliferation under basal conditions (by MTT assay) of ECs infected with recombinant miR-92a inhibitor lentivirus (H. Liu et al., 2016).

On the other hand, we have shown that miR-92a significantly reduced EPC proliferation, either in the presence or absence of VEGF. As expected, upregulation of miR-92a reduced the mitogenic effect of VEGF stimulation compared to transfection control. Our observation reproduced what was previously described by Iaconetti *et al.* for ECs (Iaconetti et al., 2012)

## Adhesion

The critical initial event for re-endothelialisation, regarding late outgrowth progenitor contribution, would be the attachment of the circulating EPCs to the denuded arterial wall. It is hypothesised that the engraftment and differentiation of EPCs depend largely on their adhesion to ECM components, such as FN, and the resultant signalling cascade that occurs on cell binding. Hence, modulating EPC adhesion activity with miR-92a inhibitor, which upregulates ITGA5, was a key consideration of ours. To accomplish this, passive *in vitro* EPC adhesion to FN, under static conditions, was tested. FN had been previously validated for EPC cultures, in fact, with superior adhesion compared to ECs (Vartanian et al., 2009). In this type of assay, the initial adhesive interaction between the cells and the substrate are said to be driven by specific integrins-ECM ligand bonding pairs (Hong, Ergezen, Lec, & Barbee, 2006). In the next hours, subsequent receptor-ligand bonds will form and quickly enhance in number, forming focal adhesions with increased tensile strength and flattening the cell (Khalili & Ahmad, 2015). Cells then start spreading beyond the projected area to reach their maximum area through expansion and adhesion strength will then become fully stable (Khalili & Ahmad, 2015). According to our results, miR-92a inhibitor significantly enhanced EPC adhesion to the FN matrix (a ligand for ITGA5). The expression of ITGA5 had been demonstrated by us and others

(Chavakis et al., 2005), and concordantly, ITGA5-KO ECs have shown reduced adhesion to FN, which can be rescued by ectopic (over)expression of ITGA5 (van der Flier et al., 2010). Given that a short termination period for the assay was used (20 mins), it is fair to assume that the relatively increased adhesion was related to miR-92a inhibitor - mediated ITGA5 upregulation. In fact, the involvement of integrin $\alpha 5\beta 1$ in late-outgrowth EPCs' interaction with ECM is in agreement with other published works (Angelos et al., 2010; Brown, Wallace, Angelos, & Truskey, 2009) with the cell contact area growing during the first 20 minutes of attachment (Brown et al., 2009).

To our knowledge increased EPC adhesion following ITGA5 overexpression induced by miR-92a inhibitor has never been attempted neither in ECs nor EPCs, but our results are in agreement (by contrast) with the observation by Bonauer and colleagues, that exogenous miR-92a transfection impairs EC adhesion to FN (Bonauer et al., 2009). Ohyagi-Hara *et al*. reported to the same observation but in cancer cells, with transfection of precursor miR-92a reducing ITGA5 expression and inhibiting cancer cell adhesion (Ohyagi-Hara et al., 2013).

## Survival

In theory, cells that successfully adhere to the ECM will have a higher chance of survival by avoiding *anoikis*, which can be defined as apoptosis caused by lack of adhesion to ECM. This enhanced adhesion capacity may play a major role in cell survival, particularly in the restenosis environment. However, our results failed to demonstrate a significant increase in $CD34^+$-derived EPC survival after miR-92a inhibitor treatment in serum-free medium. This result contrasts with the observation by Liu *et al.* in ECs, where miR-92a inhibitor significantly reduced the apoptosis rate compared with control groups (H. Liu et al., 2016). Using siRNA against KLF2 or KLF4 (miR-92a direct targets), they were able to antagonise the miR-92a inhibitor effect on the rate of EC apoptosis, directly involving this pathway in EC survival. Contrastingly, Ohyashiki *et al.* demonstrated that anti-miR-92a treatment increased apoptosis in human myeloid and lymphoid cells (Ohyashiki et al., 2010). More recently, a study in human glioma cells described an increased cell apoptosis outcome after antisense inhibition of miR-92a, via targeting the Bim gene (Niu et al., 2012). These findings suggest a differential role for miR-92a inhibitor in regulating

viability of EPCs, ECs and malignant cells, possibly through different target genes according to cell and context specificities.

When we treated $CD34^+$-derived EPCs with miR-92a, again no significant change in survival was seen when comparing with controls. Similarly, Bonauer and colleagues could not find any significant change in EC viability after miR-92a overexpression (Bonauer et al., 2009). Daniel and colleagues also reported no effect of pre-miR-92a treatment on EC apoptosis (Daniel et al., 2014). Contrastingly, there is a study by Zhang *et al.* reporting that miR-92a overexpression enhanced EC viability (under oxidative stress), through the release of Akt signalling, suggesting a vasculoprotective effect that is likely mediated through a PTEN-dependent mechanism (L. Zhang, M. Zhou, Y. Wang, et al., 2014). These findings suggest a differential role for miR-92a in regulating viability of ECs, possibly through different target genes according to context specificities, which still warrants further investigation.

## miR-92a targets which could contribute to the functional results

The studies on miRNA function have been limited by several obstacles. Given the ubiquitous nature of miRNAs it is hard to predict all their targets accurately, but with the recent development of new computational algorithms, this task has become facilitated (John et al., 2004; Lewis et al., 2003). Molecules with distinct functions like ITGA5 and ITAGV (cell-matrix interaction)(Bonauer et al., 2009), SIRT1 (histone deacetylase)(O'Donnell et al., 2005), MKK4 (mitogen kinase)(L. Zhang, M. Zhou, Y. Wang, et al., 2014) and KLF2/KFL4 (flow-induced transcription factors)(Y. Fang & Davies, 2012; H. Liu et al., 2016; Wu et al., 2011) are some of the predicted miR-92a targets that have since been validated. Curiously, all of them render an embryonic lethal phenotype if knocked down, suggesting they have significant activities in the organism (H. L. Cheng et al., 2003; D. Yang et al., 1997; J. T. Yang, Rayburn, & Hynes, 1993), only to be fine tuned by miR-92a.

We found that miR-92a inhibition enhanced VEGF-A -induced $CD34^+$-derived EPC proliferation, a result previously described in ECs and thought to be at least in part

caused by the phosphorylating activation of mitogenic ERK and JNK signalling (Iaconetti et al., 2012), a pre-requisite for EC proliferation (Salameh et al., 2005). Since miR-92a controls MKK4 levels in ECs and JNK has been shown to be phosphorylated by MKK4 (Y. Fleming et al., 2000), it has been hypothesised that miR-92a inhibitor stimulates JNK activation through de-repressing MKK4 (Iaconetti et al., 2012). Indeed, Liu and colleagues also found that treatment with miR-92a inhibitor significantly upregulated relative EC proliferation compared to controls, an effect which could be antagonised by siRNA KLF2 and KLF4 (H. Liu et al., 2016), suggesting an important role of these transcription factors in EC proliferation. Unfortunately, we could only observe an enhanced MKK4 expression trend with miR-92a inhibitor treatment, suggesting that other pathways might be involved in enhanced proliferation. Indeed, Cui and colleagues described and alternative pathway that can be accountable for enhanced proliferation in EPCs (B. Cui et al., 2011). They have shown that *in vitro* gene transfer of eNOS improved the proliferation of EPCs. Similarly, in our study we observed a miR-92a inhibitor indirectly induced eNOS expression, which could, eventually, explain the proliferation results.

Besides the pro-proliferative contribution, inhibition of miR-92a might, in theory, accelerate EPC-mediated re-endothelialisation (and hence attenuate experimental restenosis) at the injury site through additional mechanisms. SIRT1, which promotes EC angiogenesis, and ITGA5, which enables EC migration and angiogenesis (Potente, Gerhardt, & Carmeliet, 2011), are among the validated targets of miR-92a (Bonauer et al., 2009). Daniel and colleagues reported that both targets were strongly increased in arterial ECs in miR-92a inhibitor -systemically treated mice two weeks after wire-induced injury (Daniel et al., 2014), hinting that therapeutic inhibition of miR-92a stimulates re-endothelialisation, at least in part, by de-repressing the two proangiogenic factors.

SIRT1 *per se* has been shown to have an inhibitory effect on neointima formation (L. Li et al., 2011). SIRT1 deacetylation of FOXO1 inhibits its antiangiogenic activity in human vascular ECs (Potente et al., 2007) while targeting eNOS for deacetylation leads to NO production and corresponding enhanced endothelial-dependent vasodilation (Mattagajasingh et al., 2007), survival, migration and neovascularization (Aicher,

Heeschen, et al., 2003). Overexpression of SIRT1 prevents hydrogen peroxide-induced endothelial senescence suggesting that SIRT1 might prevent stress-induced endothelial dysfunction. In EPCs the expression and activity of SIRT1 also correlate inversely with senescence (Lemarie et al., 2011). However, in $CD34^+$-derived late -outgrowth EPCs we were unable to demonstrate a statistically significant upregulation of SIRT1 following miR-92a inhibitor treatment compared to control transfection, making this contribution less likely to justify the observed EPC functional enhancement.

The ECM is a non-cellular component that not only provides a physical scaffold for cells, but also triggers essential biomechanical cues that contribute towards determining EPC differentiation, proliferation, survival, polarity and migration (Caiado & Dias, 2012). In particular, the EPC transmembrane integrin α5β1 combines with FN to form a ligand-receptor complex that does not only mediate cell adhesion but can also promote cell proliferation, survival and even differentiation (Pagan et al., 2002). In 2009, Bonauer and colleagues demonstrated that ITGA5 (one of the subunits of α5β1) is a direct target of miR-92a in ECs (Bonauer et al., 2009). Ohyagi-Hara *et al.* came to the same conclusion but in cancer cells (Ohyagi-Hara et al., 2013). In our work, we have shown ITGA5 to be upregulated in $CD34^+$-derived EPCs following miR-92a antagonism. Therefore, given its interaction with ECM components, ITGA5 is considered a necessary prerequisite for vascular regeneration following injury (Koyama & Reidy, 1998; Stenzel et al., 2011) since it facilitates the adhesion, proliferation, and migration of ECs (thus, possibly EPCs as well) in the process of re-endothelialisation (Daniel et al., 2014). Moreover, vascular ECs rely heavily on their interactions with the ECM and their neighbouring cells to avoid cell death. In fact, various integrins, including $\alpha 5\beta 1$ or $\alpha V\beta 3$ have been shown to prevent apoptosis of ECs (Scatena et al., 1998; Z. Zhang, Vuori, Reed, & Ruoslahti, 1995), an effect that we were unable to see in $CD34^+$-derived EPCs using an indirect metabolic luminescence assay.

Besides $\alpha 5\beta 1$, the interaction of late-outgrowth EPCs with FN is also strongly dependent on integrins $\alpha V\beta 1$, $\alpha V\beta 3$ and $\alpha V\beta 5$ (Kokubo, Uchida, & Choi, 2007; J. Zhao, Mitrofan, Appleby, Morrell, & Lever, 2016). Since we failed to see any upregulation of ITGAV in miR-92a inhibitor treated cells (although miR-92a successfully downregulated it), ITGAV contribution to enhanced EPC adhesion in our study is less likely in comparison to ITGA5

(which was successfully upregulated following miR-92a inhibitor treatment), although others have reported that direct inhibition of $\alpha V\beta 3$- and $\alpha V\beta 5$-integrins blocks EPC-mediated re-endothelialisation of denuded arteries (Kokubo et al., 2007).

miR-92a has also been found to target KLF2 and KLF4 (Y. Fang & Davies, 2012) (genes that were not unfortunately included in my WB experiments). These transcription factors typically exert an anti-inflammatory and atheroprotective effect in ECs after injury (Y. Fang & Davies, 2012), which can modulate proliferation and survival. This is done possibly through enhanced NO production (Boon & Horrevoets, 2009; Y. Fang & Davies, 2012; Hamik et al., 2007; Iaconetti et al., 2012; Parmar et al., 2006). In fact, although eNOS is not a direct target of miR-92a, a direct correlation to ITGA5 (Bonauer et al., 2009), KLF2 (Boon et al., 2011) or KLF4 (Hamik et al., 2007) expression levels has been shown in previous studies. Also, SIRT1 was also shown to deacetylate and thereby activate eNOS (Ota et al., 2007). This off-target phospho-eNOS increased expression has been described previously for ECs as a consequence of miR-92a inhibition (Iaconetti et al., 2012). Therefore, the indirect upregulation of eNOS (which we have also observed in our study) may represent an additional effect which could contribute to the EPC-mediated enhanced re-endothelialisation following the knock-down of miR-92.

## Integrin α5 has a pivotal role in miR-92a inhibitor EPC priming

In vessels, adhesion of EPCs to injury sites are thought to involve both cell-cell and cell-ECM interactions. However, Zhao and colleagues demonstrated that under flow conditions *in vitro* late -outgrowth EPCs interact little with confluent ECs, but readily adhere to and spread where there are discontinuities in the EC monolayer, namely at gaps in the intercellular junctions between ECs (J. Zhao et al., 2016). Similarly, vascular damage *in vivo* is characterised by loss of endothelial integrity. Where the EC monolayer is disrupted, the basement membrane and its matrix components (including FN) are exposed to blood flow (Timpl, 1996). FN is an important regulator of various cellular processes including survival, differentiation, growth and migration (Hynes, 2002). FN is actively deposited in the ECM mainly by ECs and can be found circulating freely in the

plasma as well (Kaiser, Friedrich, Chavakis, Bohm, & Friedrich, 2012). FN is abundant at the site of vascular injury, a feature that might be expected to facilitate EPC incorporation (Bauters et al., 1995). The interaction between late-outgrowth EPCs with FN has been previously validated (Angelos et al., 2010; Kaiser et al., 2012) and the generated adhesion strength estimated as very strong (J. Zhao et al., 2016). In fact, late-outgrowth EPCs are much more adhesive to FN than to collagen IV, collagen I, and laminin under flow conditions (J. Zhao et al., 2016). This interaction with FN is strongly dependent on integrins $\alpha 5\beta 1$ (Angelos et al., 2010; Brown et al., 2009; Kaiser et al., 2012; J. Zhao et al., 2016). α5β1 binds to the Arg-Gly-Asp (RGD) tri-peptide motif in FN (van der Flier et al., 2010), and it is composed of α5 (ITGA5/CD49e) subunit, which undergoes post-translational cleavage in the extracellular domain to yield disulfide-linked light and heavy chains, that join with β1 (ITGB1/CD29) to form a FN receptor. Not coincidently, late-outgrowth EPCs express abundant numbers of the integrin monomers $\alpha 5$, $\alpha \mathrm{v}$, $\beta 1$, and $\beta 3$ (Chavakis et al., 2005; J. Zhao, Bolton, Randle, Bradley, & Lever, 2014), which are exactly the components of the major FN ligands $\alpha 5\beta 1$, $\alpha \mathrm{V}\beta 1$ and $\alpha \mathrm{V}\beta 3$ (Johansson, Svineng, Wennerberg, Armulik, & Lohikangas, 1997), densely present at the EPC surface (J. Zhao et al., 2014). Concordantly, Zhao *et al.* tested blocking antibodies against integrins $\alpha 5\beta 1$, $\alpha \mathrm{v}\beta 1$ and $\alpha \mathrm{v}\beta 3$ and showed a significant decrease in EPC adhesion to FN (J. Zhao et al., 2016), suggesting that the interaction between EPCs and ECM is largely mediated by these 3 integrins heterodimers. Promisingly, by using miR-92a inhibitor in $CD34^{+}$-derived EPCs we were exactly able to de-repress both ITGA5 and ITGAV monomers simultaneously, hence contributing to increased EPC adhesion to FN. Angelos and colleagues took a closer look at integrin-mediated EPC adhesion and concluded that, in fact, α5β1 seems to be the primary integrin responsible for initial cell capture to FN (Angelos et al., 2010). Their setup included adhesion experiments to FN under static and dynamic conditions where monoclonal antibodies against both α5β1 and αVβ3 were used. The adhesion of EPCs was significantly reduced relative to both static and flow controls when α5β1 integrins were blocked, which did not happen with cells blocked with anti-αVβ3. Hence, one may assume that the initial arrest of EPCs to FN is directly dependent on α5β1 and not αVβ3 integrin. Moreover, they estimated the number of α5β1 integrin receptors on the cell surface by flow cytometry to be 3 times higher than αVβ3's. Thus, the greater role of α5β1 in adhesion may,

partially reflect their increased density per EPC. EPC adhesion to FN via $\alpha5\beta_1$ integrin was further characterized using a parallel plate flow chamber (Angelos et al., 2010). FN supported cell arrest and limited EPC rolling, by making multiple small attachments via α5β1 integrin. The integrin contact area was less than the area of the cell membrane within 50 nm of separation from the surface. Once attached (maximum adhesion seen at 1.0 dyn/cm$^2$), EPCs adhered firmly with little subsequent detachment, even when exposed to 20 dyn/cm$^2$ shear stress. Further dissecting the individual effect of α5-blockade on EPCs compared to β1-blockade, Kaiser *et al.* found that α5 contribution to EPC adhesion is markedly more pronounced (Kaiser et al., 2012).

Walter and colleagues described enhanced adhesiveness of cultured human EPCs following statin treatment, an effect that was associated with the drug-induced upregulation of ITGA5 (among other integrin monomers)(Walter et al., 2002). *In vivo*, statins have been shown to accelerate reendothelialization in balloon-injured carotid arteries via enhanced BM-derived EPC engraftment. Tying everything up, Walter then showed that this effect could be abrogated by administration of RGD peptides (Walter et al., 2002), which specifically block integrin receptors (including ITGA5) on EPCs (J. M. Muller, Chilian, & Davis, 1997).

Besides anchoring cells to ECM, integrins α5β1 are known to participate in cell-surface mediated bidirectional signalling **(Figure 57)**.

**Figure 57 | Integrin conformation-function relationships.**
Representation of the conformational changes that are associated with integrin α5β1 signalling. Inside-out signaling is mediated by 1) an inactive conformation where the integrin adopts a bent conformation in which the α- and β-subunits are closely associated; 2) a primed conformation arising from intracellular signaling which culminates in the binding of talin to the β-subunit tail, causing relaxation of the leg restraints, allowing some further unbending. The latter primes the ligand-binding pocket to achieve a high-affinity conformation that is ready to accept FN; 3) an active extended conformation able to bind theFN, representing the end-point of inside-out signalling. Outside-in signalling is initiated after binding of talin and FN. As the cytoskeleton matures, tension is generated on integrin α5β1 across the cell membrane. The force applied to the integrin headpiece triggers further distancing of the heterodimer units, strengthening receptor-ligand binding and allowing the formation of stable focal adhesions and the initiation of intracellular signaling cascades which end in gene expression modulation, the end-point of outside-in signalling. Adapted from (Askari, Buckley, Mould, & Humphries, 2009) and (Ramjaun & Hodivala-Dilke, 2009). Akt - Protein Kinase B; ERK - extracellular signal-regulated kinase; FAK – focal adhesion kinase; FN – fibronectin; NFkB - factor nuclear kappa B; PI3K - Phosphoinositide 3-kinase; Rac1 - Ras-related C3 botulinum toxin substrate 1; Src - Proto-oncogene tyrosine-protein kinase.

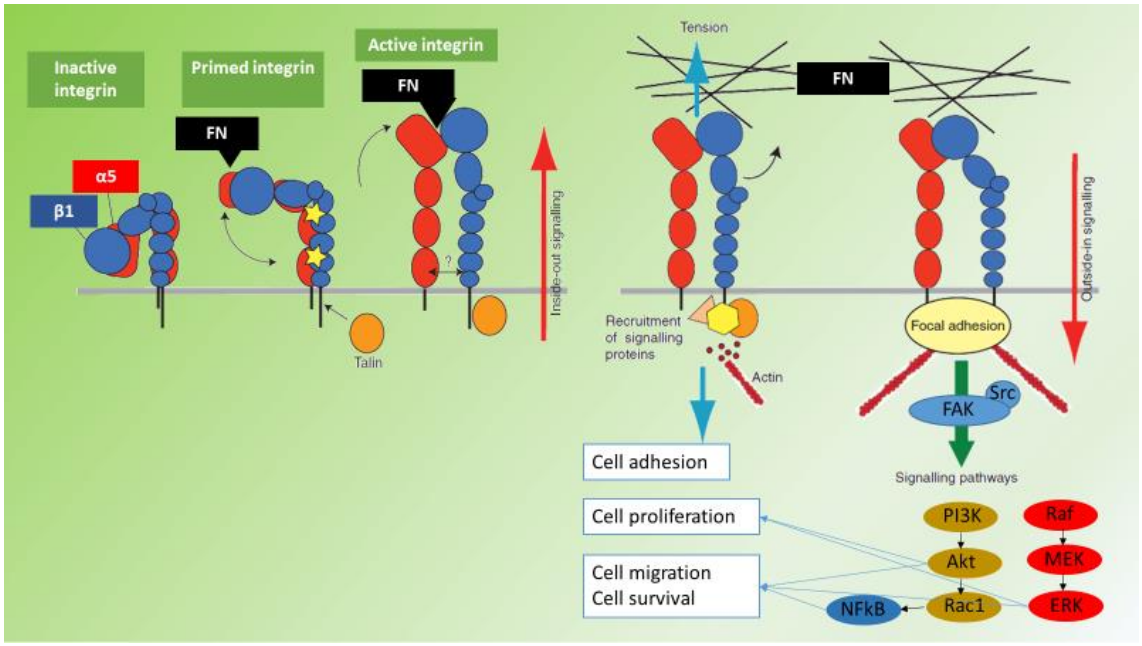


Integrins can shift between high- and low-affinity conformations for ligand binding. In an inactivated state, the α5- and a β1- chain are connected at the cytosolic end, while the extracellular heads are found in a bent-down position (Askari et al., 2009). α5β1 integrins can be activated from the cytosolic end by attachment of talin to the β1 chain. Upon talin activation the two subunits move apart, and their heads at the extracellular end assume an upright posture. Inside-out signalling allows for the interaction of α5β1 integrins with immobilised ligands, such as FN. Upon binding, the Rho *GTPase* family (including *Rho*, *Rac*, and *Cdc42*) is activated which will control stress fibre formation and the assembly of focal adhesions, involved in cell spreading and migration (Hall, 1998). Several integrins then cluster at these focal adhesion complexes, which are capable of transmitting adhesive and traction forces to the cytoplasmic actin filaments. This way, clustered integrins can convert mechanical information, such as adhesion strength and shear stress, via specific adapter proteins, into chemical signals inducing multiple cellular functions, also known as outside-in signalling. Briefly, ligand binding activates focal adhesion kinase (FAK) through direct interaction at the cytoplasmic tail of the β1-integrin subunit (Schaller, Otey, Hildebrand, & Parsons, 1995). FAK plays an essential role in several activation pathways downstream of integrins, regulating both signalling cascades and cytoskeleton changes. The signalling molecules initiate transcription of multiple genes that promote cell survival, proliferation and another key phenomenon. One of the targets of FAK is the protein kinase Src, which phosphorylates several other downstream proteins and additional sites on FAK (Ramjaun & Hodivala-Dilke, 2009).

Importantly, integrin-mediated pro-angiogenic Src activity has been observed in ECs(Zaric & Ruegg, 2005). Also, Src also plays a role in linking ECM adhesion with intercellular adhesion, which is achieved by regulating VE-cadherin activity and other components of the *adherens* junction (J. Wang & Milner, 2006). Another important target of FAK is PI3K (Sudhakar et al., 2003). In ECs, adhesion-induced PI3K activity signals via the Akt-mTOR-4E-BP1 pathway, leading to EC survival and proliferation (Sudhakar et al., 2003). Concordantly, Zhang et al. observed that inhibition of Akt phosphorylation by Ly294002 abrogated most of the protective effects of anti-miR-92a on EC-mediated angiogenesis in the setting of oxidative stress (L. Zhang, M. Zhou, G. Qin, et al., 2014). FOXO1, another downstream effector of the PI3K-Akt signalling axis, has also been implicated in angiogenesis (Ramjaun & Hodivala-Dilke, 2009). FAK can also bind p130Cas and PLC-ϒ following integrin activation (X. Zhang et al., 1999), both proteins involved in cell adhesion signalling pathways important in EC migration (Nagashima et al., 2002). α5β1 also plays a key role during the vascular remodelling and maturation of newly established vascular structures, since shear-stress has been reported to stimulate ITGA5 in ECs (Ramjaun & Hodivala-Dilke, 2009), which in turn, induces PI3K activity leading to the activation of a PLC-ϒ-PKC cascade (Sasamoto et al., 2005). Activation of the well-characterized angiogenesis ERK signalling cascade following integrin activation has also been described in ECs (Short, Talbott, & Juliano, 1998). Integrin ligation to FN induces the sequential activation of Raf, MEK and ERK (Sudhakar et al., 2003), regulating EC survival, migration and proliferation (Ramjaun & Hodivala-Dilke, 2009), although direct integrin activation of ERK has also been proposed (Roberts, Woods, Shaw, & Norman, 2003). Another established signalling pathway employed by integrins in ECs involves the activation of the NF-kB pathway (S. Klein et al., 2002). Integrin-mediated NF-kB signalling triggers the expression of a specific set of genes (S. Klein et al., 2002), conferring protection from apoptosis to ECs (Reidy, Zihlmann, Hubbell, & Hall, 2006). Among them is the prostaglandin synthesis enzyme, cyclooxygenease-2 (COX-2), which is involved in the induction of VEGF and FGF-2 growth factors, which in turn can stimulate angiogenesis (Boosani et al., 2007).

Altogether, it is easy to understand why ITGA5, the α subunit of α5β1 integrins, has been shown to mediate a variety of biological phenomena including mesoderm induction, vascular development, and neural crest development (van der Flier et al., 2010; J. T.

Yang et al., 1993). Concordantly, ITAG5-null mice die early in gestation (E10.5) partly as a result of various vascular defects (Goh, Yang, & Hynes, 1997; J. T. Yang et al., 1993). Similarly, FN-null mice also die at embryonic day (E) 9.5 exhibiting severe defects in vascular development (Francis et al., 2002). An endothelial-specific ITGA5 conditional knockout mouse (ITGA5-floxed mouse line and ablated ITGA5 in ECs using Tie2-driven expression of Cre recombinase) was specifically created to study the role of ITGA5 in vascular biology (van der Flier et al., 2010). Surprisingly, the ITGA5 conditional knockout mice were viable and lacked any immediately obvious phenotype. Characterization of ITGA5 knockout ECs suggested compensation by ITGAV by redistributing to focal adhesions, suggesting a functional overlap of these two integrins.

In summary, α5β1 is involved in several essential EC functions, such as survival, migration, proliferation and vascular remodelling (Ramjaun & Hodivala-Dilke, 2009). It is likely that the same pathways are triggered upon α5β1 integrin activation in $CD34^+$-derived late-outgrowth EPCs treated with miR-92a inhibitor, which overexpress ITGA5. Since α5β1 is the primary integrin involved in the initial cell arrest (Angelos et al., 2010) and its subunit ITGA5 is a direct target of miR-92a (Bonauer et al., 2009), we investigated whether miR-92a inhibitor functional effects on EPCs were abrogated by the knockdown of ITGA5. By using a siRNA interference strategy directed against ITGA5 we were able to successfully repress ITGA5 protein levels in miR-92a inhibitor -treated $CD34^+$-derived EPCs, without interfering significantly in other target proteins, like SIRT1. This strategy allowed us to individualize the contribution of ITGA5 for the EPC functional effects following miR-92a inhibitor treatment.

Previously, ITGA5-KO ECs have shown reduced adhesion to FN, which can be rescued by ectopic (over)expression of ITGA5 (van der Flier et al., 2010). In concordance, we have shown that miR-92a inhibitor treatment augments EPC adhesion to FN. After co-transfecting cells with both miR-92a inhibitor and si-ITGA5, the enhanced EPC adhesion was abrogated when compared to cells treated with mir-92a inhibitor alone. This results suggests that the enhanced EPC adhesion following miR-92a inhibitor priming seems to be mediated by the downstream target ITGA5, in a significant proportion.

Migration involves a coordinated sequence of adhesion and release of molecules on the cell surface as the cell moves along a chemotactic gradient. In this complex process,

ITGA5 is a critical effector. In EPCs, migration is markedly reduced when ITGA5 is blocked (Kaiser et al., 2012). Although the scratch assay results following EPC si-ITGA5 knockdown are only preliminary, they could point towards a reduction of EPC wound closure migration following si-ITGA5 + miR-92a inhibitor co-transfection compared with the condition of single miR-92a inhibitor treatment.

Remarkably, si-ITGA5 treatment had no effect on the proliferation rate of miR-92a inhibitor treated EPCs when compared to EPCs -treated with miR-92a inhibitor alone. This result suggests that ITGA5 may not be the most relevant miR-92a target when it comes to explaining the seen miR-92a inhibitor -enhanced EPC proliferation.

In all si-ITGA5 functional assays, it appears that the scrambled siRNA could have had some potential off-target effect (such as hybridizing with miR-92a inhibitor and reducing its bioavailability). That is a possibility since we were unable to reproduce the increased EPC adhesion/migration/proliferation effect following miR-92a inhibitor treatment when compared to transfection control treatment (the option for si-scrambled + miR scrambled was made in the functional assays, whereas for gene expression miR scrambled was used alone). To overcome this issue, a simultaneous ITGA5 western blot should have been performed for each assay to quantify ITGA5 abundance in all conditions. EPC ITGA5 levels in si-scrambled+miR-scrambled condition should differ from si-scrambled+miR-92a inhibitor condition.

A word of caution concerning ITGA5 overexpression. ITGA5 activation in some settings may have a negative impact. Sun *et al.*, recently, described that atheroprone flow induces ITGA5 translocation into lipid rafts in ECs and hence activation to cause activation of NLRP3 inflammasome resulting in endothelial dysfunction *in vitro* and *in vivo* (X. Sun et al., 2016). Lipid rafts are plasma membrane microdomains which are enriched in sphingolipids, cholesterol, and a variety of signaling messengers, and that interact F-actin-based cytoskeleton. Knockdown of ITGA5 seems to have ameliorated EC dysfunction in partially ligated carotid arteries of $LDLR^{-/-}$ mice. Furthermore, functional inhibition of ITGA5 in mice improved EC function in the atheroprone area. These findings have revealed a mechanism by which atheroprone flow causes endothelial dysfunction via ITGA5 activation, possibly jeopardizing our strategy of ITGA5 overexpression in $CD34^{+}$-derived EPCs for restenosis prevention. But if miR-92a inhibitor is to exert its

function only transiently following EPC transfection, long enough simply to allow for enhanced engraftment ability, then the dysfunction phenotype might not be apparent.

## The link between integrin α5 and nitric oxide in EPC priming

Human eNOS is an enzyme that is constitutively expressed mainly in ECs, which catalyses L-arginine oxidation to generate L-citrulline and NO (I. Fleming & Busse, 2003). NO is a potent vasodilator with a short half-life that contributes to vessel homoeostasis and remodelling by inducing VSMC relaxation, platelet aggregation, and leukocyte adhesion to ECs (Dimmeler et al., 1999; Rudic et al., 1998; Zhou, Chen, Fan, Jiang, & Wan, 2014). Moreover, NO production is paramount in fostering endothelial integrity and regeneration (Gareri et al., 2016), as well as regulating progenitor cell function (Chavakis et al., 2008). In fact, eNOS overexpression is known to enhance the vasculoprotective effect of EPCs (D. Kong, Melo, Mangi, et al., 2004), suggesting that our hypothesis to use a combinatorial approach with EPCs for transfer of increased NO levels may be an effective strategy to enhance endothelium regeneration in damaged vessels. This might be particularly relevant in CVD states, which are associated with reduced levels of NO bioavailability (Gallagher et al., 2007). The basal release of NO is reduced during ageing or the presence of simultaneous CVD RFs, as the activity of eNOS is suppressed in senescent ECs (Gerhard, Roddy, Creager, & Creager, 1996). As EC and EPC dysfunction cause further NO insufficiency (Ignarro, Napoli, & Loscalzo, 2002), a negative feedback loop is installed perpetuating vascular damage following injury (Evora, Baldo, Celotto, & Capellini, 2009; Ignarro et al., 2002). Moreover, impaired eNOS function is thought to be, in part, responsible for impaired mobilisation of EPCs from the BM (Padfield et al., 2010) which further contributes to the delayed vascular healing. BM cells treated with an eNOS transcriptional enhancer exhibit enhanced migratory and neovascularization capacity, when administered in a model of hind-limb ischemia, improved neovascularization (Thum, Fraccarollo, et al., 2007). Furthermore, this beneficial effect can be reversed by the use of eNOS inhibitors, strongly implicating NO in the process of vascular repair (Thum, Fraccarollo, et al., 2007). The reduced NO bioavailability can be counteracted by statins, oestrogen and EPO, all of which enhance eNOS expression, reduce senescence in ECs (Hayashi et al., 2006; Vasa, Breitschopf,

Zeiher, & Dimmeler, 2000), and are known to promote reendothelialization following vascular injury (Iwakura et al., 2003; Landmesser et al., 2004; Urao et al., 2006).

To date, there is no convincing evidence of direct regulation of eNOS by miRNAs also contributing to the remodelling process. However, recently, miR-92a has been shown to be involved in the modulation eNOS expression and activity in ECs, by repressing it (Bonauer et al., 2009; Daniel et al., 2014). Conversely, miR-92a inhibitor increases NO bioavailability in ECs (Gareri et al., 2016; Iaconetti et al., 2012; Wu et al., 2011). Therefore, it seems consensual that eNOS may also play a role in EPC-mediated endothelium regeneration following miR-92a antagonism. The inexistence of miR-92a binding sites in the 3' untranslated region of eNOS' gene suggests that a mechanism other than the direct targeting of miR-92a is involved (Wu et al., 2011). In fact, miR-92a (indirectly) -induced eNOS downregulation has been shown to be mediated by ITGA5 (Bonauer et al., 2009), KLF2 (Boon et al., 2011) and KFL4 (Hamik et al., 2007) in previous research. Furthermore, SIRT1 directly deacetylates and thereby activates eNOS and leads to more NO production (Ota et al., 2010; Rudic et al., 1998). All of these are miR-92a direct targets.

Because of the fundamental role of ITGA5 in EPC physiology we sought to understand the link between ITGA5 and eNOS in specific. As it seems, activation of eNOS can also be accomplished in a $Ca^{2+}$-independent manner, via PI3K/Akt -dependent phosphorylation (at serine 1177), which has a clear beneficial role in the number and function of EPCs (B. Cui et al., 2011; Dimmeler et al., 1999). Akt levels are reduced in senescent ECs, causing reduced eNOS phosphorylation by Akt. Therefore, as the activity of eNOS is suppressed in senescent ECs (Gerhard et al., 1996), the basal release of NO is reduced during ageing and the presence of further CVD risk factors. Importantly, Akt -mediated activation of the eNOS in ECs depends on the integrin pathway (Dimmeler, Assmus, Hermann, Haendeler, & Zeiher, 1998; Dimmeler et al., 1999). Consistent with this finding, shear stress–induced vessel relaxation is antagonised by RGD peptides, which block α5β1 integrins (J. M. Muller et al., 1997). Therefore, a miR-92a antagonising strategy aiming to enhance ITGA5 expression could presumably enhance NO bioavailability in EPCs. Indeed, in ECs, ITGA5 was found to interact with integrin- linked kinase (ILK) at the focal

adhesion which activates protein kinase B/Akt and triggers eNOS activation (Dimmeler et al., 1998; Goligorsky, Li, Brodsky, & Chen, 2002). As NO is necessary for vascular remodelling, an Akt-mediated increase in eNOS activity might represent a major determinant of vessel regeneration via EPCs. This EPC-derived NO production has been shown to exert antioxidant action and prevent further endothelial injury (L. Gao et al., 2014). Therefore, miR-92a inhibition might promote EPC function also by improving eNOS activation and NO production.

The indirect upregulation of eNOS seen after priming $CD34^+$-derived late-outgrowth EPCs with miR-92a inhibitor, possibly, accounts for some of the reported functional effects. EPC proliferation *in vitro* has previously been shown to be enhanced by eNOS gene transfer (B. Cui et al., 2011). Moreover, the activation of eNOS by Akt might explain the relevant Akt pro-proliferative effects (Dimmeler, Haendeler, Nehls, & Zeiher, 1997). Akt also seems to play a positive role in VEGF-induced EC migration (Dimmeler, Dernbach, & Zeiher, 2000). Concordantly, eNOS is required for the basal and -VEGF-induced migration of EPCs *in vitro* (Sasaki et al., 2006). In contrast, the reported enhanced EPC adhesion following miR-92a inhibitor treatment does not seem to be linked to indirectly augmented eNOS expression/activation, since adhesion experiments using NO donators by Kaiser *et al.* found no impact on adhesion of ECs (Kaiser et al., 2012).

## EPC transplantation

In an attempt to test the main thesis theory that miR-92a inhibitor would be a suitable priming strategy to enhance $CD34^+$-derived late-outgrowth engraftment in injured vessels, I resourced to a rat carotid balloon angioplasty model for proof-of-principle.

It would have been possible to use autologous $CD34^+$-derived EPCs from rat BM (instead of human EPCs), and, thus, avoid allo-immunogenicity associated with human EPC transplantation (N. Yang et al., 2011). According to Yang and colleagues, cultured MNCs from rat BM can be differentiated into early EPC-like cells in FBS, VEGF and FGF-supplemented M199 medium, or late EPC-like cells in EGM-2MV medium. Nevertheless, I have opted not to use this strategy, though, for several reasons. First, it meant

sacrificing many animals to harvest their bones. Given that only a few µL of BMB are retrieved from each bone, several samples would have to be pooled together to have enough volume to perform a MNC isolation by gradient density. Secondly, EPCs separated from MNCs exclusively by adherent culture comprise many subpopulations, therefore obtaining a uniform cell population that expressed CD34 homogeneously by MACS would be further challenging in these conditions. Thus, for the EPC transplantation experiments in rats, I proceeded with the well-characterized human $CD34^{+}$-derived late -outgrowth EPCs that I had generated from UCB, a blood source said to have less HLA immunogenicity (Riordan et al., 2007), and because the engraftment output was to be read in 24h from surgery. Moreover, most reports have found little evidence of fusion between EPCs and cells of other lineages (Koyanagi, Brandes, Haendeler, Zeiher, & Dimmeler, 2005). As an example, the proportion of ECs displaying evidence of human–mouse cell fusion is reported to be less than 3% in previous mismatch transplantation studies (S. Lee & Yoon, 2013). In fact, most recent studies have suggested that although fusion and transdifferentiation of EPCs are possible, such phenomenon is not at all prevalent (S. Lee & Yoon, 2013).

Also on the technical side, EPCs were often administered systemically in early investigations. However, more recently, experiments have tended to employ cell transplantation instead (i.e. injection directly into the injured artery), to overcome the low retention rates seen when systemically administering cells (S. Lee & Yoon, 2013). Hence, my choice for temporarily isolating the target arterial segment with combined techniques to clamp the proximal end and to ligate the distal artery against inserted balloon catheter before deploying the cells. Our results indicate that the transplantation technique appeared efficacious as proven by the fact that the DIi-labeled EPCs could be successfully deposited in the injured artery and seen by fluorescent microscopy 24h after cell administration.

Although the transplantation results are only preliminary since statistical significance could not be reached due to limited PhD time to perform more *n* numbers, in the present experiment, the engraftment of locally delivered miR-92a inhibitor -treated EPCs appeared promisingly greater compared to controls. Given the previous *in vitro*

demonstration of the role of upregulated ITGA5 (following miR-92a inhibitor treatment) in EPC-FN adhesion assay, we are lead to believe that the *in vivo* trend follows the same integrin-ECM bonding principles.

However, due to EPC scarcity in the circulation (or lack of identification parameters), there is a requirement for *ex vivo* expansion and miR-92a inhibitor treatment before primed $CD34^{+}$-derived late-outgrowth cells could provide a useful cell therapy *in vivo*. Thus, following the indication that miR-92a inhibitor might enhance EPC adhesion to injured arteries, I conducted a series of preliminary experiments **(Appendix IV)** which sought to describe the initial steps towards establishing a target tissue pre-activation strategy by transfecting miR-92a inhibitor into injured arteries. This could maximise endogenous EPC capture via ITGA5 upregulation, contributing to the prevention of post-angioplasty restenosis, instead of having to transplant pre-activated ex vivo -expanded EPCs. With target tissue modulation secured, I envisioned a NP-based strategy that could be used to transfect miR-92a inhibitor into arteries intraluminally via a stent.

# Chapter 5: General Discussion

New signalling molecules and cell types controlling the progress of restenosis are continuously being discovered. In particular, microRNAs and vascular progenitor cells have recently been shown to play a vital role in this pathophysiological process. In fact, the contribution of circulating EPCs homing to injured vessels is considered essential to promote re-endothelialisation and prevent neointima formation following PCI (Curcio et al., 2011). Moreover, it is possible that vascular wall EPCs may also contribute (Psaltis & Simari, 2015). However, EPC numbers and function among CVD patients are often intrinsically impaired leading to low engraftment rates at the target site, which could limit re-endothelialisation (Templin, Luscher, & Landmesser, 2011). Therefore, priming therapies designed to increase the ability of EPCs to engraft at the site of vascular injury are attractive and have the potential to improve the post-PCI clinical outcomes, similarly to the angiogenesis outcomes seen with primed EPCs **(Table 17)**.

**Table 17 | Priming strategies to enhance EPCs function.**
Adapted from (Haider et al., 2017). AAV: Adeno-associated virus; ECM: Extracellular matrix; EPC: Endothelial progenitor cell; HUVEC: Human umbilical vein endothelial cell; I/M: Intramyocardial; LAD: Left anterior descending; MI: Myocardial infarction; SDF-1: Stromal cell-derived factor-1α

| Study | Cell type | Preconditioning strategy | Animal model | Results of the study |
|---|---|---|---|---|
| (Yao et al., 2013) | Human umbilical cord blood-derived EPCs | Genetic modification using Ad-vector encoding for human tissue kallikrein gene | Nude mouse model of MI by LAD ligation | Decreased cardiomyocyte apoptosis with increased retention of genetically modified cells, increased capillary and arteriolar density and incorporation of the delivered cells into the blood vessels. There was significantly improved left ventricular fraction and fractional shortening |
| (Schuh et al., 2012) | EPCs isolated from rat spleen | Genetic modification using lentiviral transduction of EPCs with SDF-1α transgene | Rat heart model of acute MI by LAD ligation | Significantly increased CD31+ vascular structures, significantly improved cardiac function after I/M injection of genetically modified cells as compared with intracoronary delivery |
| (Zemani et al., 2008) | Human umbilical cord blood-derived EPCs and HUVEC | SDF-1α treatment of EPCs in vitro | Mouse model of hind limb ischemia | Intravenous administration enhanced limb angiography score by 60% as compared with the control and 25–60% increased blood flow |
| (Sen et al., 2010) | Peripheral blood-derived EPCs | Overexpression of IGF-1 using AAV vector | Rat heart model of MI by LAD ligation | Reduced myocardial apoptosis, increased cardiomyocyte proliferation, enhanced capillary density in the peri-infarct region and improved cardiac function as compared with control group |
| (Frederick et al., 2010) | EPCs cultured on ECM scaffold | Growth factor (SDF-1 α) treatment of scaffold seeded cells | Rat heart model of MI by LAD ligation | Enhanced VEGF expression in the border zone; enhanced blood vessel density, improved microvascular perfusion, attenuated remodeling, reduced scar formation and preserved cardiac function |

Priming EPCs may improve their survival, proliferation, mobilization, paracrine behavior and differentiation for enhanced repair and angiogenic potential. Various priming strategies have been reported and include, genetic modification, pretreatment with recombinant growth factor proteins, treatment with established pharmacological agents (Haider et al., 2017). Several vascular miRNAs have been identified in restenosis pathophysiology, therefore its therapeutic modulation seems feasible **(Table 18)**.

**Table 18 | Summary of recently identified miRNAs involved in (re)stenosis progression in animal models of disease and tested as targets in pre-clinical therapeutic strategies.**
Adapted from (Forte et al., 2014). LRRFIP1 - leucine-rich repeat (in Flightless 1)-interacting protein-1; MKK4 - MAPK kinase 4; Myl9 - myosin, light chain 9; ND - not determined.

| miRNAs | Animal model | Up- (↑) or down- (↓) regulation of miRNA in injured vessels | Molecular targets | Pre-clinical therapeutic strategy |
|---|---|---|---|---|
| **miR-146a** | Carotid artery balloon injury in Sprague–Dawley rats | ↑ | KLF4 | Vessel transfection with antisense miR-146a oligonucleotides in pluronic gel (S. G. Sun et al., 2011) |
| **miR-133** | Carotid artery balloon injury in Wistar rats | ↓ (early phase after injury); ↑ (late phase after injury) | Sp-1 and moesin | Vessel transfection with miR-expressing adenovirus (Torella et al., 2011) |
| **miR-424/322** | Carotid artery balloon injury in rat | ↑ | Cyclin D1 and calumenin | Vessel transfection with miRNA-expressing adenovirus (Merlet et al., 2013) |
| **miR-663** | Carotid artery ligation injury in C57BL/6N mice | ↓ | JunB and Myl9 | Vessel transfection with miR-expressing adenovirus (P. Li et al., 2013) |
| **miR-132** | Carotid artery catheter injury in Sprague–Dawley rats | ↓ (early phase after injury) ↑ (late phase after injury) | LRRFIP1 | Lipofectamine+pluronic gel-mediated delivery of miR-132 mimic (Choe et al., 2013) |
| **miR-195** | Carotid artery balloon injury in rat | ↓ | Cdc42 and cyclin D1 | Vessel transfection with miR-expressing adenovirus (Y. S. Wang et al., 2012) |
| **miR-221/222** | Carotid artery balloon injury in rat | ↑ | $p27^{Kip1}$, $p57^{Kip2}$and c-kit | Vessel transfection with antisense oligonucleotides in pluronic gel (X. Liu, Cheng, Yang, Xu, & Zhang, 2012) |
| **miR-92a** | Carotid artery balloon injury in the rat; stent deployment in rat carotid artery | ↑ | KLF4, MKK4 | Systemic infusion by tail vein of antagomiR-92a at 0, 1 and 2 days after injury (Iaconetti et al., 2012) |

miR-92a is linked to anti-angiogenic effects, via ITGA5 downregulation (Bonauer et al., 2009). α5β1 is involved in several essential EC functions, such as survival, migration, proliferation and vascular remodelling (Ramjaun & Hodivala-Dilke, 2009). It is likely that

the same pathways are triggered upon α5β1 integrin activation in $CD34^+$-derived late-outgrowth EPCs treated with miR-92a inhibitor, which overexpress ITGA5. Given that α5β1 is the primary integrin involved in the initial EPC arrest (Angelos et al., 2010), and miR-92a levels are usually high in EPCs from CAD patients (Q. Zhang et al., 2011), we thought that inhibiting miR-92a in EPCs would facilitate engraftment at the injured arterial segments by increasing its ITGA5-mediated adhesiveness to FN. EPC grafting would theoretically accelerate re-endothelialisation by paracrine and structural contribution, hence, reducing neointima formation (Walter et al., 2002).

Therefore, the overarching **aim** of this thesis was to characterise the effect of miR-92a inhibition in $CD34^+$-derived late-outgrowth EPCs, which had never been reported to the best of our knowledge.

To accomplish the objectives of this research, the following **milestones** were reached:

1. **Differentiation and characterization of $CD34^+$-derived late-outgrowth EPCs from human and porcine sources;**
2. **Characterization of gene expression and demonstration of the functional priming following miR-92a inhibitor treatment on $CD34^+$-derived late-outgrowth EPCs *in vitro* and *in vivo*, correlating it to the target ITGA5 expression**;

Soon after *in vitro* proof of concept of the EPC increased adhesiveness to FN and subsequent enhanced thriving following miR-92a inhibition, we tested the transplantation of primed human EPCs into a rat carotid injured artery for a short duration trial. The preliminary results evidenced a possible increase in engraftment capacity of the injected EPCs. Meanwhile, Iaconetti's group, and then Daniel's, attempted a systemic delivery of an inhibitor to attenuate miR-92a activity in the injured arteries and were the first to confirm that miR-92a inhibitor stimulated re-endothelialisation and decreased SMC hyperplasia, at least in part, through direct pro-proliferative effects on ECs (Daniel et al., 2014; Iaconetti et al., 2012).

Thus, it seems that the *in vitro* results from this thesis are **clinically translatable** and add important evidence to the expanding research field of therapeutic modulation of miR-

92a activity to rescue the damaged endothelium after coronary interventions via an unexplored player - EPCs. The possible role of miR-92a inhibition in post-injury restenosis prevention, taking into account the overall effect in (5.1) engrafting circulating EPCs and (5.2) other interacting partners is discussed next.

## 5.1 The role of miR-92a inhibitor in EPC-mediated regeneration of injured arteries - Direct effects in EPCs

EPC mobilisation and homing to the vascular injury site is a multi-step process involving detachment from the BM niches, entry into circulation, rolling along vessel endothelium, adhesion to denuded ECM and transmigration where they participate in re-endothelialisation (B. Cui et al., 2011; Werner et al., 2003; X. Zhao et al., 2007). However, a critical limitation for the therapeutic application of EPCs is their low number in the circulation, which is even lower in patients with CVD RFs (Fadini et al., 2006; Padfield et al., 2010; Vasa, Fichtlscherer, Aicher, et al., 2001). Moreover, EPCs isolated from patients with diabetes or hypertension exhibit a reduced activity in promoting re-endothelialisation of denuded arteries when transplanted into nude mice (Giannotti et al., 2010; Landmesser et al., 2004; Sorrentino et al., 2007), highlighting a significant limitation of current cell therapies in these patients. The functional deficits that cause these reduced *in vivo* activities are likely associated with diminished NO availability and an accelerated senescence (Giannotti et al., 2010; Sorrentino et al., 2007). Consequently, the impaired functionality of BM-derived EPCs in specific assays, such as migration or colony formation capacity *in vitro*, has been linked with disappointing outcomes in cell therapy trials (Assmus et al., 2007). Remarkably, one of the major challenges for the therapeutic application of EPCs has been the poor engraftment and cell survival rates. Numerous factors contribute to the meagre cell retention, which include exposure of the cells to inflammation, relative hypoxia, nutrient deprivation, and mechanical washout of cells from the coronary vasculature (B. Cui et al., 2011). Overall, most cells enter apoptosis within the first few days after interacting with the injury site. Therefore, an EPC priming and stabilisation strategy likely to promote longer cell

retention and engraftment can potentially be accomplished by manipulation of the integrin presentation on EPCs. Since FN, an ECM protein that may influence cellular migration and differentiation, accumulates rapidly at the site of balloon injury, an overexpression of integrins is expected to facilitate EPC incorporation (Bauters et al., 1995). EPCs' integrin expression profile has been previously described and includes the following subunits: α1, α2, α3, α4, α5, α6, α9, αv, β1, β2, β3, β5 αnd β7 (Caiado & Dias, 2012). They have been implicated in EPC mobilisation, homing, transendothelial migration, invasion, and differentiation (Caiado & Dias, 2012). Integrin α5β1 is the primary integrin involved in the initial cell arrest (Angelos et al., 2010) and its subunit ITGA5 is a direct target of miR-92a (Bonauer et al., 2009). In fact, α5β1 is involved in several other essential EC functions, such as survival, migration, proliferation and vascular remodelling (Ramjaun & Hodivala-Dilke, 2009). In EPCs, we were able to demonstrate pro-angiogenic,-migratory,-proliferative, and -adhesive effects of miR-92a inhibitor treatment on $CD34^{+}$-derived EPCs, which were partially abrogated by ITGA5 knockdown. Given that ECs and EPCs share similar processing machinery, it is likely that our reported functional effects following miR-92a inhibitor treatment in EPCs (and subsequent ITGA5 upregulation) were at least partially explained by the triggering of same EC pathways upon α5β1 integrin activation.

Briefly, ligand binding activates FAK through direct interaction at the cytoplasmic tail of the β1-integrin subunit (Schaller et al., 1995), which activates several downstream pathways downstream which are implicated in survival, proliferation and cytoskeleton changes. In fact, ITGA5 seems to even be involved in EPC differentiation to EC through FN-integrin α5β1 interaction (Caiado & Dias, 2012; Wijelath et al., 2004). The formation of VEGF/FN complexes via direct interactions with FN heparin-II domain leads firstly to the physical interaction between VEGFR-2 and integrin α5β1 (Caiado & Dias, 2012) and consequently to the activation of downstream pathways that may potentiate EPC endothelial differentiation. Moreover, in ECs, ITGA5 was found to interact with integrin-linked kinase (ILK) at the focal adhesion which activates protein kinase B/Akt and triggers eNOS activation (Dimmeler et al., 1998; Goligorsky et al., 2002). Ultimately, miR-92a inhibitor increases protein levels of serum response factor (SRF), a downstream mediator of VEGF signalling through the MEK–ERK pathway in ECs (Iaconetti et al.,

2012), which is a requirement for VEGF-induced *in vitro* angiogenesis and endothelial cells migration, proliferation, actin cytoskeleton rearrangements (Iaconetti et al., 2012)

Besides ITGA5 main role in EPC function which was our main focus of interest, several other vasculoprotective genes can be repressed by miR-92a in ECs (and in EPCs we extrapolate) and could potentially explain the observed results **(Figure 58)**.

**Figure 58 | miR-92a target genes in EPCs implicated in the post-injury restenosis response.**
Inhibition of restenosis by miR-92a antagonism involves the de-repression of the pro-angiogenic and anti-inflammatory factors SIRT1, ITGA5 and KLF2/4 in both EPCs and ECs which promotes their proliferation, migration and differentiation. Akt - Protein kinase B ; EC – endothelial cell; EPC – endothelial precursor cell; eNOS – endothelial nitric oxide synthase; ERK 1/2 - Extracellular signal–regulated kinase; ILK - Integrin-linked kinase; ITGA5 – integrin α5; ITGAV – integrin αv; JAK/STAT –Janus Kinase/Signal Transducer and Activator of Transcription; KLF2/4 - Krüppel-like factor 2/4; miR – microRNA; MKK4 - MAPK kinase 4; nF-kB – factor nuclear kappa B; (p) – phospho; SIRT1 – sirtuin 1; SOCS5 - Suppressor Of Cytokine Signaling 5; SRF – stromal release factor; VSMC – vascular smooth muscle cell.

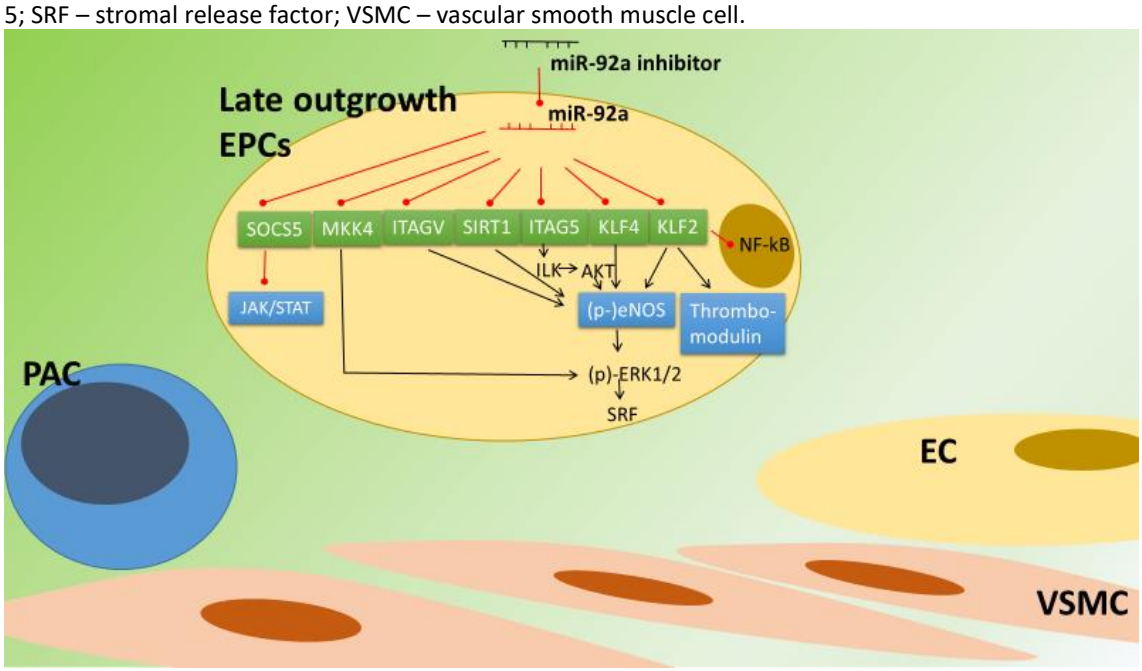


SIRT1, which prevents eNOS acetylation and inactivation (O'Donnell et al., 2005), is one such example. Overexpression of SIRT1 has been shown to reduce atherosclerotic lesion formation and to protect against neointima formation following vascular injury in mice (L. Li et al., 2011; C. Zhang, 2008). SIRT1 is part of the family of sirtuins (SIRT1 to 7), a highly conserved protein family of histone deacetylases (HDACS) that promote longevity and exert protective effects against age-related diseases such as cancer, CVDs and diabetes, through the modulation of epigenetic information by direct deacetylation of specific histone acetylation marks (D'Onofrio et al., 2015). Sirtuins play an essential role

in regulating cellular differentiation and senescence in response to nutrient availability (Potente et al., 2007). Among all sirtuins, SIRT1 is the most critical modulator of the vascular function. At vascular level, SIRT1 is the only family member shown to regulate vasodilation uniquely and the regenerative functions of ECs, EPCs and SMCs through the modulation of eNOS, forkhead box O1 (FOXO1), p53, and angiotensin II type 1 receptor (AT1R)(D'Onofrio et al., 2015). Overexpression of FoxO1 inhibits EC migration and tube formation and represses eNOS expression (Potente et al., 2005). SIRT1 deacetylation of FOXO1 inhibits its antiangiogenic activity in human vascular ECs (Potente et al., 2007), while targeting eNOS for deacetylation leads to NO production and corresponding enhanced endothelial-dependent vasodilation(Mattagajasingh et al., 2007), survival, migration and neovascularization (Aicher, Heeschen, et al., 2003). Therefore, it comes as no surprise that blocking the function of SIRT1 abolishes endothelial EC sprout formation and migration *in vitro* (Yuan et al., 2014). *In vivo*, disruption of SIRT1 gene expression in zebrafish and mice also results in dysregulated vascular growth. Numerous studies describe the protective role of SIRT1 in endothelial senescence, and conversely, SIRT1 levels progressively decline during the development of endothelial senescence (D'Onofrio et al., 2015). SIRT1 inhibits senescence by the deacetylation of FoxO proteins, which are meant to upregulate antioxidant and cytoprotective enzymes, such as catalase and MnSOD (Yamakuchi, 2012). Pharmacological or siRNA inhibition of SIRT1 induces premature senescence in ECs (Ota et al., 2007). Conversely, overexpression of SIRT1 prevents hydrogen peroxide-induced endothelial senescence suggesting that SIRT1 might prevent stress-induced endothelial dysfunction, a transversal component in several CVDs (Ota et al., 2007). In EPCs the expression and activity of SIRT1 also correlate inversely with senescence (Lemarie et al., 2011). Particularly, exposure to high glucose has been shown to reduce SIRT1 expression levels in EPCs, consequently blocking deacetylation of FOXO1 by SIRT1 and reducing eNOS phosphorylation levels(Balestrieri et al., 2008). Consistent with these findings, levels of SIRT1 protein were found to be decreased in EPC from individuals with diabetes and, especially, in patients with poor glycemic control (Balestrieri et al., 2013). *In vitro* and *ex vivo* studies revealed reduced EPC activity in the presence of hyperglycaemia which is associated with lower SIRT1 protein levels (Balestrieri et al., 2013). In fact, EPC number, differentiation ability and SIRT1 protein levels can be enhanced in patients with ST-elevation myocardial infarction

undergoing PCI provided there is an intensive peri-procedural glycaemic control (Marfella et al., 2013). Based on these considerations, it is predictable that overexpression of SIRT1 (for instance via miR-92a inhibition) would not only beneficially affect established RFs, but would also prevent endothelial dysfunction. Because SIRT1 targets several proteins in distinct pathways for deacetylation, overexpression of SIRT1 could alter the biological activity of entire signalling networks and thereby enhance EPC-mediated regeneration of injured vessels.

ITGAV is also an in silico predicted target of miR-92a (Bonauer et al., 2009). Integrins $\alpha$V$\beta$3- and $\alpha$V$\beta$5 also play a role in EPC engraftment to sites of vascular repair. $\alpha$V integrins are known to bind different ligands, including vitronectin, FN, osteopontin, fibrinogen and vWF, by binding the RGD motif (Hynes, 2002). Remarkably, EPC adhesion seems to also be mediated by $\alpha$V$\beta$3- and $\alpha$V$\beta$5-integrins, since their inhibition with cyclic RGD peptides blocks EPC-mediated re-endothelialisation of denuded arteries (Kokubo et al., 2007).

miR-92a also suppresses KLF2 and KLF4 expression by binding to their 3' UTR (H. Liu et al., 2016). Endothelial flow-induced transcription factors KLF4 and KLF2 confer a vascular anti-oxidant, vasodilatory and antithrombotic phenotype, being implicated in protection against atherogenesis (Neth, Nazari-Jahantigh, Schober, & Weber, 2013). Shear stress with a laminar flow upregulates KLFs in ECs (Nayak, Lin, & Jain, 2011) which in turn modulates the expression of over 70% of the genes that are responsive to shear stress(Fledderus et al., 2008). In swine aortic arch endothelium, a site of atherosusceptibility, both KLFs are expressed at low levels relative to protected thoracic aorta (Y. Fang & Davies, 2012). Overexpression of KLF4 in ECs activates expression of anti-inflammatory eNOS and antithrombotic thrombomodulin (Hamik et al., 2007), while KLF2 induces eNOS expression (Boon & Horrevoets, 2009; Parmar et al., 2006). Additionally, endothelial expression of KLF2 reduces cocultured SMC migration capacity via paracrine modulation (Mack et al., 2009). Fang and colleagues demonstrated that the upregulation of miR-92a expression is inversely correlated with KLF2 and KLF4 expression in atherosusceptible endothelium (Y. Fang & Davies, 2012), and then functionally validated two evolutionarily conserved miR-92a sites in KLF4 3'UTR and 1

site in KLF2 3'UTR. Atherodisruptive flow patterns are thought to increase the level of miR-92a, which in turn decreases KFLs. Overexpression of miR-92a inhibited the expression of eNOS and administration of miR-92a into mice decreased the arterial expression of KLF2 and eNOS (Wu et al., 2011). Concordantly, mouse carotid arteries receiving pre-miR-92a exhibited impaired vasodilatory response to flow (Wu et al., 2011). Knockdown of miR-92a by using an antagomir partially suppressed TNF-induced endothelial proinflammatory marker expression (monocyte chemotactic protein 1, vascular cell adhesion molecule-1, E-selectin) and upregulated eNOS through KLF4 and KLF2, therefore inhibiting TNF-induced leukocyte adhesion to ECs *in vitro*. Altogether the reported studies seem to suggest that miR-92a regulates KLF4 and KLF2 expression in arterial endothelium and contributes to phenotype heterogeneity associated with regional atherosusceptibility and protection *in vivo*. Moreover, in addition to the regulation of NO and its consequent vasodilation, the mechanism involving miR-92a targeting KLF2 may also regulate other KLF2-regulated genes such as vWF, FLK1, and Tie-2, which are essential for EC vascular functions (Wu et al., 2011). Moreover, KLF2 and KLF4 can also enhance eNOS activity, which inhibits VSMC proliferation through enhanced NO production (Boon & Horrevoets, 2009; Y. Fang & Davies, 2012; Hamik et al., 2007; Iaconetti et al., 2012; Parmar et al., 2006). In summary, several of the miR-92a direct targets like ITGA5 (Bonauer et al., 2009), SIRT1 (Ota et al., 2010; Rudic et al., 1998), KLF2 (Boon et al., 2011) and KFL4 (Hamik et al., 2007), seem to seem to downregulate eNOS. miR-92a inhibition also results in a reduction of activated NFκB through increased KLF4 expression, which probably accounts for the anti- inflammatory phenotype observed after miR-92a blockade (Loyer et al., 2014). These studies provide insight into proatherogenic functions of miR-92a under disturbed flow through suppression of KLF2/KLF4 and its key targets eNOS and thrombomodulin.

SOCS5 expression is upregulated in the aortic arch and descending aorta of normocholesterolemic mice but markedly decreased in the aortic arch of hypercholesterolemic mice, where expression of miR-92a is reported to be highest (Loyer et al., 2014). SOCS5, whose expression is induced by shear stress and which confers anti-inflammatory properties to ECs via activation of JAK-STAT pathway (Zhuang et al., 2012), was recently been validated as a miR-92a target (Loyer et al., 2014).

Inhibition of SOCS5 by siRNA was shown to increase IL-6 and monocyte chemoattractant protein-1 (MCP1) release without disturbing KLF2, KLF4, and eNOS levels, suggesting that SOCS5 directly protects against endothelial activation and overall post-injury inflammation (Loyer et al., 2014).

## 5.2 The role of miR-92a inhibitor in EPC-mediated regeneration of injured arteries: Indirect effects in EPC interacting players

In addition to their role as a structural tissue component, EPCs express many factors that contribute to tissue regeneration, including the eNOS and proangiogenic or anti-apoptotic GFs, including VEGF, hepatocyte growth factor (HGF), insulin-like growth factor 1 (IGF-1)(Urbich, Aicher, et al., 2005). GF release stimulates the recruitment of new EPCs to the injured and influences the proliferation, migration and survival of both EPCs and pre-existing mature ECs. ECs exposed to the increased NO produced by the EPCs activated by miR-92a inhibitor enhance the coverage of the injured area, while the rate of vascular VSMC proliferation and the level of platelet adhesion are significantly reduced. Thus, EPCs contribute to a surface that more closely mirrors a normal vascular endothelial phenotype via the interaction with different cellular players. In fact, EPCs, ECs and the supporting ECM exist in a state of "dynamic reciprocity" to serve and regulate each other. ECM not only provides a substrate for cell attachment and spreading, contact guidance for cell migration, and a scaffold for building tissues but also serves as a reservoir for growth factors (Davis & Senger, 2005). Zhao and colleagues found that FN provided superior adhesion for late -outgrowth EPCs compared to mature ECs, and Vartanian *et al.* revealed that EPCs deposited collagen IV, FN, and laminin to a greater extent than ECs (Vartanian et al., 2009). Therefore, primed late -outgrowth EPCs could amplify these benefits and enhance endogenous repair. Moreover, the exocytosis of miR-92a inhibitor from EPCs, can have a direct effect in other cellular players **(Figure 59)**.

**Figure 59 | miR-92a target genes in VSMCs and PACs implicated in the post-injury restenosis response.** Inhibition of restenosis by miR-92a antagonism results from the de-repression of the pro-apoptotic/pro-inflammatory MKK4 and anti-proliferative BMPR2 in VSMCs, and of the anti-inflammatory SOCS5 in PACs. BMPR2 - Bone morphogenetic protein receptor type II; EC – endothelial cell; EPC – endothelial precursor cell; ITGA5 – integrin α5; JNK – c-Jun N-terminal kinases; miR – microRNA; MKK4 - MAPK kinase 4;(p) – phospho; SOCS5 - Suppressor of Cytokine Signaling 5; VSMC – vascular smooth muscle cell.

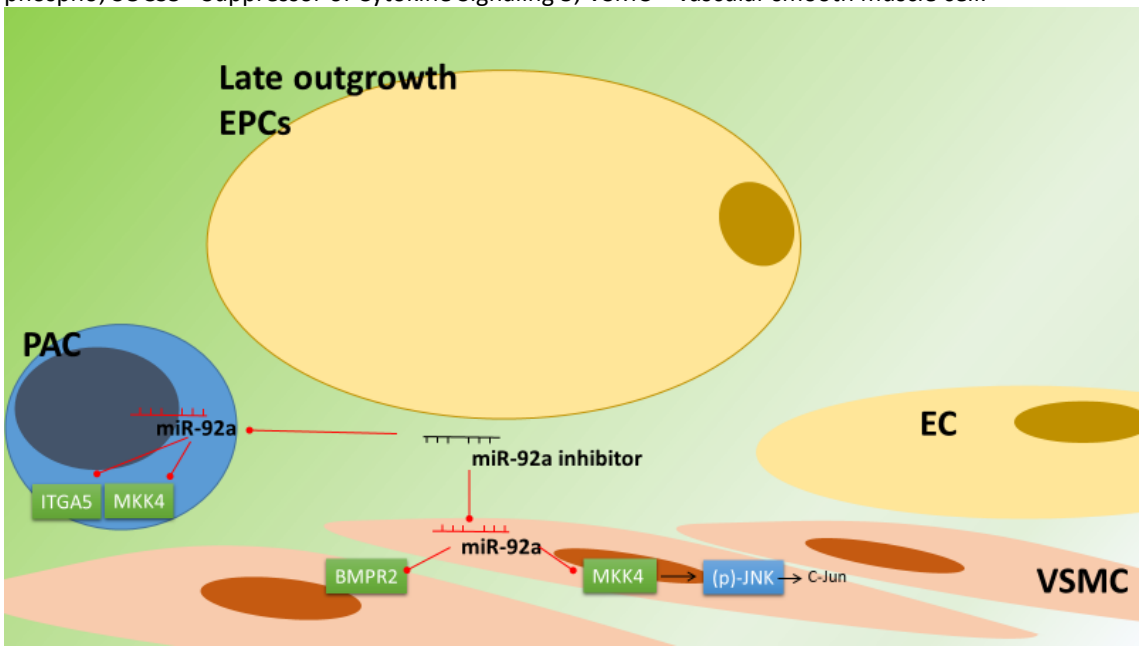


VSMC miR-92a expression is lower in comparison with ECs (Iaconetti et al., 2012), but it still plays an essential role in modulating restenosis since it exerts pro-proliferative and anti-apoptotic actions in VSMCs (L. Zhang, M. Zhou, Y. Wang, et al., 2014). miR-92a expression in VSMC is known to be low in the basal (quiescent) state, but its post-injury overexpression is protective against apoptosis induced by $H_2O_2$-mediated oxidative stress in VSMCs. This is explained mechanistically, since miR-92a targets MKK4 and JNK1, reducing their protein level. This reduction leads to attenuation of both p54 and p46 JNK activation and a significant decrease in the level of phospho-c-Jun implicated in cellular apoptosis. Moreover, JNK can also initiate TNF-α and ischemia-induced apoptosis by promoting Smac/Diablo release (Nijboer et al., 2010). JNK activation is also known to phosphorylate Bcl2 protein and hence antagonise its anti-apoptotic activity (Dhanasekaran & Reddy, 2008). In contrast, overexpression of MKK4 abrogated the antiapoptotic effects of miR-92a in VSMC under oxidative stress. In summary, MKK4 and JNK1 are down-regulated by miR-92a thus inhibiting VSMC apoptosis induced by oxidative stress. It is noteworthy that all members from the mir-17~92 cluster are upregulated in restenotic carotid arteries (miR-92a included) and all target (miR-18 being the only exception) the bone morphogenetic protein receptor type II (BMPR2)

inhibiting the proliferation of VSMCs (T. Luo et al., 2014). It was Luo and colleagues who first uncovered the crosstalk between the two critical TGF-β superfamily signalling pathways, TGF-β1/Smad3 and BMP/BMPR2, through miR-92a. Smad3 is one of core transcription factors of the profibrotic cytokine TGF-β, which enhances neointimal formation by stimulating ECM synthesis and accumulation (FN mostly)(Ryer et al., 2006; Tsai et al., 2009). Simultaneously, upregulation of Smad3 can activate the transcription of miR-17~92 cluster by binding to its promoter region. Then, miR-17~92 family members, namely miR-92a, down-regulate BMPR2, an inhibitor of VSMC proliferation, to further promote VSMC proliferation and neointimal formation in the carotid artery restenosis. These observations are in agreement with Smad3 and miR-92a being upregulated in carotid restenosis, while BMPR2 is reduced, compared with control normal arteries.

In inflammatory cells, the effect of miR-92a antagonism is still largely unknown. It appears that in macrophages miR-92a expression is blocked upon by TLR activation. The result is the reduction in the release of pro-inflammatory IL-6 and TNF-α, via the targeting of the proinflammatory MKK4. On the contrary, macrophages transfected with miR-92a inhibitor have been shown to produce higher concentrations of IL-6 and TNF-α upon LPS presentation. Moreover, in contrast to EPCs which have the expression of α5 and β1 upregulated during differentiation and α4 markedly decreased, MNCs have a higher proportion of surface α4 integrin but still present α5β1 (Kaiser et al., 2012). Therefore, localised miR-92a antagonism via an epigenetic stent can theoretically create a relative increase in their adhesive profile, further promoting an inflammatory cascade *in situ*. In summary, the effect of the delivery of miR-92a on peri-injury inflammatory cells still warrants further characterization to ascertain for its safety.

## 5.3 Limitations

The present study had some limitations that warrant discussion. The potential clinical translation of miR-92a inhibitor for EPC-mediated re-endothelialisation in the context of post-PCI injury would preferably warrant the use of EPCs from CVD patients in the pre-clinical studies. The present research used EPCs obtained from umbilical cord blood (UCB) and thus may not fully represent the impaired EPC of elderly patients with cardiovascular disease. Nevertheless, given the fact that UCB is more widely accessible and possesses a bigger pool of $C34^+$ cells when compared to peripheral blood, this strategy has often been used in many cell therapy studies reviewed elsewhere (Chong et al., 2016).

Clonally expanded $CD34^+$-derived EPCs were used for the *in vitro* validation of miR-92a inhibitor impact in cellular function. However, a major caveat to clinical translation is that it is not known whether cultured cells exist in circulation *in vivo* as such or whether they mainly represent an artificial phenotype generated by tissue culture conditions (Fadini et al., 2012). One may wonder if progenitor $CD34^+$ cells might only give rise to putative EPCs depending on an exact combination of growth factors to which the cells have been exposed *in vitro*. Future efforts should be focused on the development of a straightforward standard protocol and source to specifically define and validate EPCs so that investigators can have a benchmark for comparison (Medina et al., 2017). And if it is an artificial phenotype is it safe to use in man or have the cells been subject to mutational and epigenetic modifications? Although using MNC culture-derived EPCs in pre-clinical models seem to be safe for the animals, particularly, for EPC-mediated endothelial regeneration, there are still concerns that need to be addressed before human therapeutic application of $CD34^+$-derived EPCs.

Another limitation of our study was the use of human EPCs delivered into rat carotid artery, which prevented us from conducting long-term engraftment studies due to rejection implications. Others have used this strategy for similar short-term (24h) studies, and it to be safe and effective (Kyrtatos et al., 2009).

Together the group of highly conserved miRNAs miR-92a-1, miR-92a-2, miR 363, miR25 and miR-92b constitute the miR-92 seed family and share the same seed sequence used to design anti-miR oligonucleotides. Therefore, the used anti-miR-92a oligonucleotides may potentially have cross-targeted several other mature miRNAs. Based on the above, potential co-targeting of distinct miRNA species from the miR-92a seed family should have formally excluded in this study.

$CD34^+$- derived EPCs were generated and expanded in gelatin 1%, as others have also done (Pedroso et al., 2011). While the majority of EPC functional assays were conducted on gelatin (co-culture angiogenesis, proliferation, survival and wound healing assays), some of the EPC functional assays were performed on Fibronectin instead (cell-matrix adhesion and chemotaxis migration assays), since I wanted to scrutinize the upregulated ITGA5-FN interaction, specifically. I was unable to apply the same methodology to every functional assay due to pricing issues (Fibronectin ~630.00€ for 5mg vs Collagen powder ~41.25€ for 100g, both from SIGMA). I opted for collagen whenever a higher area of plasticware had to be coated. This constitutes a limitation for the generalization of my results, since the interaction of integrin alpha 5 subunit is expected to be different with the different ECMs.

Siavashi and colleagues scrutinized the possible role of three different natural extracellular substrates, including collagen, gelatin, and fibronectin, on multiple parameters of EPCs such as cell morphology, phenotype, clonogenic, and vasculogenic properties (Siavashi, Nassiri, Rahbarghazi, Vafaei, & Sariri, 2016). EPCs from GFP-positive mice were pre-expanded on each of these ECM substrates and then systemically transplanted into sub-lethally irradiated mice to analyse the potency of these cells for marrow reconstitution. Their results revealed considerable promise for fibronectin (FN) for EPC expansion, with maintenance of stemness characteristics, whereas gelatin and collagen matrices directed the cells toward a mature endothelial phenotype. Indeed, late EPCs pre-expanded on collagen and gelatin exhibited superior tube formation properties than EPCs pre-expanded on FN. Overall, the low angiogenic activity of the cells expanded on the FN substrate, particularly in the early stage, could be related to stable blockage of terminal differentiation of EPCs by FN. In support of this statement, we found the lowest number of $CD31^+$ mature cells on the FN matrix compared with

other matrices indicating little cell differentiation on FN. Transplantation of EPCs pre-expanded on FN resulted in widespread distribution and appropriate engraftment to various tissues with habitation in close association with the microvasculature. In addition, FN pre-expanded cells were gradually enriched in the bone marrow after transplantation, resulting in marrow repopulation and hematologic recovery, leading to improved survival of recipient mice whereas gelatin- and collagen-expanded cells failed to reconstitute the bone marrow.

It is conceivable that if EPCs in different ECM substrates exhibit different proliferation and differentiation potential leading to different reconstitution potency after *in vivo* transplantation, then EPC functional assays can be also modulated by the supporting matrix. Indeed, integrin–ECM interactions, namely, via β5-integrins, can mediate EPC paracrine factor production (Balaji et al., 2013). EPCs plated on different matrices express different cytokines levels, such as SDF-1, VEGF, monocyte chemotactic protein 1 (MCP-1), insulin-like growth factor 1, platelet-derived growth factor and macrophage inflammatory protein 1a (Balaji et al., 2013).

## 5.4 Future work

Low engraftment rates of EPCs may limit vascular regeneration (Chavakis et al., 2008; Haider et al., 2017). To increase the engraftment of cells to the target tissue either the cells could be pre-treated (e.g. modified by overexpression of genes or by incubation with small molecules) or the target tissue could be pre-activated (e.g. induction of cytokines, small molecules and miRNAs).

Having validated some interesting features of miR-92a inhibition *in vitro* in EPCs that could potentially translate into improved engraftment of these cells in the carotid injury model, we are left with some challenges for the next level - *in vivo*. AntagomiR delivery to EPCs prior to their transplantation may be quite challenging due to the need to harvest them and all protocols using short-term culture will, by their very nature, not yield sufficient numbers of EPCs for systemic therapy in the human. To treat a patient of 80 kg with a high dose cell strategy as described in some animal studies ($1 \times 10^7$ cells/25g) would require $32 \times 10^9$ cells (adjusted to body weight)(Templin et al., 2011), which exceeds the number of cells used in original clinical trials by a factor of ~3000 (Assmus et al., 2002). Therefore, progenitor cells would need to be to be expanded *in vitro* before reinjection, however, long-term culture may induce cellular senescence and introduce deviations in the phenotype of the EPC detrimental to their therapeutic efficacy. Moreover, the ideal strategy would not be to increase endogenous mobilisation nor provide increase BM-derived EPCs during transplantation, since that could hasten inflammation post-PCI or fasten the differentiation into SMC-like cells. Therefore, I envision the focus on EPC -mediated re-endothelialisation shifting to strategies aimed at maximising the recruitment and adherence of endogenous circulating EPCs to the sites of endothelial damage. Bearing all advantages and disadvantages in mind, I think that miR inhibitor delivery to the target tissue in the future might be preferred **(Table 19)**.

**Table 19 | Overview of the potential advantages and disadvantages of putative EPC-based strategies for therapeutic re-endothelialisation and restenosis prevention.**
Adapted from (Williams & Silva, 2015).

| Strategy | Advantages | Disadvantages |
|---|---|---|
| **Systemic infusion of primed EPCs** | Simple preparation of cells in solution<br>Ease of administration | Lengthy *ex vivo* expansion<br>Large number of cells required<br>Poor survival of administered cells<br>Low engraftment efficiency<br>Off-target localisation of administered cells |
| **Local bolus injection of primed EPCs** | Simple preparation of cells in solution<br>Locally delivered near site of injury<br>Fewer cells required than that for systemic infusion | Long ex vivo expansion of cells<br>Poor survival of administered cells<br>Low engraftment efficiency<br>Low retention of cells within target site |
| **Material-based deployment of EPCs and priming factors** | Targeted local delivery<br>Enhanced survival of cells due to dual delivery with small molecules<br>Greater engraftment efficiency<br>Fewer cells required than that for first two methods<br>Enhanced engraftment efficiency<br>Enhanced outward migration and function of transplanted cells | Long ex vivo expansion of cells<br>Complex preparation of cells within biomaterial system<br>Possible immune response to chosen biomaterial |
| **Deployment of priming factors in target tissue** | In situ regeneration<br>No ex vivo manipulation of cells<br>Enhanced function of endogenous cells<br>Enhanced regenerative potential by recruitment of endogenous EPCs | Approach limited by capability and functional response of endogenous cells |

I have developed several efforts in building that strategy **(Appendix IV)**. Future work will include the completion of the comparison of the Pluronic peri-adventitial delivery of miR-92a inhibitor to promote re-endothelialisation (as detected by vWF or eNOS IHC analysis and Evans blue staining) and prevent restenosis post-injury with the systemic administration previously validated for these purposes (Daniel et al., 2014; Iaconetti et al., 2012). Furthermore, to confirm the relevance of *in situ* miR-92a inhibitor -mediated ITGA5 upregulation in increasing the capture and thriving of circulating endogenous EPCs, I envisioned a BM transplantation models in nude rats. Briefly, lethally irradiated

nude rats would receive BM cells from transgenic Tie2/lacZ rats, which constitutively expressed β-galactosidase encoded by lacZ under the transcriptional regulation of an endothelium-specific promoter, Tie 2. Carotid arteries would be denuded 4 weeks after BM transplantation with the balloon angioplasty technique and the miR-92a inhibitor applied peri-adventitially using the pluronic gel. The same strategy would be used in miR-scrambled and miR-92a treated rats. X-gal staining would be performed on whole-mounted vessels to visualise and quantify BM– derived Tie2/lacZ-positive endothelial lineage cells per square millimetre of surface area. The stent coating with NP:miR-92a inhibitor would have to be developed and validated within a stent in a flow chamber with circulating porcine EPCs (engraftment validation through electronic microscopy) before advancing into the pig carotid injury model. Finally, before clinical application of this antagomiR therapy can be contemplated, further toxicology studies need to be completed.

# Appendix I – EPC differentiation from porcine bone marrow blood CD34$^+$ cells

Pig vascular biology appears to be relatively similar to that of humans (Zaragoza et al., 2011). For that reason, pigs are considered a more predictive model for CVDs and stenting outcomes than other animal models (Tsang et al., 2016). Several studies have been published about biodevices in pigs, including stents, artificial prostheses, grafts, shunts and ventricular assist devices. Additionally, the autologous transplantation of EPCs *per se* for the treatment of ischemic diseases (Dimmeler et al., 2008; Fadini, Agostini, & Avogaro, 2010; Lipinski et al., 2007) and restenosis prevention (Werner et al., 2003) is also an active area of translational research. However, as the pigs are usually immunocompetent (except for specific athymic models), human progenitor cells cannot be infused in these animals. Hence techniques for autologous EPC purification and expansion are warranted for this animal model. To date, pig cell therapy studies have relied on the infusion of pools of unselected MNCs or *ex vivo* expanded late-outgrowth EPCs derived from unselected MNCs (Chade et al., 2009; Doyle et al., 2008; Dubois et al., 2010; Tianhang et al., 2013), i.e. from heterogeneous starting populations. The use of phenotypically uncharacterized subsets of PACs derived from tissue culture is undesirable and is probably due to the fact that there are no commercially available magnetic sorting systems incorporating antibodies against porcine CD34. In fact, very few of the latter exist, and no human anti-CD34 antibody with known porcine cross-reactivity has been published to date, which complicated the implementation of an effective enrichment strategy. I described an original method, using indirect labelling, capable of enriching a primary CD34$^+$ population from pig BMB, and further differentiated them into pig CD34$^+$-derived EPCs. This strategy will enable future autologous transplantation experiments with miR-92a inhibitor transfected EPCs, and also allow the *in vitro* validation of the possible benefits of deploying a miR-92a inhibitor coated stent capable of locally transfecting engrafted EPCs. On a larger scale this

enrichment methodology might lead the way for a new generation of porcine autologous EPC transplantation trials (using primary or expanded $CD34^+$-derived EPCs).

There is only one other study, to my knowledge, reporting the isolation of these progenitors from pig BM (Layton et al., 2007). Layton *et al.* incubated cells with (mouse) anti-porcine CD34 antibodies which were then cross-linked to (goat) anti-mouse IgG microbeads, whereas, my strategy involved the incubation of cells with a (goat) anti-porcine CD34 biotinylated antibody instead, which was then made to bind with anti-biotin microbeads. Considering the success in isolating BM-derived $CD34^+$ cells, I consider BM to be an efficient and accessible source of $CD34^+$ progenitor cells for autologous use/differentiation in the pig.

# Enrichment of $CD34^+$ cells from porcine BM blood

Since *in vivo* vascular restenosis studies are long (days to weeks), human EPCs cannot be used in pigs due to immunocompatibility issues. Fortunately, the pig is large enough to allow sufficient BM cells to be harvested from its iliac crest for autologous transplantation without having to be sacrificed (unlike collection of BM blood from smaller species which must be pooled from several animal femurs). So, to test the transplantation of autologous miR-92a inhibitor-treated $CD34^+$-derived EPCs and determine the possible benefits of deploying a miR-92a inhibitor coated stent in pigs, I had to adapt techniques concerning $CD34^+$ purification and EPC differentiation to this animal model. The results of a failed isolation attempt using MACS immunomagnetic separation system with the proprietary anti-human CD34 antibody microbeads working previously for human UCB are represented in **(Figure I.1)**. There was no specific enrichment of porcine $CD34^+$ cells. Alternatively, it is possible that there was no specific labelling of porcine CD34 receptor with mouse anti-human CD34-PE conjugated antibody. Either way, I was unable to identify $CD34^+$ cells derived from pig BM using the MACS direct labelling system.

**Figure I.1 | Inability to identify CD34$^+$ cells from pig BM blood using MACS direct magnetic cell labelling.** An attempt to isolate CD34$^+$ cells from pig BM blood using MACS Immunomagnetic separation system and the proprietary mouse anti-human CD34 antibody microbeads was made, followed by flow cytometry analysis. For each set of samples, the fluorescent intensity of the isotype control was compared with the fluorescent intensity of the test sample and the corresponding histograms are presented. The results presented were obtained after one single experiment, with each condition measured in duplicate. BM – bone marrow; CD – cluster of differentiation; PE – phycoerythrin.

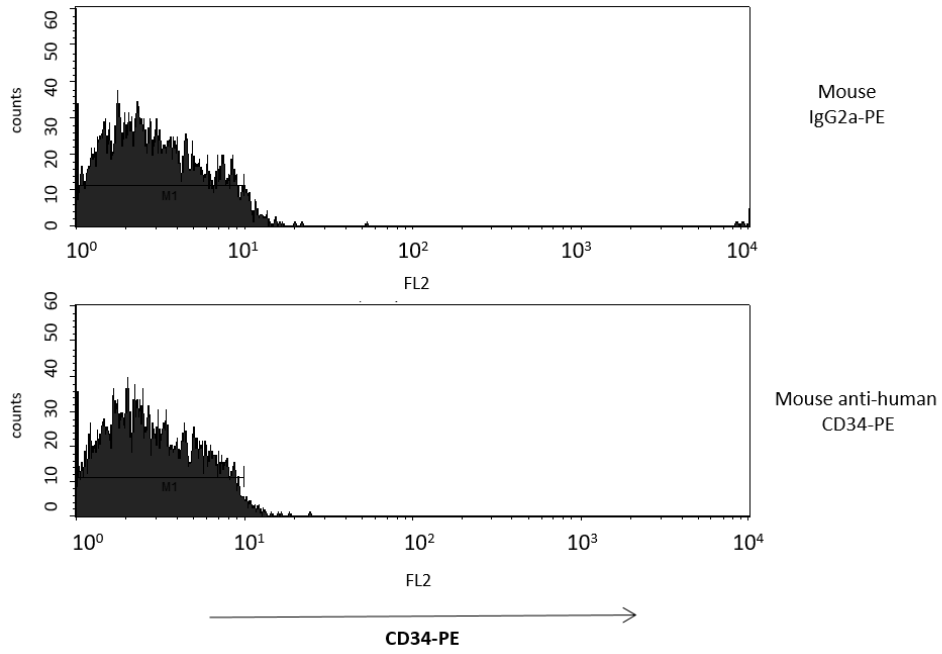


I next attempted an indirect labelling method to enrich the primary CD34$^+$ population from pig BM blood **(Table I.1)**. By using an anti-porcine biotinylated CD34 antibody and matching anti-biotin microbeads instead, I was able to successfully separate 8.945 ± 1.06 x10$^6$ CD34$^+$ cells from each pig BM unit following the previously used two-step immunomagnetic enrichment method. Cell viability after sequentially passing through the LS + MS column averaged at 87.5 % ± 2.5. By using one enrichment step only (a single microbead incubation period and a single transfer through a LS column) I was able to optimize cell viability (97% ± 1.5) with matching yield (9.2±2.42x10$^6$ CD34$^+$cells/BM unit).

**Table I.1 | Quantification of CD34$^+$ cells isolated from pig BM blood using MACS indirect magnetic cell labelling.** CD34$^+$ cells were isolated from 50 mL of pig BM blood using MACS Immunomagnetic separation system with specific modifications. For optimization purposes both single and double enrichment strategies were essayed. The total number and viability of freshly isolated CD34$^+$ cells were measured using an automatic cell counter. Data from 2 independent (double enrichment) and 3 independent (single) isolations is presented as mean values ± SEM. BM – bone marrow; CD – cluster of differentiation; MNC – mononuclear cell; SEM - standard error of the mean.

| Isolation method | MNCs (x10$^8$) | Recovered CD34$^+$ cells (x10$^6$) | Recovered cells CD34 (% of MNCs) | Viability of CD34+ recovered cells (% total cells) |
|---|---|---|---|---|
| **Two-step sorting** | 13.6 ± 0.9 | 8.945 ± 1.06 | 0.65 ± 0.03 | 87.5 ± 2.5 |
| **Single-step sorting** | 3.87 ± 1.04 | 9.2 ± 2.42 | 2.55 ± 0.49 | 97 ± 1.5 |

As for the **recovery** of CD34$^+$ cells from pig BMB, the described 2.55 % ± 0.49 (from total MNCs) is slightly lower that the only previously published 4% incidence for this animal (Layton et al., 2007). One might speculate that Layton *et al.* by using 1-week-old Landrace cross pigs (as opposed to the 3-month Yorkshire pigs that were employed in this study) might be more enriched in progenitor cells.

Pig CD34$^+$ cells recovered from BMB following single-step enrichment were 97 ± % 1.5 viable, revealing that the reduction of the protocol was the correct option also regarding **cell viability** (double labelling generated 87.5 % ± 2.5 viable cells only). Layton *et al.* did not publish the viability of pig BM CD34$^+$ cells retrieved by single-step enrichment with IgG Mouse microbeads for comparison (Layton et al., 2007).

The retrieved CD34$^+$ fraction from pig BM blood exhibited similar purity (by flow cytometry) following either enrichment methods **(Figure I.2)**. The single step labelling strategy yielded a highly pure fraction (92.72 % ± 1.17), as did the alternative double labelling (90 % ± 2.05).

**Figure I.2 | CD34$^+$ cell fractions isolated from pig BM blood using MACS indirect magnetic cell labelling are highly pure.** To determine the purity of the populations enriched for CD34 by immunomagnetic sorting, flow cytometry was used. **(A)** Representative FSC-SSC dot plots of pig BM CD34$^+$ cells and CD34$^-$ flow through are presented. For each set of samples, the fluorescent intensity of the isotype control was compared with the fluorescent intensity of the test sample and the corresponding histograms are presented. **(B)** Cells exceeding the threshold fluorescence defined by the IgG Control were quantified and considered positive for CD34. Results are presented in tabular format as mean antigen positive cells percentage ± SEM, after three independent experiments (single enrichment) and two independent experiments (two-step enrichment). Each condition was measured in duplicate. BM – bone marrow; BSA

– bovine serum albumin; CD – cluster of differentiation; FSC – forward scatter; Flt3 - Fms-like tyrosine kinase 3; HSC – hematopoietic stem cell; PBS - phosphate-buffered saline; SCF – stem cell factor; SEM - standard error of the mean; SSC – side scatter.

**A**

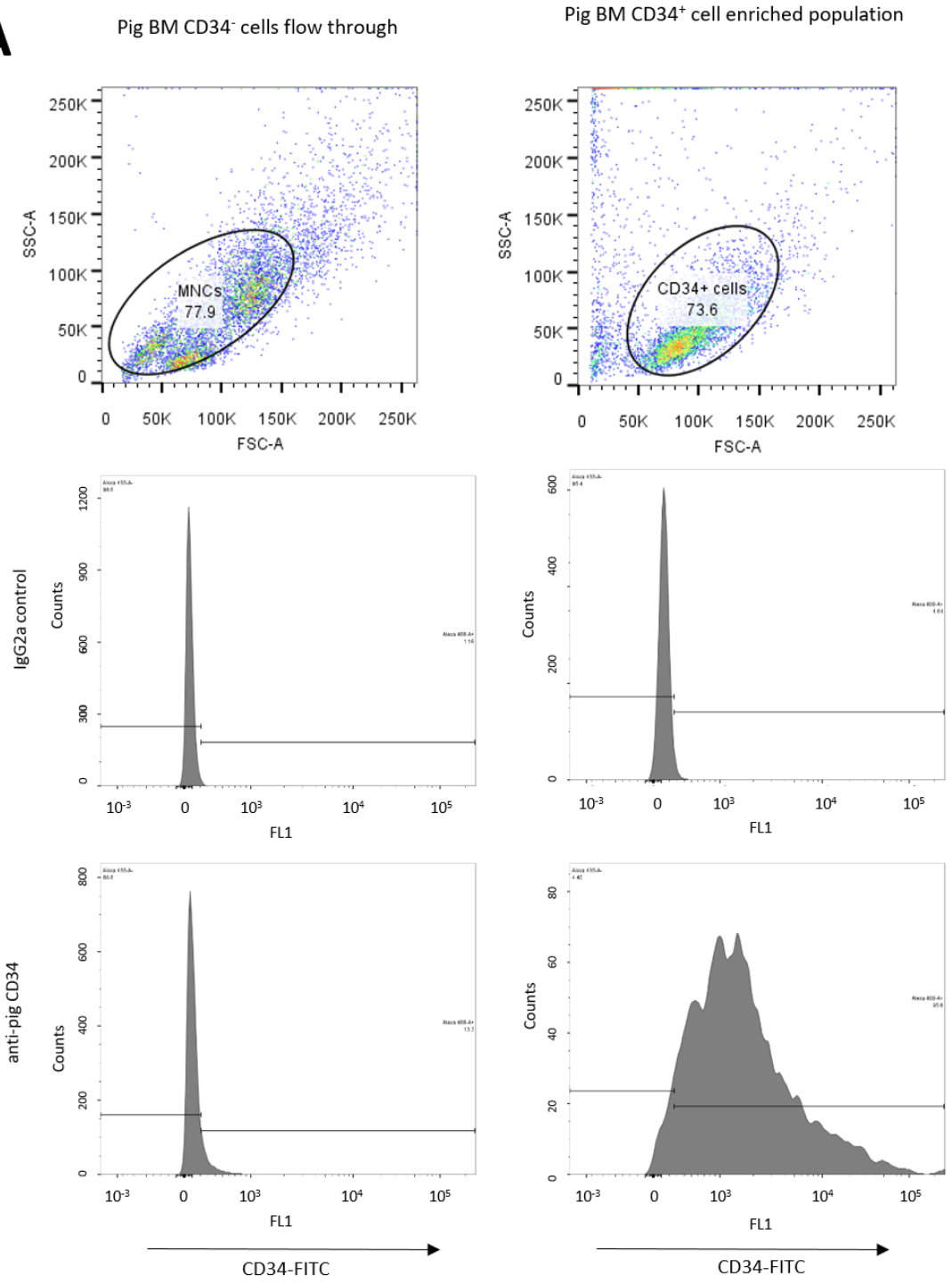


**B**

| Isolation method | Antigen | Positive cells (%) |
|---|---|---|
| **Two-step enrichment** | CD34 | 90 ± 2.05 |
| **Single-step enrichment** | CD34 | 92.72 ± 1.17 |

# Differentiation of late-outgrowth porcine EPCs from $CD34^+$ cells

I subjected the freshly isolated pig BM $CD34^+$ cells to the differentiation protocol previously established for human samples, enabling the appearance of late-outgrowth EPCs in culture **(Figure I.3)**. By day 20 of the differentiation protocol, $CD34^+$ cells had assumed a cobblestone-like morphology and became adherent to the gelatin substrate. The phenotype was further characterized by ac-LDL internalization capacity and vascular endothelial cadherin (VECAD) expression, both features displayed by pig BM $CD34^+$-derived EPCs.

**Figure I.3| Late outgrowth EPCs were successfully differentiated from pig BM blood $CD34^+$ cells.**
$CD34^+$ cells from pig BM blood were differentiated into late outgrowth. **(A)** The bright-field image on the left captures freshly isolated pig BM $CD34^+$ cells (20x). By differentiation day 7 some $CD34^+$ cells become adherent and assumed a cobblestone like morphology (see arrowed), as captured in the middle image (20x) and in the blow out (40x). After 11 days of differentiation most of the cells at the periphery were adherent, as seen in the right picture (20x). **(B)** After 20 days of cells in culture, internalization of Ac-LDL conjugated to Alexafluor-488 was demonstrated at 20x magnification. HUVECs were used as positive controls. **(C)** Further confirmation of endothelial like phenotype after 20 days of cells in culture was evident from the VECAD western blot results. **(D)** After 20 days of culture, the presence of VECAD endothelial specific marker was evaluated in pig $CD34^+$-derived EPCs by If at 60x. ac-LDL – acetylated low-density lipoprotein; CD – cluster of differentiation; DAPI - 4',6-diamidino-2-phenylindole; EPC – endothelial precursor cell; PAECs – pig aortic endothelial cells; VECAD – vascular endothelial cadherin.

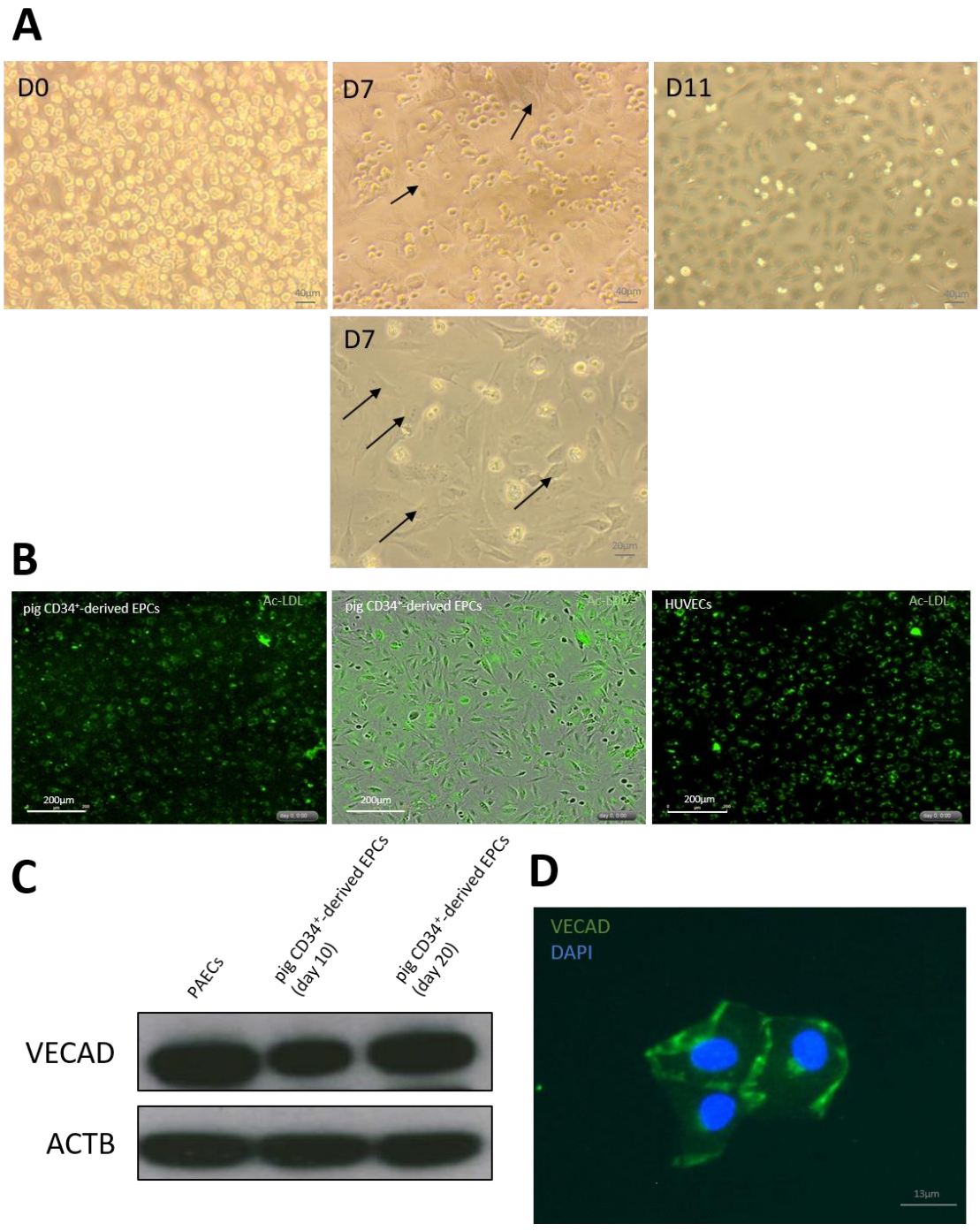
A
D0
D7
D11
D7
B
pig CD34+-derived EPCs
Ac-LDL
200μm
pig CD34+-derived EPCs
200μm
HUVECs
Ac-LDL
200μm
C
PAECs
pig CD34+-derived EPCs (day 10)
pig CD34+-derived EPCs (day 20)
VECAD
ACTB
D
VECAD
DAPI
13μm

To further illustrate endothelial commitment, I performed a Matrigel based-angiogenesis functional assay, which revealed that pig CD34$^{+}$-derived EPCs also had the ability to form tubule-like structures **(Figure I.4)**.

**Figure I.4| Pig late outgrowth CD34$^{+}$-derived EPCs showed angiogenic potential.**
The assay was performed using a Matrigel matrix with reduced growth factor content. A set of representative brightfield images (10x magnification) taken at 6h post incubation in a time-lapse imaging incubator is presented for EPCs, revealing tubule-like formation ability. HUVECs were used as positive controls and colonic SMC as negative controls. CD – cluster of differentiation; EPC – endothelial precursor cell; HUVEC - Human Umbilical Vein Endothelial Cell; SMC – smooth muscle cell.

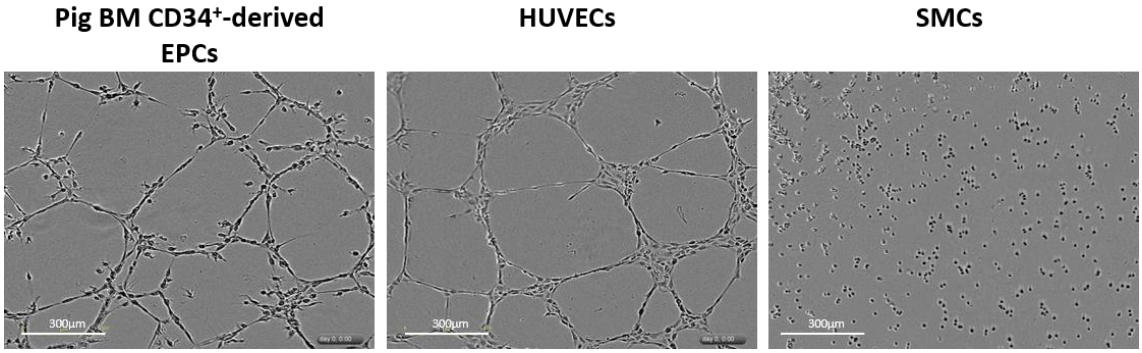


The presence of KDR (a receptor for VEGF) in preliminary flow cytometry studies, further highlighted the endothelial commitment by a significant proportion of the CD34$^{+}$-derived EPCs **(Figure I.5)**.

**Figure I.5 | KDR is present in pig BM CD34$^{+}$-derived EPCs after their differentiation.**
The presence of KDR antigen on the surface of pig BM late-outgrowth EPCs was sought by flow cytometry. **(A)** Representative FSC-SSC dot plots of EPCs at different time points are presented, as well as corresponding KDR conjugated FITC intensity histograms. **(B)** The graphic presents the percentage of KDR positive cells in the adherent fraction at the different time points in culture. **(C)** Graphical representation of fluorescence geometric mean difference to control, a surrogate of antigen mean surface density. All results are representative of 1 experiment and are therefore preliminary; all conditions were measured in duplicate. BM – bone marrow; EPC – endothelial precursor cell; FITC - Fluorescein isothiocyanate; FSC – forward scatter; IgG – Immunoglobulin; KDR – kinase insert domain receptor; SSC – side scatter.

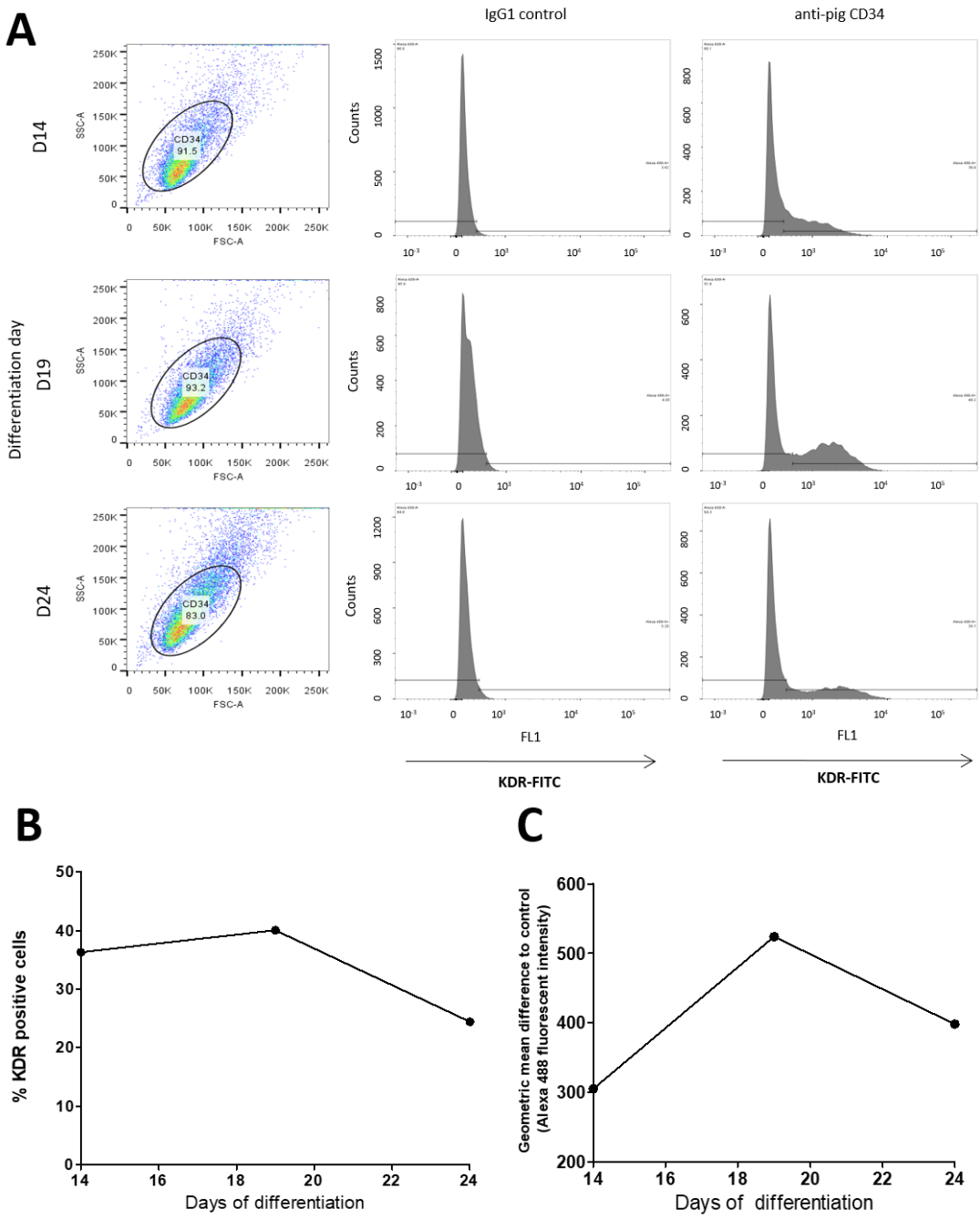


VEGF-A, the main KDR ligand, is a well described EC-specific mitogen/chemoattractant associated with vascular repair (Ferrara, 2001; Holmes et al., 2007), whereas PDGF-BB is a major growth factor released from stimulated platelets which stimulates the proliferation, migration and survival of VMSCs at the sites of vascular insults.

Both serine/threonine kinase Akt and ERK1/2 are downstream kinases which get activated by phosphorylation upon VEGF (Fujio & Walsh, 1999) and PDGF-BB (Razmara,

Heldin, & Lennartsson, 2013) stimulation of their receptors. ERK 1/2 and Akt are of particular relevance because of their strong association with the regulation of mitogenesis and activation of eNOS (Gifford et al., 2004).

ECs are rich in KDR VEGF receptor (Waltenberger, Mayr, Pentz, & Hombach, 1996). However, they are believed to lack PDGF receptors (usually present on fibroblasts and SMCs) and to be unresponsive to PDGF (Beitz, Kim, Calabresi, & Frackelton, 1991).

So, to test the activation profile of the pig BM $CD34^{+}$-derived EPCs, I challenged them with VEGF and PDGF **(Figure I.6)**. Reassuringly, the EPCs exhibited Akt and ERK phosphorylation upon VEG stimulation, but produced no response to PDGF, which is an expected feature of endothelial phenotypes ($KDR^{+}PDGFR^{-}$ cells). Both Akt and ERK 1/2 are highly expressed in HUVECs (Gifford et al., 2004).

**Figure I.6 | Pig BM CD34$^{+}$-derived EPCs exhibited phosphorylation of Akt and ERK1/2 upon VEGF stimulation.**

Cells were challenged for 10 mins with either 25 ng/mL VEGF, PDGF or SFM before its proteins were separated by SDS-PAGE, and immunoblotted with the antibodies indicated. **(A)** The single western blot is shown. **(B)** Akt and ERK1/2 phosphorylation were quantified by scanning densitometry. Phosphoprotein levels were normalised to levels of the corresponding total protein and presented in relative units. Results in this figure are derived from 1 single experiment, and therefore preliminary. PDGF – platelet derived growth factor; RU – relative units; SFM – Serum-free media; VEGF – vascular endothelial growth factor

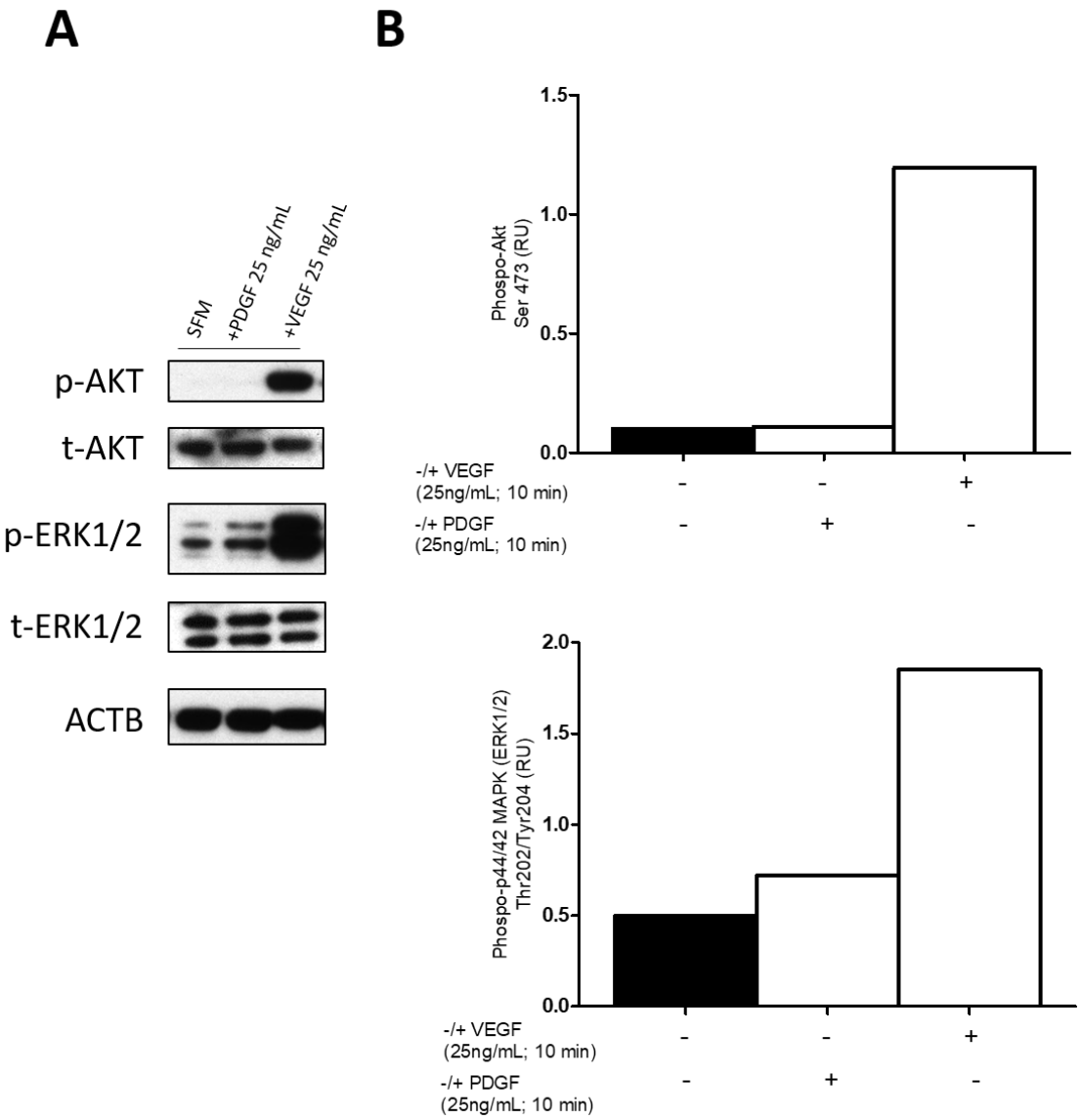

# Appendix II – Unsucessful EPC differentiation from human umbilical cord blood CD133$^+$ cells

**Figure II.1 |Late-outgrowth EPCs could not be successfully differentiated from human UCB CD133$^+$ cells.** UCB human CD133$^+$ cells could not be differentiated into late-outgrowth EPCs Bright-field images during differentiation were captured at 10x. The image represents CD133$^+$ cells still in suspension 3 weeks after isolation, at which time the differentiation culture was terminated.

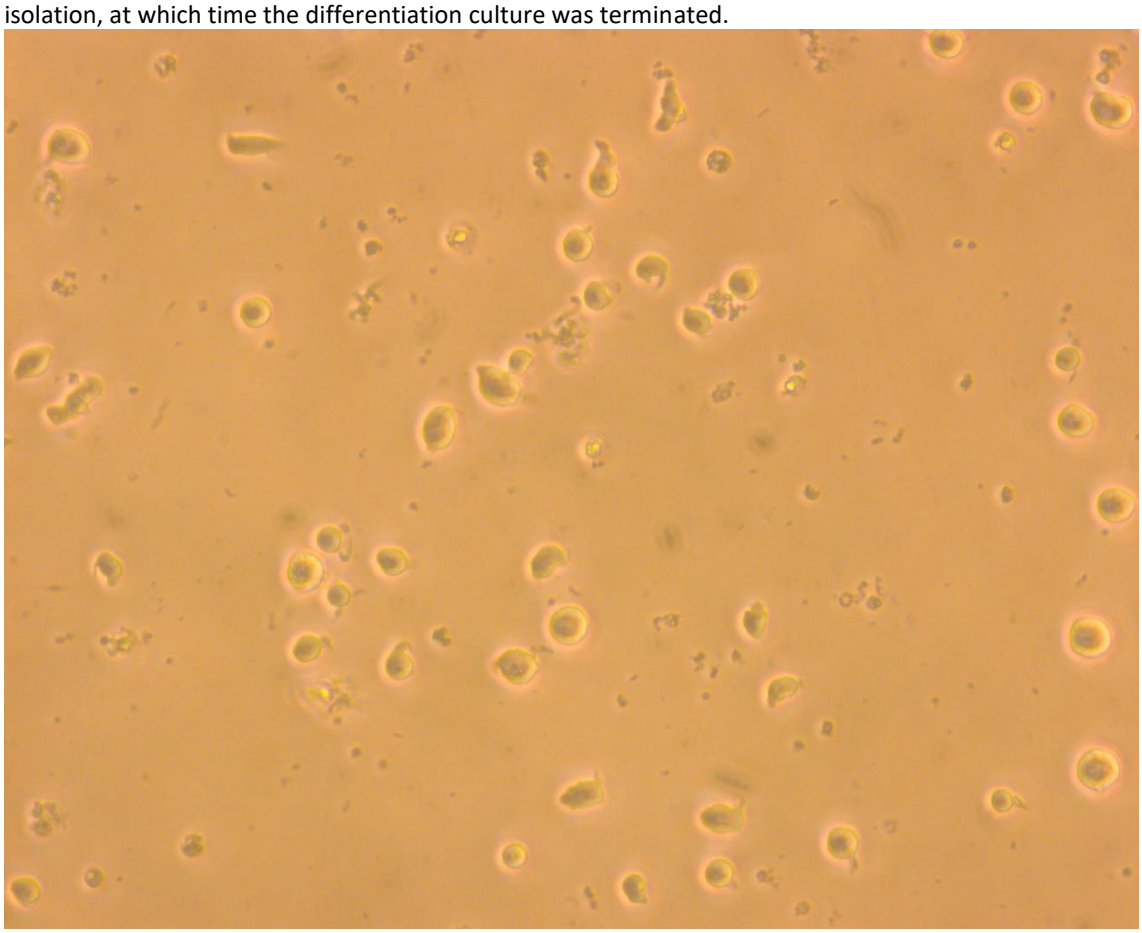

# Appendix III – Failed CD34$^{+}$-derived late outgrowth EPC transfection attempts

**Figure III.1 | CD34$^{+}$-derived EPC transfection of miR-92a (inhibitor) using SIPORT NeoFX was unsuccessful.** Human late-outgrowth EPCs (~80% confluency) were transfected in 6 well plates with 80 nM control scrambled miRNA, miR-92a-1-5p or miR-92a-1-5p inhibitor (-FITC) using SiPORT NeoFx, according to manufacturer's instructions. Following 72h knockdown in complete medium cells were lysed, proteins were separated by SDS-PAGE, and immunoblotted with the antibodies indicated. Results in this figure are preliminary and reflective of one experiment. SIPORT NeoFX was not suitable for miRNA transfection into CD34$^{+}$-derived EPCs, since no discernible change in ITGA5 levels compared to control miR scrambled transfection were seen. ACTB - β-actin; ITGA5 – Integrin α5 subunit; miR – microRNA.

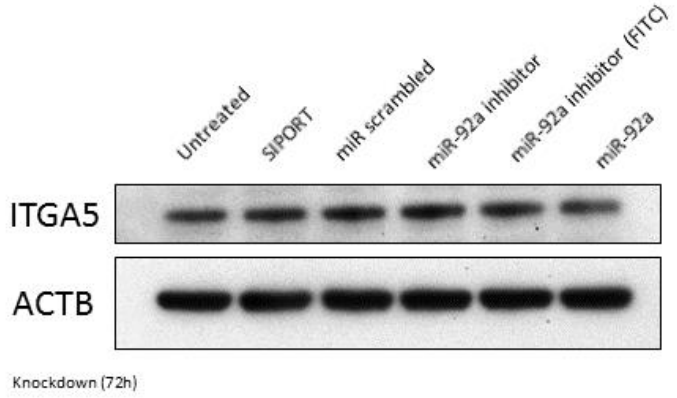


**Figure III.2 | CD34$^{+}$-derived EPC transfection of miR-92a (inhibitor) using Lipofectamine RNAimax was unsuccessful.** Human late-outgrowth EPCs (~80% confluency) were transfected in 6 well plates with 200 nM control scrambled miRNA, miR-92a-1-5p or miR-92a-1-5p inhibitor (-FITC) using Lipofectamine RNAimax, according to manufacturer's instructions. Following 72h knockdown in complete medium cells were lysed, proteins were separated by SDS-PAGE, and immunoblotted with the antibodies indicated. Results in this figure are preliminary and reflective of one experiment. Lipofectamine RNAimax was not suitable for miRNA transfection into CD34$^{+}$-derived EPCs, since no discernible change in ITGA5 levels compared to control miR scrambled transfection were seen. ACTB - β-actin; ITGA5 – Integrin α5 subunit; miR – microRNA.

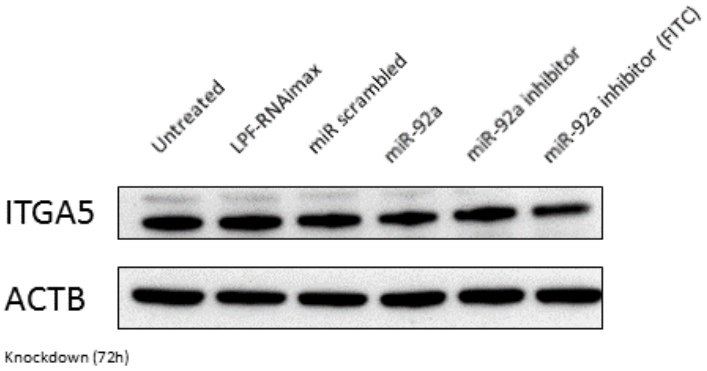

# Appendix IV: The effect of miR-92a inhibitor localised treatment on arteries and development of an nanoparticle-based delivery for EPC capture

Following the indication that miR-92a inhibitor might enhance EPC adhesion to injured arteries, this appendix chapter seeks to describe my initial steps towards establishing a target tissue pre-activation strategy by transfecting miR-92a inhibitor into injured arteries, since that harvesting of EPCs and their *in vitro* expansion before reinjection is labour intensive. Besides, tissue culture conditions could alter the phenotype of these cells. This could maximise endogenous EPC capture and thrive, contributing to the prevention of post-angioplasty restenosis, instead of having to transplant pre-activated *ex vivo* -expanded EPCs. Therefore, I developed an *in vivo* method for localized transfection of miR-92a inhibitor into the arteries using a thermo-reversible gel. Then, I sought the functional outcome of miR-92a antagonism in the injured arteries. miR-92a inhibitor presence became evident across all layers of the vascular wall 24h after deployment of the pluronic gel, and a reduced neointima formation trend was witnessed just 7 days after compared to scrambled control. Unfortunately, there was not enough time in the PhD to validate statistically the reduction in neointima formation, nor to document the enhancement in re-endothelialisation on account of increased EPC engraftment. After the neointima reduction proof-of-principle pilot experiments using the gel delivered peri-adventitially, we envisioned an NP-based strategy that could be used to transfect miR-92a inhibitor into arteries intraluminally via a stent. The intention was to incorporate a coating composed of miR-92a inhibitor complexed to biodegradable NPs into a future stent capable of a controlled miRNA release, thus priming the captured EPCs **(Figure IV.1)**. The NP -based delivery method could allow for a timed release of the miR-92a inhibitor, in a first instance enhancing EPC engraftment via ITGA5 upregulation once the rolling cells on the luminal surface were locally

transfected, and in a second stage enhancing re-endothelialisation and reducing neointima by increasing NO production.

**Figure IV.1 | Scheme of an epigenetic stent eluting NP:miR-92a inhibitor complexes.**
The diagram represents a hypothetical stent scaffold able to elute miR-92a inhibitor. This could be an efficient approach to enhance the endothelial regeneration through the promotion of the homing, survival and re-endothelialisation activity of captured EPCs (and neighbour niche), via the placement of a therapeutic biodegradable stent coated with miR-92a inhibitor complexed to biodegradable poly(lactic-co-glycolic acid) nanoparticles. miR – microRNA; NP – nanoparticles.

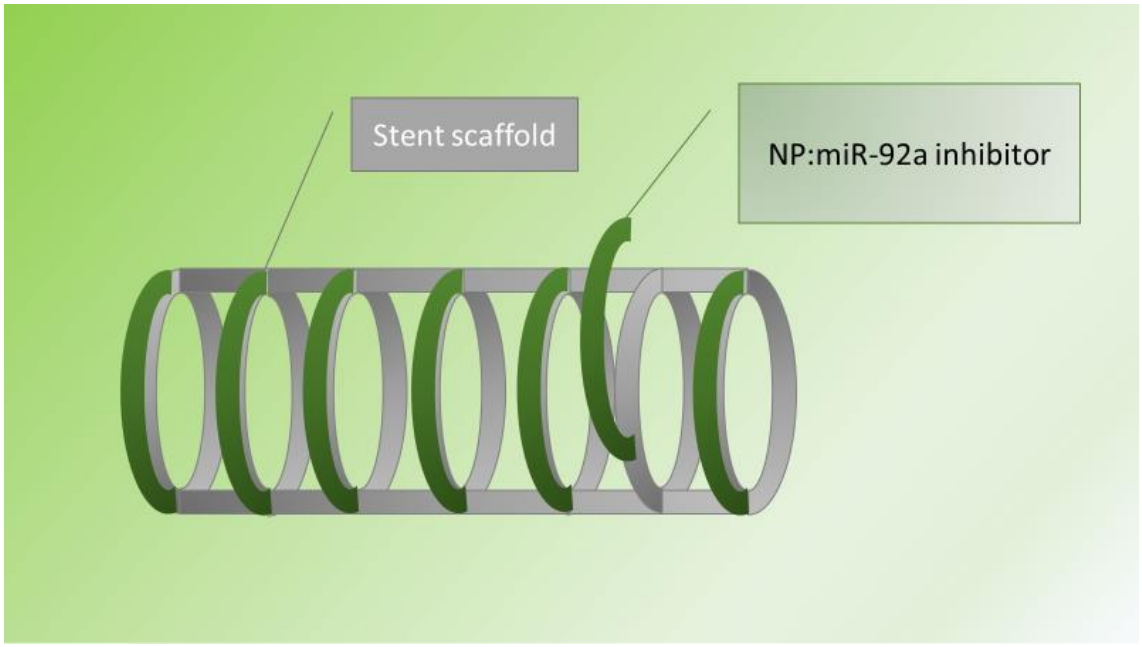


In tissue culture, miR-92a inhibitor was successfully transfected into EPCs when conjugated with the NPs, and as soon as the miRNA is released from the electrostatic bonds with the NP surface at the endosome, it seems to become available to be processed by the miRNA machinery only to produce (at least) pro-survival and pro-migratory effects. *In vivo*, NP:miR-92a were seen across the entire vascular wall following intraluminal (and peri-adventitial) arterial transfection, with preliminary results revealing a likely upregulation of miR-92a target molecules. Although the reduction in neointima formation in injured arteries following miR-92a inhibitor treatment administered systemically has been previously established (Daniel et al., 2014), it is the first time that peri-adventitial miR-92a inhibitor delivery was attempted. No publication on the functional benefits of miR-92a inhibitor transfection into EPCs using NPs as vectors was found in the literature. Moreover, it is the first time that pluronic facilitated transfection of NP:miRNAs into vessel walls is reported. Further optimization is warranted, hence the data is preliminary yet and hence discussion takes place in an appendix format only.

# miR-92a inhibitor enhances arterial angiogenesis *ex vivo*

Given that endothelial sprouting from aortic rings requires combined endothelial cell (EC) proliferation, migration, survival and tube formation (Iaconetti et al., 2012), this was considered a complete assay to extrapolate the effect of miR-92a inhibitor *ex vivo*. Therefore, endothelial-lineage cell sprouting from aortic rings embedded in a collagen matrix was quantified 7 days after transfection with miR-92a inhibitor **(Figure IV.2)**. Compared with the scrambled control, functional inhibition of miR-92a significantly increased the outgrowth area of aortic rings ($1.43x10^6$ vs. $0.67x10^6$, $p<0.001$, coverage area in pixels$^2$). Ideally outgrowth cells should have been co-stained with CD34, but unfortunately, this would not distinguish endothelial precursor cells (EPCs) from resident proangiogenic cells (PACs), as there is no specific surface marker for EPCs. Still, I was satisfied with the functional output of isolectin B4 (IBL4) staining endothelial committed cells (which comprehend EPCs (Mieno et al., 2010; Mieno et al., 2008)) following antagomiR-92a, therefore I considered useful to go through with miR-92a inhibition *in vivo* with no further *ex vivo* characterization.

**Figure IV.2| miR-92a inhibitor enhances mouse aortic angiogenesis.** Mouse aortic rings were treated with 30 nM of miR scrambled, miR-92a (5p) or miR-92a (5p) inhibitor, embedded in a collagen matrix and cultured in supplemented medium before IF analysis. **(A)** Representation of a miR-92a inhibitor transfected ring after 7 days in culture, captured at 5x. The picture reveals peripheral angiogenic aortic sprouts composed of endothelial lineage ILB4$^+$ cells, supported by a stalk of SMA actin positive cells. **(B)** Before fixation treated rings were photographed at 4x magnification, and representative brightfield images are shown, where one can observe apparently diminished and enhanced *ex vivo* aortic ring angiogenesis in miR-92a, and miR-92a inhibitor transfected samples, respectively, compared to miR-scrambled. **(C)** Quantification of the peripheral IBL4$^+$ angiogenesis network area in square pixels (subtracted digitally by the ring area itself) was performed at 2.5x IF. Results of that quantification after 3 independent experiments (3 replicates each) are plotted as means, with errors bars representing ± SEM. **P<0.01 and ***P<0.001 compared with *miR scrambled* (1-way ANOVA, Bonferroni's test for multiple comparisons). DAPI - 4',6-diamidino-2-phenylindole; IB4 – isolectin B4; IF - immunofluorescent; miR – microRNA; Si – short interfering; SEM – standard error of mean; SMA – smooth muscle actin.

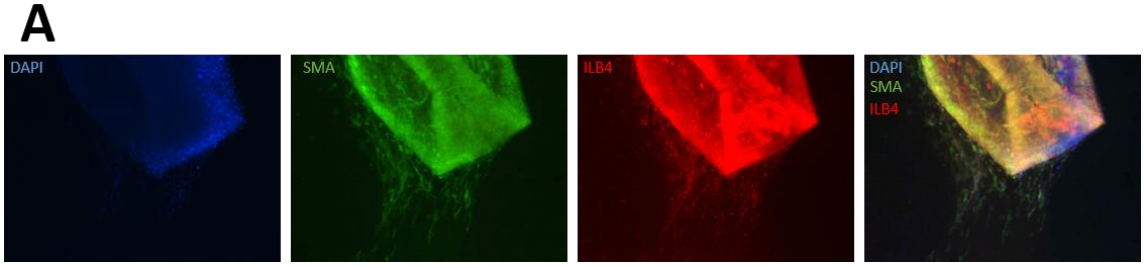

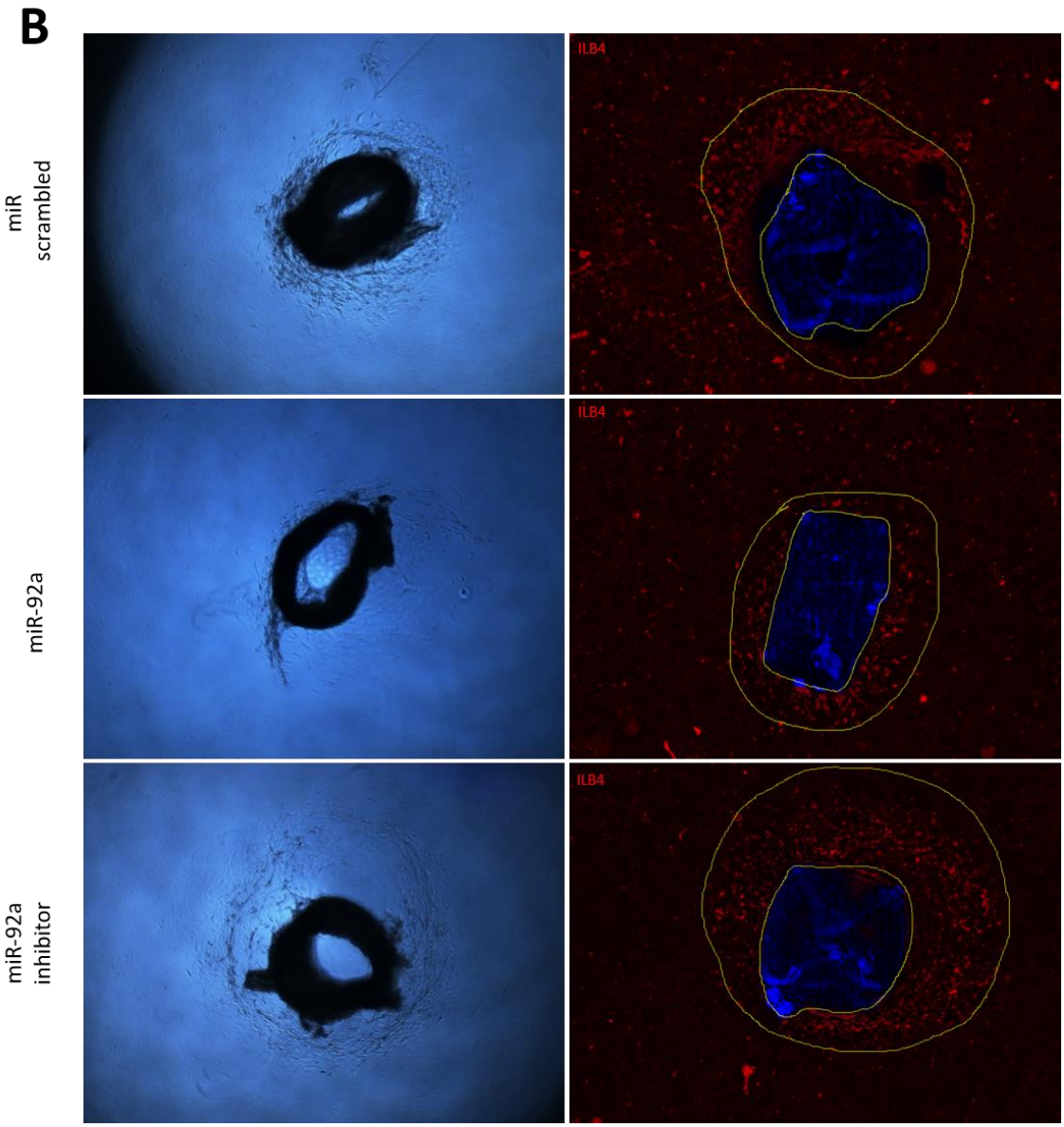
B
miR scrambled
miR-92a
miR-92a inhibitor
ILB4
ILB4
ILB4

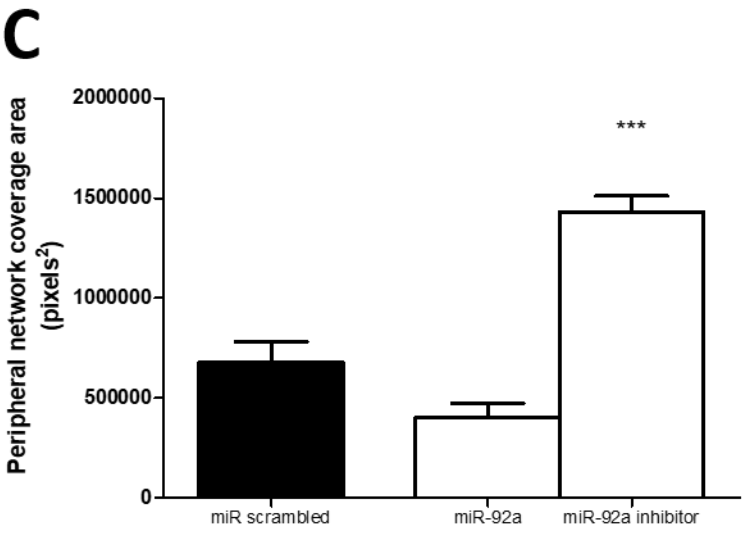
C
Peripheral network coverage area (pixels²)
2000000
1500000
1000000
500000
0
***
miR scrambled
miR-92a
miR-92a inhibitor

# Peri-adventitial gel-delivered miR-92a inhibitor is capable of arterial wall transfection *in vivo*

The *in vivo* strategy consisted in using the pluronic gel as a transfection vector for localised delivery of miR-92a inhibitor around the rat carotid artery to avoid possible systemic off-target effects, instead of delivering the microRNA (miR) via rat tail vein injection as previously attempted (Bonauer et al., 2009). Data from immunohistochemistry (IHC) and immunofluorescence (IF) demonstrated an efficient uptake of the FITC-tagged miR across the 3 arterial layers just 24h after periadventitial delivery **(Figure IV.3)**.

**Figure IV.3 | Pluronic gel periadventitial delivery is efficient at promoting rat carotid artery miR-92a inhibitor-FITC transfection.**
An uninjured rat left common carotid artery was surgically exposed so that pluronic gel containing 1 µM miR-92a (5p) inhibitor-FITC conjugated could be applied peri-adventitially onto the whole length of the vessel. The animals were sacrificed 24h postoperatively, and the artery samples were processed either by IHC or IF (anti-FITC). **(A)** Representative IHC image at 40x of a rat carotid artery treated *in vivo* with miR-92a inhibitor. **(B)** Representative IHC image at 40x of a treated artery where primary antibody staining was omitted (IHC negative control). **(C)** Representative IHC image at 40x of a non-treated artery (experimental negative control). **(D)** Representative IF image at 20x of a rat carotid artery treated *in vivo* with miR-92a inhibitor. **(E)** Representative IF image at 20x of a treated artery where primary antibody staining was omitted (IF negative control). **(F)** Representative IF image at 20x of a non-treated exposed artery (experimental negative control). DAPI - 4',6-diamidino-2-phenylindole; FITC - Fluorescein isothiocyanate; IHC – immunohistochemistry; miR – microRNA.

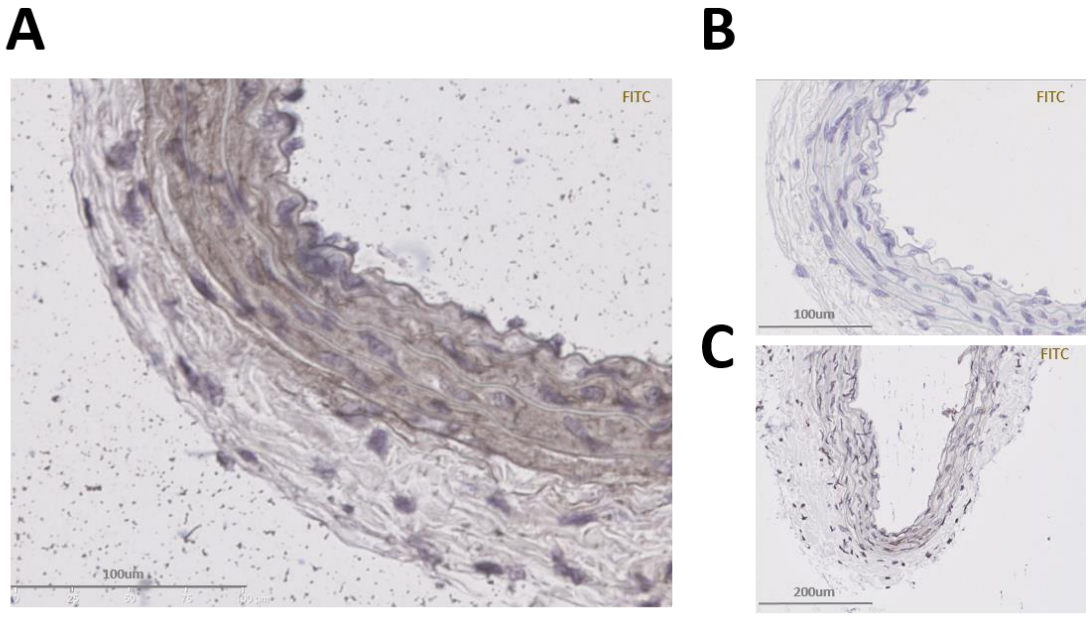

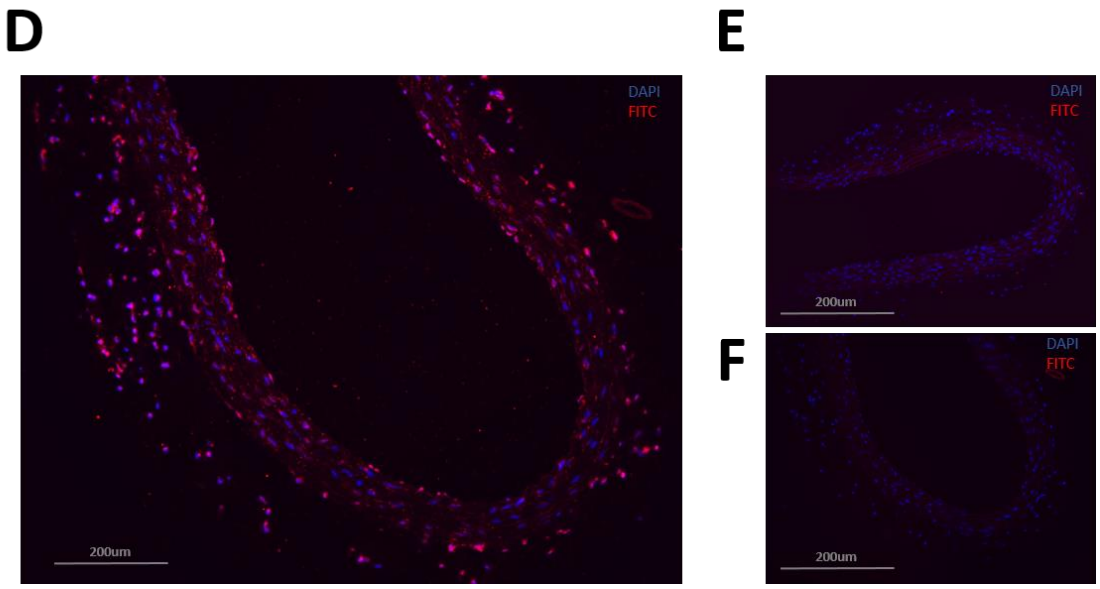


The immunostaining results were complemented by protein expression **(Figure IV.4)**, with a pilot western blot (WB) revealing a possible relative upregulation of ITGA5 following miR-92a inhibitor treatment after 48h compared to miR scrambled (124% vs. 100%, n=1). On the opposite direction, preliminary results seemed to indicate that miR-92a determined an ITGA5 downregulation just after 24h (49 % vs. 100%, n=1). Unfortunately, for time restraints related to my PhD leave coming to an end and having to return mandatorily to my clinical work as per contract, I was unable to reach the "n" numbers necessary to reach statistical significance.

**Figure IV.4 | In vivo peri-adventitial pluronic gel delivery miR-92a inhibitor seems to enhance local ITGA5 levels.**
The uninjured rat left carotid artery was surgically exposed, so that Pluronic gel containing 1µM mirR scrambled, miR-92a (5p) or miR-92a (5p) inhibitor could be applied externally. After a 24-48h post-operative period, the artery was harvested. Protein extraction involved bead-beating homogenization and retrieval of the protein lysate. Following normalisation, proteins were separated by SDS-PAGE, and **(A)** immunoblotted with the antibodies indicated. **(B)** Levels of ITGA5, were quantified during a time course by scanning densitometry and expressed as relative units compared to ACTB. Results in this figure are preliminary and reflective of one experiment. ACTB – actin beta; ITGA5 – integrin alpha 5 subunit; miR – microRNA; RU – relative units.

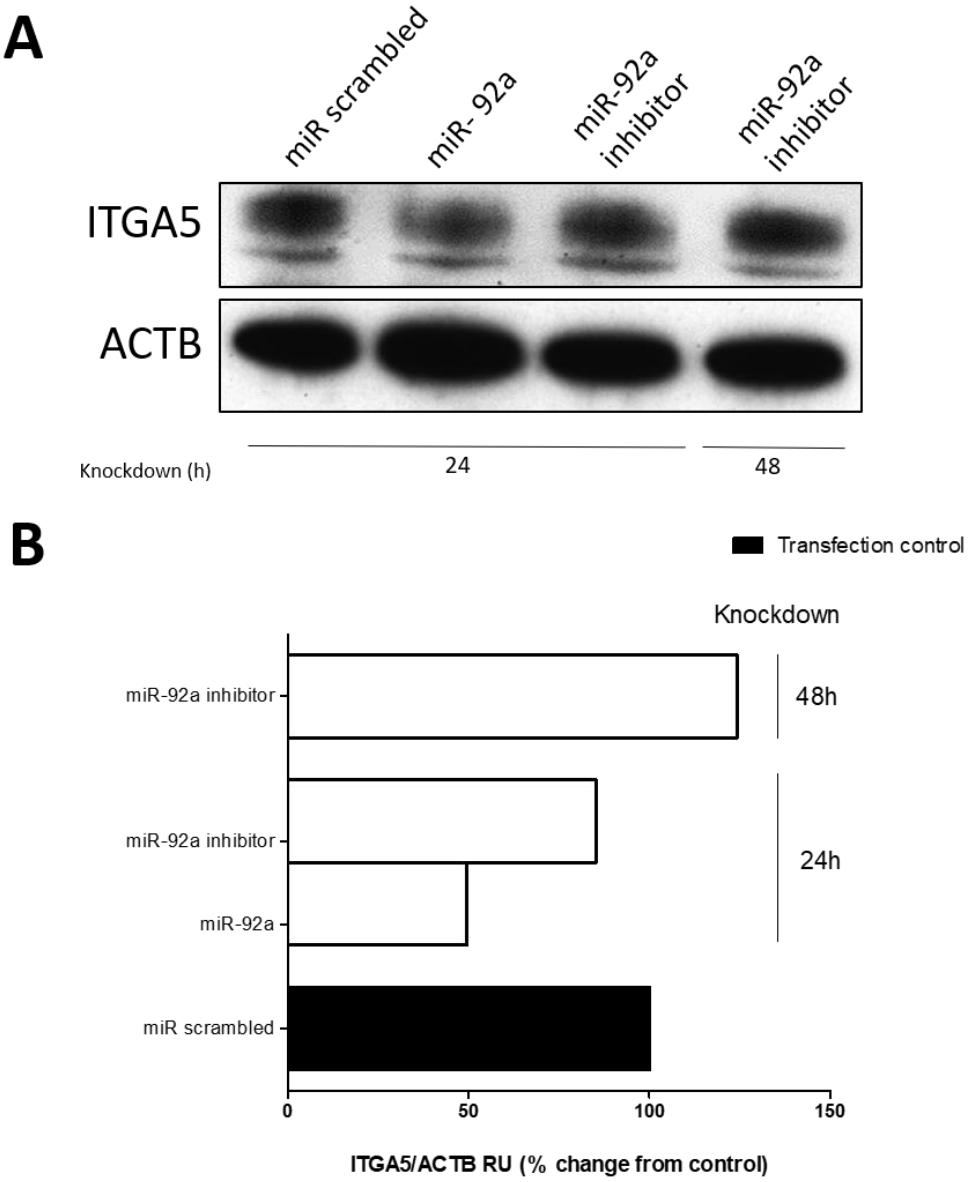
A
miR scrambled
miR- 92a
miR-92a inhibitor
miR-92a inhibitor
ITGA5
ACTB
Knockdown (h)
24
48
B
Transfection control
Knockdown
miR-92a inhibitor
miR-92a inhibitor
miR-92a
miR scrambled
48h
24h
0
50
100
150
ITGA5/ACTB RU (% change from control)

# miR-92a inhibitor localised delivery seems to mitigate post-angioplasty neointima formation

One of my original research purposes, when I started my PhD, was to demonstrate that miR-92a inhibition could prevent neointima formation following vascular injury (an effect that had never been reported), with particular contribution from EPCs, which, hypothetically, would show enhanced engraftment and re-endothelialisation activity. After inducing a balloon angioplasty injury, I investigated whether periadventitial delivery of miR-92a inhibitor caused a reduction of neointima formation. The analysis of injured arteries seemed to indicate that miR-92a antagonism could mitigate neointimal formation 7 days following the balloon injury compared to miR scrambled controls (0.3 vs. 0.63, n=1) **(Figure IV.5)**. The post-angioplasty survival was rated at 100%, with the rats demonstrating normal behaviour and welfare after returning to their environment both in control and in interventional arms. There were no local or systemic complications to report. During the entire experimental period, the animals tolerated procedures well as assessed by activity level and food and water intake, which were normal. Body weights did not differ between three groups at the end of the experiment

I was planning to reach statistical significance to demonstrate proof-of-principle, however, Iaconetti and colleagues confirmed one year into my PhD that, indeed, that *in vivo* administration of antagomiR-92a significantly enhances re-endothelialisation of injured carotid arteries and reduces neointimal formation after arterial balloon injury or stenting (Iaconetti et al., 2012). This was done via systemic administration of miR-92a inhibitor, which can potentially have undesirable off-site effects. Therefore, my focus changed from proof-of-principle to introducing specific modifications to the localised delivery of miR-92a inhibitor that could be translatable into man use and result in a safer more efficient delivery of the miRNA.

**Figure IV.5 | Pluronic gel-delivered miR-92a (5p) inhibitor treatment seems to reduce post-angioplasty stenosis.**
Following carotid balloon angioplasty, 300 µl of 1 µM miRNA were applied peri-adventitially using pluronic gel. Animals were sacrificed after 7 days, and processed arteries stained with hematoxylin and eosin in order to quantify the intima/media ratios. **(A)** Representative cross-section images of miR-scrambled treated artery (left picture) and miR-92a inhibitor (middle picture) taken at 5x and 40x magnification, compared to an uninjured rat carotid artery (right image). Dashed lines (arrowed) indicate the internal elastic lamina. **(B)** Neointima/media ratios were determined by morphometric analysis, with preliminary results from one single set of animals presented in a bar graph. miR– microRNA.

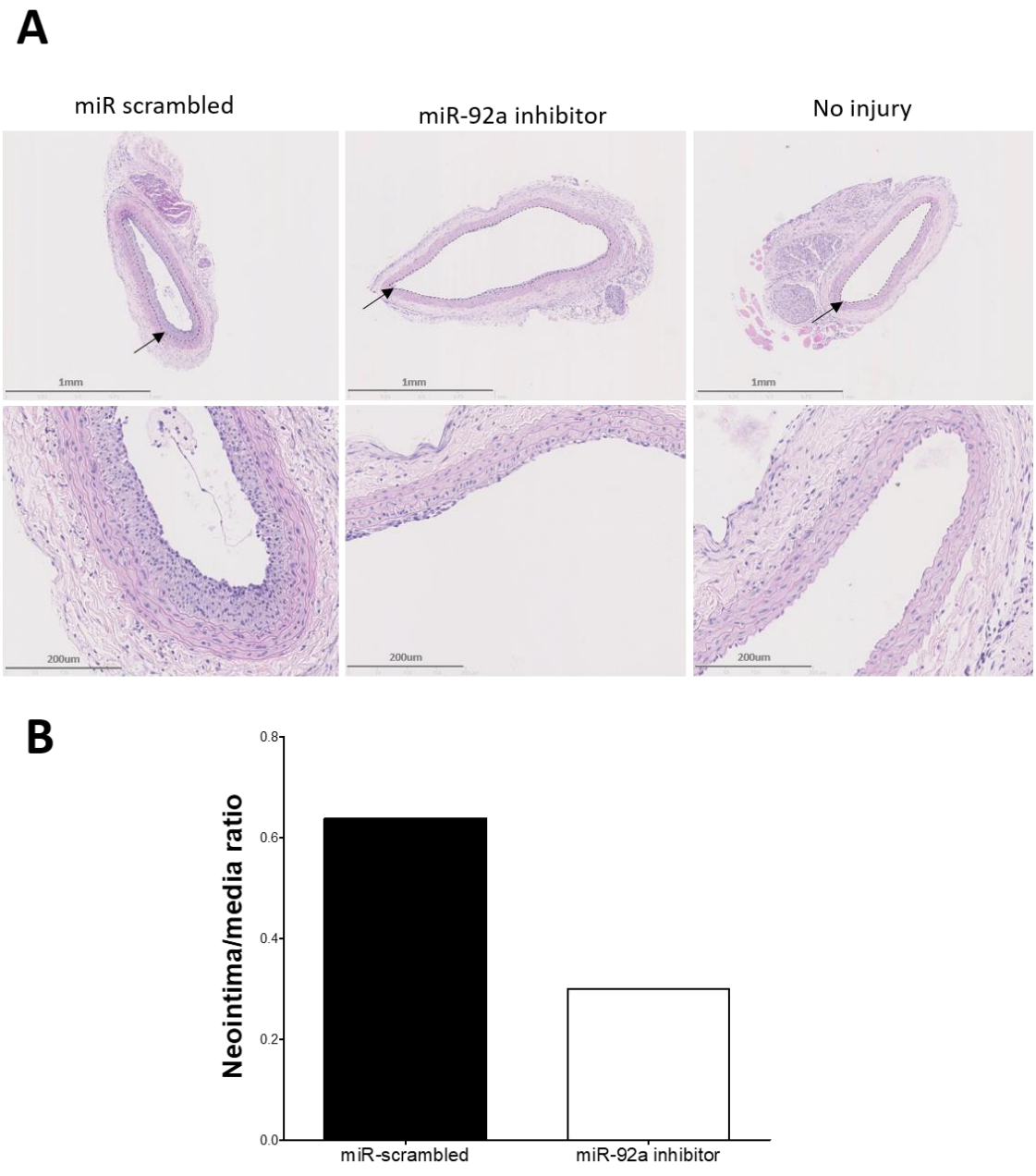


The goal became developing a NP-based transfection method which would serve as a future stent coating capable of presenting the miRNA inhibitor on the luminal surface to rolling EPCs.

# Nanoparticles for $CD34^+$-derived EPC labelling

Previously, the Portuguese group where I conducted one year of PhD had demonstrated that HUVECs could rapidly internalise protamine sulphate(PS)-coated Poly(lactic-co-glycolic acid (PLGA) nanoparticles (NPs) (Gomes et al., 2013). The optimal transfection strategy had been defined as requiring incubation with 500 μg/mL NPs for 4 hours, although in concentrations up to 1 mg/mL no substantial cytotoxicity was reported (Gomes et al., 2013). Since EPCs share many common features with ECs, I tested the same strategy with the precursor cells. To quantify labelling efficiency in EPCs, FACS was performed on cells transfected with NP-fluoresceinamine for the same period. Trypan blue was used after fixation to differentiate between the signal from membrane-associated (external) and internalised fluorochromes (internal)(McNeer et al., 2011). After quenching treatment, 99% of EPCs were fluorescein-positive, which establishes a very high transfection efficiency **(Figure IV.6)**.

After vascular injury, the vessel wall is typically a deprived milieu. One hour after balloon angioplasty, there are very few intact adventitial microvessels (Pels, Labinaz, Hoffert, & O'Brien, 1999) due to the barotrauma associated disruption, conditioning an environment poor in nutrients. Therefore, I wanted to mimic to some degree the same environment *in vitro*. However, my plans to subject EPCs in culture to deprivation conditions for longer term studies could jeopardise the feasibility of 500 μg/mL as the selected NP concentration. Therefore, I used a lower concentration (250 μg/mL) in the following experiments.

**Figure IV.6| NPs are efficiently internalised by human CD34$^{+}$-derived late -outgrowth EPCs.**
EPCs were transfected for 4 hours with 500 µg/mL NP-FITC labelled, after which cells were analysed by flow cytometry. External refers to Trypan blue quenched fluorescent signal, presumably membrane outbound NPs. **(A)** Representative FSC-SSC dot plots and histograms of non-quenched samples are presented. **(B)** Labelled cells exceeding an autofluorescence threshold were quantified and considered positive for the internalisation of NP-FITC. Results are expressed in mean values ± SEM following 3 individual experiments (each condition measured in duplicate), *** p<0.001 vs no transfection control (t-Student test). EPC – endothelial precursor cell; FITC - Fluorescein isothiocyanate; FSC – forward scatter; NP – nanoparticles; SEM – standard error mean; SSC – side scatter.

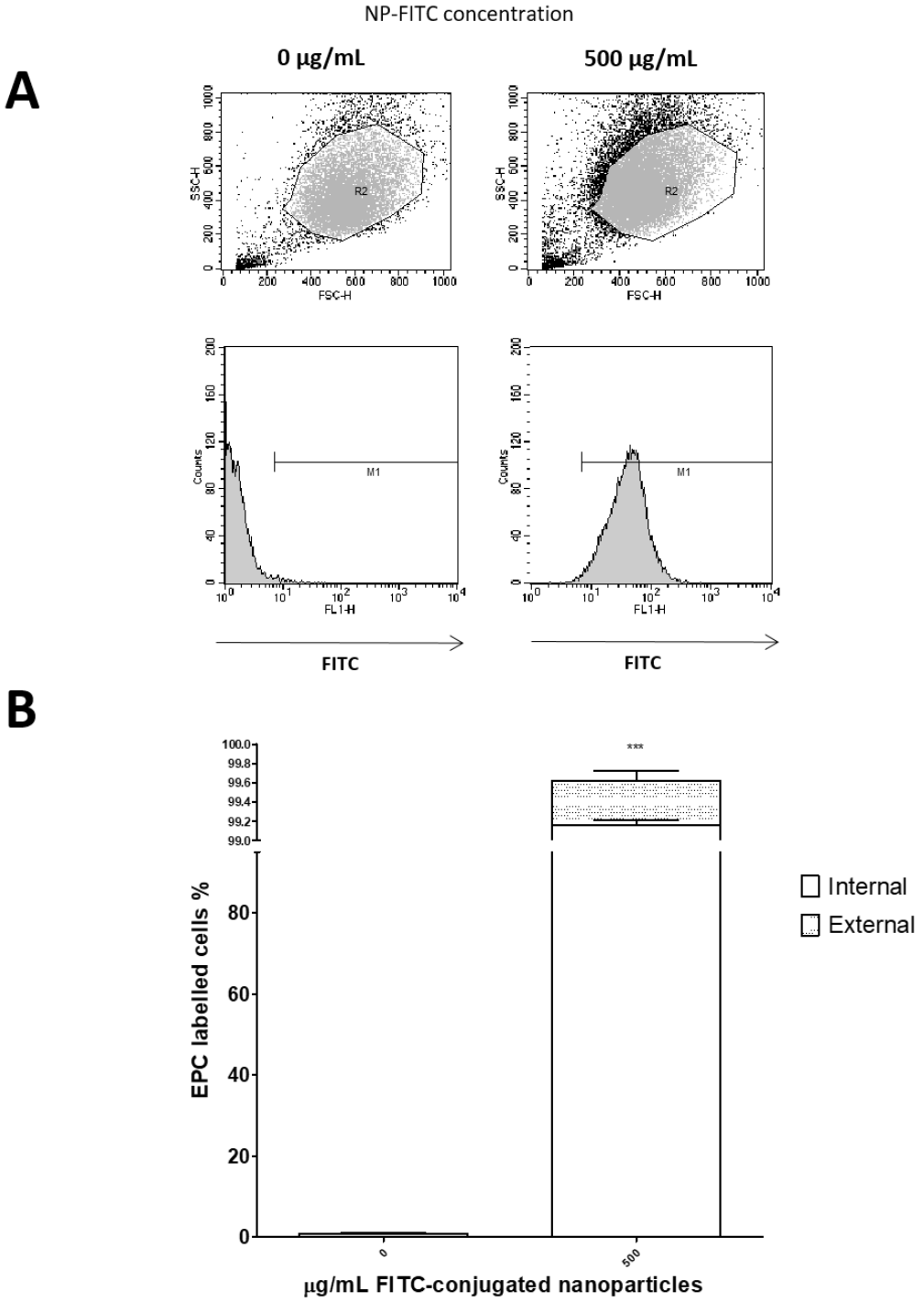

# NPs can efficiently deliver miRNAs into EPCs

Incubating NPs with miRNA produced electrostatic complexes with a mean diameter of 219 ± 14.2 nm and a zeta potential of +1.95 ± 0.99, at intracellular pH **(Table IV.1)**.

**Table IV.1 | Characterization of NPs.**
Diameter, PDI and zeta potential are properties of NPs which facilitate its internalisation. NPs were reconstituted at 500 µg/mL and complexed with miRNA at 800nM, before being diluted 1:4 for dynamic light scattering analysis in 10 mM KCl, pH 5.5. Results for the before mentioned properties are presented as means ± standard deviation, after 3 independent measurements from 3 different NP batches. NP – nanoparticle, PFCE -perfluoro-1,5-crown ether, PDI – polydispersion; PLGA – polylactic(glycol)acid, PS – protamine sulphate.

| | Diameter (nm) | PDI | Zeta potential |
|---|---|---|---|
| **NP-PFCE** | 212.9 ± 14.3 | 0.244 | -9.7 ± 0.7 |
| **NP-PFCE-PS** | 218.0 ± 9.3 | 0.381 | +7 ± 1.7 |
| **NP-PFCE-PS-miR** | 219 ± 14.2 nm | 0.267 | +1.95 ± 0.99 |

Compared to non-coated NPs, the miRNA overlayer did not significantly influence the diameter (218.0 ± 9.3 nm vs. 212.0 ± 14.3 nm, p=0.91), and so was unlikely to compromise the transfection strategy. As expected, the NP:miRNA complexes' net charge was inferior to NPs not coated with miRNAs (+1.95 ± 0.99 vs. 7± 1.7, p=0.01), as a result of the conjugation with negatively charged oligonucleotides.

PLGA NPs are known to be internalised by endocytosis (Gomes et al., 2013), therefore the fact that the NP: miRNA conjugates remained positively charged after complexation is essential for the transfection efficiency, which was next demonstrated by IF. EPCs were transfected with NPs complexed with a FITC-labelled miRNA (hsa-miR-92a-1 inhibitor) for 4h under normoxia, and 24h after that using an anti-FITC antibody we documented intracellular miRNA-associated fluorescent signal only in the condition where miRNA delivery was facilitated with NPs **(Figure IV.7)**

**Figure IV.7 | Internalisation of NP: miR complexes by human CD34$^+$-derived EPCs.**
Cellular transfection with NP:miR-92a-FITC conjugated complexes was confirmed by IF at 60x. 24h after transfection with **2)** NP at 250 µg/mL; **3)** miR-92a inhibitor-FITC 100 nM; **4)** NP-FITC 250 µg/mL; **5)** NP:miR-92a inhibitor-FITC 250 µg/mL and 100 nM respectively, cells were processed for IF. **1)** No treatment and **6)** transfection with NP:miR-92a inhibitor-FITC 250 µg/mL and 100 nM but omitting primary antibody staining were the experimental and IF negative controls, respectively. The nuclei of the cells were counter-stained with DAPI. DAPI - 4',6-diamidino-2-phenylindole, FITC - Fluorescein isothiocyanate, miRNA or miR– microRNA, NP – nanoparticle.

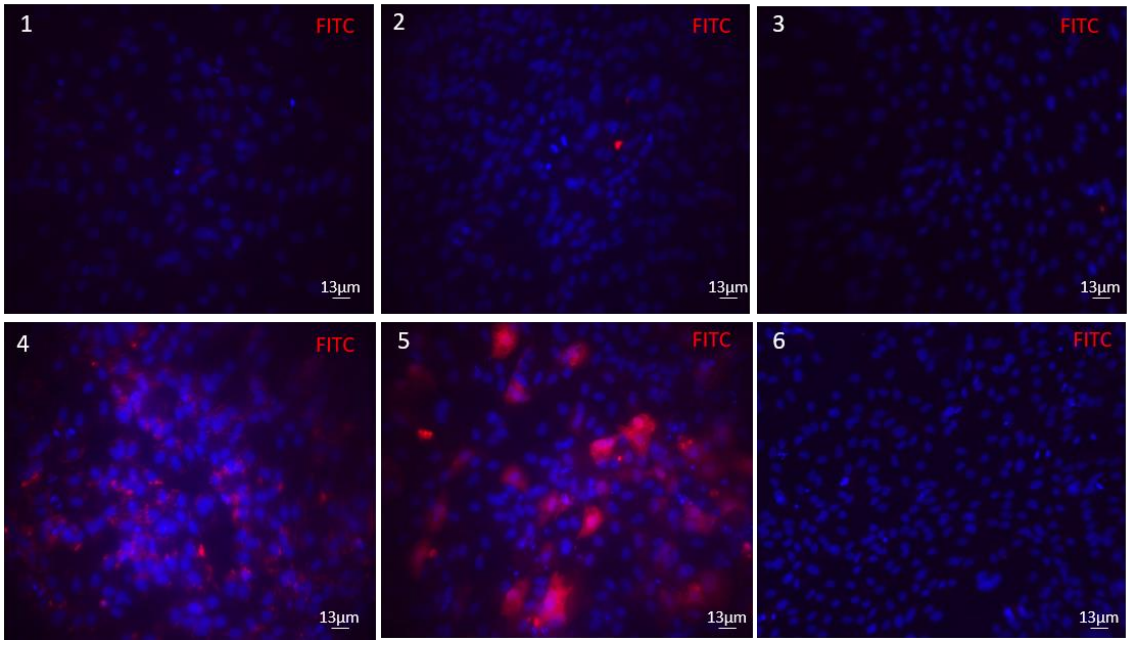


NP facilitated miRNA internalisation efficiency was quantified using FACS. When EPCs were incubated for 4h with miRNA-fluorescein labelled complexed to NPs, 81 ± 7% of the cells were labelled, and virtually no miRNA was found at the external surface **(Figure IV.7)**, demonstrating a high miRNA transfection efficiency.

**Figure IV.8 | Internalisation of NP: miR complexes by human CD34$^+$-derived EPCs.**
Transfection with NP:miR-92a-FITC complexes was confirmed by flow cytometry. Trypan blue is used to quench externally attached particles/miRNA to differentiate between the signal from membrane-associated (external) and internalised fluorochromes (internal). Treatment with miR-92a-FITC only, non-fluorescent NPs or NP:miR-92a-FITC without quenching, and omission of treatment were used as negative controls. Results are plotted as mean values ± SEM of 3 independent experiments, each condition measured in duplicate. ***P<0.001 compared with negative transfection controls (1-way ANOVA, Bonferroni's test for multiple comparisons). FITC - Fluorescein isothiocyanate, miR– microRNA, NP – nanoparticle.

**A**

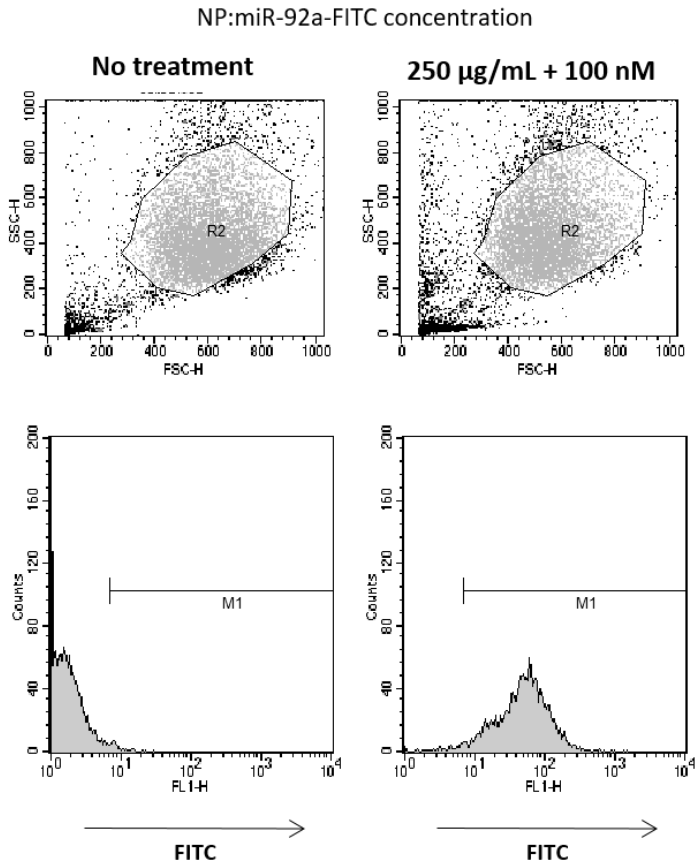
NP:miR-92a-FITC concentration
No treatment
250 µg/mL + 100 nM
SSC-H
FSC-H
R2
Counts
M1
FL1-H
FITC

**B**

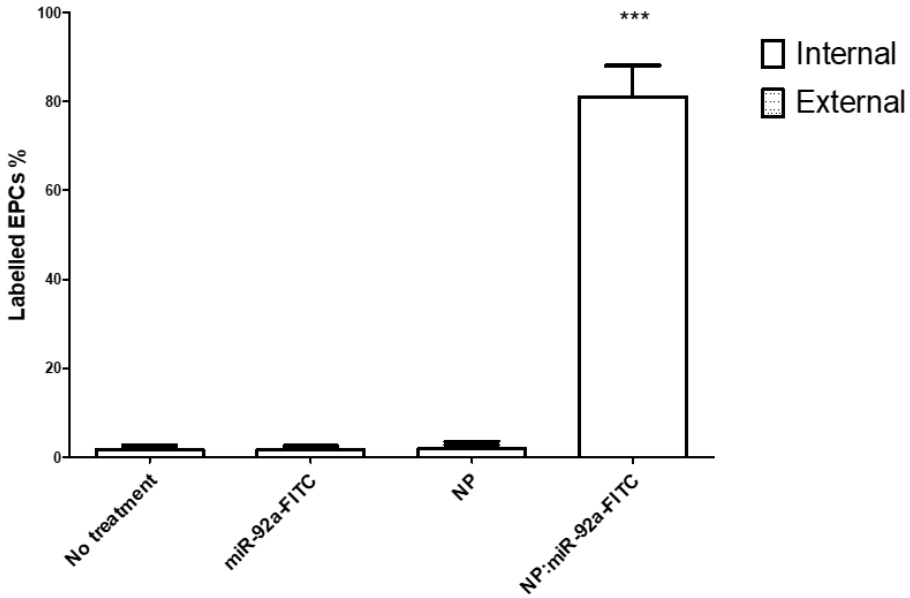
Labelled EPCs %
***
Internal
External
No treatment
miR-92a-FITC
NP
NP:miR-92a-FITC

# miR-92a is released from NPs and mediates EPC post-transcriptional modulation

Previous co-localization studies in HUVECs had shown that this specific PLGA NP formulation could present miRNAs to AGO2 and GW182 RISC proteins, which are in close interaction with the endosome membrane, thus likely promoting microRNA-RISC strand invasion (Gomes et al., 2013). Therefore, to confirm that internalised NP:miR-92a inhibitor complexes interact with the RISC machinery in EPCs, and that released miR-92a inhibitor had become readily available for processing, I conducted gene expression analysis on a miR-92a validated target, in particular, ITGA5. EPCs were incubated for 4 hours with NP:miR-92a (and its inhibitor) or NP: miR scrambled treatment, followed by 48h in serum-free culture, before evaluating mRNA levels by qRT-PCR **(Figure IV.9)**. This timing, adopted by others (Bonauer et al., 2009), presumably allows for exogenously delivered miRNAs to reach peak biological activity. The pilot results from a single experiment hint that EPCs that were transfected with NP:miR-92a had a down-regulation in the expression of ITGA5 compared to controls, whereas the inhibitor had the opposite effect on ITGA5 levels.

**Figure IV.9 | miR-92a is released from NPs complexes intracellularly.**
The gene expression profile of ITGA5 was evaluated in EPCs transfected with NP: miR complexes at 250 µg/mL and 200 nM respectively, following a 48h knockdown incubation period under starvation conditions. EPCs transfected with NP: Dy547 served as negative transfection controls. **(A)** Representative amplification plots and dissociation curves of the different transfection samples are presented for the target (ITGA5) and housekeeping (ACTB) genes. The mean minimal Ct were calculated from triplicate reactions. Blue line – experimental sample; green line – no template control sample **(B)** The target gene signal was first normalised to the housekeeping gene and then expressed about the value obtained with control transfection EPCs by using the formula $2^{-\Delta\Delta Ct}$. Results shown in the bar graphic are derived from 1 individual experiment and are therefore preliminary **(C)** Representative gel used to test primers. ACTB – actin beta; EPC – endothelial precursor cell; FITC - Fluorescein isothiocyanate; ITGA5 – integrin alpha 5 subunit; miRNA or miR– microRNA; NP – nanoparticles.

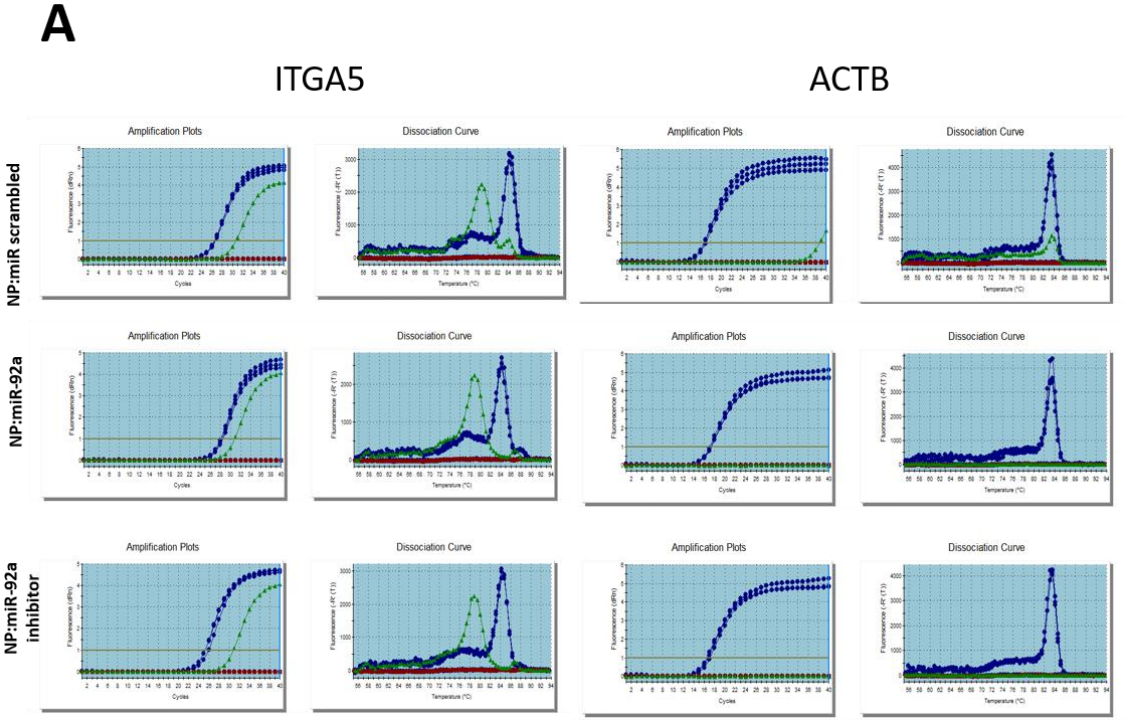
A
ITGA5
ACTB
Amplification Plots
Dissociation Curve
NP:miR scrambled
NP:miR-92a
NP:miR-92a inhibitor

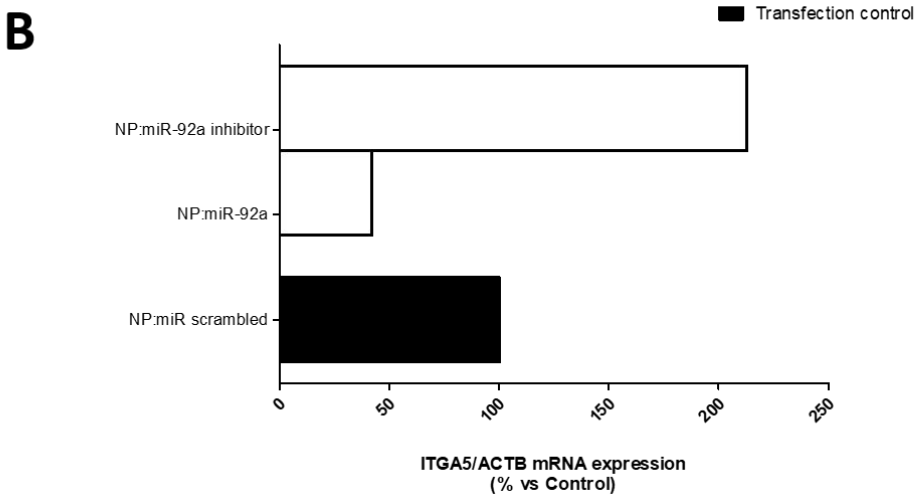
B
Transfection control
NP:miR-92a inhibitor
NP:miR-92a
NP:miR scrambled
0
50
100
150
200
250
ITGA5/ACTB mRNA expression
(% vs Control)

C

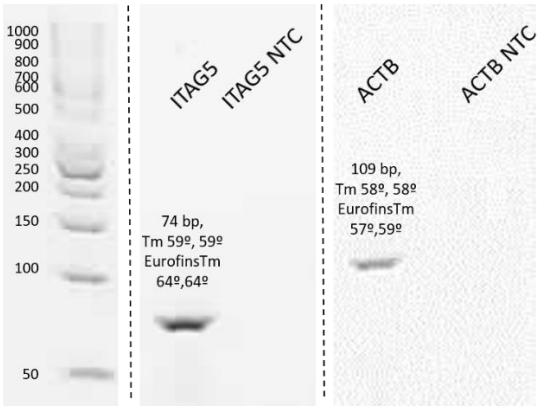


Some cellular death was still seen with 250 µg/mL compared with untreated cells. Therefore I tried an alternative transfection concentration (125 µg/mL) before leaving EPCs in serum-free medium for 48h and conducting an ATP quantitation-based survival assay **(Figure IV.10)**. The latter concentration was not detrimental (127 % ± 4 vs 100%, $p<0.01$), whereas EPCs transfected with the former concentration showed decreased survival (68 % ± 7 vs 100%, $p<0.001$).

**Figure IV.10 | A transfection NP concentration of 125 µg/mL is not detrimental for human CD34$^+$-derived EPCs.** EPC survival after transfection with NPs (125 or 250 µg/mL) for 4h, followed by 48h in starvation medium (under normoxia or hypoxia), as measured by an ATP based assay. Results represent mean values ± SEM after 5 independent experiments, ** $p< 0.01$, *** $p<0.001$ vs control transfection, t-student test). ATP – adenosine triphosphate; NP – nanoparticle; RLU - Relative light unit.

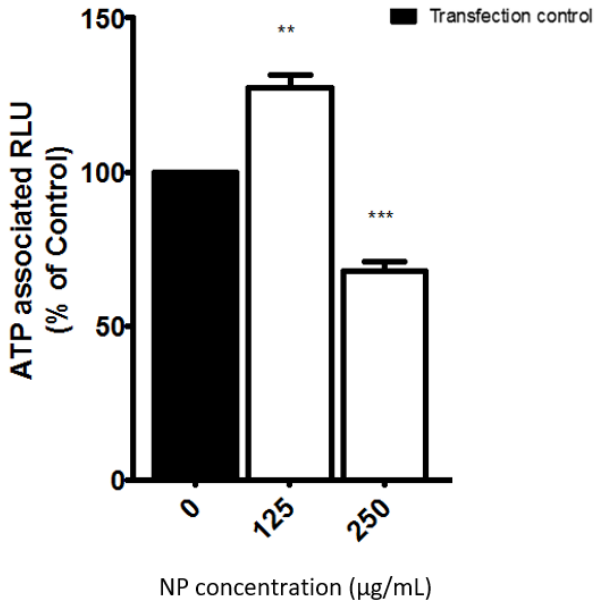


To track intracellular dynamics, EPCs were incubated 4 hours at 37ºC with serum-free medium containing NPs labelled with fluorescein amine or NPs complexed with a

fluorochrome-tagged miRNAs **(Figure IV.11)**. Dy547-labeled miRNA, a transfection control miRNA without any known human targets, was readily internalised complexed to the NPs after just 4h of incubation, whereas no intracellular miRNA signal was seen when the vector was omitted. The NPs and miRNA seemed to co-localize in complexes aggregated inside cytoplasmic vesicles distributed towards the periphery of the cell.

**Figure IV.11| Internalisation of NP: miR complexes by human CD34$^{+}$-derived EPCs.**
The intracellular distribution of NP-FITC: miR scrambled-Dy547 complexes immediately after transfection of EPCs was analysed via confocal microscopy. Representative images at 60x of the intracellular distribution of the complexes after 4h of incubation at 125 µg/mL and 100 nM respectively (top panel) versus incubation with individual components alone (bottom left - NP-FITC, bottom right - miR-Dy547), revealed that Dy547-labeled miR was readily internalized complexed to the NPs, whereas no intracellular miRNA signal was seen when the vector was omitted. Cells were stained with anti-CD31 plasmatic marker and DAPI, further evidencing that the NPs and miRNA were in close association towards the periphery of the cell. DAPI - 4',6-diamidino-2-phenylindole; CD – cluster differentiation; FITC - Fluorescein isothiocyanate; miR– microRNA; NP – nanoparticle.

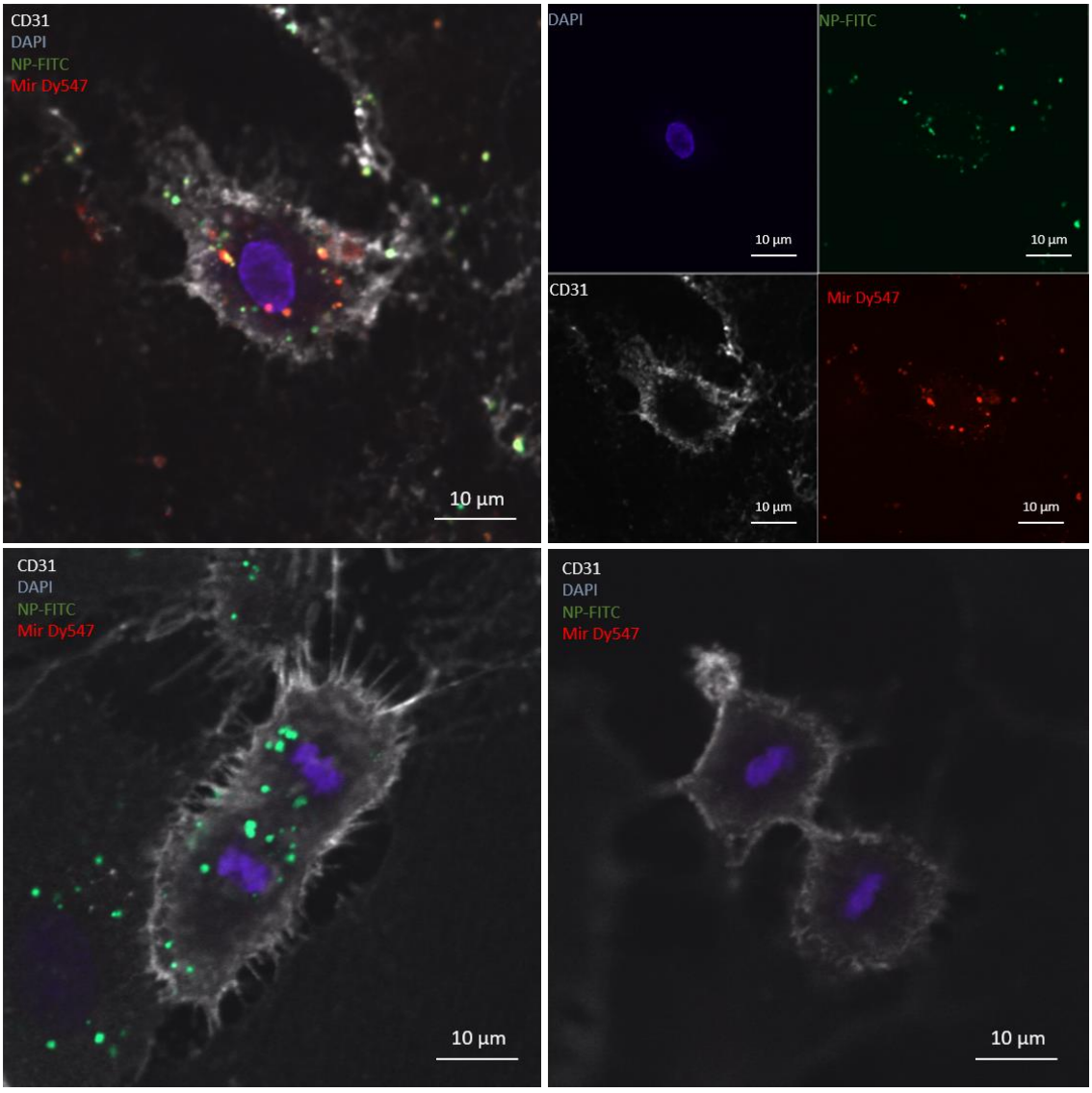

According to the confocal microscopy data, 24 h after transfection, intracellular vesicles loaded with NP:miRNAs complexes seemed to have increased in number and size, revealing a more perinuclear distribution, presumably corresponding to the early endosomal compartment, as reported previously for HUVECs (Gomes et al., 2013). Moreover, there was a lower degree of association between NPs and miRNA signal overall, thus evidencing that a good portion of the miRNA had already been released by the NPs **(Figure IV.12)**.

**Figure IV.12 | Intracellular miRNA release from NPs after 24h.**
The intracellular distribution of NP-FITC: miR scrambled-Dy547 complexes 24h after transfection of human late-outgrowth EPCs (125ug/mL and 100nM respectively) was analysed via confocal microscopy. The images at 60x revealed intracellular vesicles loaded with NP:miRNAs complexes which seemed to have increased in number and size, revealing a more perinuclear distribution, and with a lower degree of association between NPs and miRNA signal overall compared to immediately after transfection. CD – cluster of differentiation, DAPI - 4',6-diamidino-2-phenylindole; FITC - Fluorescein isothiocyanate; miR– microRNA; NP – nanoparticles.

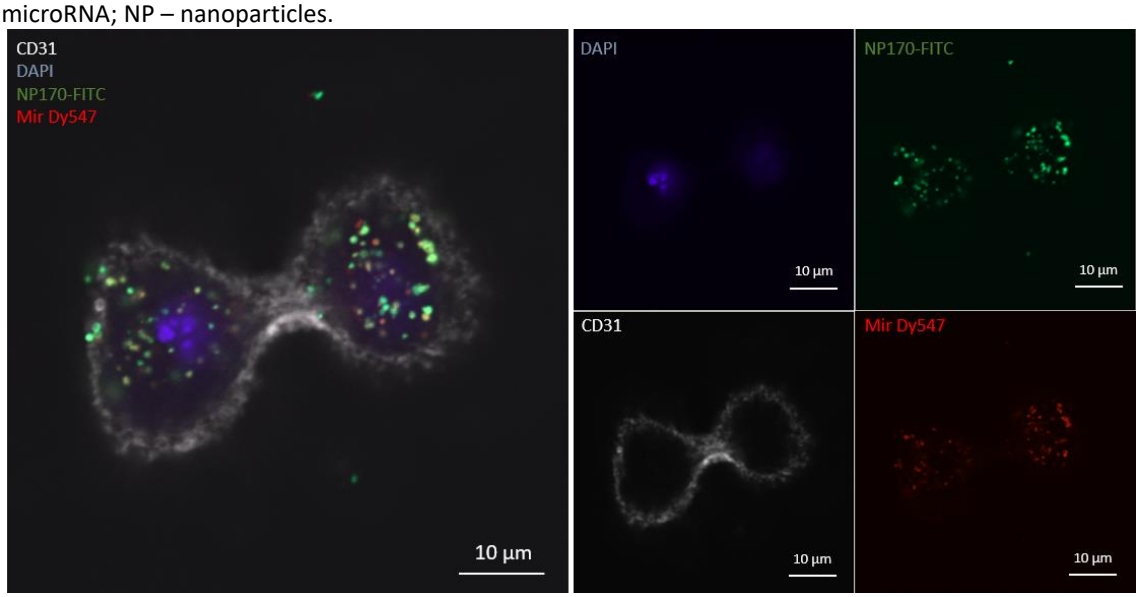


# miR-92a inhibitor containing NPs have pro-survival and –migratory effects in EPCs cultured under ischemic conditions

To demonstrate the pro-survival activity of miR-92a inhibitor, EPCs were incubated for 4 h with NP:miR-92a inhibitor and cultured under starvation for 48 h **(Figure IV.13)**. NP:miR-92a inhibitor formulation significantly increased cell survival compared to controls (128.33 ± 3.23 vs. 100%, $p < 0.001$, % of controls).

**Figure IV.13 | NP:miR-92a inhibitor exerts a pro-survival effect in human CD34$^+$-derived EPCs.**
Cells were transfected with 200nM miR-92a (5p) inhibitor complexed to NPs at 125 µg/mL. Survival in the serum-deprived medium after 48h was assessed using a Luminescent cell viability ATP-based assay. Results are plotted as means, with errors bars representing ± SEM, after 5 independent experiments (replicates of 5 were used for each experimental condition). ***P<0.001 compared with transfection control (t Student test). ATP - Adenosine triphosphate; EPC – endothelial precursor cells; miR- microRNA; NP – nanoparticle; SEM – standard error mean.

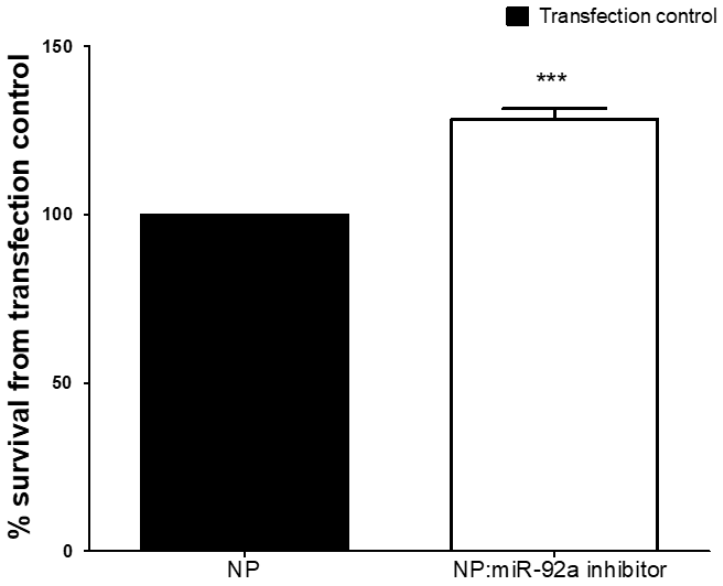


The scratch assay of cell migration was used to assess the effects of NP-miR delivery on the migration of EPCs. After a scratch had been made on a confluent cell monolayer, cells were incubated for 48h in serum free medium **(Figure IV.14)**. NP:miR-92a inhibitor transfected EPCs managed to narrow the gap area more than controls by 48h and re-establish new cell–cell contacts significantly faster than controls (3.16 ± 3 % vs. 33.5 ± 7.48 %, p<0,05, % of baseline wound area).

**Figure IV.14 | Pro-migratory effects of NP:miR-92a inhibitor in human CD34$^{+}$-derived EPCs**
Cells were transfected with NP:miR-92a (5p) inhibitor complexes at 125 µg/mL and 200 nM respectively. After overnight incubation in complete medium, the monolayer of cells was manually scratched, and cells left in serum-free medium for 48h. At the end of the follow-up, cells were photographed at 5x and the denuded area (µm$^2$) was quantified digitally. (A) Representative brightfield images of EPCs transfected with either NP (transfection control) or NP:miR-92a inhibitor after 48h. (B) Wound area after 48h quantification results after 6 independent experiments are plotted as means (conditions in duplicates), with errors bars representing ± SEM. *P<0.05 compared with NP (Student t-test). EPC- endothelial precursor cellmiR – microRNA; NP – nanoparticle; SEM – standard error of the mean.

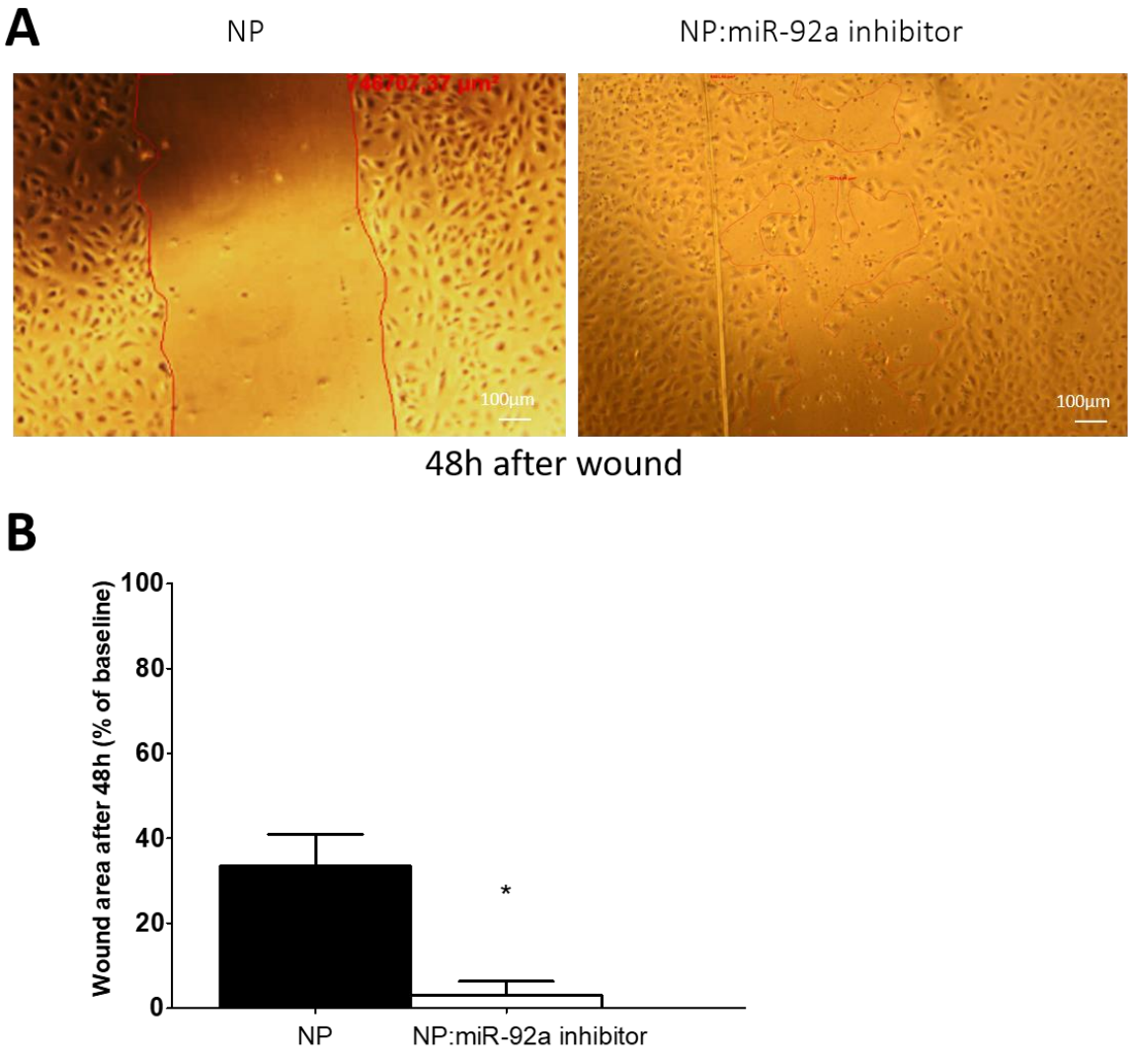

# Peri-adventitial gel delivery of NP:miR-92a inhibitor complexes results in efficient arterial wall transfection

A peri-adventitial route to deliver the NP and corresponding NP:miRNA complexes was pursued. *Ex vivo* transfection of rat carotid rings with NP-FITC (5 mg/mL) using serum free media (SFM), pluronic gel or PLGA gel, evidenced superior internalisation efficiency for medium, followed by pluronic gel, and lastly PLGA, as evaluated by a direct fluorescence assay **(Figure IV.15)**. Accordingly, we chose to pursue the *in vivo* NP delivery to the rat carotid adventitial wall using the pluronic gel, since medium would produce heavy leaking jeopardising the localised delivery method.

**Figure IV.15 | NP internalisation by the rat carotid artery via peri-adventitial gel delivery.**
Rat carotid artery segments were transfected *ex vivo* during 24h with FITC-labelled NPs resuspended at 5mg/mL either in Optimem medium, PLGA or Pluronic gel. The samples were then photographed under a fluorescent macroscope in the green channel. FITC -Fluorescein isothiocyanate; NP – nanoparticle.

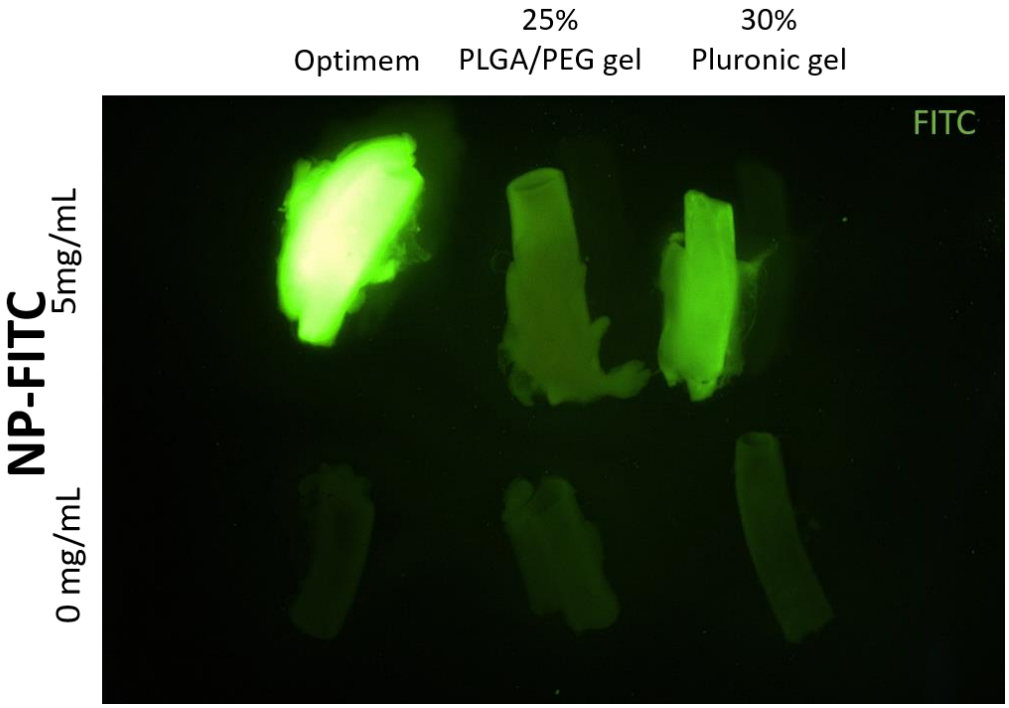


Using IF and IHC analysis, we were successful in showing NP-FITC (5mg/mL) internalisation throughout the entire vascular wall (from adventitia to intima) after just 24h following gel deposition **(Figure IV.16)**.

**Figure IV.16 | Rat carotid artery NP-FITC internalisation is efficient by pluronic gel periadventitial delivery.** Pluronic solution containing NP-FITC (5mg/mL) was applied externally to the outer surface of

the exposed LCA. The animal was allowed a 24h post-operative recovery before the LCA was harvested and processed for IF and IHC. **(A)** 20x IF pictures: 1 represents a cross-section image of an LCA treated with NP-FITC (5mg/mL in pluronic gel) via periadventitial delivery. 2-4 are representative images of controls. 2- positive control ex-vivo treated rat carotid ring segment (NP-FITC 5mg/ml in the medium for 4h); 3- negative controls non-treated rat LCA; 4- staining control ex-vivo treated rat carotid ring segment (NP-FITC 5mg/ml in the medium for 4h) where primary antibody incubation was omitted. **(B)** 10x and 40x magnification IHC pictures: 1-4 images represent the same conditions as in A). DAPI - 4',6-diamidino-2-phenylindole; FITC - Fluorescein isothiocyanate; IF – immunofluorescence; LCA – left carotid artery; miR – microRNA; NP – nanoparticles.

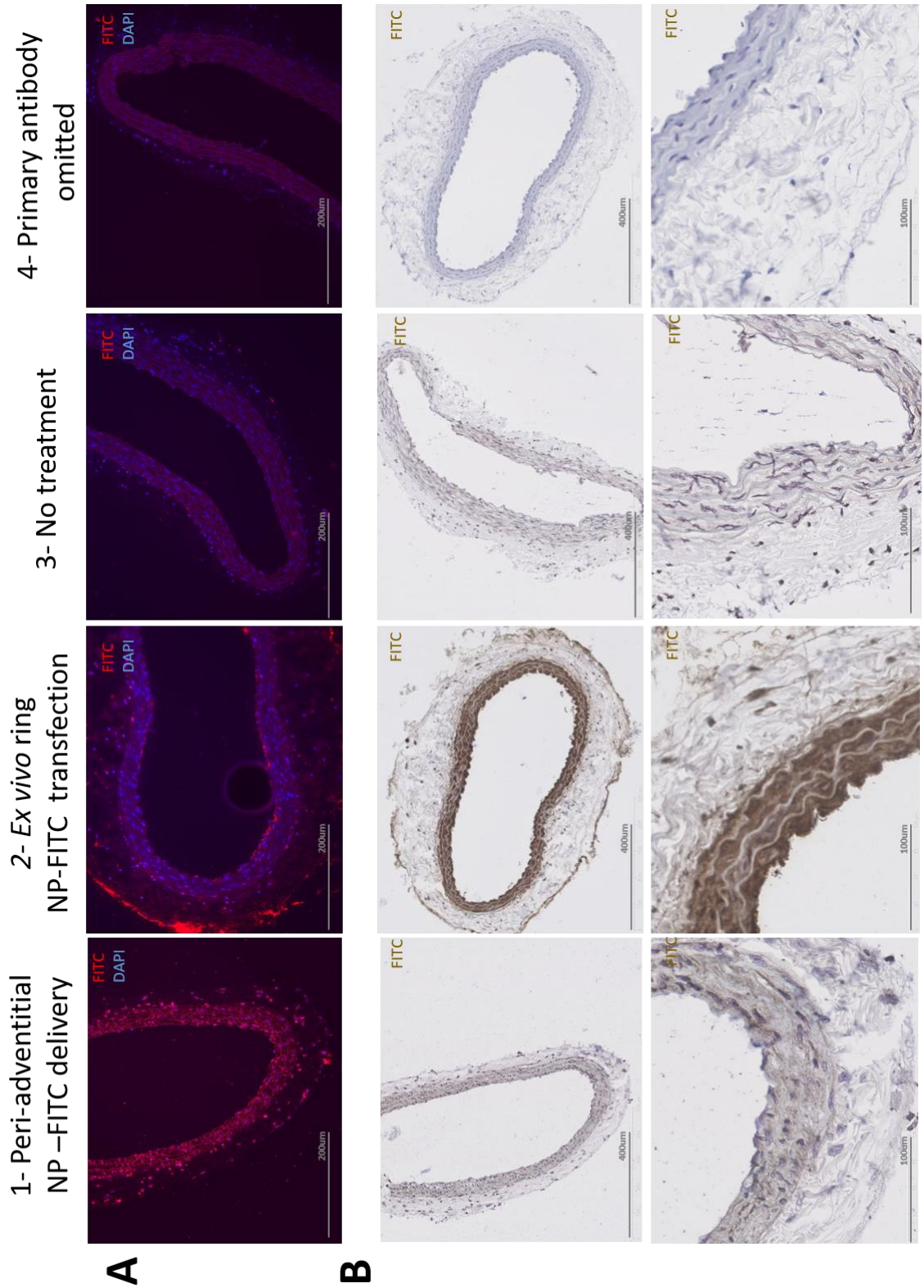

Transfecting the arterial wall with miR-92a inhibitor-FITC -labelled complexed to NPs (5mg/mL, 200nM) was also successful as indicated by IHC **(Figure IV.17)**.

**Figure IV.17 | Rat carotid artery NP:miR-92a inhibitor-FITC internalisation via peri-adventitial gel delivery.**

A periadventitial delivery of NP:miR92a inhibitor-FITC was carried out. The animal was allowed a 24h post-operative recovery before the LCA was harvested and processed for IHC. These are representative images of NP:miR-92a-FITC treated arteries via peri-adventitial pluronic gel delivery at 20x and 40x magnification. On the right the negative control is presented, where the primary antibody incubation was omitted. FITC - Fluorescein isothiocyanate; LCA – left carotid artery; miR – microRNA; NP – nanoparticles.

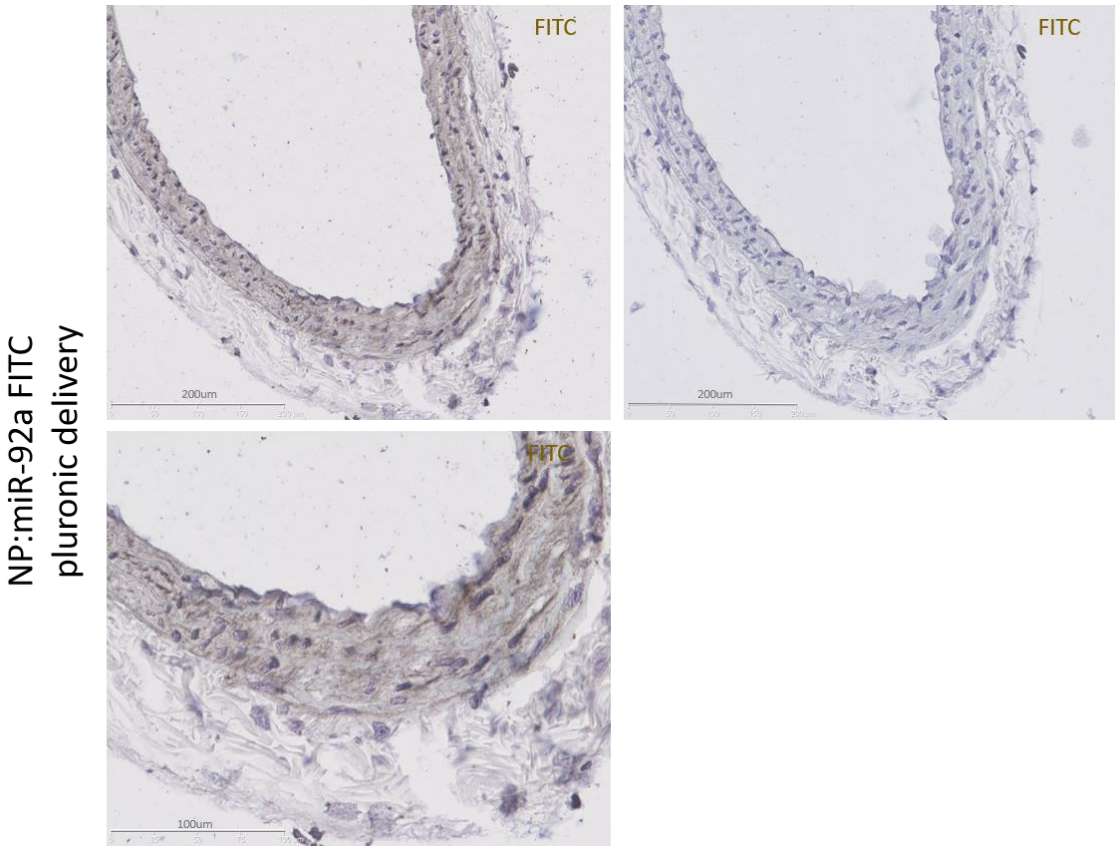


Once inside the cells, miRNA-92a inhibitor is progressively released from the NPs as hinted by miR-92a target gene regulation in a 24h post-transfection time course **(Figure IV.18)**. ITGA5, an established miR-92a target gene should be upregulated upon miR-92a inhibitor transfection (Bonauer et al., 2009). Indeed, at 24h there was an upregulation of ITGA5 levels following miR-92a inhibitor pluronic gel delivery compared to control. Also, ITGA5 levels at 24h rose higher with transfection miRNA alone than with an NP-mediated strategy, which could suggest an advantageous slow release mechanism by the NPs.

**Figure IV.18 | Pluronic gel delivery of NP:miR-92a inhibitor may be efficient at upregulating arterial ITGA5 levels after just 24h.**
Representative western blot analysis of uninjured rat carotid arteries treated with NP:miR-92a inhibitor (5mg/mL, 1µM) or miR92a inhibitor (1µM) delivered by 30% pluronic gel, against no treatment control. The animals were sacrificed 24h after surgery. This blot represents a single set of 3 paired mice. Therefore results are preliminary only. eNOS- endothelial nitric oxide synthase; ITGA5 – integrin alpha 5 subunits; miR– microRNA, NP – nanoparticles.

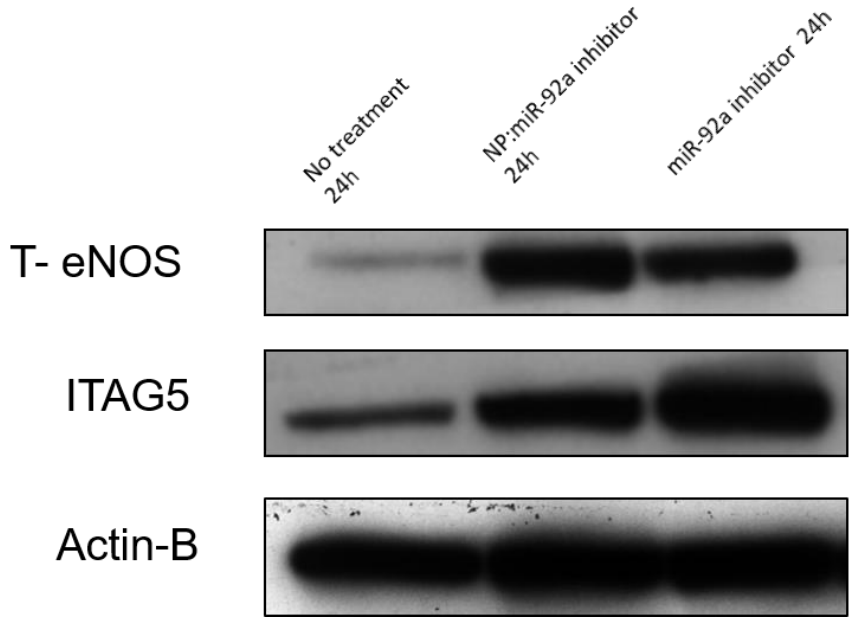


# Intra-luminal delivered NP:miR-92a inhibitor complexes are capable of arterial wall transfection

Next, the feasibility of delivering miRNA conjugated to NPs to the inner side of the arterial wall, via intraluminal infusion, was investigated. Rat carotid ring segments were used for tissue culture transfection optimisation with NP-FITC or NP:miR-92a inhibitor-FITC resuspended in medium at different concentrations **(Figure IV.19)**. The *ex vivo* titration strategy demonstrated that NPs in solution at 5 mg/mL were able to transfect the carotid segments efficiently and facilitated fluorescent miRNA delivery (1uM).

**Figure IV.19 | NP and NP:miR-92a inhibitor in suspension are internalised by the rat carotid artery.**
Rat carotid artery segments were transfected *ex vivo* during 4h in 96 well plates with increasing concentrations of **(A)** FITC-labelled NPs or **(B)** miR-92a inhibitor-FITC labelled complexed to NPs in Optimem. The samples were then photographed under a fluorescent macroscope in the green channel. FITC -Fluorescein isothiocyanate; miR – microRNA; NP – nanoparticle.

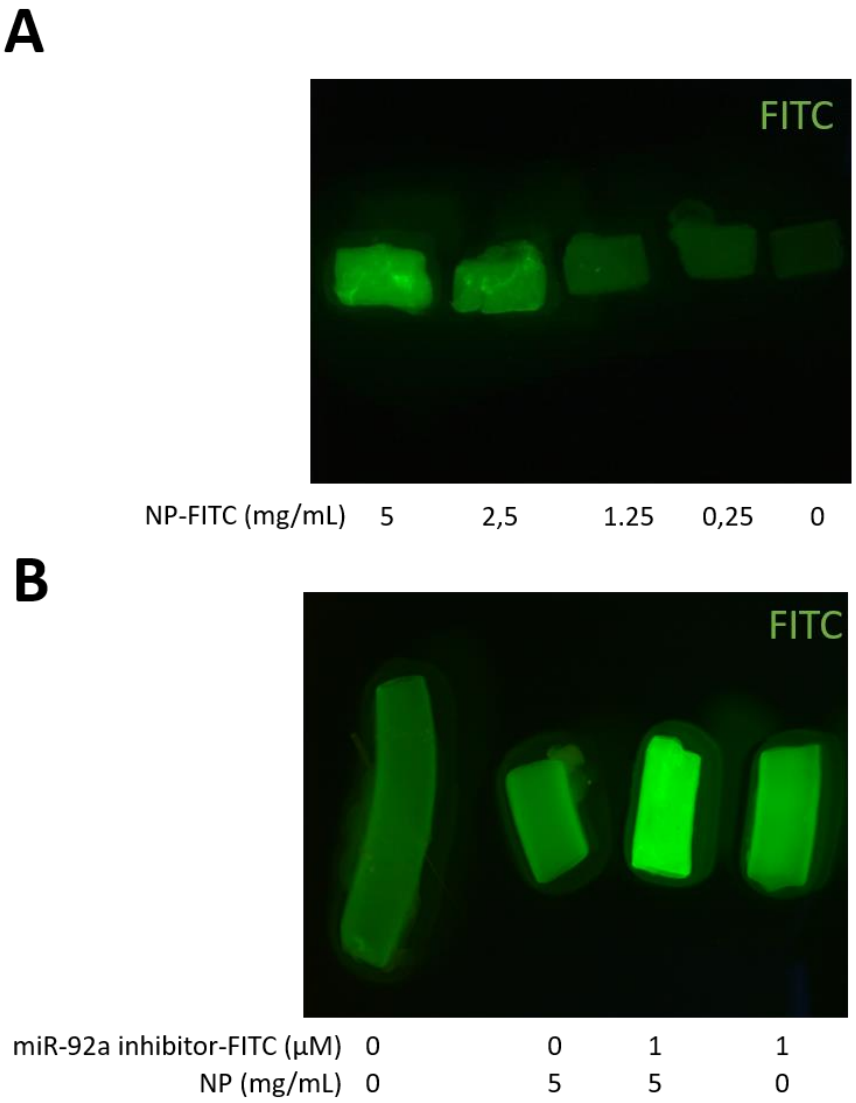


Next, intravascular delivery of the NPs to the rat carotid artery was carried out by infusing an NP-FITC labelled solution (5 mg/mL) through the arteriotomy hole at an infusion rate of 10 µl/min for a total of 20 min of occlusion time. This strategy resulted in efficient vascular wall internalisation of NPs, with a discernible pan-layer distribution pattern, as assessed 24h after infusion by IF and IHC staining **(Figure IV.20)**.

**Figure IV.20 | Rat carotid artery NP-FITC internalisation is efficient by intraluminal infusion.**
An intravascular delivery of FITC labelled NPs was carried out. The animal was allowed a 24h post-operative recovery before the LCA were harvested and processed for IF and IHC. **(A)** IF 20x pictures: 1 represents a cross-section image of an LCA treated with NP-FITC (5mg/mL in PBS) via intraluminal infusion. 2-4 are representative images of controls. 2- positive control *ex vivo* treated rat carotid ring segment (NP-FITC 5 mg/ml in the medium for 4h); 3- negative controls non-treated rat LCA; 4- staining control *ex vivo*

treated rat carotid ring segment (NP-FITC 5mg/ml in the medium for 4h) where primary antibody incubation was omitted. **(B)** IHC 10x and 40x pictures: 1-4 images represent the same conditions as in A). DAPI - 4',6-diamidino-2-phenylindole; FITC - Fluorescein isothiocyanate; IF – immunofluorescence; LCA – left carotid artery; miR – microRNA; NP – nanoparticles.

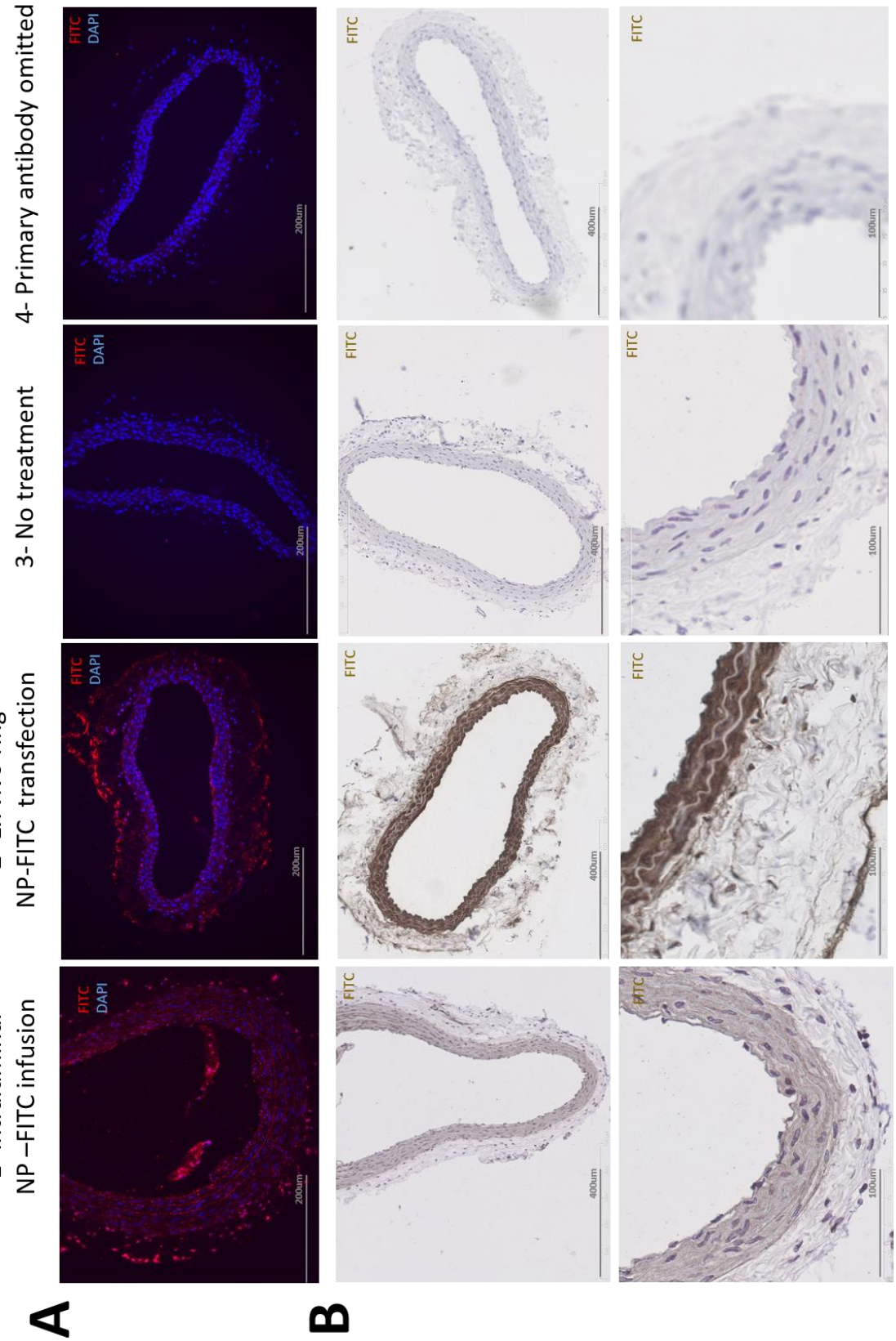

Internalisation of NPs:miR-92a inhibitor complexes (NP 5 mg/mL and miR 1 µM) was also feasible for intravascular delivery using the same interventional procedure, as demonstrated by IHC staining of treated arteries 24h post-infusion **(Figure IV.21)**. The future plans will be discussed in the global discussion chapter.

**Figure IV.21 | Rat carotid artery NP:miR-92a inhibitor internalisation via intraluminal gel delivery.**
An intraluminal delivery of NP:miR-92a inhibitor-FITC (NP 5 mg/mL and miR 1 µM) was carried out. The animal was allowed a 24h post-operative recovery before the LCA were harvested and processed for IHC. These are representative images of NP:miR-92a-FITC treated arteries via intraluminal infusion at 20x and 40x magnification. On the right the negative control is presented, where the primary antibody incubation was omitted. Given the positive FITC signal present in all layers of the artery, the intraluminal delivery strategy seemed efficient at promoting rat carotid artery NP:miR-92a-FITC internalisation. FITC - Fluorescein isothiocyanate; LCA – left carotid artery; miR – microRNA; NP – nanoparticles.

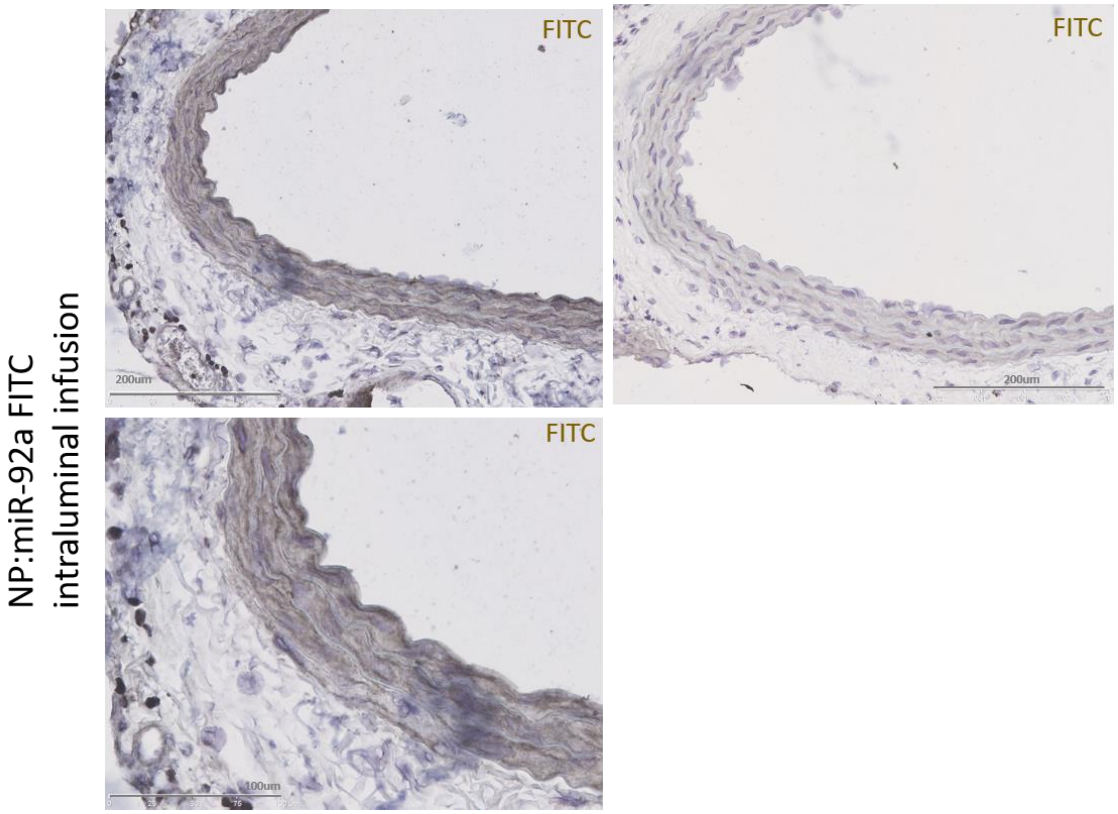

# Discussion

## Restenosis prevention by miR-92a inhibitor

Isolated aortic rings transfected with miR-92a inhibitor and cultured on Matrigel with endothelial growth medium showed significantly improved outgrowth of aortic ring cells compared with the control, as expected according to the literature (Iaconetti et al., 2012). This result pushed us to search for the effect of miR-92a inhibitor in the injured artery. One year within the PhD works, Iaconetti *et al*. published a seminal paper reporting that systemic administration of miR-92a inhibitor significantly enhanced re-endothelialisation in injured carotid arteries and reduced neointimal formation after balloon injury or stenting (Iaconetti et al., 2012). Later, Daniel *et al.* confirmed that systemic inhibition of miR-92a expression with LNA-modified antisense molecules resulted in a significant acceleration of re-endothelialisation and reduced neointima this time after wire-induced injury of the femoral artery in mice (Daniel et al., 2014). Our preliminary results regarding the reduction of neointima following the delivery of miR-92a inhibitor after experimental balloon injury seem to agree with the findings by Iaconetti *et al*. Endothelial denudation after vascular injury, and the subsequent loss of local NO synthesis could be a critical factor in the pathogenesis of restenosis. The results from Iaconetti and colleagues suggested that miR-92a inhibitor induced an increase in NO bioavailability (Gareri et al., 2016), which causes a selective increase in the EC proliferation/migration and the inhibition of VSMC proliferation (Iaconetti et al., 2012; Indolfi et al., 2002). Interestingly, our *in vitro* results seem to hint that another vascular player could contribute to the reduction of neointima, i.e., engrafting/vascular wall EPCs that show enhanced activity upon miR-92a inhibition. Cui *et al.* transplanted GFP-labeled EPCs overexpressing eNOS gene into balloon-denuded carotid arteries and found that these cells engrafted at the denuded parts of the artery, which resulted in a significantly inhibited neointimal hyperplasia (B. Cui et al., 2011). One can speculate that the NO overexpressed and released at an early stage from the regenerating endothelium and EPCs incorporating into the injured site might participate in inhibiting VSMC proliferation and migration(B. Cui et al., 2011). We too have shown a possible increase in engraftment of (miR-92a inhibitor -primed) EPCs at the injury site after

transplantation. Although, we could not show enhanced endogenous EPC engraftment following treatment of target tissue with miR-92a inhibitor (the planned experiments would surpass the remaining PhD duration), we did observe a trend towards increase in T-eNOS expression in miR-92a inhibitor treated arteries, therefore, it is conceivable that the enhanced EPC activity results obtained *in vitro* can translate into an enhanced re-endothelialisation response *in vivo* following *in-situ* transfection. We postulate that the ability of the engrafted EPCs to rapidly restore endothelial integrity at the injury site may restore endothelium-dependent NO bioavailability and suppress more efficiently the activation of VSMC proliferation and migration from the underlying media, thus resulting in attenuation of neointimal proliferation. Besides ITGA5-eNOS pathway, miR-92a has also been found to target KLF2 and KLF4 (Y. Fang & Davies, 2012) (genes that were not unfortunately included in my WB experiments since for the time of the PhD I could not find antibodies that would have good resolution in CD34+-derived EPCs). These transcription factors can also enhance eNOS activity which inhibits VSMC proliferation (Boon & Horrevoets, 2009; Y. Fang & Davies, 2012; Hamik et al., 2007; Iaconetti et al., 2012; Parmar et al., 2006). Moreover, KLF2 and KLF4 typically exert an anti-inflammatory and atheroprotective effect in ECs after injury (Y. Fang & Davies, 2012). This was elegantly shown by Hinkel and colleagues who tested leukocyte adhesion on an EC monolayer underflow after TNF-alpha activation and verified that pretreatment of either the ECs or the THP-1 cells with miR-92a inhibitor reduced leucocyte adhesion (Hinkel et al., 2013). miR-92a inhibition, by acting to de-repress KLF2 and 4, may result in the downregulation of leucocyte adhesion molecules on ECs, therefore limiting inflammatory cell infiltration.

## Systemic vs. localised miR-92a inhibitor delivery to the target tissue

The delivery approaches *per se* may vary according to the end application. In diffuse conditions, such as atherosclerosis, or for tissue targets which are not easily accessible by direct injection, systemic antagomiR delivery may be optimal (Salmena, Poliseno, Tay, Kats, & Pandolfi, 2011). Yet, one should try to minimise off-target effects by using localised deliveries, as information about tissue distribution and pharmacokinetics of

miRNAs are presently scarce and their promiscuous nature makes the side effects of long-term inhibition difficult to predict. Even though miR-92a knockout mice are viable and fertile, there are reports of increased embryonic lethality as well as growth and skeletal defects (Penzkofer et al., 2014). Moreover, the systemic administration also requires a large quantity of biomolecules.

For local regenerative applications, incorporating the miR-92a inhibitor into biomaterial scaffolds or other depots for *in situ* sustained delivery may, therefore, be preferred. An added benefit is that anti-miR approaches may be integrated with conventional regenerative biomaterial scaffolds that can simultaneously create tissue templates and provide platforms for sustained/controlled release, enabling greater spatiotemporal control over miRNA activity. One possibility to achieve the latter is to use material surface immobilizing agents, such as a stent coating that simultaneously serves as a template for the healing template and allows for local and sustained anti-miR release.

## Cell-cell miR-92a inhibitor shuttle

miRNAs have been found outside the cells in a surprisingly stable form (Polimeni et al., 2013), and it has been recently demonstrated that they can exert their regulatory function as extracellular messengers on protein expression also in recipient cells after transfer (Gareri et al., 2016). Transfer of miRNAs from cell to cell occurs mostly by means of membrane vesicles, which can be of different type and size. Exosomes (30–100 nm), shedding microvesicles (≤1000 nm) or even apoptotic bodies (50–5000 nm) are the most common. In addition to being packed into membrane vesicles, extracellular miRNAs can be loaded into high-density lipoprotein (HDL), or bound by AGO2 protein outside of vesicles (J. Zhang et al., 2015). miRNA secretion from releasing cell and subsequent uptake by a recipient cell provides a mechanism for cell-to-cell communication and exchange of material between cells (J. Zhang et al., 2015). There are 3 mechanisms of interaction between exosomes and their recipient cells described. First, the transmembrane proteins of exosomes directly interact with the signalling receptors of target cells (Munich, Sobo-Vujanovic, Buchser, Beer-Stolz, & Vujanovic, 2012). Second, the exosomes fuse with the plasma membrane of recipient cells and deliver their content into the cytoplasm (Mulcahy, Pink, & Carter, 2014). Third, the exosomes are

internalised into the recipient cells and have two fates. In one case, some engulfed exosomes may merge into endosomes and undergo transcytosis, which will move exosomes across the recipient cells and release them into neighbouring cells. In the other case, endosomes fused from engulfed exosomes will mature into lysosomes and undergo degradation (Mulcahy et al., 2014). Examples of miRNA exchange among cells involved in neointima formation are emerging in the literature. Zhou *et al.* recently showed that miR-126 is secreted by ECs in Ago2 protein complexes on atheroprone stimuli (Zhou et al., 2013). This miRNA is then internalised by VSMCs, where it inhibits the expression of proteins that normally keep the cells in a contractile and quiescent state. Additional reports uncovered miR-143/145 transfer between ECs and VSMCs through different trafficking networks (Climent et al., 2015). It was recently reported that ECs could release and transfer miR-503 to pericytes via microparticle trafficking (Caporali et al., 2015). These data are in keeping with the hypothesis that miR-92a inhibitor and NP:miR-92a inhibitor actions could be propagated across the different cell players involved in restenosis, to exert a combined anti-proliferative effect. Iaconetti and colleagues had demonstrated that miR- 92a was not expressed in VSMCs at comparable levels to other VSMC miRNAs in carotid media and adventitia. In fact, they found that the expression levels of miR-92a were significantly higher in RAO-ECs than in RAOSMCs (Iaconetti et al., 2012). MVBs, where miR-92a inhibitor and NP:miR-92a inhibitor presumably accumulate, are generated at endosomes by the inward budding of their delimiting membrane followed by the release of 100 nm vesicles into the endosomal lumen. These endosomal vesicles have a cytosolic-side inward orientation. Numerous MVB serve as a sorting station for endocytosed membrane cargo that need to be transferred to and degraded in lysosomes. As explained, other MVBs may instead fuse with the plasma membrane, resulting in secretion of their intraluminal vesicles as exosomes.

## The use of nanotechnology for interventional miR-92a inhibitor vascular delivery

The therapeutic targeting of various cardiovascular conditions using miRNA has been emerging as a novel approach in biomedicine, but the difficulty of introducing epigenetic

material into cells is a serious bottleneck in the development of this method. Limited cell penetration, unfavourable pharmacokinetics, toxicity, stability, as well as insertional mutagenesis represent some of the potential obstacles to the current *in vivo* miRNA delivery vehicles, including chemical modification, liposomes, adeno-associated virus or lentivirus (M. A. Shi & Shi, 2010). As an example, commercial liposomal transfection agents are not approved by the regulatory agencies for human use, and the viral carrier systems also have drawbacks, such as the risk of immunogenicity, random integration of oligonucleotide sequence into host chromosome, specific tissue tropism, their recombination with wild-type viruses, limited payload capacity, related toxicity, and large scale production issues (Pathak, Patnaik, & Gupta, 2009).

The enhancement of EPC functions combined with advances in tissue-engineered carrier matrices that permit embedding of EPCs and provide optimal conditions for EPC survival and endothelial outgrowth can contribute to therapeutic re-endothelialisation in wound healing. We have envisioned the use of biomaterials to (1) enhance cellular adhesion, survival, and function upon transplantation and (2) appropriately provide miRNAs with spatiotemporal control that enable enhanced recruitment/thriving of circulating progenitors. The introduction of genetic materials using nanotechnology could provide a practical alternative to the other delivery systems. In this study, I have described the development and application of biocompatible and biodegradable copolymer NPs, composed of PLGA, with approximately 200nm of diameter, capable of carrying miR-92a inhibitor on their surface for delivery into EPCs or into the arterial luminal and adventitial surface. NP-facilitated delivery of miRNA in the angioplasty-injured vascular wall could be a promising option, with several undisputed advantages over traditional transfection agents (Cyrus, Wickline, & Lanza, 2012; Gvili, Benny, Danino, & Machluf, 2007; Jukema, Ahmed, Verschuren, & Quax, 2012): (a) High internalization efficiency - small vector size in the nanoscale range bestows quicker and increased cellular uptake; (b) Biocompatibility - depending on the synthetic material, NPs can be designed to have low toxicity and immunogenicity; (c) Biodegradability, achieved by some polymer-based formulations; (d) Sustained gene delivery, which is accomplished by entrapping the biomolecules in their core, through RNAse protection mechanisms, or endosomal release modulation; (e) Targeted delivery, since NPs can be designed to target specific

cells, epitopes or intracellular localizations preferentially and hence tailored to the desired effects; (f) possibility of vector immobilization to the stent, which allows increased local concentration of the therapeutic agent at the targeted vascular segment without distal spread to non-target tissue, thereby avoiding systemic toxicity and increasing the chance of effecient gene transfection to adjacent cells. Stent-tethered vectors can better persist in tissues as they are physically protected from the shearing effect of blood flow.

Others have also sought innovative NP-mediated drug delivery for restenosis prevention. Cohen-Sacks and colleagues developed PLGA nanospheres encapsulating platelet-derived growth factor beta receptor antisense, which were successfully used in a balloon-injured rat carotid artery model (Cohen-Sacks et al., 2002). Controlled release of oligonucleotides following polymer biodegradation was achieved over a period of 1 month, resulting in inhibition of neointima formation. Nevertheless, since PLGA formulations can take long to degrade and release their encapsulated content, our strategy to coat the NP with the miRNA on the surface, and not inside the core, offers the rationale of a more rapid biological effect following post-angioplasty injury, when EPCs are engrafting, and re-endothelialisation is triggered.

## NP engineering for EPC transfection

The promise of NP systems that enable spatiotemporal control of miRNAs cues has fuelled further investigation into the kinetic delivery profile required for optimal EPC transfection *in vitro*, influencing future recruitment/re-endothelialisation at the site of vascular injury. The transfection efficiency of NPs results not only from how well these particles overcome the membrane barrier, but also the barriers outside and within the cell once they are internalised. My results indicate an EPC transfection efficiency of NP:miRNA complexes of about 80% after short-term incubation, a result which is largely related to the physicochemical optimisation performed in the NP synthesis process. Based on diameter, particles can be categorised as small (≤100 nm), medium (100–200 nm), large (201–1000 nm) or giant (≥1000 nm)(Donkuru et al., 2010). The controlled size nanoformulation used was designed to yield medium-sized NPs, designed to confer

on them a faster cell internalisation profile than large-sized particles (Pathak et al., 2009). These NP are internalised either *ex vivo* in just 4h and under 24h *in vivo*, making them useful for clinical translation. NPs were coated with specific miRNAs using a PS linker, a polycationic peptide that has been shown to condense plasmid DNA efficiently (D. Luo & Saltzman, 2000). The electrostatic interactions between the NPs and miR-92a inhibitor result in the self-folding of the oligonucleotide against the linker surface, theoretically preventing extracellular RNases from degrading the miRNA before internalisation. Optimisation of the surface charge of the NP also plays an equally important role in internalisation. A cationic substrate, PS, was coated on the NP's surface to electrostatically bind the negatively charged oligonucleotides, rendering an overall zeta potential around +2. The physicochemical properties of the resulting complex were determined by the optimisation of relative cation/anion amounts, preparation parameters (mixing speed, time, the temperature of mixing, the concentration of reactants) and material properties, such as hydrophobicity, charge density and molecular weight. The complexation masks the negative charge of the RNA molecule, thus enabling the miRNA complexes uptake by the cells. Additionally, the coating properties also dictate the electrostatic miRNA dissociation kinetics occurring at physiological pH, which will influence the concentration and duration of miR-92a inhibitor release, thereby potentially enhancing the therapeutic time window of these short-lived biomolecules. According to Gomes *et al.*, about 50% of the miRNA is still bound to the PLGA NPs inside the endosome compartment 24 h after EC transfection (Gomes et al., 2013), which correlates with my qualitative confocal microscopy results in EPCs.

## NP:miR-92a inhibitor and starvation

Several reasons underlay the fact that medium deprived of serum and VEGF was used at the different stages of the *ex vivo* assays. During the transfection period (4 h), by removing anionic proteins from the medium, we reduced the likelihood of positively charged NPs:miR-92a inhibitor complexes being sequestered, thus maximising cellular internalisation (although this might not happen *in vivo*). VEGF downregulates endogenous mir-92a expression (Iaconetti et al., 2012), which would make

interpretation of the effects of exogenous miR-92a inhibitor more complicated. The incubation period (48h) to allow time for miR-92a inhibitor processing after transfection, was performed under starvation also so to mimic the post-injury milieu better.

## NP:miRNA intracellular compartmentalization and biological activity

Studies on miRNA delivery using nanoformulations have explored NPs that accumulate in the membrane free intra-cytosolic compartment (S. J. Shi et al., 2012), as it was believed that mRNA regulation occurred largely there. However, recent data reveals that many RNA processes may be spatially restricted to the endolysosomal compartment to promote specificity and kinetic efficiency, namely miRNA maturation and mRNA regulation (D. Gibbings & Voinnet, 2010). Curiously, another NP engineering property that influenced NP:miR-92a inhibitor intracellular delivery was the composition of the biomaterial used in the NP formulation. PLGA NPs are internalised partly through fluid phase pinocytosis or clathrin-mediated endocytosis and accumulate in the endosomal compartment (Danhier et al., 2012). The intracellular pathways of internalised PLGA NPs have been characterised previously, and appear to be conserved across different epithelia (Cartiera, Johnson, Rajendran, Caplan, & Saltzman, 2009). Cartiera and colleagues demonstrated by electron microscopy that PLGA NPs colocalize with early endosomes shortly after exposure (approximately 2 hours), later to be found, over a period of 4-24 h, in other compartments within the cytoplasm, notably Golgi and endoplasmic reticulum. Interestingly, the *in-house* PS-coated PLGA nanoformulation also was shown to be incorporated into endocytic vesicles that fuse with early endosome within the first 24h following transfection (Gomes et al., 2013). Gomes and colleagues were able to coat these NPs with miRNAs, which are rapidly internalized and target the endolysosomal compartment, interacting with higher frequency with AGO2 and GW182 (proteins which are involved in the biological action of miRNAs), than liposome complexes formed by commercial reagents and miRNA, which in turn accumulate in the cell cytoplasm (Gomes et al., 2013). Interpreting the confocal microscopy internalisation data collected so far in the light of these considerations, one could speculate that PLGA copolymers also target the endosome compartment in $CD34^{+}$-derived EPCs, although the represented images are in mitosis which hampers the

analysis of the cytoplasmic distribution of the NPs. This may result in enhanced miRNA biological effect since RISC assembly and turnover also occurs at endosomes (D. Gibbings & Voinnet, 2010). The close relationship between RISC machinery and the endomembrane system seems to promote more frequent encounters between AGO2, one of the RISC incorporating proteins, and the exogenous oligonucleotides released from NPs localised in the endosome. This was demonstrated previously by Gomes et al., by quantifying NP:miRNA/AGO2 cluster association in NP:miRNA transfected cells, and comparing it to the number of AGO2/miRNA foci following liposomic delivery (Gomes et al., 2013). The latter seemed to be reduced, probably, due to the diffusion and dilution of the oligonucleotides in the cytoplasm, resulting in fewer encounters. The controlled release of the proangiogenic miR-132 from the NPs exerted described in their research had significant pro-survival and pro-angiogenic effects compared to liposomal delivery in HUVECs, raising the possibility that delivery within the endolysosomal compartment offers an excellent opportunity to enhance the biological effect of miRNAs.

More than just promoting the localised concentration of miRNA closer to the RISC machinery, NPs may in fact help in bridging the contact between both. Since AGO2 proteins are located on the cytosolic face of the endolysosomal membrane (D. Gibbings & Voinnet, 2010), the miRNA released from the NPs still has to cross the membrane. PLGA NPs are able to mediate endosome escape in a sustained manner, sometimes for days or weeks (Moynihan, Jones, Farrar, & Howard, 2001). This process is thought to be facilitated by the cationic properties of the NPs, through what is titled the “proton sponge effect”(J. G. L. Huang, T.; Gu, F. X, 2011). This effect is a temporary and localised destabilisation of the membrane resulting in the escape of NPs and/or miRNA translocation into the cytosol via transient holes. Alternatively, the miRNA release from the endolysosomal compartment may be mediated by AGO-chaperone heat shock proteins, such as HSP90. This HSPs are reported to interact with acidic phospholipid membranes to create functionally stable ATP-dependent cationic pores which could mediate the miRNA translocation from the endolysosomal compartment (Gomes et al., 2013) to the cytosolic surface of its membrane, where AGO2 and the RISC machinery is located. Immunoprecipitation studies suggest that the NPs are able to serve as a scaffold or to bridge the assembly of more Ago2-HSP90 complexes resulting in increased miRNA

translocation, especially under hypoxia, a condition that upregulates HSP90 (J. X. Chen & Meyrick, 2004).

The slow electrostatic release from the NP surface and the sustained endosome escape of the miRNA molecules, probably result in the depot release profile evidenced by the milder upregulation of ITGA5 following perivascular delivery of the inhibitor of miR-92a complexed to NPs, when compared to delivery without NP facilitation, an observation that obviously warrants a more expanded time course analysis.

## NP:miR-92a inhibitor localised delivery routes

Pluronic gel periadventitial administration has been attempted before for miRNA transfection with success (Choe et al., 2013), but to the best of our knowledge it was the first time it was used to mediate the transfection of NP:miR complexes. Pluronic F-127 is a nonionic, surfactant polyol, which consists of hydrophilic ethylene oxide (EO) and hydrophobic propylene oxide (PO) blocks that are polymerised in a basic A-B-A structure (EOx-POy-EOx) and have amphiphilic properties. The pluronic gel has been reported to enhance cell interactions, DNA transport, and transgene expression, since pluronics possess the unique ability to incorporate themselves into cell membranes in the presence of the hydrophobic poly(propylene oxide) chain (W. Fan et al., 2012). But, even when locally delivered, non-targeted drugs often do not accumulate in quantities high enough to achieve the desired effects at the cellular compartment where they could be more efficient. Accordingly, combining the transfection properties of polycationic NPs embedded within a surface-active gel seemed a logical way of enhancing internalisation and compartmentalization efficiency. In the present study, pluronic gel NP delivery demonstrated similar *ex vivo* transfection efficiency compared to incubation with NP solution, as assessed by macroscopic fluorescence intensity analysis, encouraging me to advance to *in vivo* delivery. There, the NP-facilitated delivery of miRNA within the surfactant gel to the adventitia proved to be efficient, with NP and miRNA penetration going deep into the intima after just 24h. Several trafficking combinations could account for the highly efficient miRNA tissue dissemination I have observed in such a short period. Either the peri-adventitial NP:miR-92a inhibitor or recently unbound miRNA use

a paracellular pluronic gel-facilitated route towards the intima, or they are actually internalised by adventitial and medial cells. MiR-92a inhibitor further makes their transcellular way to the innermost layer by microvesicle-mediated cell-cell communication after being released from the NPs, or NP:miR-92a inhibitor complexes travel through a typical “endocytosis–exocytosis” route. Concerning intercellular NP trafficking, there is microscopy evidence that PLGA NPs are actually prone to escape/avoid endolysosomal degradation and subsequently interact with the exocytic organelles of the cell over time: the ER, the Golgi apparatus, and secretory vesicles (Cartiera et al., 2009). In the future, a localised stent delivery could make use of an eluting matrix combining both PLGA NPs and pluronic polymer, as both biomaterials have been used in this type of platform (S. I. Jang et al., 2012; Pan, Tang, Weng, Wang, & Huang, 2007). The delivery of a miRNA with angiogenic activity conjugated to a PLGA NP delivery system which has been used in stents with good drug eluting kinetics (Luderer et al., 2011), provided the rationale to attempt NP:miR-92a inhibitor intravascular provision in the rat carotid balloon angioplasty model. No miRNA epigenetic stent has ever been described, but Blindt in 2006 deployed a stent impregnated with an integrin-binding cyclic Arg-Gly-Asp (cRGD) peptide in *in vivo* porcine models for its potential to recruit and bind EPCs to limit coronary neointimal formation (Blindt et al., 2006). EPCs express integrins with integrin-binding cRGD peptide-binding motifs on their surface. It was hypothesised that the homing and differentiation of EPCs depend largely on their adhesion to integrins and the resulting signalling cascade that occurs on cell binding. At 12 weeks, both mean neointimal area and mean percent area stenosis were significantly reduced in cRGD peptide-loaded polymer stents compared with unloaded or bare metal stents, in part by accelerating stent endothelialisation. One can speculate that if using integrin-binding peptides represents a promising target to accelerate healing after vascular injury, stents capable of upregulating ITGA5 in captured EPCs might have a similar effect.

# miR-92a inhibitor and oncogenic potential

A non-estimated quantity of miR-92a inhibitor, even if locally delivered, could leak into circulation and target multiple organs and cell types, which could alter miR-92a activity also in non-EPCs which at the time being could pose a risk mostly regarding tumorigenesis. Volinia *et al.* identified that miR-92a was markedly overexpressed in tumour tissues from a large-scale miRnome analysis (Volinia et al., 2006), while several experiments have already implicated miR-92a in tumorigenesis, namely by promoting tumour proliferation, inhibiting tumour apoptosis, and promoting tumour invasion and metastasis (M. Li et al., 2014). However, despite the need to gain further insights into the mechanisms of the miR-92a and their target genes in tumours before going into man, reassuringly, all experiments point towards an expected beneficial effect in tumour proliferation, apoptosis, and invasion/metastasis by inhibiting miR-92a. Upregulation of miR-92a could activate the PI3K/Akt/mTOR pathway, and inhibit cell apoptosis induced by chemotherapy in mantle cell lymphoma (MCL) cells; while downregulation of miR-92a could inhibit the growth of tumours in a xenograft MCL mouse model (M. Li et al., 2014). Tsuchida *et al.* demonstrated that the expression of miR-92a was increased in colon adenomas and carcinoma, and it could target Bim directly and inhibit colon carcinoma cell apoptosis, whereas miR-92a inhibitor-induced colon carcinoma cell apoptosism (Tsuchida et al., 2011). Transfection of miR-92a precursor reduced ITGA5 expression in ovarian cancer cells, which was associated with inhibition of cancer cell adhesion, and potentiation of invasion since integrins mainly mediate cell–cell and cell–ECM interactions (Missan & DiPersio, 2012). Furthermore, it was reported that miR-92a could directly target E-cadherin (CDH1), which results in lymphatic metastasis and invasion of oesophagal squamous cell carcinoma (Z. L. Chen et al., 2011). Altogether, miR-92a inhibition might be a cancer therapy strategy in the future, which is reassuring for those studying the strategy in the field of therapeutic angiogenesis, and not a risk.

# References


Abbott, J. D., Huang, Y., Liu, D., Hickey, R., Krause, D. S., & Giordano, F. J. (2004). Stromal cell-derived factor-1alpha plays a critical role in stem cell recruitment to the heart after myocardial infarction but is not sufficient to induce homing in the absence of injury. *Circulation, 110*(21), 3300-3305. doi:10.1161/01.CIR.0000147780.30124.CF

Abdellatif, M. (2012). Differential expression of microRNAs in different disease states. *Circ Res, 110*(4), 638-650. doi:10.1161/CIRCRESAHA.111.247437

Aicher, A., Brenner, W., Zuhayra, M., Badorff, C., Massoudi, S., Assmus, B., . . . Dimmeler, S. (2003). Assessment of the tissue distribution of transplanted human endothelial progenitor cells by radioactive labeling. *Circulation, 107*(16), 2134-2139. doi:10.1161/01.CIR.0000062649.63838.C9

Aicher, A., Heeschen, C., Mildner-Rihm, C., Urbich, C., Ihling, C., Technau-Ihling, K., . . . Dimmeler, S. (2003). Essential role of endothelial nitric oxide synthase for mobilization of stem and progenitor cells. *Nat Med, 9*(11), 1370-1376. doi:10.1038/nm948

Aicher, A., Rentsch, M., Sasaki, K., Ellwart, J. W., Fandrich, F., Siebert, R., . . . Heeschen, C. (2007). Nonbone marrow-derived circulating progenitor cells contribute to postnatal neovascularization following tissue ischemia. *Circ Res, 100*(4), 581-589. doi:10.1161/01.RES.0000259562.63718.35

Ambros, R. A. (2000). Simple hyperplasia of the endometrium: an evaluation of proliferative activity by Ki-67 immunostaining. *Int J Gynecol Pathol, 19*(3), 206-211.

Ambros, V., Bartel, B., Bartel, D. P., Burge, C. B., Carrington, J. C., Chen, X., . . . Tuschl, T. (2003). A uniform system for microRNA annotation. *RNA, 9*(3), 277-279.

Anand, S. (2013). A brief primer on microRNAs and their roles in angiogenesis. *Vasc Cell, 5*(1), 2. doi:10.1186/2045-824X-5-2

Angelos, M. G., Brown, M. A., Satterwhite, L. L., Levering, V. W., Shaked, N. T., & Truskey, G. A. (2010). Dynamic adhesion of umbilical cord blood endothelial progenitor cells under laminar shear stress. *Biophys J, 99*(11), 3545-3554. doi:10.1016/j.bpj.2010.10.004

Aoki, J., Serruys, P. W., van Beusekom, H., Ong, A. T., McFadden, E. P., Sianos, G., . . . Kutryk, M. J. (2005). Endothelial progenitor cell capture by stents coated with antibody against CD34: the HEALING-FIM (Healthy Endothelial Accelerated Lining Inhibits Neointimal Growth-First In Man) Registry. *J Am Coll Cardiol, 45*(10), 1574-1579. doi:10.1016/j.jacc.2005.01.048

Aoki, M., Yasutake, M., & Murohara, T. (2004). Derivation of functional endothelial progenitor cells from human umbilical cord blood mononuclear cells isolated by a novel cell filtration device. *Stem Cells, 22*(6), 994-1002. doi:10.1634/stemcells.22-6-994

Aragona, C. O., Imbalzano, E., Mamone, F., Cairo, V., Lo Gullo, A., D'Ascola, A., . . . Mandraffino, G. (2016). Endothelial Progenitor Cells for Diagnosis and Prognosis in Cardiovascular Disease. *Stem Cells Int, 2016*, 8043792. doi:10.1155/2016/8043792

Asahara, T., Murohara, T., Sullivan, A., Silver, M., van der Zee, R., Li, T., . . . Isner, J. M. (1997). Isolation of putative progenitor endothelial cells for angiogenesis. *Science, 275*(5302), 964-967.

Askari, J. A., Buckley, P. A., Mould, A. P., & Humphries, M. J. (2009). Linking integrin conformation to function. *J Cell Sci, 122*(Pt 2), 165-170. doi:122/2/165 [pii]

10.1242/jcs.018556

Assmus, B., Fischer-Rasokat, U., Honold, J., Seeger, F. H., Fichtlscherer, S., Tonn, T., . . . Registry, T.-C. (2007). Transcoronary transplantation of functionally competent BMCs is associated with a decrease in natriuretic peptide serum levels and improved survival of patients with chronic postinfarction heart failure: results of the TOPCARE-CHD Registry. *Circ Res, 100*(8), 1234-1241. doi:10.1161/01.RES.0000264508.47717.6b

Assmus, B., Rolf, A., Erbs, S., Elsasser, A., Haberbosch, W., Hambrecht, R., . . . Investigators, R.-A. (2010). Clinical outcome 2 years after intracoronary administration of bone marrow-derived progenitor cells in acute myocardial infarction. *Circ Heart Fail, 3*(1), 89-96. doi:10.1161/CIRCHEARTFAILURE.108.843243

Assmus, B., Schachinger, V., Teupe, C., Britten, M., Lehmann, R., Dobert, N., . . . Zeiher, A. M. (2002). Transplantation of Progenitor Cells and Regeneration Enhancement in Acute Myocardial Infarction (TOPCARE-AMI). *Circulation, 106*(24), 3009-3017.

Au, P., Daheron, L. M., Duda, D. G., Cohen, K. S., Tyrrell, J. A., Lanning, R. M., . . . Jain, R. K. (2008). Differential in vivo potential of endothelial progenitor cells from human umbilical cord blood and adult peripheral blood to form functional long-lasting vessels. *Blood, 111*(3), 1302-1305. doi:10.1182/blood-2007-06-094318

Awad, O., Jiao, C., Ma, N., Dunnwald, M., & Schatteman, G. C. (2005). Obese diabetic mouse environment differentially affects primitive and monocytic endothelial cell progenitors. *Stem Cells, 23*(4), 575-583. doi:10.1634/stemcells.2004-0185

Baek, D., Villen, J., Shin, C., Camargo, F. D., Gygi, S. P., & Bartel, D. P. (2008). The impact of microRNAs on protein output. *Nature, 455*(7209), 64-71. doi:10.1038/nature07242

Bahlmann, F. H., de Groot, K., Mueller, O., Hertel, B., Haller, H., & Fliser, D. (2005). Stimulation of endothelial progenitor cells: a new putative therapeutic effect of angiotensin II receptor antagonists. *Hypertension, 45*(4), 526-529. doi:10.1161/01.HYP.0000159191.98140.89

Bahlmann, F. H., De Groot, K., Spandau, J. M., Landry, A. L., Hertel, B., Duckert, T., . . . Fliser, D. (2004). Erythropoietin regulates endothelial progenitor cells. *Blood, 103*(3), 921-926. doi:10.1182/blood-2003-04-1284

Bai, H., & Wang, Z. Z. (2008). Directing human embryonic stem cells to generate vascular progenitor cells. *Gene Ther, 15*(2), 89-95. doi:10.1038/sj.gt.3303005

Baker, M., Robinson, S. D., Lechertier, T., Barber, P. R., Tavora, B., D'Amico, G., . . . Hodivala-Dilke, K. (2012). Use of the mouse aortic ring assay to study angiogenesis. *Nat Protoc, 7*(1), 89-104. doi:10.1038/nprot.2011.435

Balaji, S., King, A., Crombleholme, T. M., & Keswani, S. G. (2013). The Role of Endothelial Progenitor Cells in Postnatal Vasculogenesis: Implications for Therapeutic Neovascularization and Wound Healing. *Adv Wound Care (New Rochelle), 2*(6), 283-295. doi:10.1089/wound.2012.0398

Balestrieri, M. L., Rienzo, M., Felice, F., Rossiello, R., Grimaldi, V., Milone, L., . . . Napoli, C. (2008). High glucose downregulates endothelial progenitor cell number via SIRT1. *Biochim Biophys Acta, 1784*(6), 936-945. doi:10.1016/j.bbapap.2008.03.004

Balestrieri, M. L., Servillo, L., Esposito, A., D'Onofrio, N., Giovane, A., Casale, R., . . . Marfella, R. (2013). Poor glycaemic control in type 2 diabetes patients reduces endothelial progenitor cell number by influencing SIRT1 signalling via platelet-activating factor receptor activation. *Diabetologia, 56*(1), 162-172. doi:10.1007/s00125-012-2749-0

Bartel, D. P. (2004). MicroRNAs: genomics, biogenesis, mechanism, and function. *Cell, 116*(2), 281-297.

Bartunek, J., Vanderheyden, M., Vandekerckhove, B., Mansour, S., De Bruyne, B., De Bondt, P., . . . Wijns, W. (2005). Intracoronary injection of CD133-positive enriched bone marrow progenitor cells promotes cardiac recovery after recent myocardial infarction: feasibility and safety. *Circulation, 112*(9 Suppl), I178-183. doi:10.1161/CIRCULATIONAHA.104.522292

Basire, A., Sabatier, F., Ravet, S., Lamy, E., Mialhe, A., Zabouo, G., . . . Dignat-George, F. (2006). High urokinase expression contributes to the angiogenic properties of endothelial cells derived from circulating progenitors. *Thromb Haemost, 95*(4), 678-688.

Bassand, J. P., Hamm, C. W., Ardissino, D., Boersma, E., Budaj, A., Fernandez-Aviles, F., . . . Wijns, W. (2007). Guidelines for the diagnosis and treatment of non-ST-segment elevation acute coronary syndromes. *European heart journal, 28*(13), 1598-1660. doi:10.1093/eurheartj/ehm161

Bauersachs, J., & Thum, T. (2011). Biogenesis and regulation of cardiovascular microRNAs. *Circ Res, 109*(3), 334-347. doi:10.1161/CIRCRESAHA.110.228676

Baumheter, S., Singer, M. S., Henzel, W., Hemmerich, S., Renz, M., Rosen, S. D., & Lasky, L. A. (1993). Binding of L-selectin to the vascular sialomucin CD34. *Science, 262*(5132), 436-438.

Baumhueter, S., Dybdal, N., Kyle, C., & Lasky, L. A. (1994). Global vascular expression of murine CD34, a sialomucin-like endothelial ligand for L-selectin. *Blood, 84*(8), 2554-2565.

Bautch, V. L. (2011). Stem cells and the vasculature. *Nat Med, 17*(11), 1437-1443. doi:10.1038/nm.2539

Bauters, C., Marotte, F., Hamon, M., Oliviero, P., Farhadian, F., Robert, V., . . . Rappaport, L. (1995). Accumulation of fetal fibronectin mRNAs after balloon denudation of rabbit arteries. *Circulation, 92*(4), 904-911.

Beavers, K. R., Nelson, C. E., & Duvall, C. L. (2015). MiRNA inhibition in tissue engineering and regenerative medicine. *Adv Drug Deliv Rev, 88*, 123-137. doi:10.1016/j.addr.2014.12.006

Beeres, S. L., Atsma, D. E., van Ramshorst, J., Schalij, M. J., & Bax, J. J. (2008). Cell therapy for ischaemic heart disease. *Heart, 94*(9), 1214-1226. doi:10.1136/hrt.2008.149476

Behrendt, D., & Ganz, P. (2002). Endothelial function. From vascular biology to clinical applications. *Am J Cardiol, 90*(10C), 40L-48L.

Beitz, J. G., Kim, I. S., Calabresi, P., & Frackelton, A. R., Jr. (1991). Human microvascular endothelial cells express receptors for platelet-derived growth factor. *Proc Natl Acad Sci U S A, 88*(5), 2021-2025.

Belvedere, O., Feruglio, C., Malangone, W., Bonora, M. L., Donini, A., Dorotea, L., . . . Degrassi, A. (1999). Phenotypic characterization of immunomagnetically purified umbilical cord blood CD34+ cells. *Blood Cells Mol Dis, 25*(3-4), 141-146.

Bennett, M. R., & O'Sullivan, M. (2001). Mechanisms of angioplasty and stent restenosis: implications for design of rational therapy. *Pharmacol Ther, 91*(2), 149-166.

Bertolini, F., Mancuso, P., & Kerbel, R. S. (2005). Circulating endothelial progenitor cells. *N Engl J Med, 353*(24), 2613-2616; author reply 2613-2616.

Bianconi, V., Sahebkar, A., Kovanen, P., Bagaglia, F., Ricciuti, B., Calabro, P., . . . Pirro, M. (2018). Endothelial and cardiac progenitor cells for cardiovascular repair: A controversial paradigm in cell therapy. *Pharmacol Ther, 181*, 156-168. doi:10.1016/j.pharmthera.2017.08.004

Bikfalvi, A., Cramer, E. M., Tenza, D., & Tobelem, G. (1991). Phenotypic modulations of human umbilical vein endothelial cells and human dermal fibroblasts using two angiogenic assays. *Biol Cell, 72*(3), 275-278.

Blake, J. M., Nicoud, I. B., Weber, D., Voorhies, H., Guthrie, K. A., Heimfeld, S., & Delaney, C. (2012). Improved immunomagnetic enrichment of CD34(+) cells from umbilical cord blood using the CliniMACS cell separation system. *Cytotherapy, 14*(7), 818-822. doi:10.3109/14653249.2012.681040

Blanchet, M. R., Gold, M., Maltby, S., Bennett, J., Petri, B., Kubes, P., . . . McNagny, K. M. (2010). Loss of CD34 leads to exacerbated autoimmune arthritis through increased vascular permeability. *J Immunol, 184*(3), 1292-1299. doi:10.4049/jimmunol.0900808

Blann, A. D., Woywodt, A., Bertolini, F., Bull, T. M., Buyon, J. P., Clancy, R. M., . . . Dignat-George, F. (2005). Circulating endothelial cells. Biomarker of vascular disease. *Thromb Haemost, 93*(2), 228-235. doi:10.1160/TH04-09-0578

Blindt, R., Vogt, F., Astafieva, I., Fach, C., Hristov, M., Krott, N., . . . Weber, C. (2006). A novel drug-eluting stent coated with an integrin-binding cyclic Arg-Gly-Asp peptide inhibits neointimal hyperplasia by recruiting endothelial progenitor cells. *J Am Coll Cardiol, 47*(9), 1786-1795. doi:10.1016/j.jacc.2005.11.081

Blum A, N. S. a. B. N. (2014). Mechanistic Pathways of Atherosclerosis – Vasa Vasorum, Endothelial Progenitor Cells (Epcs) – and the Effects of 3-Hydroxy-3-Methylglutaryl-Coenzyme A (HMG-Co A) Reductase Inhibitors. *J Dis Markers, 1*(1), 6.

Bokel, C., & Brown, N. H. (2002). Integrins in development: moving on, responding to, and sticking to the extracellular matrix. *Dev Cell, 3*(3), 311-321.

Bompais, H., Chagraoui, J., Canron, X., Crisan, M., Liu, X. H., Anjo, A., . . . Uzan, G. (2004). Human endothelial cells derived from circulating progenitors display specific functional properties compared with mature vessel wall endothelial cells. *Blood, 103*(7), 2577-2584. doi:10.1182/blood-2003-08-2770

Bonauer, A., Boon, R. A., & Dimmeler, S. (2010). Vascular microRNAs. *Curr Drug Targets, 11*(8), 943-949. doi:BSP/CDT/E-Pub/00088 [pii]

Bonauer, A., Carmona, G., Iwasaki, M., Mione, M., Koyanagi, M., Fischer, A., . . . Dimmeler, S. (2009). MicroRNA-92a controls angiogenesis and functional recovery of ischemic tissues in mice. *Science, 324*(5935), 1710-1713. doi:10.1126/science.1174381

Bonauer, A., & Dimmeler, S. (2009). The microRNA-17-92 cluster: still a miRacle? *Cell Cycle, 8*(23), 3866-3873. doi:9994 [pii]

Bonello, L., Basire, A., Sabatier, F., Paganelli, F., & Dignat-George, F. (2006). Endothelial injury induced by coronary angioplasty triggers mobilization of endothelial progenitor cells in patients with stable coronary artery disease. *J Thromb Haemost, 4*(5), 979-981. doi:10.1111/j.1538-7836.2006.01858.x

Bonner, W. A., Hulett, H. R., Sweet, R. G., & Herzenberg, L. A. (1972). Fluorescence activated cell sorting. *Rev Sci Instrum, 43*(3), 404-409.

Boon, R. A., & Horrevoets, A. J. (2009). Key transcriptional regulators of the vasoprotective effects of shear stress. *Hamostaseologie, 29*(1), 39-40, 41-33.

Boon, R. A., Urbich, C., Fischer, A., Fontijn, R. D., Seeger, F. H., Koyanagi, M., . . . Dimmeler, S. (2011). Kruppel-like factor 2 improves neovascularization capacity of aged proangiogenic cells. *Eur Heart J, 32*(3), 371-377. doi:10.1093/eurheartj/ehq137

Boos, C. J., Lane, D. A., Kang, D., Goon, P. K., Blann, A. D., & Lip, G. Y. (2006). Temporal and venepuncture-related decline in circulating endothelial cell capture from mixed venous blood. *J Thromb Thrombolysis, 22*(2), 125-131. doi:10.1007/s11239-006-8422-z

Boos, C. J., Lip, G. Y., & Blann, A. D. (2006). Circulating endothelial cells in cardiovascular disease. *J Am Coll Cardiol, 48*(8), 1538-1547. doi:10.1016/j.jacc.2006.02.078

Boosani, C. S., Mannam, A. P., Cosgrove, D., Silva, R., Hodivala-Dilke, K. M., Keshamouni, V. G., & Sudhakar, A. (2007). Regulation of COX-2 mediated signaling by alpha3 type IV noncollagenous domain in tumor angiogenesis. *Blood, 110*(4), 1168-1177. doi:10.1182/blood-2007-01-066282

Bouvard, C., Gafsou, B., Dizier, B., Galy-Fauroux, I., Lokajczyk, A., Boisson-Vidal, C., . . . Helley, D. (2010). alpha6-integrin subunit plays a major role in the proangiogenic properties of endothelial progenitor cells. *Arterioscler Thromb Vasc Biol, 30*(8), 1569-1575. doi:10.1161/ATVBAHA.110.209163

Brenner, W., Aicher, A., Eckey, T., Massoudi, S., Zuhayra, M., Koehl, U., . . . Henze, E. (2004). 111In-labeled CD34+ hematopoietic progenitor cells in a rat myocardial infarction model. *J Nucl Med, 45*(3), 512-518.

Britten, M. B., Abolmaali, N. D., Assmus, B., Lehmann, R., Honold, J., Schmitt, J., . . . Zeiher, A. M. (2003). Infarct remodeling after intracoronary progenitor cell treatment in patients with acute myocardial infarction (TOPCARE-AMI): mechanistic insights from serial contrast-enhanced magnetic resonance imaging. *Circulation, 108*(18), 2212-2218. doi:10.1161/01.CIR.0000095788.78169.AF

Brock, M., Trenkmann, M., Gay, R. E., Michel, B. A., Gay, S., Fischler, M., . . . Huber, L. C. (2009). Interleukin-6 modulates the expression of the bone morphogenic protein receptor type II through a novel STAT3-microRNA cluster 17/92 pathway. *Circ Res, 104*(10), 1184-1191. doi:10.1161/CIRCRESAHA.109.197491

Brown, M. A., Wallace, C. S., Angelos, M., & Truskey, G. A. (2009). Characterization of umbilical cord blood-derived late outgrowth endothelial progenitor cells exposed to laminar shear stress. *Tissue Eng Part A, 15*(11), 3575-3587. doi:10.1089/ten.TEA.2008.0444

Buhring, H. J., Seiffert, M., Bock, T. A., Scheding, S., Thiel, A., Scheffold, A., . . . Brugger, W. (1999). Expression of novel surface antigens on early hematopoietic cells. *Ann N Y Acad Sci, 872*, 25-38; discussion 38-29.

Caiado, F., & Dias, S. (2012). Endothelial progenitor cells and integrins: adhesive needs. *Fibrogenesis Tissue Repair, 5*, 4. doi:10.1186/1755-1536-5-4

Caiado, F., Real, C., Carvalho, T., & Dias, S. (2008). Notch pathway modulation on bone marrow-derived vascular precursor cells regulates their angiogenic and wound healing potential. *PLoS One, 3*(11), e3752. doi:10.1371/journal.pone.0003752

Callaghan, M. J., Ceradini, D. J., & Gurtner, G. C. (2005). Hyperglycemia-induced reactive oxygen species and impaired endothelial progenitor cell function. *Antioxid Redox Signal, 7*(11-12), 1476-1482. doi:10.1089/ars.2005.7.1476

Campagnolo, P., Cesselli, D., Al Haj Zen, A., Beltrami, A. P., Krankel, N., Katare, R., . . . Madeddu, P. (2010). Human adult vena saphena contains perivascular progenitor cells endowed with clonogenic and proangiogenic potential. *Circulation, 121*(15), 1735-1745. doi:10.1161/CIRCULATIONAHA.109.899252

Cao, Y., Zhang, W., Gao, X., Zhang, G., Falzon, M., Townsend, C. M., Jr., . . . Ko, T. C. (2013). PTHrP is a novel mediator for TGF-beta-induced apoptosis. *Regul Pept, 184*, 40-46. doi:10.1016/j.regpep.2013.03.024

Caporali, A., Meloni, M., Nailor, A., Mitic, T., Shantikumar, S., Riu, F., . . . Emanueli, C. (2015). p75(NTR)-dependent activation of NF-kappaB regulates microRNA-503 transcription and pericyte-endothelial crosstalk in diabetes after limb ischaemia. *Nature communications, 6*, 8024. doi:10.1038/ncomms9024

Cappellari, R., D'Anna, M., Avogaro, A., & Fadini, G. P. (2016). Plerixafor improves the endothelial health balance. The effect of diabetes analysed by polychromatic flow cytometry. *Atherosclerosis, 251*, 373-380. doi:10.1016/j.atherosclerosis.2016.05.028

Carmeliet, P., Ferreira, V., Breier, G., Pollefeyt, S., Kieckens, L., Gertsenstein, M., . . . Nagy, A. (1996). Abnormal blood vessel development and lethality in embryos lacking a single VEGF allele. *Nature, 380*(6573), 435-439. doi:10.1038/380435a0

Cartiera, M. S., Johnson, K. M., Rajendran, V., Caplan, M. J., & Saltzman, W. M. (2009). The uptake and intracellular fate of PLGA nanoparticles in epithelial cells. *Biomaterials, 30*(14), 2790-2798. doi:10.1016/j.biomaterials.2009.01.057

Casamassimi, A., Balestrieri, M. L., Fiorito, C., Schiano, C., Maione, C., Rossiello, R., . . . Napoli, C. (2007). Comparison between total endothelial progenitor cell isolation versus enriched Cd133+ culture. *J Biochem, 141*(4), 503-511. doi:10.1093/jb/mvm060

Case, J., Mead, L. E., Bessler, W. K., Prater, D., White, H. A., Saadatzadeh, M. R., . . . Ingram, D. A. (2007). Human CD34+AC133+VEGFR-2+ cells are not endothelial progenitor cells but distinct, primitive hematopoietic progenitors. *Experimental hematology, 35*(7), 1109-1118. doi:10.1016/j.exphem.2007.04.002

Caveliers, V., De Keulenaer, G., Everaert, H., Van Riet, I., Van Camp, G., Verheye, S., . . . Schots, R. (2007). In vivo visualization of 111In labeled CD133+ peripheral blood stem cells after intracoronary administration in patients with chronic ischemic heart disease. *Q J Nucl Med Mol Imaging, 51*(1), 61-66.

Ceradini, D. J., Kulkarni, A. R., Callaghan, M. J., Tepper, O. M., Bastidas, N., Kleinman, M. E., . . . Gurtner, G. C. (2004). Progenitor cell trafficking is regulated by hypoxic gradients through HIF-1 induction of SDF-1. *Nat Med, 10*(8), 858-864. doi:10.1038/nm1075

Chade, A. R., Zhu, X., Lavi, R., Krier, J. D., Pislaru, S., Simari, R. D., . . . Lerman, L. O. (2009). Endothelial progenitor cells restore renal function in chronic experimental renovascular disease. *Circulation, 119*(4), 547-557. doi:10.1161/CIRCULATIONAHA.108.788653

Chaisiripoomkere, W., Jootar, S., Ungkanont, A., Jaovisidha, A., Onpun, S., & Khupulsup, K. (1999). Study of hematopoietic progenitor cells, hematological values and lymphocyte subsets in cord blood: application for cord blood transplantation. *Southeast Asian J Trop Med Public Health, 30*(4), 781-785.

Chamorro-Jorganes, A., Araldi, E., Penalva, L. O., Sandhu, D., Fernandez-Hernando, C., & Suarez, Y. (2011). MicroRNA-16 and microRNA-424 regulate cell-autonomous angiogenic functions in endothelial cells via targeting vascular endothelial growth factor receptor-2 and fibroblast growth factor receptor-1. *Arterioscler Thromb Vasc Biol, 31*(11), 2595-2606. doi:10.1161/ATVBAHA.111.236521

Chavakis, E., Aicher, A., Heeschen, C., Sasaki, K., Kaiser, R., El Makhfi, N., . . . Dimmeler, S. (2005). Role of beta2-integrins for homing and neovascularization capacity of endothelial progenitor cells. *J Exp Med, 201*(1), 63-72. doi:10.1084/jem.20041402

Chavakis, E., Hain, A., Vinci, M., Carmona, G., Bianchi, M. E., Vajkoczy, P., . . . Dimmeler, S. (2007). High-mobility group box 1 activates integrin-dependent homing of endothelial progenitor cells. *Circ Res, 100*(2), 204-212. doi:10.1161/01.RES.0000257774.55970.f4

Chavakis, E., Urbich, C., & Dimmeler, S. (2008). Homing and engraftment of progenitor cells: a prerequisite for cell therapy. *J Mol Cell Cardiol, 45*(4), 514-522. doi:10.1016/j.yjmcc.2008.01.004

Chen, J., Gu, Z., Wu, M., Yang, Y., Zhang, J., Ou, J., . . . Chen, Y. (2016). C-reactive protein can upregulate VEGF expression to promote ADSC-induced angiogenesis by activating HIF-1alpha via CD64/PI3k/Akt and MAPK/ERK signaling pathways. *Stem Cell Res Ther, 7*(1), 114. doi:10.1186/s13287-016-0377-1

Chen, J. X., & Meyrick, B. (2004). Hypoxia increases Hsp90 binding to eNOS via PI3K-Akt in porcine coronary artery endothelium. *Lab Invest, 84*(2), 182-190. doi:10.1038/labinvest.3700027

Chen, J. Z., Zhang, F. R., Tao, Q. M., Wang, X. X., Zhu, J. H., & Zhu, J. H. (2004). Number and activity of endothelial progenitor cells from peripheral blood in patients with hypercholesterolaemia. *Clin Sci (Lond), 107*(3), 273-280. doi:10.1042/CS20030389

Chen, L. J., Lim, S. H., Yeh, Y. T., Lien, S. C., & Chiu, J. J. (2012). Roles of microRNAs in atherosclerosis and restenosis. *J Biomed Sci, 19*(1), 79. doi:10.1186/1423-0127-19-79

Chen, Y. H., Lin, S. J., Lin, F. Y., Wu, T. C., Tsao, C. R., Huang, P. H., . . . Chen, J. W. (2007). High glucose impairs early and late endothelial progenitor cells by modifying nitric oxide-related but not oxidative stress-mediated mechanisms. *Diabetes, 56*(6), 1559-1568. doi:10.2337/db06-1103

Chen, Z. L., Zhao, X. H., Wang, J. W., Li, B. Z., Wang, Z., Sun, J., . . . He, J. (2011). microRNA-92a promotes lymph node metastasis of human esophageal squamous cell carcinoma via E-cadherin. *J Biol Chem, 286*(12), 10725-10734. doi:10.1074/jbc.M110.165654

Cheng, H. L., Mostoslavsky, R., Saito, S., Manis, J. P., Gu, Y., Patel, P., . . . Chua, K. F. (2003). Developmental defects and p53 hyperacetylation in Sir2 homolog (SIRT1)-deficient mice. *Proc Natl Acad Sci U S A, 100*(19), 10794-10799. doi:10.1073/pnas.1934713100

Cheng, J., Baumhueter, S., Cacalano, G., Carver-Moore, K., Thibodeaux, H., Thomas, R., . . . Lasky, L. A. (1996). Hematopoietic defects in mice lacking the sialomucin CD34. *Blood, 87*(2), 479-490.

Cheng, X. W., Kuzuya, M., Nakamura, K., Maeda, K., Tsuzuki, M., Kim, W., . . . Murohara, T. (2007). Mechanisms underlying the impairment of ischemia-induced neovascularization in matrix metalloproteinase 2-deficient mice. *Circ Res, 100*(6), 904-913. doi:10.1161/01.RES.0000260801.12916.b5

Choe, N., Kwon, J. S., Kim, J. R., Eom, G. H., Kim, Y., Nam, K. I., . . . Kook, H. (2013). The microRNA miR-132 targets Lrrfip1 to block vascular smooth muscle cell proliferation and neointimal hyperplasia. *Atherosclerosis, 229*(2), 348-355. doi:10.1016/j.atherosclerosis.2013.05.009

Chong, M. S., Ng, W. K., & Chan, J. K. (2016). Concise Review: Endothelial Progenitor Cells in Regenerative Medicine: Applications and Challenges. *Stem Cells Transl Med, 5*(4), 530-538. doi:10.5966/sctm.2015-0227

Cines, D. B., Pollak, E. S., Buck, C. A., Loscalzo, J., Zimmerman, G. A., McEver, R. P., . . . Stern, D. M. (1998). Endothelial cells in physiology and in the pathophysiology of vascular disorders. *Blood, 91*(10), 3527-3561.

Climent, M., Quintavalle, M., Miragoli, M., Chen, J., Condorelli, G., & Elia, L. (2015). TGFbeta Triggers miR-143/145 Transfer From Smooth Muscle Cells to Endothelial Cells, Thereby Modulating Vessel Stabilization. *Circ Res, 116*(11), 1753-1764. doi:10.1161/CIRCRESAHA.116.305178

Cohen-Sacks, H., Najajreh, Y., Tchaikovski, V., Gao, G., Elazer, V., Dahan, R., . . . Golomb, G. (2002). Novel PDGFbetaR antisense encapsulated in polymeric nanospheres for the treatment of restenosis. *Gene Ther, 9*(23), 1607-1616. doi:10.1038/sj.gt.3301830

Concepcion, C. P., Bonetti, C., & Ventura, A. (2012). The microRNA-17-92 family of microRNA clusters in development and disease. *Cancer J, 18*(3), 262-267. doi:10.1097/PPO.0b013e318258b60a

Connolly, J. O., Simpson, N., Hewlett, L., & Hall, A. (2002). Rac regulates endothelial morphogenesis and capillary assembly. *Mol Biol Cell, 13*(7), 2474-2485. doi:10.1091/mbc.E02-01-0006

Cooke, J. P. (2003). Flow, NO, and atherogenesis. *Proc Natl Acad Sci U S A, 100*(3), 768-770. doi:10.1073/pnas.0430082100

Cowan, C. E., Kohler, E. E., Dugan, T. A., Mirza, M. K., Malik, A. B., & Wary, K. K. (2010). Kruppel-like factor-4 transcriptionally regulates VE-cadherin expression and endothelial barrier function. *Circ Res, 107*(8), 959-966. doi:10.1161/CIRCRESAHA.110.219592

Cui, B., Huang, L., Fang, Y., Guo, R., Yin, Y., & Zhao, X. (2011). Transplantation of endothelial progenitor cells overexpressing endothelial nitric oxide synthase enhances inhibition of neointimal hyperplasia and restores endothelium-dependent vasodilatation. *Microvasc Res, 81*(1), 143-150. doi:10.1016/j.mvr.2010.09.009

Cui, Y. X., Kafienah, W., Suleiman, M. S., & Ascione, R. (2013). A new methodological sequence to expand and transdifferentiate human umbilical cord blood derived CD133+ cells into a cardiomyocyte-like phenotype. *Stem Cell Rev, 9*(3), 350-359. doi:10.1007/s12015-011-9316-9

Curcio, A., Torella, D., & Indolfi, C. (2011). Mechanisms of smooth muscle cell proliferation and endothelial regeneration after vascular injury and stenting: approach to therapy. *Circ J, 75*(6), 1287-1296.

Cutlip, D. E., Windecker, S., Mehran, R., Boam, A., Cohen, D. J., van Es, G. A., . . . Academic Research, C. (2007). Clinical end points in coronary stent trials: a case for standardized definitions. *Circulation, 115*(17), 2344-2351. doi:10.1161/CIRCULATIONAHA.106.685313

Cyrus, T., Wickline, S. A., & Lanza, G. M. (2012). Nanotechnology in interventional cardiology. *Wiley Interdiscip Rev Nanomed Nanobiotechnol, 4*(1), 82-95. doi:10.1002/wnan.154

D'Arena, G., Musto, P., Cascavilla, N., Di Giorgio, G., Zendoli, F., & Carotenuto, M. (1996). Human umbilical cord blood: immunophenotypic heterogeneity of CD34+ hematopoietic progenitor cells. *Haematologica, 81*(5), 404-409.

D'Onofrio, N., Vitiello, M., Casale, R., Servillo, L., Giovane, A., & Balestrieri, M. L. (2015). Sirtuins in vascular diseases: Emerging roles and therapeutic potential. *Biochim Biophys Acta, 1852*(7), 1311-1322. doi:10.1016/j.bbadis.2015.03.001

Danhier, F., Ansorena, E., Silva, J. M., Coco, R., Le Breton, A., & Preat, V. (2012). PLGA-based nanoparticles: an overview of biomedical applications. *J Control Release, 161*(2), 505-522. doi:10.1016/j.jconrel.2012.01.043

Daniel, J. M., Penzkofer, D., Teske, R., Dutzmann, J., Koch, A., Bielenberg, W., . . . Sedding, D. G. (2014). Inhibition of miR-92a improves re-endothelialization and prevents neointima formation following vascular injury. *Cardiovasc Res, 103*(4), 564-572. doi:10.1093/cvr/cvu162

Davis, G. E., & Senger, D. R. (2005). Endothelial extracellular matrix: biosynthesis, remodeling, and functions during vascular morphogenesis and neovessel stabilization. *Circ Res, 97*(11), 1093-1107. doi:10.1161/01.RES.0000191547.64391.e3

De Falco, E., Porcelli, D., Torella, A. R., Straino, S., Iachininoto, M. G., Orlandi, A., . . . Pesce, M. (2004). SDF-1 involvement in endothelial phenotype and ischemia-induced recruitment of bone marrow progenitor cells. *Blood, 104*(12), 3472-3482. doi:10.1182/blood-2003-12-4423

de Wynter, E. A., Coutinho, L. H., Pei, X., Marsh, J. C., Hows, J., Luft, T., & Testa, N. G. (1995). Comparison of purity and enrichment of CD34+ cells from bone marrow, umbilical cord and peripheral blood (primed for apheresis) using five separation systems. *Stem Cells, 13*(5), 524-532. doi:10.1002/stem.5530130510

Delorme, B., Basire, A., Gentile, C., Sabatier, F., Monsonis, F., Desouches, C., . . . Dignat-George, F. (2005). Presence of endothelial progenitor cells, distinct from mature endothelial cells, within human CD146+ blood cells. *Thromb Haemost, 94*(6), 1270-1279. doi:10.1160/TH05-07-0499

Dews, M., Homayouni, A., Yu, D., Murphy, D., Sevignani, C., Wentzel, E., . . . Thomas-Tikhonenko, A. (2006). Augmentation of tumor angiogenesis by a Myc-activated microRNA cluster. *Nat Genet, 38*(9), 1060-1065. doi:10.1038/ng1855

Dhanasekaran, D. N., & Reddy, E. P. (2008). JNK signaling in apoptosis. *Oncogene, 27*(48), 6245-6251. doi:10.1038/onc.2008.301

Dias, N., & Stein, C. A. (2002). Antisense oligonucleotides: basic concepts and mechanisms. *Mol Cancer Ther, 1*(5), 347-355.

Dimmeler, S., Aicher, A., Vasa, M., Mildner-Rihm, C., Adler, K., Tiemann, M., . . . Zeiher, A. M. (2001). HMG-CoA reductase inhibitors (statins) increase endothelial progenitor cells via the PI 3-kinase/Akt pathway. *J Clin Invest, 108*(3), 391-397. doi:10.1172/JCI13152

Dimmeler, S., Assmus, B., Hermann, C., Haendeler, J., & Zeiher, A. M. (1998). Fluid shear stress stimulates phosphorylation of Akt in human endothelial cells: involvement in suppression of apoptosis. *Circ Res, 83*(3), 334-341.

Dimmeler, S., Burchfield, J., & Zeiher, A. M. (2008). Cell-based therapy of myocardial infarction. *Arterioscler Thromb Vasc Biol, 28*(2), 208-216. doi:10.1161/ATVBAHA.107.155317

Dimmeler, S., Dernbach, E., & Zeiher, A. M. (2000). Phosphorylation of the endothelial nitric oxide synthase at ser-1177 is required for VEGF-induced endothelial cell migration. *FEBS Lett, 477*(3), 258-262.

Dimmeler, S., Fleming, I., Fisslthaler, B., Hermann, C., Busse, R., & Zeiher, A. M. (1999). Activation of nitric oxide synthase in endothelial cells by Akt-dependent phosphorylation. *Nature, 399*(6736), 601-605. doi:10.1038/21224

Dimmeler, S., Haendeler, J., Nehls, M., & Zeiher, A. M. (1997). Suppression of apoptosis by nitric oxide via inhibition of interleukin-1beta-converting enzyme (ICE)-like and cysteine protease protein (CPP)-32-like proteases. *J Exp Med, 185*(4), 601-607.

Dimmeler, S., & Zeiher, A. M. (2004). Vascular repair by circulating endothelial progenitor cells: the missing link in atherosclerosis? *J Mol Med (Berl), 82*(10), 671-677. doi:10.1007/s00109-004-0580-x

Doebele, C., Bonauer, A., Fischer, A., Scholz, A., Reiss, Y., Urbich, C., . . . Dimmeler, S. (2010). Members of the microRNA-17-92 cluster exhibit a cell-intrinsic antiangiogenic function in endothelial cells. *Blood, 115*(23), 4944-4950. doi:blood-2010-01-264812 [pii]

10.1182/blood-2010-01-264812

Donkuru, M., Badea, I., Wettig, S., Verrall, R., Elsabahy, M., & Foldvari, M. (2010). Advancing nonviral gene delivery: lipid- and surfactant-based nanoparticle design strategies. *Nanomedicine (Lond), 5*(7), 1103-1127. doi:10.2217/nnm.10.80

Donovan, D., Brown, N. J., Bishop, E. T., & Lewis, C. E. (2001). Comparison of three in vitro human 'angiogenesis' assays with capillaries formed in vivo. *Angiogenesis, 4*(2), 113-121.

Doran, A. C., Meller, N., & McNamara, C. A. (2008). Role of smooth muscle cells in the initiation and early progression of atherosclerosis. *Arterioscler Thromb Vasc Biol, 28*(5), 812-819. doi:10.1161/ATVBAHA.107.159327

Doyle, B., Sorajja, P., Hynes, B., Kumar, A. H., Araoz, P. A., Stalboerger, P. G., . . . Caplice, N. M. (2008). Progenitor cell therapy in a porcine acute myocardial infarction model induces cardiac hypertrophy, mediated by paracrine secretion of cardiotrophic factors including TGFbeta1. *Stem Cells Dev, 17*(5), 941-951. doi:10.1089/scd.2007.0214

Dubois, C., Liu, X., Claus, P., Marsboom, G., Pokreisz, P., Vandenwijngaert, S., . . . Janssens, S. (2010). Differential effects of progenitor cell populations on left ventricular remodeling and myocardial neovascularization after myocardial infarction. *J Am Coll Cardiol, 55*(20), 2232-2243. doi:10.1016/j.jacc.2009.10.081

Duckers, H. J., Soullie, T., den Heijer, P., Rensing, B., de Winter, R. J., Rau, M., . . . Serruys, P. W. (2007). Accelerated vascular repair following percutaneous coronary intervention by capture of endothelial progenitor cells promotes regression of neointimal growth at long term follow-up: final results of the Healing II trial using an endothelial progenitor cell capturing stent (Genous R stent). *EuroIntervention, 3*(3), 350-358.

Duinhouwer, L. E., van Rossum, B. J., van Tiel, S. T., van der Werf, R. M., Doeswijk, G. N., Haeck, J. C., . . . Bernsen, M. R. (2015). Magnetic Resonance Detection of CD34+ Cells from Umbilical Cord Blood Using a 19F Label. *PLoS One, 10*(9), e0138572. doi:10.1371/journal.pone.0138572

Durham, A. L., Speer, M. Y., Scatena, M., Giachelli, C. M., & Shanahan, C. M. (2018). Role of smooth muscle cells in vascular calcification: implications in atherosclerosis and arterial stiffness. *Cardiovasc Res, 114*(4), 590-600. doi:10.1093/cvr/cvy010

Egan, C. G., Caporali, F., Huqi, A. F., Zito, M. C., Focardi, M., Mondillo, S., . . . Sorrentino, V. (2009). Reduced levels of putative endothelial progenitor and CXCR4+ cells in coronary artery disease: kinetics following percutaneous coronary intervention and association with clinical characteristics. *Thromb Haemost, 101*(6), 1138-1146.

Eichmann, A., Corbel, C., Nataf, V., Vaigot, P., Breant, C., & Le Douarin, N. M. (1997). Ligand-dependent development of the endothelial and hemopoietic lineages from embryonic mesodermal cells expressing vascular endothelial growth factor receptor 2. *Proc Natl Acad Sci U S A, 94*(10), 5141-5146.

Erbs, S., Linke, A., Schachinger, V., Assmus, B., Thiele, H., Diederich, K. W., . . . Schuler, G. (2007). Restoration of microvascular function in the infarct-related artery by intracoronary transplantation of bone marrow progenitor cells in patients with acute myocardial infarction: the Doppler Substudy of the Reinfusion of Enriched Progenitor Cells and Infarct Remodeling in Acute Myocardial Infarction (REPAIR-AMI) trial. *Circulation, 116*(4), 366-374. doi:10.1161/CIRCULATIONAHA.106.671545

Ergun, S., & Gehling, U. M. (2007). Non-bone-marrow-derived endothelial progenitor cells: what is their exact location? *Circ Res, 101*(3), e31. doi:10.1161/CIRCRESAHA.107.157263

Estes, M. L., Mund, J. A., Mead, L. E., Prater, D. N., Cai, S., Wang, H., . . . Case, J. (2010). Application of polychromatic flow cytometry to identify novel subsets of circulating cells with angiogenic potential. *Cytometry A, 77*(9), 831-839. doi:10.1002/cyto.a.20921

Evora, P. R., Baldo, C. F., Celotto, A. C., & Capellini, V. K. (2009). Endothelium dysfunction classification: why is it still an open discussion? *Int J Cardiol, 137*(2), 175-176. doi:10.1016/j.ijcard.2008.05.031

Fabani, M. M., & Gait, M. J. (2008). miR-122 targeting with LNA/2'-O-methyl oligonucleotide mixmers, peptide nucleic acids (PNA), and PNA-peptide conjugates. *RNA, 14*(2), 336-346. doi:10.1261/rna.844108

Fadini, G. P., Agostini, C., & Avogaro, A. (2010). Autologous stem cell therapy for peripheral arterial disease meta-analysis and systematic review of the literature. *Atherosclerosis, 209*(1), 10-17. doi:10.1016/j.atherosclerosis.2009.08.033

Fadini, G. P., Agostini, C., Sartore, S., & Avogaro, A. (2007). Endothelial progenitor cells in the natural history of atherosclerosis. *Atherosclerosis, 194*(1), 46-54. doi:S0021-9150(07)00212-2 [pii]

10.1016/j.atherosclerosis.2007.03.046
Fadini, G. P., Baesso, I., Albiero, M., Sartore, S., Agostini, C., & Avogaro, A. (2008). Technical notes on endothelial progenitor cells: ways to escape from the knowledge plateau. *Atherosclerosis, 197*(2), 496-503. doi:S0021-9150(08)00012-9 [pii]

10.1016/j.atherosclerosis.2007.12.039
Fadini, G. P., Losordo, D., & Dimmeler, S. (2012). Critical reevaluation of endothelial progenitor cell phenotypes for therapeutic and diagnostic use. *Circ Res, 110*(4), 624-637. doi:10.1161/CIRCRESAHA.111.243386
Fadini, G. P., Miorin, M., Facco, M., Bonamico, S., Baesso, I., Grego, F., . . . Avogaro, A. (2005). Circulating endothelial progenitor cells are reduced in peripheral vascular complications of type 2 diabetes mellitus. *J Am Coll Cardiol, 45*(9), 1449-1457. doi:10.1016/j.jacc.2004.11.067
Fadini, G. P., Sartore, S., Albiero, M., Baesso, I., Murphy, E., Menegolo, M., . . . Avogaro, A. (2006). Number and function of endothelial progenitor cells as a marker of severity for diabetic vasculopathy. *Arterioscler Thromb Vasc Biol, 26*(9), 2140-2146. doi:10.1161/01.ATV.0000237750.44469.88
Fager, G. (1995). Thrombin and proliferation of vascular smooth muscle cells. *Circ Res, 77*(4), 645-650.
Fan, W., Wu, X., Ding, B., Gao, J., Cai, Z., Zhang, W., . . . Gao, S. (2012). Degradable gene delivery systems based on Pluronics-modified low-molecular-weight polyethylenimine: preparation, characterization, intracellular trafficking, and cellular distribution. *Int J Nanomedicine, 7*, 1127-1138. doi:10.2147/IJN.S27117
Fan, Y., Shen, F., Frenzel, T., Zhu, W., Ye, J., Liu, J., . . . Yang, G. Y. (2010). Endothelial progenitor cell transplantation improves long-term stroke outcome in mice. *Ann Neurol, 67*(4), 488-497. doi:10.1002/ana.21919
Fang, S., Wei, J., Pentinmikko, N., Leinonen, H., & Salven, P. (2012). Generation of functional blood vessels from a single c-kit+ adult vascular endothelial stem cell. *PLoS Biol, 10*(10), e1001407. doi:10.1371/journal.pbio.1001407
Fang, Y., & Davies, P. F. (2012). Site-specific microRNA-92a regulation of Kruppel-like factors 4 and 2 in atherosusceptible endothelium. *Arterioscler Thromb Vasc Biol, 32*(4), 979-987. doi:10.1161/ATVBAHA.111.244053
Felgner, P. L., Gadek, T. R., Holm, M., Roman, R., Chan, H. W., Wenz, M., . . . Danielsen, M. (1987). Lipofection: a highly efficient, lipid-mediated DNA-transfection procedure. *Proc Natl Acad Sci U S A, 84*(21), 7413-7417.
Felschow, D. M., McVeigh, M. L., Hoehn, G. T., Civin, C. I., & Fackler, M. J. (2001). The adapter protein CrkL associates with CD34. *Blood, 97*(12), 3768-3775.
Ferrara, N. (2001). Role of vascular endothelial growth factor in regulation of physiological angiogenesis. *Am J Physiol Cell Physiol, 280*(6), C1358-1366.
Fichtlscherer, S., De Rosa, S., Fox, H., Schwietz, T., Fischer, A., Liebetrau, C., . . . Dimmeler, S. (2010). Circulating microRNAs in patients with coronary artery disease. *Circ Res, 107*(5), 677-684. doi:10.1161/CIRCRESAHA.109.215566
Filipowicz, W., Bhattacharyya, S. N., & Sonenberg, N. (2008). Mechanisms of post-transcriptional regulation by microRNAs: are the answers in sight? *Nat Rev Genet, 9*(2), 102-114. doi:10.1038/nrg2290
Fina, L., Molgaard, H. V., Robertson, D., Bradley, N. J., Monaghan, P., Delia, D., . . . Greaves, M. F. (1990). Expression of the CD34 gene in vascular endothelial cells. *Blood, 75*(12), 2417-2426.
Fisher, S. A., Zhang, H., Doree, C., Mathur, A., & Martin-Rendon, E. (2015). Stem cell treatment for acute myocardial infarction. *Cochrane Database Syst Rev*(9), CD006536. doi:10.1002/14651858.CD006536.pub4
Flamme, I., & Risau, W. (1992). Induction of vasculogenesis and hematopoiesis in vitro. *Development, 116*(2), 435-439.

Fledderus, J. O., Boon, R. A., Volger, O. L., Hurttila, H., Yla-Herttuala, S., Pannekoek, H., . . . Horrevoets, A. J. (2008). KLF2 primes the antioxidant transcription factor Nrf2 for activation in endothelial cells. *Arterioscler Thromb Vasc Biol, 28*(7), 1339-1346. doi:10.1161/ATVBAHA.108.165811

Fleming, I., & Busse, R. (2003). Molecular mechanisms involved in the regulation of the endothelial nitric oxide synthase. *Am J Physiol Regul Integr Comp Physiol, 284*(1), R1-12. doi:10.1152/ajpregu.00323.2002

Fleming, Y., Armstrong, C. G., Morrice, N., Paterson, A., Goedert, M., & Cohen, P. (2000). Synergistic activation of stress-activated protein kinase 1/c-Jun N-terminal kinase (SAPK1/JNK) isoforms by mitogen-activated protein kinase kinase 4 (MKK4) and MKK7. *Biochem J, 352 Pt 1*, 145-154.

Forte, A., Rinaldi, B., Berrino, L., Rossi, F., Galderisi, U., & Cipollaro, M. (2014). Novel potential targets for prevention of arterial restenosis: insights from the pre-clinical research. *Clin Sci (Lond), 127*(11), 615-634. doi:10.1042/CS20140131

Foubert, P., Silvestre, J. S., Souttou, B., Barateau, V., Martin, C., Ebrahimian, T. G., . . . Le Ricousse-Roussanne, S. (2007). PSGL-1-mediated activation of EphB4 increases the proangiogenic potential of endothelial progenitor cells. *J Clin Invest, 117*(6), 1527-1537. doi:10.1172/JCI28338

Francis, S. E., Goh, K. L., Hodivala-Dilke, K., Bader, B. L., Stark, M., Davidson, D., & Hynes, R. O. (2002). Central roles of alpha5beta1 integrin and fibronectin in vascular development in mouse embryos and embryoid bodies. *Arterioscler Thromb Vasc Biol, 22*(6), 927-933.

Frederick, J. R., Fitzpatrick, J. R., 3rd, McCormick, R. C., Harris, D. A., Kim, A. Y., Muenzer, J. R., . . . Woo, Y. J. (2010). Stromal cell-derived factor-1alpha activation of tissue-engineered endothelial progenitor cell matrix enhances ventricular function after myocardial infarction by inducing neovasculogenesis. *Circulation, 122*(11 Suppl), S107-117. doi:10.1161/CIRCULATIONAHA.109.930404

Friedman, R. C., Farh, K. K., Burge, C. B., & Bartel, D. P. (2009). Most mammalian mRNAs are conserved targets of microRNAs. *Genome Res, 19*(1), 92-105. doi:10.1101/gr.082701.108

Friedrich, E. B., Walenta, K., Scharlau, J., Nickenig, G., & Werner, N. (2006). CD34-/CD133+/VEGFR-2+ endothelial progenitor cell subpopulation with potent vasoregenerative capacities. *Circ Res, 98*(3), e20-25. doi:10.1161/01.RES.0000205765.28940.93

Fromm, M. F. (2000). P-glycoprotein: a defense mechanism limiting oral bioavailability and CNS accumulation of drugs. *Int J Clin Pharmacol Ther, 38*(2), 69-74.

Fujii, H., Li, S. H., Szmitko, P. E., Fedak, P. W., & Verma, S. (2006). C-reactive protein alters antioxidant defenses and promotes apoptosis in endothelial progenitor cells. *Arterioscler Thromb Vasc Biol, 26*(11), 2476-2482. doi:10.1161/01.ATV.0000242794.65541.02

Fujio, Y., & Walsh, K. (1999). Akt mediates cytoprotection of endothelial cells by vascular endothelial growth factor in an anchorage-dependent manner. *J Biol Chem, 274*(23), 16349-16354.

Fujiyama, S., Amano, K., Uehira, K., Yoshida, M., Nishiwaki, Y., Nozawa, Y., . . . Matsubara, H. (2003). Bone marrow monocyte lineage cells adhere on injured endothelium in a monocyte chemoattractant protein-1-dependent manner and accelerate reendothelialization as endothelial progenitor cells. *Circ Res, 93*(10), 980-989. doi:10.1161/01.RES.0000099245.08637.CE

Fuster, V., Moreno, P. R., Fayad, Z. A., Corti, R., & Badimon, J. J. (2005). Atherothrombosis and high-risk plaque: part I: evolving concepts. *J Am Coll Cardiol, 46*(6), 937-954. doi:10.1016/j.jacc.2005.03.074

Gallagher, K. A., Liu, Z. J., Xiao, M., Chen, H., Goldstein, L. J., Buerk, D. G., . . . Velazquez, O. C. (2007). Diabetic impairments in NO-mediated endothelial progenitor cell mobilization

and homing are reversed by hyperoxia and SDF-1 alpha. *J Clin Invest, 117*(5), 1249-1259. doi:10.1172/JCI29710

Gao, D., Nolan, D. J., Mellick, A. S., Bambino, K., McDonnell, K., & Mittal, V. (2008). Endothelial progenitor cells control the angiogenic switch in mouse lung metastasis. *Science, 319*(5860), 195-198. doi:10.1126/science.1150224

Gao, L., Li, P., Zhang, J., Hagiwara, M., Shen, B., Bledsoe, G., . . . Chao, J. (2014). Novel role of kallistatin in vascular repair by promoting mobility, viability, and function of endothelial progenitor cells. *J Am Heart Assoc, 3*(5), e001194. doi:10.1161/JAHA.114.001194

Gao, M., Yao, Q., Liu, Y., Sun, F., Ma, Y., & Sun, G. (2015). Association between mobilization of circulating endothelial progenitor cells and time or degree of injury from angioplasty in patients with exertional angina: A prospective study. *Exp Ther Med, 10*(2), 809-815. doi:10.3892/etm.2015.2571

Gao, X., Yourick, J. J., & Sprando, R. L. (2017). Comparative transcriptomic analysis of endothelial progenitor cells derived from umbilical cord blood and adult peripheral blood: Implications for the generation of induced pluripotent stem cells. *Stem Cell Res, 25*, 202-212. doi:10.1016/j.scr.2017.11.004

Garcia de la Torre, N., Fernandez-Durango, R., Gomez, R., Fuentes, M., Roldan-Pallares, M., Donate, J., . . . Calle-Pascual, A. L. (2015). Expression of Angiogenic MicroRNAs in Endothelial Progenitor Cells From Type 1 Diabetic Patients With and Without Diabetic Retinopathy. *Invest Ophthalmol Vis Sci, 56*(6), 4090-4098. doi:10.1167/iovs.15-16498

Gareri, C., De Rosa, S., & Indolfi, C. (2016). MicroRNAs for Restenosis and Thrombosis After Vascular Injury. *Circ Res, 118*(7), 1170-1184. doi:10.1161/CIRCRESAHA.115.308237

Garg, R., Tellez, A., Alviar, C., Granada, J., Kleiman, N. S., & Lev, E. I. (2008). The effect of percutaneous coronary intervention on inflammatory response and endothelial progenitor cell recruitment. *Catheter Cardiovasc Interv, 72*(2), 205-209. doi:10.1002/ccd.21611

Gehling, U. M., Ergun, S., Schumacher, U., Wagener, C., Pantel, K., Otte, M., . . . Fiedler, W. (2000). In vitro differentiation of endothelial cells from AC133-positive progenitor cells. *Blood, 95*(10), 3106-3112.

Gerhard, M., Roddy, M. A., Creager, S. J., & Creager, M. A. (1996). Aging progressively impairs endothelium-dependent vasodilation in forearm resistance vessels of humans. *Hypertension, 27*(4), 849-853.

Giannotti, G., Doerries, C., Mocharla, P. S., Mueller, M. F., Bahlmann, F. H., Horvath, T., . . . Landmesser, U. (2010). Impaired endothelial repair capacity of early endothelial progenitor cells in prehypertension: relation to endothelial dysfunction. *Hypertension, 55*(6), 1389-1397. doi:10.1161/HYPERTENSIONAHA.109.141614

Gibbings, D., & Voinnet, O. (2010). Control of RNA silencing and localization by endolysosomes. *Trends Cell Biol, 20*(8), 491-501. doi:S0962-8924(10)00107-8 [pii]

10.1016/j.tcb.2010.06.001

Gibbings, D. J., Ciaudo, C., Erhardt, M., & Voinnet, O. (2009). Multivesicular bodies associate with components of miRNA effector complexes and modulate miRNA activity. *Nat Cell Biol, 11*(9), 1143-1149. doi:ncb1929 [pii]

10.1038/ncb1929

Gifford, S. M., Grummer, M. A., Pierre, S. A., Austin, J. L., Zheng, J., & Bird, I. M. (2004). Functional characterization of HUVEC-CS: Ca2+ signaling, ERK 1/2 activation, mitogenesis and vasodilator production. *J Endocrinol, 182*(3), 485-499.

Gill, M., Dias, S., Hattori, K., Rivera, M. L., Hicklin, D., Witte, L., . . . Rafii, S. (2001). Vascular trauma induces rapid but transient mobilization of VEGFR2(+)AC133(+) endothelial precursor cells. *Circ Res, 88*(2), 167-174.

Goh, K. L., Yang, J. T., & Hynes, R. O. (1997). Mesodermal defects and cranial neural crest apoptosis in alpha5 integrin-null embryos. *Development, 124*(21), 4309-4319.

Golebiewska, A., Brons, N. H., Bjerkvig, R., & Niclou, S. P. (2011). Critical appraisal of the side population assay in stem cell and cancer stem cell research. *Cell stem cell, 8*(2), 136-147. doi:10.1016/j.stem.2011.01.007

Goligorsky, M. S., Li, H., Brodsky, S., & Chen, J. (2002). Relationships between caveolae and eNOS: everything in proximity and the proximity of everything. *American journal of physiology. Renal physiology, 283*(1), F1-10. doi:10.1152/ajprenal.00377.2001

Gomes, R. S., das Neves, R. P., Cochlin, L., Lima, A., Carvalho, R., Korpisalo, P., . . . Ferreira, L. (2013). Efficient pro-survival/angiogenic miRNA delivery by an MRI-detectable nanomaterial. *ACS Nano, 7*(4), 3362-3372. doi:10.1021/nn400171w

Goussetis, E., Manginas, A., Koutelou, M., Peristeri, I., Theodosaki, M., Kollaros, N., . . . Graphakos, S. (2006). Intracoronary infusion of CD133+ and CD133-CD34+ selected autologous bone marrow progenitor cells in patients with chronic ischemic cardiomyopathy: cell isolation, adherence to the infarcted area, and body distribution. *Stem Cells, 24*(10), 2279-2283. doi:10.1634/stemcells.2005-0589

Grant, M. B., May, W. S., Caballero, S., Brown, G. A., Guthrie, S. M., Mames, R. N., . . . Scott, E. W. (2002). Adult hematopoietic stem cells provide functional hemangioblast activity during retinal neovascularization. *Nat Med, 8*(6), 607-612. doi:10.1038/nm0602-607

Green, C. E., Pearson, D. N., Camphausen, R. T., Staunton, D. E., & Simon, S. I. (2004). Shear-dependent capping of L-selectin and P-selectin glycoprotein ligand 1 by E-selectin signals activation of high-avidity beta2-integrin on neutrophils. *J Immunol, 172*(12), 7780-7790.

Gregory, R. I., Yan, K. P., Amuthan, G., Chendrimada, T., Doratotaj, B., Cooch, N., & Shiekhattar, R. (2004). The Microprocessor complex mediates the genesis of microRNAs. *Nature, 432*(7014), 235-240. doi:10.1038/nature03120

Grewal, S. S., Barker, J. N., Davies, S. M., & Wagner, J. E. (2003). Unrelated donor hematopoietic cell transplantation: marrow or umbilical cord blood? *Blood, 101*(11), 4233-4244. doi:10.1182/blood-2002-08-2510

Griese, D. P., Ehsan, A., Melo, L. G., Kong, D., Zhang, L., Mann, M. J., . . . Dzau, V. J. (2003). Isolation and transplantation of autologous circulating endothelial cells into denuded vessels and prosthetic grafts: implications for cell-based vascular therapy. *Circulation, 108*(21), 2710-2715. doi:10.1161/01.CIR.0000096490.16596.A6

Grunewald, M., Avraham, I., Dor, Y., Bachar-Lustig, E., Itin, A., Jung, S., . . . Keshet, E. (2006). VEGF-induced adult neovascularization: recruitment, retention, and role of accessory cells. *Cell, 124*(1), 175-189. doi:10.1016/j.cell.2005.10.036

Guil, S., & Caceres, J. F. (2007). The multifunctional RNA-binding protein hnRNP A1 is required for processing of miR-18a. *Nat Struct Mol Biol, 14*(7), 591-596. doi:10.1038/nsmb1250

Gulati, R., Jevremovic, D., Peterson, T. E., Chatterjee, S., Shah, V., Vile, R. G., & Simari, R. D. (2003). Diverse origin and function of cells with endothelial phenotype obtained from adult human blood. *Circ Res, 93*(11), 1023-1025. doi:10.1161/01.RES.0000105569.77539.21

Gunsilius, E., Duba, H. C., Petzer, A. L., Kahler, C. M., Grunewald, K., Stockhammer, G., . . . Gastl, G. (2000). Evidence from a leukaemia model for maintenance of vascular endothelium by bone-marrow-derived endothelial cells. *Lancet, 355*(9216), 1688-1691. doi:10.1016/S0140-6736(00)02241-8

Gvili, K., Benny, O., Danino, D., & Machluf, M. (2007). Poly(D,L-lactide-co-glycolide acid) nanoparticles for DNA delivery: waiving preparation complexity and increasing efficiency. *Biopolymers, 85*(5-6), 379-391. doi:10.1002/bip.20697

Haider, K. H., Aziz, S., & Al-Reshidi, M. A. (2017). Endothelial progenitor cells for cellular angiogenesis and repair: lessons learned from experimental animal models. *Regen Med, 12*(8), 969-982. doi:10.2217/rme-2017-0074

Hall, A. (1998). Rho GTPases and the actin cytoskeleton. *Science, 279*(5350), 509-514.

Halper, J. (2018). Basic Components of Vascular Connective Tissue and Extracellular Matrix. *Adv Pharmacol, 81*, 95-127. doi:10.1016/bs.apha.2017.08.012

Hamik, A., Lin, Z., Kumar, A., Balcells, M., Sinha, S., Katz, J., . . . Jain, M. K. (2007). Kruppel-like factor 4 regulates endothelial inflammation. *J Biol Chem, 282*(18), 13769-13779. doi:10.1074/jbc.M700078200

Hammond, S. M. (2005). Dicing and slicing: the core machinery of the RNA interference pathway. *FEBS Lett, 579*(26), 5822-5829. doi:10.1016/j.febslet.2005.08.079

Handgretinger, R., Gordon, P. R., Leimig, T., Chen, X., Buhring, H. J., Niethammer, D., & Kuci, S. (2003). Biology and plasticity of CD133+ hematopoietic stem cells. *Ann N Y Acad Sci, 996*, 141-151.

Hao, Q. L., Shah, A. J., Thiemann, F. T., Smogorzewska, E. M., & Crooks, G. M. (1995). A functional comparison of CD34 + CD38- cells in cord blood and bone marrow. *Blood, 86*(10), 3745-3753.

Harraz, M., Jiao, C., Hanlon, H. D., Hartley, R. S., & Schatteman, G. C. (2001). CD34- blood-derived human endothelial cell progenitors. *Stem Cells, 19*(4), 304-312. doi:10.1634/stemcells.19-4-304

Haug, B. H., Henriksen, J. R., Buechner, J., Geerts, D., Tomte, E., Kogner, P., . . . Einvik, C. (2011). MYCN-regulated miRNA-92 inhibits secretion of the tumor suppressor DICKKOPF-3 (DKK3) in neuroblastoma. *Carcinogenesis, 32*(7), 1005-1012. doi:10.1093/carcin/bgr073

Hausser, J., & Zavolan, M. (2014). Identification and consequences of miRNA-target interactions--beyond repression of gene expression. *Nat Rev Genet, 15*(9), 599-612. doi:10.1038/nrg3765

Hayashi, T., Matsui-Hirai, H., Miyazaki-Akita, A., Fukatsu, A., Funami, J., Ding, Q. F., . . . Iguchi, A. (2006). Endothelial cellular senescence is inhibited by nitric oxide: implications in atherosclerosis associated with menopause and diabetes. *Proc Natl Acad Sci U S A, 103*(45), 17018-17023. doi:10.1073/pnas.0607873103

Hayashita, Y., Osada, H., Tatematsu, Y., Yamada, H., Yanagisawa, K., Tomida, S., . . . Takahashi, T. (2005). A polycistronic microRNA cluster, miR-17-92, is overexpressed in human lung cancers and enhances cell proliferation. *Cancer research, 65*(21), 9628-9632. doi:10.1158/0008-5472.CAN-05-2352

He, M., Gong, Y., Shi, J., Pan, Z., Zou, H., Sun, D., . . . Li, Y. (2014). Plasma microRNAs as potential noninvasive biomarkers for in-stent restenosis. *PLoS One, 9*(11), e112043. doi:10.1371/journal.pone.0112043

Healy, L., May, G., Gale, K., Grosveld, F., Greaves, M., & Enver, T. (1995). The stem cell antigen CD34 functions as a regulator of hemopoietic cell adhesion. *Proc Natl Acad Sci U S A, 92*(26), 12240-12244.

Heinrich, E. M., & Dimmeler, S. (2012). MicroRNAs and stem cells: control of pluripotency, reprogramming, and lineage commitment. *Circ Res, 110*(7), 1014-1022. doi:10.1161/CIRCRESAHA.111.243394

Heiss, C., Keymel, S., Niesler, U., Ziemann, J., Kelm, M., & Kalka, C. (2005). Impaired progenitor cell activity in age-related endothelial dysfunction. *J Am Coll Cardiol, 45*(9), 1441-1448. doi:10.1016/j.jacc.2004.12.074

Heissig, B., Hattori, K., Dias, S., Friedrich, M., Ferris, B., Hackett, N. R., . . . Rafii, S. (2002). Recruitment of stem and progenitor cells from the bone marrow niche requires MMP-9 mediated release of kit-ligand. *Cell, 109*(5), 625-637.

Hering, B. J., Romann, D., Clarius, A., Brendel, M., Slijepcevic, M., Bretzel, R. G., & Federlin, K. (1989). Bovine islets of Langerhans. Potential source for transplantation? *Diabetes, 38 Suppl 1*, 206-208.

Herrmann, M., Binder, A., Menzel, U., Zeiter, S., Alini, M., & Verrier, S. (2014). CD34/CD133 enriched bone marrow progenitor cells promote neovascularization of tissue engineered constructs in vivo. *Stem Cell Res, 13*(3 Pt A), 465-477. doi:10.1016/j.scr.2014.10.005

Hildbrand, P., Cirulli, V., Prinsen, R. C., Smith, K. A., Torbett, B. E., Salomon, D. R., & Crisa, L. (2004). The role of angiopoietins in the development of endothelial cells from cord blood CD34+ progenitors. *Blood, 104*(7), 2010-2019. doi:10.1182/blood-2003-12-4219

Hill, J. M., Zalos, G., Halcox, J. P., Schenke, W. H., Waclawiw, M. A., Quyyumi, A. A., & Finkel, T. (2003). Circulating endothelial progenitor cells, vascular function, and cardiovascular risk. *N Engl J Med, 348*(7), 593-600. doi:10.1056/NEJMoa022287

Hinkel, R., Penzkofer, D., Zuhlke, S., Fischer, A., Husada, W., Xu, Q. F., . . . Dimmeler, S. (2013). Inhibition of microRNA-92a protects against ischemia/reperfusion injury in a large-animal model. *Circulation, 128*(10), 1066-1075. doi:10.1161/CIRCULATIONAHA.113.001904

Hirschi, K. K., Ingram, D. A., & Yoder, M. C. (2008). Assessing identity, phenotype, and fate of endothelial progenitor cells. *Arterioscler Thromb Vasc Biol, 28*(9), 1584-1595. doi:10.1161/ATVBAHA.107.155960

Holmes, K., Roberts, O. L., Thomas, A. M., & Cross, M. J. (2007). Vascular endothelial growth factor receptor-2: structure, function, intracellular signalling and therapeutic inhibition. *Cell Signal, 19*(10), 2003-2012. doi:10.1016/j.cellsig.2007.05.013

Hong, S., Ergezen, E., Lec, R., & Barbee, K. A. (2006). Real-time analysis of cell-surface adhesive interactions using thickness shear mode resonator. *Biomaterials, 27*(34), 5813-5820. doi:10.1016/j.biomaterials.2006.07.031

Horisawa, E., Kubota, K., Tuboi, I., Sato, K., Yamamoto, H., Takeuchi, H., & Kawashima, Y. (2002). Size-dependency of DL-lactide/glycolide copolymer particulates for intra-articular delivery system on phagocytosis in rat synovium. *Pharm Res, 19*(2), 132-139.

Hossain, A., Kuo, M. T., & Saunders, G. F. (2006). Mir-17-5p regulates breast cancer cell proliferation by inhibiting translation of AIB1 mRNA. *Mol Cell Biol, 26*(21), 8191-8201. doi:10.1128/MCB.00242-06

Hou, D., Youssef, E. A., Brinton, T. J., Zhang, P., Rogers, P., Price, E. T., . . . March, K. L. (2005). Radiolabeled cell distribution after intramyocardial, intracoronary, and interstitial retrograde coronary venous delivery: implications for current clinical trials. *Circulation, 112*(9 Suppl), I150-156. doi:10.1161/CIRCULATIONAHA.104.526749

Hristov, M., Erl, W., & Weber, P. C. (2003). Endothelial progenitor cells: mobilization, differentiation, and homing. *Arterioscler Thromb Vasc Biol, 23*(7), 1185-1189. doi:10.1161/01.ATV.0000073832.49290.B5

Hristov, M., & Weber, C. (2008). Endothelial progenitor cells in vascular repair and remodeling. *Pharmacol Res, 58*(2), 148-151. doi:10.1016/j.phrs.2008.07.008

Hristov, M., Zernecke, A., Bidzhekov, K., Liehn, E. A., Shagdarsuren, E., Ludwig, A., & Weber, C. (2007). Importance of CXC chemokine receptor 2 in the homing of human peripheral blood endothelial progenitor cells to sites of arterial injury. *Circ Res, 100*(4), 590-597. doi:01.RES.0000259043.42571.68 [pii]

10.1161/01.RES.0000259043.42571.68

Hristov, M., Zernecke, A., Liehn, E. A., & Weber, C. (2007). Regulation of endothelial progenitor cell homing after arterial injury. *Thromb Haemost, 98*(2), 274-277.

Hu, Y., Davison, F., Zhang, Z., & Xu, Q. (2003). Endothelial replacement and angiogenesis in arteriosclerotic lesions of allografts are contributed by circulating progenitor cells. *Circulation, 108*(25), 3122-3127. doi:10.1161/01.CIR.0000105722.96112.67

Huang, J. G. L., T.; Gu, F. X. (2011). Emerging Nanomaterials for Targeting Subcellular Organelles. *6*.

Huang, P. H., Chen, Y. H., Chen, Y. L., Wu, T. C., Chen, J. W., & Lin, S. J. (2007). Vascular endothelial function and circulating endothelial progenitor cells in patients with cardiac syndrome X. *Heart, 93*(9), 1064-1070. doi:10.1136/hrt.2006.107763

Huang, Z., Huang, D., Ni, S., Peng, Z., Sheng, W., & Du, X. (2010). Plasma microRNAs are promising novel biomarkers for early detection of colorectal cancer. *Int J Cancer, 127*(1), 118-126. doi:10.1002/ijc.25007

Humphries, J. D., Byron, A., & Humphries, M. J. (2006). Integrin ligands at a glance. *J Cell Sci, 119*(Pt 19), 3901-3903. doi:119/19/3901 [pii]

10.1242/jcs.03098

Hur, J., Yang, H. M., Yoon, C. H., Lee, C. S., Park, K. W., Kim, J. H., . . . Kim, H. S. (2007). Identification of a novel role of T cells in postnatal vasculogenesis: characterization of endothelial progenitor cell colonies. *Circulation, 116*(15), 1671-1682. doi:10.1161/CIRCULATIONAHA.107.694778

Hur, J., Yoon, C. H., Kim, H. S., Choi, J. H., Kang, H. J., Hwang, K. K., . . . Park, Y. B. (2004). Characterization of two types of endothelial progenitor cells and their different contributions to neovasculogenesis. *Arterioscler Thromb Vasc Biol, 24*(2), 288-293. doi:10.1161/01.ATV.0000114236.77009.06

Hutter, R., Carrick, F. E., Valdiviezo, C., Wolinsky, C., Rudge, J. S., Wiegand, S. J., . . . Sauter, B. V. (2004). Vascular endothelial growth factor regulates reendothelialization and neointima formation in a mouse model of arterial injury. *Circulation, 110*(16), 2430-2435. doi:10.1161/01.CIR.0000145120.37891.8A

Hutvagner, G., Simard, M. J., Mello, C. C., & Zamore, P. D. (2004). Sequence-specific inhibition of small RNA function. *PLoS Biol, 2*(4), E98. doi:10.1371/journal.pbio.0020098

Hynes, R. O. (2002). Integrins: bidirectional, allosteric signaling machines. *Cell, 110*(6), 673-687.

Iaconetti, C., Gareri, C., Polimeni, A., & Indolfi, C. (2013). Non-coding RNAs: the "dark matter" of cardiovascular pathophysiology. *Int J Mol Sci, 14*(10), 19987-20018. doi:10.3390/ijms141019987

Iaconetti, C., Polimeni, A., Sorrentino, S., Sabatino, J., Pironti, G., Esposito, G., . . . Indolfi, C. (2012). Inhibition of miR-92a increases endothelial proliferation and migration in vitro as well as reduces neointimal proliferation in vivo after vascular injury. *Basic Res Cardiol, 107*(5), 296. doi:10.1007/s00395-012-0296-y

Ignarro, L. J., Napoli, C., & Loscalzo, J. (2002). Nitric oxide donors and cardiovascular agents modulating the bioactivity of nitric oxide: an overview. *Circ Res, 90*(1), 21-28.

Ii, M., Takenaka, H., Asai, J., Ibusuki, K., Mizukami, Y., Maruyama, K., . . . Losordo, D. W. (2006). Endothelial progenitor thrombospondin-1 mediates diabetes-induced delay in reendothelialization following arterial injury. *Circ Res, 98*(5), 697-704. doi:10.1161/01.RES.0000209948.50943.ea

Ikutomi, M., Sahara, M., Nakajima, T., Minami, Y., Morita, T., Hirata, Y., . . . Sata, M. (2015). Diverse contribution of bone marrow-derived late-outgrowth endothelial progenitor cells to vascular repair under pulmonary arterial hypertension and arterial neointimal formation. *J Mol Cell Cardiol, 86*, 121-135. doi:10.1016/j.yjmcc.2015.07.019

Imanishi, T., Moriwaki, C., Hano, T., & Nishio, I. (2005). Endothelial progenitor cell senescence is accelerated in both experimental hypertensive rats and patients with essential hypertension. *J Hypertens, 23*(10), 1831-1837.

Imbert, A. M., Belaaloui, G., Bardin, F., Tonnelle, C., Lopez, M., & Chabannon, C. (2006). CD99 expressed on human mobilized peripheral blood CD34+ cells is involved in transendothelial migration. *Blood, 108*(8), 2578-2586. doi:10.1182/blood-2005-12-010827

Indolfi, C., Torella, D., Coppola, C., Curcio, A., Rodriguez, F., Bilancio, A., . . . Chiariello, M. (2002). Physical training increases eNOS vascular expression and activity and reduces restenosis after balloon angioplasty or arterial stenting in rats. *Circ Res, 91*(12), 1190-1197.

Ingram, D. A., Caplice, N. M., & Yoder, M. C. (2005). Unresolved questions, changing definitions, and novel paradigms for defining endothelial progenitor cells. *Blood, 106*(5), 1525-1531. doi:10.1182/blood-2005-04-1509

Ingram, D. A., Mead, L. E., Moore, D. B., Woodard, W., Fenoglio, A., & Yoder, M. C. (2005). Vessel wall-derived endothelial cells rapidly proliferate because they contain a

complete hierarchy of endothelial progenitor cells. *Blood, 105*(7), 2783-2786. doi:10.1182/blood-2004-08-3057

Ingram, D. A., Mead, L. E., Tanaka, H., Meade, V., Fenoglio, A., Mortell, K., . . . Yoder, M. C. (2004). Identification of a novel hierarchy of endothelial progenitor cells using human peripheral and umbilical cord blood. *Blood, 104*(9), 2752-2760. doi:10.1182/blood-2004-04-1396

Inoue, T., Sata, M., Hikichi, Y., Sohma, R., Fukuda, D., Uchida, T., . . . Node, K. (2007). Mobilization of CD34-positive bone marrow-derived cells after coronary stent implantation: impact on restenosis. *Circulation, 115*(5), 553-561. doi:10.1161/CIRCULATIONAHA.106.621714

Inoue, T., Taguchi, I., Abe, S., Toyoda, S., Nakajima, K., Sakuma, M., & Node, K. (2011). Activation of matrix metalloproteinase-9 is associated with mobilization of bone marrow-derived cells after coronary stent implantation. *Int J Cardiol, 152*(3), 332-336. doi:10.1016/j.ijcard.2010.07.028

Issler, O., & Chen, A. (2015). Determining the role of microRNAs in psychiatric disorders. *Nat Rev Neurosci, 16*(4), 201-212. doi:10.1038/nrn3879

Iwaguro, H., Yamaguchi, J., Kalka, C., Murasawa, S., Masuda, H., Hayashi, S., . . . Asahara, T. (2002). Endothelial progenitor cell vascular endothelial growth factor gene transfer for vascular regeneration. *Circulation, 105*(6), 732-738.

Iwakura, A., Luedemann, C., Shastry, S., Hanley, A., Kearney, M., Aikawa, R., . . . Losordo, D. W. (2003). Estrogen-mediated, endothelial nitric oxide synthase-dependent mobilization of bone marrow-derived endothelial progenitor cells contributes to reendothelialization after arterial injury. *Circulation, 108*(25), 3115-3121. doi:10.1161/01.CIR.0000106906.56972.83

Jaatinen, T., & Laine, J. (2007). Isolation of mononuclear cells from human cord blood by Ficoll-Paque density gradient. *Curr Protoc Stem Cell Biol, Chapter 2*, Unit 2A 1. doi:10.1002/9780470151808.sc02a01s1

Jang, J. H., Kim, S. K., Choi, J. E., Kim, Y. J., Lee, H. W., Kang, S. Y., . . . Kim, H. C. (2007). Endothelial progenitor cell differentiation using cryopreserved, umbilical cord blood-derived mononuclear cells. *Acta Pharmacol Sin, 28*(3), 367-374. doi:10.1111/j.1745-7254.2007.00519.x

Jang, S. I., Kim, J. H., Kim, M., Yang, S., Jo, E. A., Lee, J. W., . . . Lee, D. K. (2012). Porcine feasibility and safety study of a new paclitaxel-eluting biliary stent with a Pluronic-containing membrane. *Endoscopy, 44*(9), 825-831. doi:10.1055/s-0032-1309881

Janic, B., & Arbab, A. S. (2012). Cord blood endothelial progenitor cells as therapeutic and imaging probes. *Imaging Med, 4*(4), 477-490. doi:10.2217/iim.12.35

Janic, B., Guo, A. M., Iskander, A. S., Varma, N. R., Scicli, A. G., & Arbab, A. S. (2010). Human cord blood-derived AC133+ progenitor cells preserve endothelial progenitor characteristics after long term in vitro expansion. *PLoS One, 5*(2), e9173. doi:10.1371/journal.pone.0009173

Jevnaker, A. M., Khuu, C., Kjole, E., Bryne, M., & Osmundsen, H. (2011). Expression of members of the miRNA17-92 cluster during development and in carcinogenesis. *J Cell Physiol, 226*(9), 2257-2266. doi:10.1002/jcp.22562

Ji, R., Cheng, Y., Yue, J., Yang, J., Liu, X., Chen, H., . . . Zhang, C. (2007). MicroRNA expression signature and antisense-mediated depletion reveal an essential role of MicroRNA in vascular neointimal lesion formation. *Circ Res, 100*(11), 1579-1588. doi:10.1161/CIRCRESAHA.106.141986

Jiang, M., He, B., Zhang, Q., Ge, H., Zang, M. H., Han, Z. H., . . . Yin, X. Y. (2010). Randomized controlled trials on the therapeutic effects of adult progenitor cells for myocardial infarction: meta-analysis. *Expert opinion on biological therapy, 10*(5), 667-680. doi:10.1517/14712591003716437

Jiang, Y., Wang, H. Y., Li, Y., Guo, S. H., Zhang, L., & Cai, J. H. (2015). Peripheral blood miRNAs as a biomarker for chronic cardiovascular diseases (vol 4, pg 5026, 2014). *Scientific Reports, 5*. doi:ARTN 8178

10.1038/srep08178

Jin, H., Aiyer, A., Su, J., Borgstrom, P., Stupack, D., Friedlander, M., & Varner, J. (2006). A homing mechanism for bone marrow-derived progenitor cell recruitment to the neovasculature. *J Clin Invest, 116*(3), 652-662. doi:10.1172/JCI24751

Jin, H. Y., Gonzalez-Martin, A., Miletic, A. V., Lai, M., Knight, S., Sabouri-Ghomi, M., . . . Xiao, C. (2015). Transfection of microRNA Mimics Should Be Used with Caution. *Front Genet, 6*, 340. doi:10.3389/fgene.2015.00340

Johansson, S., Svineng, G., Wennerberg, K., Armulik, A., & Lohikangas, L. (1997). Fibronectin-integrin interactions. *Front Biosci, 2*, d126-146.

John, B., Enright, A. J., Aravin, A., Tuschl, T., Sander, C., & Marks, D. S. (2004). Human MicroRNA targets. *PLoS Biol, 2*(11), e363. doi:10.1371/journal.pbio.0020363

Jukema, J. W., Ahmed, T. A., Verschuren, J. J., & Quax, P. H. (2012). Restenosis after PCI. Part 2: prevention and therapy. *Nat Rev Cardiol, 9*(2), 79-90. doi:10.1038/nrcardio.2011.148

Jukema, J. W., Verschuren, J. J., Ahmed, T. A., & Quax, P. H. (2012). Restenosis after PCI. Part 1: pathophysiology and risk factors. *Nat Rev Cardiol, 9*(1), 53-62. doi:10.1038/nrcardio.2011.132

Kachamakova-Trojanowska, N., Bukowska-Strakova, K., Zukowska, M., Dulak, J., & Jozkowicz, A. (2015). The real face of endothelial progenitor cells - Circulating angiogenic cells as endothelial prognostic marker? *Pharmacol Rep, 67*(4), 793-802. doi:10.1016/j.pharep.2015.05.017

Kaiser, R., Friedrich, D., Chavakis, E., Bohm, M., & Friedrich, E. B. (2012). Effect of hypoxia on integrin-mediated adhesion of endothelial progenitor cells. *J Cell Mol Med, 16*(10), 2387-2393. doi:10.1111/j.1582-4934.2012.01553.x

Kalka, C., Masuda, H., Takahashi, T., Gordon, R., Tepper, O., Gravereaux, E., . . . Asahara, T. (2000). Vascular endothelial growth factor(165) gene transfer augments circulating endothelial progenitor cells in human subjects. *Circ Res, 86*(12), 1198-1202.

Kalka, C., Masuda, H., Takahashi, T., Kalka-Moll, W. M., Silver, M., Kearney, M., . . . Asahara, T. (2000). Transplantation of ex vivo expanded endothelial progenitor cells for therapeutic neovascularization. *Proc Natl Acad Sci U S A, 97*(7), 3422-3427. doi:10.1073/pnas.070046397

Kane, N. M., Meloni, M., Spencer, H. L., Craig, M. A., Strehl, R., Milligan, G., . . . Baker, A. H. (2010). Derivation of endothelial cells from human embryonic stem cells by directed differentiation: analysis of microRNA and angiogenesis in vitro and in vivo. *Arterioscler Thromb Vasc Biol, 30*(7), 1389-1397. doi:10.1161/ATVBAHA.110.204800

Kang, S., Yang, Y. J., Li, C. J., & Gao, R. L. (2008). Effects of intracoronary autologous bone marrow cells on left ventricular function in acute myocardial infarction: a systematic review and meta-analysis for randomized controlled trials. *Coronary artery disease, 19*(5), 327-335. doi:10.1097/MCA.0b013e328300dbd3

Kang, Y., Wang, F., Feng, J., Yang, D., Yang, X., & Yan, X. (2006). Knockdown of CD146 reduces the migration and proliferation of human endothelial cells. *Cell Res, 16*(3), 313-318. doi:10.1038/sj.cr.7310039

Karshovska, E., Zernecke, A., Sevilmis, G., Millet, A., Hristov, M., Cohen, C. D., . . . Schober, A. (2007). Expression of HIF-1alpha in injured arteries controls SDF-1alpha mediated neointima formation in apolipoprotein E deficient mice. *Arterioscler Thromb Vasc Biol, 27*(12), 2540-2547. doi:10.1161/ATVBAHA.107.151050

Katare, R., Riu, F., Mitchell, K., Gubernator, M., Campagnolo, P., Cui, Y., . . . Madeddu, P. (2011). Transplantation of human pericyte progenitor cells improves the repair of infarcted heart through activation of an angiogenic program involving micro-RNA-132. *Circ Res, 109*(8), 894-906. doi:10.1161/CIRCRESAHA.111.251546

Katoh, T., Sakaguchi, Y., Miyauchi, K., Suzuki, T., Kashiwabara, S., Baba, T., & Suzuki, T. (2009). Selective stabilization of mammalian microRNAs by 3' adenylation mediated by the cytoplasmic poly(A) polymerase GLD-2. *Genes Dev, 23*(4), 433-438. doi:10.1101/gad.1761509

Kawamoto, A., Iwasaki, H., Kusano, K., Murayama, T., Oyamada, A., Silver, M., . . . Losordo, D. W. (2006). CD34-positive cells exhibit increased potency and safety for therapeutic neovascularization after myocardial infarction compared with total mononuclear cells. *Circulation, 114*(20), 2163-2169. doi:10.1161/CIRCULATIONAHA.106.644518

Kawasaki, K., Watabe, T., Sase, H., Hirashima, M., Koide, H., Morishita, Y., . . . Miyazawa, K. (2008). Ras signaling directs endothelial specification of VEGFR2+ vascular progenitor cells. *J Cell Biol, 181*(1), 131-141. doi:10.1083/jcb.200709127

Kebir, A., Harhouri, K., Guillet, B., Liu, J. W., Foucault-Bertaud, A., Lamy, E., . . . Blot-Chabaud, M. (2010). CD146 short isoform increases the proangiogenic potential of endothelial progenitor cells in vitro and in vivo. *Circ Res, 107*(1), 66-75. doi:10.1161/CIRCRESAHA.109.213827

Kee, H. J., Kwon, J. S., Shin, S., Ahn, Y., Jeong, M. H., & Kook, H. (2011). Trichostatin A prevents neointimal hyperplasia via activation of Kruppel like factor 4. *Vascul Pharmacol, 55*(5-6), 127-134. doi:10.1016/j.vph.2011.07.001

Kekarainen, T., Mannelin, S., Laine, J., & Jaatinen, T. (2006). Optimization of immunomagnetic separation for cord blood-derived hematopoietic stem cells. *BMC Cell Biol, 7*, 30. doi:10.1186/1471-2121-7-30

Khalili, A. A., & Ahmad, M. R. (2015). A Review of Cell Adhesion Studies for Biomedical and Biological Applications. *Int J Mol Sci, 16*(8), 18149-18184. doi:10.3390/ijms160818149

Khan, A. A., Betel, D., Miller, M. L., Sander, C., Leslie, C. S., & Marks, D. S. (2009). Transfection of small RNAs globally perturbs gene regulation by endogenous microRNAs. *Nature biotechnology, 27*(6), 549-555. doi:10.1038/nbt.1543

Khvorova, A., Reynolds, A., & Jayasena, S. D. (2003). Functional siRNAs and miRNAs exhibit strand bias. *Cell, 115*(2), 209-216.

Kijima, Y., Ishikawa, M., Sunagawa, T., Nakanishi, K., Kamei, N., Yamada, K., . . . Ochi, M. (2009). Regeneration of peripheral nerve after transplantation of CD133+ cells derived from human peripheral blood. *J Neurosurg, 110*(4), 758-767. doi:10.3171/2008.3.17571

Kim, D. H., Saetrom, P., Snove, O., Jr., & Rossi, J. J. (2008). MicroRNA-directed transcriptional gene silencing in mammalian cells. *Proc Natl Acad Sci U S A, 105*(42), 16230-16235. doi:10.1073/pnas.0808830105

Kipshidze, N., Dangas, G., Tsapenko, M., Moses, J., Leon, M. B., Kutryk, M., & Serruys, P. (2004). Role of the endothelium in modulating neointimal formation: vasculoprotective approaches to attenuate restenosis after percutaneous coronary interventions. *J Am Coll Cardiol, 44*(4), 733-739. doi:10.1016/j.jacc.2004.04.048

Klein, D., Weisshardt, P., Kleff, V., Jastrow, H., Jakob, H. G., & Ergun, S. (2011). Vascular wall-resident CD44+ multipotent stem cells give rise to pericytes and smooth muscle cells and contribute to new vessel maturation. *PLoS One, 6*(5), e20540. doi:10.1371/journal.pone.0020540

Klein, S., de Fougerolles, A. R., Blaikie, P., Khan, L., Pepe, A., Green, C. D., . . . Giancotti, F. G. (2002). Alpha 5 beta 1 integrin activates an NF-kappa B-dependent program of gene expression important for angiogenesis and inflammation. *Mol Cell Biol, 22*(16), 5912-5922.

Kokubo, T., Uchida, H., & Choi, E. T. (2007). Integrin alpha(v)beta(3) as a target in the prevention of neointimal hyperplasia. *J Vasc Surg, 45 Suppl A*, A33-38. doi:10.1016/j.jvs.2007.02.069

Kolh, P., & Wijns, W. (2011). Joint ESC/EACTS guidelines on myocardial revascularization. *J Cardiovasc Med (Hagerstown), 12*(4), 264-267. doi:10.2459/JCM.0b013e328344e647

Kondo, T., Hayashi, M., Takeshita, K., Numaguchi, Y., Kobayashi, K., Iino, S., . . . Murohara, T. (2004). Smoking cessation rapidly increases circulating progenitor cells in peripheral

blood in chronic smokers. *Arterioscler Thromb Vasc Biol, 24*(8), 1442-1447. doi:10.1161/01.ATV.0000135655.52088.c5

Kong, D., Melo, L. G., Gnecchi, M., Zhang, L., Mostoslavsky, G., Liew, C. C., . . . Dzau, V. J. (2004). Cytokine-induced mobilization of circulating endothelial progenitor cells enhances repair of injured arteries. *Circulation, 110*(14), 2039-2046. doi:10.1161/01.CIR.0000143161.01901.BD

Kong, D., Melo, L. G., Mangi, A. A., Zhang, L., Lopez-Ilasaca, M., Perrella, M. A., . . . Dzau, V. J. (2004). Enhanced inhibition of neointimal hyperplasia by genetically engineered endothelial progenitor cells. *Circulation, 109*(14), 1769-1775. doi:10.1161/01.CIR.0000121732.85572.6F

Kong, F., Garcia, A. J., Mould, A. P., Humphries, M. J., & Zhu, C. (2009). Demonstration of catch bonds between an integrin and its ligand. *J Cell Biol, 185*(7), 1275-1284. doi:10.1083/jcb.200810002

Koyama, H., & Reidy, M. A. (1998). Expression of extracellular matrix proteins accompanies lesion growth in a model of intimal reinjury. *Circ Res, 82*(9), 988-995.

Koyanagi, M., Brandes, R. P., Haendeler, J., Zeiher, A. M., & Dimmeler, S. (2005). Cell-to-cell connection of endothelial progenitor cells with cardiac myocytes by nanotubes: a novel mechanism for cell fate changes? *Circ Res, 96*(10), 1039-1041. doi:10.1161/01.RES.0000168650.23479.0c

Krause, D. S., Fackler, M. J., Civin, C. I., & May, W. S. (1996). CD34: structure, biology, and clinical utility. *Blood, 87*(1), 1-13.

Krutzfeldt, J., Kuwajima, S., Braich, R., Rajeev, K. G., Pena, J., Tuschl, T., . . . Stoffel, M. (2007). Specificity, duplex degradation and subcellular localization of antagomirs. *Nucleic Acids Res, 35*(9), 2885-2892. doi:10.1093/nar/gkm024

Krutzfeldt, J., Rajewsky, N., Braich, R., Rajeev, K. G., Tuschl, T., Manoharan, M., & Stoffel, M. (2005). Silencing of microRNAs in vivo with 'antagomirs'. *Nature, 438*(7068), 685-689. doi:nature04303 [pii]

10.1038/nature04303

Kuchen, S., Resch, W., Yamane, A., Kuo, N., Li, Z., Chakraborty, T., . . . Casellas, R. (2010). Regulation of microRNA expression and abundance during lymphopoiesis. *Immunity, 32*(6), 828-839. doi:10.1016/j.immuni.2010.05.009

Kuehbacher, A., Urbich, C., & Dimmeler, S. (2008). Targeting microRNA expression to regulate angiogenesis. *Trends Pharmacol Sci, 29*(1), 12-15. doi:S0165-6147(07)00277-5 [pii]

10.1016/j.tips.2007.10.014

Kunz, G. A., Liang, G., Cuculi, F., Gregg, D., Vata, K. C., Shaw, L. K., . . . Peterson, E. D. (2006). Circulating endothelial progenitor cells predict coronary artery disease severity. *Am Heart J, 152*(1), 190-195. doi:10.1016/j.ahj.2006.02.001

Kurpisz, M., Czepczynski, R., Grygielska, B., Majewski, M., Fiszer, D., Jerzykowska, O., . . . Siminiak, T. (2007). Bone marrow stem cell imaging after intracoronary administration. *Int J Cardiol, 121*(2), 194-195. doi:10.1016/j.ijcard.2006.08.062

Kyrtatos, P. G., Lehtolainen, P., Junemann-Ramirez, M., Garcia-Prieto, A., Price, A. N., Martin, J. F., . . . Lythgoe, M. F. (2009). Magnetic tagging increases delivery of circulating progenitors in vascular injury. *JACC Cardiovasc Interv, 2*(8), 794-802. doi:10.1016/j.jcin.2009.05.014

Lai, E. C. (2002). Micro RNAs are complementary to 3' UTR sequence motifs that mediate negative post-transcriptional regulation. *Nat Genet, 30*(4), 363-364. doi:10.1038/ng865

Lam, A. (2012). The next generation of miRNA modulators: new mirVana™ miRNA mimics and inhibitors. Retrieved from http://cgs.hku.hk/portal/files/GRC/Events/Seminars/2012/20120606/mirvana%20microrna%20mimic%20and%20inhibitors%20jun2012%20for%20cgs%20.pdf

Landmesser, U., Engberding, N., Bahlmann, F. H., Schaefer, A., Wiencke, A., Heineke, A., . . . Drexler, H. (2004). Statin-induced improvement of endothelial progenitor cell mobilization, myocardial neovascularization, left ventricular function, and survival after experimental myocardial infarction requires endothelial nitric oxide synthase. *Circulation, 110*(14), 1933-1939. doi:10.1161/01.CIR.0000143232.67642.7A

Lanuti, P., Rotta, G., Almici, C., Avvisati, G., Budillon, A., Doretto, P., . . . Miscia, S. (2016). Endothelial progenitor cells, defined by the simultaneous surface expression of VEGFR2 and CD133, are not detectable in healthy peripheral and cord blood. *Cytometry A, 89*(3), 259-270. doi:10.1002/cyto.a.22730

Lanza, F., Healy, L., & Sutherland, D. R. (2001). Structural and functional features of the CD34 antigen: an update. *J Biol Regul Homeost Agents, 15*(1), 1-13.

Larsen, K., Cheng, C., Tempel, D., Parker, S., Yazdani, S., den Dekker, W. K., . . . Duckers, H. J. (2012). Capture of circulatory endothelial progenitor cells and accelerated re-endothelialization of a bio-engineered stent in human ex vivo shunt and rabbit denudation model. *Eur Heart J, 33*(1), 120-128. doi:10.1093/eurheartj/ehr196

Lasala, J. M., Cox, D. A., Dobies, D., Muhlestein, J. B., Katopodis, J. N., Revtyak, G., . . . Physicians, A. P. (2008). Usage patterns and 2-year outcomes with the TAXUS express stent: results of the US ARRIVE 1 registry. *Catheter Cardiovasc Interv, 72*(4), 433-445. doi:10.1002/ccd.21618

Laufs, U., Werner, N., Link, A., Endres, M., Wassmann, S., Jurgens, K., . . . Nickenig, G. (2004). Physical training increases endothelial progenitor cells, inhibits neointima formation, and enhances angiogenesis. *Circulation, 109*(2), 220-226. doi:10.1161/01.CIR.0000109141.48980.37

Lavergne, M., Vanneaux, V., Delmau, C., Gluckman, E., Rodde-Astier, I., Larghero, J., & Uzan, G. (2011). Cord blood-circulating endothelial progenitors for treatment of vascular diseases. *Cell Prolif, 44 Suppl 1*, 44-47. doi:10.1111/j.1365-2184.2010.00722.x

Layton, D. S., Strom, A. D., O'Neil, T. E., Broadway, M. M., Stephenson, G. L., Morris, K. R., . . . Bean, A. G. (2007). Development of an anti-porcine CD34 monoclonal antibody that identifies hematopoietic stem cells. *Experimental hematology, 35*(1), 171-178. doi:10.1016/j.exphem.2006.08.019

Lee, R. C., Feinbaum, R. L., & Ambros, V. (1993). The C. elegans heterochronic gene lin-4 encodes small RNAs with antisense complementarity to lin-14. *Cell, 75*(5), 843-854.

Lee, S., & Yoon, Y. S. (2013). Revisiting cardiovascular regeneration with bone marrow-derived angiogenic and vasculogenic cells. *Br J Pharmacol, 169*(2), 290-303. doi:10.1111/j.1476-5381.2012.01857.x

Lee, Y., Ahn, C., Han, J., Choi, H., Kim, J., Yim, J., . . . Kim, V. N. (2003). The nuclear RNase III Drosha initiates microRNA processing. *Nature, 425*(6956), 415-419. doi:10.1038/nature01957

Lee, Y. S., Pressman, S., Andress, A. P., Kim, K., White, J. L., Cassidy, J. J., . . . Carthew, R. W. (2009). Silencing by small RNAs is linked to endosomal trafficking. *Nat Cell Biol, 11*(9), 1150-1156. doi:10.1038/ncb1930

Lei, L. C., Huo, Y., Li, J. P., Li, X. X., Han, Y. Y., Wang, H. Z., & Zhu, Y. (2007). [Activities of circulating endothelial progenitor cells in patients with in-stent restenosis]. *Zhonghua Yi Xue Za Zhi, 87*(48), 3394-3398.

Lemarie, C. A., Shbat, L., Marchesi, C., Angulo, O. J., Deschenes, M. E., Blostein, M. D., . . . Schiffrin, E. L. (2011). Mthfr deficiency induces endothelial progenitor cell senescence via uncoupling of eNOS and downregulation of SIRT1. *Am J Physiol Heart Circ Physiol, 300*(3), H745-753. doi:10.1152/ajpheart.00321.2010

Lennox, K. A., & Behlke, M. A. (2011). Chemical modification and design of anti-miRNA oligonucleotides. *Gene Ther, 18*(12), 1111-1120. doi:10.1038/gt.2011.100

Leone, A. M., Rutella, S., Bonanno, G., Abbate, A., Rebuzzi, A. G., Giovannini, S., . . . Crea, F. (2005). Mobilization of bone marrow-derived stem cells after myocardial infarction

and left ventricular function. *Eur Heart J, 26*(12), 1196-1204. doi:10.1093/eurheartj/ehi164

Leone, A. M., Rutella, S., Bonanno, G., Contemi, A. M., de Ritis, D. G., Giannico, M. B., . . . Crea, F. (2006). Endogenous G-CSF and CD34+ cell mobilization after acute myocardial infarction. *Int J Cardiol, 111*(2), 202-208. doi:10.1016/j.ijcard.2005.06.043

Leone, A. M., Rutella, S., Giannico, M. B., Perfetti, M., Zaccone, V., Brugaletta, S., . . . Crea, F. (2008). Effect of intensive vs standard statin therapy on endothelial progenitor cells and left ventricular function in patients with acute myocardial infarction: Statins for regeneration after acute myocardial infarction and PCI (STRAP) trial. *Int J Cardiol, 130*(3), 457-462. doi:10.1016/j.ijcard.2008.05.036

Leone, A. M., Valgimigli, M., Giannico, M. B., Zaccone, V., Perfetti, M., D'Amario, D., . . . Crea, F. (2009). From bone marrow to the arterial wall: the ongoing tale of endothelial progenitor cells. *Eur Heart J, 30*(8), 890-899. doi:10.1093/eurheartj/ehp078

Leor, J., & Marber, M. (2006). Endothelial progenitors: a new Tower of Babel? *J Am Coll Cardiol, 48*(8), 1588-1590. doi:10.1016/j.jacc.2006.07.032

Lev, E. I., Leshem-Lev, D., Mager, A., Vaknin-Assa, H., Harel, N., Zimra, Y., . . . Kornowski, R. (2010). Circulating endothelial progenitor cell levels and function in patients who experienced late coronary stent thrombosis. *Eur Heart J, 31*(21), 2625-2632. doi:10.1093/eurheartj/ehq184

Lewis, B. P., Shih, I. H., Jones-Rhoades, M. W., Bartel, D. P., & Burge, C. B. (2003). Prediction of mammalian microRNA targets. *Cell, 115*(7), 787-798.

Li, B., Sharpe, E. E., Maupin, A. B., Teleron, A. A., Pyle, A. L., Carmeliet, P., & Young, P. P. (2006). VEGF and PlGF promote adult vasculogenesis by enhancing EPC recruitment and vessel formation at the site of tumor neovascularization. *FASEB J, 20*(9), 1495-1497. doi:10.1096/fj.05-5137fje

Li, L., Liu, H., Xu, C., Deng, M., Song, M., Yu, X., . . . Zhao, X. (2017). VEGF promotes endothelial progenitor cell differentiation and vascular repair through connexin 43. *Stem Cell Res Ther, 8*(1), 237. doi:10.1186/s13287-017-0684-1

Li, L., Zhang, H. N., Chen, H. Z., Gao, P., Zhu, L. H., Li, H. L., . . . Liang, C. C. (2011). SIRT1 acts as a modulator of neointima formation following vascular injury in mice. *Circ Res, 108*(10), 1180-1189. doi:10.1161/CIRCRESAHA.110.237875

Li, M., Guan, X., Sun, Y., Mi, J., Shu, X., Liu, F., & Li, C. (2014). miR-92a family and their target genes in tumorigenesis and metastasis. *Exp Cell Res, 323*(1), 1-6. doi:10.1016/j.yexcr.2013.12.025

Li, P., Zhu, N., Yi, B., Wang, N., Chen, M., You, X., . . . Sun, J. (2013). MicroRNA-663 regulates human vascular smooth muscle cell phenotypic switch and vascular neointimal formation. *Circ Res, 113*(10), 1117-1127. doi:10.1161/CIRCRESAHA.113.301306

Li, Q., Zhang, X., Peng, Y., Chai, H., Xu, Y., Wei, J., . . . Huang, D. (2013). Comparison of the sorting efficiency and influence on cell function between the sterile flow cytometry and immunomagnetic bead purification methods. *Prep Biochem Biotechnol, 43*(2), 197-206. doi:10.1080/10826068.2012.719846

Li, Z. (2013). CD133: a stem cell biomarker and beyond. *Exp Hematol Oncol, 2*(1), 17. doi:10.1186/2162-3619-2-17

Liang, C. C., Park, A. Y., & Guan, J. L. (2007). In vitro scratch assay: a convenient and inexpensive method for analysis of cell migration in vitro. *Nat Protoc, 2*(2), 329-333. doi:10.1038/nprot.2007.30

Liao, Y., Geyer, M. B., Yang, A. J., & Cairo, M. S. (2011). Cord blood transplantation and stem cell regenerative potential. *Experimental hematology, 39*(4), 393-412. doi:10.1016/j.exphem.2011.01.002

LifeTecnhologies. (2012). New tools for microRNA functional analysis. *BioProbes.* Retrieved from https://www.thermofisher.com/content/dam/LifeTech/migration/files/technical-reference-library/newsletters-journals/bioprobes/bioprobes-67.par.49444.file.dat/bioprobes-67-mirvana.pdf

Lim, L. P., Lau, N. C., Garrett-Engele, P., Grimson, A., Schelter, J. M., Castle, J., . . . Johnson, J. M. (2005). Microarray analysis shows that some microRNAs downregulate large numbers of target mRNAs. *Nature, 433*(7027), 769-773. doi:10.1038/nature03315

Lin, R. Z., Dreyzin, A., Aamodt, K., Dudley, A. C., & Melero-Martin, J. M. (2011). Functional endothelial progenitor cells from cryopreserved umbilical cord blood. *Cell Transplant, 20*(4), 515-522. doi:10.3727/096368910X532729

Lin, X., Zhan, J. K., Wang, Y. J., Tan, P., Chen, Y. Y., Deng, H. Q., & Liu, Y. S. (2016). Function, Role, and Clinical Application of MicroRNAs in Vascular Aging. *Biomed Res Int, 2016*, 6021394. doi:10.1155/2016/6021394

Lin, Y., Weisdorf, D. J., Solovey, A., & Hebbel, R. P. (2000). Origins of circulating endothelial cells and endothelial outgrowth from blood. *J Clin Invest, 105*(1), 71-77. doi:10.1172/JCI8071

Lipinski, M. J., Biondi-Zoccai, G. G., Abbate, A., Khianey, R., Sheiban, I., Bartunek, J., . . . Vetrovec, G. W. (2007). Impact of intracoronary cell therapy on left ventricular function in the setting of acute myocardial infarction: a collaborative systematic review and meta-analysis of controlled clinical trials. *J Am Coll Cardiol, 50*(18), 1761-1767. doi:10.1016/j.jacc.2007.07.041

Liu, H., Li, G., Zhao, W., & Hu, Y. (2016). Inhibition of MiR-92a May Protect Endothelial Cells After Acute Myocardial Infarction in Rats: Role of KLF2/4. *Med Sci Monit, 22*, 2451-2462.

Liu, N., & Olson, E. N. (2010). MicroRNA regulatory networks in cardiovascular development. *Dev Cell, 18*(4), 510-525. doi:10.1016/j.devcel.2010.03.010

Liu, N. M., Siu, K. L., Youn, J. Y., & Cai, H. (2016). Attenuation of neointimal formation with netrin-1 and netrin-1 preconditioned endothelial progenitor cells. *J Mol Med (Berl)*. doi:10.1007/s00109-016-1490-4

Liu, S. Q., Li, Z. L., Cao, Y. X., Li, L., Ma, X., Zhao, X. G., . . . Yuan, B. X. (2011). Transfusion of autologous late-outgrowth endothelial cells reduces arterial neointima formation after injury. *Cardiovasc Res, 90*(1), 171-181. doi:10.1093/cvr/cvq395

Liu, X., Cheng, Y., Yang, J., Xu, L., & Zhang, C. (2012). Cell-specific effects of miR-221/222 in vessels: molecular mechanism and therapeutic application. *J Mol Cell Cardiol, 52*(1), 245-255. doi:10.1016/j.yjmcc.2011.11.008

Liu, X., Hao, L., Li, D., Zhu, L., & Hu, S. (2015). Long non-coding RNAs and their biological roles in plants. *Genomics Proteomics Bioinformatics, 13*(3), 137-147. doi:10.1016/j.gpb.2015.02.003

Liu, X., Li, Y., Liu, Y., Luo, Y., Wang, D., Annex, B. H., & Goldschmidt-Clermont, P. J. (2010). Endothelial progenitor cells (EPCs) mobilized and activated by neurotrophic factors may contribute to pathologic neovascularization in diabetic retinopathy. *Am J Pathol, 176*(1), 504-515. doi:10.2353/ajpath.2010.081152

Liu, Z. J., Tian, R., An, W., Zhuge, Y., Li, Y., Shao, H., . . . Velazquez, O. C. (2010). Identification of E-selectin as a novel target for the regulation of postnatal neovascularization: implications for diabetic wound healing. *Ann Surg, 252*(4), 625-634. doi:10.1097/SLA.0b013e3181f5a079

Liu, Z. J., & Velazquez, O. C. (2008). Hyperoxia, endothelial progenitor cell mobilization, and diabetic wound healing. *Antioxid Redox Signal, 10*(11), 1869-1882. doi:10.1089/ars.2008.2121

Llevadot, J., Murasawa, S., Kureishi, Y., Uchida, S., Masuda, H., Kawamoto, A., . . . Asahara, T. (2001). HMG-CoA reductase inhibitor mobilizes bone marrow--derived endothelial progenitor cells. *J Clin Invest, 108*(3), 399-405. doi:10.1172/JCI13131

Logie, J. J., Ali, S., Marshall, K. M., Heck, M. M., Walker, B. R., & Hadoke, P. W. (2010). Glucocorticoid-mediated inhibition of angiogenic changes in human endothelial cells is not caused by reductions in cell proliferation or migration. *PLoS One, 5*(12), e14476. doi:10.1371/journal.pone.0014476

Lombardo, M. F., Iacopino, P., Cuzzola, M., Spiniello, E., Garreffa, C., Ferrelli, F., . . . Irrera, G. (2012). Type 2 diabetes mellitus impairs the maturation of endothelial progenitor cells and increases the number of circulating endothelial cells in peripheral blood. *Cytometry A, 81*(10), 856-864. doi:10.1002/cyto.a.22109

Loyer, X., Potteaux, S., Vion, A. C., Guerin, C. L., Boulkroun, S., Rautou, P. E., . . . Tedgui, A. (2014). Inhibition of microRNA-92a prevents endothelial dysfunction and atherosclerosis in mice. *Circ Res, 114*(3), 434-443. doi:10.1161/CIRCRESAHA.114.302213

Luderer, F., Lobler, M., Rohm, H. W., Gocke, C., Kunna, K., Kock, K., . . . Sternberg, K. (2011). Biodegradable sirolimus-loaded poly(lactide) nanoparticles as drug delivery system for the prevention of in-stent restenosis in coronary stent application. *J Biomater Appl, 25*(8), 851-875. doi:10.1177/0885328209360696

Luo, D., & Saltzman, W. M. (2000). Synthetic DNA delivery systems. *Nature biotechnology, 18*(1), 33-37. doi:10.1038/71889

Luo, T., Cui, S., Bian, C., & Yu, X. (2014). Crosstalk between TGF-beta/Smad3 and BMP/BMPR2 signaling pathways via miR-17-92 cluster in carotid artery restenosis. *Mol Cell Biochem, 389*(1-2), 169-176. doi:10.1007/s11010-013-1938-6

Lyden, D., Hattori, K., Dias, S., Costa, C., Blaikie, P., Butros, L., . . . Rafii, S. (2001). Impaired recruitment of bone-marrow-derived endothelial and hematopoietic precursor cells blocks tumor angiogenesis and growth. *Nat Med, 7*(11), 1194-1201. doi:10.1038/nm1101-1194

Ma, N., Ladilov, Y., Moebius, J. M., Ong, L., Piechaczek, C., David, A., . . . Steinhoff, G. (2006). Intramyocardial delivery of human CD133+ cells in a SCID mouse cryoinjury model: Bone marrow vs. cord blood-derived cells. *Cardiovasc Res, 71*(1), 158-169. doi:10.1016/j.cardiores.2006.03.020

Ma, Z. L., Mai, X. L., Sun, J. H., Ju, S. H., Yang, X., Ni, Y., & Teng, G. J. (2009). Inhibited atherosclerotic plaque formation by local administration of magnetically labeled endothelial progenitor cells (EPCs) in a rabbit model. *Atherosclerosis, 205*(1), 80-86. doi:10.1016/j.atherosclerosis.2008.07.048

Mack, P. J., Zhang, Y., Chung, S., Vickerman, V., Kamm, R. D., & Garcia-Cardena, G. (2009). Biomechanical Regulation of Endothelium-dependent Events Critical for Adaptive Remodeling. *J Biol Chem, 284*(13), 8412-8420. doi:10.1074/jbc.M804524200

Maehara, Y., Anai, H., Tamada, R., & Sugimachi, K. (1987). The ATP assay is more sensitive than the succinate dehydrogenase inhibition test for predicting cell viability. *Eur J Cancer Clin Oncol, 23*(3), 273-276.

Maia, J., Santos, T., Aday, S., Agasse, F., Cortes, L., Malva, J. O., . . . Ferreira, L. (2011). Controlling the neuronal differentiation of stem cells by the intracellular delivery of retinoic acid-loaded nanoparticles. *ACS Nano, 5*(1), 97-106. doi:10.1021/nn101724r

Maltby, S., Freeman, S., Gold, M. J., Baker, J. H., Minchinton, A. I., Gold, M. R., . . . McNagny, K. M. (2011). Opposing roles for CD34 in B16 melanoma tumor growth alter early stage vasculature and late stage immune cell infiltration. *PLoS One, 6*(4), e18160. doi:10.1371/journal.pone.0018160

Marboeuf, P., Corseaux, D., Mouquet, F., Van Belle, E., Jude, B., & Susen, S. (2008). Inflammation triggers colony forming endothelial cell mobilization after angioplasty in chronic lower limb ischemia. *J Thromb Haemost, 6*(1), 195-197. doi:10.1111/j.1538-7836.2007.02783.x

Marcelis, C. L., Hol, F. A., Graham, G. E., Rieu, P. N., Kellermayer, R., Meijer, R. P., . . . de Brouwer, A. P. (2008). Genotype-phenotype correlations in MYCN-related Feingold syndrome. *Hum Mutat, 29*(9), 1125-1132. doi:10.1002/humu.20750

Marcola, M., & Rodrigues, C. E. (2015). Endothelial progenitor cells in tumor angiogenesis: another brick in the wall. *Stem Cells Int, 2015*, 832649. doi:10.1155/2015/832649

Marfella, R., Rizzo, M. R., Siniscalchi, M., Paolisso, P., Barbieri, M., Sardu, C., . . . Balestrieri, M. L. (2013). Peri-procedural tight glycemic control during early percutaneous coronary

intervention up-regulates endothelial progenitor cell level and differentiation during acute ST-elevation myocardial infarction: effects on myocardial salvage. *Int J Cardiol, 168*(4), 3954-3962. doi:10.1016/j.ijcard.2013.06.053

Massa, M., Campanelli, R., Bonetti, E., Ferrario, M., Marinoni, B., & Rosti, V. (2009). Rapid and large increase of the frequency of circulating endothelial colony-forming cells (ECFCs) generating late outgrowth endothelial cells in patients with acute myocardial infarction. *Experimental hematology, 37*(1), 8-9. doi:10.1016/j.exphem.2008.09.007

Massberg, S., Konrad, I., Schurzinger, K., Lorenz, M., Schneider, S., Zohlnhoefer, D., . . . Gawaz, M. (2006). Platelets secrete stromal cell-derived factor 1alpha and recruit bone marrow-derived progenitor cells to arterial thrombi in vivo. *J Exp Med, 203*(5), 1221-1233. doi:10.1084/jem.20051772

Mattagajasingh, I., Kim, C. S., Naqvi, A., Yamamori, T., Hoffman, T. A., Jung, S. B., . . . Irani, K. (2007). SIRT1 promotes endothelium-dependent vascular relaxation by activating endothelial nitric oxide synthase. *Proc Natl Acad Sci U S A, 104*(37), 14855-14860. doi:10.1073/pnas.0704329104

Mauri, L., Silbaugh, T. S., Wolf, R. E., Zelevinsky, K., Lovett, A., Zhou, Z., . . . Normand, S. L. (2008). Long-term clinical outcomes after drug-eluting and bare-metal stenting in Massachusetts. *Circulation, 118*(18), 1817-1827. doi:10.1161/CIRCULATIONAHA.108.781377

McKenzie, A. J., Hoshino, D., Hong, N. H., Cha, D. J., Franklin, J. L., Coffey, R. J., . . . Weaver, A. M. (2016). KRAS-MEK Signaling Controls Ago2 Sorting into Exosomes. *Cell Rep, 15*(5), 978-987. doi:10.1016/j.celrep.2016.03.085

McNeer, N. A., Chin, J. Y., Schleifman, E. B., Fields, R. J., Glazer, P. M., & Saltzman, W. M. (2011). Nanoparticles deliver triplex-forming PNAs for site-specific genomic recombination in CD34+ human hematopoietic progenitors. *Mol Ther, 19*(1), 172-180. doi:10.1038/mt.2010.200

Medina, R. J., Barber, C. L., Sabatier, F., Dignat-George, F., Melero-Martin, J. M., Khosrotehrani, K., . . . Stitt, A. W. (2017). Endothelial Progenitors: A Consensus Statement on Nomenclature. *Stem Cells Transl Med, 6*(5), 1316-1320. doi:10.1002/sctm.16-0360

Medina, R. J., O'Neill, C. L., Sweeney, M., Guduric-Fuchs, J., Gardiner, T. A., Simpson, D. A., & Stitt, A. W. (2010). Molecular analysis of endothelial progenitor cell (EPC) subtypes reveals two distinct cell populations with different identities. *BMC Med Genomics, 3*, 18. doi:10.1186/1755-8794-3-18

Meister, G. (2013). Argonaute proteins: functional insights and emerging roles. *Nat Rev Genet, 14*(7), 447-459. doi:10.1038/nrg3462

Melero-Martin, J. M., Khan, Z. A., Picard, A., Wu, X., Paruchuri, S., & Bischoff, J. (2007). In vivo vasculogenic potential of human blood-derived endothelial progenitor cells. *Blood, 109*(11), 4761-4768. doi:10.1182/blood-2006-12-062471

Melnik, K., Nakamura, M., Comella, K., Lasky, L. C., Zborowski, M., & Chalmers, J. J. (2001). Evaluation of eluents from separations of CD34+ cells from human cord blood using a commercial, immunomagnetic cell separation system. *Biotechnol Prog, 17*(5), 907-916. doi:10.1021/bp010079r

Melo, S. A., Sugimoto, H., O'Connell, J. T., Kato, N., Villanueva, A., Vidal, A., . . . Kalluri, R. (2014). Cancer exosomes perform cell-independent microRNA biogenesis and promote tumorigenesis. *Cancer Cell, 26*(5), 707-721. doi:10.1016/j.ccell.2014.09.005

Meneveau, N., Deschaseaux, F., Seronde, M. F., Chopard, R., Schiele, F., Jehl, J., . . . Davani, S. (2011). Presence of endothelial colony-forming cells is associated with reduced microvascular obstruction limiting infarct size and left ventricular remodelling in patients with acute myocardial infarction. *Basic Res Cardiol, 106*(6), 1397-1410. doi:10.1007/s00395-011-0220-x

Merlet, E., Atassi, F., Motiani, R. K., Mougenot, N., Jacquet, A., Nadaud, S., . . . Marchand, A. (2013). miR-424/322 regulates vascular smooth muscle cell phenotype and neointimal formation in the rat. *Cardiovasc Res, 98*(3), 458-468. doi:10.1093/cvr/cvt045

Michaud, S. E., Dussault, S., Haddad, P., Groleau, J., & Rivard, A. (2006). Circulating endothelial progenitor cells from healthy smokers exhibit impaired functional activities. *Atherosclerosis, 187*(2), 423-432. doi:10.1016/j.atherosclerosis.2005.10.009

Mieno, S., Boodhwani, M., Robich, M. P., Clements, R. T., Sodha, N. R., & Sellke, F. W. (2010). Effects of diabetes mellitus on VEGF-induced proliferation response in bone marrow derived endothelial progenitor cells. *J Card Surg, 25*(5), 618-625. doi:10.1111/j.1540-8191.2010.01086.x

Mieno, S., Clements, R. T., Boodhwani, M., Sodha, N. R., Ramlawi, B., Bianchi, C., & Sellke, F. W. (2008). Characteristics and function of cryopreserved bone marrow-derived endothelial progenitor cells. *Ann Thorac Surg, 85*(4), 1361-1366. doi:10.1016/j.athoracsur.2007.12.006

Mills, L., Tellez, C., Huang, S., Baker, C., McCarty, M., Green, L., . . . Bar-Eli, M. (2002). Fully human antibodies to MCAM/MUC18 inhibit tumor growth and metastasis of human melanoma. *Cancer research, 62*(17), 5106-5114.

Mills, N. L., Tura, O., Padfield, G. J., Millar, C., Lang, N. N., Stirling, D., . . . Newby, D. E. (2009). Dissociation of phenotypic and functional endothelial progenitor cells in patients undergoing percutaneous coronary intervention. *Heart, 95*(24), 2003-2008. doi:10.1136/hrt.2008.163162

Miltenyi, S., Muller, W., Weichel, W., & Radbruch, A. (1990). High gradient magnetic cell separation with MACS. *Cytometry, 11*(2), 231-238. doi:10.1002/cyto.990110203

Miraglia, S., Godfrey, W., Yin, A. H., Atkins, K., Warnke, R., Holden, J. T., . . . Buck, D. W. (1997). A novel five-transmembrane hematopoietic stem cell antigen: isolation, characterization, and molecular cloning. *Blood, 90*(12), 5013-5021.

Missan, D. S., & DiPersio, M. (2012). Integrin control of tumor invasion. *Crit Rev Eukaryot Gene Expr, 22*(4), 309-324.

Moreno, P. R., Sanz, J., & Fuster, V. (2009). Promoting mechanisms of vascular health: circulating progenitor cells, angiogenesis, and reverse cholesterol transport. *J Am Coll Cardiol, 53*(25), 2315-2323. doi:S0735-1097(09)01121-8 [pii]

10.1016/j.jacc.2009.02.057

Moynihan, J. S., Jones, D. H., Farrar, G. H., & Howard, C. R. (2001). A novel microencapsulated peptide vaccine against hepatitis B. *Vaccine, 19*(23-24), 3292-3300.

Mulcahy, L. A., Pink, R. C., & Carter, D. R. (2014). Routes and mechanisms of extracellular vesicle uptake. *J Extracell Vesicles, 3*. doi:10.3402/jev.v3.24641

Muller, A. M., Medvinsky, A., Strouboulis, J., Grosveld, F., & Dzierzak, E. (1994). Development of hematopoietic stem cell activity in the mouse embryo. *Immunity, 1*(4), 291-301.

Muller, J. M., Chilian, W. M., & Davis, M. J. (1997). Integrin signaling transduces shear stress--dependent vasodilation of coronary arterioles. *Circ Res, 80*(3), 320-326.

Mulligan-Kehoe, M. J., & Simons, M. (2014). Vasa vasorum in normal and diseased arteries. *Circulation, 129*(24), 2557-2566. doi:10.1161/CIRCULATIONAHA.113.007189

Mund, J. A., Estes, M. L., Yoder, M. C., Ingram, D. A., Jr., & Case, J. (2012). Flow cytometric identification and functional characterization of immature and mature circulating endothelial cells. *Arterioscler Thromb Vasc Biol, 32*(4), 1045-1053. doi:10.1161/ATVBAHA.111.244210

Munich, S., Sobo-Vujanovic, A., Buchser, W. J., Beer-Stolz, D., & Vujanovic, N. L. (2012). Dendritic cell exosomes directly kill tumor cells and activate natural killer cells via TNF superfamily ligands. *Oncoimmunology, 1*(7), 1074-1083. doi:10.4161/onci.20897

Murohara, T., Asahara, T., Silver, M., Bauters, C., Masuda, H., Kalka, C., . . . Isner, J. M. (1998). Nitric oxide synthase modulates angiogenesis in response to tissue ischemia. *J Clin Invest, 101*(11), 2567-2578. doi:10.1172/JCI1560

Muscari, C., Gamberini, C., Basile, I., Bonafe, F., Valgimigli, S., Capitani, O., . . . Caldarera, C. M. (2010). Comparison between Culture Conditions Improving Growth and Differentiation

of Blood and Bone Marrow Cells Committed to the Endothelial Cell Lineage. *Biol Proced Online, 12*(1), 9023. doi:10.1007/s12575-009-9023-y

Nagashima, K., Endo, A., Ogita, H., Kawana, A., Yamagishi, A., Kitabatake, A., . . . Mochizuki, N. (2002). Adaptor protein Crk is required for ephrin-B1-induced membrane ruffling and focal complex assembly of human aortic endothelial cells. *Mol Biol Cell, 13*(12), 4231-4242. doi:10.1091/mbc.E02-04-0181

Naito, H., Kidoya, H., Sakimoto, S., Wakabayashi, T., & Takakura, N. (2012). Identification and characterization of a resident vascular stem/progenitor cell population in preexisting blood vessels. *EMBO J, 31*(4), 842-855. doi:10.1038/emboj.2011.465

Nayak, L., Lin, Z., & Jain, M. K. (2011). "Go with the flow": how Kruppel-like factor 2 regulates the vasoprotective effects of shear stress. *Antioxid Redox Signal, 15*(5), 1449-1461. doi:10.1089/ars.2010.3647

Nazari-Jahantigh, M., Wei, Y., & Schober, A. (2012). The role of microRNAs in arterial remodelling. *Thromb Haemost, 107*(4), 611-618. doi:10.1160/TH11-12-0826

Neth, P., Nazari-Jahantigh, M., Schober, A., & Weber, C. (2013). MicroRNAs in flow-dependent vascular remodelling. *Cardiovasc Res, 99*(2), 294-303. doi:10.1093/cvr/cvt096

Nguyen, V. A., Furhapter, C., Obexer, P., Stossel, H., Romani, N., & Sepp, N. (2009). Endothelial cells from cord blood CD133+CD34+ progenitors share phenotypic, functional and gene expression profile similarities with lymphatics. *J Cell Mol Med, 13*(3), 522-534. doi:10.1111/j.1582-4934.2008.00340.x

Nielsen, J. S., & McNagny, K. M. (2008). Novel functions of the CD34 family. *J Cell Sci, 121*(Pt 22), 3683-3692. doi:10.1242/jcs.037507

Nielsen, J. S., & McNagny, K. M. (2009). CD34 is a key regulator of hematopoietic stem cell trafficking to bone marrow and mast cell progenitor trafficking in the periphery. *Microcirculation, 16*(6), 487-496. doi:10.1080/10739680902941737

Nijboer, C. H., van der Kooij, M. A., van Bel, F., Ohl, F., Heijnen, C. J., & Kavelaars, A. (2010). Inhibition of the JNK/AP-1 pathway reduces neuronal death and improves behavioral outcome after neonatal hypoxic-ischemic brain injury. *Brain Behav Immun, 24*(5), 812-821. doi:10.1016/j.bbi.2009.09.008

Nishiwaki, Y., Yoshida, M., Iwaguro, H., Masuda, H., Nitta, N., Asahara, T., & Isobe, M. (2007). Endothelial E-selectin potentiates neovascularization via endothelial progenitor cell-dependent and -independent mechanisms. *Arterioscler Thromb Vasc Biol, 27*(3), 512-518. doi:10.1161/01.ATV.0000254812.23238.2b

Niu, H., Wang, K., Zhang, A., Yang, S., Song, Z., Wang, W., . . . Wang, Y. (2012). miR-92a is a critical regulator of the apoptosis pathway in glioblastoma with inverse expression of BCL2L11. *Oncol Rep, 28*(5), 1771-1777. doi:10.3892/or.2012.1970

Nobbmann, U., Connah, M., Fish, B., Varley, P., Gee, C., Mulot, S., . . . Harding, S. E. (2007). Dynamic light scattering as a relative tool for assessing the molecular integrity and stability of monoclonal antibodies. *Biotechnol Genet Eng Rev, 24*, 117-128.

O'Donnell, K. A., Wentzel, E. A., Zeller, K. I., Dang, C. V., & Mendell, J. T. (2005). c-Myc-regulated microRNAs modulate E2F1 expression. *Nature, 435*(7043), 839-843. doi:10.1038/nature03677

Obad, S., dos Santos, C. O., Petri, A., Heidenblad, M., Broom, O., Ruse, C., . . . Kauppinen, S. (2011). Silencing of microRNA families by seed-targeting tiny LNAs. *Nat Genet, 43*(4), 371-378. doi:10.1038/ng.786

Obernosterer, G., Leuschner, P. J., Alenius, M., & Martinez, J. (2006). Post-transcriptional regulation of microRNA expression. *RNA, 12*(7), 1161-1167. doi:10.1261/rna.2322506

Oh, I. Y., Yoon, C. H., Hur, J., Kim, J. H., Kim, T. Y., Lee, C. S., . . . Kim, H. S. (2007). Involvement of E-selectin in recruitment of endothelial progenitor cells and angiogenesis in ischemic muscle. *Blood, 110*(12), 3891-3899. doi:10.1182/blood-2006-10-048991

Ohtani, K., Vlachojannis, G. J., Koyanagi, M., Boeckel, J. N., Urbich, C., Farcas, R., . . . Dimmeler, S. (2011). Epigenetic regulation of endothelial lineage committed genes in pro-

angiogenic hematopoietic and endothelial progenitor cells. *Circ Res, 109*(11), 1219-1229. doi:10.1161/CIRCRESAHA.111.247304

Ohyagi-Hara, C., Sawada, K., Kamiura, S., Tomita, Y., Isobe, A., Hashimoto, K., . . . Kimura, T. (2013). miR-92a inhibits peritoneal dissemination of ovarian cancer cells by inhibiting integrin alpha5 expression. *Am J Pathol, 182*(5), 1876-1889. doi:10.1016/j.ajpath.2013.01.039

Ohyashiki, J. H., Umezu, T., Kobayashi, C., Hamamura, R. S., Tanaka, M., Kuroda, M., & Ohyashiki, K. (2010). Impact on cell to plasma ratio of miR-92a in patients with acute leukemia: in vivo assessment of cell to plasma ratio of miR-92a. *BMC research notes, 3*, 347. doi:10.1186/1756-0500-3-347

Olive, V., Jiang, I., & He, L. (2010). mir-17-92, a cluster of miRNAs in the midst of the cancer network. *Int J Biochem Cell Biol, 42*(8), 1348-1354. doi:10.1016/j.biocel.2010.03.004

Omidi, Y., Hollins, A. J., Benboubetra, M., Drayton, R., Benter, I. F., & Akhtar, S. (2003). Toxicogenomics of non-viral vectors for gene therapy: a microarray study of lipofectin- and oligofectamine-induced gene expression changes in human epithelial cells. *J Drug Target, 11*(6), 311-323. doi:10.1080/10611860310001636908

Osella, M., Bosia, C., Cora, D., & Caselle, M. (2011). The role of incoherent microRNA-mediated feedforward loops in noise buffering. *PLoS Comput Biol, 7*(3), e1001101. doi:10.1371/journal.pcbi.1001101

Ota, H., Akishita, M., Eto, M., Iijima, K., Kaneki, M., & Ouchi, Y. (2007). Sirt1 modulates premature senescence-like phenotype in human endothelial cells. *J Mol Cell Cardiol, 43*(5), 571-579. doi:10.1016/j.yjmcc.2007.08.008

Ota, H., Eto, M., Ogawa, S., Iijima, K., Akishita, M., & Ouchi, Y. (2010). SIRT1/eNOS axis as a potential target against vascular senescence, dysfunction and atherosclerosis. *J Atheroscler Thromb, 17*(5), 431-435.

Otsuka, M., Zheng, M., Hayashi, M., Lee, J. D., Yoshino, O., Lin, S., & Han, J. (2008). Impaired microRNA processing causes corpus luteum insufficiency and infertility in mice. *J Clin Invest, 118*(5), 1944-1954. doi:10.1172/JCI33680

Ott, I., Keller, U., Knoedler, M., Gotze, K. S., Doss, K., Fischer, P., . . . Oostendorp, R. A. (2005). Endothelial-like cells expanded from CD34+ blood cells improve left ventricular function after experimental myocardial infarction. *FASEB J, 19*(8), 992-994. doi:10.1096/fj.04-3219fje

Ouchi, N., Kihara, S., Arita, Y., Nishida, M., Matsuyama, A., Okamoto, Y., . . . Matsuzawa, Y. (2001). Adipocyte-derived plasma protein, adiponectin, suppresses lipid accumulation and class A scavenger receptor expression in human monocyte-derived macrophages. *Circulation, 103*(8), 1057-1063.

Owens, G. K. (1995). Regulation of differentiation of vascular smooth muscle cells. *Physiol Rev, 75*(3), 487-517.

Ozsolak, F., Poling, L. L., Wang, Z., Liu, H., Liu, X. S., Roeder, R. G., . . . Fisher, D. E. (2008). Chromatin structure analyses identify miRNA promoters. *Genes Dev, 22*(22), 3172-3183. doi:10.1101/gad.1706508

Padfield, G. J., Newby, D. E., & Mills, N. L. (2010). Understanding the role of endothelial progenitor cells in percutaneous coronary intervention. *J Am Coll Cardiol, 55*(15), 1553-1565. doi:S0735-1097(10)00505-X [pii]

10.1016/j.jacc.2009.10.070

Pagan, I., Khosla, J., Li, C. M., & Sannes, P. L. (2002). Effect of growth factor-fibronectin matrix interaction on rat type II cell adhesion and DNA synthesis. *Exp Lung Res, 28*(2), 69-84.

Pakala, R., Willerson, J. T., & Benedict, C. R. (1997). Effect of serotonin, thromboxane A2, and specific receptor antagonists on vascular smooth muscle cell proliferation. *Circulation, 96*(7), 2280-2286.

Palmer, R. M., Ferrige, A. G., & Moncada, S. (1987). Nitric oxide release accounts for the biological activity of endothelium-derived relaxing factor. *Nature, 327*(6122), 524-526. doi:10.1038/327524a0

Pan, C. J., Tang, J. J., Weng, Y. J., Wang, J., & Huang, N. (2007). Preparation and characterization of rapamycin-loaded PLGA coating stent. *J Mater Sci Mater Med, 18*(11), 2193-2198. doi:10.1007/s10856-007-3075-9

Paprocka, M., Krawczenko, A., Dus, D., Kantor, A., Carreau, A., Grillon, C., & Kieda, C. (2011). CD133 positive progenitor endothelial cell lines from human cord blood. *Cytometry A, 79*(8), 594-602. doi:10.1002/cyto.a.21092

Parmar, K. M., Larman, H. B., Dai, G., Zhang, Y., Wang, E. T., Moorthy, S. N., . . . Garcia-Cardena, G. (2006). Integration of flow-dependent endothelial phenotypes by Kruppel-like factor 2. *J Clin Invest, 116*(1), 49-58. doi:10.1172/JCI24787

Pasquinelli, A. E., Reinhart, B. J., Slack, F., Martindale, M. Q., Kuroda, M. I., Maller, B., . . . Ruvkun, G. (2000). Conservation of the sequence and temporal expression of let-7 heterochronic regulatory RNA. *Nature, 408*(6808), 86-89. doi:10.1038/35040556

Patel, J., Donovan, P., & Khosrotehrani, K. (2016). Concise Review: Functional Definition of Endothelial Progenitor Cells: A Molecular Perspective. *Stem Cells Transl Med, 5*(10), 1302-1306. doi:10.5966/sctm.2016-0066

Patenaude, A., Parker, J., & Karsan, A. (2010). Involvement of endothelial progenitor cells in tumor vascularization. *Microvasc Res, 79*(3), 217-223. doi:10.1016/j.mvr.2010.01.007

Pathak, A., Patnaik, S., & Gupta, K. C. (2009). Recent trends in non-viral vector-mediated gene delivery. *Biotechnol J, 4*(11), 1559-1572. doi:10.1002/biot.200900161

Pedroso, D. C., Tellechea, A., Moura, L., Fidalgo-Carvalho, I., Duarte, J., Carvalho, E., & Ferreira, L. (2011). Improved survival, vascular differentiation and wound healing potential of stem cells co-cultured with endothelial cells. *PLoS One, 6*(1), e16114. doi:10.1371/journal.pone.0016114

Peichev, M., Naiyer, A. J., Pereira, D., Zhu, Z., Lane, W. J., Williams, M., . . . Rafii, S. (2000). Expression of VEGFR-2 and AC133 by circulating human CD34(+) cells identifies a population of functional endothelial precursors. *Blood, 95*(3), 952-958.

Pelagiadis, I., Relakis, K., Kalmanti, L., & Dimitriou, H. (2012). CD133 immunomagnetic separation: effectiveness of the method for CD133(+) isolation from umbilical cord blood. *Cytotherapy, 14*(6), 701-706. doi:10.3109/14653249.2012.663487

Peled, A., Grabovsky, V., Habler, L., Sandbank, J., Arenzana-Seisdedos, F., Petit, I., . . . Alon, R. (1999). The chemokine SDF-1 stimulates integrin-mediated arrest of CD34(+) cells on vascular endothelium under shear flow. *J Clin Invest, 104*(9), 1199-1211. doi:10.1172/JCI7615

Pellet-Many, C., Frankel, P., Evans, I. M., Herzog, B., Junemann-Ramirez, M., & Zachary, I. C. (2011). Neuropilin-1 mediates PDGF stimulation of vascular smooth muscle cell migration and signalling via p130Cas. *Biochem J, 435*(3), 609-618. doi:BJ20100580 [pii]

10.1042/BJ20100580

Pelliccia, F., Cianfrocca, C., Rosano, G., Mercuro, G., Speciale, G., & Pasceri, V. (2010). Role of endothelial progenitor cells in restenosis and progression of coronary atherosclerosis after percutaneous coronary intervention: a prospective study. *JACC Cardiovasc Interv, 3*(1), 78-86. doi:10.1016/j.jcin.2009.10.020

Pelosi, E., Valtieri, M., Coppola, S., Botta, R., Gabbianelli, M., Lulli, V., . . . Peschle, C. (2002). Identification of the hemangioblast in postnatal life. *Blood, 100*(9), 3203-3208. doi:10.1182/blood-2002-05-1511

Pels, K., Labinaz, M., Hoffert, C., & O'Brien, E. R. (1999). Adventitial angiogenesis early after coronary angioplasty : correlation with arterial remodeling. *Arterioscler Thromb Vasc Biol, 19*(2), 229-238.

Penzkofer, D., Bonauer, A., Fischer, A., Tups, A., Brandes, R. P., Zeiher, A. M., & Dimmeler, S. (2014). Phenotypic characterization of miR-92a-/- mice reveals an important function of miR-92a in skeletal development. *PLoS One, 9*(6), e101153. doi:10.1371/journal.pone.0101153

Perin, E. C., & Silva, G. V. (2009). Autologous cell-based therapy for ischemic heart disease: clinical evidence, proposed mechanisms of action, and current limitations. *Catheter Cardiovasc Interv, 73*(3), 281-288. doi:10.1002/ccd.21807

Petty, R. D., Sutherland, L. A., Hunter, E. M., & Cree, I. A. (1995). Comparison of MTT and ATP-based assays for the measurement of viable cell number. *J Biolumin Chemilumin, 10*(1), 29-34. doi:10.1002/bio.1170100105

Piper, R. C., & Katzmann, D. J. (2007). Biogenesis and function of multivesicular bodies. *Annu Rev Cell Dev Biol, 23*, 519-547. doi:10.1146/annurev.cellbio.23.090506.123319

Plow, E. F., Haas, T. A., Zhang, L., Loftus, J., & Smith, J. W. (2000). Ligand binding to integrins. *J Biol Chem, 275*(29), 21785-21788. doi:10.1074/jbc.R000003200

Pober, J. S. (2012). Just the FACS or stalking the elusive circulating endothelial progenitor cell. *Arterioscler Thromb Vasc Biol, 32*(4), 837-838. doi:10.1161/ATVBAHA.112.246280

Polimeni, A., De Rosa, S., & Indolfi, C. (2013). Vascular miRNAs after balloon angioplasty. *Trends Cardiovasc Med, 23*(1), 9-14. doi:10.1016/j.tcm.2012.08.004

Potente, M., Gerhardt, H., & Carmeliet, P. (2011). Basic and therapeutic aspects of angiogenesis. *Cell, 146*(6), 873-887. doi:10.1016/j.cell.2011.08.039

Potente, M., Ghaeni, L., Baldessari, D., Mostoslavsky, R., Rossig, L., Dequiedt, F., . . . Dimmeler, S. (2007). SIRT1 controls endothelial angiogenic functions during vascular growth. *Genes Dev, 21*(20), 2644-2658. doi:10.1101/gad.435107

Potente, M., Urbich, C., Sasaki, K., Hofmann, W. K., Heeschen, C., Aicher, A., . . . Dimmeler, S. (2005). Involvement of Foxo transcription factors in angiogenesis and postnatal neovascularization. *J Clin Invest, 115*(9), 2382-2392. doi:10.1172/JCI23126

Prokopi, M., Pula, G., Mayr, U., Devue, C., Gallagher, J., Xiao, Q., . . . Mayr, M. (2009). Proteomic analysis reveals presence of platelet microparticles in endothelial progenitor cell cultures. *Blood, 114*(3), 723-732. doi:10.1182/blood-2009-02-205930

Psaltis, P. J., Harbuzariu, A., Delacroix, S., Holroyd, E. W., & Simari, R. D. (2011). Resident vascular progenitor cells--diverse origins, phenotype, and function. *J Cardiovasc Transl Res, 4*(2), 161-176. doi:10.1007/s12265-010-9248-9

Psaltis, P. J., & Simari, R. D. (2015). Vascular wall progenitor cells in health and disease. *Circ Res, 116*(8), 1392-1412. doi:10.1161/CIRCRESAHA.116.305368

Qin, G., Ii, M., Silver, M., Wecker, A., Bord, E., Ma, H., . . . Losordo, D. W. (2006). Functional disruption of alpha4 integrin mobilizes bone marrow-derived endothelial progenitors and augments ischemic neovascularization. *J Exp Med, 203*(1), 153-163. doi:10.1084/jem.20050459

Quirici, N., Soligo, D., Caneva, L., Servida, F., Bossolasco, P., & Deliliers, G. L. (2001). Differentiation and expansion of endothelial cells from human bone marrow CD133(+) cells. *Br J Haematol, 115*(1), 186-194.

Rafii, S., & Lyden, D. (2003). Therapeutic stem and progenitor cell transplantation for organ vascularization and regeneration. *Nat Med, 9*(6), 702-712. doi:10.1038/nm0603-702

Rafii, S., Shapiro, F., Rimarachin, J., Nachman, R. L., Ferris, B., Weksler, B., . . . Asch, A. S. (1994). Isolation and characterization of human bone marrow microvascular endothelial cells: hematopoietic progenitor cell adhesion. *Blood, 84*(1), 10-19.

Rajagopal, V., & Rockson, S. G. (2003). Coronary restenosis: a review of mechanisms and management. *Am J Med, 115*(7), 547-553.

Ramagli, L. S. (1999). Quantifying protein in 2-D PAGE solubilization buffers. *Methods Mol Biol, 112*, 99-103.

Ramjaun, A. R., & Hodivala-Dilke, K. (2009). The role of cell adhesion pathways in angiogenesis. *Int J Biochem Cell Biol, 41*(3), 521-530. doi:10.1016/j.biocel.2008.05.030

Rapozzi, V., Cogoi, S., & Xodo, L. E. (2006). Antisense locked nucleic acids efficiently suppress BCR/ABL and induce cell growth decline and apoptosis in leukemic cells. *Mol Cancer Ther, 5*(7), 1683-1692. doi:10.1158/1535-7163.MCT-06-0006

Rautou, P. E., Vion, A. C., Amabile, N., Chironi, G., Simon, A., Tedgui, A., & Boulanger, C. M. (2011). Microparticles, vascular function, and atherothrombosis. *Circ Res, 109*(5), 593-606. doi:10.1161/CIRCRESAHA.110.233163

Razmara, M., Heldin, C. H., & Lennartsson, J. (2013). Platelet-derived growth factor-induced Akt phosphorylation requires mTOR/Rictor and phospholipase C-gamma1, whereas S6 phosphorylation depends on mTOR/Raptor and phospholipase D. *Cell Commun Signal, 11*(1), 3. doi:10.1186/1478-811X-11-3

Reddy, M. K., Vasir, J. K., Hegde, G. V., Joshi, S. S., & Labhasetwar, V. (2007). Erythropoietin induces excessive neointima formation: a study in a rat carotid artery model of vascular injury. *J Cardiovasc Pharmacol Ther, 12*(3), 237-247. doi:10.1177/1074248406297326

Rehman, J., Li, J., Orschell, C. M., & March, K. L. (2003). Peripheral blood "endothelial progenitor cells" are derived from monocyte/macrophages and secrete angiogenic growth factors. *Circulation, 107*(8), 1164-1169.

Rehman, J., Li, J., Parvathaneni, L., Karlsson, G., Panchal, V. R., Temm, C. J., . . . March, K. L. (2004). Exercise acutely increases circulating endothelial progenitor cells and monocyte-/macrophage-derived angiogenic cells. *J Am Coll Cardiol, 43*(12), 2314-2318. doi:10.1016/j.jacc.2004.02.049

Reidy, M., Zihlmann, P., Hubbell, J. A., & Hall, H. (2006). Activation of cell-survival transcription factor NFkappaB in L1Ig6-stimulated endothelial cells. *J Biomed Mater Res A, 77*(3), 542-550. doi:10.1002/jbm.a.30590

Reyes, M., Dudek, A., Jahagirdar, B., Koodie, L., Marker, P. H., & Verfaillie, C. M. (2002). Origin of endothelial progenitors in human postnatal bone marrow. *J Clin Invest, 109*(3), 337-346. doi:10.1172/JCI14327

Richardson, M. R., & Yoder, M. C. (2011). Endothelial progenitor cells: quo vadis? *J Mol Cell Cardiol, 50*(2), 266-272. doi:10.1016/j.yjmcc.2010.07.009

Riessen, R., Wight, T. N., Pastore, C., Henley, C., & Isner, J. M. (1996). Distribution of hyaluronan during extracellular matrix remodeling in human restenotic arteries and balloon-injured rat carotid arteries. *Circulation, 93*(6), 1141-1147.

Riordan, N. H., Chan, K., Marleau, A. M., & Ichim, T. E. (2007). Cord blood in regenerative medicine: do we need immune suppression? *J Transl Med, 5*, 8. doi:10.1186/1479-5876-5-8

Roberts, M. S., Woods, A. J., Shaw, P. E., & Norman, J. C. (2003). ERK1 associates with alpha(v)beta 3 integrin and regulates cell spreading on vitronectin. *J Biol Chem, 278*(3), 1975-1985. doi:10.1074/jbc.M208607200

Robinson, C. J., & Stringer, S. E. (2001). The splice variants of vascular endothelial growth factor (VEGF) and their receptors. *J Cell Sci, 114*(Pt 5), 853-865.

Roca-Cusachs, P., Gauthier, N. C., Del Rio, A., & Sheetz, M. P. (2009). Clustering of alpha(5)beta(1) integrins determines adhesion strength whereas alpha(v)beta(3) and talin enable mechanotransduction. *Proc Natl Acad Sci U S A, 106*(38), 16245-16250. doi:10.1073/pnas.0902818106

Rodriguez-Menocal, L., St-Pierre, M., Wei, Y., Khan, S., Mateu, D., Calfa, M., . . . Vazquez-Padron, R. I. (2009). The origin of post-injury neointimal cells in the rat balloon injury model. *Cardiovasc Res, 81*(1), 46-53. doi:10.1093/cvr/cvn265

Rohde, E., Bartmann, C., Schallmoser, K., Reinisch, A., Lanzer, G., Linkesch, W., . . . Strunk, D. (2007). Immune cells mimic the morphology of endothelial progenitor colonies in vitro. *Stem Cells, 25*(7), 1746-1752. doi:10.1634/stemcells.2006-0833

Rohde, E., Malischnik, C., Thaler, D., Maierhofer, T., Linkesch, W., Lanzer, G., . . . Strunk, D. (2006). Blood monocytes mimic endothelial progenitor cells. *Stem Cells, 24*(2), 357-367. doi:10.1634/stemcells.2005-0072

Rossig, L., Urbich, C., Bruhl, T., Dernbach, E., Heeschen, C., Chavakis, E., . . . Dimmeler, S. (2005). Histone deacetylase activity is essential for the expression of HoxA9 and for endothelial commitment of progenitor cells. *J Exp Med, 201*(11), 1825-1835. doi:10.1084/jem.20042097

Rossig, L., Urbich, C., & Dimmeler, S. (2004). Endothelial progenitor cells at work: not mature yet, but already stress-resistant. *Arterioscler Thromb Vasc Biol, 24*(11), 1977-1979. doi:10.1161/01.ATV.0000146815.54702.75

Roura, S., Pujal, J. M., Galvez-Monton, C., & Bayes-Genis, A. (2015). Impact of umbilical cord blood-derived mesenchymal stem cells on cardiovascular research. *Biomed Res Int, 2015*, 975302. doi:10.1155/2015/975302

Rowand, J. L., Martin, G., Doyle, G. V., Miller, M. C., Pierce, M. S., Connelly, M. C., . . . Terstappen, L. W. (2007). Endothelial cells in peripheral blood of healthy subjects and patients with metastatic carcinomas. *Cytometry A, 71*(2), 105-113. doi:10.1002/cyto.a.20364

Rudic, R. D., Shesely, E. G., Maeda, N., Smithies, O., Segal, S. S., & Sessa, W. C. (1998). Direct evidence for the importance of endothelium-derived nitric oxide in vascular remodeling. *J Clin Invest, 101*(4), 731-736. doi:10.1172/JCI1699

Ryer, E. J., Hom, R. P., Sakakibara, K., Nakayama, K. I., Nakayama, K., Faries, P. L., . . . Kent, K. C. (2006). PKCdelta is necessary for Smad3 expression and transforming growth factor beta-induced fibronectin synthesis in vascular smooth muscle cells. *Arterioscler Thromb Vasc Biol, 26*(4), 780-786. doi:10.1161/01.ATV.0000209517.00220.cd

Sabatel, C., Malvaux, L., Bovy, N., Deroanne, C., Lambert, V., Gonzalez, M. L., . . . Struman, I. (2011). MicroRNA-21 exhibits antiangiogenic function by targeting RhoB expression in endothelial cells. *PLoS One, 6*(2), e16979. doi:10.1371/journal.pone.0016979

Sadahira, Y., Ruan, F., Hakomori, S., & Igarashi, Y. (1992). Sphingosine 1-phosphate, a specific endogenous signaling molecule controlling cell motility and tumor cell invasiveness. *Proc Natl Acad Sci U S A, 89*(20), 9686-9690.

Sakurai, H., Kawabata, K., Sakurai, F., Nakagawa, S., & Mizuguchi, H. (2008). Innate immune response induced by gene delivery vectors. *Int J Pharm, 354*(1-2), 9-15. doi:10.1016/j.ijpharm.2007.06.012

Salameh, A., Galvagni, F., Bardelli, M., Bussolino, F., & Oliviero, S. (2005). Direct recruitment of CRK and GRB2 to VEGFR-3 induces proliferation, migration, and survival of endothelial cells through the activation of ERK, AKT, and JNK pathways. *Blood, 106*(10), 3423-3431. doi:10.1182/blood-2005-04-1388

Salati, S., Zini, R., Bianchi, E., Testa, A., Mavilio, F., Manfredini, R., & Ferrari, S. (2008). Role of CD34 antigen in myeloid differentiation of human hematopoietic progenitor cells. *Stem Cells, 26*(4), 950-959. doi:10.1634/stemcells.2007-0597

Salmena, L., Poliseno, L., Tay, Y., Kats, L., & Pandolfi, P. P. (2011). A ceRNA hypothesis: the Rosetta Stone of a hidden RNA language? *Cell, 146*(3), 353-358. doi:10.1016/j.cell.2011.07.014

Sasaki, K., Heeschen, C., Aicher, A., Ziebart, T., Honold, J., Urbich, C., . . . Dimmeler, S. (2006). Ex vivo pretreatment of bone marrow mononuclear cells with endothelial NO synthase enhancer AVE9488 enhances their functional activity for cell therapy. *Proc Natl Acad Sci U S A, 103*(39), 14537-14541. doi:10.1073/pnas.0604144103

Sasamoto, A., Nagino, M., Kobayashi, S., Naruse, K., Nimura, Y., & Sokabe, M. (2005). Mechanotransduction by integrin is essential for IL-6 secretion from endothelial cells in response to uniaxial continuous stretch. *Am J Physiol Cell Physiol, 288*(5), C1012-1022. doi:10.1152/ajpcell.00314.2004

Sata, M., Saiura, A., Kunisato, A., Tojo, A., Okada, S., Tokuhisa, T., . . . Nagai, R. (2002). Hematopoietic stem cells differentiate into vascular cells that participate in the pathogenesis of atherosclerosis. *Nat Med, 8*(4), 403-409. doi:10.1038/nm0402-403

Sato, Y., Kanno, S., Oda, N., Abe, M., Ito, M., Shitara, K., & Shibuya, M. (2000). Properties of two VEGF receptors, Flt-1 and KDR, in signal transduction. *Ann N Y Acad Sci, 902*, 201-205; discussion 205-207.

Scatena, M., Almeida, M., Chaisson, M. L., Fausto, N., Nicosia, R. F., & Giachelli, C. M. (1998). NF-kappaB mediates alphavbeta3 integrin-induced endothelial cell survival. *J Cell Biol, 141*(4), 1083-1093.

Schaller, M. D., Otey, C. A., Hildebrand, J. D., & Parsons, J. T. (1995). Focal adhesion kinase and paxillin bind to peptides mimicking beta integrin cytoplasmic domains. *J Cell Biol, 130*(5), 1181-1187.

Scheubel, R. J., Zorn, H., Silber, R. E., Kuss, O., Morawietz, H., Holtz, J., & Simm, A. (2003). Age-dependent depression in circulating endothelial progenitor cells in patients undergoing coronary artery bypass grafting. *J Am Coll Cardiol, 42*(12), 2073-2080.

Schlingemann, R. O., Rietveld, F. J., de Waal, R. M., Bradley, N. J., Skene, A. I., Davies, A. J., . . . Ruiter, D. J. (1990). Leukocyte antigen CD34 is expressed by a subset of cultured endothelial cells and on endothelial abluminal microprocesses in the tumor stroma. *Lab Invest, 62*(6), 690-696.

Schmeisser, A., Garlichs, C. D., Zhang, H., Eskafi, S., Graffy, C., Ludwig, J., . . . Daniel, W. G. (2001). Monocytes coexpress endothelial and macrophagocytic lineage markers and form cord-like structures in Matrigel under angiogenic conditions. *Cardiovasc Res, 49*(3), 671-680.

Schmeisser, A., Graffy, C., Daniel, W. G., & Strasser, R. H. (2003). Phenotypic overlap between monocytes and vascular endothelial cells. *Adv Exp Med Biol, 522*, 59-74.

Schmidt-Lucke, C., Fichtlscherer, S., Aicher, A., Tschope, C., Schultheiss, H. P., Zeiher, A. M., & Dimmeler, S. (2010). Quantification of circulating endothelial progenitor cells using the modified ISHAGE protocol. *PLoS One, 5*(11), e13790. doi:10.1371/journal.pone.0013790

Schmidt-Lucke, C., Rossig, L., Fichtlscherer, S., Vasa, M., Britten, M., Kamper, U., . . . Zeiher, A. M. (2005). Reduced number of circulating endothelial progenitor cells predicts future cardiovascular events: proof of concept for the clinical importance of endogenous vascular repair. *Circulation, 111*(22), 2981-2987. doi:10.1161/CIRCULATIONAHA.104.504340

Schober, A., Karshovska, E., Zernecke, A., & Weber, C. (2006). SDF-1alpha-mediated tissue repair by stem cells: a promising tool in cardiovascular medicine? *Trends Cardiovasc Med, 16*(4), 103-108. doi:10.1016/j.tcm.2006.01.006

Schuh, A., Kroh, A., Konschalla, S., Liehn, E. A., Sobota, R. M., Biessen, E. A., . . . Sasse, A. (2012). Myocardial regeneration by transplantation of modified endothelial progenitor cells expressing SDF-1 in a rat model. *J Cell Mol Med, 16*(10), 2311-2320. doi:10.1111/j.1582-4934.2012.01539.x

Scolnik, M. P., Morilla, R., de Bracco, M. M., Catovsky, D., & Matutes, E. (2002). CD34 and CD117 are overexpressed in AML and may be valuable to detect minimal residual disease. *Leuk Res, 26*(7), 615-619.

Seeger, F. H., Zeiher, A. M., & Dimmeler, S. (2013). MicroRNAs in stem cell function and regenerative therapy of the heart. *Arterioscler Thromb Vasc Biol, 33*(8), 1739-1746. doi:10.1161/ATVBAHA.113.300138

Sekiguchi, H., Ii, M., & Losordo, D. W. (2009). The relative potency and safety of endothelial progenitor cells and unselected mononuclear cells for recovery from myocardial infarction and ischemia. *J Cell Physiol, 219*(2), 235-242. doi:10.1002/jcp.21672

Sen, S., Merchan, J., Dean, J., Ii, M., Gavin, M., Silver, M., . . . Aikawa, R. (2010). Autologous transplantation of endothelial progenitor cells genetically modified by adeno-associated viral vector delivering insulin-like growth factor-1 gene after myocardial infarction. *Hum Gene Ther, 21*(10), 1327-1334. doi:10.1089/hum.2010.006

Shalaby, F., Rossant, J., Yamaguchi, T. P., Gertsenstein, M., Wu, X. F., Breitman, M. L., & Schuh, A. C. (1995). Failure of blood-island formation and vasculogenesis in Flk-1-deficient mice. *Nature, 376*(6535), 62-66. doi:10.1038/376062a0

Shan, S. W., Lee, D. Y., Deng, Z., Shatseva, T., Jeyapalan, Z., Du, W. W., . . . Yang, B. B. (2009). MicroRNA MiR-17 retards tissue growth and represses fibronectin expression. *Nat Cell Biol, 11*(8), 1031-1038. doi:10.1038/ncb1917

Shanahan, C. M., & Weissberg, P. L. (1998). Smooth muscle cell heterogeneity: patterns of gene expression in vascular smooth muscle cells in vitro and in vivo. *Arterioscler Thromb Vasc Biol, 18*(3), 333-338.

Shao, R., Bao, S., Bai, X., Blanchette, C., Anderson, R. M., Dang, T., . . . Wang, X. F. (2004). Acquired expression of periostin by human breast cancers promotes tumor angiogenesis through up-regulation of vascular endothelial growth factor receptor 2 expression. *Mol Cell Biol, 24*(9), 3992-4003.

Sharifi, M., Salehi, R., Gheisari, Y., & Kazemi, M. (2013). Inhibition of MicroRNA miR-92a Inhibits Cell Proliferation in Human Acute Promyelocytic Leukemia. *Turk J Haematol, 30*(2), 157-162. doi:10.4274/Tjh.2012.0171

Sharma, S. Y., M. (2010). Gene silencing of E-selectin block recruitment of endothelial progenitor cell to vascular endothelium under flow. *J. Biomedical Science and Engineering, 3*, 5. doi:10.4236/jbise.2010.36077

Shen, B., Delaney, M. K., & Du, X. (2012). Inside-out, outside-in, and inside-outside-in: G protein signaling in integrin-mediated cell adhesion, spreading, and retraction. *Curr Opin Cell Biol, 24*(5), 600-606. doi:10.1016/j.ceb.2012.08.011

Shi, M., Ishikawa, M., Kamei, N., Nakasa, T., Adachi, N., Deie, M., . . . Ochi, M. (2009). Acceleration of skeletal muscle regeneration in a rat skeletal muscle injury model by local injection of human peripheral blood-derived CD133-positive cells. *Stem Cells, 27*(4), 949-960. doi:10.1002/stem.4

Shi, M. A., & Shi, G. P. (2010). Intracellular delivery strategies for microRNAs and potential therapies for human cardiovascular diseases. *Sci Signal, 3*(146), pe40. doi:scisignal.3146pe40 [pii]

10.1126/scisignal.3146pe40

Shi, Q., Rafii, S., Wu, M. H., Wijelath, E. S., Yu, C., Ishida, A., . . . Hammond, W. P. (1998). Evidence for circulating bone marrow-derived endothelial cells. *Blood, 92*(2), 362-367.

Shi, S. J., Zhong, Z. R., Liu, J., Zhang, Z. R., Sun, X., & Gong, T. (2012). Solid lipid nanoparticles loaded with anti-microRNA oligonucleotides (AMOs) for suppression of microRNA-21 functions in human lung cancer cells. *Pharm Res, 29*(1), 97-109. doi:10.1007/s11095-011-0514-6

Shi, Y., O'Brien, J. E., Fard, A., Mannion, J. D., Wang, D., & Zalewski, A. (1996). Adventitial myofibroblasts contribute to neointimal formation in injured porcine coronary arteries. *Circulation, 94*(7), 1655-1664.

Shigoka, M., Tsuchida, A., Matsudo, T., Nagakawa, Y., Saito, H., Suzuki, Y., . . . Kuroda, M. (2010). Deregulation of miR-92a expression is implicated in hepatocellular carcinoma development. *Pathol Int, 60*(5), 351-357. doi:10.1111/j.1440-1827.2010.02526.x

Shim, Y., Nam, M. H., Hyuk, S. W., Yoon, S. Y., & Song, J. M. (2015). Concurrent hypermulticolor monitoring of CD31, CD34, CD45 and CD146 endothelial progenitor cell markers for acute myocardial infarction. *Anal Chim Acta, 853*, 501-507. doi:10.1016/j.aca.2014.10.036

Short, S. M., Talbott, G. A., & Juliano, R. L. (1998). Integrin-mediated signaling events in human endothelial cells. *Mol Biol Cell, 9*(8), 1969-1980.

Shyy, J. Y., & Chien, S. (2002). Role of integrins in endothelial mechanosensing of shear stress. *Circ Res, 91*(9), 769-775.

Siavashi, V., Nassiri, S. M., Rahbarghazi, R., Vafaei, R., & Sariri, R. (2016). ECM-Dependence of Endothelial Progenitor Cell Features. *J Cell Biochem, 117*(8), 1934-1946. doi:10.1002/jcb.25492

Sidney, L. E., Branch, M. J., Dunphy, S. E., Dua, H. S., & Hopkinson, A. (2014). Concise review: evidence for CD34 as a common marker for diverse progenitors. *Stem Cells, 32*(6), 1380-1389. doi:10.1002/stem.1661

Siemerink, M. J., Klaassen, I., Vogels, I. M., Griffioen, A. W., Van Noorden, C. J., & Schlingemann, R. O. (2012). CD34 marks angiogenic tip cells in human vascular endothelial cell cultures. *Angiogenesis, 15*(1), 151-163. doi:10.1007/s10456-011-9251-z

Sieuwerts, A. M., Klijn, J. G., & Foekens, J. A. (1997). Assessment of the invasive potential of human gynecological tumor cell lines with the in vitro Boyden chamber assay: influences of the ability of cells to migrate through the filter membrane. *Clin Exp Metastasis, 15*(1), 53-62.

Sieveking, D. P., Buckle, A., Celermajer, D. S., & Ng, M. K. (2008). Strikingly different angiogenic properties of endothelial progenitor cell subpopulations: insights from a novel human angiogenesis assay. *J Am Coll Cardiol, 51*(6), 660-668. doi:10.1016/j.jacc.2007.09.059

Silber, S., Damman, P., Klomp, M., Beijk, M. A., Grisold, M., Ribeiro, E. E., . . . de Winter, R. J. (2011). Clinical results after coronary stenting with the Genous Bio-engineered R stent: 12-month outcomes of the e-HEALING (Healthy Endothelial Accelerated Lining Inhibits Neointimal Growth) worldwide registry. *EuroIntervention, 6*(7), 819-825. doi:10.4244/EIJV6I7A141

Simard, T., Jung, R. G., Motazedian, P., Di Santo, P., Ramirez, F. D., Russo, J. J., . . . Hibbert, B. (2017). Progenitor Cells for Arterial Repair: Incremental Advancements towards Therapeutic Reality. *Stem Cells Int, 2017*, 8270498. doi:10.1155/2017/8270498

Siomi, H., & Siomi, M. C. (2009). RISC hitches onto endosome trafficking. *Nat Cell Biol, 11*(9), 1049-1051. doi:ncb0909-1049 [pii]

10.1038/ncb0909-1049

Siomi, H., & Siomi, M. C. (2010). Posttranscriptional regulation of microRNA biogenesis in animals. *Mol Cell, 38*(3), 323-332. doi:S1097-2765(10)00251-0 [pii]

10.1016/j.molcel.2010.03.013

Slovinska, L., Novotna, I., Kubes, M., Radonak, J., Jergova, S., Cigankova, V., . . . Cizkova, D. (2011). Umbilical cord blood cells CD133+/CD133- cultivation in neural proliferation media differentiates towards neural cell lineages. *Arch Med Res, 42*(7), 555-562. doi:10.1016/j.arcmed.2011.10.003

Small, E. M., & Olson, E. N. (2011). Pervasive roles of microRNAs in cardiovascular biology. *Nature, 469*(7330), 336-342. doi:10.1038/nature09783

Solovey, A., Lin, Y., Browne, P., Choong, S., Wayner, E., & Hebbel, R. P. (1997). Circulating activated endothelial cells in sickle cell anemia. *N Engl J Med, 337*(22), 1584-1590. doi:10.1056/NEJM199711273372203

Solovey, A. N., Gui, L., Chang, L., Enenstein, J., Browne, P. V., & Hebbel, R. P. (2001). Identification and functional assessment of endothelial P1H12. *J Lab Clin Med, 138*(5), 322-331. doi:10.1067/mlc.2001.118519

Sorrentino, S. A., Bahlmann, F. H., Besler, C., Muller, M., Schulz, S., Kirchhoff, N., . . . Landmesser, U. (2007). Oxidant stress impairs in vivo reendothelialization capacity of endothelial progenitor cells from patients with type 2 diabetes mellitus: restoration by the peroxisome proliferator-activated receptor-gamma agonist rosiglitazone. *Circulation, 116*(2), 163-173. doi:10.1161/CIRCULATIONAHA.106.684381

Stein, A., Mohr, F., Laux, M., Thieme, S., Lorenz, B., Cetindis, M., . . . Ott, I. (2012). Erythropoietin-induced progenitor cell mobilisation in patients with acute ST-segment-elevation myocardial infarction and restenosis. *Thromb Haemost, 107*(4), 769-774. doi:10.1160/TH11-08-0552

Stellos, K., & Gawaz, M. (2007). Platelet interaction with progenitor cells: potential implications for regenerative medicine. *Thromb Haemost, 98*(5), 922-929.
Stenmark, K. R., Yeager, M. E., El Kasmi, K. C., Nozik-Grayck, E., Gerasimovskaya, E. V., Li, M., . . . Frid, M. G. (2013). The adventitia: essential regulator of vascular wall structure and function. *Annu Rev Physiol, 75*, 23-47. doi:10.1146/annurev-physiol-030212-183802
Stenvang, J., Petri, A., Lindow, M., Obad, S., & Kauppinen, S. (2012). Inhibition of microRNA function by antimiR oligonucleotides. *Silence, 3*(1), 1. doi:10.1186/1758-907X-3-1
Stenzel, D., Lundkvist, A., Sauvaget, D., Busse, M., Graupera, M., van der Flier, A., . . . Gerhardt, H. (2011). Integrin-dependent and -independent functions of astrocytic fibronectin in retinal angiogenesis. *Development, 138*(20), 4451-4463. doi:10.1242/dev.071381
Strehlow, K., Werner, N., Berweiler, J., Link, A., Dirnagl, U., Priller, J., . . . Nickenig, G. (2003). Estrogen increases bone marrow-derived endothelial progenitor cell production and diminishes neointima formation. *Circulation, 107*(24), 3059-3065. doi:10.1161/01.CIR.0000077911.81151.30
Strilic, B., Kucera, T., Eglinger, J., Hughes, M. R., McNagny, K. M., Tsukita, S., . . . Lammert, E. (2009). The molecular basis of vascular lumen formation in the developing mouse aorta. *Dev Cell, 17*(4), 505-515. doi:10.1016/j.devcel.2009.08.011
Suarez, Y., Fernandez-Hernando, C., Yu, J., Gerber, S. A., Harrison, K. D., Pober, J. S., . . . Sessa, W. C. (2008). Dicer-dependent endothelial microRNAs are necessary for postnatal angiogenesis. *Proc Natl Acad Sci U S A, 105*(37), 14082-14087. doi:10.1073/pnas.0804597105
Sudhakar, A., Sugimoto, H., Yang, C., Lively, J., Zeisberg, M., & Kalluri, R. (2003). Human tumstatin and human endostatin exhibit distinct antiangiogenic activities mediated by alpha v beta 3 and alpha 5 beta 1 integrins. *Proc Natl Acad Sci U S A, 100*(8), 4766-4771. doi:10.1073/pnas.0730882100
Sun, S. G., Zheng, B., Han, M., Fang, X. M., Li, H. X., Miao, S. B., . . . Wen, J. K. (2011). miR-146a and Kruppel-like factor 4 form a feedback loop to participate in vascular smooth muscle cell proliferation. *EMBO Rep, 12*(1), 56-62. doi:10.1038/embor.2010.172
Sun, X., Fu, Y., Gu, M., Zhang, L., Li, D., Li, H., . . . Zhu, Y. (2016). Activation of integrin alpha5 mediated by flow requires its translocation to membrane lipid rafts in vascular endothelial cells. *Proc Natl Acad Sci U S A, 113*(3), 769-774. doi:10.1073/pnas.1524523113
Sunada, H., Masuda, M., & Fujiwara, K. (1993). Preservation of differentiated phenotypes in cultured aortic endothelial cells by malotilate and phosphoascorbic acid. *Eur J Cell Biol, 60*(1), 48-56.
Sylvestre, Y., De Guire, V., Querido, E., Mukhopadhyay, U. K., Bourdeau, V., Major, F., . . . Chartrand, P. (2007). An E2F/miR-20a autoregulatory feedback loop. *J Biol Chem, 282*(4), 2135-2143. doi:10.1074/jbc.M608939200
Szmitko, P. E., Kutryk, M. J., Stewart, D. J., Strauss, M. H., & Verma, S. (2006). Endothelial progenitor cell-coated stents under scrutiny. *Can J Cardiol, 22*(13), 1117-1119.
Takahashi, T., Kalka, C., Masuda, H., Chen, D., Silver, M., Kearney, M., . . . Asahara, T. (1999). Ischemia- and cytokine-induced mobilization of bone marrow-derived endothelial progenitor cells for neovascularization. *Nat Med, 5*(4), 434-438. doi:10.1038/7434
Takamiya, M., Okigaki, M., Jin, D., Takai, S., Nozawa, Y., Adachi, Y., . . . Matsubara, H. (2006). Granulocyte colony-stimulating factor-mobilized circulating c-Kit+/Flk-1+ progenitor cells regenerate endothelium and inhibit neointimal hyperplasia after vascular injury. *Arterioscler Thromb Vasc Biol, 26*(4), 751-757. doi:10.1161/01.ATV.0000205607.98538.9a
Takizawa, S., Nagata, E., Nakayama, T., Masuda, H., & Asahara, T. (2016). Recent Progress in Endothelial Progenitor Cell Culture Systems: Potential for Stroke Therapy. *Neurol Med Chir (Tokyo), 56*(6), 302-309. doi:10.2176/nmc.ra.2016-0027

Tanaka, M., Oikawa, K., Takanashi, M., Kudo, M., Ohyashiki, J., Ohyashiki, K., & Kuroda, M. (2009). Down-regulation of miR-92 in human plasma is a novel marker for acute leukemia patients. *PLoS One, 4*(5), e5532. doi:10.1371/journal.pone.0005532

Tang, D., Lu, J., Walterscheid, J. P., Chen, H. H., Engler, D. A., Sawamura, T., . . . Chen, C. H. (2008). Electronegative LDL circulating in smokers impairs endothelial progenitor cell differentiation by inhibiting Akt phosphorylation via LOX-1. *J Lipid Res, 49*(1), 33-47. doi:10.1194/jlr.M700305-JLR200

Taniguchi, N., Nakamura, T., Sawada, T., Matsubara, K., Furukawa, K., Hadase, M., . . . Matsubara, H. (2010). Erythropoietin prevention trial of coronary restenosis and cardiac remodeling after ST-elevated acute myocardial infarction (EPOC-AMI): a pilot, randomized, placebo-controlled study. *Circ J, 74*(11), 2365-2371.

Templin, C., Luscher, T. F., & Landmesser, U. (2011). Cell-based cardiovascular repair and regeneration in acute myocardial infarction and chronic ischemic cardiomyopathy-current status and future developments. *Int J Dev Biol, 55*(4-5), 407-417. doi:10.1387/ijdb.103219ct

Thomson, J. M., Newman, M., Parker, J. S., Morin-Kensicki, E. M., Wright, T., & Hammond, S. M. (2006). Extensive post-transcriptional regulation of microRNAs and its implications for cancer. *Genes Dev, 20*(16), 2202-2207. doi:10.1101/gad.1444406

Thum, T. (2012). MicroRNA therapeutics in cardiovascular medicine. *EMBO Mol Med, 4*(1), 3-14. doi:10.1002/emmm.201100191

Thum, T., Fleissner, F., Klink, I., Tsikas, D., Stichtenoth, D., Ertl, G., & Bauersachs, J. (2007). Growth hormone treatment improves markers of systemic nitric oxide bioavailability via the insulin-like growth factor-1 Importance for endothelial progenitor cells. *J Stem Cells Regen Med, 2*(1), 115-116.

Thum, T., Fraccarollo, D., Schultheiss, M., Froese, S., Galuppo, P., Widder, J. D., . . . Bauersachs, J. (2007). Endothelial nitric oxide synthase uncoupling impairs endothelial progenitor cell mobilization and function in diabetes. *Diabetes, 56*(3), 666-674. doi:10.2337/db06-0699

Thum, T., Tsikas, D., Stein, S., Schultheiss, M., Eigenthaler, M., Anker, S. D., . . . Bauersachs, J. (2005). Suppression of endothelial progenitor cells in human coronary artery disease by the endogenous nitric oxide synthase inhibitor asymmetric dimethylarginine. *J Am Coll Cardiol, 46*(9), 1693-1701. doi:10.1016/j.jacc.2005.04.066

Tianhang, L., Bo, W., Zhengmao, L., Tao, P., Hong, Z., Xuchao, X., . . . Guoen, F. (2013). Autologous transplantation of endothelial progenitor cells to prevent multiple organ dysfunction syndromes in pig. *J Trauma Acute Care Surg, 74*(2), 508-515. doi:10.1097/TA.0b013e3182703420

Timmermans, F., Plum, J., Yoder, M. C., Ingram, D. A., Vandekerckhove, B., & Case, J. (2009). Endothelial progenitor cells: identity defined? *J Cell Mol Med, 13*(1), 87-102. doi:10.1111/j.1582-4934.2008.00598.x

Timmermans, F., Van Hauwermeiren, F., De Smedt, M., Raedt, R., Plasschaert, F., De Buyzere, M. L., . . . Vandekerckhove, B. (2007). Endothelial outgrowth cells are not derived from CD133+ cells or CD45+ hematopoietic precursors. *Arterioscler Thromb Vasc Biol, 27*(7), 1572-1579. doi:10.1161/ATVBAHA.107.144972

Timpl, R. (1996). Macromolecular organization of basement membranes. *Curr Opin Cell Biol, 8*(5), 618-624.

Tintut, Y., Alfonso, Z., Saini, T., Radcliff, K., Watson, K., Bostrom, K., & Demer, L. L. (2003). Multilineage potential of cells from the artery wall. *Circulation, 108*(20), 2505-2510. doi:10.1161/01.CIR.0000096485.64373.C5

Tomlinson, M. J., Tomlinson, S., Yang, X. B., & Kirkham, J. (2013). Cell separation: Terminology and practical considerations. *J Tissue Eng, 4*, 2041731412472690. doi:10.1177/2041731412472690

Torella, D., Iaconetti, C., Catalucci, D., Ellison, G. M., Leone, A., Waring, C. D., . . . Indolfi, C. (2011). MicroRNA-133 controls vascular smooth muscle cell phenotypic switch in vitro

and vascular remodeling in vivo. *Circ Res, 109*(8), 880-893. doi:10.1161/CIRCRESAHA.111.240150

Torsney, E., Mandal, K., Halliday, A., Jahangiri, M., & Xu, Q. (2007). Characterisation of progenitor cells in human atherosclerotic vessels. *Atherosclerosis, 191*(2), 259-264. doi:10.1016/j.atherosclerosis.2006.05.033

Treguer, K., Heinrich, E. M., Ohtani, K., Bonauer, A., & Dimmeler, S. (2012). Role of the microRNA-17-92 cluster in the endothelial differentiation of stem cells. *J Vasc Res, 49*(5), 447-460. doi:10.1159/000339429

Tsai, S., Hollenbeck, S. T., Ryer, E. J., Edlin, R., Yamanouchi, D., Kundi, R., . . . Kent, K. C. (2009). TGF-beta through Smad3 signaling stimulates vascular smooth muscle cell proliferation and neointimal formation. *Am J Physiol Heart Circ Physiol, 297*(2), H540-549. doi:10.1152/ajpheart.91478.2007

Tsang, H. G., Rashdan, N. A., Whitelaw, C. B., Corcoran, B. M., Summers, K. M., & MacRae, V. E. (2016). Large animal models of cardiovascular disease. *Cell Biochem Funct, 34*(3), 113-132. doi:10.1002/cbf.3173

Tsuchida, A., Ohno, S., Wu, W., Borjigin, N., Fujita, K., Aoki, T., . . . Kuroda, M. (2011). miR-92 is a key oncogenic component of the miR-17-92 cluster in colon cancer. *Cancer Sci, 102*(12), 2264-2271. doi:10.1111/j.1349-7006.2011.02081.x

Tulis, D. A. (2007). Rat carotid artery balloon injury model. *Methods Mol Med, 139*, 1-30.

Tura, O., Skinner, E. M., Barclay, G. R., Samuel, K., Gallagher, R. C., Brittan, M., . . . Mills, N. L. (2013). Late outgrowth endothelial cells resemble mature endothelial cells and are not derived from bone marrow. *Stem Cells, 31*(2), 338-348. doi:10.1002/stem.1280

Urao, N., Okigaki, M., Yamada, H., Aadachi, Y., Matsuno, K., Matsui, A., . . . Matsubara, H. (2006). Erythropoietin-mobilized endothelial progenitors enhance reendothelialization via Akt-endothelial nitric oxide synthase activation and prevent neointimal hyperplasia. *Circ Res, 98*(11), 1405-1413. doi:10.1161/01.RES.0000224117.59417.f3

Urbich, C., Aicher, A., Heeschen, C., Dernbach, E., Hofmann, W. K., Zeiher, A. M., & Dimmeler, S. (2005). Soluble factors released by endothelial progenitor cells promote migration of endothelial cells and cardiac resident progenitor cells. *J Mol Cell Cardiol, 39*(5), 733-742. doi:10.1016/j.yjmcc.2005.07.003

Urbich, C., Dernbach, E., Reissner, A., Vasa, M., Zeiher, A. M., & Dimmeler, S. (2002). Shear stress-induced endothelial cell migration involves integrin signaling via the fibronectin receptor subunits alpha(5) and beta(1). *Arterioscler Thromb Vasc Biol, 22*(1), 69-75.

Urbich, C., & Dimmeler, S. (2004). Endothelial progenitor cells: characterization and role in vascular biology. *Circ Res, 95*(4), 343-353. doi:10.1161/01.RES.0000137877.89448.78

95/4/343 [pii]

Urbich, C., Heeschen, C., Aicher, A., Dernbach, E., Zeiher, A. M., & Dimmeler, S. (2003). Relevance of monocytic features for neovascularization capacity of circulating endothelial progenitor cells. *Circulation, 108*(20), 2511-2516. doi:10.1161/01.CIR.0000096483.29777.50

Urbich, C., Heeschen, C., Aicher, A., Sasaki, K., Bruhl, T., Farhadi, M. R., . . . Dimmeler, S. (2005). Cathepsin L is required for endothelial progenitor cell-induced neovascularization. *Nat Med, 11*(2), 206-213. doi:10.1038/nm1182

Urbich, C., Kuehbacher, A., & Dimmeler, S. (2008). Role of microRNAs in vascular diseases, inflammation, and angiogenesis. *Cardiovasc Res, 79*(4), 581-588. doi:10.1093/cvr/cvn156

Vajkoczy, P., Blum, S., Lamparter, M., Mailhammer, R., Erber, R., Engelhardt, B., . . . Hatzopoulos, A. K. (2003). Multistep nature of microvascular recruitment of ex vivo-expanded embryonic endothelial progenitor cells during tumor angiogenesis. *J Exp Med, 197*(12), 1755-1765. doi:10.1084/jem.20021659

Valadi, H., Ekstrom, K., Bossios, A., Sjostrand, M., Lee, J. J., & Lotvall, J. O. (2007). Exosome-mediated transfer of mRNAs and microRNAs is a novel mechanism of genetic exchange between cells. *Nat Cell Biol, 9*(6), 654-659. doi:10.1038/ncb1596

Valgimigli, M., Rigolin, G. M., Fucili, A., Porta, M. D., Soukhomovskaia, O., Malagutti, P., . . . Ferrari, R. (2004). CD34+ and endothelial progenitor cells in patients with various degrees of congestive heart failure. *Circulation, 110*(10), 1209-1212. doi:10.1161/01.CIR.0000136813.89036.21

van Beem, R. T., Verloop, R. E., Kleijer, M., Noort, W. A., Loof, N., Koolwijk, P., . . . Zwaginga, J. J. (2009). Blood outgrowth endothelial cells from cord blood and peripheral blood: angiogenesis-related characteristics in vitro. *J Thromb Haemost, 7*(1), 217-226. doi:10.1111/j.1538-7836.2008.03192.x

van Beusekom, H. M., Ertas, G., Sorop, O., Serruys, P. W., & van der Giessen, W. J. (2012). The Genous endothelial progenitor cell capture stent accelerates stent re-endothelialization but does not affect intimal hyperplasia in porcine coronary arteries. *Catheter Cardiovasc Interv, 79*(2), 231-242. doi:10.1002/ccd.22928

Van Craenenbroeck, E. M., Conraads, V. M., Van Bockstaele, D. R., Haine, S. E., Vermeulen, K., Van Tendeloo, V. F., . . . Hoymans, V. Y. (2008). Quantification of circulating endothelial progenitor cells: a methodological comparison of six flow cytometric approaches. *J Immunol Methods, 332*(1-2), 31-40. doi:10.1016/j.jim.2007.12.006

van der Flier, A., Badu-Nkansah, K., Whittaker, C. A., Crowley, D., Bronson, R. T., Lacy-Hulbert, A., & Hynes, R. O. (2010). Endothelial alpha5 and alphav integrins cooperate in remodeling of the vasculature during development. *Development, 137*(14), 2439-2449. doi:10.1242/dev.049551

Vartanian, K. B., Kirkpatrick, S. J., McCarty, O. J., Vu, T. Q., Hanson, S. R., & Hinds, M. T. (2009). Distinct extracellular matrix microenvironments of progenitor and carotid endothelial cells. *J Biomed Mater Res A, 91*(2), 528-539. doi:10.1002/jbm.a.32225

Vasa, M., Breitschopf, K., Zeiher, A. M., & Dimmeler, S. (2000). Nitric oxide activates telomerase and delays endothelial cell senescence. *Circ Res, 87*(7), 540-542.

Vasa, M., Fichtlscherer, S., Adler, K., Aicher, A., Martin, H., Zeiher, A. M., & Dimmeler, S. (2001). Increase in circulating endothelial progenitor cells by statin therapy in patients with stable coronary artery disease. *Circulation, 103*(24), 2885-2890.

Vasa, M., Fichtlscherer, S., Aicher, A., Adler, K., Urbich, C., Martin, H., . . . Dimmeler, S. (2001). Number and migratory activity of circulating endothelial progenitor cells inversely correlate with risk factors for coronary artery disease. *Circ Res, 89*(1), E1-7.

Vaughan, E. E., Liew, A., Mashayekhi, K., Dockery, P., McDermott, J., Kealy, B., . . . O'Brien, T. (2012). Pretreatment of endothelial progenitor cells with osteopontin enhances cell therapy for peripheral vascular disease. *Cell Transplant, 21*(6), 1095-1107. doi:10.3727/096368911X623880

Ventura, A., Young, A. G., Winslow, M. M., Lintault, L., Meissner, A., Erkeland, S. J., . . . Jacks, T. (2008). Targeted deletion reveals essential and overlapping functions of the miR-17 through 92 family of miRNA clusters. *Cell, 132*(5), 875-886. doi:10.1016/j.cell.2008.02.019

Venturini, L., Battmer, K., Castoldi, M., Schultheis, B., Hochhaus, A., Muckenthaler, M. U., . . . Scherr, M. (2007). Expression of the miR-17-92 polycistron in chronic myeloid leukemia (CML) CD34+ cells. *Blood, 109*(10), 4399-4405. doi:10.1182/blood-2006-09-045104

Verma, S., Kuliszewski, M. A., Li, S. H., Szmitko, P. E., Zucco, L., Wang, C. H., . . . Kutryk, M. J. (2004). C-reactive protein attenuates endothelial progenitor cell survival, differentiation, and function: further evidence of a mechanistic link between C-reactive protein and cardiovascular disease. *Circulation, 109*(17), 2058-2067. doi:10.1161/01.CIR.0000127577.63323.24

Volinia, S., Calin, G. A., Liu, C. G., Ambs, S., Cimmino, A., Petrocca, F., . . . Croce, C. M. (2006). A microRNA expression signature of human solid tumors defines cancer gene targets. *Proc Natl Acad Sci U S A, 103*(7), 2257-2261. doi:10.1073/pnas.0510565103

von der Leyen, H. E., Gibbons, G. H., Morishita, R., Lewis, N. P., Zhang, L., Nakajima, M., . . . Dzau, V. J. (1995). Gene therapy inhibiting neointimal vascular lesion: in vivo transfer of endothelial cell nitric oxide synthase gene. *Proc Natl Acad Sci U S A, 92*(4), 1137-1141.

Vono, R., Spinetti, G., Gubernator, M., & Madeddu, P. (2012). What's new in regenerative medicine: split up of the mesenchymal stem cell family promises new hope for cardiovascular repair. *J Cardiovasc Transl Res, 5*(5), 689-699. doi:10.1007/s12265-012-9395-2

Vormoor, J., Lapidot, T., Pflumio, F., Risdon, G., Patterson, B., Broxmeyer, H. E., & Dick, J. E. (1994). Immature human cord blood progenitors engraft and proliferate to high levels in severe combined immunodeficient mice. *Blood, 83*(9), 2489-2497.

Voyta, J. C., Via, D. P., Butterfield, C. E., & Zetter, B. R. (1984). Identification and isolation of endothelial cells based on their increased uptake of acetylated-low density lipoprotein. *J Cell Biol, 99*(6), 2034-2040.

Waltenberger, J., Mayr, U., Pentz, S., & Hombach, V. (1996). Functional upregulation of the vascular endothelial growth factor receptor KDR by hypoxia. *Circulation, 94*(7), 1647-1654.

Walter, D. H., Haendeler, J., Reinhold, J., Rochwalsky, U., Seeger, F., Honold, J., . . . Dimmeler, S. (2005). Impaired CXCR4 signaling contributes to the reduced neovascularization capacity of endothelial progenitor cells from patients with coronary artery disease. *Circ Res, 97*(11), 1142-1151. doi:10.1161/01.RES.0000193596.94936.2c

Walter, D. H., Rittig, K., Bahlmann, F. H., Kirchmair, R., Silver, M., Murayama, T., . . . Isner, J. M. (2002). Statin therapy accelerates reendothelialization: a novel effect involving mobilization and incorporation of bone marrow-derived endothelial progenitor cells. *Circulation, 105*(25), 3017-3024.

Walter, D. H., Schachinger, V., Elsner, M., Mach, S., Auch-Schwelk, W., & Zeiher, A. M. (2000). Effect of statin therapy on restenosis after coronary stent implantation. *Am J Cardiol, 85*(8), 962-968.

Wang, C. H., Cherng, W. J., Yang, N. I., Kuo, L. T., Hsu, C. M., Yeh, H. I., . . . Stanford, W. L. (2008). Late-outgrowth endothelial cells attenuate intimal hyperplasia contributed by mesenchymal stem cells after vascular injury. *Arterioscler Thromb Vasc Biol, 28*(1), 54-60. doi:10.1161/ATVBAHA.107.147256

Wang, C. H., Verma, S., Hsieh, I. C., Chen, Y. J., Kuo, L. T., Yang, N. I., . . . Cherng, W. J. (2006). Enalapril increases ischemia-induced endothelial progenitor cell mobilization through manipulation of the CD26 system. *J Mol Cell Cardiol, 41*(1), 34-43. doi:10.1016/j.yjmcc.2006.03.006

Wang, D., Li, L. K., Dai, T., Wang, A., & Li, S. (2018). Adult Stem Cells in Vascular Remodeling. *Theranostics, 8*(3), 815-829. doi:10.7150/thno.19577

Wang, D., Wang, A., Wu, F., Qiu, X., Li, Y., Chu, J., . . . Li, S. (2017). Sox10(+) adult stem cells contribute to biomaterial encapsulation and microvascularization. *Sci Rep, 7*, 40295. doi:10.1038/srep40295

Wang, H., Yin, Y. G., Huang, H., Zhao, X. H., Yu, J., Wang, Q., . . . Ding, S. F. (2016). Transplantation of EPCs overexpressing PDGFR-beta promotes vascular repair in the early phase after vascular injury. *BMC Cardiovasc Disord, 16*(1), 179. doi:10.1186/s12872-016-0353-9

Wang, J., & Milner, R. (2006). Fibronectin promotes brain capillary endothelial cell survival and proliferation through alpha5beta1 and alphavbeta3 integrins via MAP kinase signalling. *J Neurochem, 96*(1), 148-159. doi:10.1111/j.1471-4159.2005.03521.x

Wang, S. H., Lin, S. J., Chen, Y. H., Lin, F. Y., Shih, J. C., Wu, C. C., . . . Chen, Y. L. (2009). Late outgrowth endothelial cells derived from Wharton jelly in human umbilical cord reduce neointimal formation after vascular injury: involvement of pigment epithelium-derived factor. *Arterioscler Thromb Vasc Biol, 29*(6), 816-822. doi:10.1161/ATVBAHA.109.184739

Wang, X., Chen, J., Tao, Q., Zhu, J., & Shang, Y. (2004). Effects of ox-LDL on number and activity of circulating endothelial progenitor cells. *Drug Chem Toxicol, 27*(3), 243-255. doi:10.1081/DCT-120037505

Wang, Y., Sheng, G., Juranek, S., Tuschl, T., & Patel, D. J. (2008). Structure of the guide-strand-containing argonaute silencing complex. *Nature, 456*(7219), 209-213. doi:10.1038/nature07315

Wang, Y. S., Wang, H. Y., Liao, Y. C., Tsai, P. C., Chen, K. C., Cheng, H. Y., . . . Juo, S. H. (2012). MicroRNA-195 regulates vascular smooth muscle cell phenotype and prevents neointimal formation. *Cardiovasc Res, 95*(4), 517-526. doi:10.1093/cvr/cvs223

Werner, N., Junk, S., Laufs, U., Link, A., Walenta, K., Bohm, M., & Nickenig, G. (2003). Intravenous transfusion of endothelial progenitor cells reduces neointima formation after vascular injury. *Circ Res, 93*(2), e17-24. doi:10.1161/01.RES.0000083812.30141.74

Werner, N., Kosiol, S., Schiegl, T., Ahlers, P., Walenta, K., Link, A., . . . Nickenig, G. (2005). Circulating endothelial progenitor cells and cardiovascular outcomes. *N Engl J Med, 353*(10), 999-1007. doi:10.1056/NEJMoa043814

Werner, N., & Nickenig, G. (2006). Influence of cardiovascular risk factors on endothelial progenitor cells: limitations for therapy? *Arterioscler Thromb Vasc Biol, 26*(2), 257-266. doi:01.ATV.0000198239.41189.5d [pii]

10.1161/01.ATV.0000198239.41189.5d

Werner, N., Priller, J., Laufs, U., Endres, M., Bohm, M., Dirnagl, U., & Nickenig, G. (2002). Bone marrow-derived progenitor cells modulate vascular reendothelialization and neointimal formation: effect of 3-hydroxy-3-methylglutaryl coenzyme a reductase inhibition. *Arterioscler Thromb Vasc Biol, 22*(10), 1567-1572.

Wijelath, E. S., Rahman, S., Murray, J., Patel, Y., Savidge, G., & Sobel, M. (2004). Fibronectin promotes VEGF-induced CD34 cell differentiation into endothelial cells. *J Vasc Surg, 39*(3), 655-660. doi:10.1016/j.jvs.2003.10.042

Williams, P. A., & Silva, E. A. (2015). The Role of Synthetic Extracellular Matrices in Endothelial Progenitor Cell Homing for Treatment of Vascular Disease. *Ann Biomed Eng, 43*(10), 2301-2313. doi:10.1007/s10439-015-1400-x

Williamson, K., Stringer, S. E., & Alexander, M. Y. (2012). Endothelial progenitor cells enter the aging arena. *Front Physiol, 3*, 30. doi:10.3389/fphys.2012.00030

Winter, J., Jung, S., Keller, S., Gregory, R. I., & Diederichs, S. (2009). Many roads to maturity: microRNA biogenesis pathways and their regulation. *Nat Cell Biol, 11*(3), 228-234. doi:10.1038/ncb0309-228

Wojakowski, W., Pyrlik, A., Krol, M., Buszman, P., Ochala, A., Milewski, K., . . . Tendera, M. (2013). Circulating endothelial progenitor cells are inversely correlated with in-stent restenosis in patients with non-ST-segment elevation acute coronary syndromes treated with EPC-capture stents (JACK-EPC trial). *Minerva Cardioangiol, 61*(3), 301-311.

Woods, K., Thomson, J. M., & Hammond, S. M. (2007). Direct regulation of an oncogenic micro-RNA cluster by E2F transcription factors. *J Biol Chem, 282*(4), 2130-2134. doi:10.1074/jbc.C600252200

Wu, W., Xiao, H., Laguna-Fernandez, A., Villarreal, G., Jr., Wang, K. C., Geary, G. G., . . . Shyy, J. Y. (2011). Flow-Dependent Regulation of Kruppel-Like Factor 2 Is Mediated by MicroRNA-92a. *Circulation, 124*(5), 633-641. doi:10.1161/CIRCULATIONAHA.110.005108

Xiao, C., Srinivasan, L., Calado, D. P., Patterson, H. C., Zhang, B., Wang, J., . . . Rajewsky, K. (2008). Lymphoproliferative disease and autoimmunity in mice with increased miR-17-92 expression in lymphocytes. *Nat Immunol, 9*(4), 405-414. doi:10.1038/ni1575

Xu, J., Liu, X., Jiang, Y., Chu, L., Hao, H., Liua, Z., . . . Liu, Z. (2008). MAPK/ERK signalling mediates VEGF-induced bone marrow stem cell differentiation into endothelial cell. *J Cell Mol Med, 12*(6A), 2395-2406. doi:10.1111/j.1582-4934.2008.00266.x

Xu, Q. (2008). Stem cells and transplant arteriosclerosis. *Circ Res, 102*(9), 1011-1024. doi:102/9/1011 [pii]

10.1161/CIRCRESAHA.108.171488

Yamaguchi, J., Kusano, K. F., Masuo, O., Kawamoto, A., Silver, M., Murasawa, S., . . . Asahara, T. (2003). Stromal cell-derived factor-1 effects on ex vivo expanded endothelial progenitor cell recruitment for ischemic neovascularization. *Circulation, 107*(9), 1322-1328.

Yamaguchi, T. P., Dumont, D. J., Conlon, R. A., Breitman, M. L., & Rossant, J. (1993). flk-1, an flt-related receptor tyrosine kinase is an early marker for endothelial cell precursors. *Development, 118*(2), 489-498.

Yamakuchi, M. (2012). Endothelial senescence and microRNA. *Biomol Concepts, 3*(3), 213-223. doi:10.1515/bmc-2011-0042

Yang, D., Tournier, C., Wysk, M., Lu, H. T., Xu, J., Davis, R. J., & Flavell, R. A. (1997). Targeted disruption of the MKK4 gene causes embryonic death, inhibition of c-Jun NH2-terminal kinase activation, and defects in AP-1 transcriptional activity. *Proc Natl Acad Sci U S A, 94*(7), 3004-3009.

Yang, J. T., Rayburn, H., & Hynes, R. O. (1993). Embryonic mesodermal defects in alpha 5 integrin-deficient mice. *Development, 119*(4), 1093-1105.

Yang, N., Li, D., Jiao, P., Chen, B., Yao, S., Sang, H., . . . Qin, S. (2011). The characteristics of endothelial progenitor cells derived from mononuclear cells of rat bone marrow in different culture conditions. *Cytotechnology, 63*(3), 217-226. doi:10.1007/s10616-010-9329-2

Yang, W., Chendrimada, T. P., Wang, Q., Higuchi, M., Seeburg, P. H., Shiekhattar, R., & Nishikura, K. (2006). Modulation of microRNA processing and expression through RNA editing by ADAR deaminases. *Nat Struct Mol Biol, 13*(1), 13-21. doi:10.1038/nsmb1041

Yang, W. J., Yang, D. D., Na, S., Sandusky, G. E., Zhang, Q., & Zhao, G. (2005). Dicer is required for embryonic angiogenesis during mouse development. *J Biol Chem, 280*(10), 9330-9335. doi:10.1074/jbc.M413394200

Yang, X., Coriolan, D., Murthy, V., Schultz, K., Golenbock, D. T., & Beasley, D. (2005). Proinflammatory phenotype of vascular smooth muscle cells: role of efficient Toll-like receptor 4 signaling. *Am J Physiol Heart Circ Physiol, 289*(3), H1069-1076. doi:10.1152/ajpheart.00143.2005

Yao, Y., Sheng, Z., Li, Y., Fu, C., Ma, G., Liu, N., . . . Chao, L. (2013). Tissue kallikrein-modified human endothelial progenitor cell implantation improves cardiac function via enhanced activation of akt and increased angiogenesis. *Lab Invest, 93*(5), 577-591. doi:10.1038/labinvest.2013.48

Ye, E. A., & Steinle, J. J. (2015). miR-15b/16 protects primary human retinal microvascular endothelial cells against hyperglycemia-induced increases in tumor necrosis factor alpha and suppressor of cytokine signaling 3. *J Neuroinflammation, 12*, 44. doi:10.1186/s12974-015-0265-0

Yin, A. H., Miraglia, S., Zanjani, E. D., Almeida-Porada, G., Ogawa, M., Leary, A. G., . . . Buck, D. W. (1997). AC133, a novel marker for human hematopoietic stem and progenitor cells. *Blood, 90*(12), 5002-5012.

Yin, H., Kanasty, R. L., Eltoukhy, A. A., Vegas, A. J., Dorkin, J. R., & Anderson, D. G. (2014). Non-viral vectors for gene-based therapy. *Nat Rev Genet, 15*(8), 541-555. doi:10.1038/nrg3763

Yin, Y., Liu, H., Wang, F., Li, L., Deng, M., Huang, L., & Zhao, X. (2015). Transplantation of cryopreserved human umbilical cord blood-derived endothelial progenitor cells induces recovery of carotid artery injury in nude rats. *Stem Cell Res Ther, 6*, 37. doi:10.1186/s13287-015-0022-4

Yoder, M. C. (2012). Human endothelial progenitor cells. *Cold Spring Harb Perspect Med, 2*(7), a006692. doi:10.1101/cshperspect.a006692

Yoder, M. C., Mead, L. E., Prater, D., Krier, T. R., Mroueh, K. N., Li, F., . . . Ingram, D. A. (2007). Redefining endothelial progenitor cells via clonal analysis and hematopoietic stem/progenitor cell principals. *Blood, 109*(5), 1801-1809. doi:10.1182/blood-2006-08-043471

Yoon, C. H., Hur, J., Park, K. W., Kim, J. H., Lee, C. S., Oh, I. Y., . . . Kim, H. S. (2005). Synergistic neovascularization by mixed transplantation of early endothelial progenitor cells and late outgrowth endothelial cells: the role of angiogenic cytokines and matrix metalloproteinases. *Circulation, 112*(11), 1618-1627. doi:10.1161/CIRCULATIONAHA.104.503433

Yoshioka, T., Takahashi, M., Shiba, Y., Suzuki, C., Morimoto, H., Izawa, A., . . . Ikeda, U. (2006). Granulocyte colony-stimulating factor (G-CSF) accelerates reendothelialization and reduces neointimal formation after vascular injury in mice. *Cardiovasc Res, 70*(1), 61-69. doi:10.1016/j.cardiores.2005.12.013

Young, P. E., Baumhueter, S., & Lasky, L. A. (1995). The sialomucin CD34 is expressed on hematopoietic cells and blood vessels during murine development. *Blood, 85*(1), 96-105.

Yu, Z., Wang, C., Wang, M., Li, Z., Casimiro, M. C., Liu, M., . . . Pestell, R. G. (2008). A cyclin D1/microRNA 17/20 regulatory feedback loop in control of breast cancer cell proliferation. *J Cell Biol, 182*(3), 509-517. doi:10.1083/jcb.200801079

Yuan, Q., Bai, Y. P., Shi, R. Z., Liu, S. Y., Chen, X. M., Chen, L., . . . Hu, C. P. (2014). Regulation of endothelial progenitor cell differentiation and function by dimethylarginine dimethylaminohydrolase 2 in an asymmetric dimethylarginine-independent manner. *Cell Biol Int, 38*(9), 1013-1022. doi:10.1002/cbin.10288

Zampetaki, A., Kirton, J. P., & Xu, Q. (2008). Vascular repair by endothelial progenitor cells. *Cardiovasc Res, 78*(3), 413-421. doi:cvn081 [pii]

10.1093/cvr/cvn081

Zampetaki, A., & Mayr, M. (2012). MicroRNAs in vascular and metabolic disease. *Circ Res, 110*(3), 508-522. doi:10.1161/CIRCRESAHA.111.247445

Zaragoza, C., Gomez-Guerrero, C., Martin-Ventura, J. L., Blanco-Colio, L., Lavin, B., Mallavia, B., . . . Egido, J. (2011). Animal models of cardiovascular diseases. *J Biomed Biotechnol, 2011*, 497841. doi:10.1155/2011/497841

Zargham, R. (2008). Preventing restenosis after angioplasty: a multistage approach. *Clin Sci (Lond), 114*(4), 257-264. doi:10.1042/CS20070228

Zargham, R., Pepin, J., & Thibault, G. (2007). alpha8beta1 Integrin is up-regulated in the neointima concomitant with late luminal loss after balloon injury. *Cardiovasc Pathol, 16*(4), 212-220. doi:10.1016/j.carpath.2007.01.010

Zaric, J., & Ruegg, C. (2005). Integrin-mediated adhesion and soluble ligand binding stabilize COX-2 protein levels in endothelial cells by inducing expression and preventing degradation. *J Biol Chem, 280*(2), 1077-1085. doi:10.1074/jbc.M410006200

Zemani, F., Silvestre, J. S., Fauvel-Lafeve, F., Bruel, A., Vilar, J., Bieche, I., . . . Boisson-Vidal, C. (2008). Ex vivo priming of endothelial progenitor cells with SDF-1 before transplantation could increase their proangiogenic potential. *Arterioscler Thromb Vasc Biol, 28*(4), 644-650. doi:10.1161/ATVBAHA.107.160044

Zengin, E., Chalajour, F., Gehling, U. M., Ito, W. D., Treede, H., Lauke, H., . . . Ergun, S. (2006). Vascular wall resident progenitor cells: a source for postnatal vasculogenesis. *Development, 133*(8), 1543-1551. doi:10.1242/dev.02315

Zhang, C. (2008). MicroRNAs: role in cardiovascular biology and disease. *Clin Sci (Lond), 114*(12), 699-706. doi:10.1042/CS20070211

Zhang, C. (2010). MicroRNAs in vascular biology and vascular disease. *J Cardiovasc Transl Res, 3*(3), 235-240. doi:10.1007/s12265-010-9164-z

Zhang, C., Zhou, C., Wu, X. J., Yang, M., Yang, Z. H., Xiong, H. Z., . . . Li, X. N. (2014). Human CD133-positive hematopoietic progenitor cells initiate growth and metastasis of colorectal cancer cells. *Carcinogenesis, 35*(12), 2771-2777. doi:10.1093/carcin/bgu192

Zhang, J., Li, S., Li, L., Li, M., Guo, C., Yao, J., & Mi, S. (2015). Exosome and exosomal microRNA: trafficking, sorting, and function. *Genomics Proteomics Bioinformatics, 13*(1), 17-24. doi:10.1016/j.gpb.2015.02.001

Zhang, L., Huang, J., Yang, N., Greshock, J., Megraw, M. S., Giannakakis, A., . . . Coukos, G. (2006). microRNAs exhibit high frequency genomic alterations in human cancer. *Proc Natl Acad Sci U S A, 103*(24), 9136-9141. doi:10.1073/pnas.0508889103

Zhang, L., Zhou, M., Qin, G., Weintraub, N. L., & Tang, Y. (2014). MiR-92a regulates viability and angiogenesis of endothelial cells under oxidative stress. *Biochem Biophys Res Commun, 446*(4), 952-958. doi:10.1016/j.bbrc.2014.03.035

Zhang, L., Zhou, M., Wang, Y., Huang, W., Qin, G., Weintraub, N. L., & Tang, Y. (2014). miR-92a inhibits vascular smooth muscle cell apoptosis: role of the MKK4-JNK pathway. *Apoptosis, 19*(6), 975-983. doi:10.1007/s10495-014-0987-y

Zhang, Q., Kandic, I., & Kutryk, M. J. (2011). Dysregulation of angiogenesis-related microRNAs in endothelial progenitor cells from patients with coronary artery disease. *Biochem Biophys Res Commun, 405*(1), 42-46. doi:10.1016/j.bbrc.2010.12.119

Zhang, X., Chattopadhyay, A., Ji, Q. S., Owen, J. D., Ruest, P. J., Carpenter, G., & Hanks, S. K. (1999). Focal adhesion kinase promotes phospholipase C-gamma1 activity. *Proc Natl Acad Sci U S A, 96*(16), 9021-9026.

Zhang, Z., Vuori, K., Reed, J. C., & Ruoslahti, E. (1995). The alpha 5 beta 1 integrin supports survival of cells on fibronectin and up-regulates Bcl-2 expression. *Proc Natl Acad Sci U S A, 92*(13), 6161-6165.

Zhao, J., Bolton, E. M., Randle, L., Bradley, J. A., & Lever, A. M. (2014). Functional characterization of late outgrowth endothelial progenitor cells in patients with end-stage renal failure. *Transpl Int, 27*(5), 437-451. doi:10.1111/tri.12277

Zhao, J., Mitrofan, C. G., Appleby, S. L., Morrell, N. W., & Lever, A. M. (2016). Disrupted Endothelial Cell Layer and Exposed Extracellular Matrix Proteins Promote Capture of Late Outgrowth Endothelial Progenitor Cells. *Stem Cells Int, 2016*, 1406304. doi:10.1155/2016/1406304

Zhao, X., Huang, L., Yin, Y., Fang, Y., & Zhou, Y. (2007). Autologous endothelial progenitor cells transplantation promoting endothelial recovery in mice. *Transpl Int, 20*(8), 712-721. doi:10.1111/j.1432-2277.2007.00497.x

Zhao, Y., Vanhoutte, P. M., & Leung, S. W. (2015). Vascular nitric oxide: Beyond eNOS. *J Pharmacol Sci, 129*(2), 83-94. doi:10.1016/j.jphs.2015.09.002

Zhou, J., Chen, L., Fan, Y., Jiang, J., & Wan, J. (2014). Atorvastatin increases endothelial progenitor cells in balloon-injured mouse carotid artery. *Can J Physiol Pharmacol, 92*(5), 369-374. doi:10.1139/cjpp-2013-0292

Zhou, J., Li, Y. S., Nguyen, P., Wang, K. C., Weiss, A., Kuo, Y. C., . . . Chien, S. (2013). Regulation of Vascular Smooth Muscle Cell Turnover by Endothelial Cell-Secreted MicroRNA-126: Role of Shear Stress. *Circ Res, 113*(1), 40-51. doi:10.1161/CIRCRESAHA.113.280883

Zhou, J., Wang, K. C., Wu, W., Subramaniam, S., Shyy, J. Y., Chiu, J. J., . . . Chien, S. (2011). MicroRNA-21 targets peroxisome proliferators-activated receptor-alpha in an autoregulatory loop to modulate flow-induced endothelial inflammation. *Proc Natl Acad Sci U S A, 108*(25), 10355-10360. doi:10.1073/pnas.1107052108

Zhu, S., Deng, S., Ma, Q., Zhang, T., Jia, C., Zhuo, D., . . . Dong, C. (2013). MicroRNA-10A* and MicroRNA-21 modulate endothelial progenitor cell senescence via suppressing high-mobility group A2. *Circ Res, 112*(1), 152-164. doi:10.1161/CIRCRESAHA.112.280016

Zhuang, G., Wu, X., Jiang, Z., Kasman, I., Yao, J., Guan, Y., . . . Ferrara, N. (2012). Tumour-secreted miR-9 promotes endothelial cell migration and angiogenesis by activating the JAK-STAT pathway. *EMBO J, 31*(17), 3513-3523. doi:10.1038/emboj.2012.183

Ziegelhoeffer, T., Fernandez, B., Kostin, S., Heil, M., Voswinckel, R., Helisch, A., & Schaper, W. (2004). Bone marrow-derived cells do not incorporate into the adult growing vasculature. *Circ Res, 94*(2), 230-238. doi:10.1161/01.RES.0000110419.50982.1C

Zorzi, P., Aplin, A. C., Smith, K. D., & Nicosia, R. F. (2010). Technical Advance: The rat aorta contains resident mononuclear phagocytes with proliferative capacity and proangiogenic properties. *J Leukoc Biol, 88*(5), 1051-1059. doi:10.1189/jlb.0310178